Approaches to the Synthesis of Chiral and Amino-substituted BODIPY Dyes

By

Rua Bandar Alnoman

A thesis submitted in partial fulfilment of the requirements for the degree of

Doctor of Philosophy

July 2016

Abstract

Boron dipyrromethenes (BODIPYs) have attracted considerable attention due to their fluorescence properties, including high fluorescence quantum yields and absorption coefficients, good photochemical stability and narrow absorption and emission bandwidths. Because of these properties, they have found extensive use for in vivo imaging, analyte sensing, photodynamic therapy, solar cells and light harvesting arrays. This thesis is divided in two parts. Part one covers the synthesis of functionalised chiral BODIPYs whilst part two involves investigations into the synthesis and application of aminoBODIPY via metal catalysed amination reactions.

Four approaches to the synthesis of novel chiral BODIPY dyes were investigated. The axially chiral BODIPY dye with C2-symmetry **I** was synthesised via Suzuki coupling of the corresponding 2,6-dibromoBODIPY with 2-methoxyphenyl boronic acid. The unsymmetrical axially chiral BODIPY **II** was synthesized via Suzuki coupling of the corresponding 2-bromoBODIPY with phenyl boronic acid. Unfortunately, attempted resolution of these chiral systems by analytical chiral HPLC was unsuccessful.

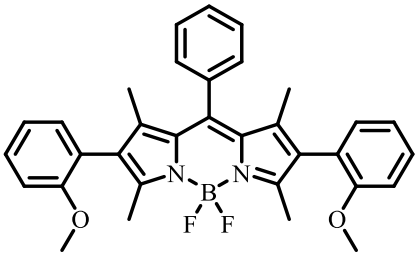

I

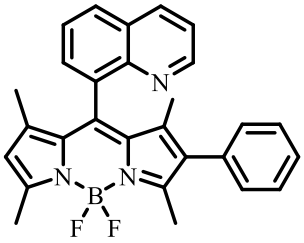

II

The new helically chiral BODIPYs **IIIa-c** were synthesised. Resolution of racemic helically chiral BODIPYs **IIIa** and **IIIb** was successfully accomplished by preparative chiral HPLC.

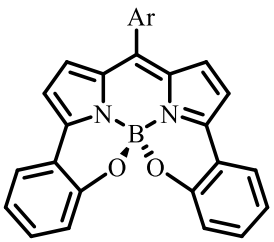

IIIa-c

IIIa, Ar=4-MeC_6H_4
IIIb, Ar=2-pyridyl
IIIc, Ar=4-$(C_8H_{17}O)C_6H_4$

Electronic circular dichroism (ECD) spectra of both (*M*) and (*P*) isomers of **IIIa** and **IIIb** were measured by Prof. W. Herrebout (University of Antwerp). Comparison of the measured and computationally predicted ECD spectra allowed the absolute configuration of each of the enantiomeric samples of **IIIa-b** to be established. The CPL spectra of both (*M*) and (*P*) isomers of **IIIa** and **IIIb** were recorded by Prof. R. D. Peacock (University of Glasgow). The $|g_{lum}|$ of **IIIa** at 637 nm is 0.0043 and **IIIb** at 675 nm is 0.0042, which are among the largest so far reported for a simple BODIPY fluorophore in solution.

We designed and synthesized the mono-strapped BODIPY **V** scaffold via sequential regioselective functionalisation of the unsymmetrical BODIPY **IV**. Resolution of *N,N,F,O*-BODIPY **V** by analytical chiral HPLC gave two peaks confirming that single enantiomers of this compound should be accessible.

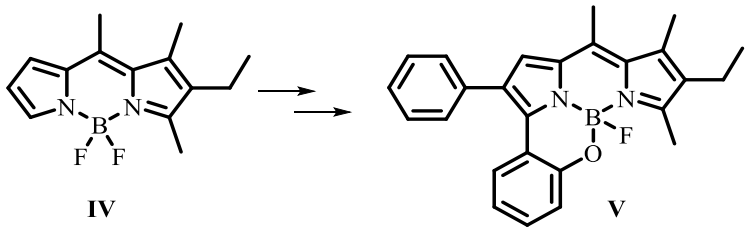

IV **V**

The 8-anisyl-substituted BODIPY **VI** was synthesized using a standard synthetic route, regioselective iodination with ICl then gave the 2-iodo-substituted BODIPY **VII**. We unexpectedly found that copper catalysed nucleophilic substitution of the 2-iodoBODIPY **VII** produced the 3-amino BODIPYs **VIIIa-n** in good yield. The reactions occurred successfully for a range of primary and secondary alkyl and aryl amines and even with benzamide, albeit in low yield.

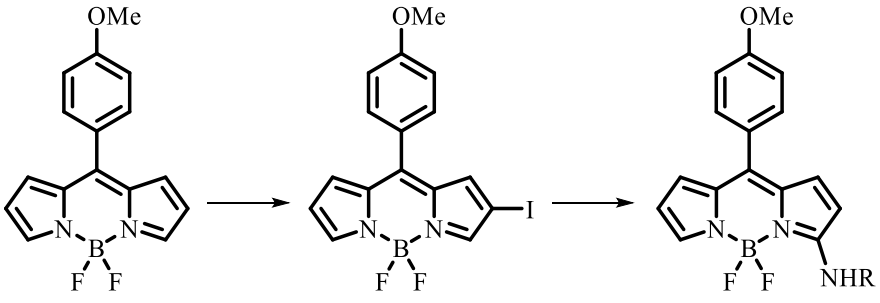

VI **VII** **VIIIa-n**

2-aminoBODIPYs **Xa-e** have been prepared successfully via Buchwald–Hartwig amination of the 2-iodoBODIPY **IX** (fully blocked). The presence of the nitrogen group

in the 2-position gives a broadened red-shifted absorption maximum and quenched fluorescence.

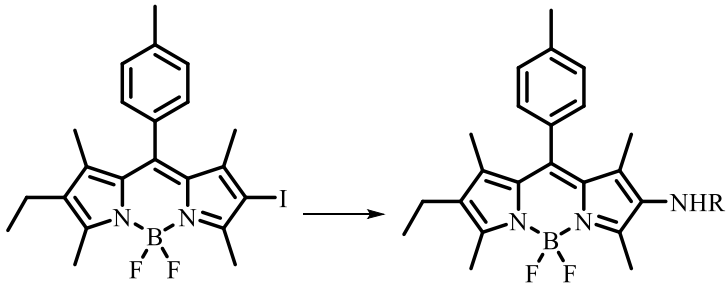

IX **Xa-e**

This palladium catalysed amination was used to prepare the 2-nitroaniline-substituted BODIPY **XI**. Reduction of the nitro group by hydrogenation gave the novel fluorescence-quenched 2-aminoaniline-substituted BODIPY **XII**. Reaction of this compound with triphosgene gave the corresponding benzimidazolone-substituted BODIPY **XIII**. The bright yellow fluorescence of the triphosgene reaction product **XIII** can be easily visualized by the naked eye. The detection limit for phosgene was determined to be 160 nM in solution at room temperature.

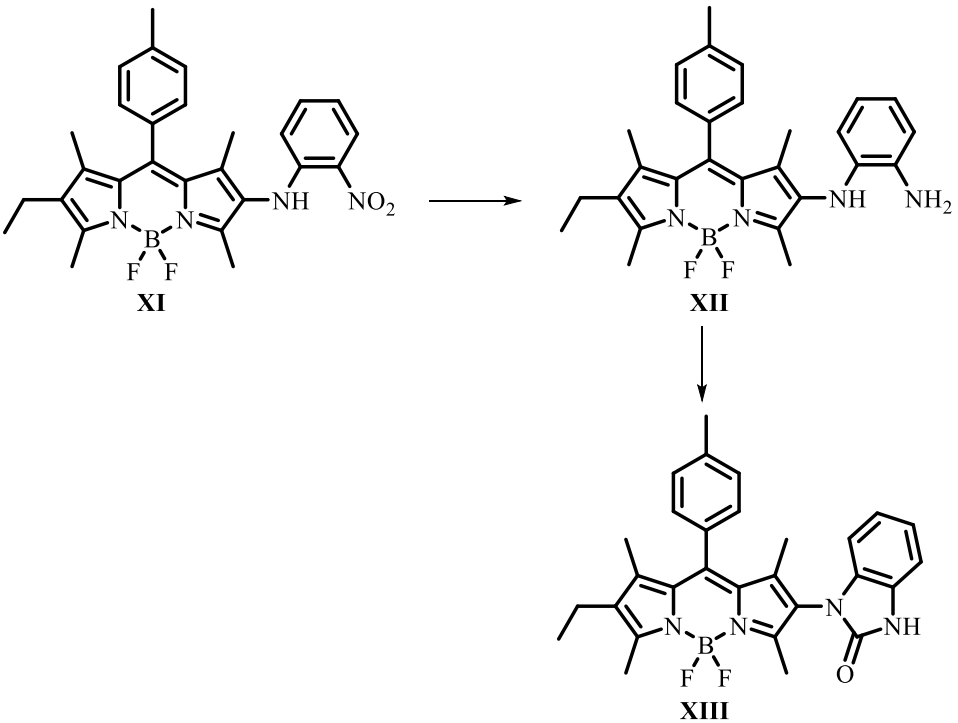

XI **XII** **XIII**

Dedication

I would like to dedicate this work to my father, Bandar Alnoman; to my mother, Hedayat Bokhari; to my brothers and sisters; to my wonderful husband, Moaz Zulali; and to my children, Omar and Joanne.

Acknowledgement

In the Name of Allah, the Most Gracious, the Most Merciful,

I would like to express my gratitude to Allah (God) for giving me the opportunity, determination, and strength to do this work.

I would like to express my deepest appreciation to my supervisor, Dr. Julian Knight, for his continuous support, guidance and encouragement over the course of my PhD and related research. I could not have imagined having a better advisor and mentor for my PhD study.

Many thanks also to my second supervisor, Dr. Michael Hall, for his support, guidance, knowledge, and experience from which I benefited from so greatly. I would like to thank Professor Anthony Harriman for his assistance with the measurements, Dr Corrine Wills for assistance with NMR spectroscopy, and Dr Paul G. Waddell for X-ray crystallography analysis. I would like to thank all the past and present members in the Dr. Julian Knight research group, for all the good times and memories.

Special thanks are directed to the Taibah University for providing scholarship funds and financial support. I also would like to thank Newcastle University for providing me with all the necessary facilities.

Finally, I would like to thank my entire family for their love, support, extraordinary encouragement, and assistance over the past few years. A special thank you goes to my husband for supporting me through these times, as I could not have been as successful without his flexibility and support.

Publications from this work

1. J. G. Knight, R. B. Alnoman, and Paul G. Waddell, *Org. Biomol. Chem.*, 2015, **13**, 3819-3829.
2. R. B. Alnoman, S. Rihn, D. C. O'Connor, F. A. Black, B. Costello, P. G. Waddell, W. Clegg, R. D. Peacock, W. Herrebout, J. G. Knight, and M. J. Hall, *Chem. Eur. J.*, 2016, **22**, 93-96.

List of Abbreviations

Ar	Aryl
atm	Atmosphere(s)
BINAP	2,2′-Bis(diphenylphosphino)-1,1′-binaphthalene
Boc	Di-t-butyl dicarbonate
BODIPY	Boron dipyrrin, 4,4-difluoro-4-bora-3a,4a-diaza-s-indacene
°C	Degree Celsius
cat	Catalytic
CD	Circular dichroism
cm^{-1}	Wavenumber(s)
CPL	Circularly polarized luminescence
DCE	Dichloroethane
DCM	Dichloromethane
DDQ	2,3-Dichloro-5,6-dicyano-1,4-benzoquinone
DMF	*N*,*N*-Dimethyl formamide
DMSO	Dimethylsulfoxide
d-PET	Donor photoinduced electron transfer
ee	Enantiomeric excess
eq	Equivalent
Et_2O	Diethyl Ether
EtOAc	Ethyl acetate
EtOH	Ethanol
ε	molar extinction coefficient
g	Gram
H-KITPHOS	11-dicyclohexylphosphino-12-phenyl-9,10-dihydro-9,10-ethenoanthracene
h	Hour/s
HPLC	High-performance liquid chromatography
IR	Infra-red
i-Pr_2NEt	*N*,*N*-Diisopropyethylamine
MeOH	Methanol

mg	Milligram
mL	Millilitre
mmol	Millimole
N_2	Nitrogen
NMR	Nuclear magnetic resonance
NBS	*N*-bromosuccinimide
PeT	Photoinduced electron transfer
$Pd_2(dba)_3$	Tris(dibenzylideneacetone)dipalladium(0)
$Pd(OAc)_2$	Palladium(II) acetate
ϕ	Quantum yield
S_0	Ground state
S_1	First excited state
SPhos	2-Dicyclohexylphosphino-2',6'-dimethoxybiphenyl
S_NAr	Nucleophilic aromatic substitution
TFA	Trifluoroacetic acid
THF	Tetrahydrofuran
TLC	Thin layer chromatography
UV	Ultraviolet
XPhos	2-Dicyclohexylphosphino-2′,4′,6′-triisopropylbiphenyl

Table of contents

Chapter 1: Introduction

1.1. General introduction to fluorescence

Luminescence is the emission of ultraviolet, visible or infrared photons from any substance, which occurs from an electronically excited state.[1–3] There are various types of luminescence, i.e. photoluminescence, radioluminescence, chemiluminescence, electroluminescence, and thermoluminescence, which are classified according to the mode of excitation.[1–3] Photoluminescence is the emission of the light from a material after absorption of photons. Photoluminescence is formally divided into two types: phosphorescence and fluorescence, which are determined by the nature of the excited state.

The phenomenon of fluorescence was introduced in the middle of the nineteenth century by the British scientist Sir George Gabriel Stokes.[2] Fluorescence is defined as the radiative emission of a photon by a substance from the first excited singlet state (S_1) to the ground singlet state (S_0), which can be schematically explained by the Jablonski energy level diagram (Figure 1.1).

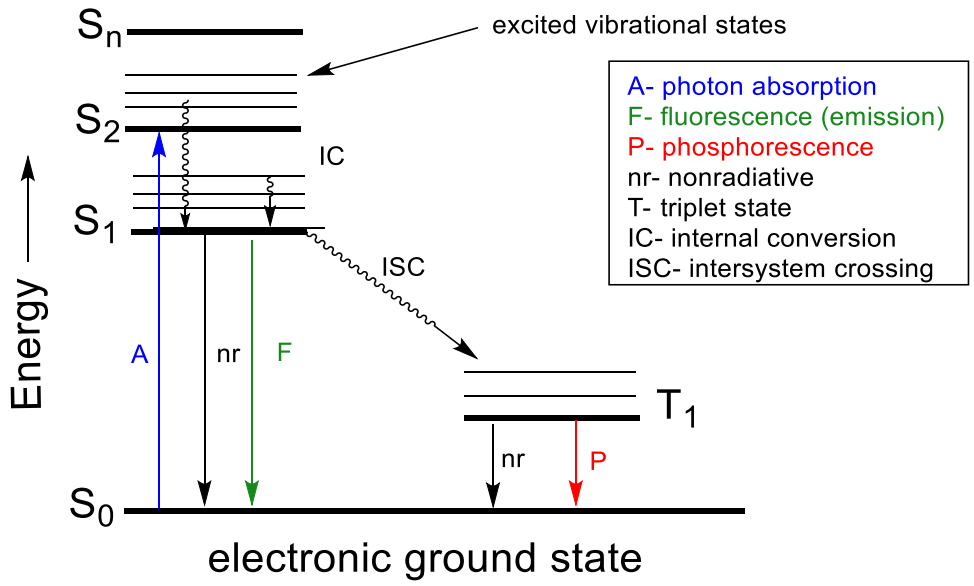

Figure 1.1: Jablonski energy level diagram.[1]

As shown in the Jablonski diagram bold horizontal lines correspond to the electronic states and above these the thin horizontal lines represent vibrational sublevels. Normally,

electrons are in the ground state (S_0). When incoming light with appropriate energy interacts with an electron in the molecule the photon may be absorbed, causing the electron to jump to an excited state (S_1 or S_2) and this process is very fast (10^{-15} second). The electron then loses energy due to the vibration of the molecule. This process is called internal conversion and the electron falls to the lowest electronic level (S_1). Finally the electron may return to one of the vibrational sub-levels of the ground state (S_0) by releasing light. Fluorescence is characterised by its emission spectrum, quantum yield and lifetime.

Quantum yield (Φ_F) is a measure of the efficiency of a fluorescent system. It is the ratio of the total number of emitted photons over the total number of absorbed photons.[1] The quantum yield (Φ_F) is expressed as a number or a percentage, with the maximum being 1 or 100%. It is common to measure the fluorescence quantum yield by comparison to a reference compound whose quantum yield has been accurately determined by direct measurement. In this case, the quantum yield of the sample is calculated according to Equation 1.1.

$$\Phi_{sample} = \Phi_{reference} \left(F_{sample} \left(1-10^{-A_{reference}}\right)\eta^2_{sample} / F_{reference} \left(1-10^{-A_{sample}}\right)\eta^2_{reference}\right).$$[4,5]

Equation 1.1

Here, Φ is the fluorescence quantum yield for the sample or reference, A is the absorption intensity at the excitation wavelength, F is the fluorescence area and η is the solvent refractive index.

The fluorescence lifetime is also important, it is a measure of the time that a fluorophore remains in its excited state (S_1) before returning to the ground state (S_0).[1,2]

1.2. General introduction to fluorophores

Over the past few decades, fluorescent compounds have continued to attract the attention of researchers due to their spectral and physicochemical properties.[6] The term fluorophore refers to a fluorescent molecule that can re-emit light upon light excitation. There are two different classes: intrinsic (that occur naturally) and extrinsic (typically synthetic) and each has its own properties.[2]

There are many organic dyes in common use including rhodamine,[7] fluorescein,[8] alexa,[9] ethidium,[10] cyanine,[11] and BODIPYs (Figure 1.2). Fluorescein is an example of a fluorescent dye which has been used as a fluorescent tracer for many applications. Fluorescein isothiocyanate is a reactive derivative of fluorescein dye which is commonly used to tag a target nucleophile.

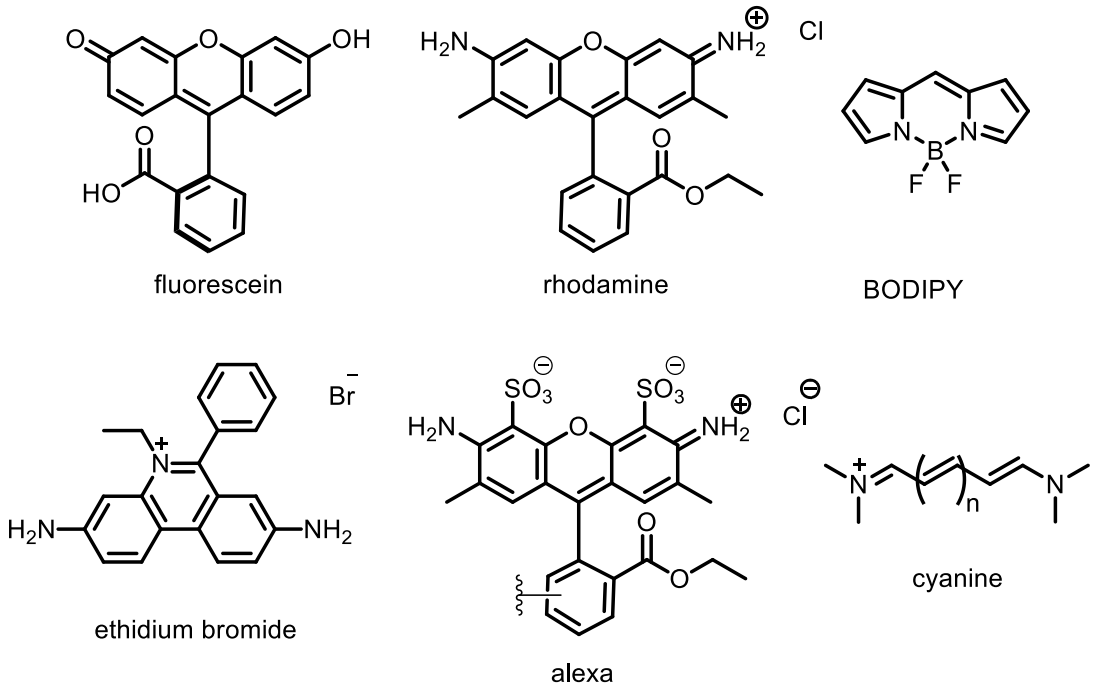

Figure 1.2: Structures of organic fluorescent dyes.

Rhodamine is another example of a fluorescent dye which can be used as a tracer dye within water to determine the direction and rate of flow and transport. There are many different Rhodamine derivatives such as Rhodamine B and Rhodamine 6G.

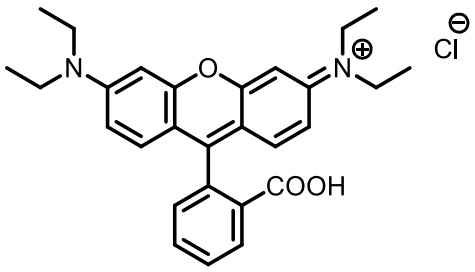

Rhodamine B

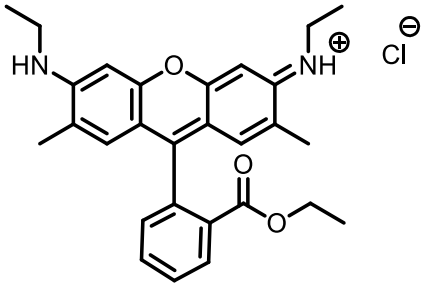

Rhodamine 6G

1.3. Borondipyrromethene Difluoride (BODIPY)

1.3.1. Background and structure

4,4-Difluoro-4-bora-3a,4a-diaza-s-indacene **1.1** (abbreviated to BODIPY), shown below, is the central heterocyclic core of a large family of fluorescent compounds.[12] In 1968, Treibs and Kreuzer synthesized the first BODIPY dye.[9] However, this discovery was not used until the 1990s when Boyer and co-workers realized that BODIPY dyes could be used as possible fluorescent probes.

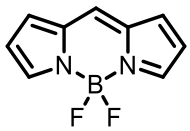

BODIPY **1.1**

Scheme 1.1 shows the numbering of a dipyrromethane **1.2**, a dipyrrin **1.3** and a boron dipyrrin **1.1**.[13] The numbering of a BODIPY core is different from that of a dipyrrin and a dipyrromethane.[12,13] The 8-position in the BODIPY core is often referred to as the meso site.[6,13]

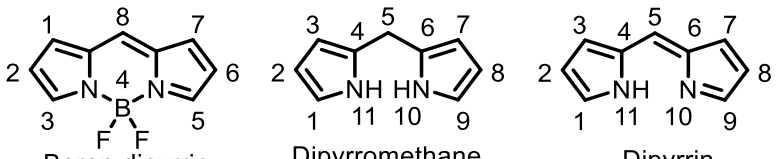

Scheme 1.1: Structure and numbering of a dipyrromethane **1.2**, a dipyrrin **1.3** and a boron dipyrrin **1.1**.[6]

In recent years, the number of published data on the synthesis and properties of BODIPYs has been increasing rapidly (Figure 1.3). According to the Web of Science Citation report, 6105 articles have been published on BODIPY as a topic since 1989.

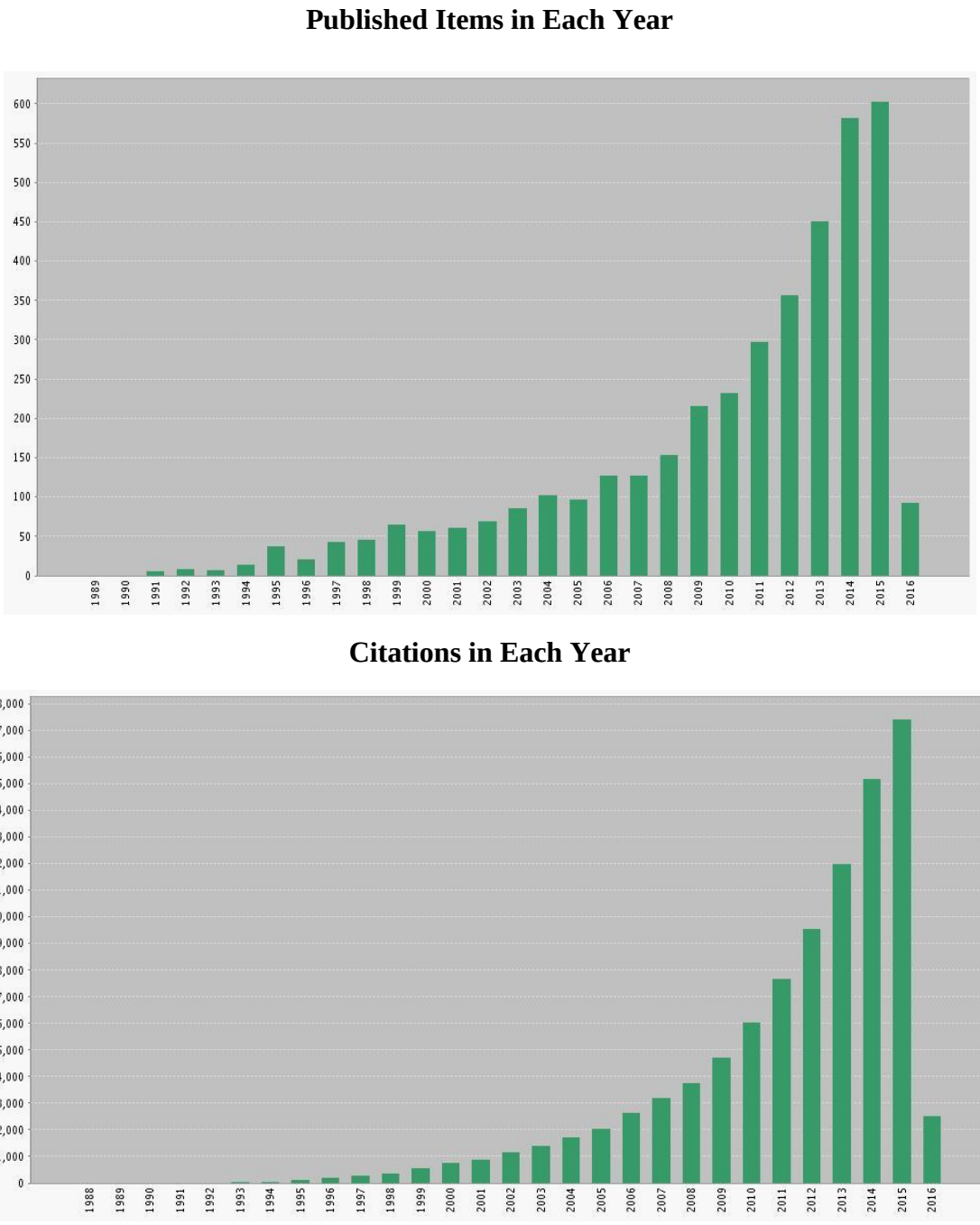

Figure 1.3: Web of Science citation report of the number of publications and citations resulting from searching "BODIPY" as the topic.

Also, in reviewing the literature, a number of reviews on BODIPY dyes have been published because of the fast increase in their popularity over the last few years. For instance, in 2007, Loudet and Burgess[12] reviewed the synthesis and spectroscopic properties of different types of BODIPY dyes and their derivatives.

In 2008, Ziessel[6] and co-workers discussed the chemistry and photophysical properties of BODIPY dyes. In 2011, Boyle and co-workers[14] reported a review on using BODIPYs as fluorescent components of novel light active materials. Awuah and You,[15] in 2012, provided an overview BODIPY dyes as photosensitizers for photodynamic therapy of cancer. Boens, Leen and Dehaen[16] described the synthesis of different BODIPYs as fluorescent indicators. In 2014, Shen[17] published a review on structural modification strategies for synthesis of long wavelength absorbing BODIPY dyes. In 2015, Ravikanth[18] discussed the synthesis, properties and applications of halogenated BODIPY dyes containing halogens at the pyrrole carbons of the BODIPY core.

1.3.2. General properties of BODIPY

Boron dipyrromethenes **1.1** tend to absorb light in the visible range, and are often characterised by sharp absorption and emission spectra with high molar extinction coefficient, high quantum yields of fluorescence and narrow absorption and emission bandwidths.[12] Also, they are soluble in most organic solvents and mostly insensitive to the solvent polarity and pH of their environment. They are stable under physiological conditions, display low toxicity, high photostability and resistance to chemical degradation.[12] The photophysical properties of the BODIPYs can be affected by introducing different substituents at the various positions of the BODIPY core as shown in Figure 1.4. The symmetrical alkylated BODIPYs **1.4** and **1.5** have not been reported.[12] The fluorescence quantum yields for **1.6**, **1.7**, **1.8** and **1.9** were reported in the literature and could be used as a reference to which other BODIPYs can be compared.[12] Also, the unsymmetrically substituted BODIPYs **1.9** and **1.10** have been synthesised. Comparing compounds **1.6** and **1.7** with compound **1.8**, alkylation at the 2,6-position generally leads to red-shift of absorption and emission maxima but lower quantum yield.[12]

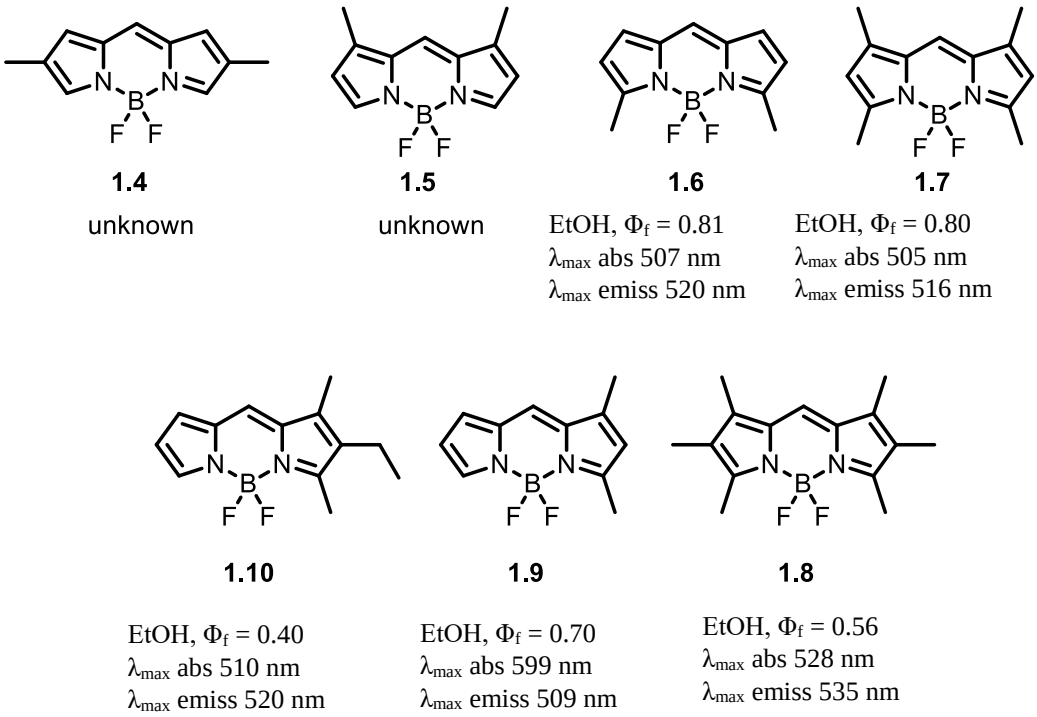

Figure 1.4: Different alkyl substitution on the core BODIPY dye.[12]

The presence of the aryl group at the meso-position of the 1,7-substituted BODIPY **1.13** leads to a slightly lower fluorescence quantum yield and red-shift of absorption and emission maxima compared to BODIPY **1.7**.[12] However, the fluorescence quantum yield of BODIPYs **1.11** and **1.12** are appreciably less than BODIPY **1.6**. Such differences are usually referred to the presence of 1,7-substituents which prevent free rotation of the aryl group, thus reducing loss of energy from the excited states through non-radiative processes.[12]

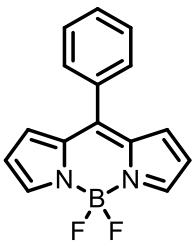

1.11

MeOH, Φ_f =0.06
λ_{max} abs 501 nm
λ_{max} emiss 517 nm

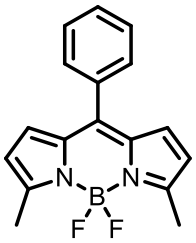

1.12

MeOH, Φ_f = 0.19
λ_{max} abs 508 nm
λ_{max} emiss 521 nm

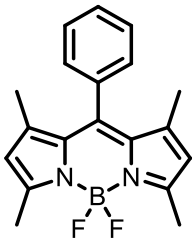

1.13

MeOH, Φ_f = 0.65
λ_{max} abs 508 nm
λ_{max} emiss 598 nm

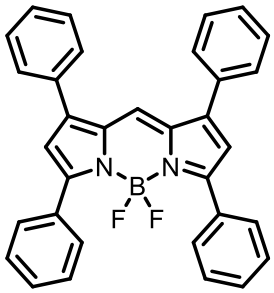

1.14

THF, Φ_f = 0.92
λ_{max} abs 571 nm
λ_{max} emiss 601

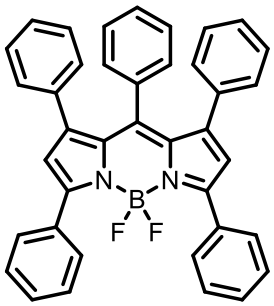

1.15

THF, Φ_f = 0.31
λ_{max} abs 561 nm
λ_{max} emiss 597 nm

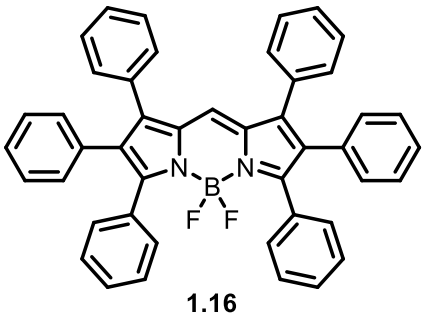

1.16

THF, Φ_f = 0.96
λ_{max} abs 576 nm
λ_{max} emiss 608 nm

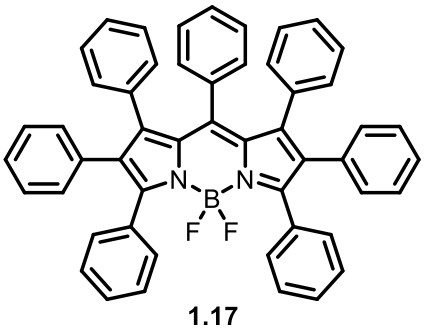

1.17

THF, Φ_f = 0.2
λ_{max} abs 573 nm
λ_{max} emiss 613 nm

Figure 1.5: Different alkyl and aryl substitution at the pyrrole carbons of the BODIPY core.[12,17,19]

Polyphenylated BODIPYs **1.14-1.17** have been synthesised.[17–21] Arylation at the pyrrole carbons of the BODIPY core leads to red-shifted absorption and emission maxima and increased quantum yield for these compounds (compare **1.14** with **1.7**, and **1.16** with **1.8**) as seen in Figure 1.5.

Moreover, it has found that the replacement of the fluorine atoms with aryl or alkyne groups such as BODIPY **1.19** and **1.20** produced only minor changes in the absorption and emission maxima as compared to parent BODIPY **1.18** (Figure 1.6).[12]

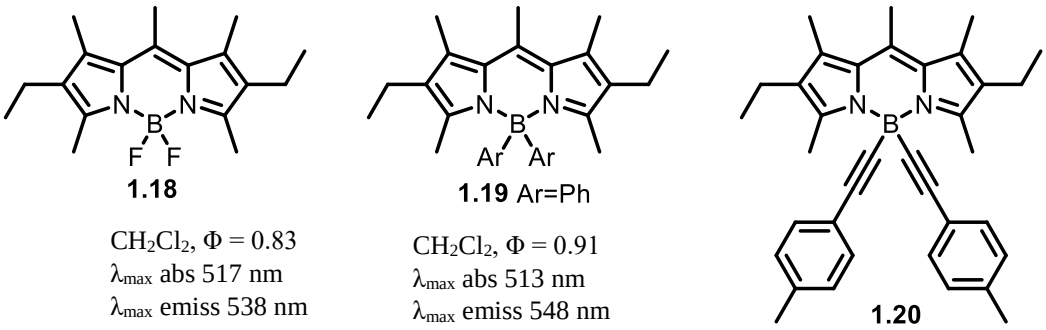

Figure 1.6: Example of the replacement of the two fluorine atom with aryl or alkyne group.[12]

Addition of alkoxy groups to the boron centre has also been reported in the literature.[22,23] For example, the replacement of the fluorine atoms in the BODIPY **1.21** with various alcohols produced *O*-BODIPYs **1.22-1.24** and the presence of alkoxy group cause little change to the photophysics (Figure 1.7).[22,23]

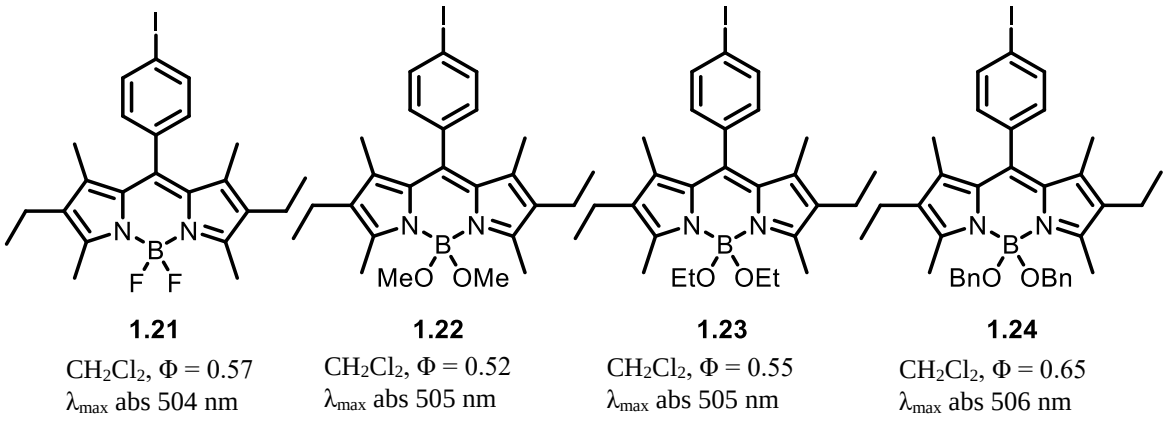

Figure 1.7: Example of the replacement of the two fluorine atoms with alkoxy groups.[23]

Conversion of the 3,5-di(methoxyphenyl)BODIPYs **1.25** and **1.26** into the corresponding *O*-chelated derivative **1.27** and **1.28** leads to a significant increase in quantum yield of fluorescence and red shifted absorption and emission maxima. This is probably due to structure rigidification and a decrease in the dihedral angle between the aryl ring and the BODIPY core.[17]

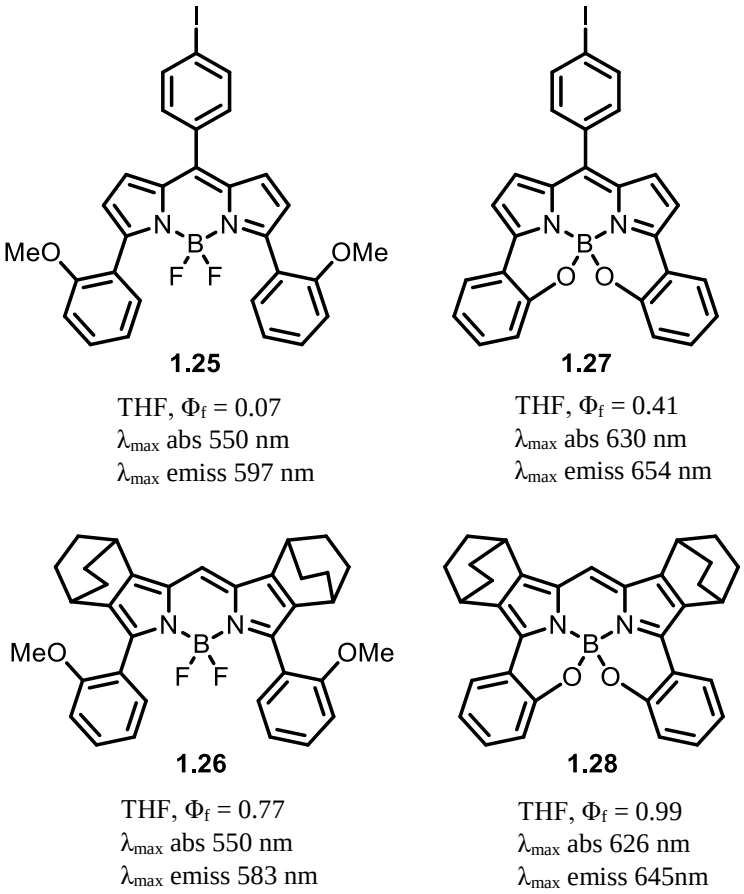

Figure 1.8: Examples of O-chelated BODIPYs.[17]

1.3.3. General synthetic routes to BODIPY dyes

As mentioned earlier, Treibs and Kreuzer synthesised the first BODIPY in 1968.[24] The reaction between acetic anhydride and 2,4-dimethyl pyrrole in the presence of boron trifluoride diethyl etherate ($BF_3.OEt_2$) gave a mixture of highly fluorescent compounds **1.29** and **1.30** (Scheme 1.2).

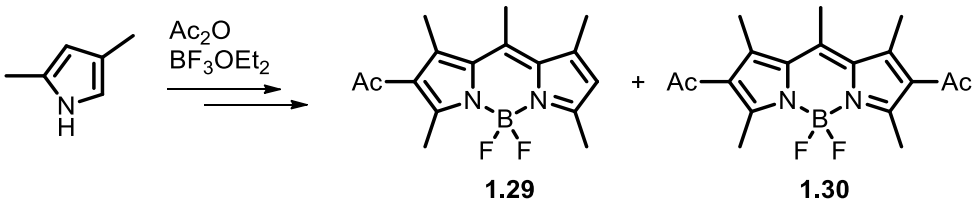

1.29 1.30

Scheme 1.2: Synthesis of the first BODIPYs **1.29** and **1.30** by Triebs et al.[24]

BODIPY derivatives can be synthesized by using various different synthetic methods, and the most obvious approaches are well known from porphyrin research. Synthetic approaches to the BODIPY core usually start from the condensation of a simple pyrrole with a highly electrophilic carbonyl compound, such as an acyl chloride, acid anhydride or aldehyde. However, the instability of the intermediate (unsubstituted dipyrromethene), which can undergo porphyrin formation or polymerization leads to the use of a 2-substituted pyrrole in most of the routes. Burgess[12] describes the synthesis of BODIPY dyes using three major routes: from pyrrole and aldehyde, from pyrrole and acid chloride, and from pyrrole and ketopyrrole.

1.3.3.1. From aldehyde

A straightforward approach to simple symmetrical BODIPY compounds is the acid catalysed condensation of an aldehyde **1.31** with two molecules of a pyrrole to afford a dipyrromethane **1.32**.[16] To avoid a polymerization in this reaction the pyrrole is used as the solvent[25] while the reaction with substituted pyrrole does not require excess pyrrole and occurs in normal organic solvent. The dipyrromethane **1.32** is oxidized immediately after preparation to generate the corresponding dipyrromethene **1.33** which is less stable. Subjecting the dipyrromethene **1.33** to a base, such as triethylamine (Et_3N) or diisopropylethylamine ($i\text{-}Pr_2NEt$), and boron trifluoride diethyl etherate ($BF_3.OEt_2$) generates the symmetric BODIPY dyes **1.34**, as shown in Scheme 1.3.

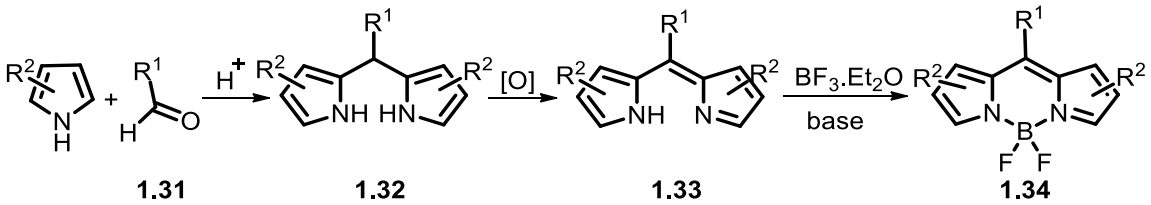

1.31 **1.32** **1.33** **1.34**

Scheme 1.3: General synthetic route to the symmetrical BODIPY from aldehyde.

Numerous BODIPY dyes have been synthesized from readily available pyrroles by using this synthetic method, which allows variation of the substituents on both the pyrrole (R^2) and meso (R^1) carbon atoms. Moreover, it has been found that substituents on the pyrrole, specifically on the 1-and 7- positions of the BODIPY, restrict rotation of an aromatic group attached at the meso-position. The resulting orthogonal geometry results in a reduction of the electronic coupling between the 8-substituent and the dye.[16] Many researchers have performed this method in a one-pot process without isolation of the intermediates. For example, Vicente[26] synthesised BODIPY **1.35** from the reaction between substituted pyrrole and aldehydes.

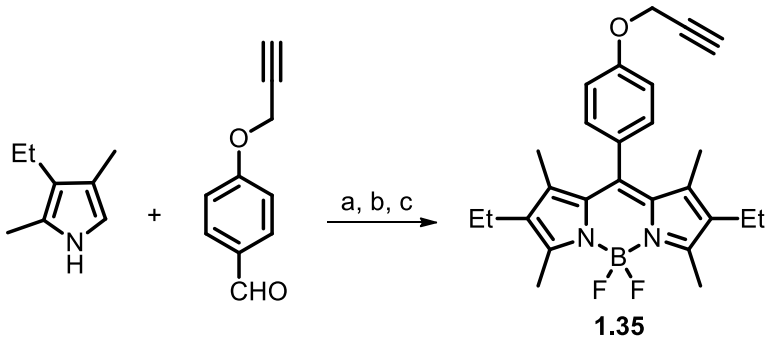

1.35

Scheme 1.4: Synthesis of BODIPY **1.35**. Reagent and conditions; a) TFA and CH_2Cl_2; b) DDQ; c) NEt_3, $BF_3.OEt_2$, 84%.[26]

1.3.3.2. From carboxylic acid

A more efficient route for the synthesis of symmetrical BODIPY cores is by acid-catalysed condensation of pyrroles with an acylium equivalent **1.36** such as an acid chloride, anhydride or an orthoester (Scheme 1.5).[16] Often, the acylpyrrole intermediate **1.37** is not isolated, because it reacts with an excess of the pyrrole under acidic conditions to form a dipyrromethene **1.38**. Treatment of the dipyrromethene intermediate **1.38** with base, and boron trifluoride diethyl etherate ($BF_3.OEt_2$) affords the symmetric BODIPY dye **1.39**, as shown in Scheme 1.5.

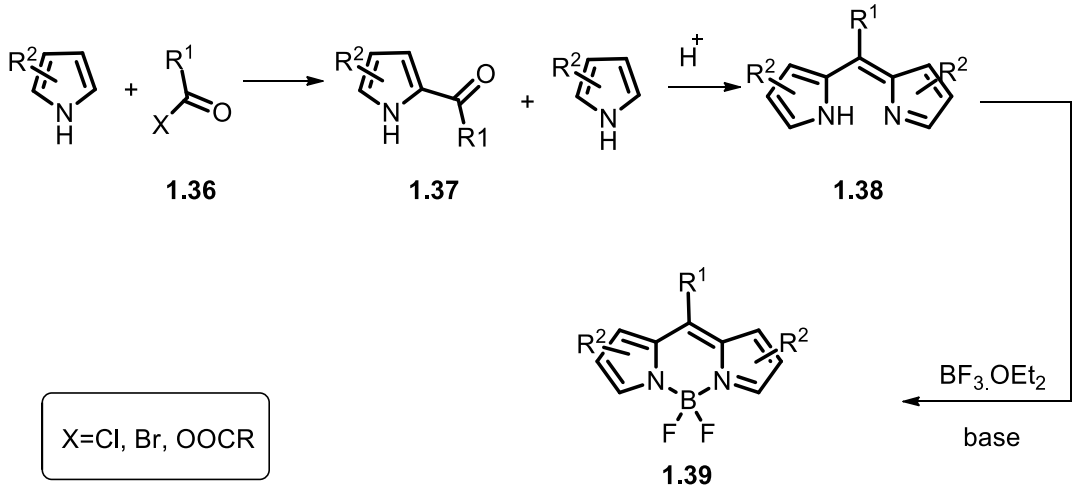

Scheme 1.5: General synthetic route to symmetrical BODIPYs by from acylation of pyrrole followed by condensation and complexation.

The advantage of this approach is that it does not require an oxidation step, and the formation of the BODIPY can be performed in a one-pot without isolation of the dipyrromethane. The disadvantage of this method is in the reaction conversion which is not always complete and this leads to a challenging purification. An example is the synthesis of BODIPYs **1.41a-d** in one-pot from 2,4-dimethyl-3-ethylpyrrole and acid chlorides **1.40a-d** (Scheme 1.6).[27]

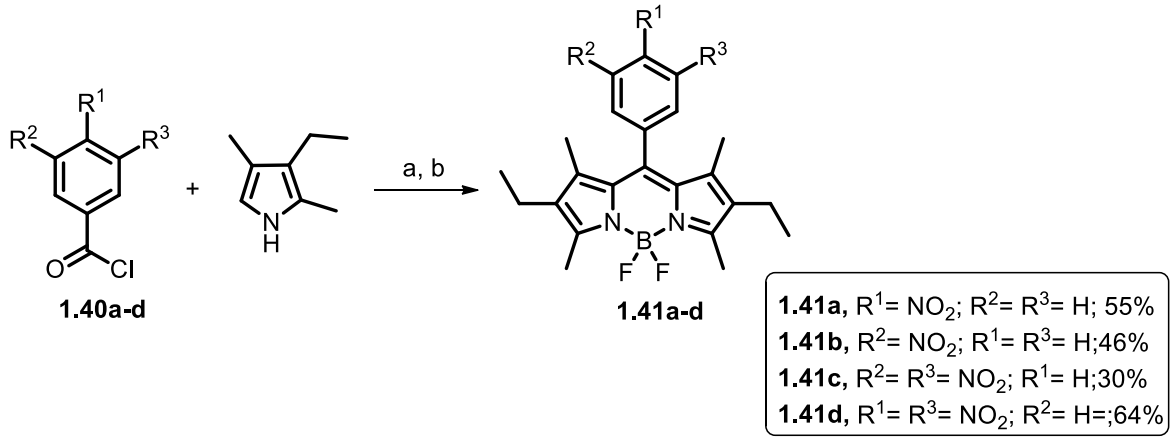

Scheme 1.6: Synthesis of BODIPY **1.41a-d** from acyl chlorides. Reagent and conditions; a) CH_2Cl_2, r.t., 72 h; b) NEt_3, $BF_3.OEt_2$, r.t., 24 h.

1.3.3.3. From a ketopyrrole

Unsymmetrical BODIPY compounds, unsubstituted or substituted at the 8-position cannot be prepared by using the two previous methods. They can be formed via condensation of a ketopyrrole with a second pyrrole in the presence of a Lewis acid followed by complexation in the presence of $BF_3.OEt_2$ and base to give unsymmetrical BODIPYs **1.42** (Scheme 1.7).

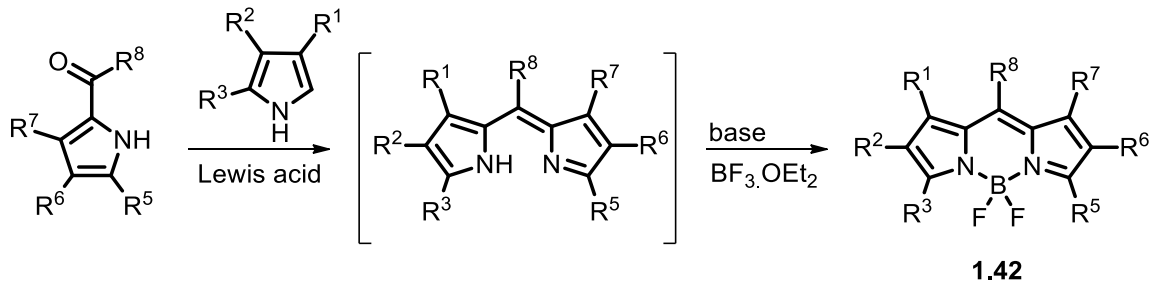

Scheme 1.7: Synthesis of unsymmetrical BODIPY **1.42** from ketopyrrole.

This method is advantageous because no oxidation step is required. Also, in this method symmetrical or unsymmetrical BODIPYs can be prepared in one-pot without isolation of the unstable dipyrromethene hydrochloride salt intermediate which can be difficult. Although BODIPYs are prepared in one-pot with no isolation, this approach does require isolation of the ketopyrrole intermediate in order to synthesise the unsymmetrical BODIPY.

For instance, Duportail[28] applied this method in the synthesis of symmetrical BODIPY **1.45**. The ketopyrrole **1.43** was synthesised by the reaction of 4-iodobenzoyl chloride with the magnesium salt of 2,4-dimethylpyrrole (formed by deprotonation with MeMgBr). Then, condensation of ketopyrrole **1.43** with another equivalent of 2,4-dimethylpyrrole in the presence of $POCl_3$ gave dipyrromethene **1.44**. Finally, complexation the dipyrromethene with $BF_3.OEt_2$ in the presence of triethylamine produced the symmetrical BODIPY **1.45** (Scheme 1.8).

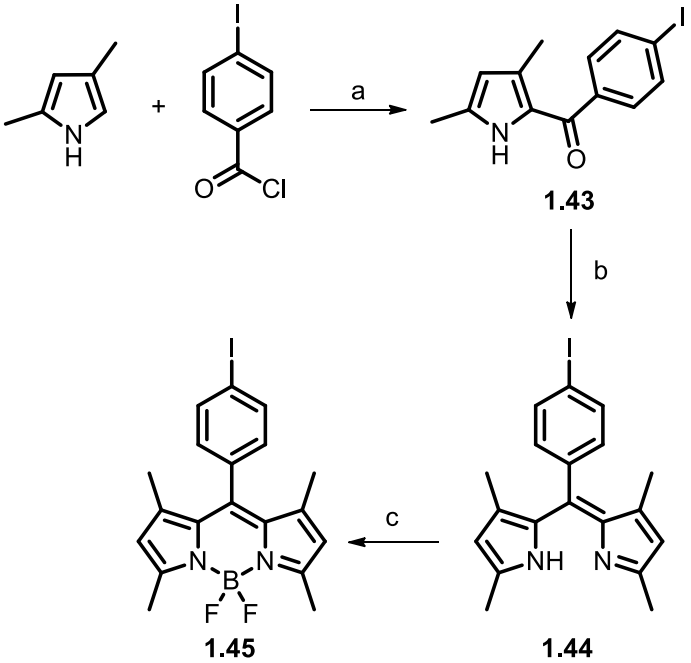

Scheme 1.8: Synthesis of symmetrical BODIPY **1.45**. Conditions and reagents; a) MeMgBr, Et_2O, 35 °C, 30 min, 81%; b) 2,4-dimethylpyrrole, $POCl_3$, CH_2Cl_2/pentane, 0 °C, r.t., 24 h, 46 %; c) $BF_3.OEt_2$, NEt_3, toluene, 80 °C, 30 min, 80 %.[16]

A similar approach was used by Chang[29] in order to synthesise unsymmetrical BODIPY **1.46**. In this case, BODIPY **1.46** was synthesised in a one-pot reaction without isolation of the dipyrromethene intermediate by condensation of 2-formylpyrrole with 2,4-dimethylpyrrole in the presence of $POCl_3$, followed by BF_2 chelation leading to BODIPY **1.46** (Scheme 1.9).

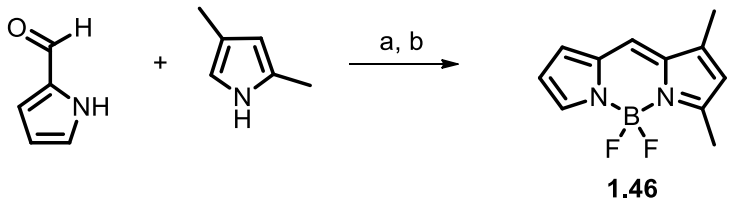

1.46

Scheme 1.9: Synthesis of unsymmetrical BODIPY **1.46**. Conditions and reagents; a) 2,4-dimethylpyrrole, $POCl_3$, CH_2Cl_2, -5 °C, 3 h, r.t., 3 h; b) $BF_3.OEt_2$, NEt_3, r.t., 3 h, 51 %.[29]

1.4. Some applications of functionalized BODIPYs

Design and development of near-infrared (NIR) BODIPY dyes has gained considerable research interest over the past decade because of rapid developments in various optical imaging and bioanalytical techniques, such as nucleic acid detection, in vivo imaging, DNA sequencing, gel electrophoresis, vascular mapping and tissue perfusion.[30]

There are a number of commercially available BODIPY scaffolds which can be connected to proteins, peptides, oligonucleotides, lipids, polystyrene microspheres and dextran (Table 1.1). By standard chemical reactions succinimidyl esters of BODIPY acids and carboxylic acids can be converted into fluorescent amides, acid halides, or esters.

Table 1.1: Examples of commercially available BODIPY dyes.

Dye name	Chemical structure	Absorption max (nm)	Emission max (nm)
BODIPY 630/650 (Life Technologies Inc.)	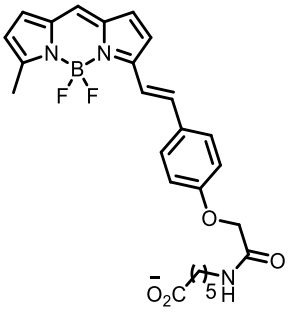	625	640
BODIPY 650/665 (Life Technologies Inc.)	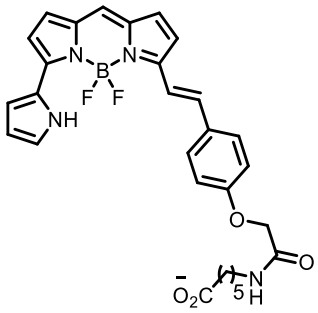	646	660
BODIPY FL-X (ThermoFisher Scientific)	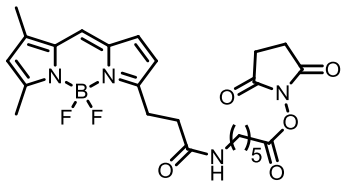	501	510
BODIPY 665/676 (ThermoFisher Scientific)	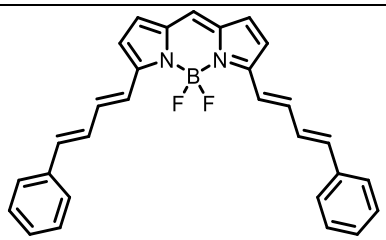	605	676
BODIPY TR-X (ThermoFisher Scientific)	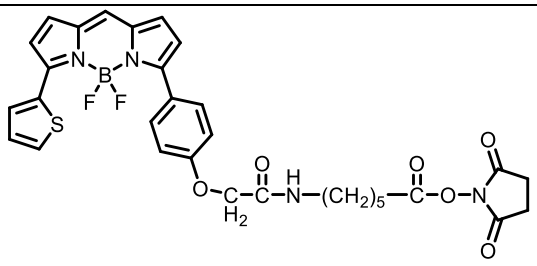	591	620

Owing to their favourable characteristics, BODIPY dyes can act as an important component in many different applications. Figure 1.9 shows some applications of

functionalised BODIPYs in which R^1, R^7, R^3 and R^6 may extend the delocalisation and/or carry other functional groups.

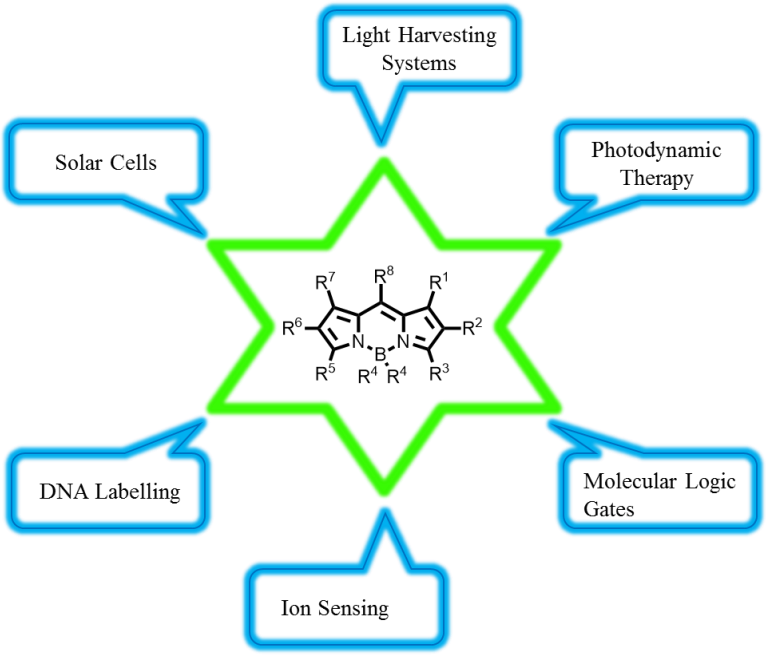

Figure 1.9: Applications of BODIPY Dyes.[31–34]

BODIPY dyes have been used in a photodynamic therapy (PDT) which is a potential treatment for cancer and other localized diseases that uses a photosensitizer agent, a visible or near-visible light and oxygen as elements in its mechanism of action.

For example, O'Shea and his group[35] have disclosed a new class of potential photodynamic therapy agent, the BF_2-chelated azadipyrromethenes **1.47** and synthesised a sequence of a supramolecular photonic therapeutic agent (SPTA) analogues **1.48-1.50** with pH-responsive amine receptors. They described a new method for achieving photodynamic therapy selectivity based upon the reversible off/on switching of the main therapeutic property (generation of singlet oxygen) of a SPTA (Figure 1.11).[35]

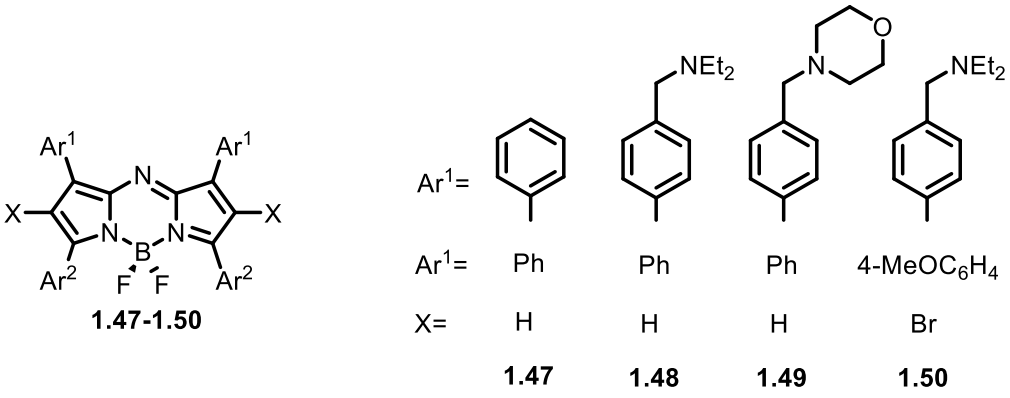

Figure 1.10: Structure of aza BODIPYs.[35]

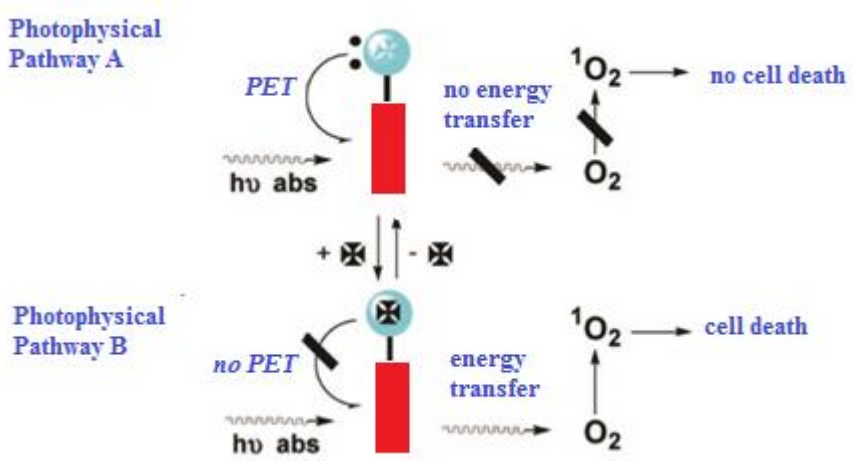

Figure 1.11: "Design and function of an SPTA. Blue circle, substrate-specific receptor. Red rectangle, photosensitizer. Black cross, substrate".[35] (Adapted from S. O. McDonnell, M. J. Hall, L. T. Allen, A. Byrne, W. M. Gallagher, and D. F. O'Shea, J. *Am. Chem. Soc*. 2005, **127**, 16360-16361).

BODIPY dyes have also been developed as a sensitizer in dye-sensitized solar cell (DSSC) systems which are a new type of low cost photovoltaic (solar) cell that absorbs visible light to produce electricity. The DSSC device consists of glass sheet (transparent conducting indium tin oxide (ITO) or fluorine doped tin oxide (FTO)), a semiconducting electrode (n-type TiO_2, p-type NiO), a dye sensitizer (which is able to harvest light and transfer electrons), redox mediator (I^-/I_3^- or Co^{II}/Co^{III} complexes) and a counter electrode (carbon or Pt) (Figure 1.12).

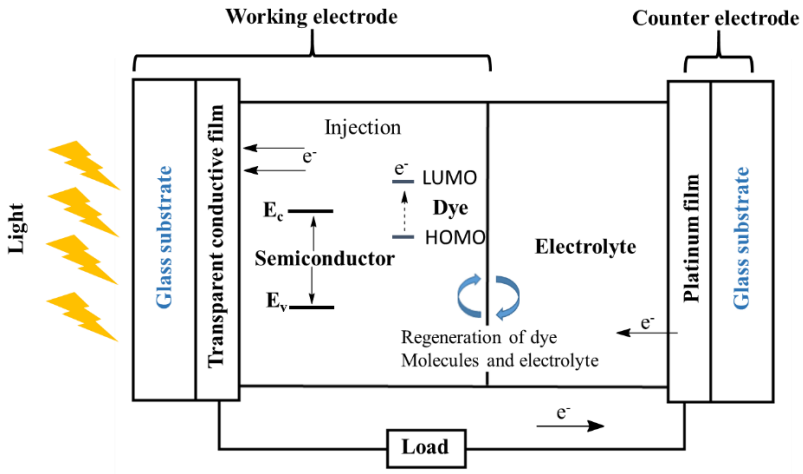

Figure 1.12: "Schematic diagram of the energy flow in a DSSC".[36] (Adapted from S. S. P. Singh, and T. Gayathri, *Eur. J. Org. Chem*. 2014, 4689-4707)

The first BODIPY photosensitizers **1.51** and **1.52** for DSSCs were reported by Fukuzumi and his group.[36] The percentage power conversion efficiency (η) of these compounds is 0.16% and 0.13% respectively.

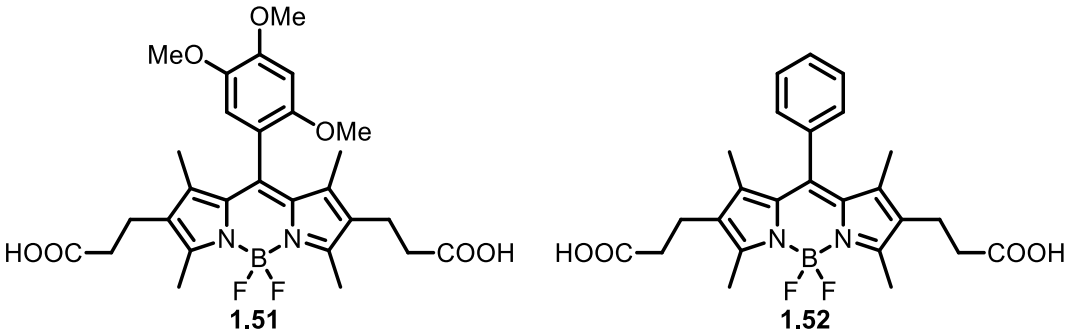

Figure 1.13: Structure of sensitizers **1.51** and **1.52**.

Kubo et al.[37] have designed and synthesised sensitizers **1.53-1.55** (Figure 1.14) which involve thienyl-cyanoacrylic acid units and reported their efficiency in a DSSC setup. The cell based on BODIPY **1.55** has a good conversion efficiency (6.06%) which is the highest value for BODIPY-based DSSCs has been reported up to date .[37]

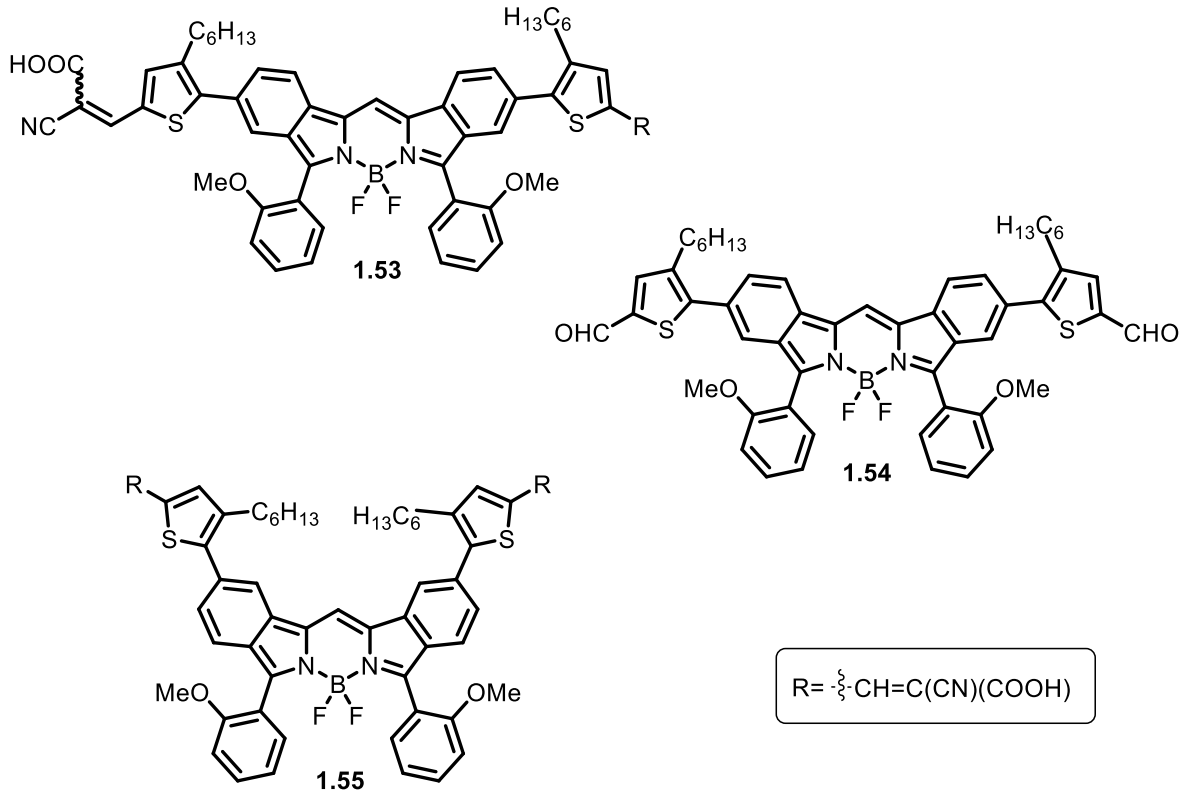

Figure 1.14: Structure of sensitizer **1.53**, **1.54** and **1.55**.[37]

BODIPY dyes have been widely used to target biological molecules such as amino acids, nucleotides, DNAs, RNAs, lipids and proteins.[38–40] There are many examples in the literature of the synthesis of BODIPYs dyes containing different reactive groups for protein labelling.[41] A succinimidyl ester is one of the most commonly used groups for conjugation of BODIPYs to amino acids (specifically lysines). A BODIPY-succinimidyl ester can react with amino groups in the protein producing an amide bond and releasing *N*-hydroxysuccinimide as shown in Figure 1.15a.[41]

Also, several BODIPY compounds containing an isothiocyanate group have been reported in the literature. The nucleophilic reaction between the amino group of an amino acid (specifically lysines) and the isothiocyanate group of an BODIPY leads to formation of a thiourea linkage as seen in Figure 1.15b.[41]

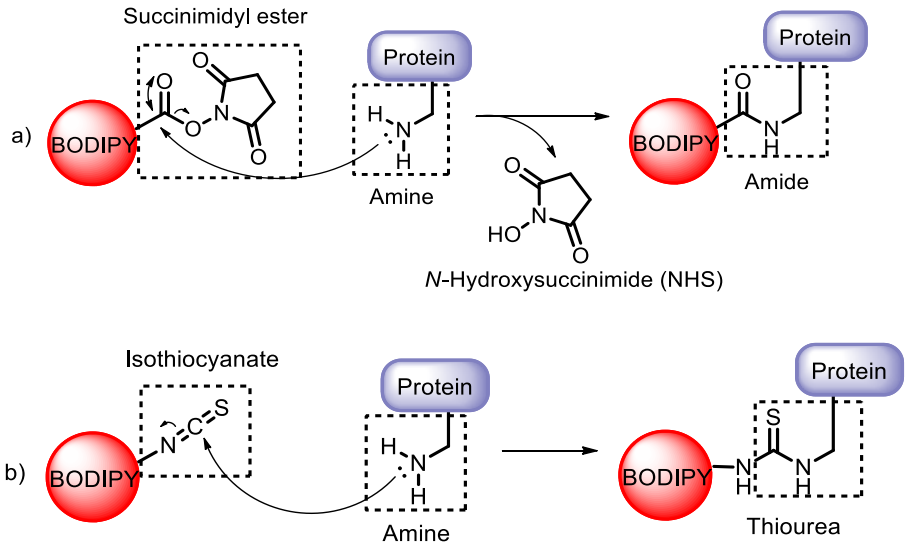

Figure 1.15: General mechanisms of amine labelling with succinimidyl ester and isothiocyanate functionalised BODIPYs.[41] (Adapted from L. C. D. D. L. Rezende, S. Emery and F. Emery, *Orbital Elec. J. Chem*, 2013, **5**, 62–83.).

The reactivity of iodoacetamide and maleimide toward sulfhydryl groups of amino acid residues (specifically cysteine) has also been described in the literature.[41] Figure 1.16a and b illustrate the mechanism of sulfhydryl labeling with iodoacetamide and maleimide BODIPY derivatives.

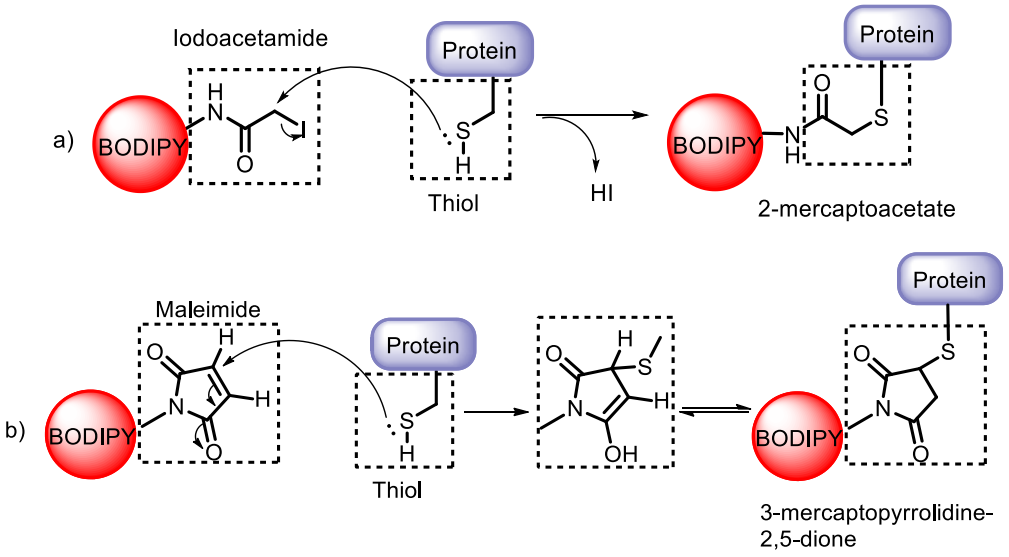

Figure 1.16: General mechanism of sulfhydryl labelling with iodoacetamide and malemaide functionalised BODIPY derivatives.[41] (Adapted from L. C. D. D. L. Rezende, S. Emery and F. Emery, *Orbital Elec. J. Chem*, 2013, **5**, 62–83.).

1.5. Goals and objectives

This project aimed to synthesize functionalized BODIPY dyes. The first part of the research focuses on the synthesis of novel chiral BODIPY dyes in which chirality is intimately associated with the BODIPY core in order to maximise the likelihood of enantioselective modification of the optical properties in response to the two enantiomeric forms of a chiral analyte. Ultimately, this approach might be used in the development of high throughput screening of enantiomeric excess and the use of this methodology may be applied, for example, in the development of novel chiral catalysts and the optimisation of reaction conditions.

In the second part, investigation into the synthesis and application of amino-substituted BODIPYs via metal catalysed amination reactions are described as a new strategy towards fluorescence-quenched BODIPY dyes. Such fluorescence-quenched systems are highly useful for many different applications in which fluorescence 'switch on' can be achieved in response to an analyte.

Chapter 2: Synthesis of chiral BODIPY dyes

2.1. Introduction

Chiral compounds can exist as two non-superimposable mirror image forms which are termed enantiomers. In general, enantiomers have the same physical properties like refractive index, UV, solubility, IR, NMR, X-ray diffraction pattern and density. However, the two enantiomers are not identical in chiroptical properties such as optical rotatory dispersion, optical rotation and circular dichroism.[42,43]

Each enantiomer often shows very different pharmacological, physiological, pharmacokinetic and pharmacodynamic properties.[42] For instance, there were a number of adverse effects when using racemic dopa for the treatment of Parkinson's disease such as nausea and anorexia. It was subsequently found that the drug must be marketed as a single enantiomer (L)-dopa because (D)-dopa is ineffective and quite toxic.[44]

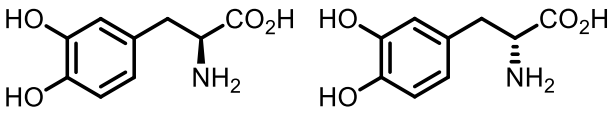

L-dopa **D-dopa**

Molecular chirality can be divided into four types: central, axial, planar and helical.[42,43] Examples of the four different types of chiral molecules are shown in Figure 2.1. In all cases the two mirror images of the molecules cannot be superimposed. The first type and the most common is central chirality which usually created by an atom with four different groups. Axial chirality is a stereoisomerism resulting from the nonplanar arrangement of four substituents about an axis. This kind of chirality can be observed in atropisomeric biaryl compounds such as BINAP and BINOL due to restricted rotation between the aryl-aryl single bond. Planar chirality is a stereoisomerism resulting from the arrangement of out of plane substituents with respect to the plane. Helical chirality is a special type of axial chirality in which the molecules twist (like a cork-screw) and can therefore be right handed or left handed.

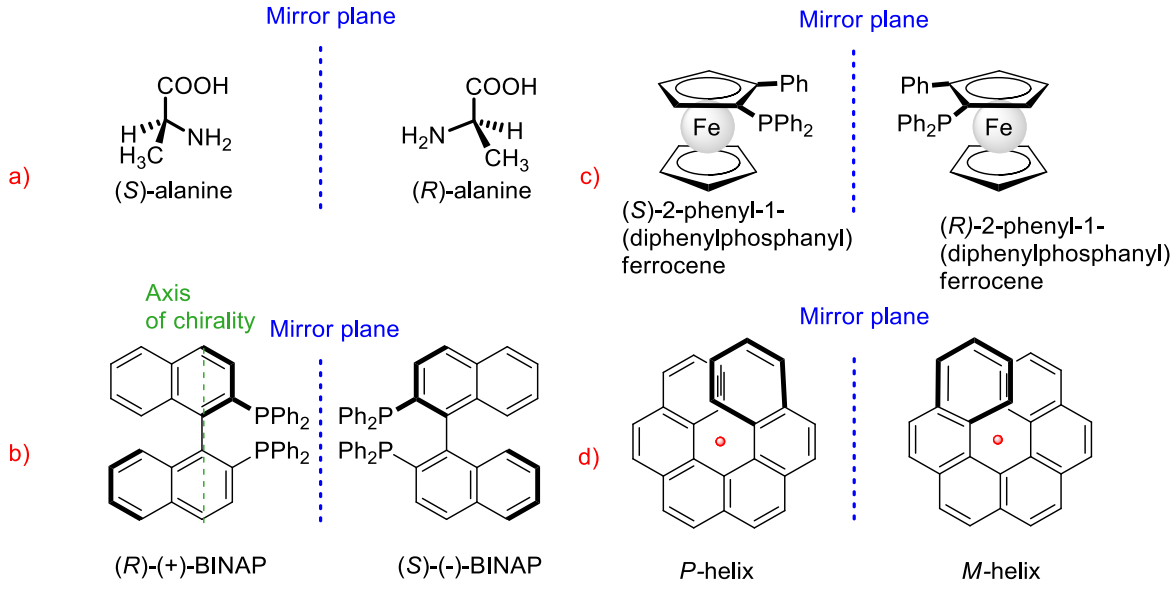

Figure 2.1: examples of the four different types of chiral molecules a) central, b) axial, c) planar, d) helical.[42,43]

A variety of methods are used for determination of enantiomeric composition.[45] Chromatography techniques have been used for many years for quantification of ee and for enantiomer separations. For instance, chiral high-performance liquid chromatography (HPLC), capillary electrophoresis (CE) and chiral gas chromatography (GC) are used to attempt high-throughput screening (HTS) of ee values.[45,46] These methods have produced the most accurate measurements. However, a major limitation of these methods is the long elution times and the sequential nature of the method when used for multiple analyses.

Alternative methods for determining ee are the use of liquid crystals (LCs) via visual detection and by spectroscopic measurements. A major disadvantage of these methods is that they require derivatization of analytes or substrates. Another approach to the determination of ee is the use of enzymes and antibodies which feature high selectivity and inherent chirality.[45] However, these techniques suffer from a lack of generality.

Recently, researchers have turned to optical methods which are more accurate, precise, and user-friendly. The use of fluorescent molecular sensors for the measurement of the enantiomeric excess of chiral chemical compounds has several advantages. For example, measurement can be made rapidly thus avoiding time consuming chromatography. Also, optical methods offer the possibility of real-time measurement, amenability to automation, inexpensive instrumentation, virtually no waste and low-cost reagents.[47] Therefore, these sensors have been used for (HTS) to determine a compound's stability to racemization under different conditions and to rapidly detect the enantioselectivity of chemical reaction products.[45]

There are several important features must be present in sensor molecules such as:-

1. Suitable groups that will bind reversibly with the target species, for instance;acidic/basic groups, hydrogen bonding groups or polar groups.[47]
2. A signal must be formed by the host-guest interaction.[47]
3. The signal transduction and groups conferring recognition must be organized in an interactive conformation, so binding with a target species results in signal generation.[47]

Enantiomeric fluorescent sensors give different responses by reaction or interaction with chiral molecules (Figure 2.2).[48] One enantiomer of a given chiral selector molecule can interact with a chiral analyte containing a fluorescent group, thus forming distereomeric complexes of different structure and stability (Figure 2.2a). Moreover, fluorescent compounds can be used to produce an enantioselective response in the presence of both non-fluorescent and fluorescent analytes (Figure 2.2b).[48] Consequently, there are many fluorophores that have been used for this purpose such as cyclodextrin, cyclic urea, binaphthol, calixarene and crown ethers. Most commonly chirality is introduced into these compounds as atropisomerism using biphenyls, cumulenes and allenes.

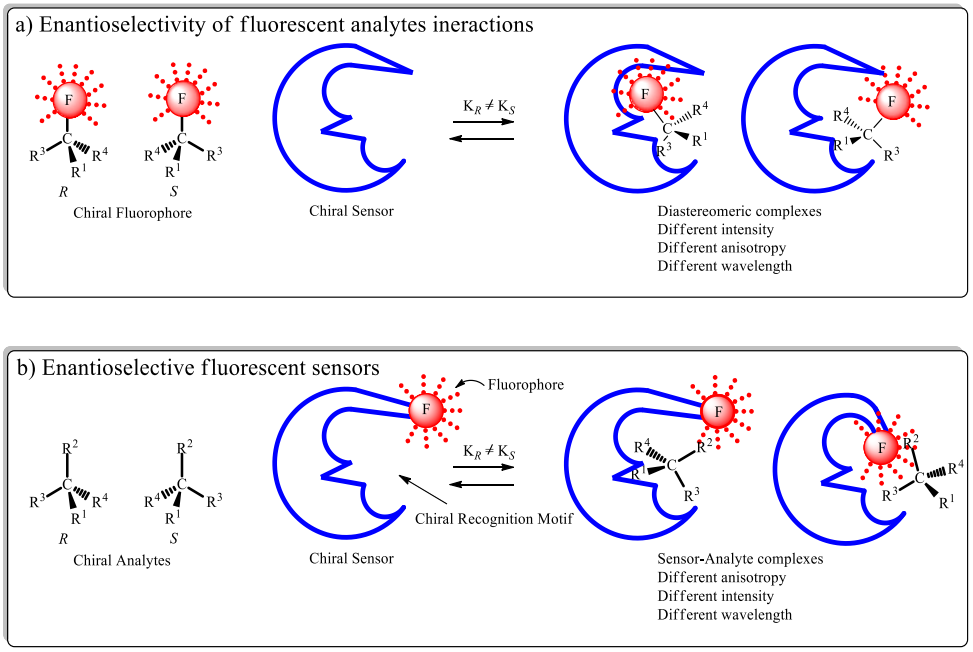

Figure 2.2: Two different schemes for inducing an enantioselective fluorescence response.[48]

Boron dipyrromethenes (BODIPYs) have found extensive use in imaging and sensing due to their fluorescence properties. Few different chiral BODIPYs have been synthesized and their structure, electrochemical and spectroscopic properties have been investigated.[49–54] However, there is one report of the use of chiral BODIPY species for enantioselective applications.[54] The binaphthol BODIPY derivative **2.1** is optically active and shows chiral discrimination towards the enantiomers of α-methylbenzylamine by display of different fluorescence quenching rates of the BODIPY fluorescence.[54]

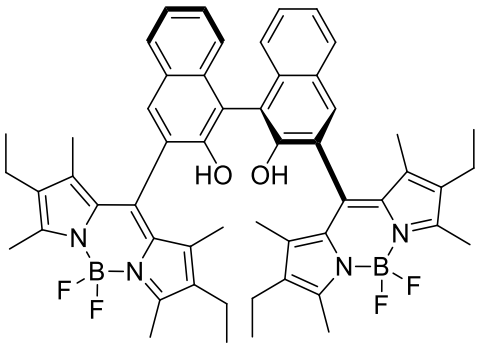

2.1

It was found that specific changes of the BODIPY fluorescence signal were generated by the interaction between the α-methylbenzylamine quencher and the 1,1'-binaphthalene receptor. A decrease of the intensity of the fluorescence band was detected by addition of

(*R*) - and (*S*)-1-phenylethylamine respectively. The efficiency of the quenching process for (*S*) - and (*R*)-1-phenylethylamine (PEA) were examined. The equation for static quenching was used to analyze the experimental data.[54]

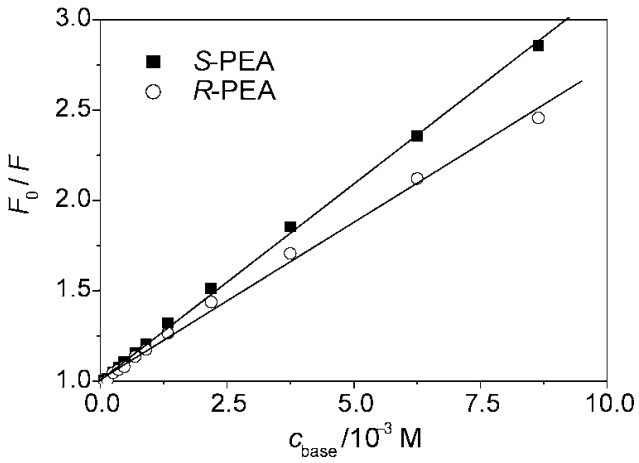

Figure 2.3: Plots for the quenching of **2.1** with *R*-PEA and *S*-PEA in acetonitrile.[54]

Figure 2.3 shows the corresponding plots for the quenching of **2.1** with (*R*)- and (*S*)-1-phenylethylamine. The different slopes indicate the suitability of **2.1** as a chirally discriminating sensor for optically active amines. The steeper slope for quenching of **2.1** with (*S*)-PEA in acetonitrile, based on a higher association constant (K_S = 226 M^{-1}) for (*S*)-PEA–**2.1** as compared to (*R*)-PEA–**2.1** (K_S = 161 M^{-1}), suggests that association of the S-PEA and **2.1** is more effective. The ratio of K_S(R-S)/K_S(R-R) = 1.40 is relatively high for amine complexes of a simple binaphthol receptor unit and obviously demonstrates the potential of **2.1** as an enantioselective sensor molecule.[54]

In this project, we aimed to synthesise functionalised BODIPYs in which chirality is intimately associated with the BODIPY core in order to maximise the likelihood of enantioselective modification of the optical properties in response to the two enantiomeric forms of a chiral analyte. Therefore, this chapter is discussed several approaches to the synthesis of chiral BODIPY dyes.

2.2. Axially chiral BODIPYs

More recent attention has focused on the synthesis of axially chiral BODIPY dyes.[49–52] For instance, Akkaya explored a new chiral system based on rotationally hindered di-BODIPY core.[50] They synthesised rac-BODIPY **2.2** and separated the enantiomers by HPLC using a chiral stationary phase (Chiralcel-OD column) (Figure 2.4).[50] As shown in Figure 2.5 the circular dichroism spectrum has been used to establish successful separation of the two enantiomers **2.2a** and **2.2b**).

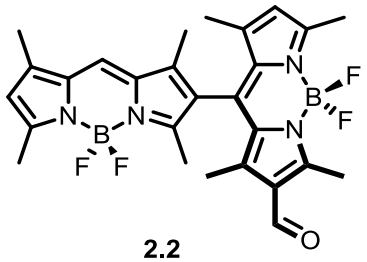

2.2

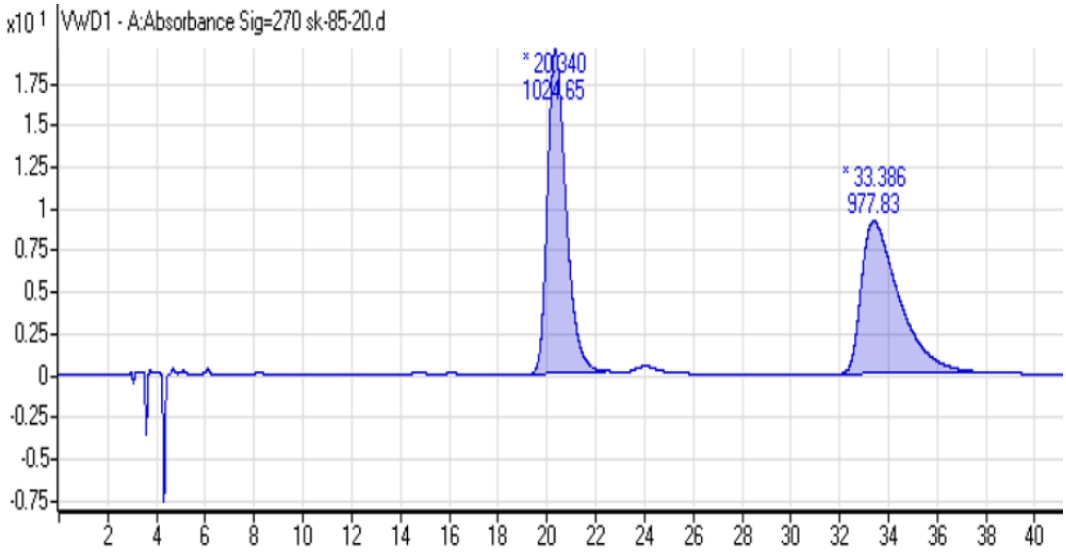

Figure 2.4: HPLC separation of BODIPY **2.2** to **2.2a** (20.3 min) and **2.2 b** (33.4 min).[50]

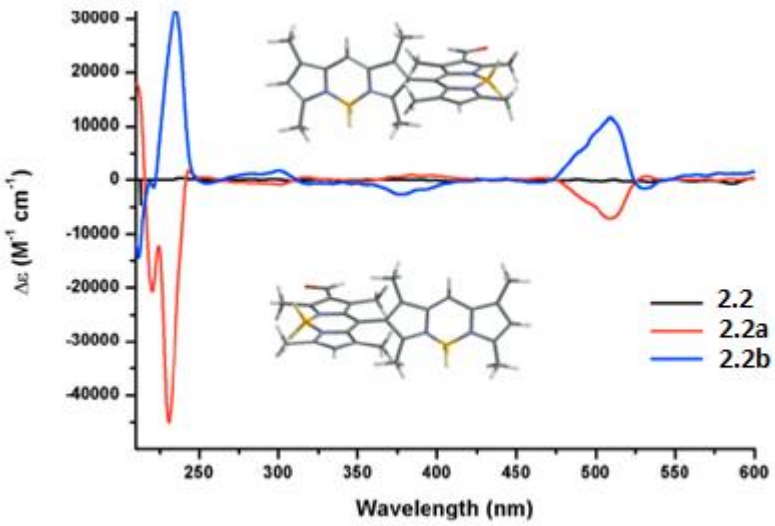

Figure 2.5: Circular dichroism spectra of rac-BODIPY **2.2** and the two enantiomers.[50]

In 2014, Hall[51] reported the synthesis, resolution and determination of the absolute configuration of axially chiral BODIPY **2.3** as shown in Figure 2.6 and 2.7.[51]

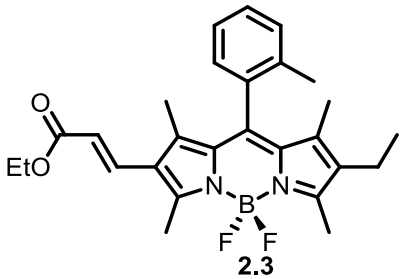

2.3

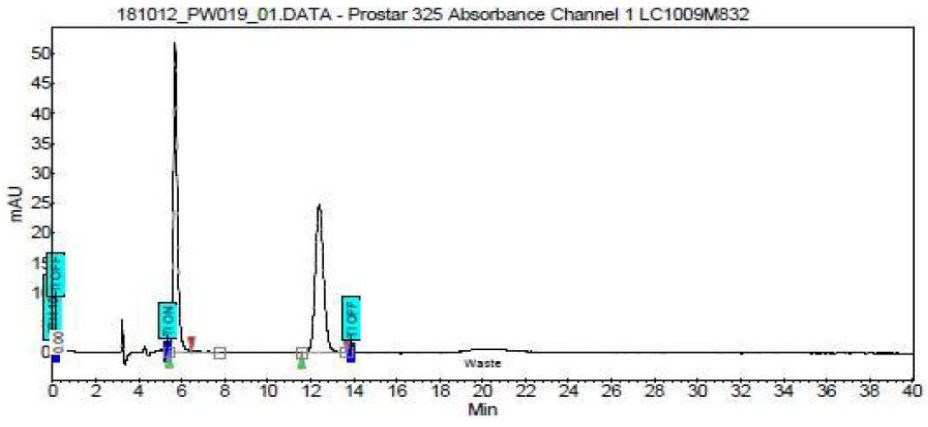

Figure 2.6: HPLC separation of BODIPY **2.3** to the two enantiomers.[51]

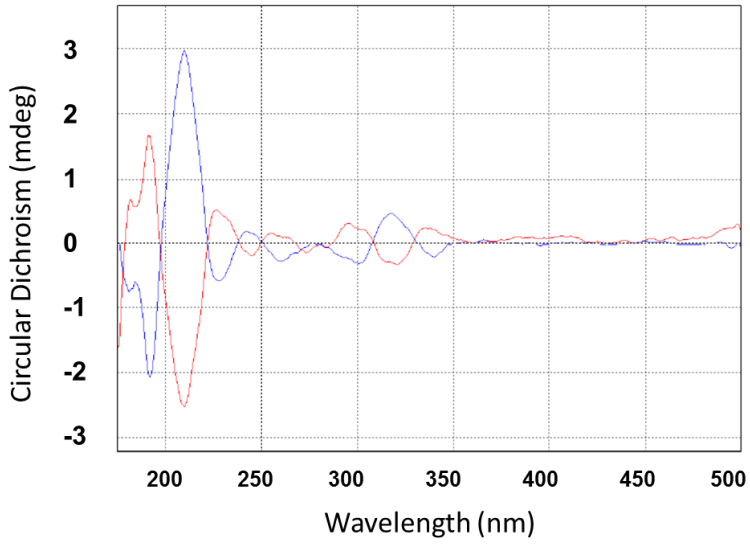

Figure 2.7: ECD spectra of **2.3**-(+) and **2.3**-(-).[51]

2.2.1. Synthesis of axially chiral BODIPY dyes with C2-symmetry

Due to restricted rotation around the pyrrole-aryl bonds, the BODIPY **2.6** was expected to be chiral (see later). A synthetic route to 2,6-bis(2-methoxyphenyl)BODIPY **2.6** is shown in Scheme 2.1.

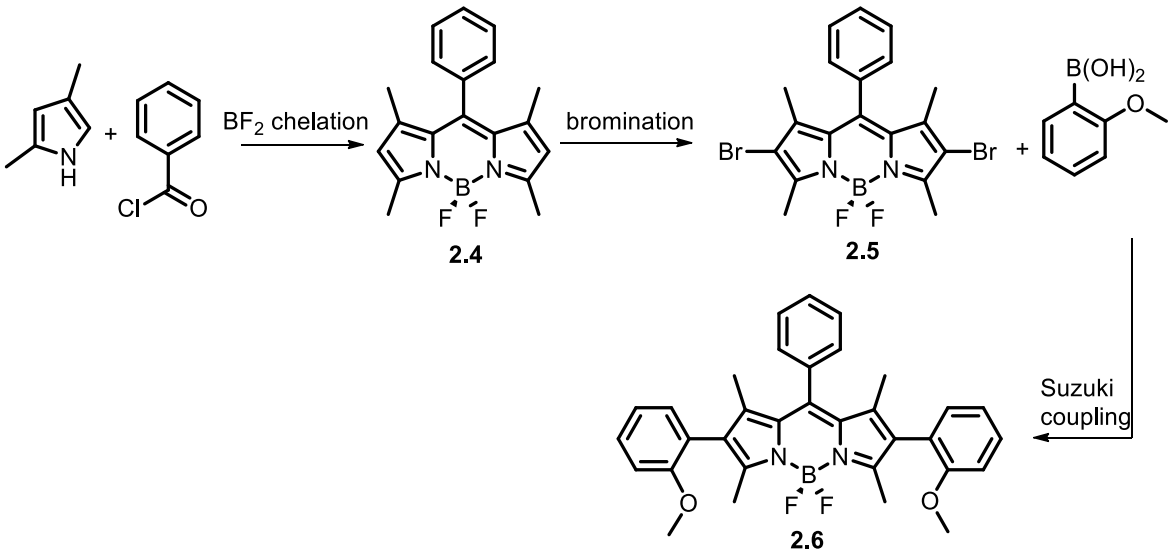

Scheme 2.1: Synthetic approach to the synthesis of 2,6-bis(2-methoxyphenyl)BODIPY **2.6**.

Synthesis of symmetrical BODIPYs can be accomplished by starting with different acyl chlorides or aryl aldehydes both of which are commercially available. Using a literature

procedure,[55] the one-pot condensation of benzoyl chloride with two equivalents of 2,4-dimethyl pyrrole was used to synthesise the symmetrical BODIPY **2.4**. Initially, 2,4-dimethylpyrrole and benzoyl chloride were stirred at room temperature, followed by BF_2 chelation by treatment with boron trifluoride diethyl etherate ($BF_3.OEt_2$) in the presence of *N*,*N*-diisopropylethylamine (i-$PrNEt_2$) to produce the symmetrical BODIPY **2.4** (Scheme **2.2**).

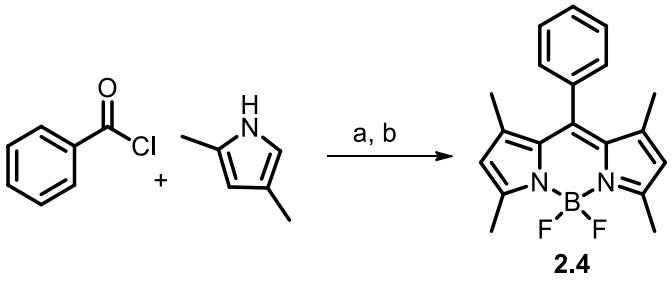

2.4

Scheme 2.2: Synthesis of 8-phenyl BODIPY **2.4**. Conditions and reagents: a) DCM, 16 h, r.t; b) $BF_3.OEt_2$, i-Pr_2NEt, 0 ℃, 1 h, 40%.

It is perhaps not surprising that the most common method for the synthesis of halogenated BODIPY dyes relies on direct electrophilic halogenation. Using a literature[56] procedure, the 2,6-dibromoBODIPY **2.5** was prepared by reaction of the 8-phenylBODIPY **2.4** with Br_2 (Scheme **2.3**). Purification using column chromatography gave the desired 2,6-dibromoBODIPY **2.5** in high yield (90%). Crystals of 2,6-dibromoBODIPY **2.5** were obtained by slow evaporation from a mixture of ethyl acetate and petrol (1:3). The crystal structure shown in figure **2.8** was obtained through single crystal X-ray crystallography.

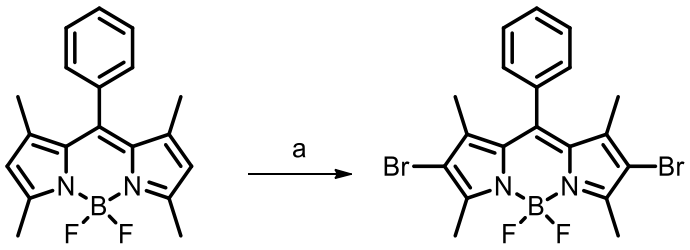

2.4 **2.5**

Scheme 2.3: Synthesis of 8-phenylBODIPY **2.5**. Conditions and reagents: a) Br_2, DCM, r.t., 3 h, 90%.

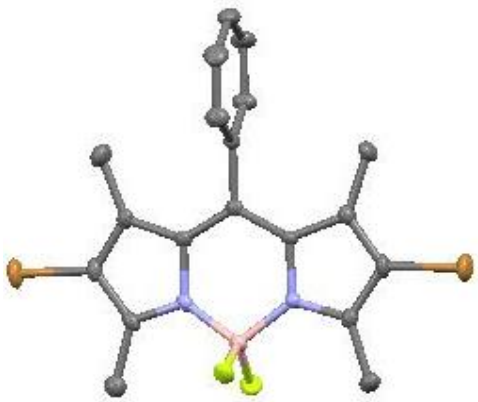

Figure 2.8: Molecular structure of 2,6-dibromoBODIPY **2.5**. Hydrogen atoms have been omitted for clarity.

The synthesis of halogenated BODIPYs has been reported as a useful reaction which can be followed by various transition metal catalysed cross-coupling reactions or nucleophilic substitution. 2,6-Bis(2-methoxyphenyl) BODIPY **2.6** was synthesized via a Suzuki coupling reaction. 2,6-DibromoBODIPY **2.5** was reacted with 2-methoxybenzeneboronic acid in the presence of $Pd(OAc)_2$ and H-KITPHOS **2.7**[57] in toluene to form BODIPY **2.6** in 25%.

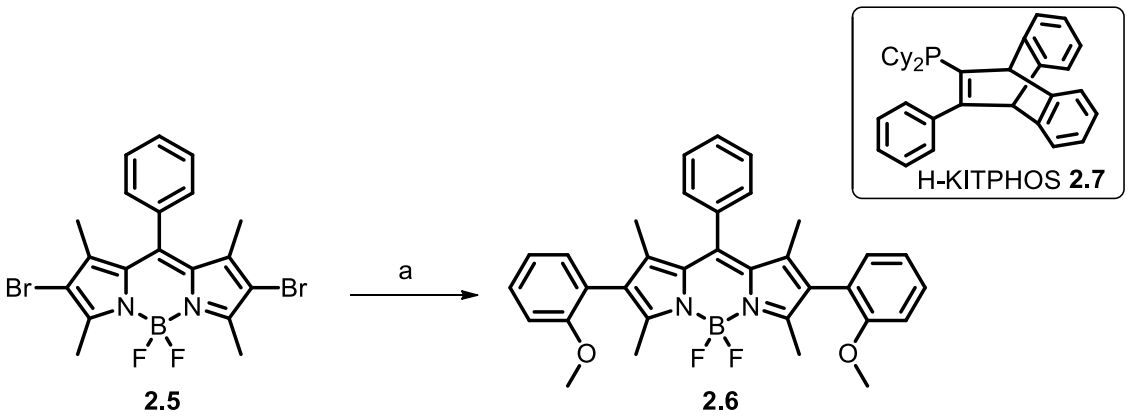

Scheme 2.4: Synthesis of 2,6-bis(2-methoxyphenyl) BODIPY **2.6**. Conditions and reagents: a) H-KITPHOS **2.7** (12 mol %), $Pd(OAc)_2$ (5 mol %), K_3PO_4 (4 eq), toluene, reflux, 20 h, 25%.

In this reaction we expected to form a diastereomeric mixture of the *syn*-**2.6** and *anti*-**2.6** isomers of 2,6-bis(2-methoxyphenyl) BODIPY but this was not evident from the ^{1}H NMR spectrum of the product. ^{19}F NMR spectroscopy is a useful tool to distinguish between the two isomers because it can distinguish different fluorine chemical environments.

In general, the ^{19}F NMR spectrum shows four peaks (1:1:1:1 quartet) for symmetrical F_2-BODIPY dyes, resulting from the coupling of the two identical fluorine atoms with the single boron (I = 3/2) nucleus. For instance, the ^{19}F NMR spectrum for phenyl-BODIPY **2.4**, recorded in $CDCl_3$, is reported to consist of four peaks, clearly indicating that the fluorine atoms reside in identical environments (Figure 2.9).

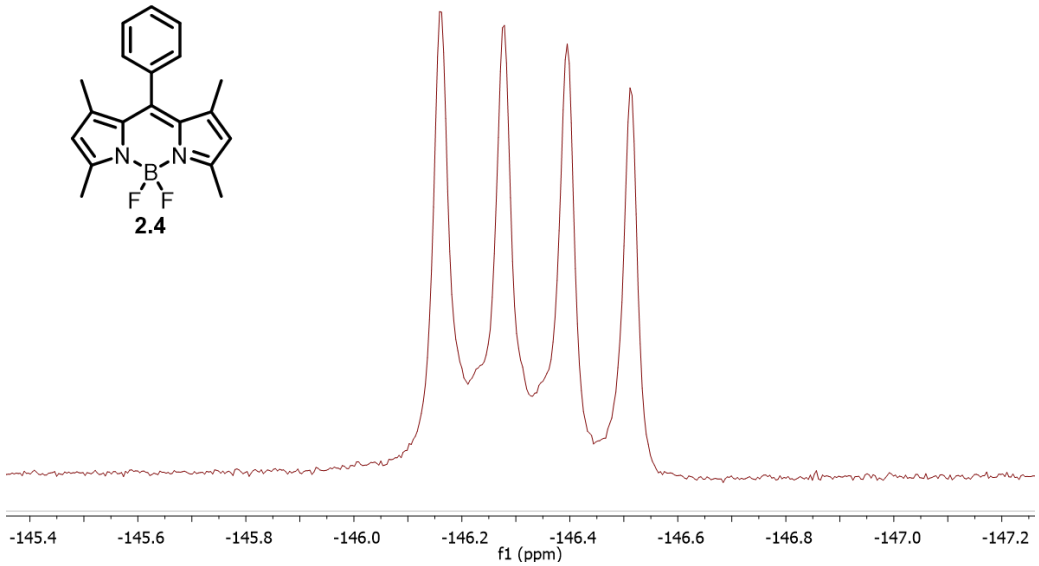

Figure 2.9: ^{19}F NMR spectrum reported for phenyl-BODIPY **2.4** in $CDCl_3$.

In 2008, Benniston published a paper[58] in which they synthesised the symmetric quinone substituted BODIPY **2.9** for detection of reactive oxygen species (ROS) and monitoring lipid oxidation in living cells (Scheme 2.5).[58]

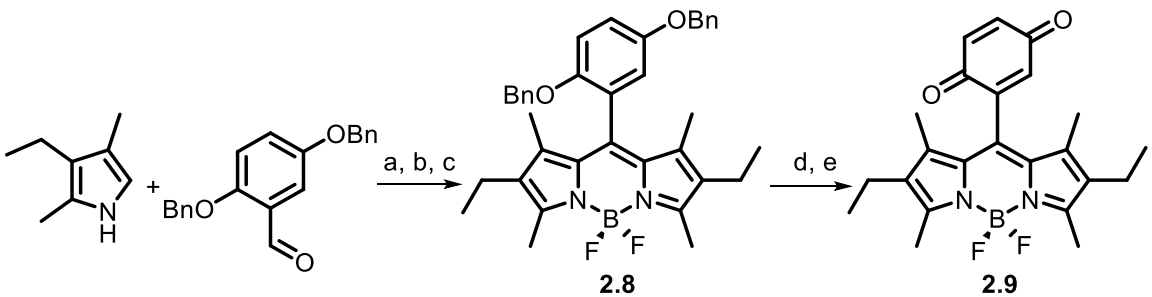

Scheme 2.5: Synthesis of 8-quinone BODIPY **2.8**. Conditions and reagents: a) TFA, DCM, r.t., 24 h. b) DDQ, 24h. c) $BF_3.OEt_2$, i-Pr_2NEt, r.t., 6 h, 50%. d) H_2 (4 atm), Pd/C (10 mol%), DCM/MeOH,. (d) THF, DDQ, r.t., 82%.[58]

The ^{19}F NMR spectrum for the symmetrical BODIPY **2.9** consists of 16 peaks due to the two different fluorine atoms coupling to each other and also coupling to the boron atom, indicating that the fluorines are diastereotopic. (Figure 2.10).[58]

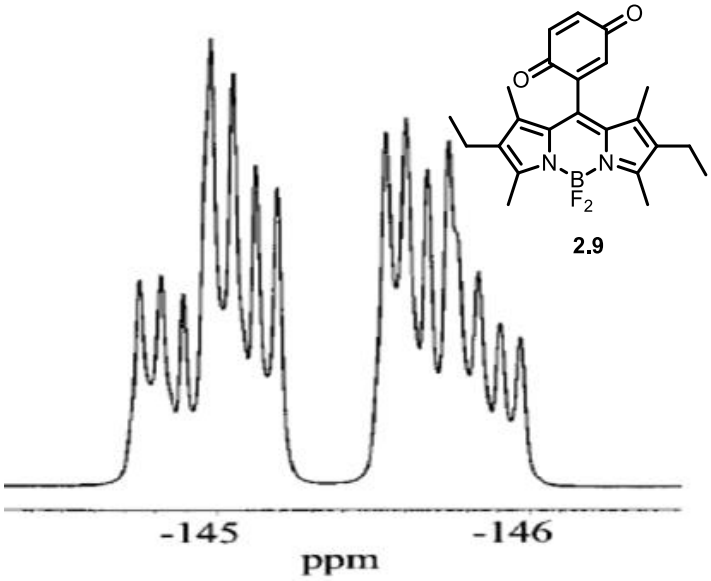

Figure 2.10: ^{19}F NMR spectrum reported for BODIPY **2.9** in $CDCl_3$.[58]

Benniston reported the same phenomenon in BODIPY **2.11**. Even though BODIPY **2.11** contains hydrogens at the 1 and 7 positions, free rotation of the 8-phenanthrene substituent appears to be restricted as indicated by the double quartet in the ^{19}F NMR spectrum of BODIPY **2.11** (Scheme 2.6).[59]

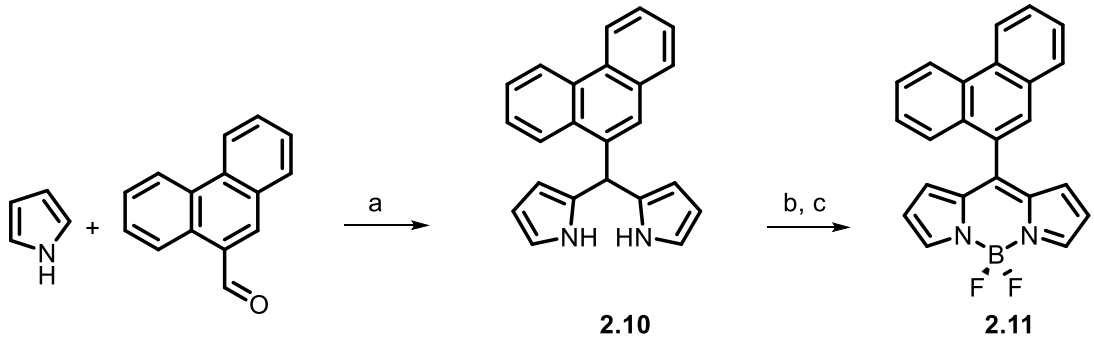

Scheme 2.6: Synthesis of 8-phenanthrene substituted BODIPY **2.11**. Conditions and reagents: a) TFA, r.t., 90 h, 54%. b) DDQ, DCM, 90 min. c) $BF_3.OEt_2$, i-Pr_2NEt, r.t., 20 h, 55%.[59]

Therefore, in the case of BODIPY **2.6**, due to restricted rotation around the pyrrole-aryl bond, the *anti* diastereoisomer was expected to be chiral. The ^{19}F NMR spectrum for the

2,6-bis(2-methoxyphenyl) BODIPY **2.6** showed 20 peaks and corresponds to a diastereomeric mixture (50 : 50 ratio) of the *syn*-**2.6** and *anti*-**2.6** isomers (Figure 2.11).

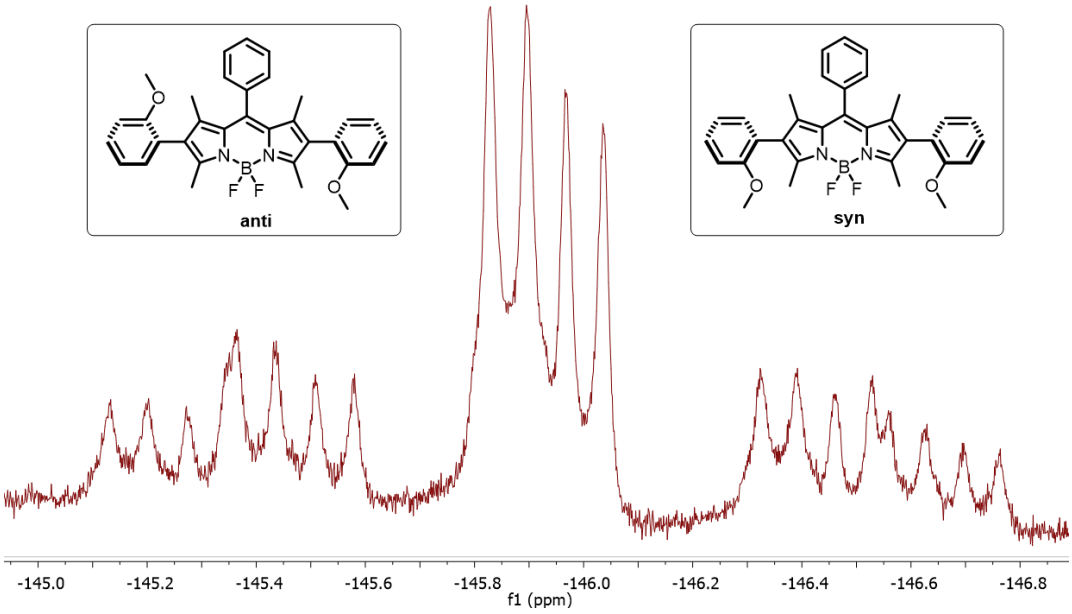

Figure 2.11: ^{19}F NMR spectrum for the mixture of isomers of 2,6-bis-(2-methoxyphenyl)BODIPY **2.6**.

In order to measure the barrier to rotation for the 2-methoxyphenyl group a variable temperature (VT) ^{19}F NMR experiment was performed using toluene-d_8 from 298 to 373 K (Figure 2.12). However, no sign of coalescence or broadening of the peaks was observed which indicates that restricted rotation of the 2-methoxyphenyl/BODIPY bond, even at high temperature results in the two fluorine atoms being inequivalent. This restriction is caused by a combination of the steric bulk of the 2-methoxy groups together with the 1,3,5,7 methyl groups.

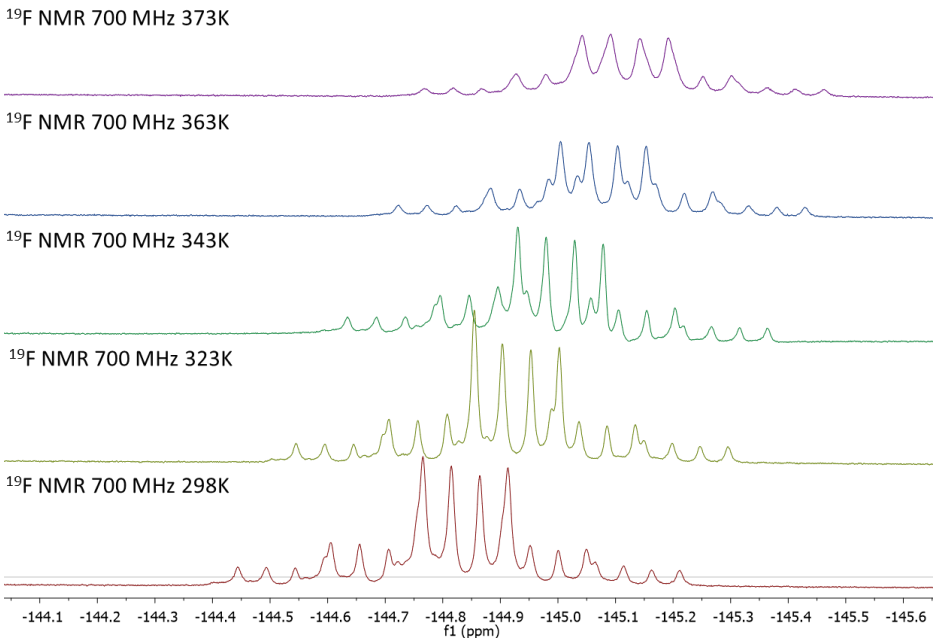

Figure 2.12: ^{19}F VT NMR spectra of the mixture of isomers of 2,6-bis-(2-methoxyphenyl)BODIPY **2.6**, in d_8-toluene.

2.2.1.1. Chiral resolution

Chiral resolution, also called chiral separation, is a process used to separate the two enantiomers of a racemic compound. There are a several different methods by which enantiomers can be separated such as creation of diastereomers by reaction of the enantiomers with an enantiomerically pure chiral compound; the resulting diastereoisomers can be purified for example by standard column chromatography or by crystallization (common for diastereoisomeric salts). Chiral column chromatography is frequently used as an analytical tool to measure the ratio of enantiomers but can also be used preparatively.

2.2.1.2. Chiral HPLC separation

In direct chiral chromatographic separation the two enantiomers are placed in a chiral environment. As a matter of principle, chiral selectors are employed in the stationary phase and/or the mobile phase, which produce diastereomeric interactions with the enantiomeric analytes which consequently elute at different rates. The enantiomer which interacts less strongly with the stationary phase will elute more quickly.

Unfortunately, attempts to separate **2.6** syn and the two enantiomers of **2.6** anti by chiral HPLC were not successful as shown in Figure 2.13.

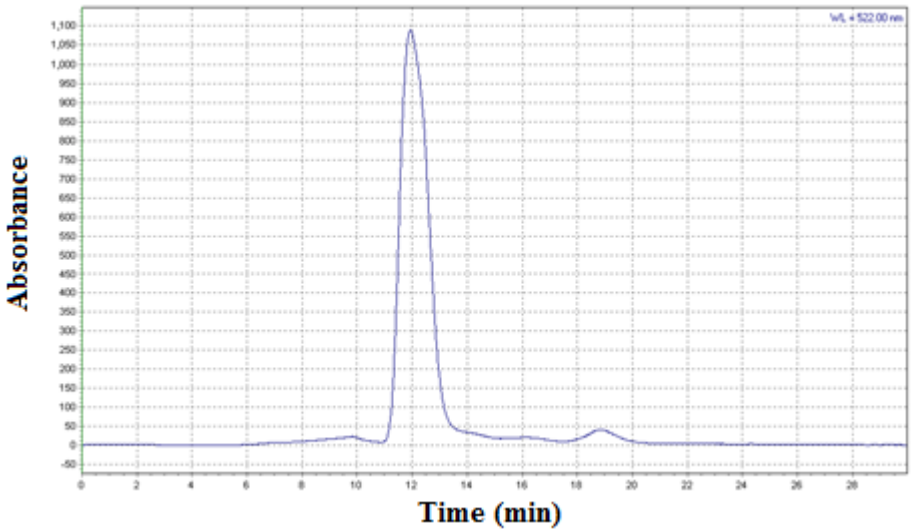

Figure 2.13: Attempted HPLC separation of the stereoisomers of BODIPY **2.6**. Daicel Chiralpk OB column (25 cm x 0.46 cm) hexane:isopropanol (80:20); 0.5 mL min^{-1}.

2.2.1.3. Photophysical data for 2,6-bis(2-methoxyphenyl) BODIPY 2.6

The UV and fluorescence spectra of BODIPYs **2.4-2.6** were measured in $CHCl_3$ at room temperature (Table 2.1). Rhodamine 6G was used as the reference compound for determination of fluorescence quantum yields (rhodamine 6G Φ_f= 0.95, λ_{ex}= 479 or 496 nm, in ethanol).

Table 2.1. Photophysical data of the BODIPYs **2.4-6** in $CHCl_3$.

BODIPY	λ_{abs} (max)/nm	$\varepsilon/10^4$ $M^{-1}cm^{-1}$	λ_{em} (max)/nm	Φ_f (λ_{ex})
2.4	502	3.74	511	0.57(479)
2.5	530	5.67	543	0.46(496)
2.6	578	7.15	591	0.98(496)

Figure 2.14 shows the absorption and emission spectra of parent BODIPY **2.4** and of 2,6-dibromoBODIPY **2.5** and BODIPY **2.6**. As Table 2.1 illustrates all of these BODIPY dyes showed strong absorption bands. In comparison to the parent BODIPY **2.4**, the presence of bromine atoms (heavy atoms) at the 2 and 6 positions of the BODIPY core leads to a 28 nm (1052 cm^{-1}) red-shift of the absorption maximum and a 32 nm (1153 cm^{-1}) red-shift of the emission maximum. Also, the presence of the 2-methoxyphenyl group in the position 2 and 6 leads to red-shift by 76 nm (2619 cm^{-1}) of the absorption and red-shift by 80 nm (2649 cm^{-1}) of the emission maximum.

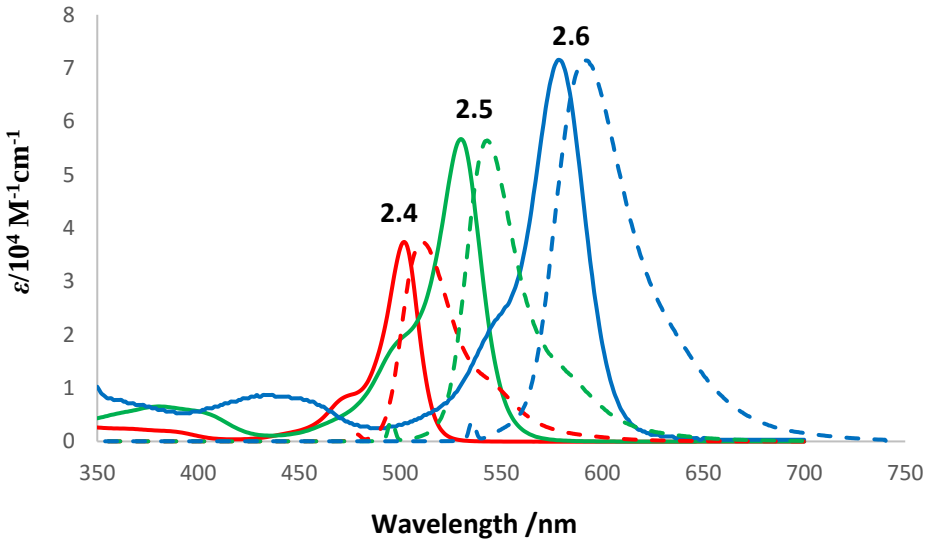

Figure 2.14: Absorption spectrum (solid lines) in terms of the molar absorption coefficient (ε) and normalised fluorescence spectrum (dashed lines) for **2.4** (—), **2.5** (—), and **2.6** (—) in $CHCl_3$.

Due to the formation of 1:1 diastereoisomeric mixture, and the failure of attempted isomer separation by chiral HPLC, this BODIPY was not pursued further.

2.2.2. Synthesis of unsymmetrical axially chiral BODIPY dyes

In order to avoid the diastereoisomer separation problem we decided to synthesise a 1 and 7 substituted BODIPY with an 8-quinoline group at the meso position (8 position). The restricted rotation between 8-quinoline and the substituents in positions 1 and 7 leads to the potential for atropisomerism as long as the BODIPY is unsymmetrically substituted. A functionalized axially chiral BODIPY such as **2.15** might interact enantioselectively with a chiral analyte. The two enantiomers of the chiral 8-quinolinyl substituted BODIPY **2.15** might even be resolved by crystallization of diastereoisomeric salts formed using an enantiopure chiral acid, or simply by chiral HPLC.

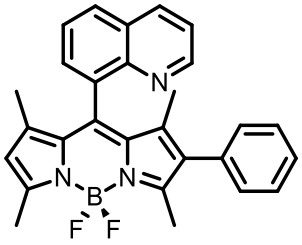

2.15

Functionalization at the meso position can be achieved simply by acid catalyzed condensation of a pyrrole with a suitably substituted acyl chloride or aryl aldehyde. The first step in the synthesis of BODIPY **2.15** is acid catalysed condensation of 2,4-dimethylpyrrole with quinoline-8-carbonyl chloride **2.12** which is not commercially available. In general, acyl chlorides are prepared by treating the corresponding carboxylic acid with thionyl chloride, phosphorus pentachloride, or phosphorus trichloride. By using the literature procedure,[60] quinolinecarboxylic acid was treated with 6 equivalents of thionyl chloride at room temperature for 2 days, followed by the addition of hexane to induce precipitation of the hydrochloride salt of the quinoline-8-carbonyl chloride **2.12** (Scheme 2.7). The crude product was used immediately due to its expected sensitivity towards hydrolysis.

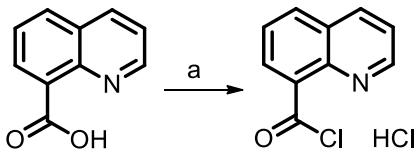

2.12

Scheme 2.7: Synthesis of the quinoline-8-carbonyl chloride **2.12**. Conditions and reagents: a) $SOCl_2$ (12 eq), r.t., 48 h.

BODIPY **2.13** was synthesised using a non-oxidative method via condensation of 2,4-dimethylpyrrole with quinoline-8-carbonyl chloride **2.12** in presence of i-$PrNEt_2$ in DCM.[53] The presumed dipyrromethene intermediate was converted directly to the BODIPY **2.13** without isolation by treatment with i-Pr_2NEt and boron trifluoride etherate ($BF_3.OEt_2$) (Scheme 2.8).

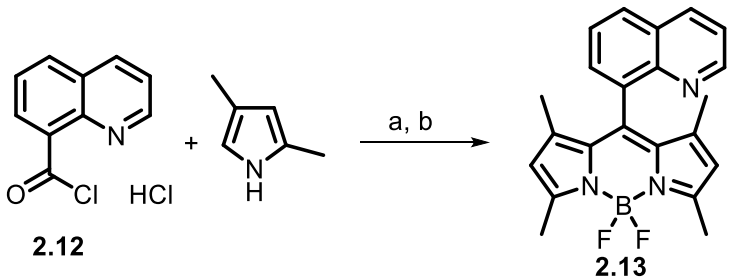

2.12 **2.13**

Scheme 2.8: Synthesis of the BODIPY **2.13**. Conditions and reagents: a) 2,4-dimethylpyrrole (2 eq), DCM, r.t., 24 h. b) i-Pr_2NEt (6.8 eq), $BF_3.OEt_2$ (7.7 eq), 0℃, 1 h, 85%.

The ^{19}F NMR spectrum of **2.13** BODIPY showed 16 peaks which are typical of this class of BODIPY (Figure 2.15). Based on restricted rotation of the 8-quinoline ring in the meso-position (or 8-position) the two fluorine atoms are non-identical and therefore couple to each other and also to the boron atom.

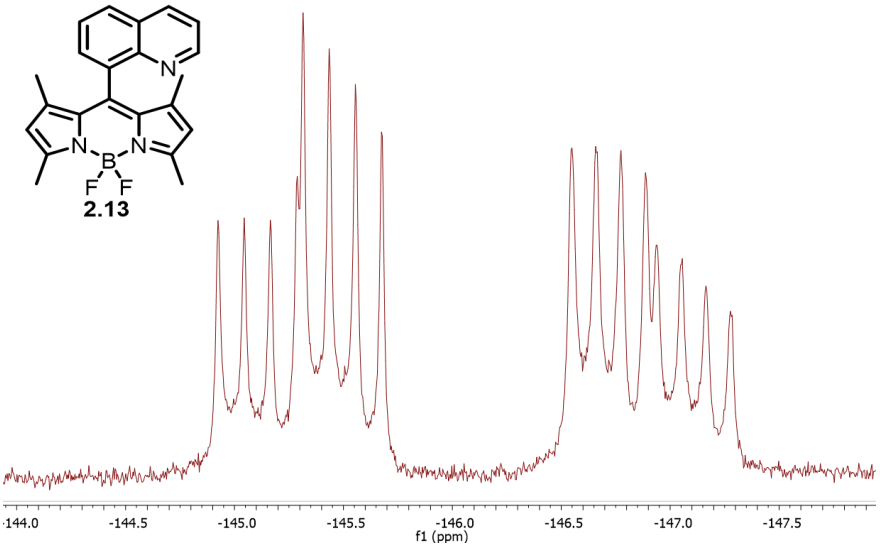

Figure 2.15: ^{19}F NMR spectrum of BODIPY **2.13** (282 MHz, $CDCl_3$).

Desymmetrization of the BODIPY **2.13** is required in order to form an axially chiral system. We decided to desymmetrise **2.13** by bromination of one of the two pyrrole units of the BODIPY. Mono-halogenation of BODIPY is challenging to achieve without any double halogenation. Jia-Hai reported a method[61] for the mono- and di-bromonation of BODIPY using $CuBr_2$ as the brominating agent. Using this procedure,[61] the novel 2-bromoBODIPY **2.14** was synthesized in 60% yield via electrophilic substitution of BODIPY **2.13** with $CuBr_2$, potassium carbonate in acetonitrile under oxygen atmosphere (1 atm, balloon) at room temperature for 24 h (Scheme 2.9). This 2-bromoBODIPY **2.14** allows further functionalization by coupling reactions such as Heck and Suzuki.

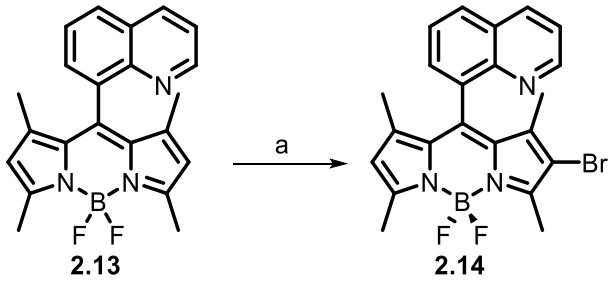

Scheme 2.9: Synthesis of the 2-bromo BODIPY **2.14**. Conditions and reagents: a) $CuBr_2$ (1.5 eq), K_2CO_3 (3 eq), MeCN, r.t., 24 h, 60%.

Suzuki coupling of the 2-bromoBODIPY **2.14** with phenylboronic acid gave the unsymmetrical axially chiral BODIPY **2.15** in good yield (86%) (Scheme 2.10).

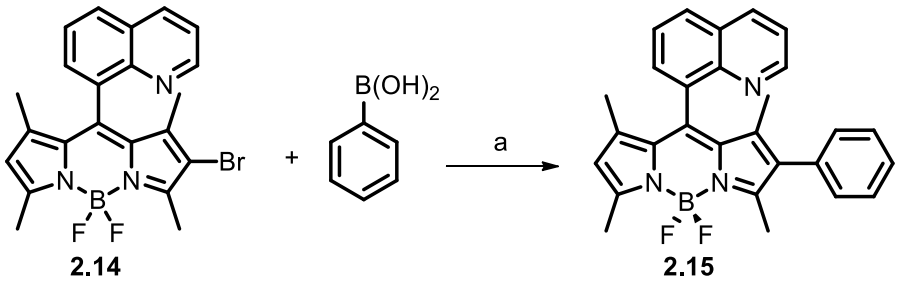

Scheme 2.10: Synthesis of the 2-phenyl BODIPY **2.15**. Conditions and reagents: a) phenylboronic acid (3 eq), $Pd(PPh_3)_4$ (5 mol %), THF, toluene, water, 80 ℃, 24 h, 86%.

Although, in principle, the quinoline **2.15** might be resolved by fractional crystallisation of diastereoisomeric salts using an enantiopure chiral acid, this would be difficult on a small scale. For this reason we decided to resolve the two enantiomers using analytical chiral HPLC. Unfortunately, attempts to separate the enantiomers of BODIPY **2.15** in this way were unsuccessful. Figure 2.16 shows the best separation which was achieved.

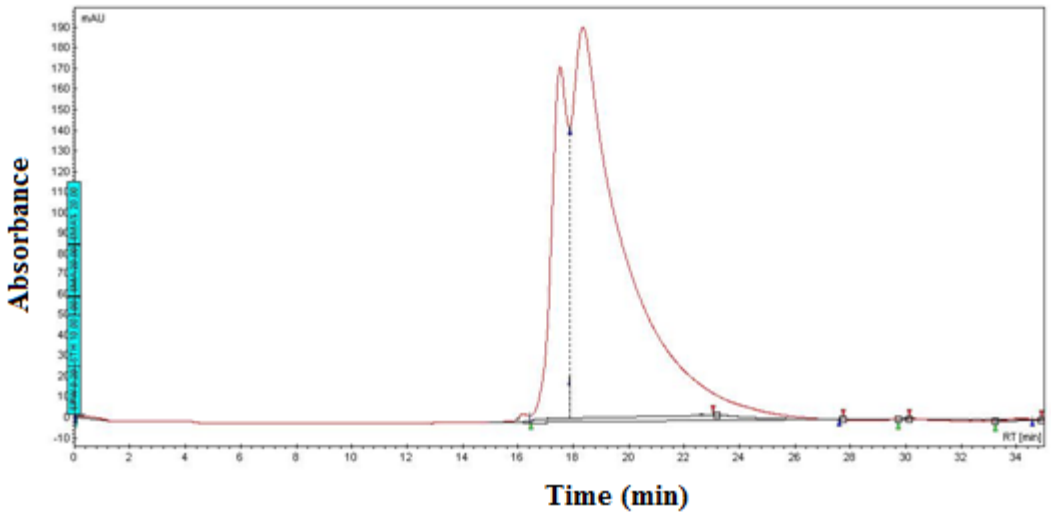

Figure 2.16: Attempted HPLC resolution of BODIPY **2.15**. Daicel Chiralpk OB column (25 cm x 0.46 cm), hexane:isopropanol (80:20) 0.5 mL min^{-1}.

2.2.2.1. Photophysical data of the 2-phenyl BODIPY 2.15.

The UV and fluorescence spectra of BODIPYs **2.13-2.15** were measured in $CHCl_3$ at room temperature (Table 2.2). Rhodamine 6G was used as the reference compound for determination of fluorescence quantum yields (rhodamine 6G Φ_f= 0.95, λ_{ex}= 479 or 496 nm, in ethanol).

Table 2.2. Photophysical data of the BODIPYs **2.13-15**.

BODIPY	λ_{abs} (max)/nm	$\varepsilon/10^4$ $M^{-1}cm^{-1}$	λ_{em} (max)/nm	Φ_f (λ_{ex})
2.13	506	6.03	517	0.75(479)
2.14	518	9.68	532	0.83(496)
2.15	518	7.06	531	0.86(496)

Figure 2.17 shows the absorption and emission spectra of parent quinoline-substituted BODIPY **2.13** and of the 2-bromoBODIPY **2.14** and 2-phenyl BODIPY **2.15**. As Table 2.2 illustrates all of these BODIPY dyes showed strong absorption bands. In comparison to the parent BODIPY **2.14**, the presence of bromine atom (heavy atom) at the 2 position of the BODIPY core leads to a 12 nm (457 cm^{-1}) red-shift of the absorption maximum and a 15 nm

(510 cm^{-1}) red-shift of the emission maximum. However, there was no significant further red-shift of the absorption and emission maximum in the presence of the phenyl group in the position 2 of the core BODIPY.

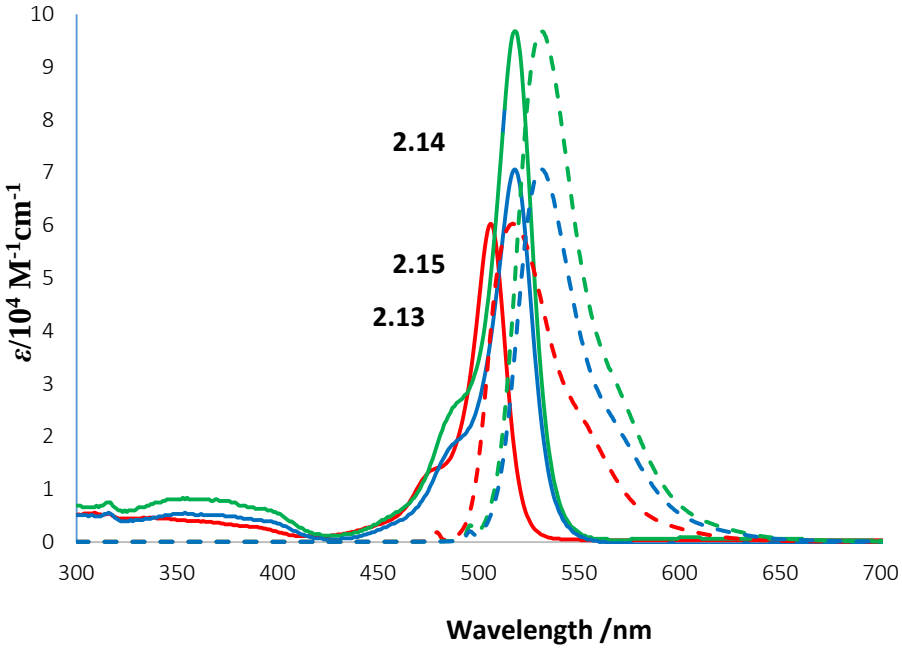

Figure 2.17: Absorption spectrum (solid lines) in terms of the molar absorption coefficient (ε) and normalised fluorescence spectrum (deshed lines) for **2.13** (—), **2.14** (—), and **2.15** (—) in $CHCl_3$.

Although the axially chiral BODIPY **2.15** was successfully prepared in 2 steps from BODIPY **2.13**, attempts to resolve BODIPY **2.15** into its separate enantiomers by chiral HPLC have so far been unsuccessful. It is possible that resolution of this quinoline derivative might be possible by fractional crystallisation of distereisomeric salts formed by treatment with an enantiopure chiral acid but this would require a larger quantity of the BODIPY than was available from our initial synthesis.

2.3. Helically chiral BODIPY

2.3.1. Approach to synthesis of functionalized Aza BODIPY dyes

Exchange of the meso-carbon atom of BODIPY dyes for a nitrogen atom generates a sub-class of BODIPY called aza-BODIPY. The first aza dipyrromethene chromophore was synthesized in the 1940s,[62–64] but the aza-BODIPY species was not reported until 1994.[65] Interest in the aza-BODIPY species has increased due to their photophysical properties; in particular it has been found that inclusion of the meso-nitrogen produces a large red shift of the absorption and emission bands in the 650-850 nm range, with high molar extinction coefficient, and moderate to high fluorescence quantum yields.[6,16,35,60,66–72] O'Shea reported the conversion of tetraarylazadipyrromethenes **2.16** into BF_2 chelates **2.17** and application for photodynamic therapy (Scheme 2.11).[35,66]

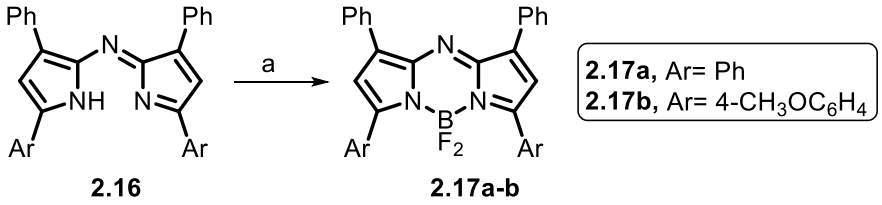

2.16 **2.17a-b**

Scheme 2.11: Synthesis of the aza-BODIPY dyes **2.17**. Conditions and reagents: a) $BF_3.OEt_2$, i-Pr_2NEt, DCM, 16 h, r.t.

O'Shea subsequently reported a new class of aza-BODIPY **2.19**, in which the cyclisation of the two oxygen atoms of the aryl substituents of the BODIPY **2.18** onto the boron atom renders the molecule chiral (Scheme 2.12).[72]

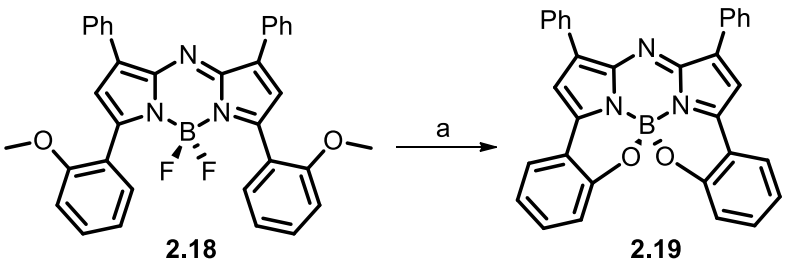

Scheme 2.12. Synthesis of Near-IR fluorophores **2.19**. Conditions and reagents: a) BBr_3, DCM, 0-25℃, 12 h.[72]

Symmetrical aza-BODIPY derivatives **2.21** were synthesized by using the synthetic route in Scheme 2.13. We aimed in this project to synthesise a functionalized aza-BODIPY and then study potential uses of these chiral dyes.

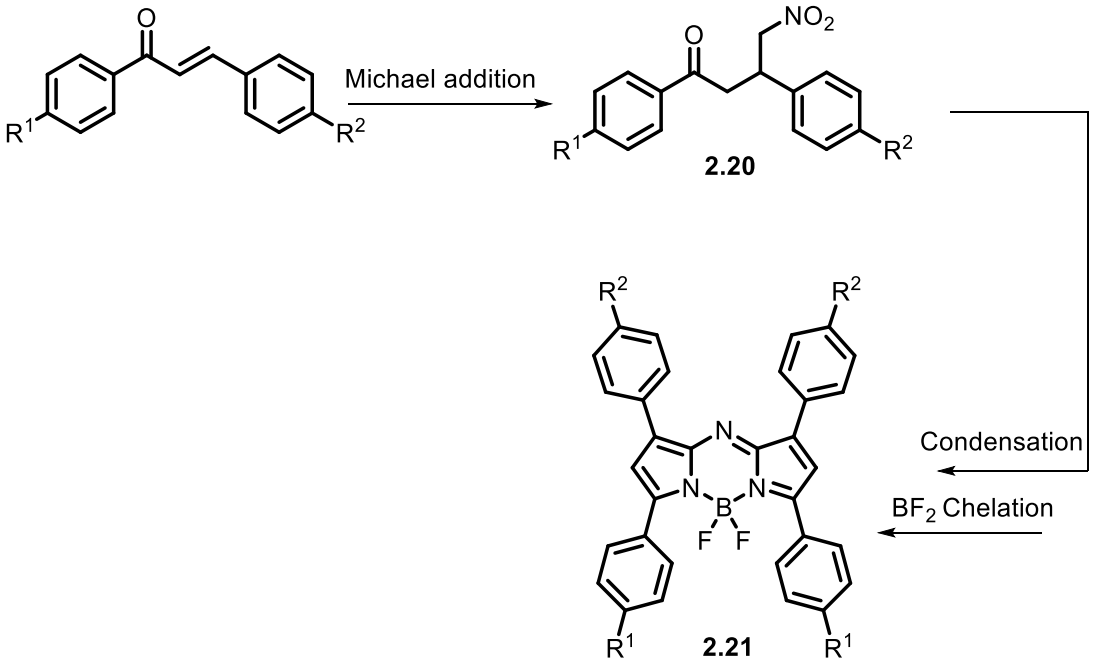

Scheme 2.13: General synthetic approach to the synthesis of an aza-bodipy dye.[72]

Before attempting the synthesis of more highly functionalized *N,N,O,O*-aza-BODIPYs we started with the synthesis of the known[72] *N,N,O,O*-aza-BODIPY compounds **2.25a, b** to gain familiarity with the synthetic route (Scheme 2.14) and the properties of the key *N,N,O,O*-aza-BODIPY core.

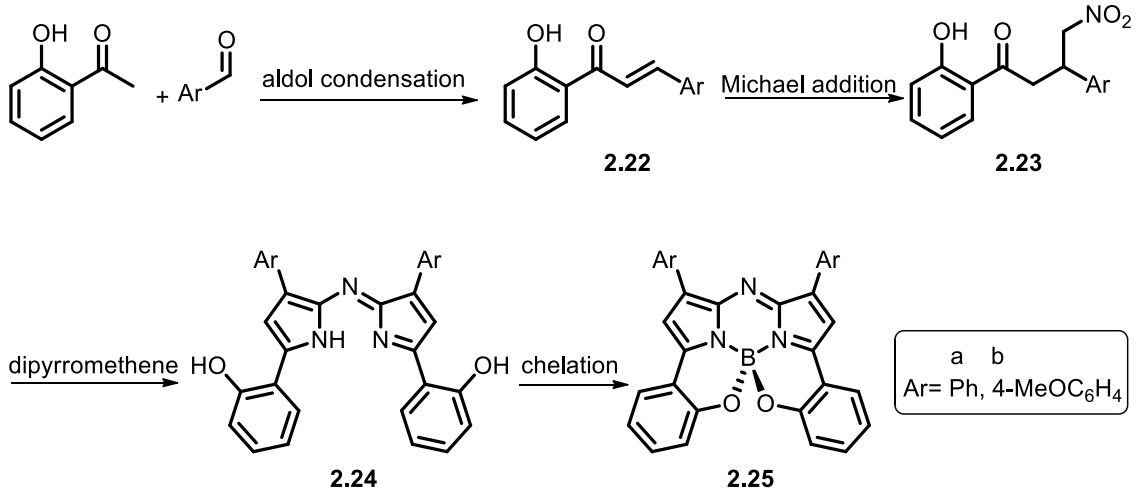

Scheme 2.14: Four steps for the synthesis of *N,N,O,O*-aza-BODIPY **2.25a-b**.

Initially, by using a literature procedure the aldol condensation between 2'-hydroxyacetophenone and aldehyde was carried out by treatment with sodium hydroxide (Scheme 2.15). The expected chalcone derivatives **2.22a, b** were formed in good yield.[73,74] The ^{1}H NMR spectrum of the product showed the appearance of the signals corresponding to the two protons on the alkene (**2.22a**, 7.92 and 7.66 ppm; **2.22b**, 7.91 and 7.57) and the coupling constant between these protons (**2.22a**, 15.5 H_z; **2.22b**, 15.4 H_z) indicated that the configuration of the double bond was *E*.

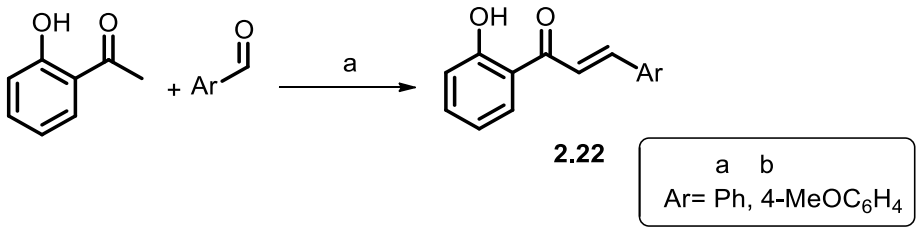

Scheme 2.15: Synthesis of chalcone derivatives **2.22**.[73,74] Conditions and reagents: a) NaOH, MeOH, 48 h, r.t., (**2.22a**, 52%; **2.22b**, 54%).

Michael addition to form compound **2.23a,b** was accomplished by treatment of chalcone derivatives **2.22a,b** with nitromethane and diethylamine (Scheme 2.16).[72] The ^{1}H NMR spectrum of the crude product mixture showed disappearance of the signals corresponding to the two vinylic hydrogens and appearance of a signal corresponding to the CH_2 which is α to the NO_2 (**2.23a**, Ar = Ph, 3.64 – 3.39 ppm). The crude products were recrystallized from methanol to give **2.23a** and **2.23b** in good yields 55 and 80% respectively.

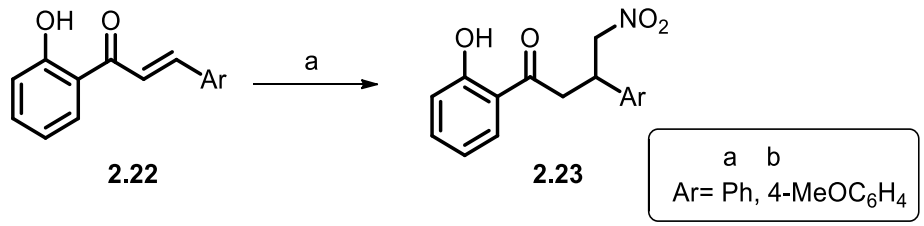

Scheme 2.16: Synthesis of compounds **2.23**.[72] Conditions and reagents: a) $MeNO_2$ (4 eq), Et_2NH, MeOH, 17 h, reflux, (**2.23a**, 55%; **2.23b**, 80%).[72]

Tetraarylazadipyrromethenes **2.24a, b** were synthesized by treating diaryl-γ-nitro ketones **2.23a,b** with excess of ammonium acetate in cumene under reflux for 3 hours.[72] The products **2.24a, b** were isolated by trituration with cold methanol in low yield (**2.24a,** 11% and **2.24b**, 20%) as blue solids.[72] The ^{1}H NMR spectrum of the pure product showed appearance of the signal corresponding to the CH on the position 3 (**2.24a,** Ar = Ph, 7.28 ppm; **2.24b,** Ar = 4-$MeOC_6H_4$, 7.78ppm).

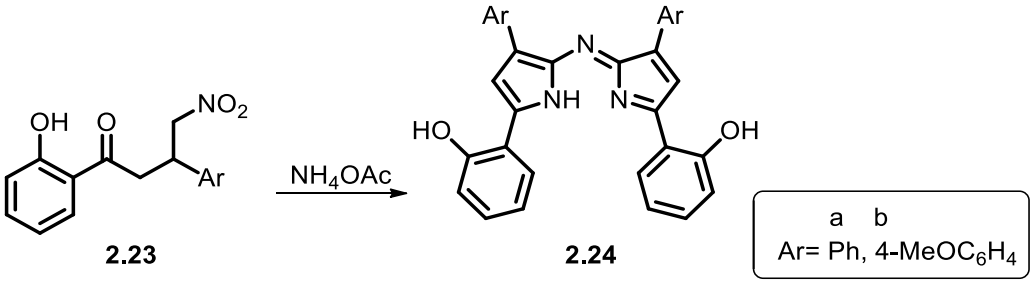

Scheme 2.17: Synthesis of tetraarylazadipyrromethenes **2.24**. Conditions and reagents: a) NH_4OAc (35 eq), cumene, 3 h, reflux, (**2.24a**, 11%; **2.24b**, 20%).[72]

The aza-BODIPY compounds **2.25a, b** were synthesized by treatment of compounds **2.24a, b** with i-Pr_2NEt and BF_3.Et_2O in toluene (Scheme 2.18).[72] The target compounds **2.25a** and **2.25b** were formed by BF_2 chelation and intramolecular phenolic oxygen fluorine displacement in good yields (82 and 73% respectively).

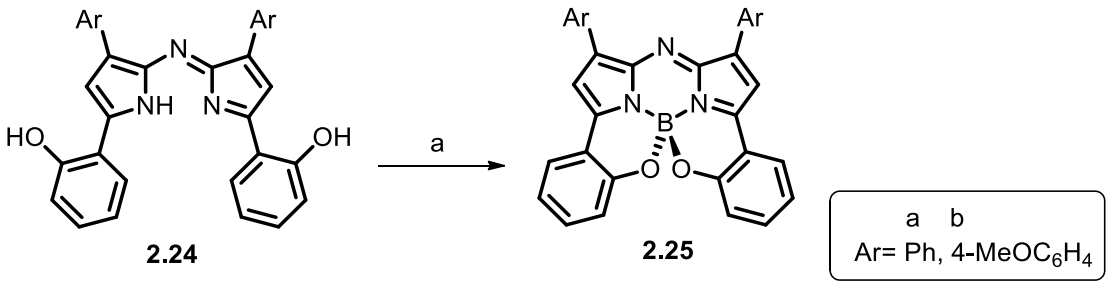

Scheme 2.18: Synthesis of aza-BODIPY compounds **2.25**.[35] Conditions and reagents: a) i-Pr_2NEt (14 eq), BF_3.OEt_2 (10 eq), toluene, 2 h, reflux, (**2.25a**, 82%; **2.25b**, 73%).

The preparation of aza-BODIPY **2.25a**, **b** succeeded in a good yield. However, these compounds have no functional groups which could interact with a chiral molecule. Therefore, we decided to prepare a more highly functionalized aza-BODIPY **2.26** for potential applications to enantioselective sensing. The two enantiomers of the chiral aza-BODIPY **2.26** might be resolved by simply by chiral HPLC.

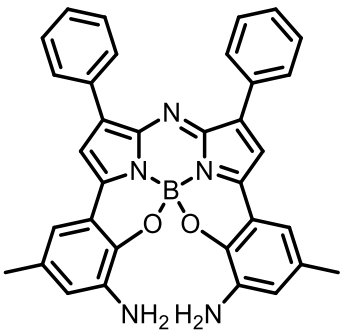

2.26

We envisioned that aza-BODIPY **2.26** could be obtained starting from the commercially available 2-hydroxy-5-methyl-3-nitroacetophenone and benzaldehyde. Aldol condensation of these two compounds in ethanol gave 1-(2-hydroxy-5-methyl-3nitrophenyl)-3-phenylpropenone **2.27** in 89% yield (Scheme 2.19).

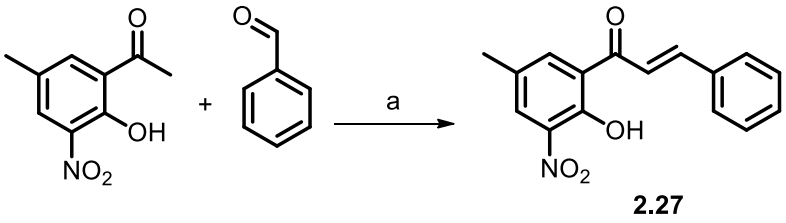

Scheme 2.19: Synthesis of chalcone derivative **2.27.** Conditions and reagents: a) KOH (3 eq), EtOH, r.t., 24 h, 89%.

Michael addition reaction of the resulting chalcone **2.27** with nitromethane in diethylamine and methanol successfully produced the γ-nitroketone **2.28** in a good yield 73% (Scheme 2.20).

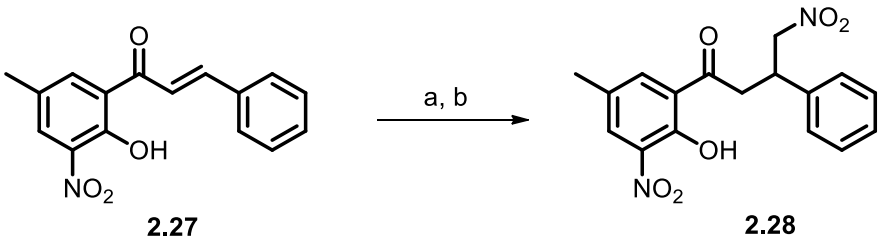

Scheme 2.20: synthesis of compound **2.26**. Conditions and reagents: a) Et_2NH (4 eq), $MeNO_2$ (4 eq), MeOH, reflux, 17 h; b) r.t., HCl (2M), 73%.

The most challenging step in the synthesis of aza-BODIPYs is preparation of the aza-dipyrrin. We attempted to synthesise **2.29** following O'Shea's conditions[72] by treatment of compound **2.28** with ammonium acetate in cumene under reflux for 3 hours. Unfortunately, the dark crude product was insoluble in a range of organic solvents. ^1H NMR spectrum in D_2O indicated a very complex mixture of compounds.

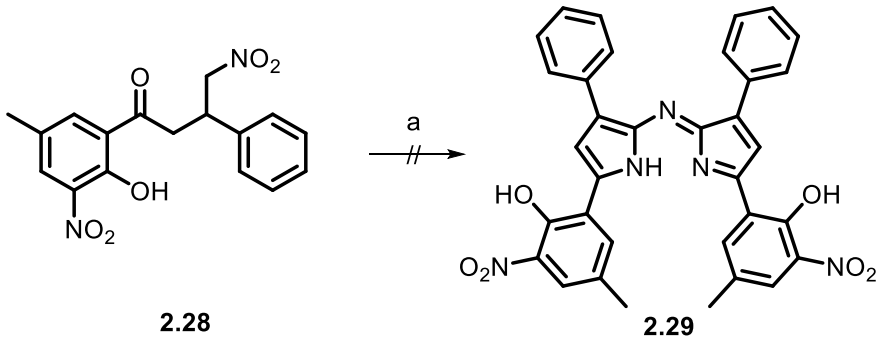

Scheme 2.21: synthesis of compound **2.29**. Conditions and reagents: a) NH_4OAc (35 eq), cumene, 3 h, reflux.

We then examined Gray's conditions[71] to make **2.29** by performing the reaction in 1-butanol as a solvent under reflux for 24 h, nevertheless, similar insoluble dark crude material was observed with a highly complex ^{1}H NMR spectrum. A possible explanation for this might be the presence of two NO_2 groups in the Michael addition product **2.28**. A mechanism for the formation of aza-dipyrrins from nitromethane was proposed by O'Shea in 2012.[70] As Scheme 2.22 shows, the start of the reaction to form aza-dipyrrin involves the formation of enamine intermediate **2.32** from Michael addition product **2.30** and ammonia, followed by nucleophilic addition to produce intermediate **2.33**. Three potential routes then lead from **2.33** to the aza-dipyrrin **2.36**.

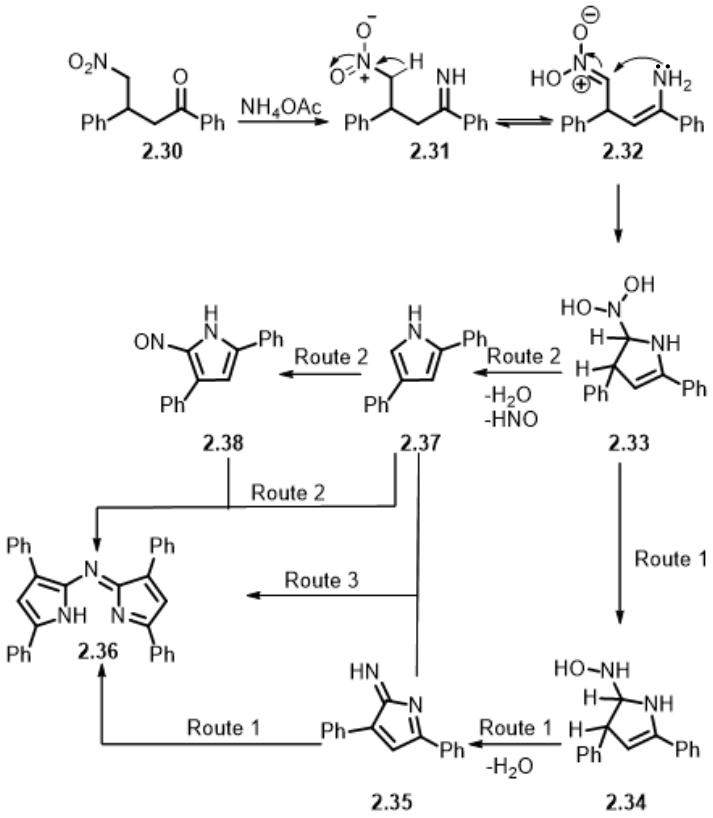

Scheme 2.22: Three different proposed routes for the synthesis of aza-dipyrrins.[70]

Since the formation of aza-dipyrrin **2.29** was unsuccessful by using the Michael addition product **2.28**, we decided to hydrogenate the NO_2 group of the 2-hydroxy-5-methyl-3-nitroacetophenone followed by protection of the resulting NH_2 group to prevent any complication during the formation of the aza-dipyrrin.

Following a literature procedure,[75] the nitro group of 2-hydroxy-5-methyl-3-nitroacetophenone was reduced to 2-hydroxy-5-methyl-3-aminoacetophenone **2.39** using $SnCl_2.2H_2O$ in absolute ethanol. Purification using column chromatography gave the desired compound **2.39** in good yield (75%) (Scheme 2.23).

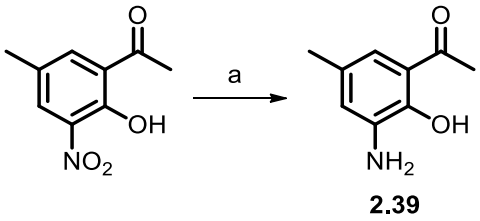

2.39

Scheme 2.23: Synthesis of compound **2.39**. Conditions and reagents: a) $SnCl_2.2H_2O$ (5 eq), EtOH, 4 h, reflux, 75%.

Treatment of the reduced compound **2.39** with di-*tert*-butyl dicarbonate (Boc) and triethylamine in DCM produced the protected compound **2.40** in low yield 30% (Scheme 2.24).

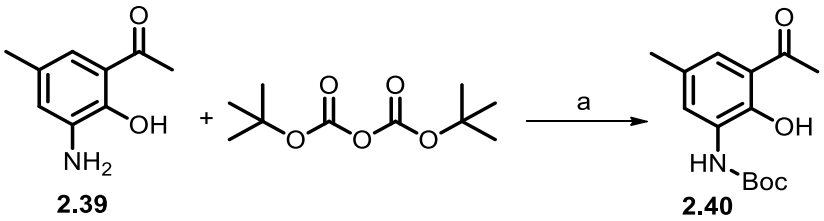

2.39 **2.40**

Scheme 2.24: Synthesis of protected compound **2.40**. Conditions and reagents: a) Di-*tert*-butyl dicarbonate (1.1 eq), NEt_3 (1.1 eq), DCM, r.t., 48 h, 30%.

Unfortunately, the aldol condensation reaction of compound **2.40** with benzaldehyde failed to form the expected chalcone derivative **2.41** (Scheme 2.25).

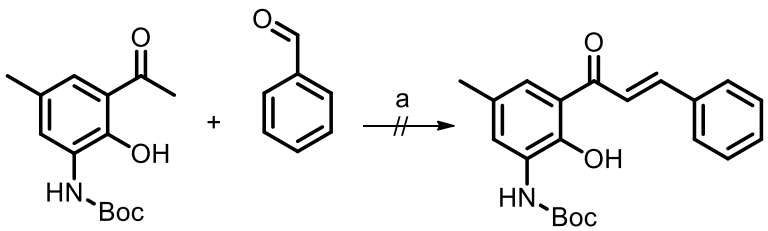

2.40 **2.41**

Scheme 2.25: Attempt to synthesis of chalcone **2.41**. Conditions and reagents: a) KOH (3 eq), EtOH, r.t., 24 h.

The known aza-BODIPY compounds **2.25a, b** were synthesized successfully, nevertheless, all attempts for synthesis of the functionalized aza-BODIPY **2.26** proved unsuccessful. There are some disadvantages in the synthesis of aza-BODIPYs. For instance, the yield of formation of the aza-dipyrrins **2.24a, b** is very low. It has been reported that aza-BODIPYs can only be synthesized from heavily substituted pyrroles, such as ring annelated pyrroles or 2,4-diarylpyrroles.[16] Also, there are few 2-hydroxyacetophenone derivatives which are commercially available thus limiting the ease with which structural variation can be accomplished. Therefore, we decided to exchange of the central nitrogen atom of the aza-BODIPYs with a C atom (C-meso) to form the corresponding helically chiral *N,N,O,O*-BODIPYs.

2.3.2. Synthesis of helically chiral *N,N,O,O*-BODIPY dyes.

Burgess[76] reported the synthesis and investigation of the *N,N,O,O*-BODIPY structure. This compound is helically chiral due to the chelation to boron which prevents rotation of the aryl rings about the pyrrole rings. The two enantiomers of this compound were not resolved, nonetheless, the reported HPLC analysis of the rac **2.42** on a Pirkle column showed two peaks which indicates that separation is possible. In general, this ring system gives a red-shifted and sharper fluorescence emission than the ordinary BODIPY.

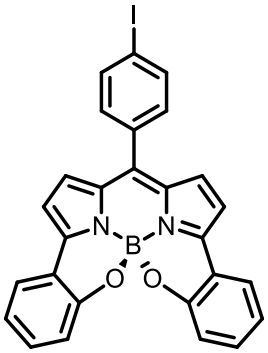

2.42

In 2008, Kung successfully synthesised and characterized a water soluble *O*-chelated BODIPY **2.43**, for targeting β-amyloid plaques.[77] In addition, Kubo prepared *O*-chelated BODIPY **2.44** which can work as a light-harvesting sensitizer in polymeric solar cells.[78]

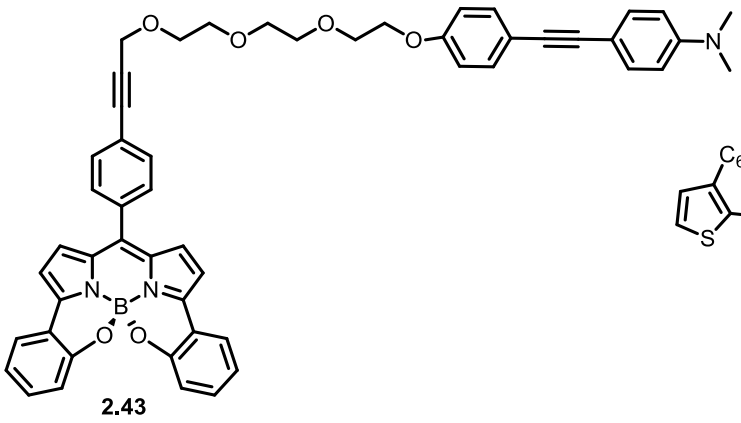

2.43

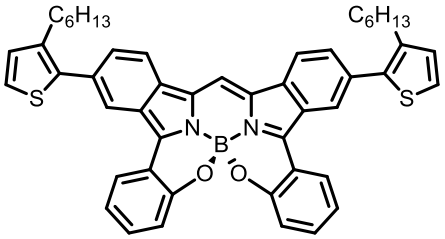

2.44

A considerable number of *O*-chelated BODIPYs have been reported in the literature.[77,79–84] However, there is no report of the use of *O*-chelated BODIPY species for enantioselective applications or use as chiroptical dyes. Interestingly, the separation of the two enantiomers and information about the chiral properties of these molecules (*O*-chelated BODIPY) has not been reported. Therefore, we aimed to synthesise *O*-chelated BODIPY derivatives followed by resolution of these racemic helically chiral BODIPYs to give single enantiomers, and then study the chiral properties of these molecules in their excited state.

In general, only one synthetic approach to *O*-chelated BODIPYs has been investigated (Scheme 2.26).[77–83] Suzuki coupling of (2-methoxyphenyl)boronic acid with 2-bromo-*N*-Boc pyrrole followed by Boc deprotection gives the 2-arylpyrrole **2.46**. Then, condensation of an aryl chloride with pyrrole **2.46** affords the dipyrromethene **2.47**. Subjecting the dipyrromethene **2.47** to base and boron trifluoride etherate affords the BODIPY complex **2.48**. Finally, double demethylation of BODIPY **2.48** affords *O*-chelated BODIPY **2.49** (Scheme 2.26). Therefore, our first approach toward the synthesis of *O*-chelated BODIPYs followed this route.

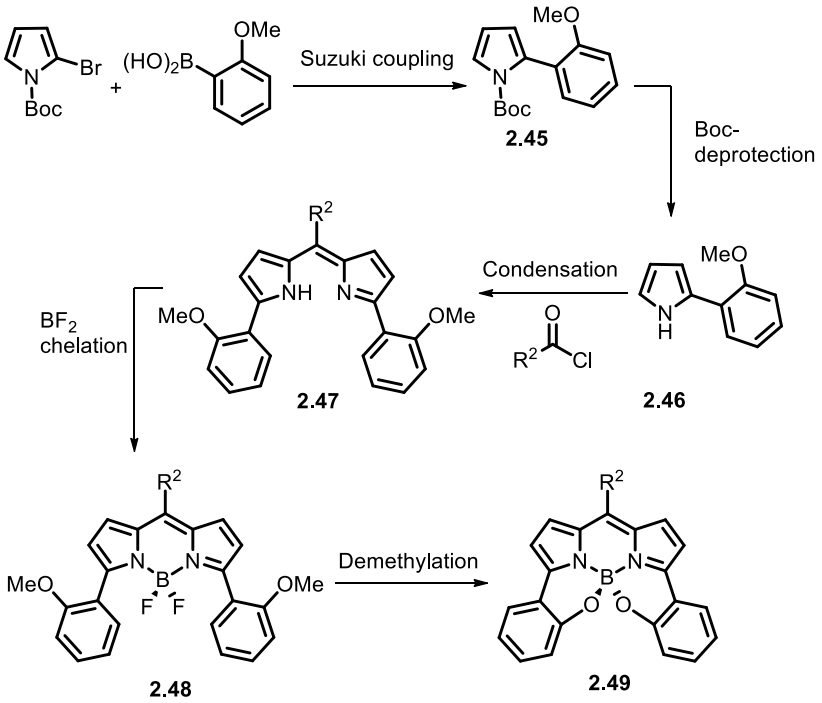

Scheme 2.26: General synthetic approach to the synthesis of *O*-chelated BODIPYs **2.49**.

The commercially available pyrrole was reacted with 1,3-dibromo-5,5-dimethylhydantoin **2.50** in the presence of azoisobutyronitrile (AIBN) in THF at -78℃ to give brominated pyrrole, followed by Boc-protection by using triethylamine, di-*tert*-butyl dicarbonate and a catalytic amount of 4-dimethylaminopyridine[84] to give a 70:30 ratio of the *N*-Boc-2-bromopyrrole **2.51** as major product together with a minor amount of *N*–Boc-3-bromopyrrole **2.52** which were not separable by column chromatography.

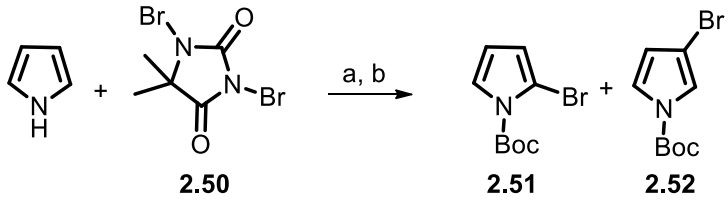

Scheme 2.27: Synthesis of *N*-Boc-2-bromopyrrole **2.51**. Conditions and reagents: a) DBDMH (1 eq), THF, AIBN (2 mol %), -78℃, 2 h; b) Et_3N (0.8 eq), Di-*tert*-butyl dicarbonate (2.8 eq), DMAP (2 mol%), r.t., 16 h (**2.51**, 65%; **2.52**, 20%).

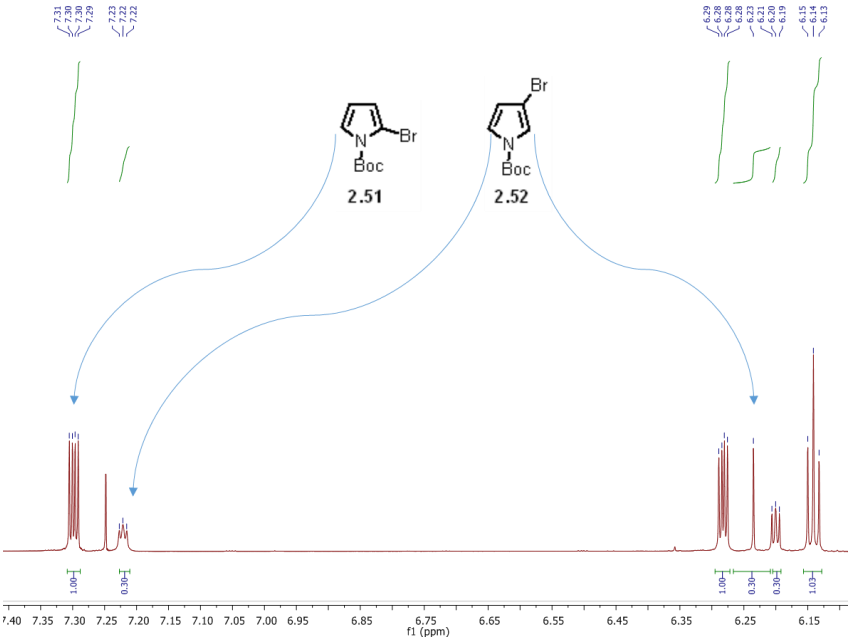

Figure 2.18: ^{1}H NMR spectrum of a mixture of *N*-Boc-2-bromopyrrole **2.51** and **2.52**.

Tert-butyl 2-(2-methoxyphenyl)-1H-pyrrole-1-carboxylate **2.45** was synthesized via Suzuki coupling reaction. Initially, a mixture of *N*-Boc-2 and 3-bromopyrrole **2.51** and **2.52** were reacted with 2-methoxybenzeneboronic acid in the presence of $Pd(PPh_3)_4$ and Na_2CO_3 in methanol. The crude product was purified using column chromatography to give **2.45** as a light grey solid in good yield (73%).

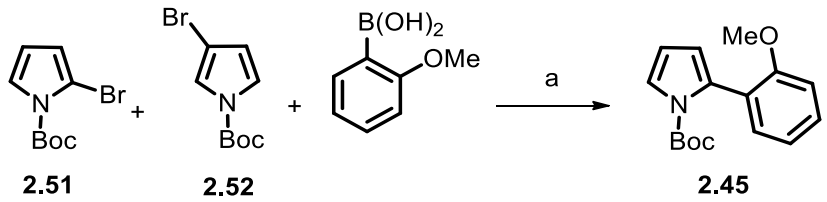

Scheme 2.28: Synthesis of *tert*-butyl 2-(2-methoxyphenyl)-1H-pyrrole-1-carboxylate **2.45**. Conditions and reagents: a) 2-methoxyphenylboronic acid (1 eq), $Pd(PPh_3)_4$ (5 mol%), Na_2CO_3 (2 eq), toluene, MeOH, 80 ℃, 20 h, 73%.

Deprotection of the *N*-Boc group to give the pyrrole **2.46** was accomplished by treatment with sodium methoxide in a mixture of methanol and THF at room temperature for 6 h.[85] The crude product was purified using column chromatography to give **2.46** as a light green solid in 50% yield.

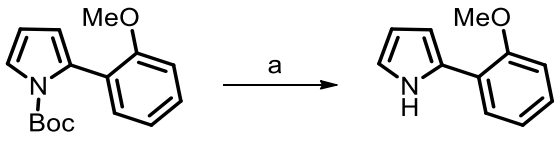

2.45 **2.46**

Scheme 2.29: Synthesis of 2-(2-methoxyphenyl)-1H-pyrrole **2.46**. Conditions and reagents: a) NaOMe (3 eq), THF, MeOH, r.t., 20 h, 50%.

Our initial attempt to form symmetrical BODIPY **2.49** was via condensation of pyrrole **2.46** with 4-methylbenzoyl chloride to give dipyrromethene **2.47** (Scheme 2.30). The crude product was purified using column chromatography to give **2.47** as a grey solid in 20% yield.

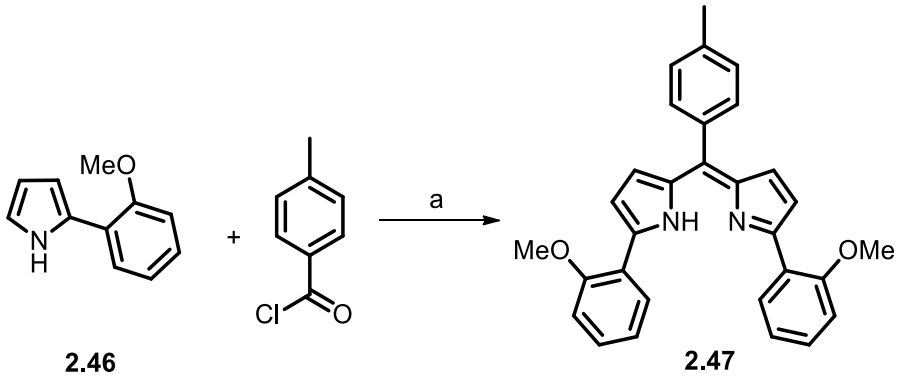

2.46 **2.47**

Scheme 2.30: Synthesis of symmetrical dipyrromethene **2.47**. Conditions and reagents: a) 4-methylbenzoyl chloride (1 eq), DCE, 85℃, 3 h, 20%.

The dipyrromethene **2.47** was synthesized successfully. However, there are some disadvantages in this synthetic route. For instance, the difficulties in the purification and handling of 2-bromopyrrole **2.51**. In addition, the yield of the Boc deprotection reaction and formation of dipyrromethene is very low. Therefore, we developed an alternative synthetic route. This new approach involves the synthesis of the symmetrical dipyrromethane **2.54** followed by double bromination reaction and DDQ oxidation to give a 1,9-dibromodipyrromethene followed by formation of the symmetrical 3,5-dibromoBODIPY **2.56**. Suzuki coupling with ortho-methoxyphenyl boronic acid to give BODIPY **2.48**. Finally, demethylation of the aryl ether with BBr_3 should result in the replacement of the B-F bonds with B-O bonds to give BODIPY **2.49** (Scheme 2.31).

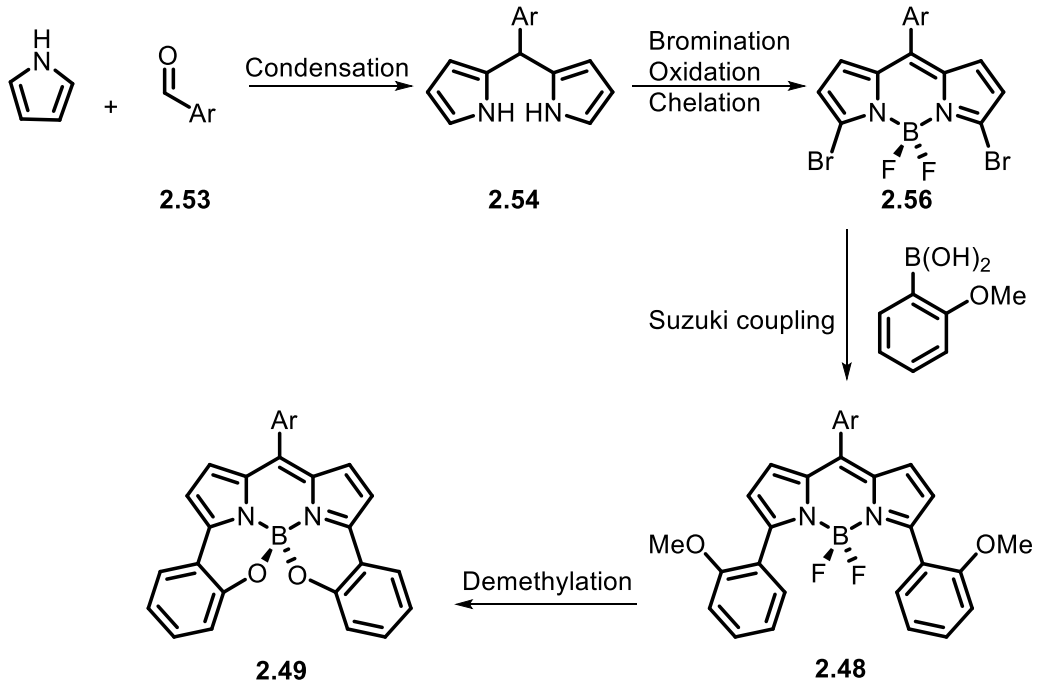

Scheme 2.31: General synthetic approach to the synthesis of *O*-chelated chiral BODIPYs.

Condensation of *p*-tolualdehyde **2.53a** with pyrrole in the presence of catalytic $BF_3.OEt_2$ proceeded to give the corresponding dipyrromethane[86] **2.54a** (Scheme 2.32). The reaction mixture was stirred for 30 min at room temperature, resulting in complete disappearance of the aldehyde by TLC. The ^1H NMR spectrum of the crude reaction mixture showed the appearance of the signal corresponding to the CH at the meso position as a singlet at 5.47 ppm.

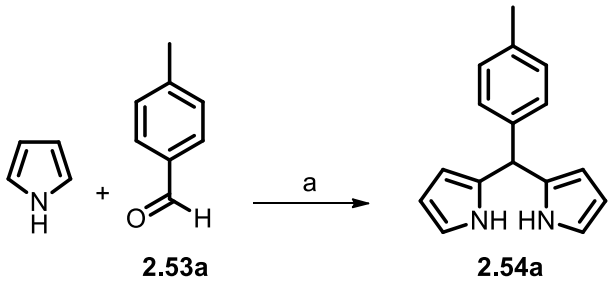

Scheme 2.32: Synthesis of symmetrical dipyrromethane **2.54a**. Conditions and reagents: a) *p*-tolualdehyde **2.53a** (1 eq), pyrrole (25 eq), $BF_3.OEt_2$ (10 mol%), r.t., 30 min., 69%.

1,9-dibromo-5-(4-methylphenyl)dipyrromethene **2.55a** was synthesized as reported in the literature[87] via the selective addition of an electrophilic brominating agent to the 1 and 9 positions of compound **2.54a** followed by oxidation. Thus, compound **2.54a** was treated with of *N*-bromosuccinimide at -78℃ for 1 h. Then, the crude product was oxidized with 1 equivalent of DDQ at room temperature for 10 min. The dipyrromethene **2.55a** was

isolated in 80% yield by flash column chromatography. Then, BF_2 chelation by treatment 1,9-dibromodipyrromethene **2.55a** with boron trifluoride diethyl etherate ($BF_3.OEt_2$) in the presence of *N*,*N*-diisopropylethylamine[87] (i-Pr_2NEt) gave the fluorescent BF_2 complex **2.56a** in a good yield (Scheme 2.33).

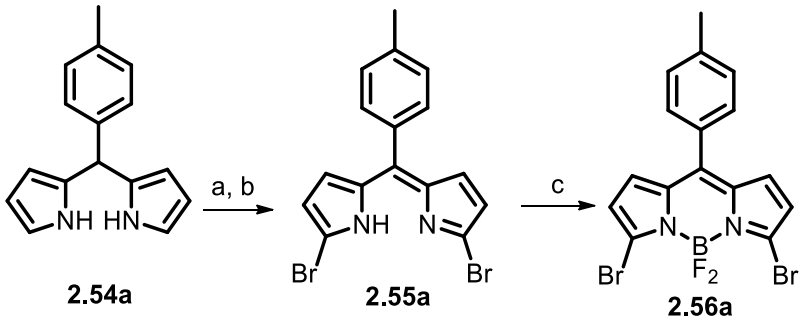

Scheme 2.33: Synthesis of symmetrical 3,5-dibromoBODIPY **2.56a**. Conditions and reagents: a) NBS (2 eq), THF, -78 ℃, 1 h; b) DDQ (1 eq), THF, 10 min., r.t., 80%; c) i-Pr_2NEt (7 eq), $BF_3.OEt_2$ (7 eq), r.t., 31 h, 86 %.

Crystals of compound **2.56a** were obtained by slow evaporation from a mixture of chloroform and hexane (1:3). The crystal structure shown in Figure 2.19 was obtained through single crystal X-ray crystallography.

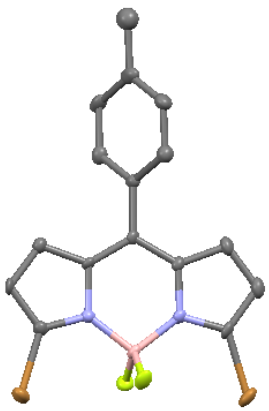

Figure 2.19: Molecular structure of 3,5-dibromoBODIPY **2.56a**, confirming the bromination reaction occurred at positions 3 and 5. Hydrogen atoms have been omitted for clarity.

Suzuki coupling to form compound **2.48a** was accomplished using conditions reported by Hao for related compounds.[56] The 3,5-dibromo-BODIPY **2.56a** was treated with 3 equivalents of 2-methoxybenzeneboronic acid in toluene in the presence of $Pd(PPh_3)_4$ as catalyst and Na_2CO_3, under reflux for 4 h (Scheme 2.34). The crude material was purified using column chromatography. The diarylated BODIPY **2.48a** was generated in high

yield (98%). The signal for the 6 protons of the two methoxy groups was observed as a singlet at 3.70 ppm in the ^{1}H NMR spectrum.

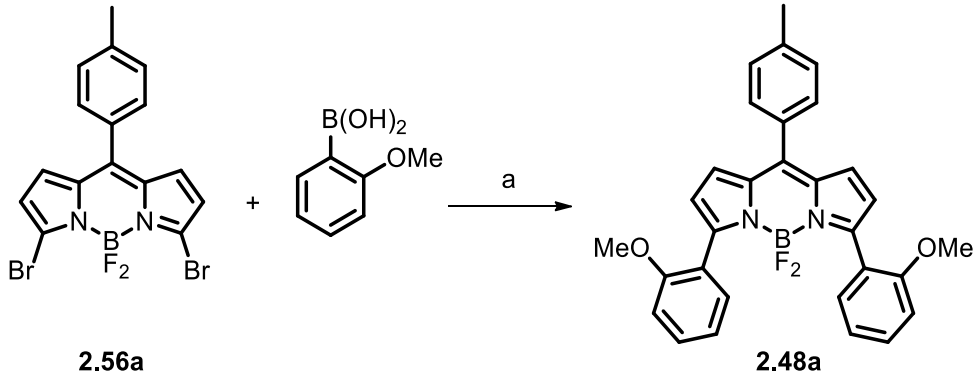

Scheme 2.34: Synthesis of symmetrical compound **2.48a**. Conditions and reagents: a) 2-methoxybenzeneboronic acid (3 eq), $Pd(PPh_3)_4$ (5 mol%), Na_2CO_3 (4 eq), toluene, 4 h, reflux, 98%.

Following Kung's procedure,[77] double demethylation of the aryl ether **2.48a** was accomplished by treatment with 10 equivalents of BBr_3. The crude product was purified using column chromatography to give **2.49a** as a dark red solid. The ^{1}H NMR spectrum of this novel compound showed loss of the signal corresponding to the two methoxy groups.

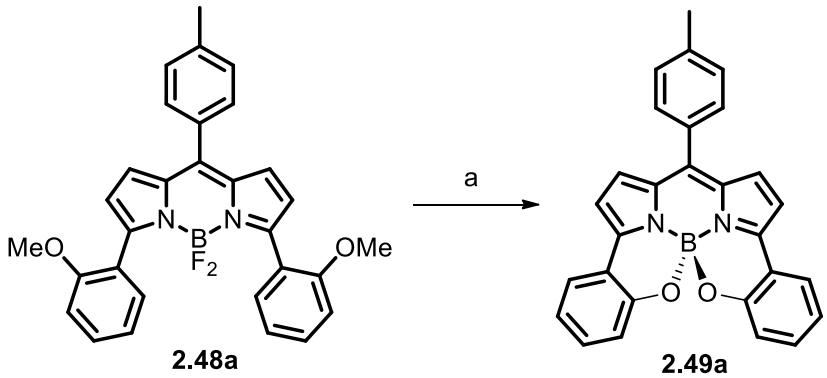

Scheme 2.35: Synthesis of *N,N,O,O*-BODIPY **2.49a**. Conditions and reagents: BBr_3 (10 eq), CH_2Cl_2, r.t., 5 h, 96%.

Crystals of **2.49a** were obtained by slow evaporation from a mixture of chloroform and hexane (1:3). The X-ray crystal structure reveals significant twisting of the *N,N,O,O*-BODIPY **2.49a**; the twist angle between the planes defined by the two pyrrolic rings is 9.8°. The O-B-O angle is 107.91°, but the N1-B-O2 and N2-B-O1 angles are 115.06 and 115.11°, respectively. However, the N-B-N angle is 105.53° which is pinched inward.

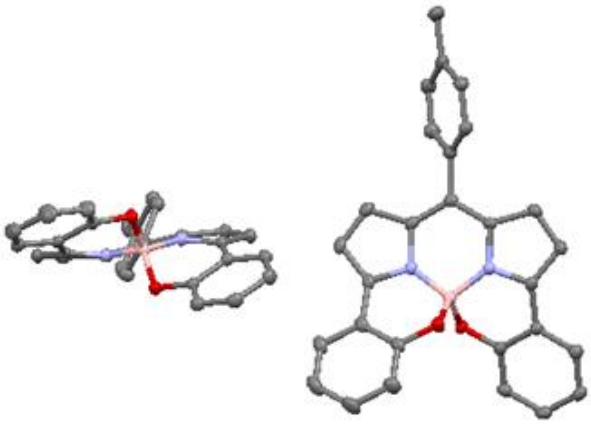

Figure 2.20: Two views of one molecule in the molecular structure of *N,N,O,O*-BODIPY **2.49a** showing the helical chirality of the molecule. Hydrogen atoms have been omitted for clarity.

The preparation of *N,N,O,O*-BODIPY **2.49a** succeeded in a good yield. However, this compound has no functional group which could interact with a chiral molecule. Substitution at the pyrrolic positions is more difficult than functionalization at the meso position which can be achieved simply by acid catalysed condensation of pyrrole with suitably substituted acyl chlorides or aryl aldehydes.

We decided to attach a 2-pyridyl group at the meso-position by using an activated 2-picolinic acid derivative or pyridine 2-carboxaldehyde to form *N,N,O,O*-BODIPY **2.49b**. The two enantiomers of the chiral 2-pyridyl substituted BODIPY **2.49b** might be resolved by crystallization of diastereoisomeric salts formed using an enantiopure chiral acid, or simply by chiral HPLC.

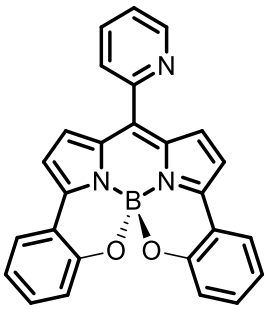

2.49b

Following the success in preparing helically chiral *N,N,O,O*-BODIPY **2.49a** through our developed synthetic route, we decided to apply a similar approach to form *N,N,O,O*-BODIPY **2.49b**.

Condensation of picolinaldehyde **2.53b** with pyrrole proceeded to give the corresponding dipyrromethane **2.54b** in a good yield (62%) (Scheme 2.36).

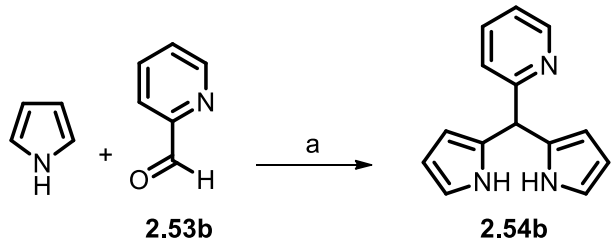

Scheme 2.36: Synthesis of symmetrical dipyrromethane **2.54b**. Conditions and reagents: a) Picolinaldehyde **2.53b** (1 eq), pyrrole (25 eq), $BF_3.OEt_2$ (10 mol%), r.t., 24 h., 62%.

As scheme 2.37 illustrates, 3,5-dibromo-8-(2-pyridyl)BODIPY **2.56b** was synthesized via the regioselective bromination at the 1 and 9 positions of dipyrromethane **2.54b** with *N*-bromosuccinimide to give 1,9-dibromo-5-(2-pyridyl)dipyrromethane **2.55b** in 76% yield. Then, the pure product was oxidized with DDQ at room temperature for an hour and this was followed by BF_2 chelation with *N*,*N*-diisopropylethylamine (i-Pr_2NEt) and boron trifluoride diethyl etherate ($BF_3.OEt_2$) to produce symmetrical 3,5-dibromoBODIPY **2.56b**.

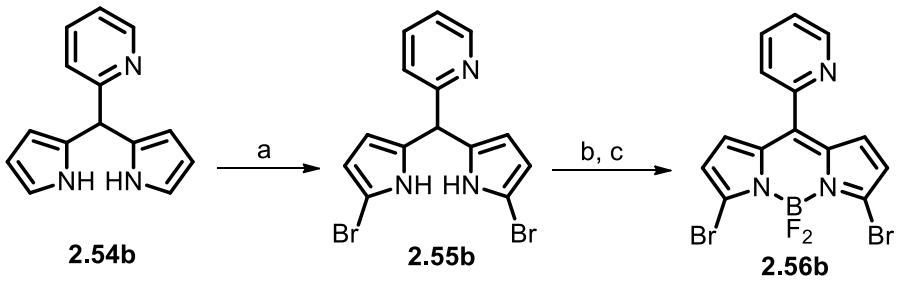

Scheme 2.37: Synthesis of symmetrical 3,5 dibromoBODIPY **2.56b**. Conditions and reagents: a) NBS (2 eq), THF, -78℃, 1 h, 76%; b) DDQ (1 eq), toluene, 1 h, r.t; c) i-Pr_2NEt (7 eq), $BF_3.OEt_2$ (7 eq), r.t., 31 h, 50%.

3,5-Bis(2-methoxyphenyl) BODIPY **2.48b** was synthesized via Suzuki coupling reaction. Initially, 3,5-dibromo BODIPY **2.56b** was treated with 2-methoxybenzeneboronic acid in the presence of $Pd(PPh_3)_4$, and Na_2CO_3 in water and toluene under reflux for 26 h. This resulted in unreacted 3,5-dibromo BODIPY **2.56b** and 2-methoxybenzeneboronic acid. Therefore, a different catalyst and reaction conditions were used. 2-Dicyclohexylphosphino-2',6'-dimethoxybiphenyl (S-Phos) was added to $Pd(OAc)_2$ in toluene at room temperature for 30 min. Three equivalents of 2-methoxybenzeneboronic acid, 3,5-dibromo BODIPY **2.56b** and four equivalents K_3PO_4

were added (Scheme 2.38). The reaction mixture was refluxed for 4 h, resulting in complete disappearance of the 3,5-dibromo BODIPY **2.56b**. The pink crude product was purified by column chromatography to give the product **2.48b** as pink solid in 81% (Scheme 2.38).

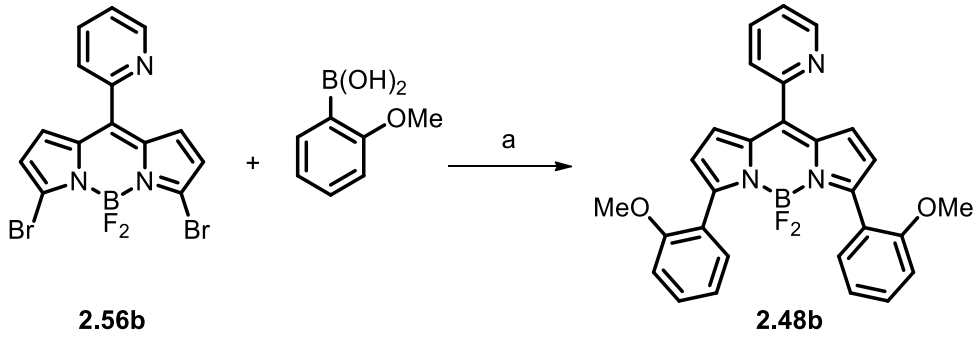

Scheme 2.38: Synthesis of symmetrical compound **2.48b**. Conditions and reagents: a) 2-methoxybenzeneboronic acid (3 eq), SPhos (12.5 mol%), $Pd(OAc)_2$ (5 mol%), K_3PO_4 (4 eq), toluene, 4 h, reflux, 81%.

Finally, double demethylation of the aryl ether **2.48b** was accomplished by treatment with excess of BBr_3 (Scheme 2.39). The crude product was purified using column chromatography to give **2.49b** as a dark red solid in 60% yield.

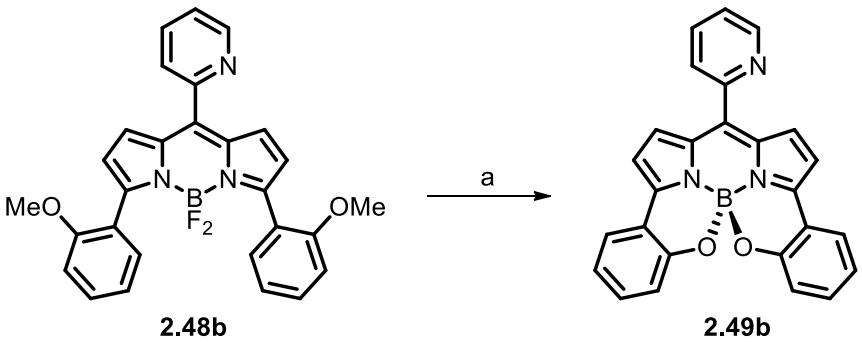

Scheme 2.39: Synthesis of *N,N,O,O*-BODIPY **2.49b**. Conditions and reagents: BBr_3 (10 eq), CH_2Cl_2, r.t., 5 h, 60%.

The final symmetrical *N,N,O,O*-BODIPY which was considered incorporates a lipophilic long-chain alkoxy substituent on the meso-aryl group (**2.49c**). Such a compound might be of use, for example, for selective incorporation into lipid layers or micelles. Condensation of 4-octyloxybenzaldehyde **2.53c** with pyrrole in presence of $BF_3.OEt_2$proceeded to give the corresponding dipyrromethane **2.54c** in high yield (89%) (Scheme 2.40).

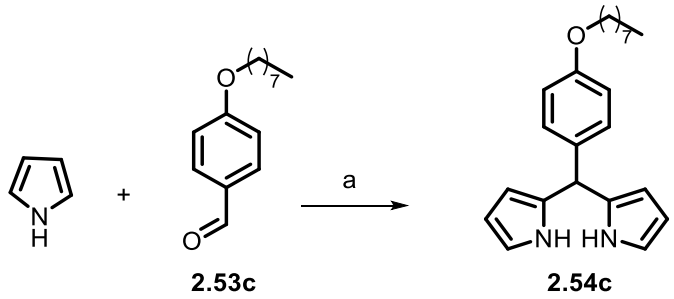

2.53c 2.54c

Scheme 2.40: Synthesis of symmetrical dipyrromethane **2.54c**. Conditions and reagents: a) 4-Octyloxybenzaldehyde **2.53c** (1 eq), pyrrole (25 eq), $BF_3.OEt_2$ (10 mol%), r.t., 24 h., 62%.

3,5-DibromoBODIPY **2.56c** was then synthesised in one-pot with no isolation of the intermediates. Dipyrromethane **2.45c** was treated with *N*-bromosuccinimide for 1 h, followed by oxidation with DDQ and then BF_2 chelation with boron trifluoride diethyl etherate ($BF_3.OEt_2$) in the presence of *N*,*N*-diisopropylethylamine (i-Pr_2NEt). Purification using column chromatography gave 3,5-dibromoBODIPY **2.56c** in 61% yield (Scheme 2.41).

The next task was Suzuki coupling reaction of the 3,5-dibromoBODIPY **2.56c** with 2-methoxybenzeneboronic acid. Buchwald[88] has reported the use of the palladacycle **3.54** in conjunction with the bulky, electron rich XPhos ligand for highly efficient Suzuki coupling reaction. The catalyst is activated via dissociation of chloride and reductive elimination of the carbocycle to produce the monoligated Pd(0)XPhos active catalyst.

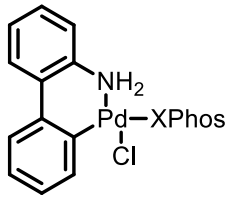

3.54

This catalyst was applied to the Suzuki coupling of dibromoBODIPY **2.56c**. The crude material was purified using column chromatography to generate BODIPY **2.48c** as a pink solid in 60%. Finally, double demethylation of the aryl ether **2.48c** was accomplished by treatment with 12 equivalents of BBr_3. The crude product was purified using column chromatography to give *N*,*N*,*O*,*O*-BODIPY **2.49c** as a dark red solid (Scheme 2.41).

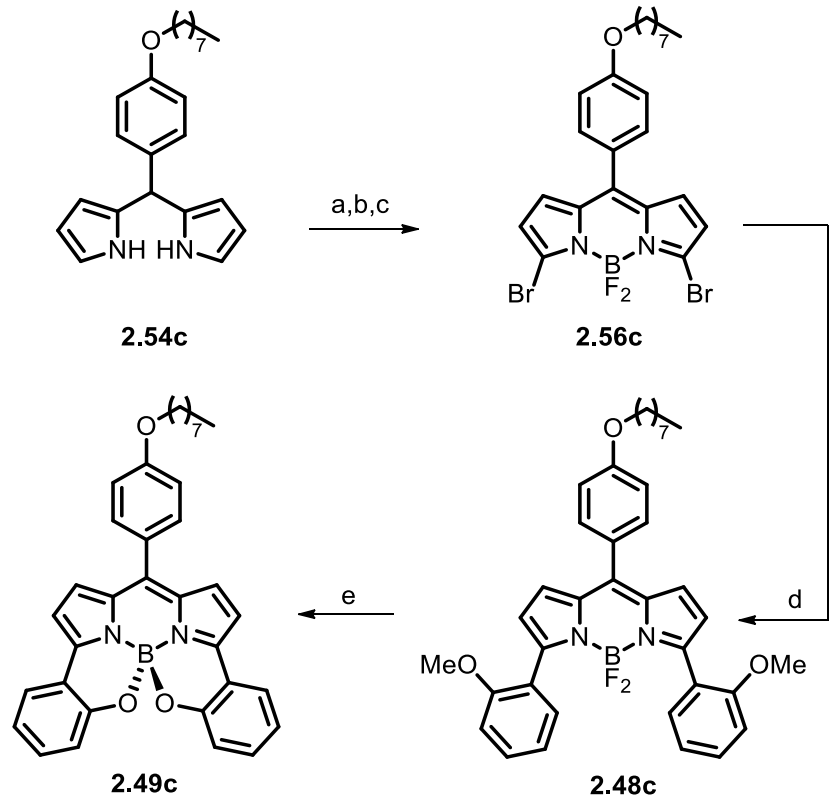

Scheme 2.41: Synthesis of *N,N,O,O*-BODIPY **2.49c**. Conditions and reagents: a) NBS (2.4 eq), THF, -78℃, 1 h; b) DDQ (1 eq), 1 h, r.t; c) i-Pr_2NEt (6 eq), BF_3.OEt_2 (8 eq), DCM, r.t., 3 h, 61%; d) 2-methoxybenzeneboronic acid (3 eq), LPd(XPhos)Cl **3.54** (5 mol%), K_3PO_4 (2 eq), THF-water, 6 h, reflux, 60%; e) BBr_3 (10 eq), CH_2Cl_2, 0℃ to r.t., 5 h, 67%.

In order to shorten the synthetic route, we examined different conditions to make *N,N,O,O*-BODIPY **2.49c** by performing the Suzuki reaction using 2-hydroxybenzeneboronic acid instaed of 2-methoxybenzeneboronic acid (Scheme 2.42). We hoped that the Suzuki coupling between 3,5-dibromoBODIPY **2.56c** and 2-hydroxybenzeneboronic acid might lead directly to the formation of the strapped BODIPY **2.49c**. This might happen by nucleophilic substitution of the two fluorine atoms with 2-hydroxyphenyl groups to form the chelated BODIPY **2.49c** with loss of HF.

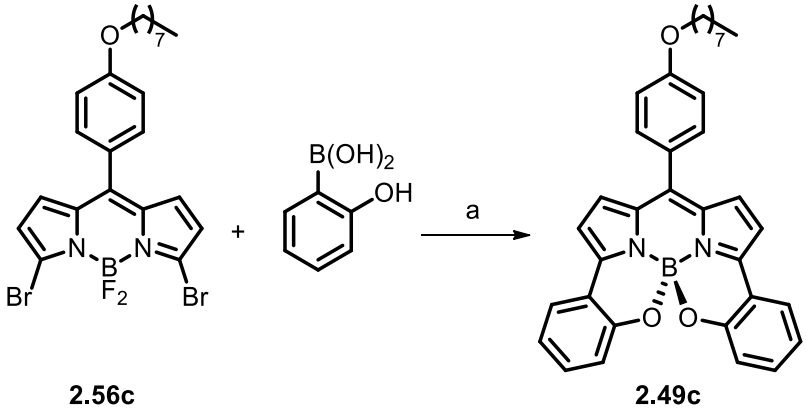

2.56c **2.49c**

Scheme 2.42: Attempted synthesis of *N,N,O,O*-BODIPY **2.49c**.a) 2-methoxybenzeneboronic acid (3 eq), LPd(XPhos)Cl **3.54** (5 mol%), K_3PO_4 (2 eq), THF-water, 6 h, reflux.

TLC analysis of the reaction indicated a mixture of the required product **2.49c** and a new material. Purification using column chromatography gave the desired strapped BODIPY **2.49c** as a minor product together with a major amount of a new purple product which was not completely purified. Attempts to further purify this material by crystallisation were not successful, probably as a result of the presence of a long alkyl chain. The ^{1}H NMR spectrum of this slightly impure purple compound showed 16 peaks corresponding to the aromatic protons which have different chemical shifts compared to the BODIPY **2.49c** (Figure 2.21). It is possible that the reaction between 3,5-dibromoBODIPY **2.56c** and 2-hydroxybenzeneboronic acid produced the *C,O*-coordinated BODIPY **2.49d** (Scheme 2.43). A similar reaction has been observed by Rebecca Clarke (Dr Hall's research group, Newcastle University) and in that case the product was confirmed by X-ray crystallography.

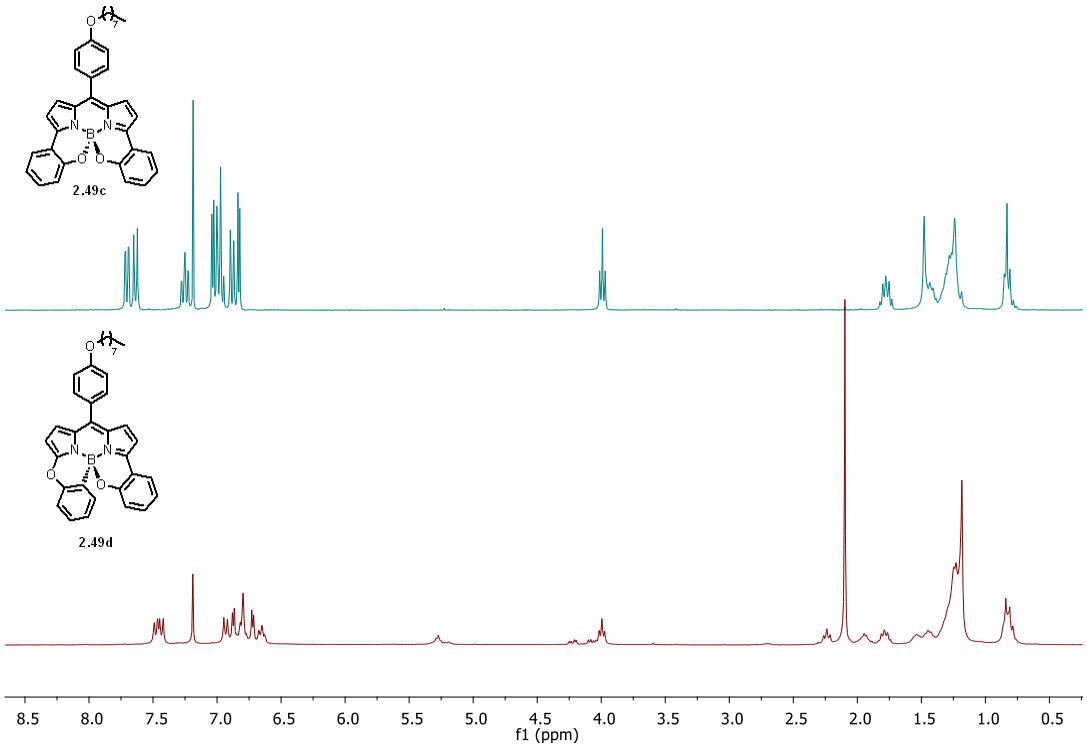

Figure 2.21: ^{1}H NMR spectra of *N,N,O,O*-BODIPY **2.49c** and BODIPY **2.49d**.

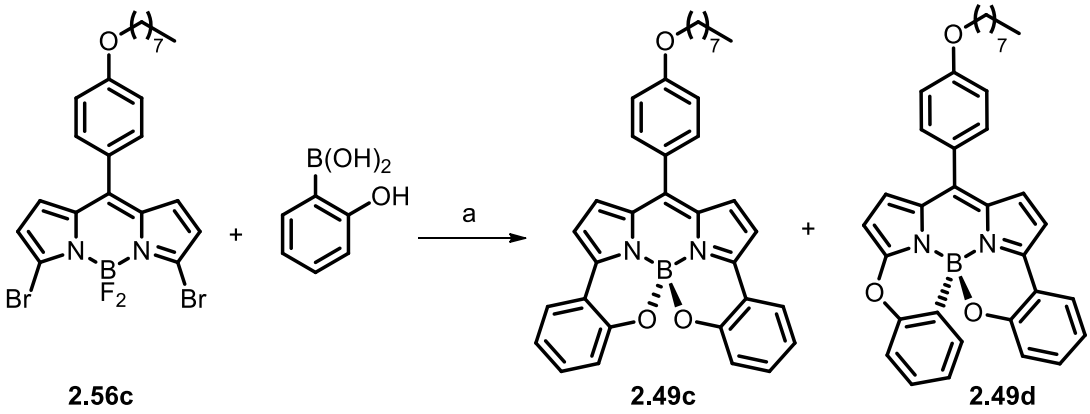

Scheme 2.43: Synthesis of *N,N,O,O*-BODIPY **2.49c** and possible co-product *N,N,O,C*-BODIPY **2.49d**.a) 2-methoxybenzeneboronic acid (3 eq), LPd(XPhos)Cl **3.54** (5 mol%), K_3PO_4 (2 eq), THF-water, 6 h, reflux.

The formation of *C,O*-coordinated BODIPY **2.49d** might occur via the mechanisms shown in (Scheme 2.44). In general, 3,5-halogenated BODIPY compounds are very reactive toward a nucleophilic substitution reaction. Therefore, the first step is mono-nucleophilic substitution between the dibromo BODIPY **2.56c** and 2-hydroxybenzeneboronic acid. In fact a second nucleophilic substitution reaction is usually

more difficult because the lone-pair of electrons of the 3-alkoxy group are delocalized into the aromatic π electron system which strongly reduces its electrophilicity.

The second step is Suzuki coupling reaction between mono-bromo BODIPY and the excess of 2-hydroxybenzeneboronic acid in presence of LPd(XPhos)Cl **3.54** and K_3PO_4. Finally, replacement of the BF_2 with the tethered boronic acid is consistent with the literature.[80] The last step is cyclisation with loss of water. Future work will investigate the optimised conditions for the synthesis of this type of *N*,*N*,*C*,*O*-BODIPY type.

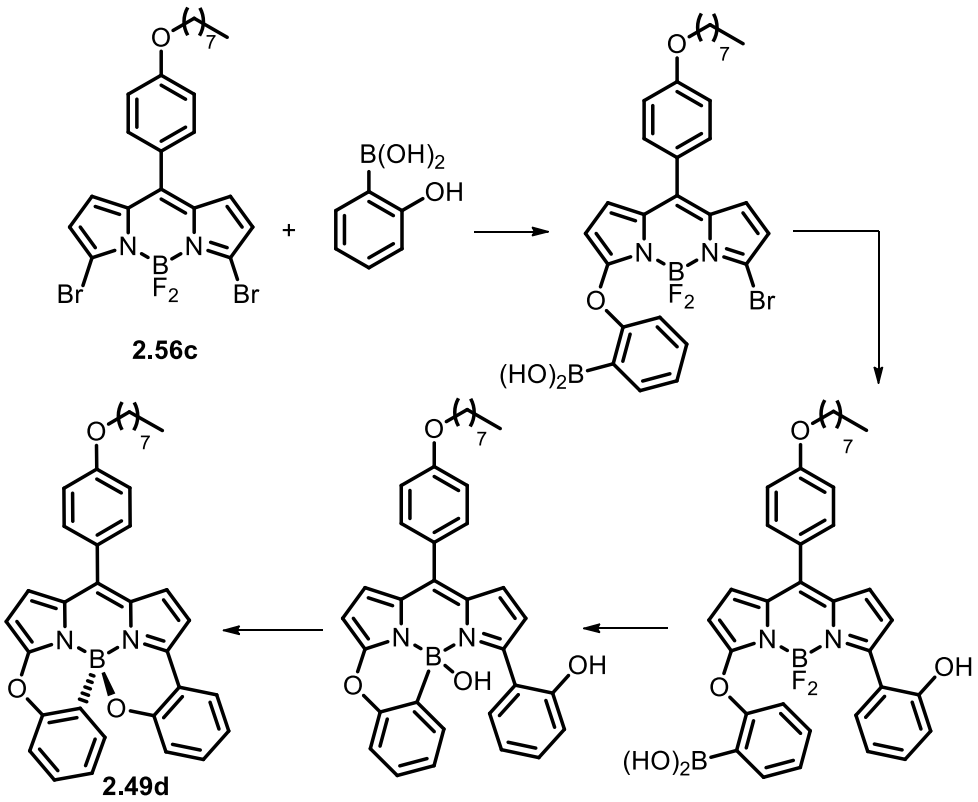

Scheme 2.44: Proposed mechanism of formation *N*,*N*,*O*,*C*-BODIPY **2.49d**.

2.3.2.2. Photophysical properties of helically chiral *N,N,O,O*-BODIPYs

2.3.2.2.1. UV Absorption and Fluorescence of the helically chiral *N,N,O,O*-BODIPYs

In reviewing the literature, the photophysical properties of helically chiral *N,N,O,O*-BODIPYs have been reported in detail.[77–83] All of the reported *N,N,O,O*-BODIPY derivatives show good to high fluorescence quantum yield and a red shift of the absorption and emission maxima in comparison to the corresponding *N,N*-BODIPY systems. A possible explanation for this might be due to the chelation of the bottom aryl rings which rigidifies the system and extends the conjugation. For comparison the photophysical properties for the novel parent BODIPY **2.48a** were measured (Table 2.3). As Figure 2.22 shows, the absorption and emission spectra are sharp and narrow bands.

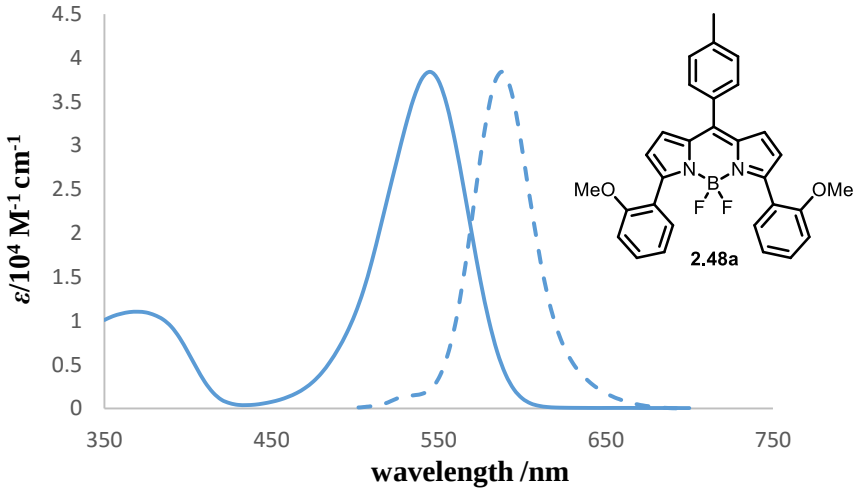

Figure 2.22: Absorption spectrum (solid line) in terms of the molar absorption coefficient (ε) and normalised fluorescence spectrum (hashed line) for BODIPY **2.48a**, recorded in $CHCl_3$ at room temperature, with an excitation wavelength of 500 nm.

The novel *N,N,O,O*-BODIPYs **2.49a, 2.49b** and **2.49c**, are red coloured and appear to be highly fluorescent under UV at 365 nm. The photophysical data, including absorption and fluorescence maxima, were collected for all three *N,N,O,O*-BODIPYs (Table 2.3). Mg[TPP] in toluene was used as the standard for measuring Φ_f. The absorption and emission spectra of *N,N,O,O*-BODIPYs **2.49a, 2.49b** and **2.49c** are represented in Figure 2.23.

Table 2.3: Absorption and fluorescence data for compounds **2.48a** and **2.49a-c**.[a]

No	8-Aryl group	λmax(abs)/ nm	λmax(em) [λex]/nm	$\varepsilon/10^4$ M^{-1} cm^{-1}	Φ_f[b]/ $CHCl_3$	Φ_f/ CH_3CN
2.48a	4-MeC_6H_4	545	588[490]	3.84	0.65	-
2.49a	4-MeC_6H_4	622	637[565]	4.00	0.56	0.52
2.49b	2-pyridyl	643	675[565]	2.82	0.26	0.28
2.49c	4-$OctOC_6H_4$	619	636[565]	6.34	0.48	-

a All values measured in $CHCl_3$. b Relative to Mg[TPP] (Φ_f= 0.15 , 565 nm, toluene).[89]

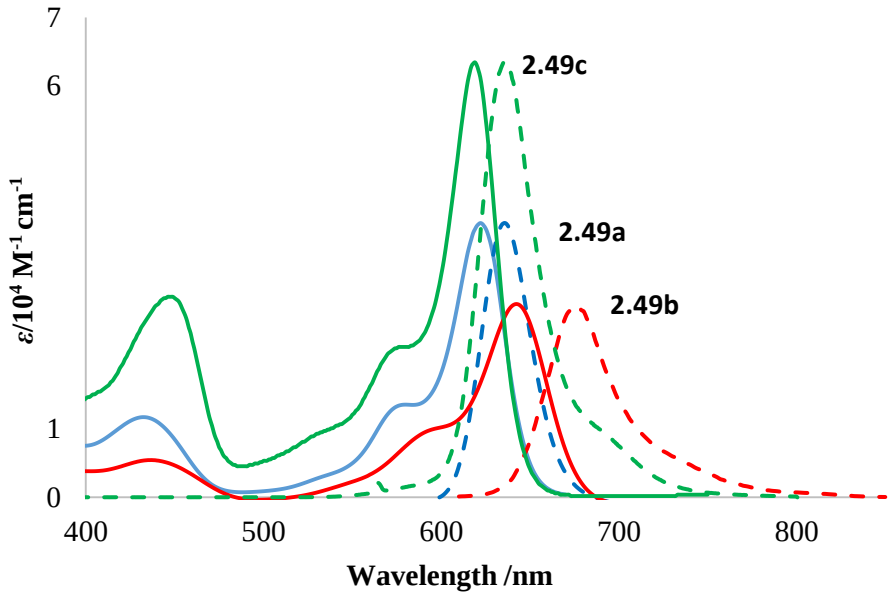

Figure 2.23: Absorption spectrum (solid lines) in terms of the molar absorption coefficient (ε) and normalised fluorescence spectrum (hashed lines) for **2.49a** (—), **2.49b** (—), and **2.49c** (—) in $CHCl_3$.

As Table 2.3 illustrates the low-energy maxima (*λ*abs) of **2.49a**, **2.49b** and **2.49c** are 622 nm, 643 and 619 nm respectively and all of these BODIPY dyes showed strong absorption bands. In comparison to the BODIPY **2.48a**, the chelation of the bottom aryl rings onto the BODIPY **2.49a** leads to red-shifts of both the absorption and emission maxima. The most significant shifts can be seen in the 2-pyridyl-substituted compound **2.49b** for which the absorption maximum is red shifted by 98 nm (2796 cm^{-1}) and the emission maximum by 87 nm (2192 cm^{-1}).

The helically chiral *N,N,O,O*-BODIPY **2.49a** was used as an example of this system for meausuring the excited-singlet state lifetime (τ). The excited-singlet state lifetime (τ) of BODIPY **2.49a** in 2-methyltetrahydrofuran (MTHF) at room temperature is 10 ns. It is interesting to note that the replacement of the two fluorine atoms with oxygen leads to a significant increase in the τ compared to BODIPYs **2.57**-**2.60**.[90,91] Moreover, strapping results in an unsually long lifetime for a BODIPY. The τ of **2.49a** was recorded by Patrycja Stachelek (Prof. A Harriman's group, Newcastle University).

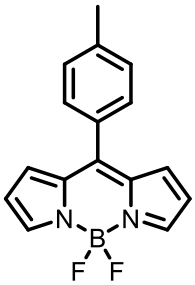

2.57

τ: 0.15 ns

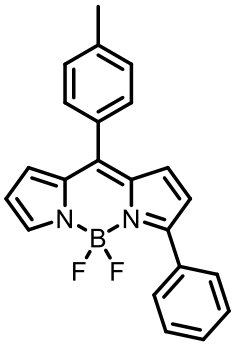

2.58

τ: 0.092 ns

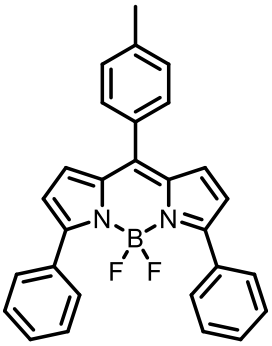

2.59

τ: 2.1 ns

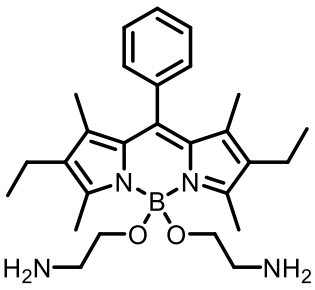

2.60

τ: 4.76 ns

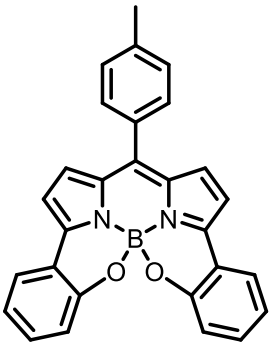

2.49a

τ: 10 ns

We decided to examine chiral HPLC as a method for resolution of the helically chiral BODIPY's **2.49a** and **2.49b**. Separation of **2.49a** by chiral HPLC using a Daicel Chiralcel OD-H column (25 cm × 0.46 cm); hexane:isopropanol (80:20) as the eluent gave two peaks in a 1:1 ratio confirming that **2.49a** was racemic (Figure 2.24).

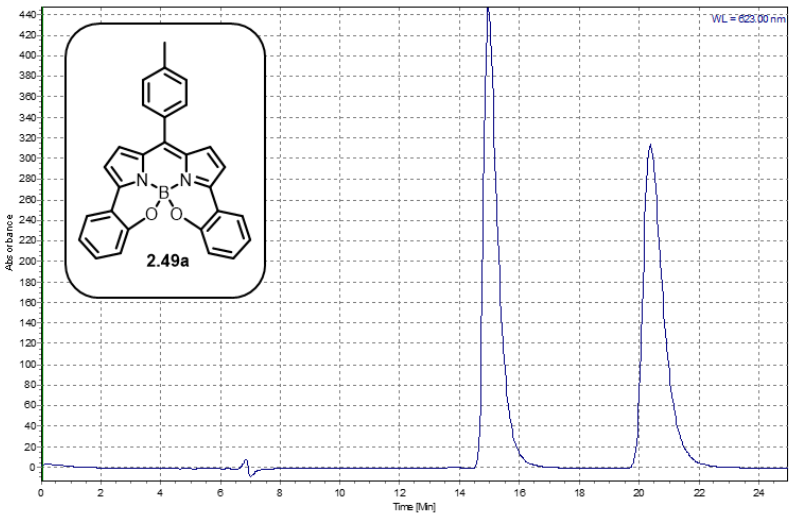

Figure 2.24: Chiral HPLC trace of **2.49a**. Daicel Chiralcel OD-H column (25 cm x 0.46 cm); hexane:isopropanol (80:20); 0.5 mL min^{-1}

Analysis of the helically chiral BODIPY **2.49b** under the same conditions gave similar HPLC trace. These results illustrated that the helically chiral BODIPYs were separable by chiral HPLC.

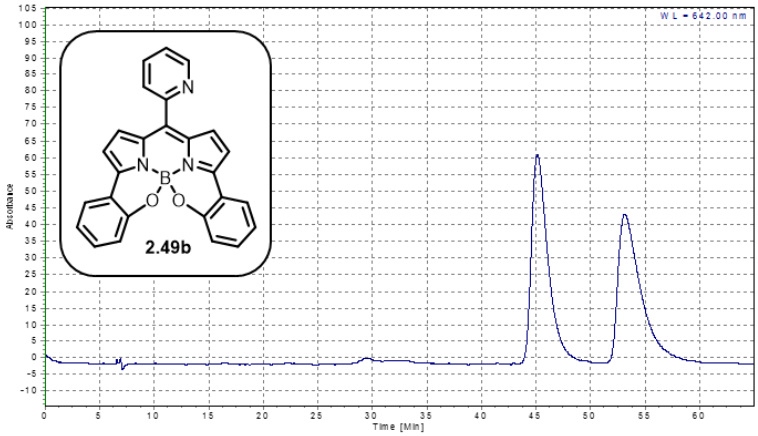

Figure 2.25: Chiral HPLC trace of **2.49b**. Daicel Chiralcel OD-H column (25 cm x 0.46 cm); hexane:isopropanol (80:20); 0.5 mL min^{-1}.

We succeeded in the separation of small amounts of the two enantiomers of BODIPYs **2.49a** and **2.49b** which were then used to examine their chiroptical properties.

2.3.2.3. Chiroptical properties of the helically chiral *N,N,O,O*-BODIPYs

The term chiroptical/chiroptic refers to optical techniques which use absorption, emission or refraction of anisotropic radiation for exploration of chiral substances.[92] There are several chiroptical techniques which can differentiate between the two enantiomers such as optical rotatory dispersion (ORD), circular dichroism (CD) and circular polarization of luminescence (CPL).[92–94]

2.3.2.3.1. Electronic Circular Dichroism (ECD) of the helically chiral *N,N,O,O*-BODIPYs.

Circular Dichroism (CD) is a spectroscopic technique which measures differences in the absorption of left and right handed circularly polarised light by a molecule which contains one or more chiral chromophores.[94]

After the resolution of **2.49a** and **2.49b** by chiral HPLC, the absorption spectra of the two enantiomers of **2.49a** and **2.49b** were recorded as shown in Figure 2.26. Then the two enantiomers of **2.49a** and **2.49b** were submitted to Electronic Circular Dichroism (ECD). Electronic circular dichroism (ECD) spectra of both (*M*) and (*P*) isomers of **2.49a** and **2.49b** were measured by Prof. W. Herrebout (University of Antwerp).

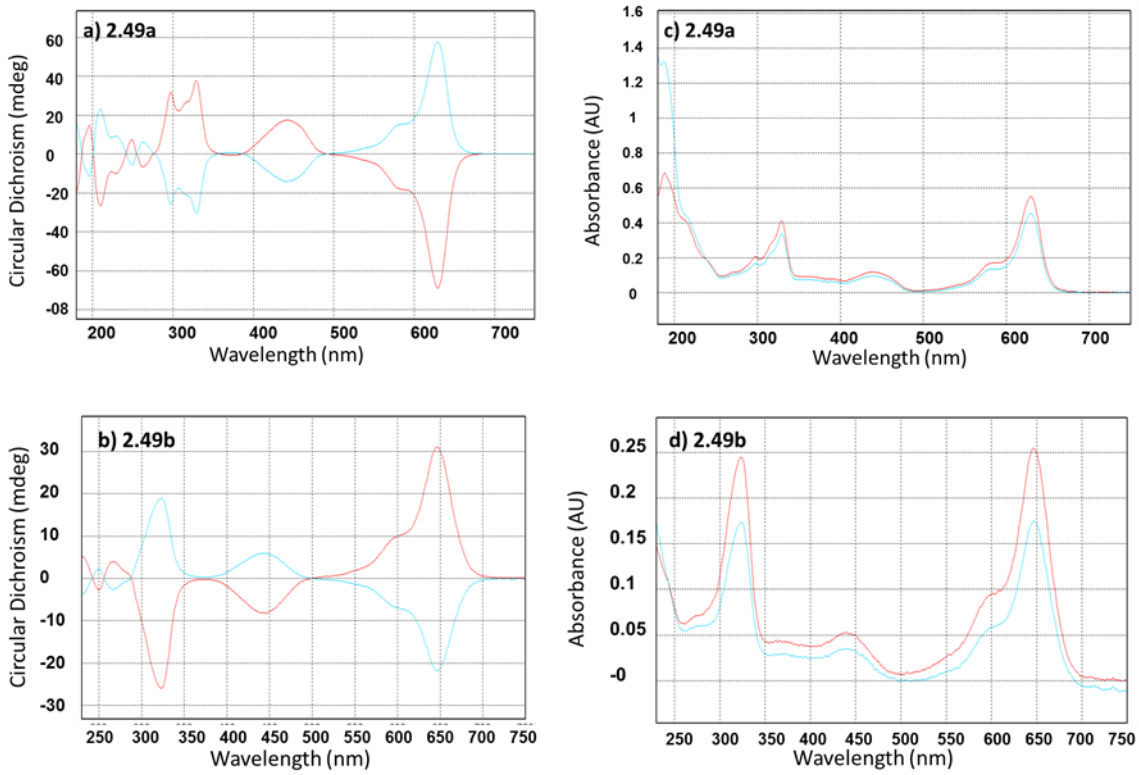

Figure 2.26: a) CD spectra of **(*P*)-2.49a** red (A) and **(*M*)-2.49a** cyan (B) after baseline correction; **b)** CD spectra of **(*P*)-2.49b** red (A) and **(*M*)-2.49b** cyan (B) after baseline correction**; c)** Absorbance spectra of **(*M*)-2.49a** red (A) and **(*P*)-2.49a** cyan (B) [hexane]; **d)** Absorbance spectra of **(*M*)-2.49b** red (A) and **(*P*)-2.49b** cyan (B) [$CHCl_3$] after baseline correction.

Electronic circular dichroism (ECD) spectra were measured of both (*M*) and (*P*) isomers of **2.49a** and **2.49b** in hexane or chloroform as appropriate at 20℃ for ~5.5 to 6 minutes, by using an Applied Photophysics Ltd. Chirascan-plus spectrometer. In each case mirror image ECD spectra were obtained from the corresponding enantiomers and showed that (*M*) and (*P*) isomers of **2.49a** and **2.49b** are enantiomers. Also, the major peaks of the electronic circular dichroism (ECD) spectra aligned well with those of the absorption spectra (Figure 2.27).

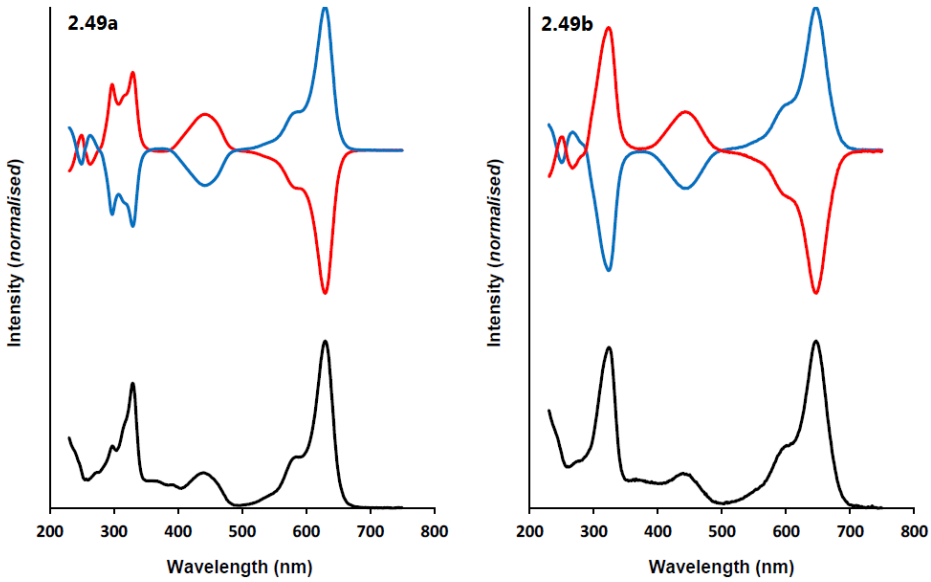

Figure 2.27: Normalised ECD (red and blue) and UV−vis absorption spectra (black): (**2.49a**) (*M*)-**2.49a** (red) and (*P*)-**2.49a** (blue) [hexane], (**2.49b**) (*M*)- **2.49b** (red) and (*P*)- **2.49b** (blue) [$CHCl_3$].

Boltzmann weighted ECD spectra, for samples **(*P*)-2.49(a-b)** were calculated (Figure 2.28) to determine the absolute configuration to the resolved enantiomers of **2.49a-b**. The agreement between experimental and calculated ECD allowed the absolute configuration of each of the enantiomeric samples of **2.49a-b** to be established. Calculation were performed by Prof. W. Herrebout (University of Antwerp).

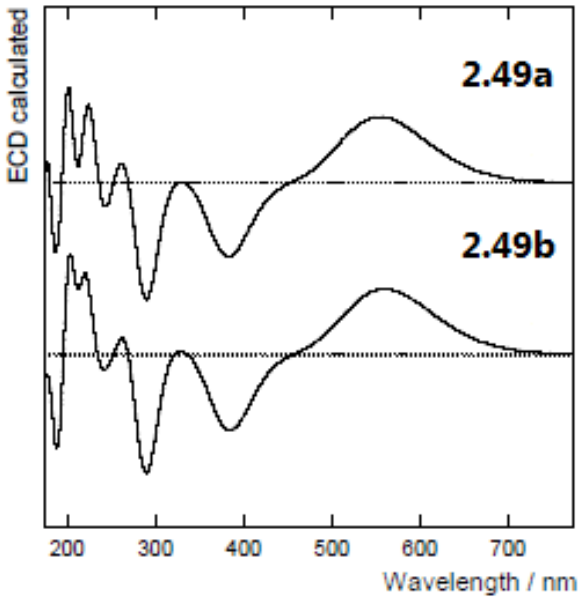

Figure 2.28: Calculated ECD spectra of **(*P*)-2.49a** and **(*P*)-2.49b**.

2.3.2.3.2. Circular Polarization of Luminescence (CPL) of the helically chiral *N,N,O,O*-BODIPYs

Circularly polarized luminescence (CPL) is a spectroscopic technique which measures differences in the emission of left and right handed circularly polarised radiation by chiral luminescent systems.[92,93] The magnitude of CPL is measured by the luminescence dissymmetry factor $g_{lum} = 2(I_L - I_R)/(I_L + I_R)$, where I_L and I_R the luminescence intensities of left and right circularly polarized components, respectively.[92,93]

In recent years, the interest in CPL has grown due to its use as a valuable source of information on the geometry of the excited state and also its application in the development and improvement of numerous photonic tools, such as display devices including optical storage and processing system, 3D optical displays, spintronics-based devices, CPL lasers, security tags, biological probes and signatures and enantioselective CPL sensors.[95]

The circularly polarized luminescence (CPL) of helically chiral *N,N,O,O*-BODIPY systems has not been reported. The CPL spectra of both (*M*) and (*P*) isomers of **2.49a** and **2.49b** were recorded by Prof. R. D. Peacock (University of Glasgow). The CPL was performed by using a home built instrument constructed around a Fluoromax 2. The CPL spectra were recorded of both (*M*) and (*P*) isomers of **2.49a** and **2.49b** in MeCN and excited at 540 nm. As is evident from Figure 2.29, it can be seen that both (*M*) and (*P*) isomers of **2.49a** and **2.49b** show mirror-image CPL and also show maxima matching the maximum visible emission of the *N,N,O,O*-BODIPYs. The spectra are an average of five scans. As is common for reports of the CPL spectra of most transition-metal and chiral organic chromophores, the solid line in the CPL plot is drawn to show the luminescence spectral line shape (Figure 2.29). The $|g_{lum}|$ of **2.49a** at 637 nm is 0.0043 and for **2.49b** at 675 nm is 0.0042, which is in the range of most CPL compounds from 10^{-5} to 10^{-2}.[96–98] The $|g_{lum}|$ values for these compounds include the largest so far reported for a simple BODIPY fluorophore in solution.

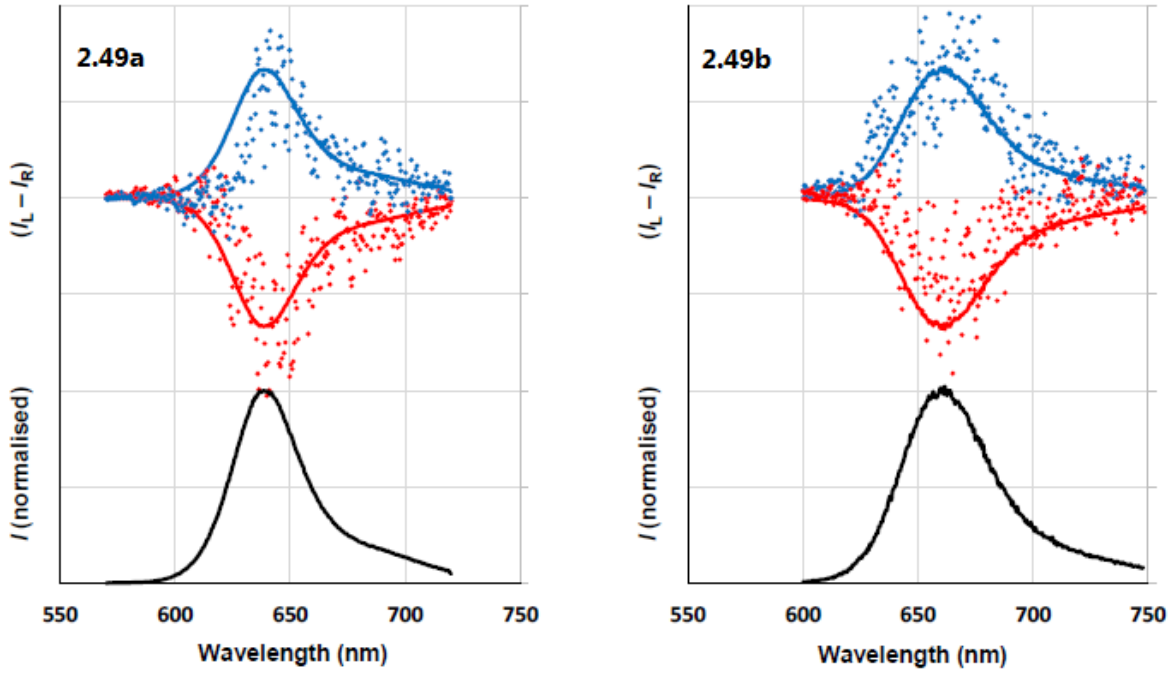

Figure 2.29: Normalised CPL spectra (red and blue) and normalised fluorescence spectra (black) shown (MeCN, excitation 540 nm): (**2.49a**) (*M*)-**2.49a** (red) and (*P*)- **2.49a** (blue), (**2.49b**) (*M*)- **2.49b** (red) and (*P*)- **2.49b** (blue).

We have successfully synthesised helically chiral *N*,*N*,*O*,*O*-BODIPY **2.49a-b** and measured their absorption, emission, molar absorption coefficient and quantum yield ϕ_F. We also succeeded in the separation of the two enantiomers of BODIPYs **2.49a** and **2.49b** by chiral HPLC and recorded the ECD and CPL spectra. Next we turned our attention to the synthesis of a new helically chiral *N*,*N*,*N*,*N*-BODIPY **2.63**.

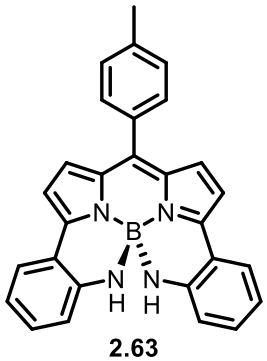

2.63

2.3.3. Approaches to helically chiral *N,N,N,N*-BODIPY dyes.

Up to now, the synthesis of helically chiral *N,N,N,N*-BODIPYs has not been reported. Formation of the *N*-B chelated product might cause significant effects on the position of the absorption and emission maxima. Therefore, we decided to synthesise the helically chiral *N,N,N,N*-BODIPY **2.63** as an example of this novel system. Also, we aimed to study the photophysical properties of this new system in order to understand the effect of *N*-*N* chelation on the BODIPY core.

We have designed a synthetic route for *N,N,N,N*-BODIPYs as shown in Scheme 2.45. Suzuki coupling of a 3,5-dibromoBODIPY **2.56a** with 2-nitrophenylboronic acid, followed by hydrogenation and then fluorine replacement affords *N*-chelated BODIPYs. The two enantiomers of the helical chiral *N,N,N,N*-BODIPYs might be resolved by chiral HPLC in the same way as the corresponding *N,N,O,O*-chelated system.

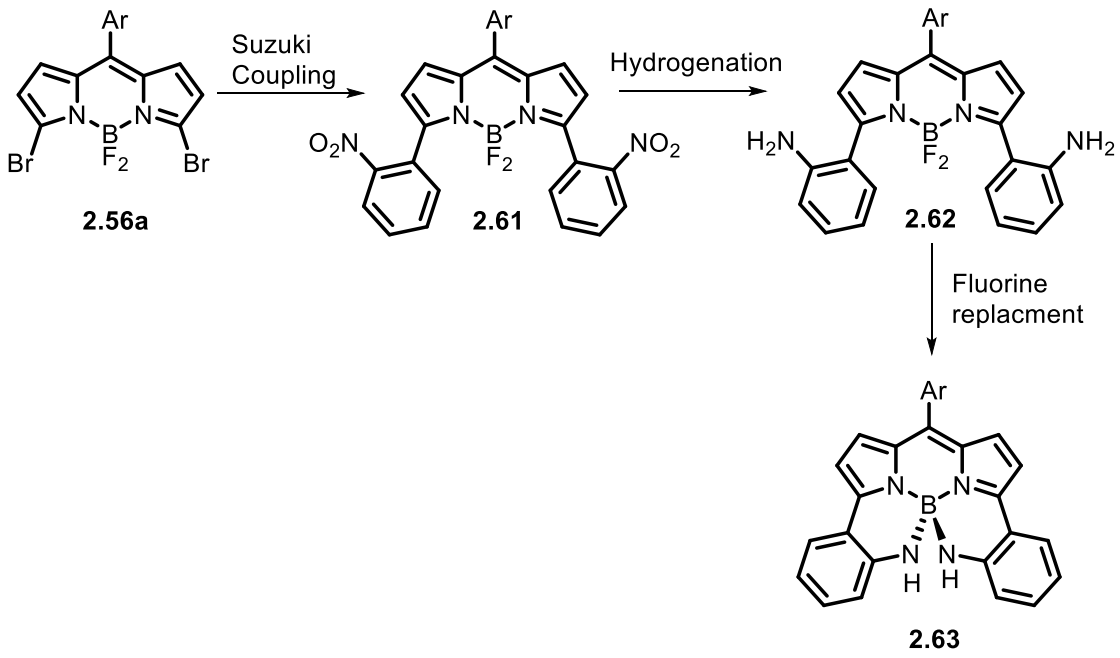

Scheme 2.45: General synthetic approach for the synthesis of helically chiral *N,N,N,N*-BODIPYs.

Suzuki coupling reaction to form compound **2.61** was accomplished by treatment of 3.5-dibromo-BODIPY **2.56a** with 3 equivalents of 2-nitrobenzeneboronic acid in THF and water in the presence of the cyclometalated catalyst precursor LPd(XPhos)Cl **3.54** (Scheme 2.46). The crude material was purified using column chromatography to generate BODIPY **2.61** as a dark orange solid in 75%.

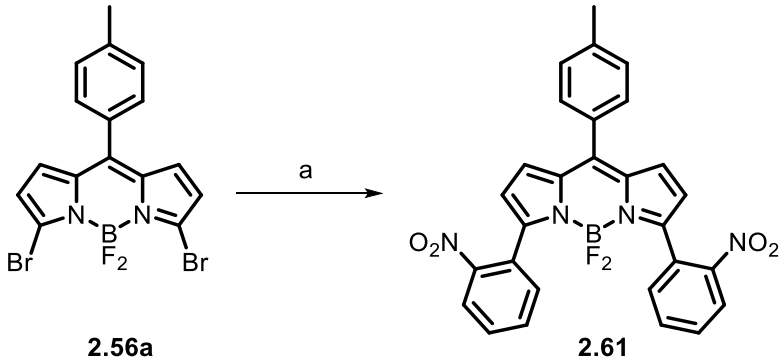

2.56a **2.61**

Scheme 2.46: Synthesis of symmetrical compound **2.61**. Conditions and reagents: a) 2-nitrobenzeneboronic acid (3 eq), LPd(XPhos)Cl **3.54** (5 mol%), K_3PO_4 (4 eq), THF-water, 6 h, reflux, 75%.

Hydrogenation of the nitroaryl-BODIPY **2.61** by using Pd/C and H_2 in DCM and MeOH for 2 h at room temperature produced the BODIPY **2.62** as a dark purple solid in high yield (80%) (Scheme 2.47).

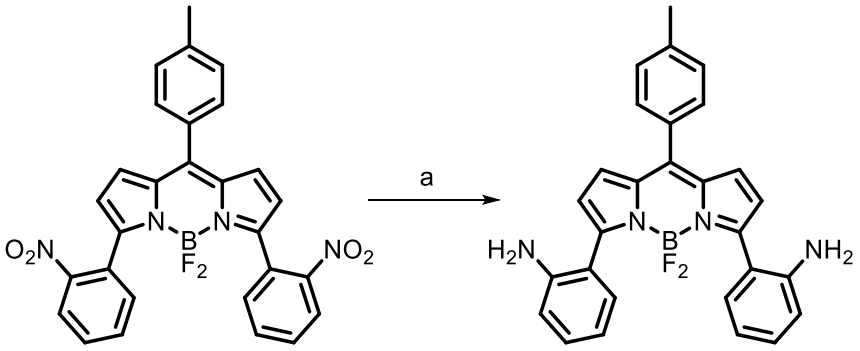

2.61 **2.62**

Scheme 2.47: Synthesis of BODIPY **2.62**. Conditions and reagents: a) H_2 (1 atm), 10% Pd/C, MeOH-CH_2Cl_2, r.t., 2 h (80%).

Our initial attempt to effect the replacement of the two fluorine atoms to give helically chiral *N,N,N,N*-BODIPY **2.63** involved treating BODIPY **2.62** with Cs_2CO_3 in 1,4-dioxane at 95℃ under nitrogen for 16 h (Scheme 2.48). After 4 hours, TLC of the reaction mixture indicated formation of a new compound together with starting material. After a further 12 h, however, the resulting mixture showed several spots on the TLC. The ^{1}H and ^{11}B NMR spectra of the crude product were complicated with no sign of the desired product. Unfortunately due to time constraints the synthesis of helically chiral *N,N,N,N*-BODIPY **2.63** was not completed. It is possible that the use of i-Pr_2NEt or even with $BF_3.OEt_2$might be more successful.

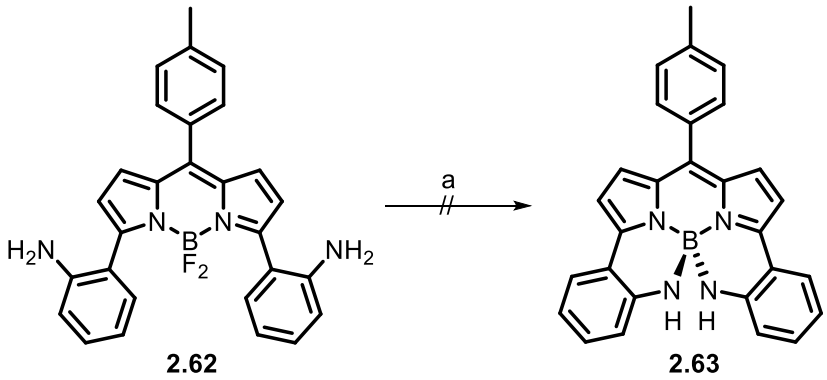

Scheme 2.48: Attempted synthesis of *N,N,N,N*-BODIPY **2.63**. Conditions and reagents: BODIPY **2.62** (0.100 mmol), Cs_2CO_3 (5 eq), 1,4-dioxane (2 mL), 95 ℃, 16 h.

2.3.4. Synthesis of half strapped *N,N,O,F*-BODIPY dyes

The previous section 2.3.2 has provided interesting results concerning the formation and separation of *N,N,O,O*-BODIPY derivatives. Next, we turned our attention to prepare `half strapped` *N,N,O,F*-BODIPYs which might be expected to have an emission wavelength less red-shifted a the previous *N,N,O,O*-BODIPYs. So far, very little attention has been paid to the synthesis of mono-strapped BODIPYs.[80,99–101]

An early example of this type of BODIPY was reported by Nabeshima[80] in 2009 when the free ligand **2.64** was treated with arylboronic acids to afford the half strapped BODIPYs **2.65a-c** (Scheme 2.49).

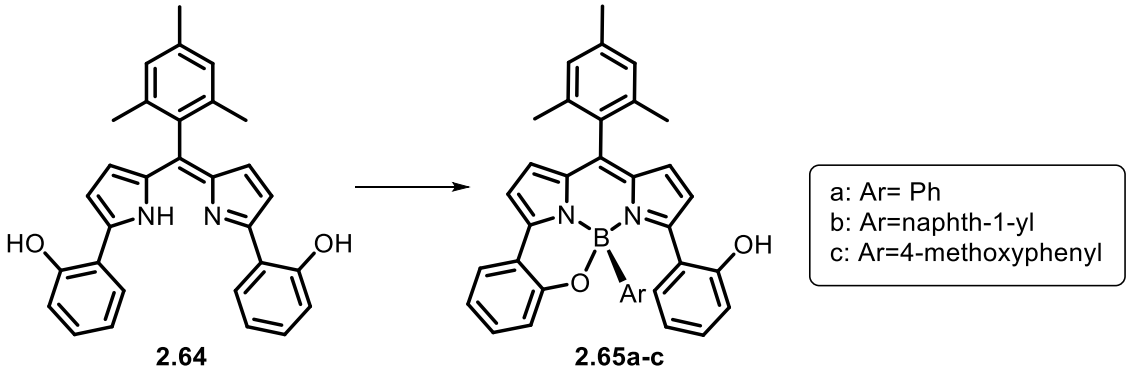

Scheme 2.49: Synthesis of *N,N,O,C*-BODIPY **2.65a-c**.[80]

Kovtun[60] reported a new method for synthesis of this type of BODIPY by treating 3-acetaldehyde BODIPY **2.66** with boron trifluoride diethyl etherate ($BF_3.OEt_2$) in toluene under reflux (Scheme 2.50). BODIPY **2.67** is presumably formed by trapping of the corresponding enol. The increase in conjugation, and the loss of HF may help to make the strapping favourable.

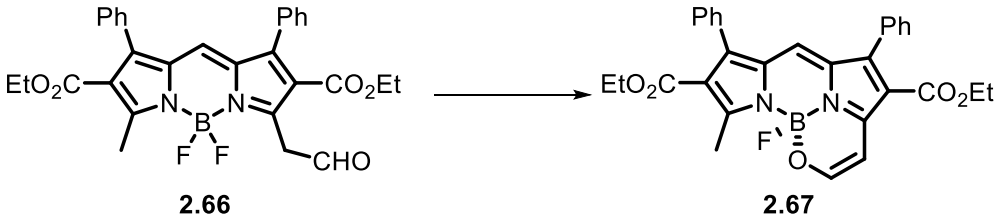

Scheme 2.50: Synthesis of *N,N,O,F*-BODIPY **2.67**.

Our target molecule was the *N,N,O,F*-BODIPY **2.74** which could not be prepared by following Kovtun's approach[60], nor using Nabeshima's approach[80]. The proposed synthetic route for *N,N,O,F*-BODIPYs is shown in Scheme 2.51.

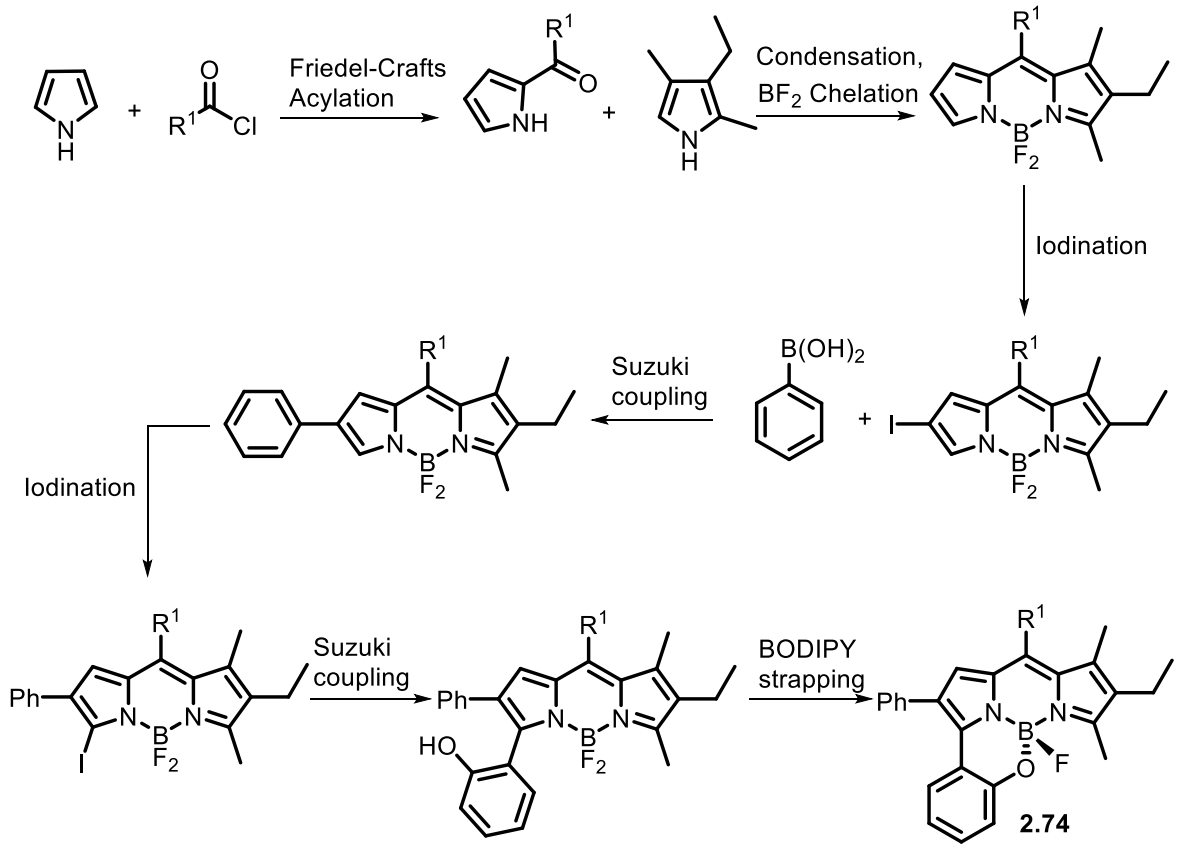

Scheme 2.51: General synthetic approach or the synthesis of *N,N,O,F*-BODIPYs **2.74**.

In 2013, Min Ji described an efficient solvent free procedure for preparing 2-acylpyrroles by using zinc oxide (ZnO) as an inexpensive and nontoxic Lewis acid catalyst.[102] Following this procedure, Friedel-Crafts acylation of pyrrole with p-toluoyl chloride or acetyl chloride in the presence of ZnO gave the ketone **2.67a-b** in 55 and 53% yield respectively (scheme 2.52).

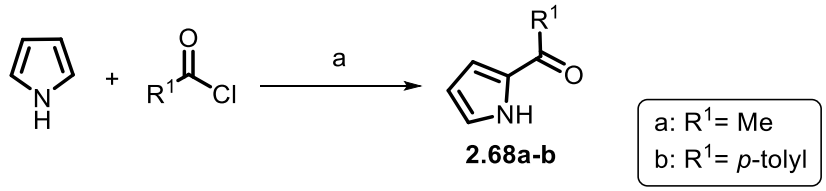

Scheme 2.52: Synthesis of 2-ketopyrrole **2.68a-b**. Conditions and reagents; a) ZnO (25 mol%), r.t., 5 min., **2.68a** 55% and **2.68b** 53%.

The next step was the BF_2 chelation of ketopyrrole **2.68a-b**. The condensation of the ketopyrrole **2.68a-b** with 3-ethyl-2,4-dimethylpyrrole in the presence of borontrifluoride diethyl etherate ($BF_3.OEt_2$) and Hünig's base (i-Pr_2NEt) produced the unsymmetrical BODIPYs **2.69a-b** (Scheme 2.53). This method has been reported in the synthesis of other BODIPY's previously.[103]

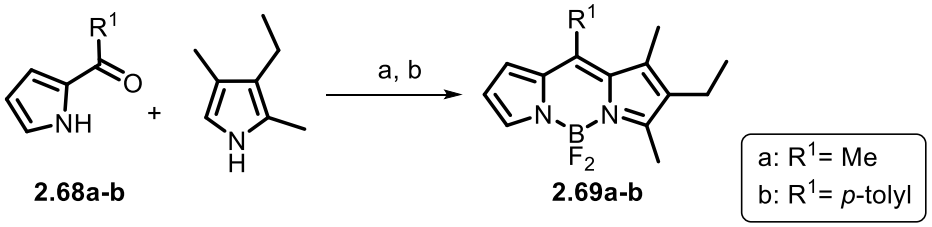

Scheme 2.53: Synthesis of unsymmetrical BODIPY **2.69a-b**. Conditions and reagents; a) 3-ethyl-2,4-dimethylpyrrole (1.1 eq), $BF_3.OEt_2$ (0.1 mol%), CH_2Cl_2, r.t., 1 h; b) $BF_3.OEt_2$ (8 eq), i-Pr_2NEt (1.1 eq), r.t., 16 h, **2.69a** 66% and **2.69b** 55%.

The regioselective iodination of the BODIPY **2.69a** will occur at the 2 position (as discussed in chapter 3).[56] The BODIPYs **2.69a-b** were treated with NIS in DCM for 16 h. The crude products were purified using column chromatography to give **2.70a-b** in good yield of 60 and 85% respectively (Scheme 2.54).

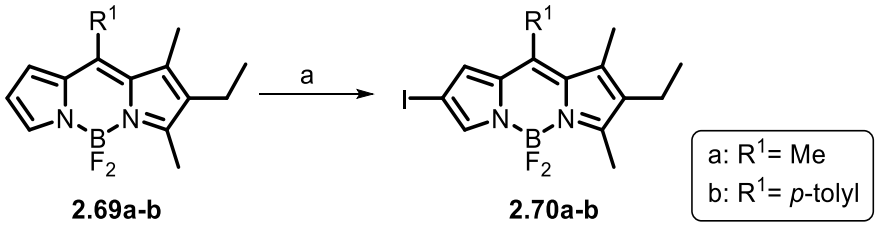

Scheme 2.54: Synthesis of 2-iodoBODIPY **2.70a-b**. Conditions and reagents; a) NIS (1.7 eq), CH_2Cl_2, r.t., 16 h, **2.70a** 60% and **2.70b** 85%.

The unsymmetrical BODIPY **2.71** was synthesised via palladium catalysed Suzuki cross coupling. In the first attempt, 2-iodoBODIPY **2.70a** was treated with phenylboronic acid (1.3 equivalents) in presence $Pd(PPh_3)_4$ (10 mol %) and Na_2CO_3 (2 equivalents) in toluene under reflux for 4 h to afford BODIPY **2.71** in low yield (25%). In the second attempt we used the highly efficient cyclometalated precatalyst Pd(Xphos)Cl[88] **3.54** and K_3PO_4 in THF and water under reflux for 16 h (Scheme 2.55). The crude product was purified using column chromatography to give **2.71** as red solid in high yield (83%) (Scheme 2.55).

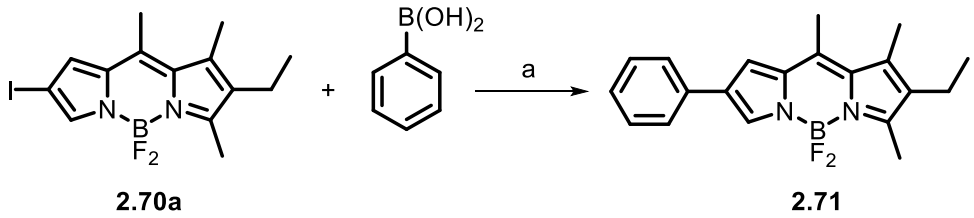

Scheme 2.55: Synthesis of unsymmetrical BODIPY **2.71**. Conditions and reagents; a) Phenylboronic acid (2 eq), LPd(XPhos)Cl **3.54** (2 mol%), K_3PO_4 (2 eq), THF-water, 16 h, reflux, 83%.

The structure of unsymmetrical BODIPY **2.71** was confirmed unambiguously by X-ray structure determination after crystal growth through slow diffusion of petroleum ether into a solution of the BODIPY in DCM (Figure 2.30).

Figure 2.30: Molecular structure of BODIPY **2.71**. Hydrogen atoms have been omitted for clarity.

To the unsymmetrical BODIPY **2.71** another regioselective iodination with NIS in DCM was completed, affording 3-iodoBODIPY **2.72** as a dark red solid in 78% yield (Scheme 2.56).

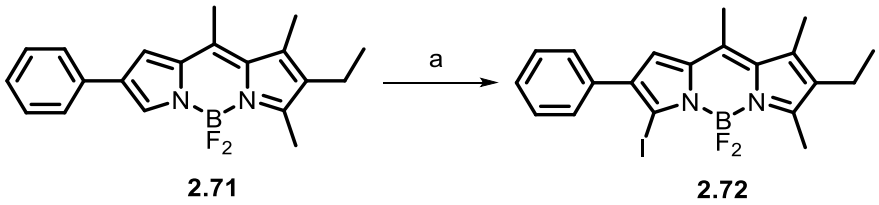

Scheme 2.56: Synthesis of 3-iodoBODIPY **2.72**. Conditions and reagents; a) NIS (1.3 equivalents), CH_2Cl_2, r.t., 16 h, 78%.

^{1}H NMR spectrum was used to determine that the reaction had been completed regioselectively. The ^{1}H NMR spectrum of the product showed the disappearance of one signal at 7.8 ppm which corresponds to the proton at the 3 position and the proton at the 1 position was shifted upfield upon incorporation of iodine.

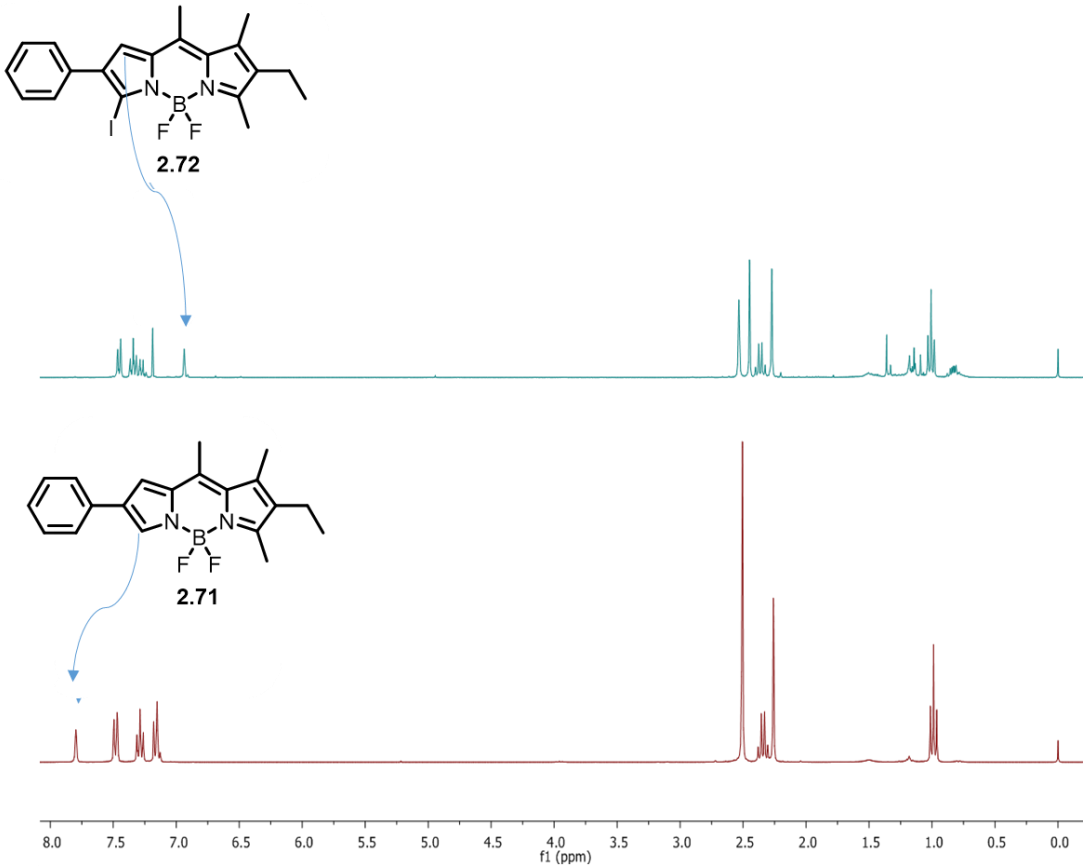

Figure 2.31: ^{1}H NMR spectra of 3-iodoBODIPY **2.72** and BODIPY **2.71**.

It was hoped that the second Suzuki coupling between the 3-iodoBODIPY **2.72** and 2-hydroxybenzeneboronic acid would lead to the formation of the half strapped BODIPY **2.74**. This might happen by nucleophilic substitution of one fluorine atom by the 2-hydroxyphenyl group with loss of HF. However, the resulting product from the second Suzuki coupling was actually the unstrapped BODIPY **2.73** as seen in Scheme 2.57.

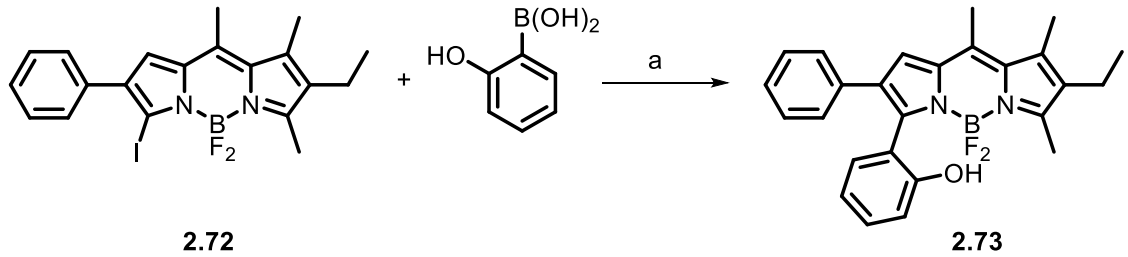

2.72 **2.73**

Scheme 2.57: Synthesis of unsymmetrical BODIPY **2.73**. Conditions and reagents; a) 2-Hydroxyphenylboronic acid (2 eq), LPd(XPhos)Cl **3.54** (2 mol%), K_3PO_4 (2 eq), THF-water, 16 h, reflux, 25%.

This was confirmed by ^{11}B NMR which shows a triplet peak at 0.58, this indicates that the core boron atom is still coupled to two fluorine atoms (Figure 2.32).

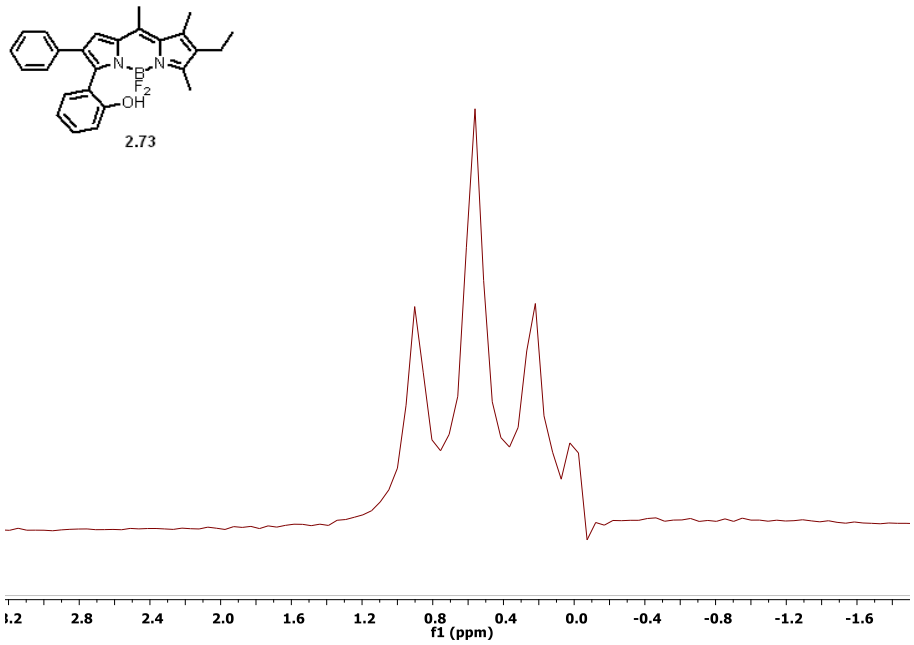

Figure 2.32: ^{11}B NMR spectrum of BODIPY **2.73** (96 MHz, $CDCl_3$).

What was surprising is that the ^{19}F NMR spectrum (Figure 2.33) shows two double quartet peaks. As explained earlier in this chapter, this pattern results from the fluorine atoms coupling to the boron atom and also coupling to each other. This implies that the two fluorine atoms are in different environments. The two different environment may be

formed because of steric hindrance around the BODIPY structure leading to restricted rotation around the pyrrole-phenol bond. Alternatively, it may be that a hydrogen-bond exists between the phenol OH group and one of the fluorine atoms, again restricting rotation.

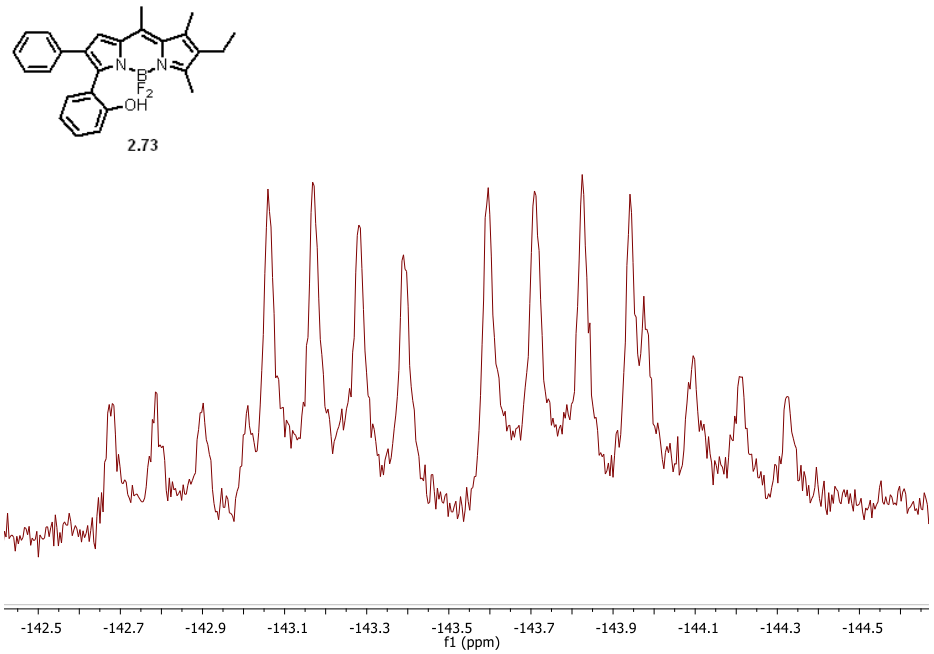

Figure 2.33: ^{19}F NMR spectrum of BODIPY **2.73** (282MHz, $CDCl_3$).

In order to prepare the half strapped BODIPY we followed Kovtun's method, as they formed a mono-strapped 3-enol BODIPY derivative using $BF_3.OEt_2$ in toluene. We first attempted the reaction on a very small scale in an NMR tube, following the progress by ^{11}B and ^{19}F NMR. The BODIPY **2.73** was dissolved in $CDCl_3$ and then once $BF_3.OEt_2$ was added the solution colour changed from orange to a deep red colour. The crude ^{11}B NMR and ^{19}F NMR spectra indicated the formation of the product, however, it appeared to decompose over time, and this may be due to the generation of HF. Therefore, in the second attempt we decided to add a base to prevent such acidic conditions from forming. The BODIPY **2.73** was treated with i-Pr_2NEt and then $BF_3.OEt_2$ in DCM (Scheme 2.58). The reaction was followed by TLC until disappearance of all the starting material. The crude product was purified using column chromatography to afford the strapped BODIPY **2.74** in 50% yield.

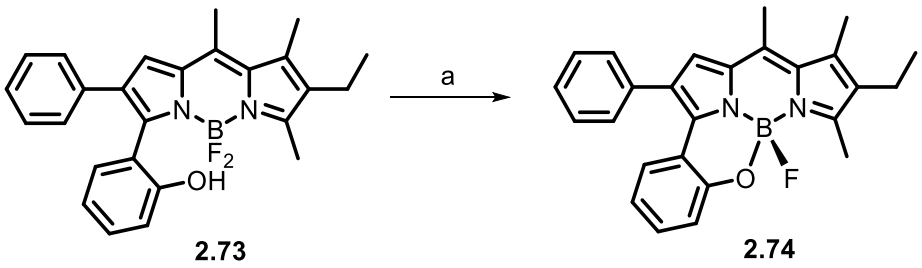

Scheme 2.58: Synthesis of half strapped BODIPY **2.74**. Conditions and reagents; a) i-Pr_2NEt (1 eq), $BF_3.OEt_2$ (1 eq), DCM, 10 min, reflux, 50%.

The ^{11}B NMR spectrum of the half strapped BODIPY **2.74** shows a doublet peak, this indicates that the core boron atom is coupled to one fluorine atom (Figure 2.34).

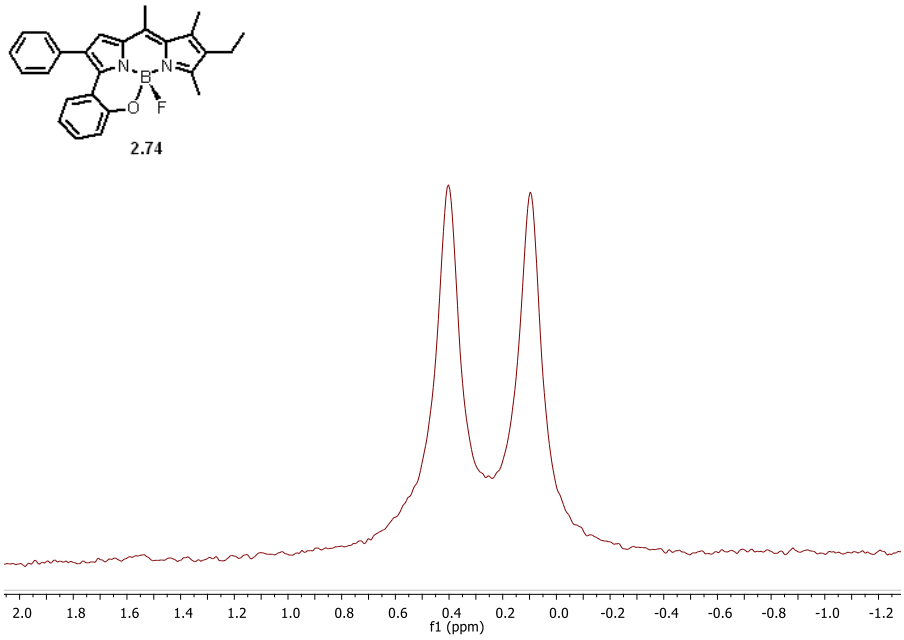

Figure 2.34: ^{11}B NMR spectrum of BODIPY **2.74** (160 MHz, $CDCl_3$).

2.3.4.1. Chiral HPLC Separation

Chiral HPLC separation of the two enantiomers of *N*,*N*,*F*,*O*-BODIPY **2.74** was investigated. HPLC of BODIPY **2.74** using a Daicel Chiralcel OD-H column (25 cm × 0.46 cm); hexane:isopropanol (80:20) as the eluent successfully produced two well resolved peaks as shown in Figure 2.35.

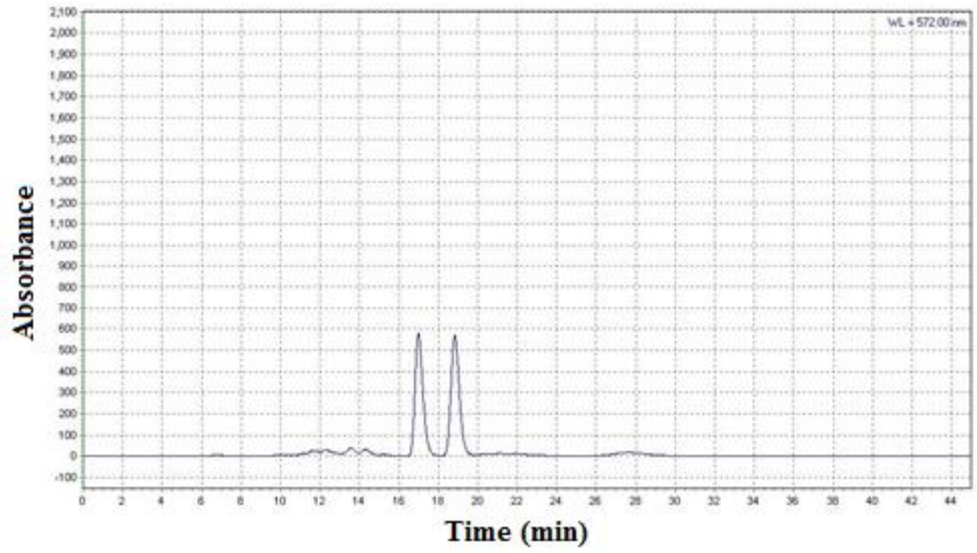

Figure 2.35: Chiral HPLC trace of **2.74**. Daicel Chiralcel OD-H column (25 cm x 0.46 cm); hexane:iso-propanol (80:20); 0.5 mL min^{-1}.

The chiral *N*,*N*,*F*,*O*-BODIPY **2.74** has been successfully synthesised through the use of our designed route. Unfortunately, due to time constraints and lack of material further spectroscopic analysis has not yet been performed.

2.3.4.2. Photophysical data of parent BODIPY 2.69a and BODIPY 2.73

The UV and fluorescence spectra were measured for BODIPY **2.69a** and **2.73** in $CHCl_3$ at room temperature (Table 2.4). Rhodamine 6G was used as the reference compound for determination of fluorescence quantum yields (rhodamine 6G $\Phi_{f=}$ 0.95, $\lambda_{ex=}$ 479 or 496 nm, in ethanol).

Table 2.4: Photophysical data of the selected BODIPYs in $CHCl_3$.

BODIPY	λ_{abs} (max)/nm	$\varepsilon/10^4$ $M^{-1}cm^{-1}$	λ_{em} (max)/nm	Φ_f (λ_{ex})
2.69a	502	4.59	515	0.55(479)
2.73	530	5.04	567	0.56(496)

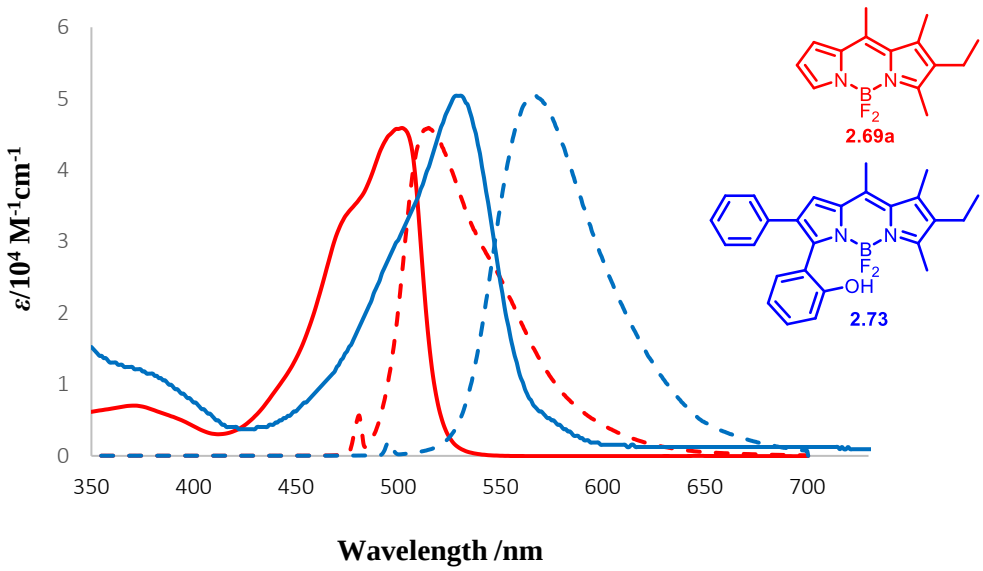

Figure 2.36: Absorption spectrum (solid lines) in terms of the molar absorption coefficient (ε) and normalised fluorescence spectrum (hashed lines) for **2.69a** (—), and **2.73** (—) in $CHCl_3$.

Figure 2.36 shows the absorption and emission spectra of parent BODIPY **2.69a** and of BODIPY **2.73**. As Table 2.4 illustrates both of these BODIPY dyes showed strong absorption bands. In comparison to the parent BODIPY **2.69a**, the presence of aromatic rings in both the 3- and 2-positions of the BODIPY core leads to a 28 nm (1053 cm^{-1}) red-shift of the absorption maximum and a 52 nm (1781 cm^{-1}) red-shift of the emission maximum. Future effort will involve synthesis of the *N,N,F,O*-BODIPY **2.74** on a larger scale, to measure the absorption and emission spectra and also to separate the two

enantiomers. Overall, these encouraging results indicate that the synthesis of activated chiral *N*,*N*,*F*,*O*-BODIPYs is worth investigated in the future.

2.4. Conclusion

The BODIPY system has come a long way from its initial discovery, and is now well established as a useful fluorophore. Many synthetic approaches and structural variations have been reported in literature. However, there are few reports of the use of chiral BODIPY species for enantioselective applications. During this research to synthesise functionalised chiral BODIPYs for enantioselective sensing we have disclosed a range of novel chiral systems.

The 2,6-bis(2-methoxyphenyl) BODIPY **2.6** was synthesized via Suzuki coupling reaction, by coupling of the corresponding 2,6-dibromo BODIPY with 2-methoxyphenyl boronic acid. ^{19}F NMR of the product indicated that a 1:1 mixture of diastereoisomers was formed, presumably corresponding to compounds in which the methoxy groups are either *syn*- or *anti*- to each other.

The axially chiral quinoline-BODIPY **2.15** has been successfully synthesised from readily available starting materials by regioselective monobromination at the 2-position of the BODIPY core. Suzuki coupling reaction gave the axially chiral quinoline-BODIPY **2.15**. However, all attempts separate the enantiomeric BODIPYs were unsuccessful.

The known aza-BODIPY compounds **2.25a, b** were synthesized successfully, nevertheless, attempts to synthesise more heavily functionalized aza-BODIPY **2.26** proved unsuccessful.

Helically chiral *N,N,O,O*-BODIPYs **2.49a-c** were synthesised using modular approach. These compounds showed very desirable spectral properties, such as high molar absorption coefficients and good quantum yields of fluorescence. The two enantiomers of **2.49a** and **2.49** were separated by chiral HPLC. The ECD spectra of the two enantiomers of BODIPYs **2.49a** and **2.49b** were recorded and in combination with computational modelling allowed the absolute configuration of each of the enantiomeric samples of **2.49a-b** to be established. Moreover, CPL spectra of each of the enantiomeric samples of **2.49a-b** were recorded.

We attempted to synthesise helically chiral *N,N,N,N*-BODIPY **2.63**, however, due to time constraints successful conditions for the final boron chelation step have yet to be identified.

Finally, the mono-strapped BODIPY scaffold **2.74** was synthesised and was analysed by ^{1}H, ^{11}B, ^{19}F NMR, all of which confirmed the correct product. Separation of *N,N,F,O*-BODIPY **2.74** by analytical chiral HPLC gave two peaks confirming that **2.74** was racemic. This indicated that the *N,N,F,O*-BODIPY **2.74** is separable by chiral HPLC.

Chapter 3: Synthesis of aminoBODIPYs via metal catalyzed amination

3.1. Introduction

It is perhaps not surprising that many electrophilic substitution reactions into the BODIPY core have been reported including halogenation,[56] sulfonation,[12] and nitration.[12] The synthesis of halogenated BODIPYs has been reported as a useful reaction which can be followed by various transition metal catalysed cross-coupling reactions or by nucleophilic substitution. The most common approach to introduce amine substituents on the BODIPY core is nucleophilic substitution (S_NAr) of a BODIPY carrying a good leaving group (e.g. methoxy, halogen, or methylthio).[6,104] A nucleophilic substitution (S_NAr) of a BODIPY can only occur in the 1, 3 ,5, 7 and 8 (meso) positions due to the electronic requirements of S_NAr.[104,105] As shown in Figure 3.1, a nucleophile can attack these positions to form an intermediate anion in which the negative charge may be delocalized on to one of the nitrogen atoms of the core BODIPY.[105] This may explain why there are few reports of 2-amino-substituted BODIPYs.

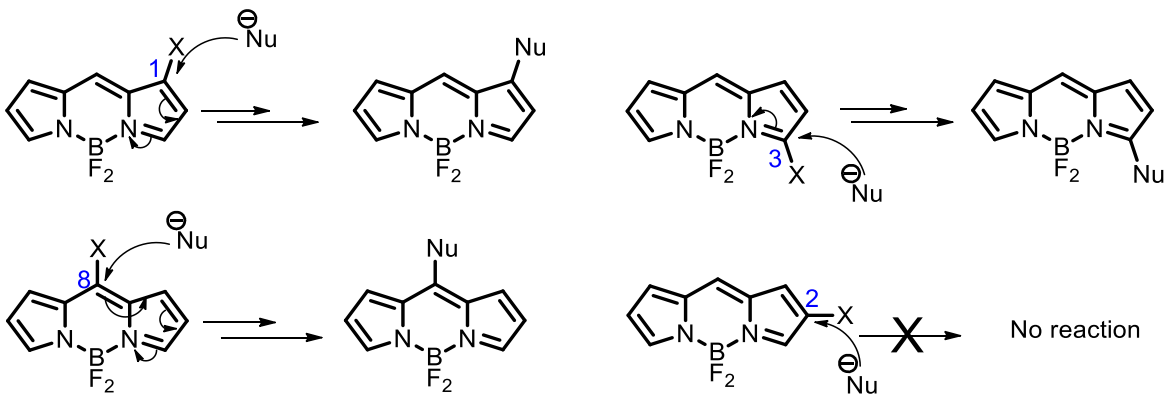

Figure 3.1: Nucleophilic substitution (S_NAr) at each portion of a BODIPY core.

Likewise, an unusual example of S_NAr, oxidative nucleophilic hydrogen substitution by amines, occurs in the electron poor 3,5-positions of unhalogenated BODIPYs **3.1** in the presence of a suitable oxidizing agent (permanganate, CAN, DDQ, or O_2). This approach is limited to primary and secondary alkyl amines (Scheme 3.1).[106]

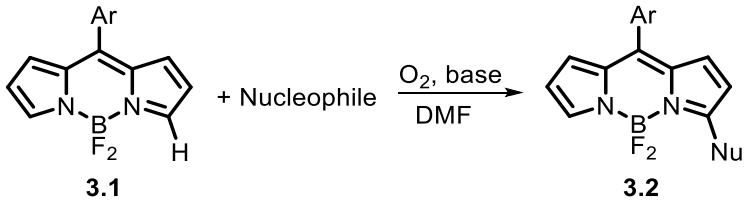

Scheme 3.1: Direct oxidative hydrogen substitution on a BODIPY dye **3.1**.

The 2-amino group has been introduced by nitration followed by reduction. The electrophilic substitution of BODIPY **3.3** with HNO_3 in Ac_2O produced the 2-nitroBODIPY **3.4** together with a minor amount of the 3-nitroBODIPY **3.5**. However, this approach is limited to the parent 2-NH_2 substituent (Scheme 3.2).[107]

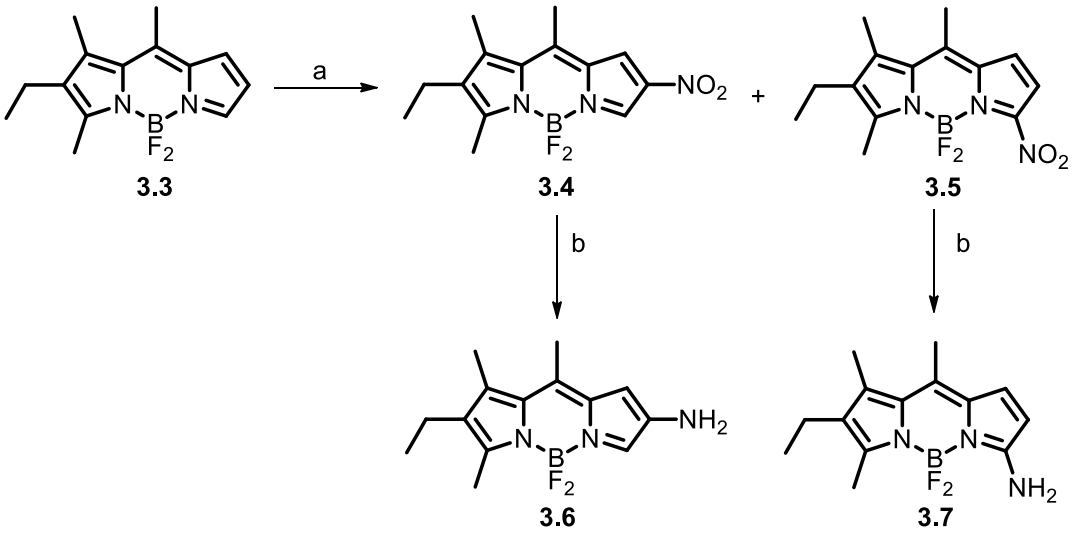

Scheme 3.2: Synthesis of 2-amino BODIPY **3.6**. a) HNO_3, Ac_2O, 0 ℃, b) H_2, Pd/C.

Introduction of 2-NH_2 has also been reported by palladium-catalysed coupling of a 2-bromoBODIPY **3.8** with benzophenone imine followed by hydrolysis of the resulting 2-iminoBODIPY **3.9**. This approach is also structurally limited and uses a rather high palladium loading (5 – 40 mol %) (Scheme 3.3).[108]

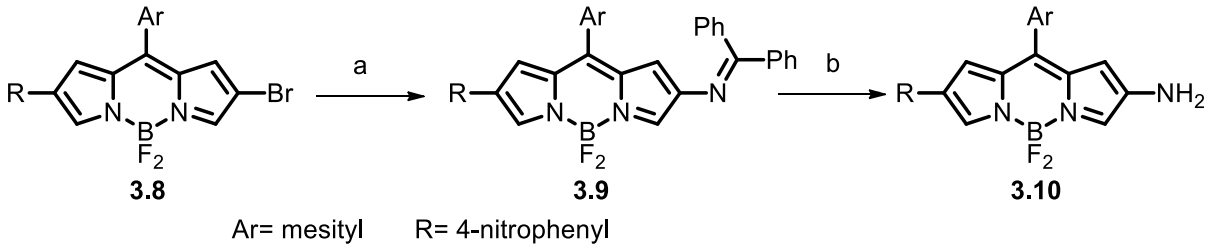

Scheme 3.3: Synthesis of 2-aminoBODIPY **3.10**. Conditions; (a) benzophenone imine (1.5 eq), Cs_2CO_3 (2.0 eq), Xantphos (40 mol%), Pd_2dba_3 $CHCl_3$ (20 mol%), dioxane, 100 ℃, 2 h, (b) HCl (1 M), THF, 60 ℃, 1 h.

Introduction of an amino group onto the BODIPY core causes significant effects on the position of the absorption and emission maxima, and it quenches the fluorescence quantum yield because of intramolecular charge transfer or photoelectron transfer.[109] This electron donation can be reduced by co-ordination of the nitrogen lone pair to a Lewis or Brønsted acid, leading to restoration of the BODIPY fluorescence (switch on sensors).[110] We envisaged that 2-aminoBODIPYs might be synthesised by metal catalysed amination of the corresponding 2-halogeno derivatives (Scheme 3.4).

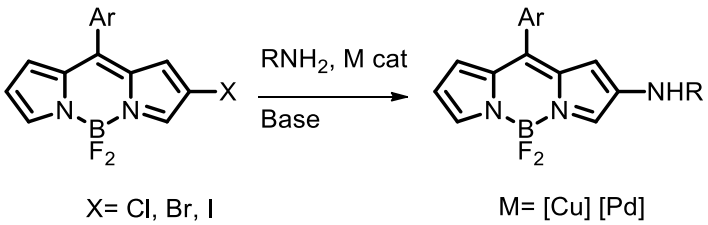

Scheme 3.4: General scheme for metal catalysed amination.

This chapter describes the results of our investigation into metal catalysed amination of 2-halogeno BODIPYs.

3.2. Copper catalysed amination of aryl halides

The Ullmann condensation is a reaction between an aryl halide and an amine, thioether or phenol in the presence of a copper catalyst and base to synthesise the corresponding aryl amine, thioether or ether compounds **3.11**, respectively (Scheme 3.5).[111–113] In 1904, Fritz Ullmann reported the first copper mediated aromatic nucleophilic substitution reaction. The original method for the coupling reaction requires the use of stoichiometric amounts of copper salts and high reaction temperatures.

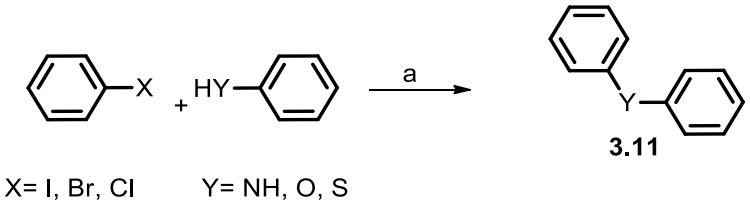

Scheme 3.5: Cu(I) or Cu(II) salts, base, ligand, solvent, 100-300 ℃.

3.2.1. Proposed mechanistic hypotheses for Ullmann condensation reaction

The exact nature (oxidation state) of the Cu-intermediate remains under debate. [111–113] There are four different proposed mechanisms for the Ullmann condensation reaction, which can be classified into two main categories: those in which the oxidation state of copper remains constant and those in which the oxidation state changes throughout the mechanistic cycle. The four different strategies are shown in Scheme 3.6:[111–113]

(1) Oxidative addition of aryl halide to Cu(I) resulting in an intermediate Cu(III) species (Scheme 3.6, a).

(2) Formation of aryl radical intermediates *via* halide atom transfer (Scheme 3.6, d).

(3) Formation of aryl radical intermediates *via* single electron transfer (Scheme 3.6, b).

(4) σ-bond metathesis through a four-centre intermediate (Scheme 3.6, e).

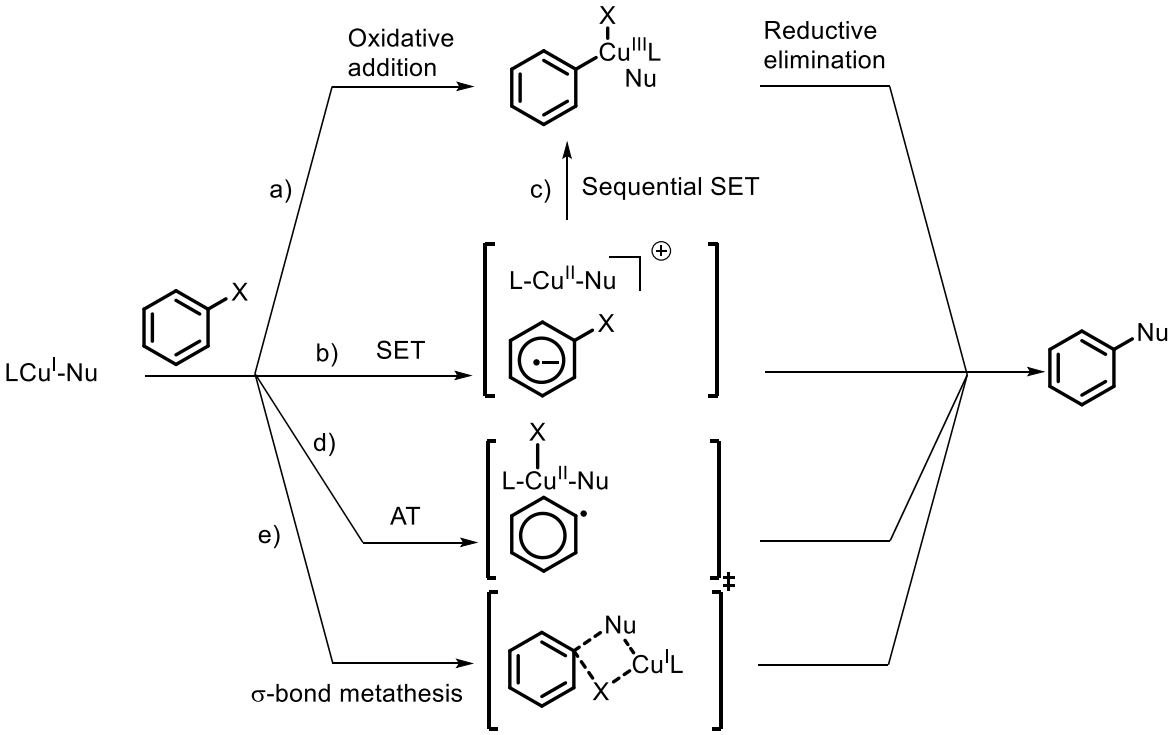

Scheme 3.6: Four mechanisms pathway for Ullmann condensation.

A considerable amount of literature has been published on copper catalyzed amination of halogenobenzene derivatives. However, there is little published data on the amination of 3-halogeno-5-membered heteroaromatic compounds.[114–120]

For instance, in 2001, Buchwald and his co-workers[115] developed an inexpensive copper catalyst system for the amination of aryl halides by using diamine ligand, a weak base and non-polar solvent. For example, they synthesised *N*-thiophen-3-yl benzamide **3.12** by using copper iodide and 1,2 diaminocyclohexane as ligand in the presence of K_3PO_4 in dioxane at 110℃ (Scheme 3.7).

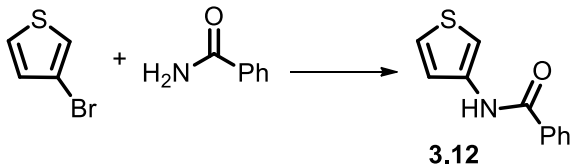

Scheme 3.7: Synthesis of *N*-thiophen-3-yl benzamide **3.12.** Conditions and reagents; 3-bromothiophene (1.00 mmol), benzamide (1.20 mmol), CuI (10 mol%), 1,2-diaminocyclohexane (10 mol%), K_3PO_4 (2.0 mmol), dioxane, 110 ℃, 15 h, 96%.[115]

In 2002, Padwa and Grawford[117] applied Buchwald amidation conditions to 2 and 3-substituted bromofurans and bromothiophenes by using *N*,*N*-dimethylethylenediamine as a ligand (Scheme 3.8).

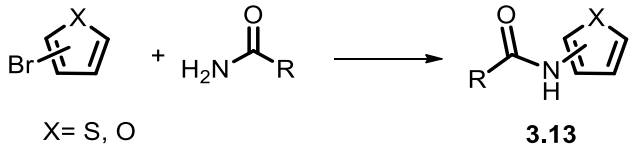

Scheme 3.8: General scheme for copper catalysed amidation of 2- and 3-bromothiophene. Conditions and reagents; CuI (1 mol%), *N*,*N*-dimethylethylenediamine (10 mol%), K_3PO_4 (4 eq), dioxane, 110 ℃ (97-81%).[117]

In addition, Twieg (2005) found that *N*,*N*-dimethylethanolamine (deanol) is a useful solvent and ligand for copper catalyzed amination (Scheme 3.9).[114]

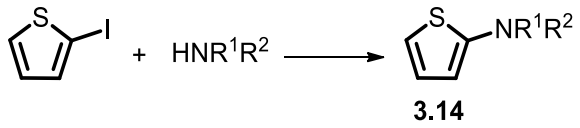

Scheme 3.9: *N*,*N*-dimethylethanolamine, Cu metal (10 mol%), $K_3PO_4.H_2O$ (2 eq) 60-75℃, 10-24 h.[114]

Surprisingly, there is no report of copper catalysed amination of 2 and 6 halogeno BODIPYs. A general synthetic route to 2-aminoBODIPY is shown in Scheme **3.10**.

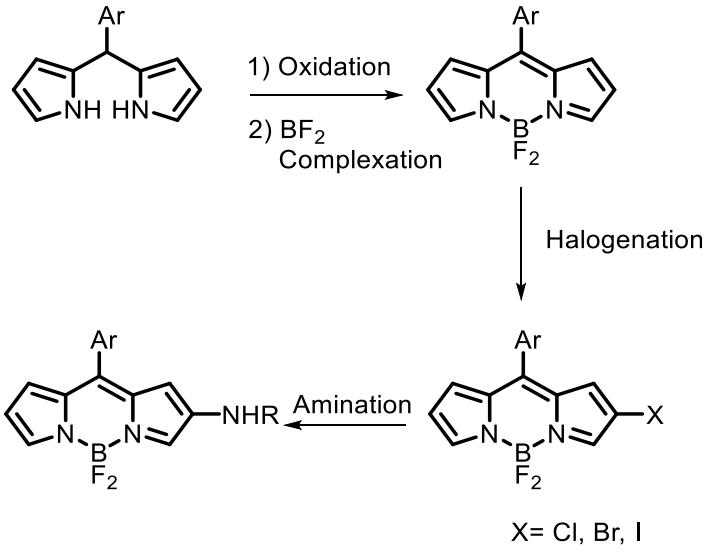

Scheme 3.10: A general synthetic route to 2-aminoBODIPY.

3.3. Synthesis of an 8-arylBODIPY 3.16

Using a literature procedure, the 8-arylBODIPY **3.16** was synthesized through a condensation of anisaldehyde and pyrrole in the presence of boron trifluoride-etherate ($BF_3.OEt_2$) as catalyst to form dipyrromethane **3.15**,[121] followed by oxidation with 2,3-dichloro-5,6-dicyano-1,4-benzoquinone (DDQ) to the corresponding dipyrromethene and then the BF_2 chelation by treatment with boron trifluoride diethyl etherate ($BF_3.OEt_2$) in the presence of *N*,*N*-diisopropylethylamine (i-Pr_2NEt) (Scheme 3.11).

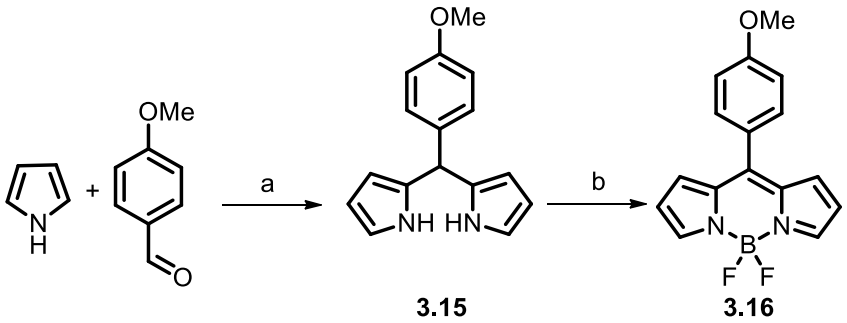

Scheme 3.11: Synthesis of 8-arylBODIPY **3.16**. Conditions and reagents; a) $BF_3.OEt_2$, r.t., 4 h (87%), b) DDQ, CH_2Cl_2, 0 °C, 30 min, $BF_3.OEt_2$, i-Pr_2NEt, r.t., 2 h (77%);

3.4. Synthesis of the 2-iodoBODIPY 3.17

Halogenated BODIPYs can be synthesized by using three different synthetic strategies: by using a suitably halogenated pyrrole, by halogenation of a dipyrromethane precursor or by electrophilic substitution onto the pre-formed BODIPY.[6,18] Several reports have shown that it is possible to introduce halogens on to the BODIPY core regioselectively.[18] Indeed, the halogenation of BODIPYs should be controlled by electronic and steric factors.[122] According to Burgess (2007) the 1 and 7 positions of an 8-arylBODIPY are sterically hindered, because of the bulky aryl group at the 8-position, and also due to the large size of the halogen atom (Figure 3.2).[12,122] In addition to being less sterically hindered, the 2 and 6 positions of the BODIPY are the most susceptible to electrophilic attack due to having the lower positive charge. [108]

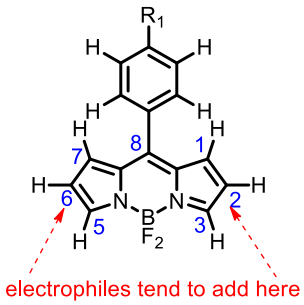

Figure 3.2: Electrophilic attack on unsubstituted 8-aryl BODIPY.

Regioselective iodination[122] of BODIPY **3.16** with ICl produced the 2-iodo-substituted BODIPY **3.17** together with a minor amount of the 2,6-diiodide **3.18** which were separable by column chromatography (Scheme 3.12).

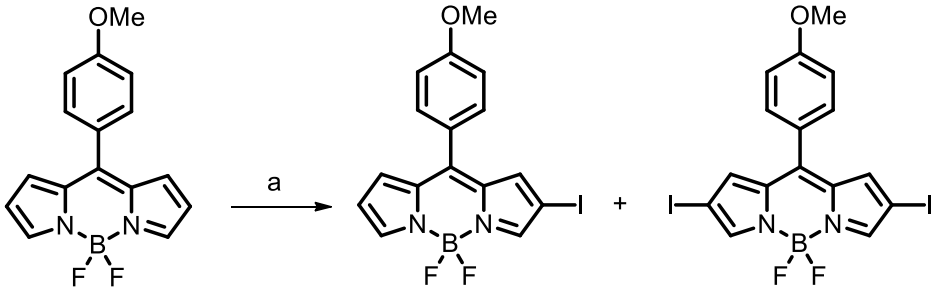

Scheme 3.12: Synthesis of 2-iodoBODIPY **3.17**. Conditions and reagents; (a) ICl, CH_2Cl_2–MeOH, r.t., 2 h (**3.17**, 65%; **3.18**, 15%).

The regioselectivity of the halogenation was confirmed by X-ray structure, after crystal growth through slow diffusion of hexane into a solution of the BODIPY in chloroform, which confirmed that the iodide was introduced on to position 2 then 6 regioselectively (Figure 3.3).

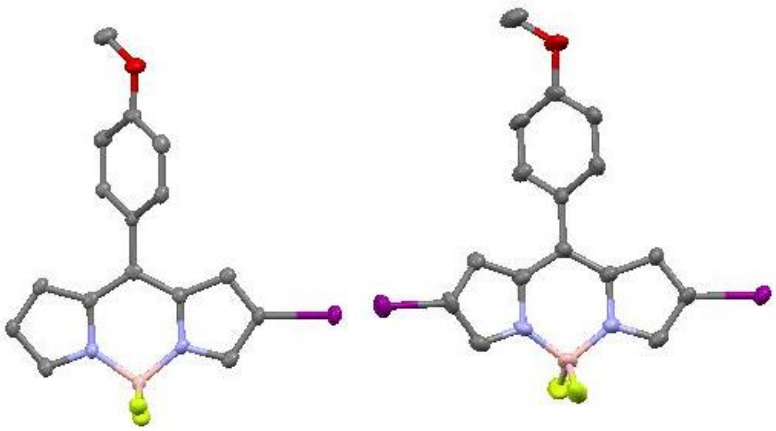

Figure 3.3: Molecular structure of BODIPY **3.17** and **3.18**, confirming the regioselectivity of the halogenation. Hydrogen atoms have been omitted for clarity.

3.5. Attempted synthesis of 2-amino BODIPY via Copper catalysed amination

In the first attempt we followed Twieg's procedure,[114] 1.5 equivalents of hexylamine were added to the 2-iodoBODIPY **3.17**, in the presence of Cu (5 mol%), CuI (5 mol%) and 2 equivalents of K_3PO_4 in *N*,*N*-dimethylethanolamine at 80 ℃ for 48 h. We were delighted to observe that amination had occurred, but in only 16% yield. In the ^{1}H NMR spectrum, we were expecting to observe the same or slight shifting for the two signals of the CH in positions 3 and 5 at 8.0 and 7.8 ppm. However, the ^{1}H NMR spectrum of the product showed the disappearance of one signal at 8.0 ppm (Figure 3.4). Surprisingly, it was found that the amination had occurred in the 3-position (Scheme 3.13).

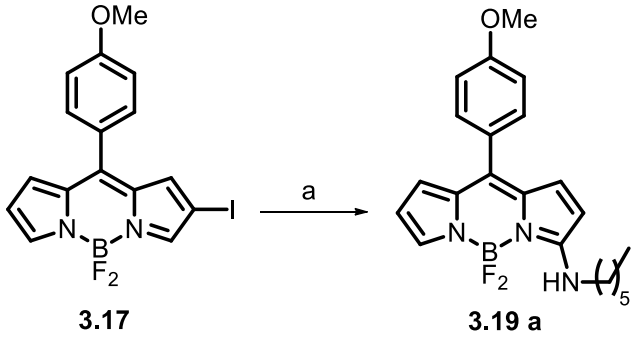

3.17 **3.19 a**

Scheme 3.13: Cu/CuI catalysed amination of BODIPY **3.17**. Conditions and reagents; (a) *N*-hexylamine (1.5 eq), Cu metal (5 mol%), CuI (5 mol%), K_3PO_4 (2.0 eq), *N*,*N*-dimethylethanolamine, 80℃, 48 h, 16%.

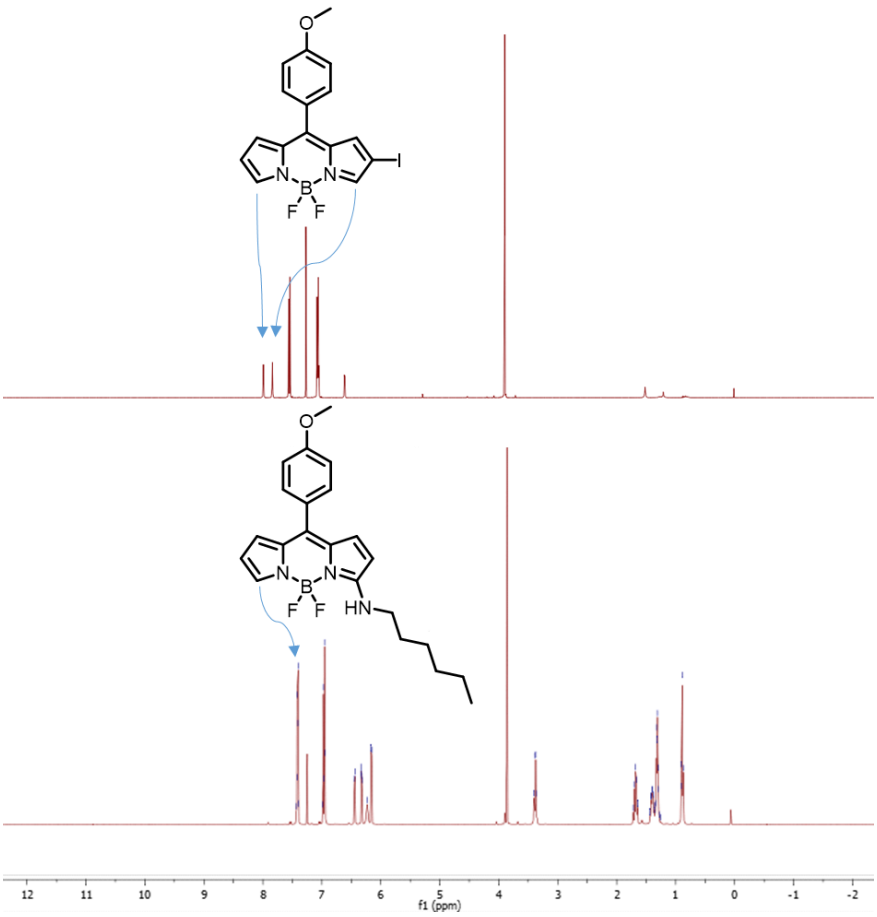

Figure 3.4: ^{1}H NMR spectra of 2-iodoBODIPY **3.17** and BODIPY **3.19a**.

The regioselectivity of amination of the 2-iodoBODIPY **3.17** was confirmed by X-ray structure determination, after crystal growth through slow diffusion of petroleum ether into a solution of the BODIPY in DCM, which confirmed that the hexylamine was introduced on to position 3 (Figure 3.5).

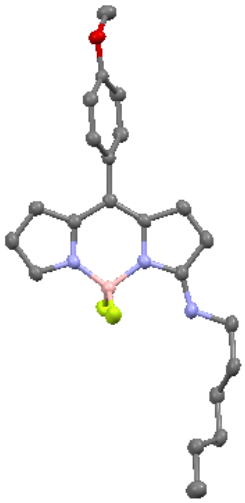

Figure 3.5: Molecular structure of 3-hexylaminoBODIPY **3.19a**, confirming the amination reaction occurred at position 3. Hydrogen atoms have been omitted for clarity.

3.5.1. Screening of ligand

Many different ligands have been reported for copper catalysed amination reactions such as ligands **L1**, **L2**, **L3** and **L4** (Figure 3.6).

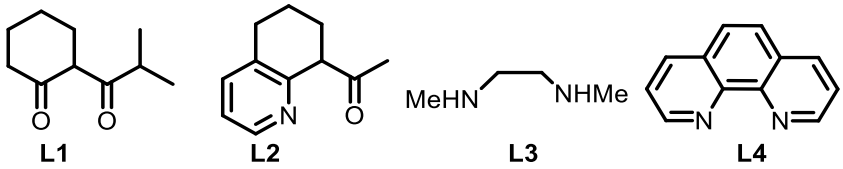

Figure 3.6: Ligands screened in the amination of BODIPY.

In 2006 Buchwald reported that the use of the diketone ligand **L1** allows the amination reaction of aryl halides with aliphatic amines to occur under mild conditions. The catalyst is formed easily in situ by combining ligand **L1** with CuI (Scheme 3.14).[123]

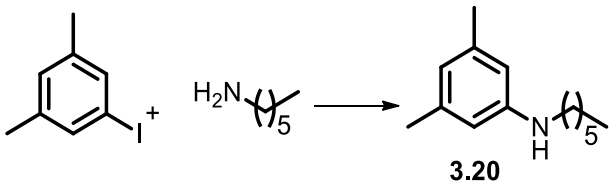

Scheme 3.14: Buchwald amination using **L1**.[123] Conditions and reagents; 5 mol% CuI, 20 mol% **L1**, Cs_2CO_3 (2 eq), DMF, r.t., 98%.

In 2009, Ding studied the use of 2-pyridinyl β-ketone ligand **L2** in the CuI-catalyzed amination and found that good yields were obtained by using a weak base and non-polar solvent at room temperature (Scheme 3.15).[124]

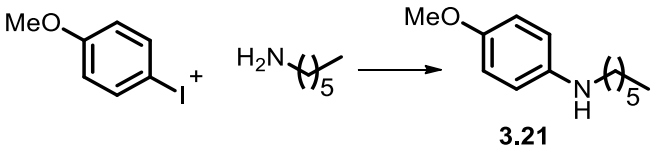

3.21

Scheme 3.15: Ding amination using **L2**.[124] Conditions and reagents; 10 mol% CuI, 20 mol% **L2**, Cs_2CO_3 (2 eq), DMF, Ar, r.t., 97%.

Diamine ligands such as *N,N'*-dimethyl ethylenediamine **L3,** ethylenediamine and 1,10-phenanthroline **L4** are also useful in Cu-catalyzed C-N bond formation.[125,126] In order to optimise the yield of synthesis 3-aminoBODIPY **3.19** we screened a series of bidentate ligands **L1-L4** as shown in Table 3.1. The choice of catalyst and ligand loading, base and solvent were taken from Buchwald's report[123] using **L1**. The choice of 80℃ was based on a first temperature screening reaction using **L3** which showed that no reaction was observed with hexylamine at 25 or 50℃. Also, it was established that no reaction at room temperature occurred with hexylamine for any of these ligands.

Table 3.1: Ligand variation in the amination of BODIPY **3.17**.

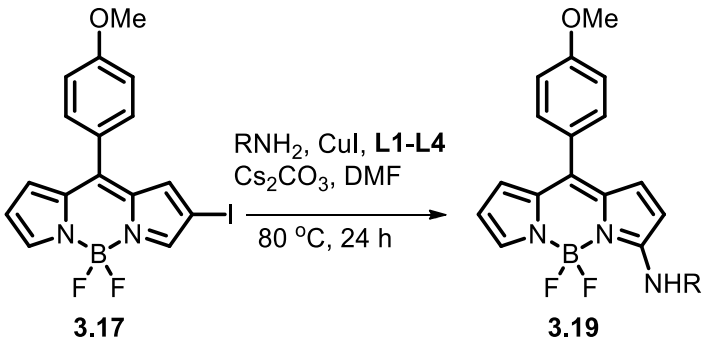

Entry	R	Ligand	Product	Isolated yield
1	$CH_3(CH_2)_5$	**L1**	**3.19a**	30
2	$CH_3(CH_2)_5$	**L2**	**3.19a**	20
3	$CH_3(CH_2)_5$	**L3**	**3.19a**	35
4	$CH_3(CH_2)_5$	**L4**	**3.19a**	60
5	4-MeC_6H_4	**L1**	**3.19b**	6
6	4-MeC_6H_4	**L2**	**3.19b**	70
7	4-MeC_6H_4	**L3**	**3.19b**	30
8	4-MeC_6H_4	**L4**	**3.19b**	84
9	PhCO	**L1**	**3.19c**	6
10	PhCO	**L2**	**3.19c**	11
11	PhCO	**L3**	**3.19c**	10
12	PhCO	**L4**	**3.19c**	15

Conditions and reagents: BODIPY **3.17** (0.25 mmol), amine or amide (0.47 mmol), CuI (5 mol%), ligand (20 mol%), Cs_2CO_3 (0.47 mmol), DMF (0.8 mL), 80℃, 24 h.

The catalytic activity of the chosen ligands was evaluated by reaction of the 2-iodoBODIPY **3.17** with *n*-hexylamine, *p*-toluidine and benzamide at 80℃ to give the corresponding 3-substituted BODIPY **3.19a**, **3.19b** and **3.19c** respectively. From Table 3.1 it is clear that the ligand **L4** (1,10-phenanthroline) gives the highest yield regardless of the nature of the nucleophile. Good yields were obtained in the case of *n*-hexylamine (60%) and *p*-toluidine (80%) and also the reaction was successful even in the case of the

much more weakly nucleophilic benzamide (15%). The ketopyridine **L2** and dimethylethylenediamine **L3** also successfully promoted the copper-catalysed amination reaction with moderate yields (20-70%). Interestingly, diketone (**L1**) showed much lower efficiency, although it contains a bidentate chelating centre.

3.5.2. Scope of the amination of the 2-iodoBODIPY 3.16

Subsequently, to explore the scope of the copper catalyzed nucleophilic substitution reaction, 5 mol% CuI, 20 mol% **L4** in DMF with Cs_2CO_3 as the base at 80 ˚C for 2 h were used as the general conditions in the reaction of the 2-iodoBODIPY **3.17** with a range of different amines (Table 3.2).

Different primary alkyl amines including *n*-hexylamine, benzylamine, 2-thiophenyl ethyl amine and cyclohexylamine were reacted successfully in good yield (entries 1 and 4-6). Also, good yields were obtained with secondary alkyl amines such as morpholine and pyrrolidine (entries 7 and 8). High yields were achieved for electron rich primary anilines including 4-methylphenyl amine and 4-methoxyphenyl amine (entries 2 and 10). However, slightly lower yields were obtained in the case of the less nucleophilic electron deficient anilines (entries 11-13) and the yields were slightly lower with the more sterically hindered 2-methoxy substituted aniline (entry 9) and a secondary aniline methylphenylamine (entry 14). One interesting finding was that in many cases the 3-aminoBODIPY **3.19** was accompanied by formation of a small amount of the corresponding 3-amino-6-iodoBODIPY **3.22** (Table 3.2). The structure of 3-hexylamino-6-iodoBODIPY **3.22a** was confirmed unambiguously by X-ray structure determination (Figure 3.7).

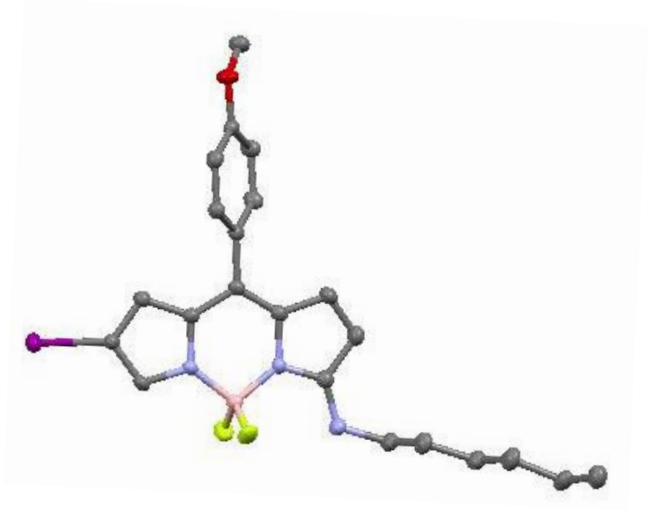

Figure 3.7: molecular structure of 3-hexylamino-6-iodoBODIPY **3.22a**. Hydrogen atoms have been omitted for clarity.

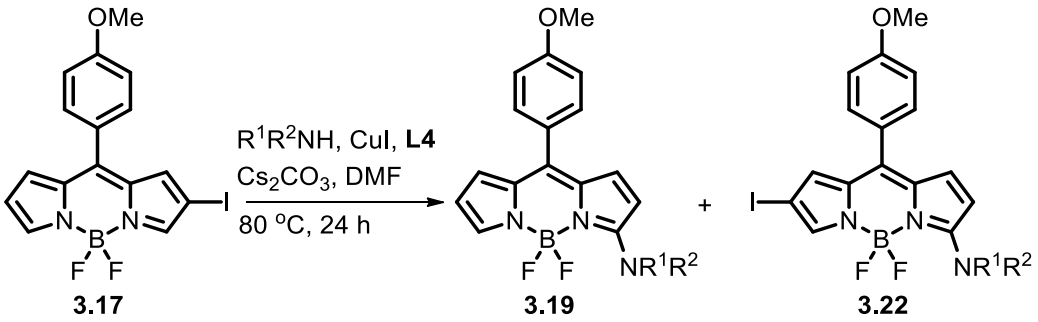

Table 3.2: Scope of the amination of the 2-iodoBODIPY **3.17**.

Entry	R^1	R^2	Product	Isolated yield	
				3.19	**3.22**
1	$CH_3(CH_2)_5$	H	**3.19a/3.22a**	60	5
2	4-MeC_6H_4	H	**3.19b/3.22b**	84	5
3	PhCO	H	**3.19c**	15	-
4	$PhCH_2$	H	**3.19d**	64	-
5	2-ThiophenylCH_2CH_2	H	**3.19e**	65	-
6	Cyclohexyl	H	**3.19f/3.22f**	78	4
7	$O(CH_2CH_2)_2$		**3.19g**	85	-
8	$CH_2CH_2CH_2CH_2$		**3.19h/3.22h**	87	4
9	2-$MeOC_6H_4$	H	**3.19i**	60	-
10	4-$MeOC_6H_4$	H	**3.19j/3.22j**	78	6
11	4-ClC_6H_4	H	**3.19k/3.22k**	66	13
12	4-NCC_6H_4	H	**3.19l/3.22l**	77	15
13	2-Pyridyl	H	**3.19m/3.22m**	60	14
14	Ph	Me	**3.19n**	40	-

Conditions and reagents: BODIPY **3.17** (0.25 mmol), amine or amide (0.47 mmol), CuI (5 mol%), ligand **L4** (20 mol%), Cs_2CO_3 (0.47 mmol), DMF (0.8 mL), 80℃, 24 h. The second entry refers to the yield of 6-iodo by-product **3.22**, where isolated.

3.6. Synthesis of the 2-bromoBODIPY 3.23

Using a literature procedure,[56] the 2-bromoBODIPY **3.23** was prepared by reaction of the 8-(4-methoxyphenyl)BODIPY **3.16** with NBS in DCM at room temperature for 90 min (Scheme 3.16). Purification using column chromatography gave the desired 2-bromoBODIPY **3.23** in high yield (73%).

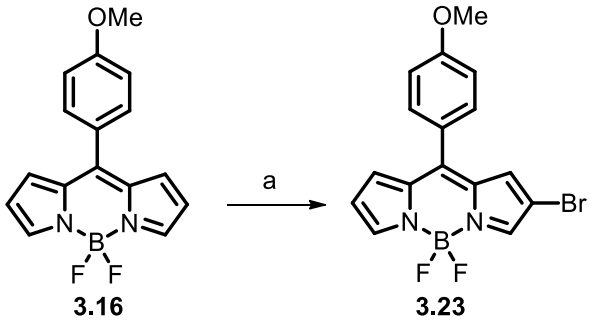

Scheme 3.16: Synthesis of 2-bromoBODIPY **3.23**. Conditions and reagents; (a) NBS, CH_2Cl_2, r.t., 90 min. (73%).

The copper catalysed nucleophilic amination was attempted by applying the same reaction conditions, using phenanthroline (**L4**), to the reaction of the 2-bromoBODIPY **3.23** with pyrrolidine to give the 3-(pyrrolidin-1-yl)BODIPY **3.19h** in 80% yield, together with the corresponding 6-bromo-3-(pyrrolidin-1yl)BODIPY **3.24** in 5% yield (scheme 3.17).

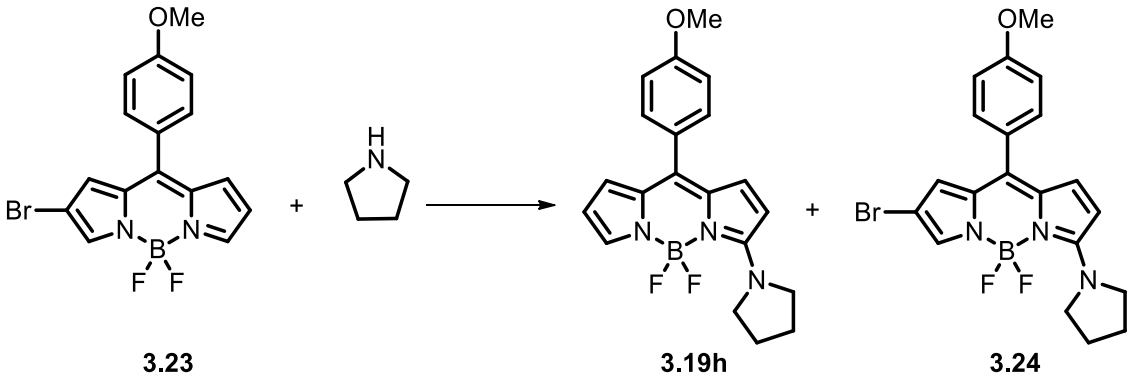

Scheme 3.17: synthesis of 3-(pyrrolidin-1-yl)BODIPY **3.19h** and 6-bromo-3-(pyrrolidin-1yl)BODIPY **3.24**. Conditions and reagents; pyrrolidine (2.0 eq), CuI (5 mol%), 1,10-phenanthroline **L4** (20 mol%), Cs_2CO_3 (2.0 eq), DMF, 80℃, 24 h.

The structure of the 3-pyrrolidinyl product **3.19h** was confirmed by X-ray structure determination (Figure 3.8).

Figure 3.8: molecular structure of 3-(pyrrolidin-1-yl)BODIPY **3.19h**. Hydrogen atoms have been omitted for clarity.

The high yields of amination regardless of the nature of the halogen support a straightforward nucleophilic substitution mechanism.

3.7. Attempted synthesis of a 3,5-diaminoBODIPY

The synthesis of a 3,5-diaminoBODIPY via copper catalysed double amination of the 2,6-diiodoBODIPY **3.18** was attempted. Attempts using both a primary aniline and pyrrolidine were unsuccessful (Table 3.3). In both cases the unreacted diiodoBODIP **3.18** was recovered under these reaction conditions and there was no sign of any singly aminated product, which may be due to the higher degree of steric hindrance in this reaction in comparison to the successful reaction using 2-iodoBODIPY.

Table 3.3: All attempts carried out for synthesis of a 3,5-diaminoBODIPY.

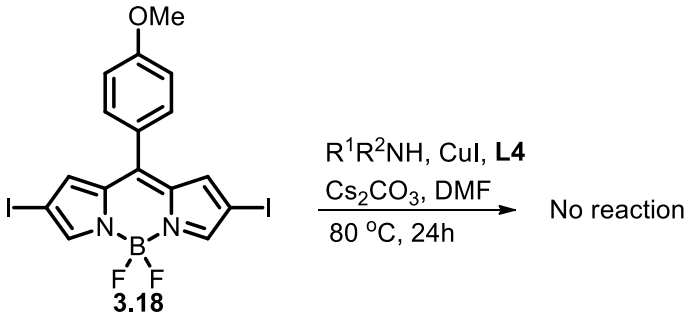

Entry	R^1	R^2	Product
1	4-$MeOC_6H_4$	H	No product
2	$CH_2CH_2CH_2CH_2$		No product

Conditions and reagents: BODIPY **3.18** (0.25 mmol), amine (0.47 mmol), CuI (5 mol%), 1,10-phenanthroline **L4** (20 mol%), Cs_2CO_3 (0.47 mmol), DMF (0.8 mL), 80℃, 24 h.

3.8. Mechanism of reaction

In order to explore the reaction mechanism, we have tried to determine the role of each component in the amination reaction. The reaction between 2-iodoBODIPY **3.17** and pyrrolidine was repeated using the same reaction conditions with omission of each component in turn. As shown in Table 3.4, in the absence of cooper iodide no reaction occurred between 2-iodoBODIPY **3.17** and pyrrolidine. When the ligand was omitted then the amination product **3.19h** was formed in 50% yield together with 3% of the 2-iodo-5-(pyrrolidin-1yl)BODIPY **3.22h**. Also, in the absence of added base (Cs_2CO_3) the product **3.19h** was formed in low yield together with the by-product **3.22h** (14% and 10% respectively). Therefore, copper is essential for the amination to occur and the base and ligand improve the reaction conversion.

Table 3.4: Investigation of the role of each component in the amination reaction.

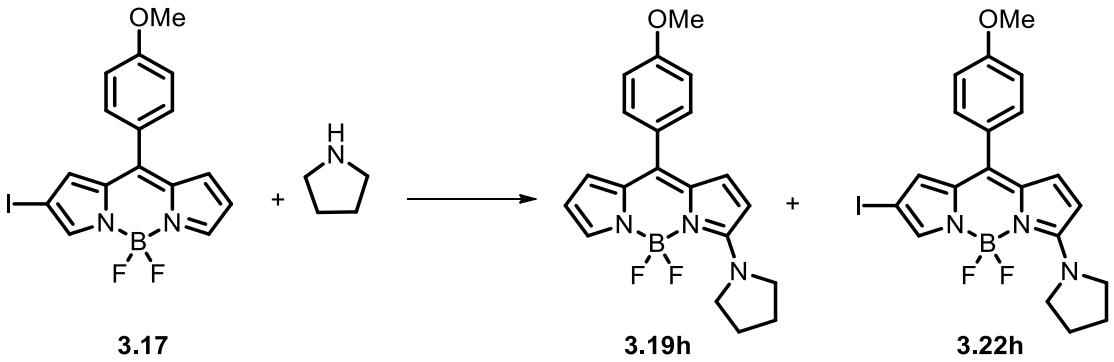

3.17 **3.19h** **3.22h**

Starting material	CuI	L4	Cs_2CO_3	Outcome
3.17	X	X	✓	Starting material
	X	✓	✓	Starting material
	✓	✓	X	**3.19h** (15%) **3.22h** (10%)
	✓	X	✓	**3.19h** (50%) **3.22h** (3%)

Conditions and reagents: BODIPY **3.17** (0.25 mmol), amine (0.47 mmol), CuI (5 mol%), 1,10-phenanthroline **L4** (20 mol%), Cs_2CO_3 (0.47 mmol), DMF (0.8 mL), 80℃, 24 h.

Since iodoBODIPY compounds are known to act as initiators for photooxidation,[127] the reaction between the 2-iodoBODIPY **3.17** and 4-cyanoaniline was repeated with careful exclusion of light and also with a 5-cycle freeze-pump-thaw sequence to degas the solution. This did not significantly change the yields of the products (**3.17l** and **3.22l**) and so it is unlikely that the reaction is photoinitiated or requires the presence of dioxygen. We considered three different mechanisms for this copper catalysed nucleophilic substitution reaction.

A first possibility involves a base-catalysed halogen dance[128] (BCHD). Based-catalyzed halogen dance (BCHD) reactions, also referred to as halogen-dance (HD), halogen migration or halogen scrambling were first found by chance in 1953.[129] The base catalysed halogen dance (BCHD) reaction represents a base induced reaction of a haloaromatic compound in which a halogen atom moves to a new position in the product. Halogen dance reactions are an excellent synthetic tool which empower functionalization of positions which are otherwise difficult to address. There is a large volume of published studies describing the mechanism of BCHD reactions. Figure 3.9 describes the general equation of the halogen dance reaction.

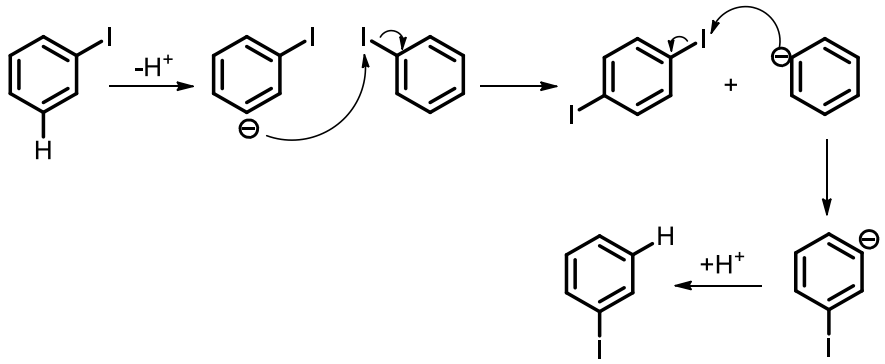

Figure 3.9: the general mechanism of the halogen dance reaction.

In the case of 2-iodoBODIPY **3.17**, the first step of a halogen dance would be formation of an anion by deprotonation of 2-iodoBODIPY **3.17** in the 5-position. The resulting anion **3.17a** can abstract iodine from the 2-iodoBODIPY **3.17** to give 2,5-diiodoBODIPY **3.25** and the newly formed anion **3.26**. These two species can react again to form anion **3.27** followed by protonation to give 3-iodoBODIPY **3.28**. After amination of 3-iodoBODIPY **3.28**, 3-aminoBODIPY **3.19** can obtained as shown in Scheme 3.18.

In principle the deprotonation and subsequent halogen migration could occur on any of the BODIPY positions; only when the halogen reaches the 3-position can it be displaced by the nucleophile, leading to the observed product.

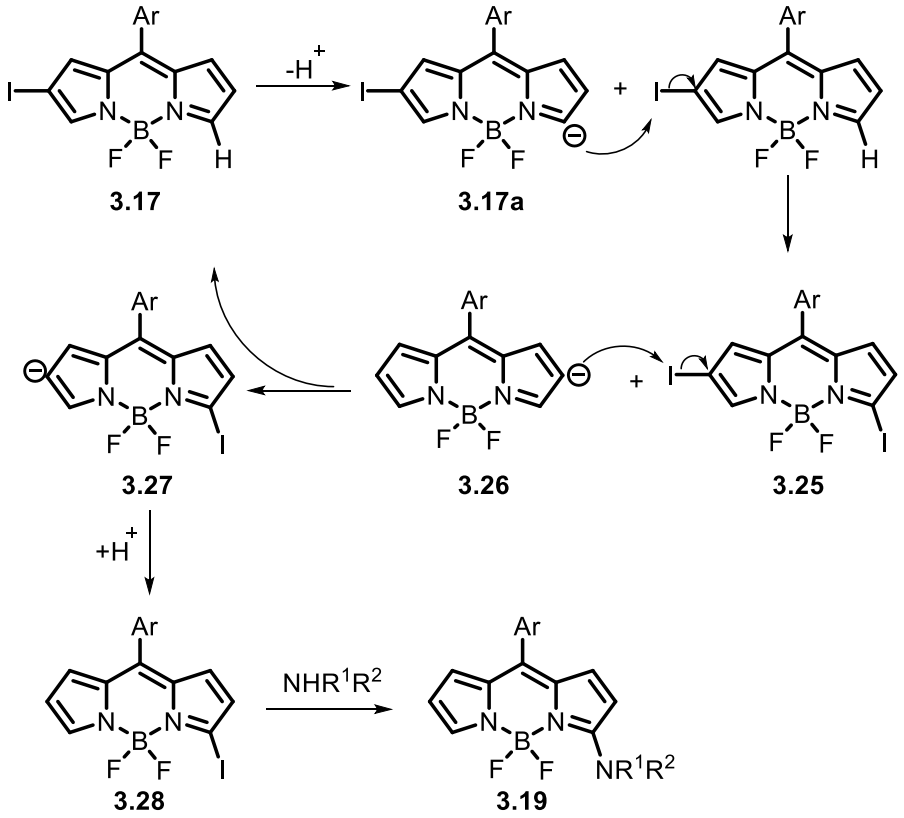

Scheme 3.18: Possible mechanistic pathway involving base catalysed halogen dance of BODIPY.

According to the proposed halogen dance mechanism (Scheme 3.18), deprotonation of the unhalogenated compound **3.16** followed by abstraction of iodine from the 2,6-diiodide **3.18** would be expected to allow both compounds to enter into the halogen dance manifold. In order to establish whether the reaction between 2-iodoBODIPY and amines occurs by a halogen dance mechanism, the unhalogenated BODIPY **3.16** was treated with the 2,6-diiodide **3.18** and pyrrolidine under the same reaction conditions, however, no aminated product was observed and the unreacted starting materials were isolated (Scheme 3.19).

This observation, together with the high yield obtained even with the 2-bromoBODIPY **3.23**, suggest that a halogen dance mechanism is not involved.

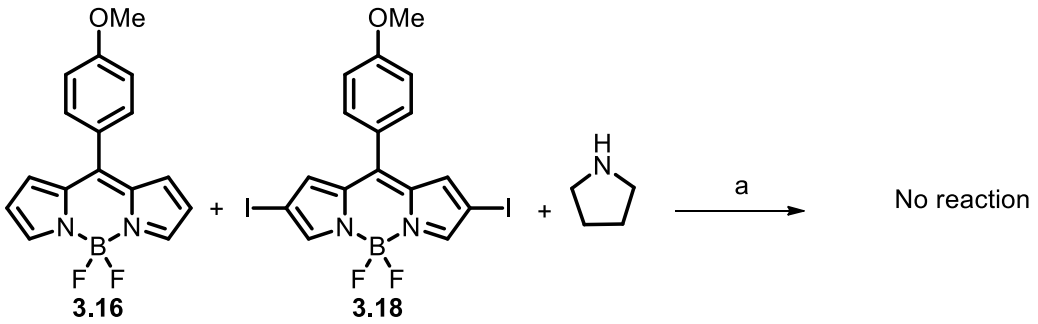

Scheme 3.19: Attempted copper catalysed amination of a 1:1 mixture of the BODIPY **3.16** and the 2,6-diiodide **3.18** with pyrrolidine; Conditions and reagents; pyrrolidine (2 eq), CuI (5 mol%), 1,10-phenanthroline **L4** (20 mol%), Cs_2CO_3 (2 eq), DMF, 80℃, 24 h.

A second possibility is that the loss of iodine from C-2 is a reductive process, linked to oxidation of the copper (I) catalyst[130] [e.g. via a copper (I)/copper (III) cycle or single electron transfers involving copper (II)] (Scheme 3.20). Such a mechanism would provide the oxidant required for the known direct nucleophilic hydrogen displacement by the amine[106] and could explain formation of the iodinated by-product **3.22** by direct nucleophilic hydrogen displacement reaction at the 5-postion of the iodoBODIPY **3.17**. The unreactivity of the 2,6-diiodide **3.18** is hard to explain by this mechanism, since it might be expected to be just as good an oxidant for the copper as the monoiodoBODIPY **3.17**.

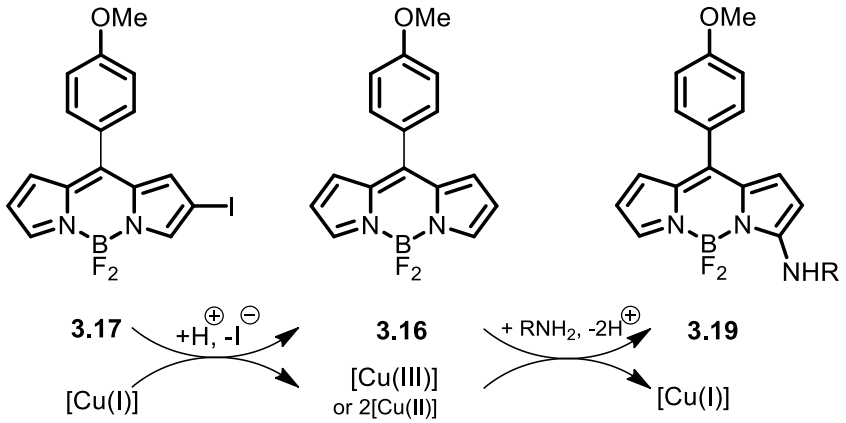

Scheme 3.20: Possible mechanistic pathway involving a copper redox cycle.

Scheme 3.21 shows a third mechanistic possibility which involves initial nucleophilic attack at C-3. The necessity for copper catalysis (Table 3.4) suggests that the nucleophile might be an amido copper species such as **3.29**.[131] The resulting anion **3.30** might be copper-bound, corresponding to an amidocupration, but may be delocalised over the

BODIPY π-system. In order to produce the product, iodide must be lost and this requires protonation at C-2 to give **3.31** followed by base-mediated elimination of HI. This mechanism does not account for the formation of the 5-amino-2-iodoBODIPY by-product **3.22**.

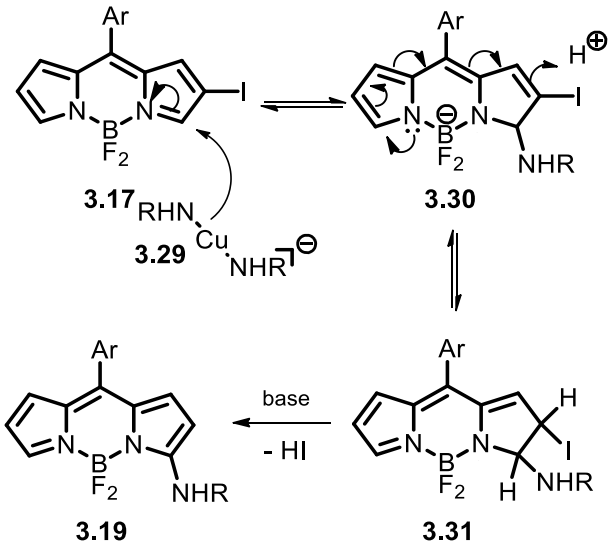

Scheme 3.21: Possible mechanistic pathway initiated by nucleophilic attack at 3-position.

Observation of the 2-iodo-5-aminoBODIPY by-product **3.22** suggests initial attack might occur at the 5-postion of the iodoBODIPY **3.17** rather than at the 3-position (Scheme 3.22).

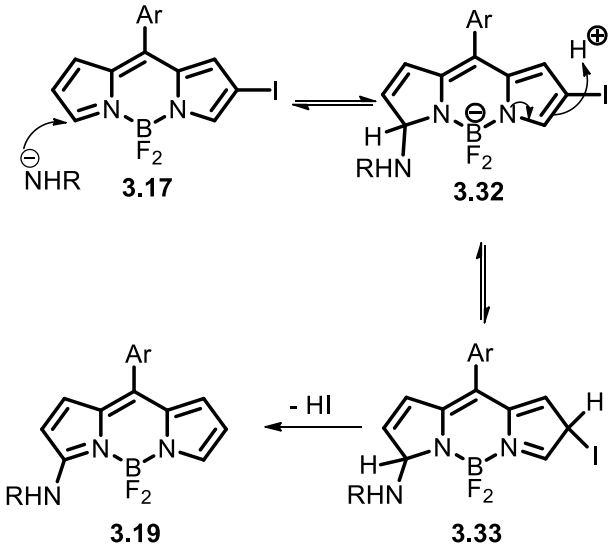

Scheme 3.22: Possible mechanistic pathway initiated by nucleophilic attack at 5-position.

Formation of the by-product **3.22** is an oxidative process requiring the formal loss of hydride from iodoBODIPY **3.17** and thus the yield of **3.22** might be expected to be increased in the presence of oxygen, which is not observed. Direct oxidative nucleophilic hydrogen substitution by amines occurs in the 3-position of unhalogenated 8-arylBODIPYs but requires a stoichiometric oxidant (DDQ, CAN, permanganate, or O_2) and is reported to be successful for primary and secondary alkyl amines but to fail in the case of anilines (Scheme 3.23).[106]

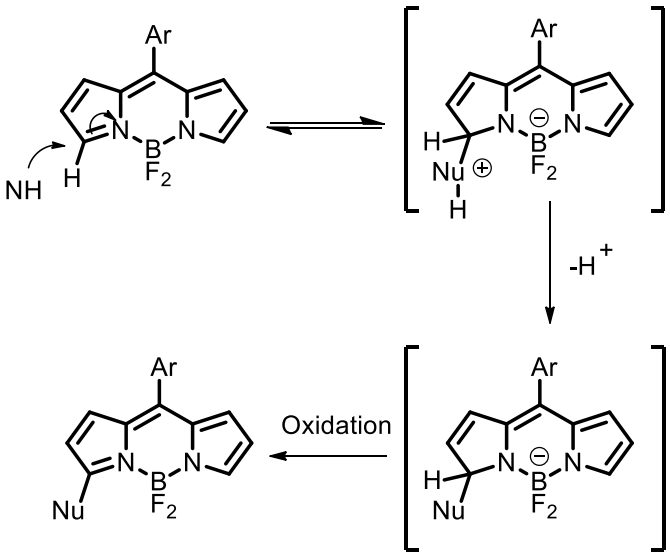

Scheme 3.23: Direct oxidative nucleophilic hydrogen substitution by amines.[106]

In order to investigate the position of the nucleophilic attack the unsymmetrical BODIPY **3.34** was synthesised via zinc oxide mediated Friedel-Crafts acylation of pyrrole followed by reaction of the resulting ketone **2.68b** with 2,4-dimethylpyrrole in the presence of boron trifluoride-etherate (Scheme 3.24). Iodination with NIS was moderately regioselective in favour of substitution on the more electron rich, methylated, ring to give a mixture of mono-iodoBODIPYs **3.35** and **3.36** in a ratio of 6:1 respectively. The 2-iodoBODIPY **3.35**, in which the 5-position is blocked by a methyl group, did not react under the amination conditions. This observation suggest that initial nucleophilic attack actually occurs at C-5 of the 2-iodoBODIPY, however it was also found that the reaction between 2-iodoBODIPY **3.36**, in which the 5-position is free, and pyrrolidine did not form any amination product under the amination conditions. A possible explanation for these results may be the presence of the electron donating methyl groups in C1 and C3 of the BODIPYs is sufficient to disfavour nucleophilic attack by the amine. It is noteworthy

that the direct oxidative hydrogen displacement was reported only on BODIPYs lacking any substituent except at the 8-position. [106]

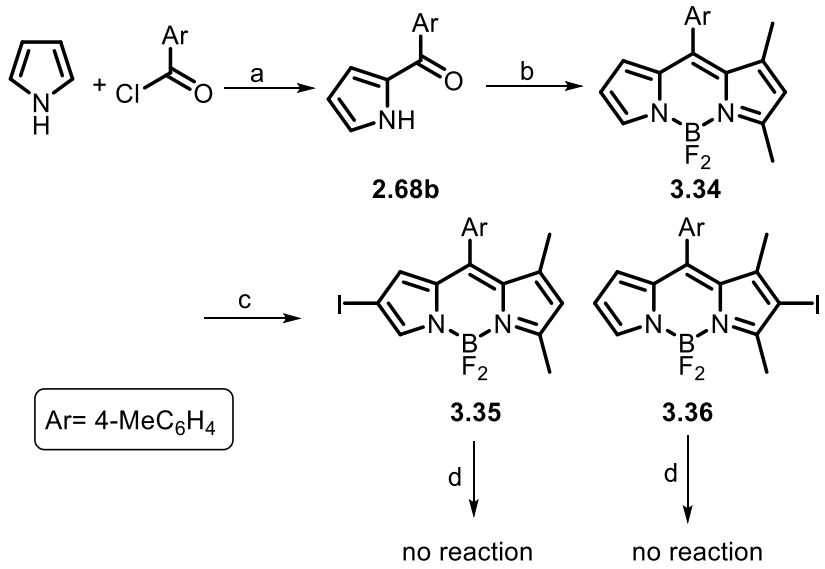

Scheme 3.24: Conditions and reagents; a) ZnO, r.t., 5 min (55%); b) 2,4-dimethylpyrrole, $BF_3.OEt_2$, i-Pr_2NEt, CH_2Cl_2, r.t., 24 h (84%); c) NIS, CH_2Cl_2, r.t., 21 h (**3.35**, 13%; **3.36**, 74%); d) pyrrolidine (2 eq), CuI (5 mol%), 1,10-phenanthroline **L4** (20 mol%), Cs_2CO_3 (2 eq), DMF, 80℃, 24 h.

3.9. Synthesis of 6-deuterio-2-iodoBODIPY

Due to the failure of the reactions between pyrrolidine and BODIPY **3.35** or **3.36** we decided to synthesise isotopically labeled compounds to investigate the position of the nucleophilic attack. The synthesis of isotopically labelled compounds is very important for detailed mechanistic studies of many chemical reactions. The most common stable isotopes used in research include ^{13}C, ^{18}O, ^{2}H (Deuterium or D) and ^{15}N. A radical mediated halogen deuterium exchange is one of the most common methods for deuteration, and the mechanism of the reaction is described in Figure 3.10.

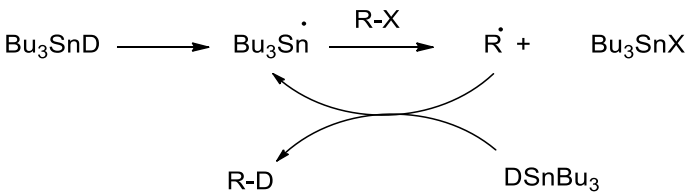

Figure 3.10: The proposed reaction mechanism of the halogen-deuterium exchange.[36]

Radical-mediated deuteration of the diiodoBODIPY **3.18** was attempted using tributyltin deuteride in deuterobenzene (Table 3.5, entry 1). The reaction mixture was degassed by

a 5-cycle freeze-pump-thaw sequence and also with careful exclusion of light before heating but no dehalogenated product **3.39** was observed. Mutsumi (2011) has reported[132] the use of THF-d_8 as the deuterium source in presence of tributyltin hydride (Bu_3SnH) for high yielding deuterium-halogen exchange in aromatic iodides (Scheme 3.25).

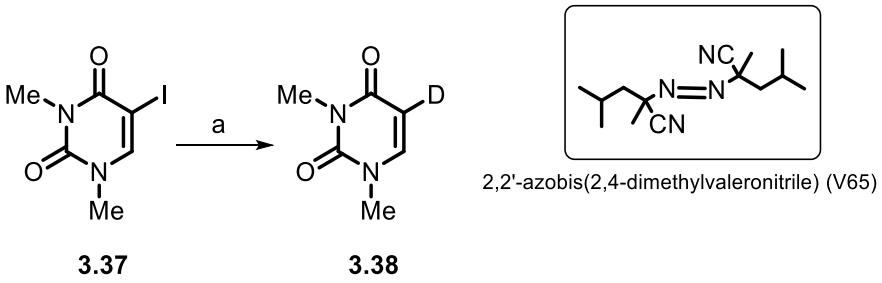

3.37 **3.38**

Scheme 3.25: THF-d_8 mediated radical deuteration.[132] Conditions and reagents; Bu_3SnH (1.2 eq), V-65 (0.2 eq), THF-d_8, 2 h, reflux, 62%.

In the second attempt we followed the Mutsumi procedure,[132] by treating diiodo BODIPY **3.18** with Bu_3SnH and AIBN as the initiator in THF-d_8 as the D source at 66℃ for 18 h, However, no product was observed in the ^1H NMR spectrum of the crude material as all starting material was recovered. Finally, we used Bu_3SnD instate of Bu_3SnH; again no product **3.39** was observed in the ^1H NMR spectrum of the crude material and the starting material was still present.

Table 3.5: All attempts carried out for synthesis of 6-deuterio-2-iodoBODIPY **3.39**

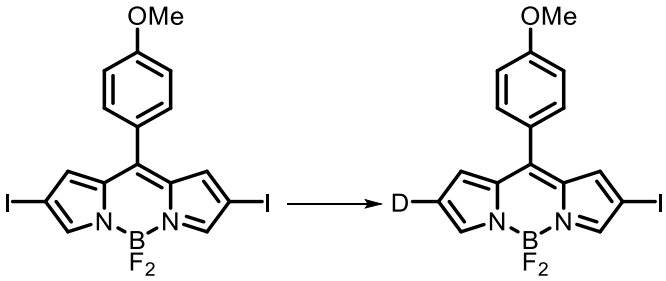

Attempts	Reaction conditions	Product
1	BODIPY **3.18** (0.18 mmol), $(C_4H_9)_3SnD$ (0.22 mmol), AIBN (0.018 mmol), benzene-d_6, 80 ℃, 18 h	No reaction
2	BODIPY **3.18** (0.4 mmol), $(C_4H_9)_3SnH$ (0.47 mmol), AIBN (0.079 mmol), THF-d_8, 66 ℃, 18 h	No reaction
3	BODIPY **3.18** (0.4 mmol), $(C_4H_9)_3SnD$ (0.47 mmol), AIBN (0.079 mmol), THF-d_8, 66 ℃, 18h	No reaction

May (2001), has reported a convenient method for the deuteration of compound **3.40** by using 10% Pd/C, Et_3N and deuterium gas in ethyl acetate to form compound **3.41** in an excellent yield (96%).[133]

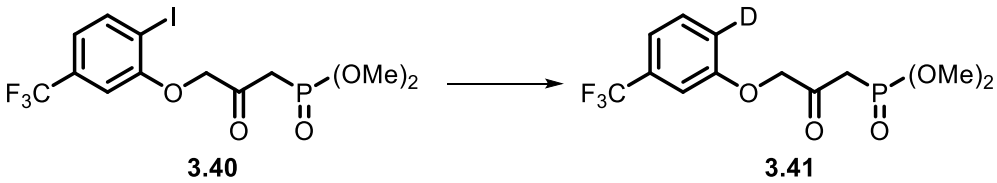

Scheme 3.26: Synthesis of deuterated phenoxyketophosphonate **3.41**. Conditions and reagents; D_2, Pd/C, EtOAc, r.t., 2 h, 96%.

Following this literature procedure, the deuteration of 2,6-diiodoBODIPY **3.18** was carried out by using Pd/C and D_2 (1 atm, balloon) in DCM and MeOH for 5 h at room temperature (Scheme 3.27). The 6-deuterio-2-iodoBODIPY **3.39** was formed in 60% yield together with 17% of the 2,6-dideuteriated BODIPY **3.42** which were separable by column chromatography.

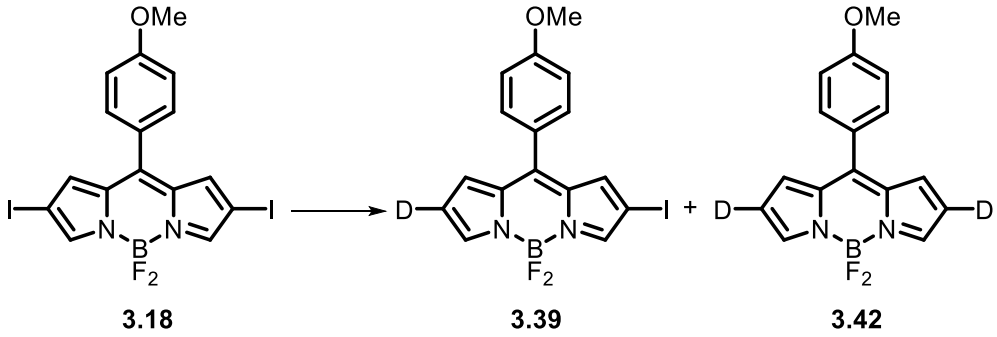

Scheme 3.27: Synthesis of deuterioBODIPY **3.39**. Conditions and reagents; D_2 (1 atm), Pd/C, CH_2Cl_2-MeOH, r.t., 5 h (**3.39**, 60%; **3.42**, 17%).

The 6-deuterio-2-iodoBODIPY **3.39** was reacted with pyrrolidine in the presence of CuI, **L4** and Cs_2CO_3 in DMF at 80℃ for 24 h to give a 70:30 ratio of the 3-amino-6-deuterioBODIPY **3.43** together with the regioisomeric 3-amino-2-deuterioBODIPY **3.44** (Scheme 3.28).

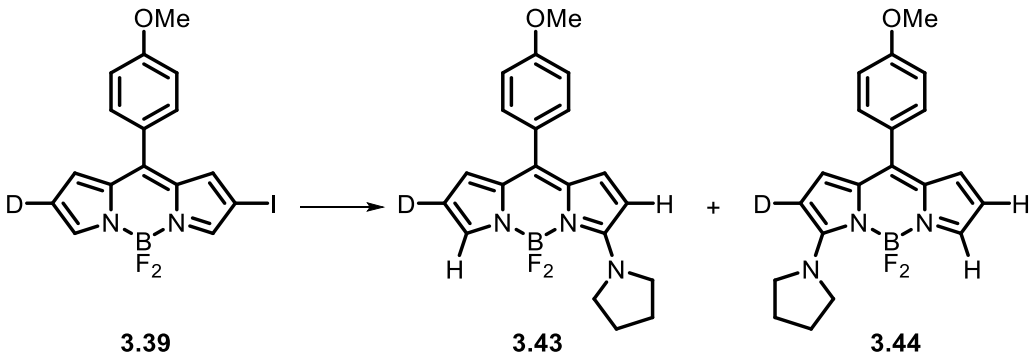

Scheme 3.28: Synthesis of 3-amino-6-deuterioBODIPY **3.43**. Conditions and reagents; pyrrolidine (2.0 rq), CuI (5 mol%), 1,10-phenanthroline **L4** (20 mol%), Cs_2CO_3 (2.0 rq), DMF, 80℃, 24 h (95%; **3.43:3.44** = 70:30).

The ratio of regioisomeric mono-duterated aminoBODIPYs **3.43** and **3.44** was measured by ^{1}H NMR integration of the 2-H signal at δ 6.06 ppm (0.7 H) which indicates 30% deuteration at the 2-position (Figure 3.11). Likewise, integration of the resonance at δ 6.79 ppm (1.3 H for 5-H and 5′-H) indicates 70% deuteration at the 5-position.

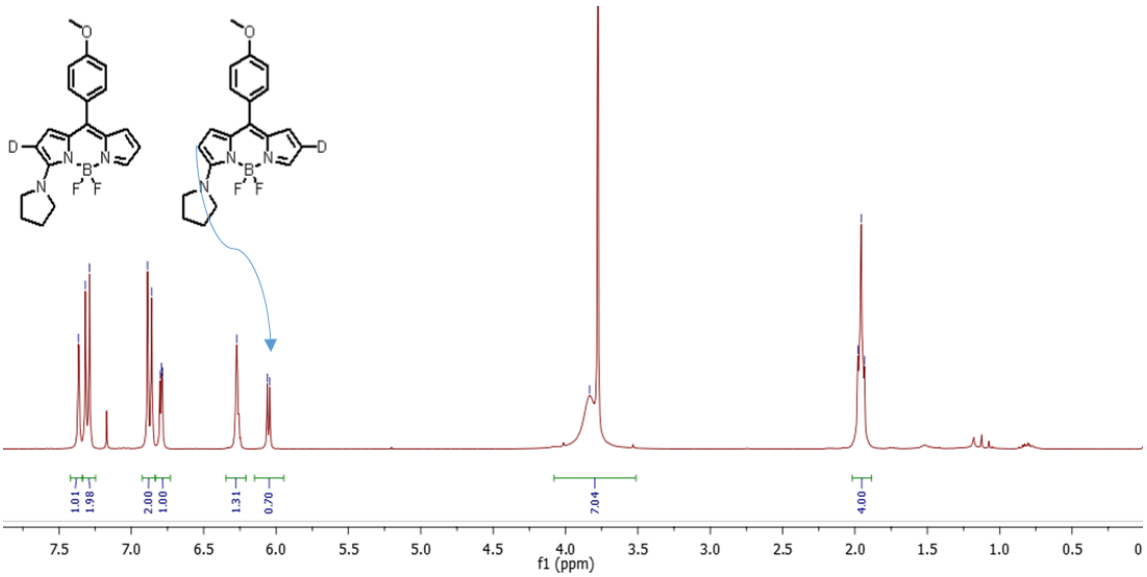

Figure 3.11: ^{1}H NMR spectrum of a mixture of amino-6-deuterioBODIPY **3.43** and **3.44** (500 MHz, $CDCl_3$).

Formation of 3-amino-6-deuterioBODIPY **3.43** as the major product is consistent with the straightforward nucleophilic substitution mechanism involving attack at C-3 (as shown in Scheme 3.21), but the presence of the regioisomeric 2-deuteriated product **3.44** indicates a minor pathway involving nucleophilic attack by the amine at C-5 in the iodoBODIPY **3.39**. The unequal ratio of products **3.43:3.44** rules out any mechanisms involving prior dehalogenation to produce the unsubstituted BODIPY **3.45** in situ (Scheme 3.29).

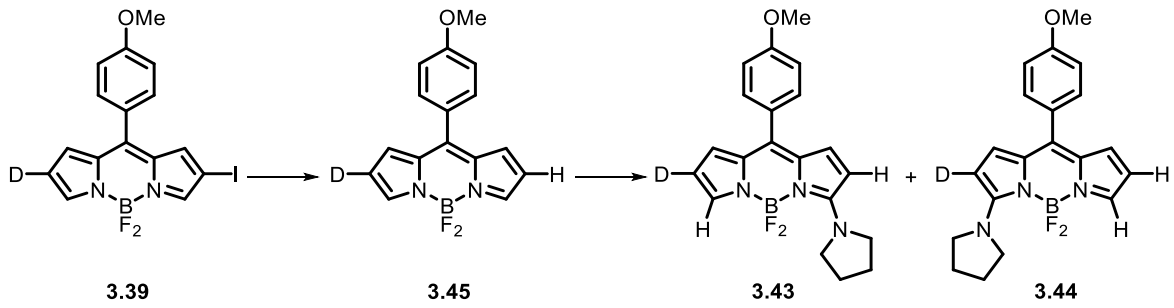

Scheme 3.29: Possible mechanistic pathway involving prior dehalogenation of BODIPY **3.39**.

Although synthesis of 3-aminoBODIPYs was successful, due to the failure to form 2-aminoBODIPYs via copper catalysed amination, we decided to attempt the synthesis of 2-aminoBODIPYs by using palladium catalysed Buchwald-Hartwig amination.

3.10. Palladium catalysed amination of aryl halides

Buchwald-Hartwig cross coupling is a reaction between aryl halides or trifluoromethanesulfonates and amines in the presence of a palladium catalyst and base to synthesise the corresponding aryl amines. In 1983, Migita and co-workers reported the first palladium catalysed formation of aryl C-N bonds.[134]

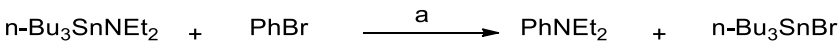

Scheme 3.30: First palladium catalysed amination. Conditions and reagents: a) PhBr (1 eq), Bu_3SnNEt_2 (1.5 eq), $PdCl_2(o\text{-tolyl}_3P)_2$ (0.01 eq), toluene, 100 ℃, 3 h.

In 1995, Buchwald developed a new catalytic procedure based on Migita's amination method.[135] The main disadvantage of these early methods is that both methods used a stoichiometric amount of heat and moisture sensitive tributyltin amides as coupling reagent. In 1995, Hartwig[136] and Buchwald[137] concurrently discovered that the amination can occur by replacing a toxic aminotin species with the free amine if one uses a strong hindered base such as sodium *tert*-butoxide, which formed the corresponding sodium amide in situ by deprotonating the palladium-coordinated amine.

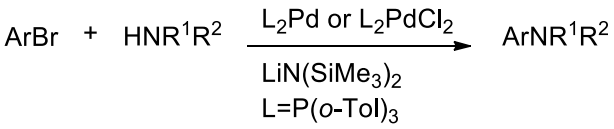

Scheme 3.31: General equation for formation of arylamines by using Pd catalyst.

As shown in Figure 3.12 the initial step in catalytic cycle of Buchwald reaction is generating the LnPd(0) catalyst in situ which can readily undergo an oxidative addition into the carbon-halogen bond of the aryl halide substrate to give an ArPdXL complex.[41] The amine nucleophile then coordinates to Pd(II) and is subsequently deprotonated by the base. The final step in the Buchwald catalytic cycle is reductive elimination, forming the amino aryl product and regenerating the active catalyst.[138]

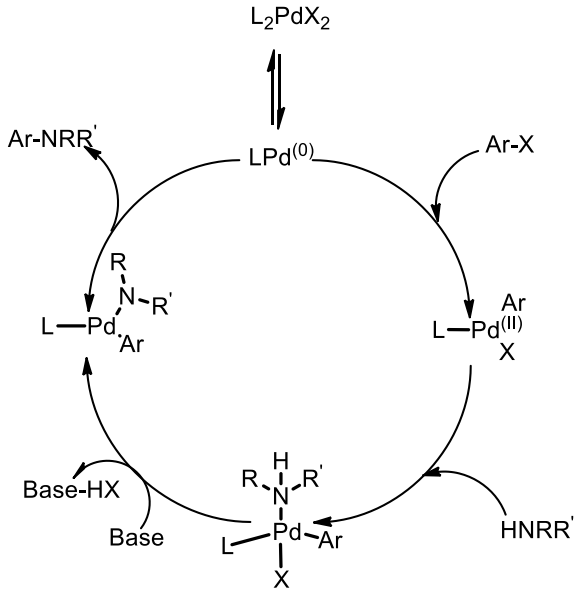

Figure 3.12: Buchwald-Hartwig Amination Reaction Mechanism.[138]

As mentioned previously (section 3.1), Hiroto[108] and his group prepared 2-amino-8-mesityl BODIPY **3.10** via palladium-catalysed imination of 2-bromoBODIPY **3.8** with benzophenone imine to form an imino BODIPY followed by hydrolysis with aqueous HCl.[108]

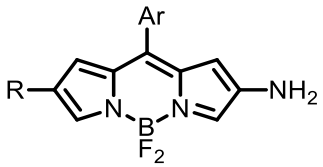

3.10

Ar= mesityl **3.10a** R= H
3.10b R= 4-nitrophenyl

We modified Hiroto's procedure[108] by using an amine instead of benzophenone imine in order to produce 2-aminoBODIPYs. We attempted to synthesise 2-aminoBODIPY **3.46** following Hiroto's conditions, 1.5 equivalents of *p*-toluidine were added to the 2-iodoBODIPY **3.17** in the presence of Xantphos, $Pd_2(dba)_3$-$CHCl_3$ and Cs_2CO_3 in 1,4-dioxane at 95℃ for 16 h (Scheme 3.32). TLC analyses of the reaction indicated a complex mixture of products, including unreacted starting material. There was no sign of the desired 2-aminoBODIPY in the ^{1}H NMR spectrum of the crude material.

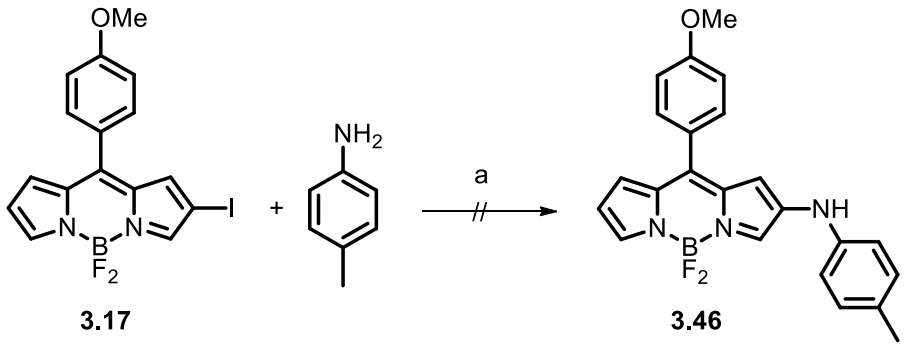

Scheme 3.32: Attempted amination of 2-iodoBODIPY **3.17**. Conditions and reagents: a) $Pd_2(dba)_3.CHCl_3$ (20 mol%), Xantphos (40 mol%), Cs_2CO_3 (1.7 equivalents), 1,4-dioxane, 95℃, 16 h.

Due to the failure of the reaction between *p*-toludine and 3,5-unsubstituted BODIPY **3.17**, we decided to synthesise a BODIPY **3.50** in which the 1, 3, 5 and 7 positions are blocked by substitutions, followed by iodination and then amination. Two different routes to synthesis of 2-iodoBODIPY **3.50** were investigated as shown in Scheme 3.33.

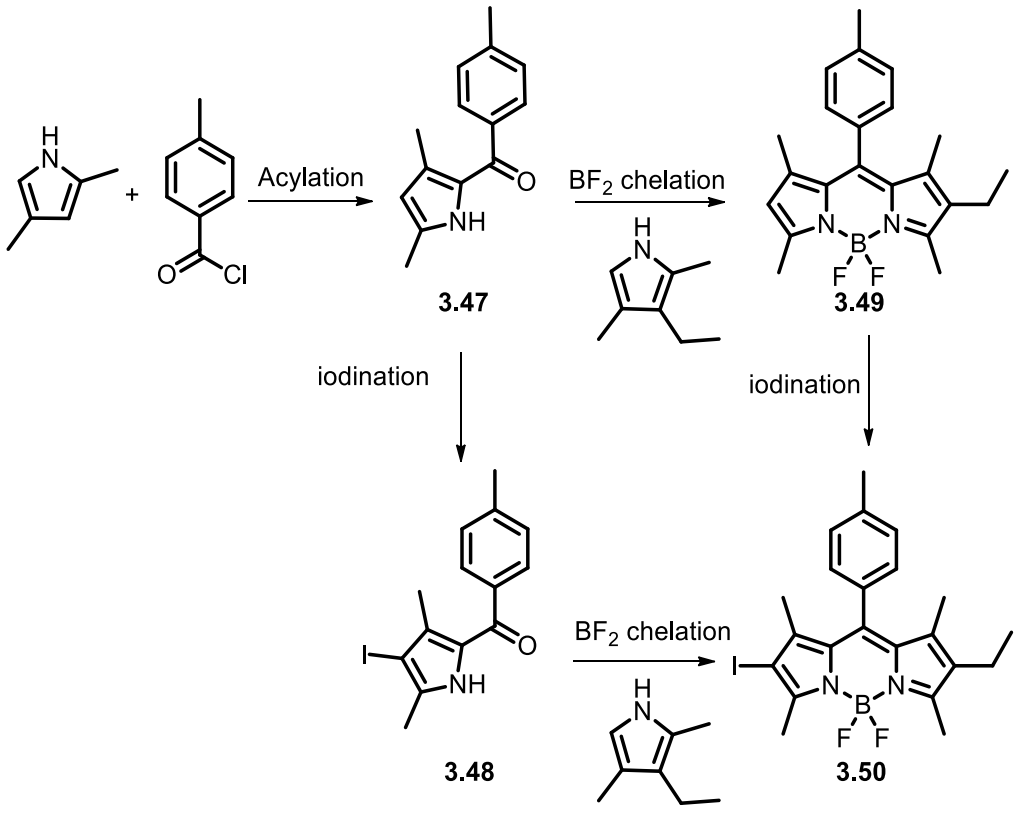

Scheme 3.33: Synthetic approaches to the synthesis of 2-iodoBODIPY **3.50**.

3.11. Synthesis of a 2-iodoBODIPY 3.50

The initial step in the synthesis of fully blocked BODIPY **3.50** was the synthesis of 2-ketopyrrole **3.47**. Following a literature procedure,[51] deprotonation of 2,4-dimethylpyrrole by MeMgBr as a base followed by selective C-2 acylation with *p*-toluoyl chloride produced the 2-ketopyrrole **3.47** in 40% yield (Scheme 3.34).

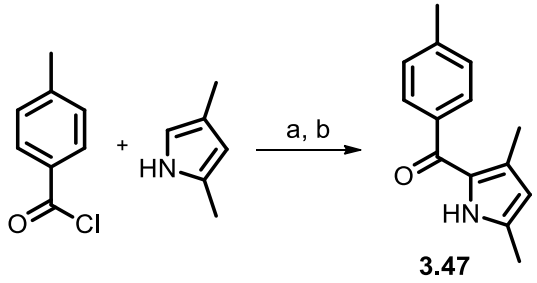

Scheme 3.34: Synthesis of 2-ketopyrrole **3.47.** Conditions and reagents; a) THF, MeMgCl (1.1 eq), reflux, 1 h. b) *p*-toluoyl chloride (1.3 eq), r.t., 24 h, 40%.

In order to increase the reaction yield and reduce the reaction time we followed the Min Ji procedure for Friedel-Crafts acylation of 2,4-dimethylpyrrole with *p*-toluoyl chloride in the presence of ZnO to produce 2-acylpyrrole **3.47** in an improved yield of 55% (Scheme 3.35).

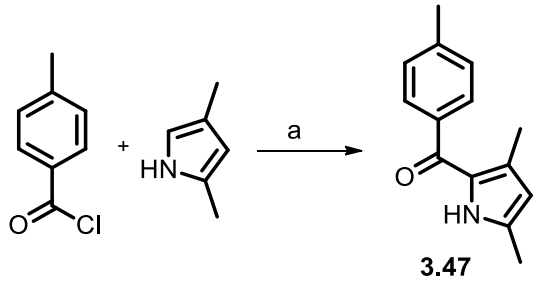

Scheme 3.35: Synthesis of 2-ketopyrrole **3.47**. Conditions and reagents; a) ZnO (25 mol%), r.t., 5 h, 55%.

The next step, electrophilic iodination of 2-ketopyrrole **3.47** was be anticipated to be straightforward as just one reactive site is available to be iodinated. 3-Iodo-2-ketopyrrole **3.48** was synthesised in excellent yield by treating 2-ketopyrrole **3.47** with *N*-iodosuccinimide in DCM (Scheme 3.36).

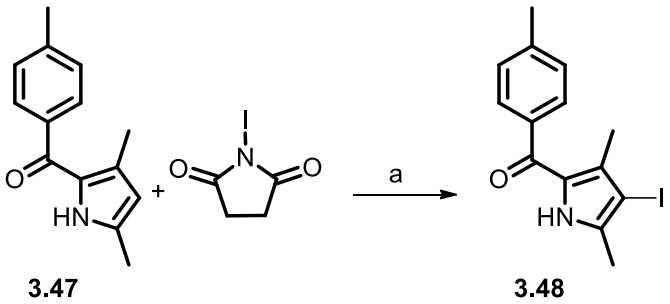

3.47 3.48

Scheme 3.36: Synthesis of 3-iodo-2-ketopyrrole **3.48**. Conditions and reagents; a) NIS (1.1 eq), DCM, r.t., 2 h, 98%.

Condensation of the 3-iodo-2-ketopyrrole **3.48** with 3-ethyl-2,4-dimethylpyrrole in the presence of borontrifluoride etherate as catalyst to form the intermediate dipyrromethene was followed by in situ conversion to the BODIPY **3.50** by further treatment with borontrifluoride etherate and Hünig's base. Purification using column chromatography gave the desired 2-iodoBODIPY **3.50** in 50%, together with the dehalogenated BODIPY **3.49** in 30% (Scheme 3.37).

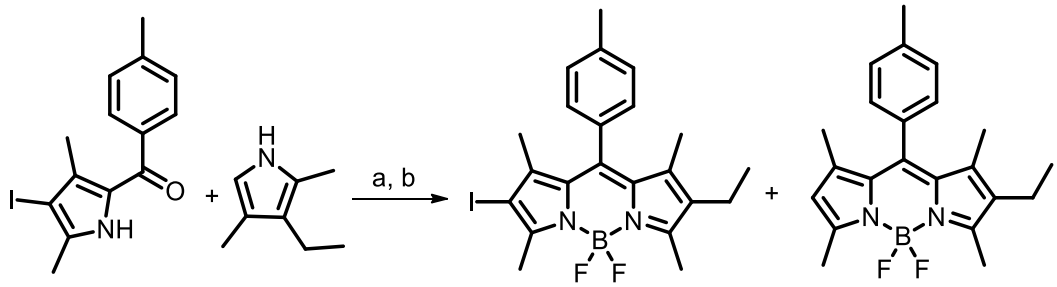

3.48 3.50 3.49

Scheme 3.37: Synthesis of 2-iodoBODIPY **3.50**. Conditions and reagents; a) 3-ethyl-2,4-dimethylpyrrole, $BF_3.OEt_2$, DCM, r.t., 2 h; b) $BF_3.OEt_2$, i-Pr_2NEt, CH_2Cl_2, r.t., 4 h, (**3.50**, 50%, **3.49**, 30%).

The synthesis of 2-iodoBODIPY **3.50** was successful, however, due to difficulties in the separation of the product **3.50** and the deiodinated BODIPY **3.49** which have a very close R*f* values on TLC we decided to synthesise 2-iodoBODIPY **3.50** by using a modified route. The second route involved the synthesis of the unhalogenated BODIPY **3.49** followed by electrophilic iodination with *N*-iodosuccinimide to give the iodoBODIPY **3.50**.

BODIPY **3.49** was prepared according to a previous procedure[139] by BF_3 mediated condensation of the ketopyrrole **3.47** and dimethylethylpyrrole followed by further treatment with borontrifluoride etherate and Hünig's base (Scheme 3.38).

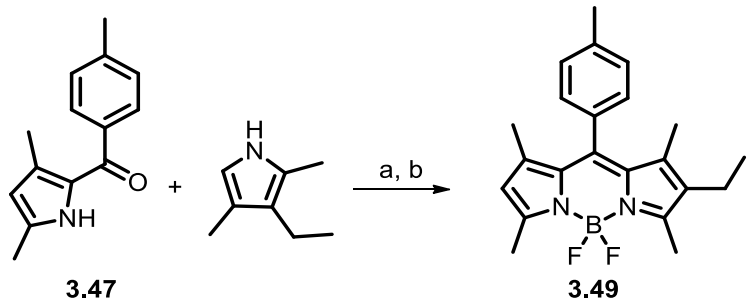

3.47 **3.49**

Scheme 3.38: Synthesis of BODIPY **3.49**. Conditions and reagents; a) 3-ethyl-2,4-dimethylpyrrole, $BF_3.OEt_2$, DCM, r.t., 2 h; b) $BF_3.OEt_2$, i-Pr_2NEt, CH_2Cl_2, r.t., 4 h, 86%.

Using a literature procedure,[140] the 2-iodoBODIPY **3.50** was then prepared by reaction of the BODIPY **3.49** with NIS in DCM at room temperature for 4 h (Scheme 3.39). Purification by column chromatography gave the desired 2-iodoBODIPY **3.50** in high yield (80%).

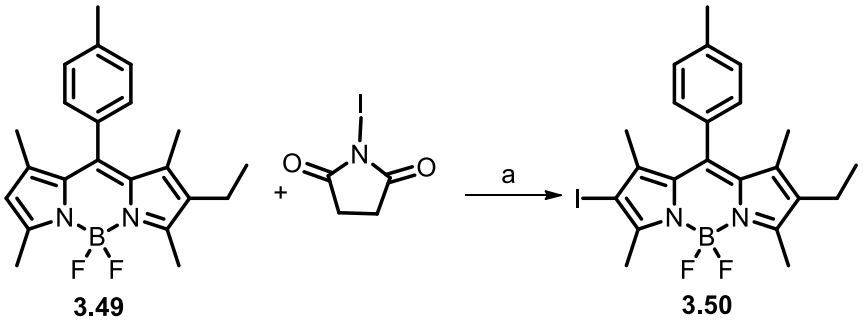

3.49 **3.50**

Scheme 3.39: Synthesis of 2-iodoBODIPY **3.50**. Conditions and reagents; a) NIS (1.1 eq), DCM, r.t., 4 h, 80%.

3.12. Synthesis of 2 aminoBODIPYs via Palladium catalysed amination

Our initial attempt to form a 2-aminoBODIPY from the 2-iodoBODIPY **3.50** was by modifying Hiroto's and Shinokubo's procedure[108] (as detailed previously). Much to our delight we indeed observed formation of the 2-aminoBODIPY **3.51** upon stirring the fully blocked BODIPY **3.50** with 4-methoxyaniline in the presence of Xantphos, Pd_2dba_3-$CHCl_3$ and Cs_2CO_3 in 1,4-dioxane at 95℃ for 16 h, however, the yield was moderate (36%) (Scheme 3.40). This model system was then optimized with respect to the influence of different ligands **L5-L8**, Pd sources, bases and temperature.

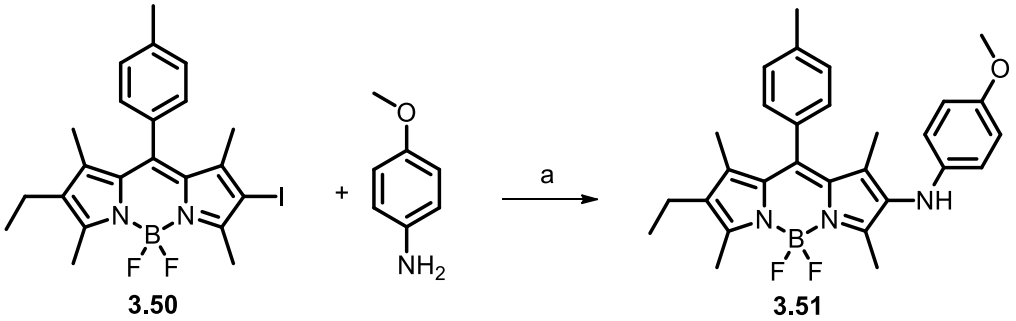

Scheme 3.40: Amination of 2-iodoBODIPY **3.50**. Conditions and reagents; $Pd_2dba_3.CHCl_3$ (20 mol%), Xantphos (1.1 mol per mol Pd), Cs_2CO_3 (1.7 eq), 1,4-dioxane, 95℃, 16 h, 36%.

3.12.1 Screening of the ligand

In general, the key features of Buchwald amination cross coupling mechanism are; the activation of the catalyst, oxidative addition, transmetalation and reductive elimination. The role of the ligands in Pd-catalysed C-N cross coupling reactions are summarized in Table 3.6.[141]

Table 3.6: the catalytically active species in Buchwald amination reactions

Step of catalytic cycle	Roles of ligands
Preactivation	Generation of LnPd(0)catalyst and protection of Pd(0) from deactivation
Oxidative addition	Promotion of oxidation addition is essential for less reactive substrates
Reductive elimination	Required to remove the product from the coordination shell of Pd

As Table 3.6 illustrates, the catalytically active species in Buchwald amination reactions is the LnPd(0) species, with Pd in the zero oxidation state.[141] Most catalysts will require activation to form LnPd(0) species in solution before entering the catalytic cycle. Therefore, Pd-catalysed C-N cross-coupling is controlled by ligand design. To date there have been a huge number of ligands used for Buchwald amination reactions such as diphosphines and biphenylmonophosphine ligands.

Buchwald reported that the combination of BINAP as a ligand and $Pd_2(dba)_3$ in the presence of NaOtBu as a base formed an efficient catalyst system for the cross-coupling of amines with aryl bromides (Scheme 3.41).[142]

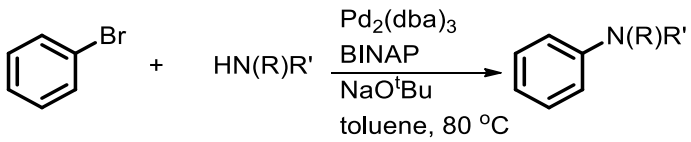

Scheme 3.41: General scheme for amination using BINAP as ligand.[142]

Buchwald has developed a range of bulky dialkyl biarylmonophosphines for palladium catalysed coupling reactions, including amination.[143–145] The particular features of these ligands, typified by XPhos (**L7**) and SPhos (**L8**), are: the electron-rich nature promotes oxidative addition of challenging substrates, such as aryl chlorides; the large steric bulk of the ligands accelerates reductive elimination and also promotes formation of the monoligated. $L_1Pd(0)$ species; and a weak interaction between the metal and the second ring of the biaryl unit stabilises the low-coordinate metal species.

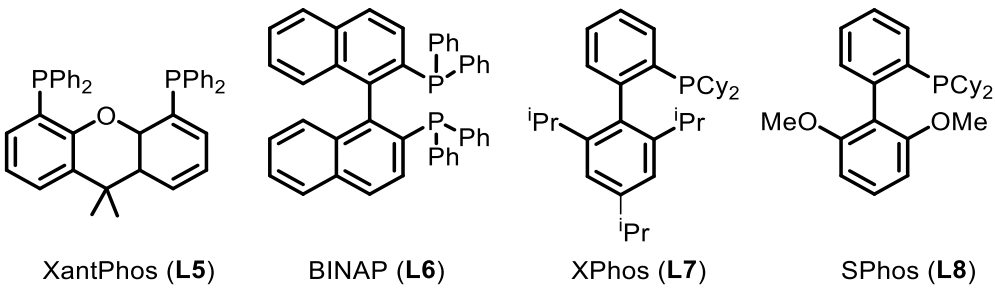

Figure 3.13: Ligands screened in the Buchwald amination of BODIPY **3.50**.

We started with the ligand screening of **L5-L8** (Figure 3.13) using 4-methoxyaniline. Figure 3.14 shows the results of the amination of the 2-iodoBODIPY **3.50**. The choice of solvent, base, temperature (110℃), Pd source and its loading were taken from Hiroto's

and Shinokubo's report using XantPhos **L5** as ligand. As mentioned earlier, $Pd_2(dba)_3$ together with XantPhos formed 2-aminoBODIPY **3.51** in a moderate yield of 36% (Figure 3.14). While using *rac*-BINAP **L6** as ligand reduced the yield of the product **3.50** to 5% (Figure 3.14). The use of the biphenyl derivatives with bulky alkyl groups at phosphorus, XPhos **L7** and SPhos **L8**, produced much improved product yields (71% and 80% respectively) (Figure 3.14). We further optimized the reaction condition by varying the Pd source.

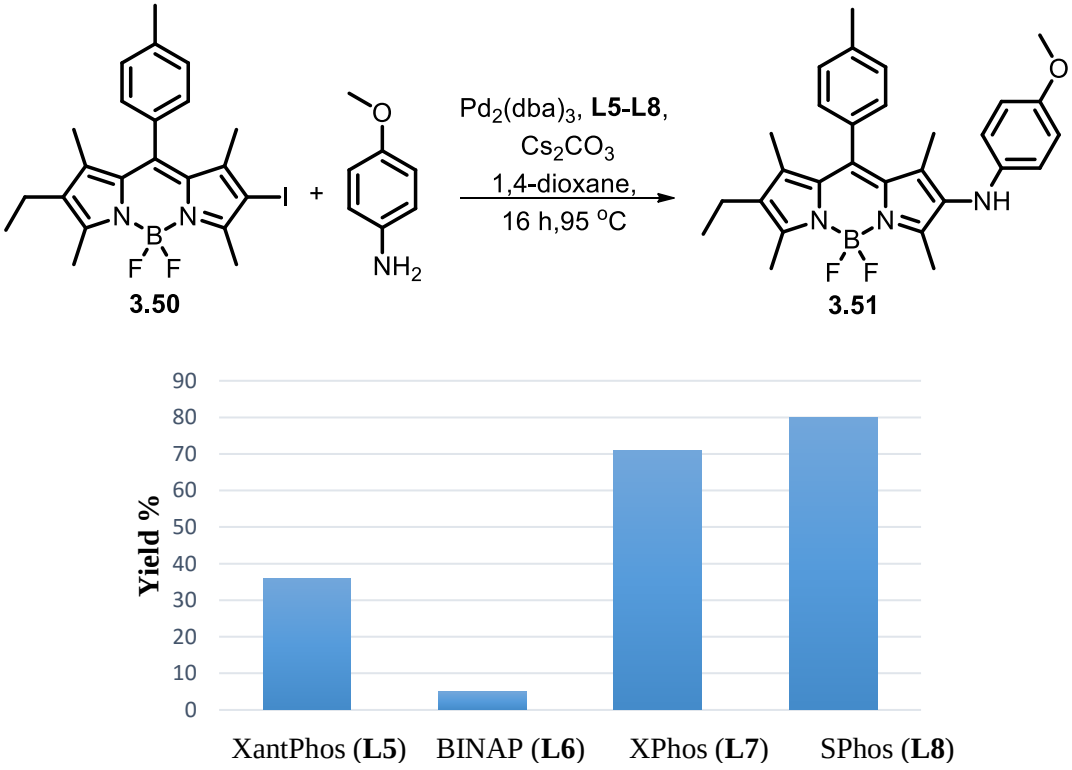

Figure 3.14: Ligand effects in the palladium-catalysed amination of 2-iodoBODIPY **3.50**. Conditions and reagents: BODIPY **3.50** (0.23 mmol), 4-$MeOC_6H_4NH_2$ (1.01 mmol), $Pd_2(dba)_3$ (10 mol%), ligand **L5-L8** (1.1 mol per mol Pd), Cs_2CO_3 (0.35 mmol), 1,4-dioxane (2 mL), 95 ℃, 16 h.

3.12.2 Screening of Pd source

In general, the activation of catalysts takes place as impulsive coordination transformations using either $Pd(OAc)_2$ or $Pd_2(dba)_3$ as the palladium source.[146] This activation can either be through a reduction step if the palladium source is in the +2 oxidation state, such as $Pd(OAc)_2$ or through ligand dissociation if the palladium source is already in the zero oxidation state, such as $Pd_2(dba)_3$.

In recent years, there has been an increasing interest in the development of a new series of Pd(I) and Pd (II) precatalysts[147,148] which are stable and which release monoligated

Pd(0) by simple procedures. In 2008, Buchwald and his group[149] developed a new class of Pd precatalysts such as **3.52** that are useful for Suzuki cross coupling of aryl chlorides.

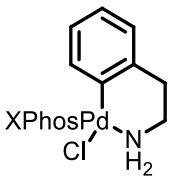

3.52

However, it is obtained in several steps. Moreover, the activation of this precatalyst with weak bases is slow and occurs only at high temperatures. Buchwald[148] subsequently developed precatalyst (XPhosPdCl) **3.53**, its activation with weak base occurs at room temperature and it is easily synthesised in one pot reaction as shown in Scheme 3.42. This precatalyst is useful for the fast and efficient Suzuki coupling reaction of unstable boronic acids.

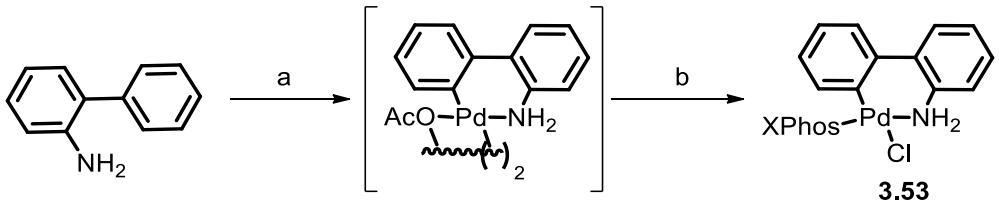

3.53

Scheme 3.42: Synthesis of Precatalyst **3.53**, Conditions and reagents: a) $Pd(OAc)_2$, toluene, 60℃, b) LiCl, acetone, r.t., then XPhos, r.t., 83%.[148]

However, this type of precatalyst (**3.53**) cannot be generated with larger ligands such as BrettPhos and *t*BuXphos. Moreover, these precatalysts are not stable in solution for long periods of time. In 2013, Buchwald designed and synthesised the μ-OMs dimer[88] (LPdOMs) (**3.54**) from commercially available 2-aminobiphenyl and treated this with different ligands to afford the corresponding precatalysts.[88]

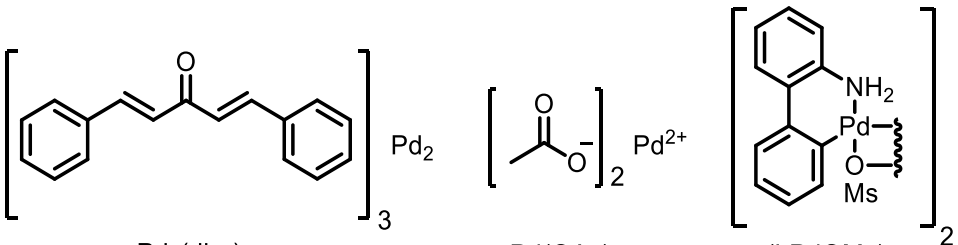

$Pd_2(dba)_3$ $Pd(OAc)_2$ $(LPdOMs)_2$

3.54

Figure 3.15: Pd sources screened in the Buchwald amination of BODIPY **3.50**.

As shown in Figure 3.16, the yield of the 2-aminoBODIPY **3.50** dropped to 19% from 80% due to changing the Pd source from $Pd_2(dba)_3$ to $Pd(OAc)_2$. However, the use of the μ-OMs dimer $(LPdOMs)_2$ **3.54** produced an excellent yield of the 2-aminoBODIPY **3.50** (96%). Therefore, the combination of μ-OMs dimer $(LPdOMs)_2$ **3.54** (10 mol%) and SPhos **L8** in presence of Cs_2CO_3 in dioxane at 95℃ was optimal.

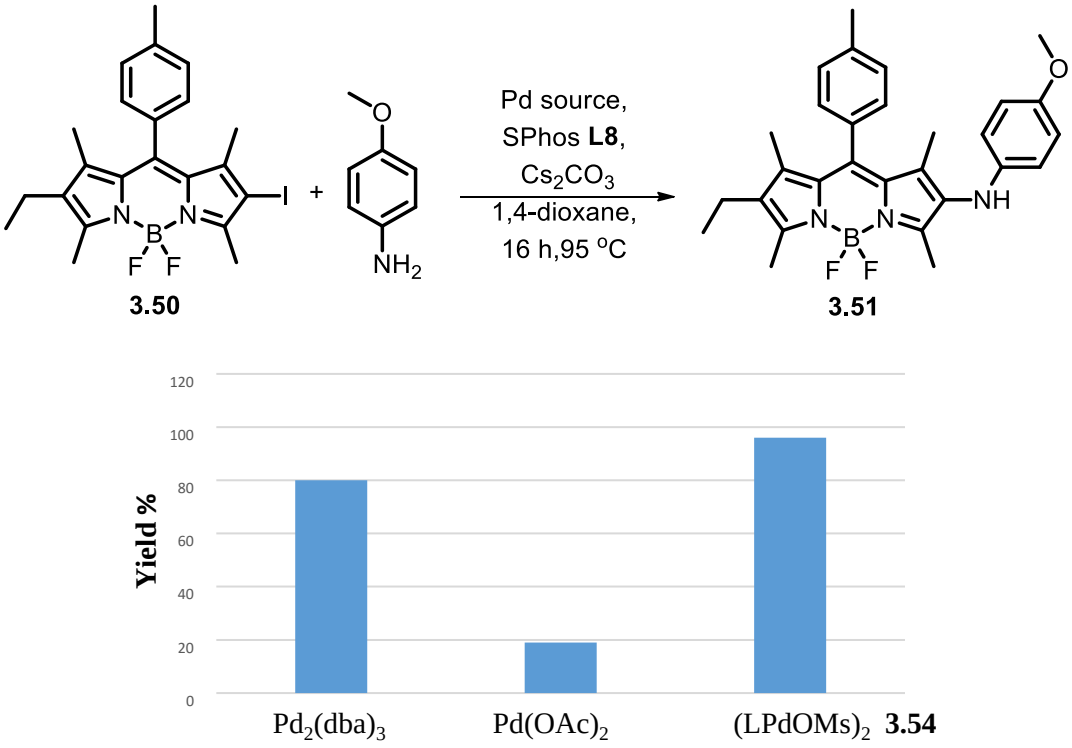

Figure 3.16: Pd source effects in the palladium-catalysed amination of 2-iodoBODIPY **3.50**. Conditions and reagents: BODIPY **3.50** (0.23 mmol), 4-$MeOC_6H_4NH_2$ (1.01 mmol), Pd source (10 mol%), SPhos **L8** (1.1 mol per mol Pd), Cs_2CO_3 (0.35 mmol), 1,4-dioxane (2 mL), 95 ℃, 16 h.

It was then shown (Table 3.7) that a reduction of the palladium loading from 10 mol% down to 1.2 mol% resulted in a slight drop in yield (from 96% to 81%, entries 1–4) but further reduction to 0.5 mol% and 0.1 mol% was unsuccessful (entries 5,6).

Table 3.7: Pd source loading effects in the palladium-catalysed amination of 2-iodoBODIPY **3.50**.

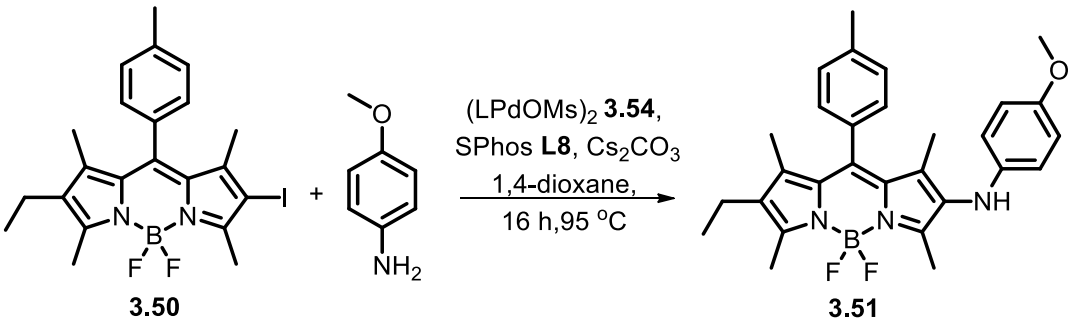

Entry	%Pd	Yield%
1	10	96
2	5	94
3	2.5	92
4	1.2	81
5	0.5	10
6	0.1	No reaction

Conditions and reagents: BODIPY **3.50** (0.23 mmol), 4-$MeOC_6H_4NH_2$ (1.01 mmol), $(LPdOMs)_2$ **3.54** (10-0.1mol%), SPhos **L8** (1.1 mol per mol Pd), Cs_2CO_3 (0.35 mmol), 1,4-dioxane (2 mL), 95 ℃, 16 h.

3.12.4 Screening of base and temperature

We further optimized the reaction conditions by varying base and temperature. On examining the effect of changing the base to K_3PO_4 a decrease in the yield was observed, to 60% compared to the 82% on using Cs_2CO_3. However, on employing KF the reaction did not proceed (Table 3.8).

Table 3.8: Base effects in the palladium-catalyzed amination of 2-iodoBODIPY **3.50**.

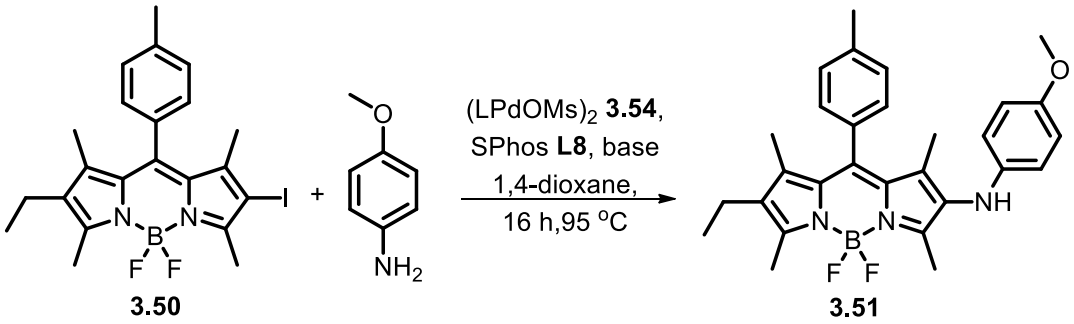

Entry	Base	Yield%
1	Cs_2CO_3	80
2	K_3PO_4	60
3	KF	No reaction

Conditions and reagents: BODIPY **3.50** (0.23 mmol), 4-$MeOC_6H_4NH_2$ (1.01 mmol), $(LPdOMs)_2$ **3.54** (1.2mol%), SPhos **L8** (1.1 mol per mol Pd), base (0.35 mmol), 1,4-dioxane (2 mL), 95 ℃, 16 h.

The effect of the reaction temperature on the yield of the 2-aminoBODIPY **3.51** was studied in the temperature range 20 to 95℃. Figure 3.17 shows that the percentage yield of the 2-aminoBODIPY **3.50** decreased with decrease in the reaction temperature from 95 to 20℃.

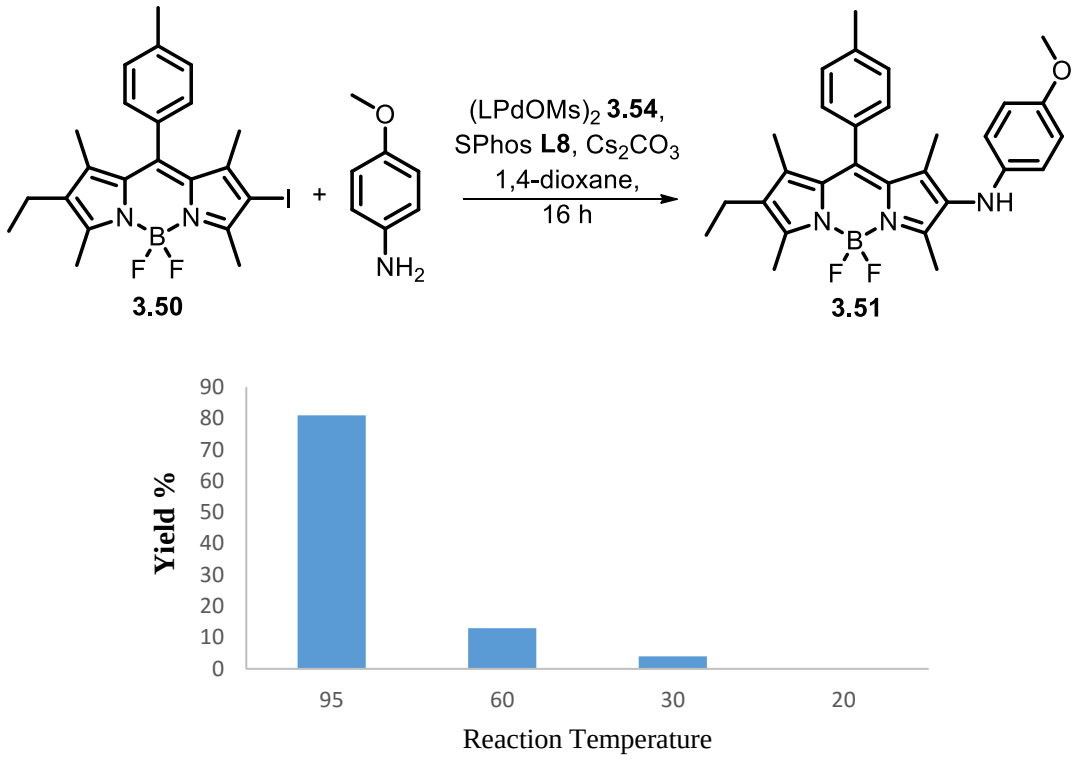

Figure 3.17: Reaction temperature effects in the palladium-catalyzed amination of 2-iodoBODIPY. Conditions and reagents: BODIPY **3.50** (0.203 mmol), 4-$MeOC_6H_4NH_2$ (1.01 mmol), $(LPdOMs)_2$ **3.54** (1.2 mol%), SPhos **L8** (1.1 mol per mol Pd), Cs_2CO_3 (0.345 mmol), 1,4-dioxane (2 mL), 20-95 ℃, 16 h.

Overall, after screening of different ligand, Pd sources, bases and reaction temperatures, the combination of SPhos **L8** as a ligand, μ-OMs dimer $(LPdOMs)_2$ **3.54** (1.2 mol%), Cs_2CO_3 as a base and 1,4-dioxane as a solvent at 95℃ for 16 h was an efficient system for the Buchwald amination of the 2-iodoBODIPY **3.50**. These conditions were applied to the reaction of the 2-iodoBODIPY **3.50** with a range of amines (Figure 3.18).

3.12.5. Scope of the amination of the 2-iodoBODIPY 3.49

Having established the optimized reaction conditions, the scope of the Buchwald-coupling was then explored by using a series of different amines. As shown in Figure 3.18, the aniline with electron donating substituents afforded the desired products (**3.51** and **3.57**) in excellent yield. Also, good yields were obtained even with anilines with electron withdrawing substituents (**3.55**, **3.56**) and the sterically hindering substituents (**3.57**). However in the case of a primary alkylamine (n-hexylamine), the yield obtained was low (**3.58**), and attempts to use secondary alkyl amines (pyrrolidine and morpholine) were unsuccessful.

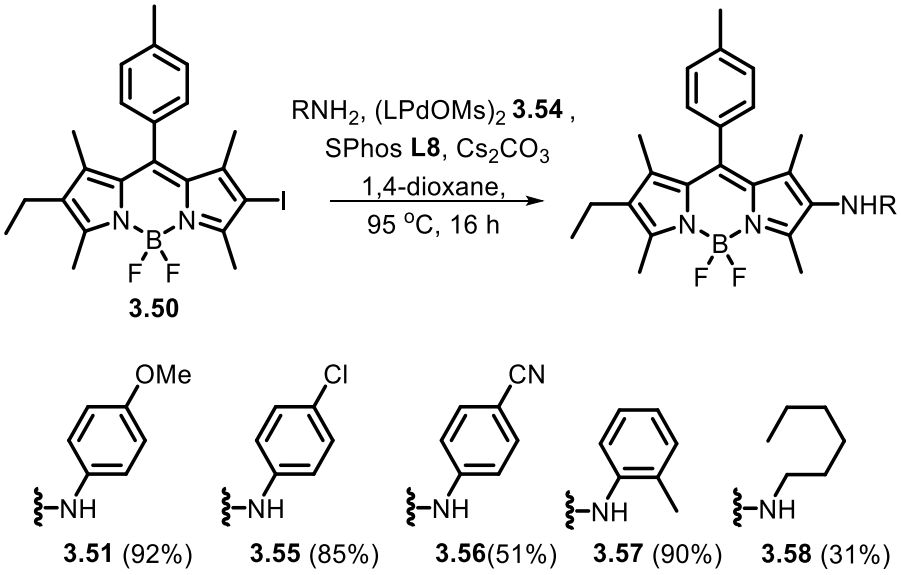

Figure 3.18: Amination of 2-iodoBODIPY **3.50**. Conditions and reagents: BODIPY **3.50** (0.23 mmol), amine (1.01 mmol), $(LPdOMs)_2$ **3.54** (1.2 mol%), SPhos **L8** (1.1 mol per mol Pd), Cs_2CO_3 (0.345 mmol), 1,4-dioxane (2 mL), 95 ℃, 16 h.

3.13. Spectroscopic properties

3.13.1. Photophysical properties of the 3-aminoBODIPYs

One of the features of BODIPY compounds is that structural modifications may be easily made, which affords additional opportunities to vary their optical properties. In reviewing the literature, most simple BODIPY derivatives display a strong absorption band at 530 (± 20 nm) and weaker absorption bands (around 350 nm) with sharp and narrow bands in the absorption spectra. However, the absorption maxima of substituted BODIPY's are strongly affected by the electronic nature of the substituents.[104]

Moreover, the intensity of fluorescence of substituted BODIPYs can be affected by a wide variety of processes.[150-151] For instance, photoinduced electron transfer (PeT) often results in fluorescence quenching due to an attached electron donor substituent,[12] an example is shown below (Figure 3.19).

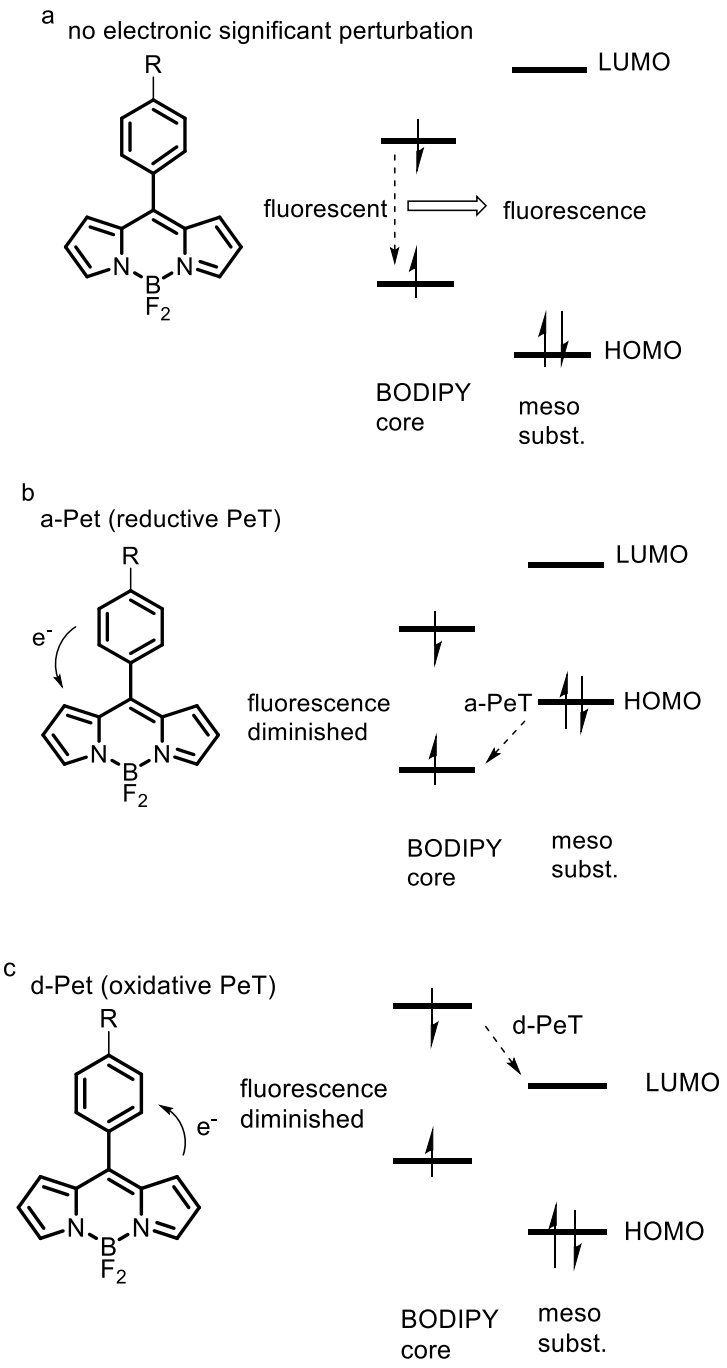

Figure 3.19: Electron Transfer: energy level diagram.[12]

In general, when the BODIPY acts as the electron acceptor, the HOMO of the BODIPY should be lower than the HOMO of the donor (such as an amine group) so that an electron from the donor can be transferred to the BODIPY and fill its singly occupied HOMO resulting in fluorescence quenching and a weakly fluorescent or nonfluorescent BODIPY.[16]

However, coordination of the electron donor group to the analyte may stabilise and lower its HOMO energy below that of the BODIPY HOMO and thus electron transfer is reduced and fluorescence is turned on.[16]

Figure 3.20 illustrates a specific example in which the 8-substituted bodipy **3.59**[152] is used as photoinduced electron transfer (PET) fluorescence sensor for Zn^{2+}. The lone pair of the electrons on the amine quenches the fluorescence of the excited state in the free BODIPY **3.59**. However, addition of zinc ions disrupts the PeT quenching due to coordination of the lone pair with the metal.[152]

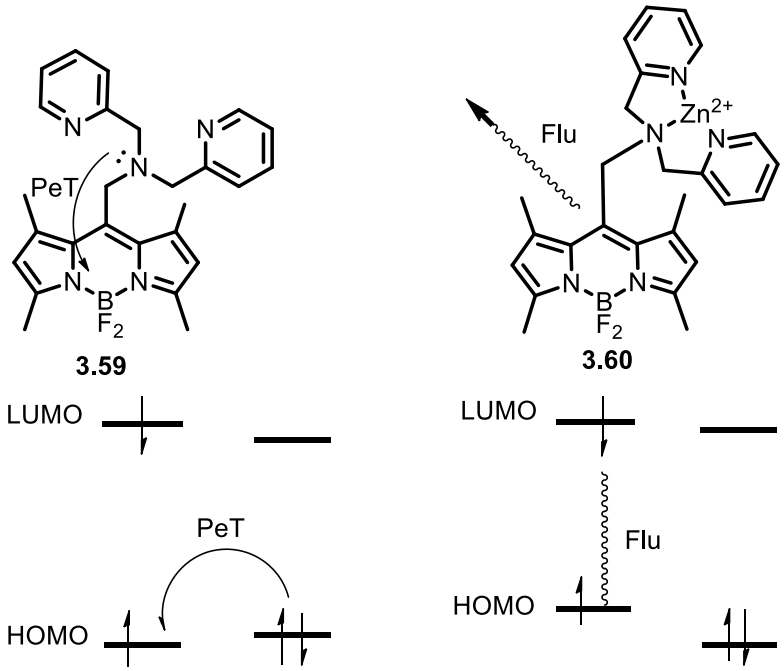

Figure 3.20: An example of a BODIPY-based Zn^{2+} switch, which works by fluorescent quenching *via* a photoinduced electron transfer.[152]

A decrease in fluorescence is often observed in the presence of heavy atom substituents on a BODIPY core (e.g. I, Br) because heavy atoms increase the possibility of intersystem crossing.[153]

The installation of electron-donating groups on BODIPY leads to an increase in the molar absorption coefficient and red-shift of the absorption and fluorescence spectrum and reduced quantum yield. Also, introduction of electro-donating groups generally leads to broad spectra. The presence of lone pairs of electrons on the nitrogen or oxygen atoms does not change the π-π^* nature of the transitions of the parent BODIPY, but they may be involved directly in π bonding with the BODIPY system. The photophysical properties

of 3-amino-substituted BODIPYs have previously been reported in detail.[56,107,108,122,154–168]

The photophysical properties of non-aminated BODIPY **3.16** and 3-aminoBODIPY derivatives were measured in THF at room temperature (Table 3.9). Rhodamine 6G was used as the reference compound, for determination of fluorescence quantum yields (rhodamine 6G Φ_f= 0.95, λ_{ex}= 470-510 nm, in ethanol).[169]

Table 3.9: Absorption and fluorescence data for compounds **3.16**, **3.19a-n** in THF.

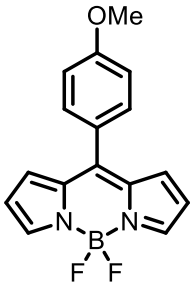

3.16

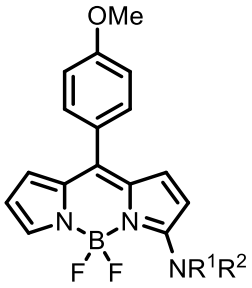

3.19

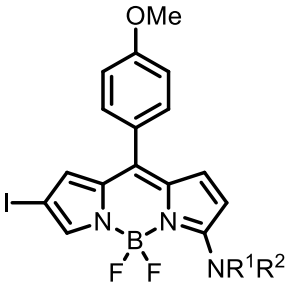

3.22

BODIPY	R^1	R^2	λ_{abs} (max) /nm	$\varepsilon/10^4$ M^{-1} cm^{-1}	λ_{em} (max) /nm	Φf (λex)
3.16	-		494	4.59	508	0.075(479)
3.19a	$CH_3(CH_2)_5$	H	493	3.51	525	0.026(484)
3.22a	$CH_3(CH_2)_5$	H	508	2.09	524	0.058(484)
3.19b	4-MeC_6H_4	H	500	4.34	—	—
3.19c	PhCO	H	522	4.69	534	0.050(492)
3.19d	$PhCH_2$	H	498	3.43	525	0.030(484)
3.19e	2-ThiophenylCH_2CH_2	H	496	3.09	528	0.033(485)
3.19f	Cyclohexyl	H	496	3.56	525	0.015(484)
3.19g	$O(CH_2CH_2)_2$		484	3.23	—	—
3.19h	$CH_2CH_2CH_2CH_2$		476	4.15	540	0.005(490)
3.19i	2-$MeOC_6H_4$	H	500	3.07	—	—
3.19j	4-$MeOC_6H_4$	H	501	1.99	—	—
3.19k	4-ClC_6H_4	H	508	4.53	565	0.007(475)
3.19l	4-NCC_6H_4	H	533	5.34	557	0.015(500)
3.19m	2-Pyridyl	H	527	3.44	549	0.022(497)
3.19n	Ph	Me	500	1.95	—	—

The absorption and fluorescence data for non-aminated BODIPY **3.16** and 3-aminoBODIPYs **3.19** are summarized in Table 3.9. Figure 3.21 shows the absorption and emission spectra of non-aminated BODIPY **3.16** and of 3-aminoBODIPY **3.19a** (R= n-Hex) and **3.19I** (R= 4-CNC_6H_4), with the remaining absorption spectra for **3.19b-h** and **3.19j-n** are given in the appendix.

As Table 3.9 illustrates the majority of these BODIPY dyes showed strong absorption bands. In comparison to the parent BODIPY **3.16**, the presence of an amino group at the 3 position of the BODIPY core leads to an up to 40 nm (1481 cm^{-1}) red-shift of the absorption maximum and an up to 57 nm (1986 cm^{-1}) red-shift of the emission maximum. Consistent with the literature, all of the 3-aminoBODIPY derivatives show low fluorescent quantum yield, and some are non-fluorescent. A possible explanation for this might be attributed to photoinduced electron transfer (PeT) which often results in fluorescence quenching due to the electron donating effect of the amine group.

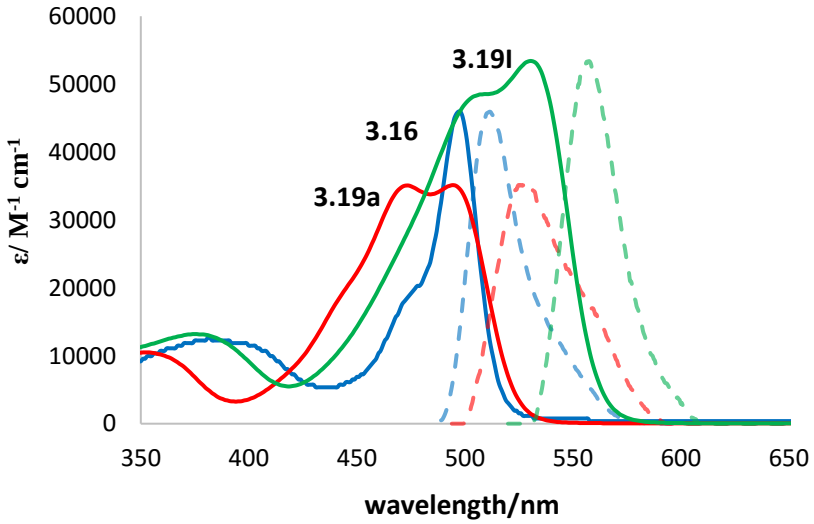

Figure 3.21: Absorption spectrum (soild lines) in terms of the molar absorption coefficient (ε) and normalised fluorescence spectrum (dashed lines) for **3.16** (—), **3.19a** (—), and **3.19I** (—) in THF.

3.13.2. Photophysical properties of the 2-aminoBODIPYs

In reviewing the literature, the photophysical properties of 2-aminoBODIPYs have not been reported in detail. Therefore, in order to understand the effect of incorporating the NH group in the 2-positon on the BODIPY fluorophore, the photophysical properties for the novel parent BODIPY **3.49** was measured. As Figure 3.22 shows, the absorption and emission spectra are sharp and narrow band.

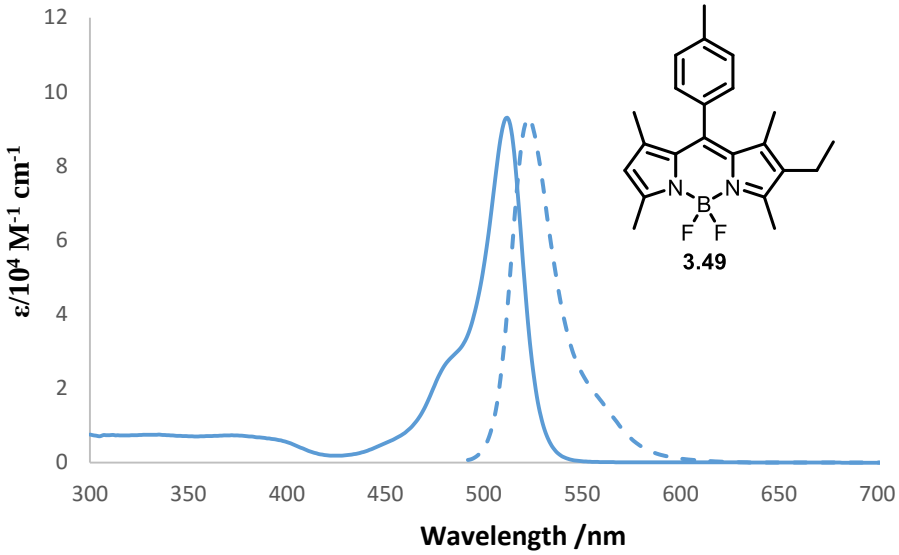

Figure 3.22: The absorption spectrum (solid line) in terms of the molar absorption coefficient (ε) and the normalised fluorescence spectrum (dashed line) of the parent BODIPY **3.49**, recorded in THF at room temperature, with an excitation wavelength of 487 nm.

The absorption and emission data for the 2-aminoBODIPY compounds and the parent unsubstituted compound **3.49** are summarized in Table 3.10.

Table 3.10: Photophysical data of the 2-aminoBODIPYs.

BODIPY	R	λ_{abs} (max)/nm	$\varepsilon/10^4$ M^{-1} cm^{-1}	λ_{em} (max)/nm	Φ_f (λ_{ex})
3.49	-	512	9.30	523	0.97(487)
3.51	4-$MeOC_6H_4$	523	1.83	-	-
3.55	4-ClC_6H_4	524	2.51	-	-
3.56	4-NCC_6H_4	520	3.60	-	-
3.57	2-MeC_6H_4	523	2.91	-	-
3.58	$CH_3(CH_2)_5$	524	2.39	-	-

The absorption spectra of 2-aminoBODIPYs **3.51** and **3.55-3.58** are represented in Figure 3.23. The majority of these BODIPY dyes showed strong absorption bands. In comparison to the parent BODIPY **3.49**, the presence of an amino group at the 2-position of the BODIPY core leads to very broad peaks, an up to 12 nm (447 cm^{-1}) red-shift of the absorption maximum and the molar absorption coefficients are lower, but still typical of BODIPY compounds (Figure 3.23).

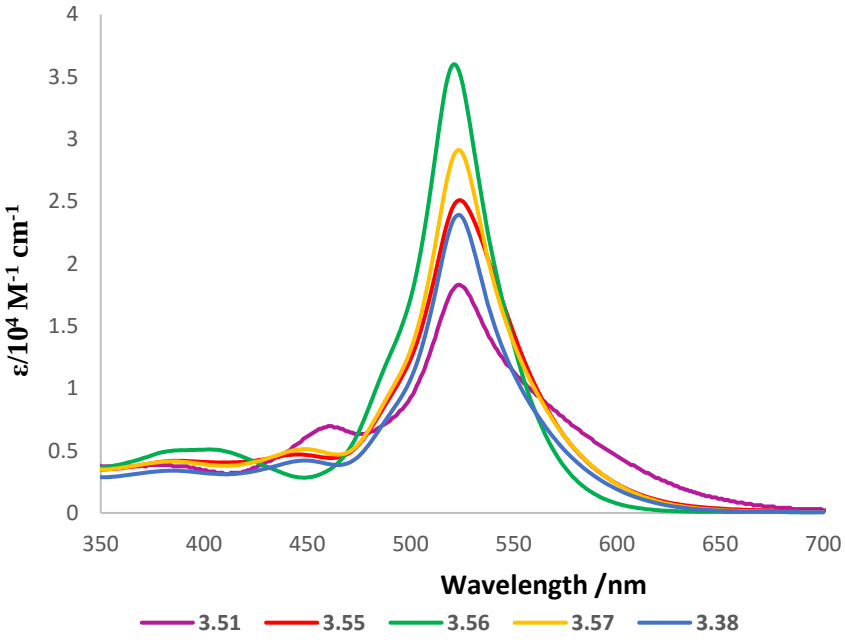

Figure 3.23: The absorption spectrum in terms of the molar absorption coefficient (ε) of the 2-aminoBODIPY **3.51** and **3.55-3.58**, recorded in THF at room temperature.

The novel 2-aminoBODIPY **3.51** and **3.55-8**, are dark purple coloured and appear to be not fluorescent during column chromatography. We attempted to measure the

fluorescence quantum yields of 2-aminoBODIPYs **3.51** and **3.55-8** in tetrahydrofuran and toluene, however, the fluorescence of 2-aminoBODIPYs **3.51** and **3.55-8** is essentially completely quenched. As discussed earlier, all of the 3-aminoBODIPYs show low fluorescent quantum yield, however incorporation of the amino group in the 2-position has an even stronger deleterious effect on the fluorescence properties of the molecules. The electron releasing capacity of the amino group at the 2-position appears to be strong enough to prompt a charge transfer state, which generally quenches the fluorescence emission.

3.13.2.1. Absorption data for 2-aminoBODIPY 3.51 (R= 4-MeOC$_6$H$_4$) in different solvents

The absorption spectra of 2-aminoBODIPY **3.51** in other solvents (Figure 3.24) are very similar to that in THF which all show two main absorption bands: (1) in the visible wavelength region, the 0-0 band of a strong S_0-S_1 transition with a maximum ranging from 520 to 525 nm (Table 3.11) and shoulder on the high-energy side, which is attributed to the 0-1 vibrational band of the same transition. The wavelengths of these absorption maxima (Table 3.11) are very similar to those of 3-aminoBODIPY derivatives.[56,107,108,122,154–168] As mentioned earlier, the absorption spectra are dependent on solvent polarity; the maximum being red-shifted (by ~5 nm) when the solvent is changed from acetonitrile (520 nm) to toluene (525 nm). (2) Additionally, a weaker, broad absorption band is found in the UV at about 464 nm, the position of which is not appreciably affected by solvent polarity.

This band is also attributed to the S_0-S_1 transition but involving a vibronic state of higher energy than that in the shoulder described above.

Table 3.11: Absorption spectral data of compound **3.51** in different solvents

BODIPY	Solvent	λ_{abs}(max)/nm	$\varepsilon/10^4$ $M^{-1}cm^{-1}$
3.51	Toluene	525	3.95
	CH_2Cl_2	523	4.53
	THF	523	2.99
	EtOH	522	3.36
	MeCN	520	3.53

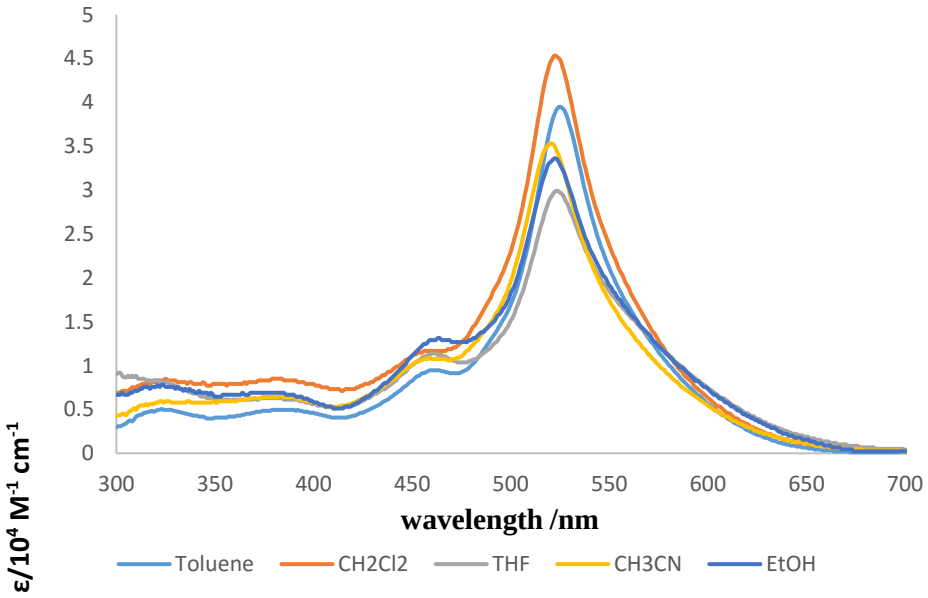

Figure 3.24: Absorption spectrum in terms of the molar absorption coefficient (ε) for 2-aminoBODIPY **3.51** in different solvents.

In addition to these features, a pronounced low-energy 'tail' is evident and appears to be more significant as the solvent polarity is increased. This might be due to a charge transfer state. To try to help confirm the validity of this analysis, the absorption spectrum was fitted to a series of Gaussian components (peak fitting was performed by Prof. A. Harriman, Newcastle University). Figure 3.25 shows the experimental and fitted spectra for the 2-(4-methoxyaniline)-BODIPY **3.51** in toluene and acetonitrile. The experimental data is well reproduced by a combination of components (Figure 3.25):

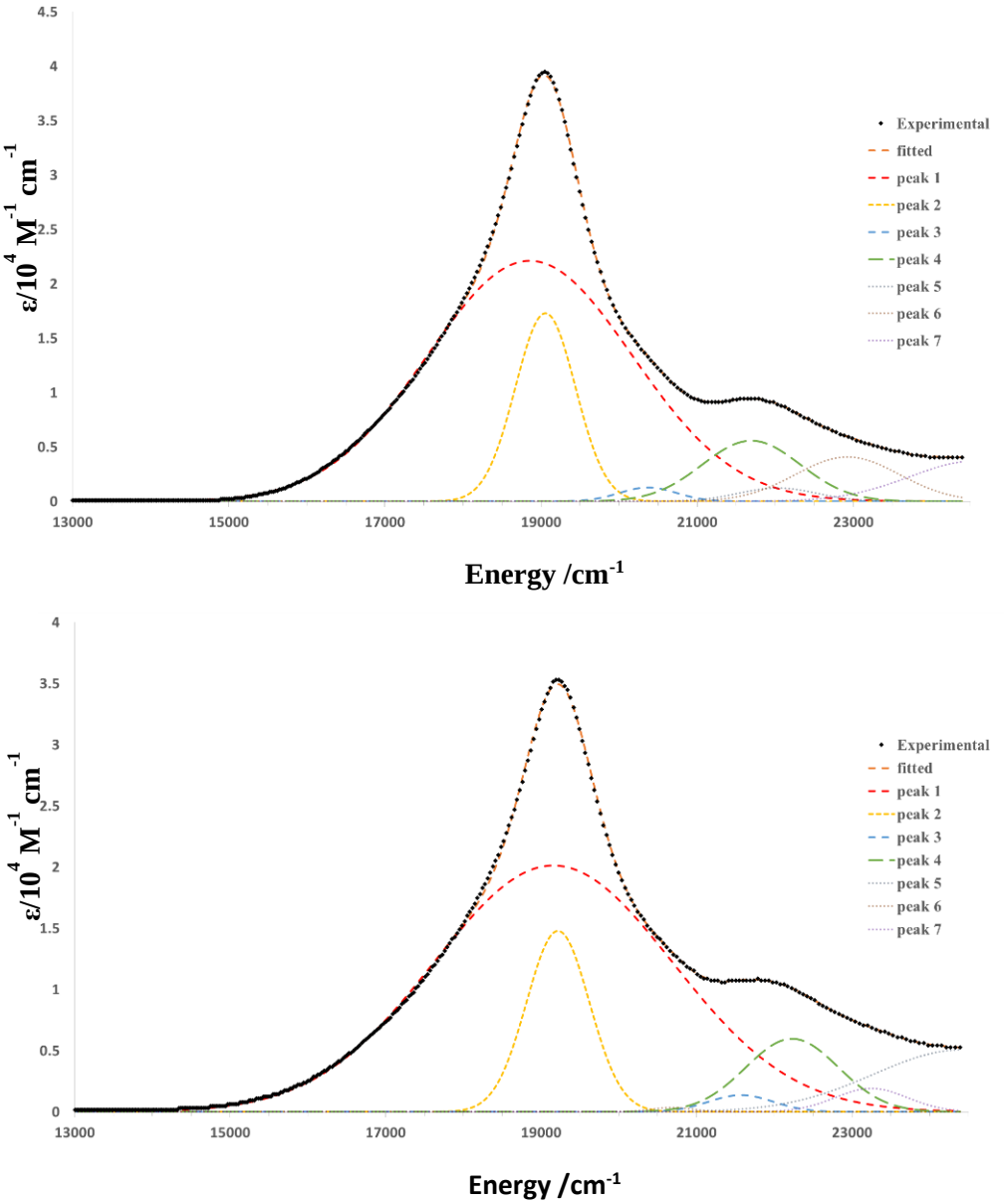

Figure 3.25: Peak fitting of absorption spectra for 2-aminoBODIPY **3.51** in toluene (top) and MeCN (bottom).

(1) A broad, low energy band (Peak 1) attributed to charge transfer. This band moves to higher energy as the solvent polarizability increases (ν_{max} = 18,855 cm^{-1} in toluene, 19,156 cm^{-1} in MeCN). The relatively small shift in energy observed between solvents of significantly different polarizability suggests that the ground state is already rather polar and that excitation does not lead to a dramatic change in polarity. A calculation (DFT at the B3LYP/6-31 G (d) level, appling the polarizable continuum model with solvent = toluene) indicated a ground state dipole moment of 4.6 D. The solvent reorganisation energy (λ_{CT}) can be calculated

from the full width at half maximum (FWHM) of the band, according to Equation 3.1.[170]

$$\lambda_{CT} = (FWHM)^2/[16 \ln 2 K_B T] \qquad \textbf{Equation 3.1.}^{170}$$

K_B= Boltzmann's constant = 0.6950 $cm^{-1}K^{-1}$

The FWHM of the charge-transfer band (Peak 1) in toluene is 3086.6 cm^{-1}, corresponding to λ_{CT} = 4,218 cm^{-1} (at 293 K). In acetonitrile, the FWHM is 3613.9 cm^{-1}, which corresponds to λ_{CT} = 5,783 cm^{-1}. This solvent dependence of the reorganisation energy is as expected for a charge-transfer transition.

(2) A sharper band (Peak 2) corresponding to the S_0-S_1 transition of the BODIPY ($\pi \rightarrow \pi^*$). This is also blue shifted on moving from toluene (ν_{max} = 19,055 cm^{-1}) to MeCN (ν_{max} = 19,215 cm^{-1}) but considerably less so than the CT band, as expected of a transition which does not lead to significant charge redistribution. Likewise, The FWHM of this band is less solvent dependent (906.2 cm^{-1} in toluene, 952.0 cm^{-1} in MeCN) as expected.

(3) Peak 3, corresponding to the shoulder of the the S_0-S_1 BODIPY transition, and attributed to the 0-1 vibrational band. In toluene, this band is centred at 20,368 cm^{-1}. This is 1,314 cm^{-1} higher in energy than the main 0-0 band and presumably corresponds to a low energy torsional mode.

(4) Peak 4, corresponding to a higher energy vibrational band. In toluene this band is centred at 21,691 cm^{-1}. This is 2,636 cm^{-1} higher in energy than the main 0-0 band and may correspond to the N-H stretch of the amine.

The remaining three Gaussians (Peaks 5-7) centred at higher energies, included to fit the model closely to the experimental data, are not interpreted.

3.13.2.2. Crystal structure determination of 3.57

Further structural confirmation of 2-aminoBODIPY was performed through X-ray crystallography. A crystal of the 2-methylaniline-derived **3.57** was grown by slow evaporation of a solution in hexane/DCM. The orientation of the 2-methylphenyl moiety is rotated out of the dipyrrolyl plane with a dihedral angle (C10, C8, C24 and C25) of 82.7° (2) for compound **3.57**. In addition, the crystal structure confirmed that the amine group and the BODIPY core are not coplanar, the calculated twist angle between the aniline and the BODIPY core (dihedral angle C12, N3, C2 and C3) is 75.3° (2).

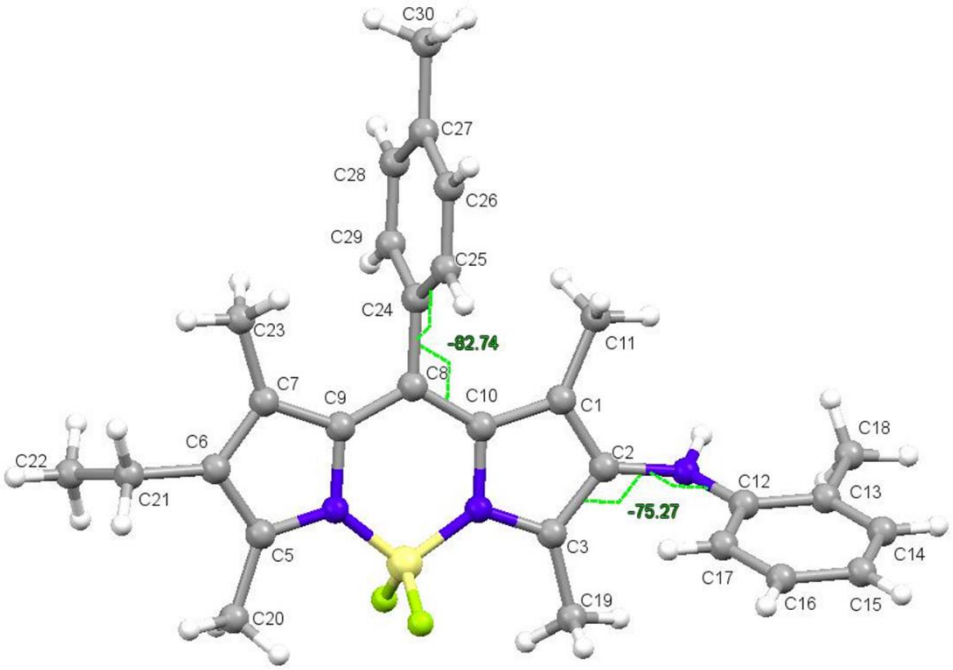

Figure 3.26: molecular structure of 2-aminoBODIPY **3.57**. Hydrogen atoms have been omitted for clarity.

3.13.2.3. Electrochemical properties of the 2-aminoBODIPYs 3.51 and 3.58

In general, the unsubstituted BODIPY is electron deficient and the electrochemical properties display one reversible reduction, one irreversible reduction and a poorly defined oxidation wave.[171,172] However, introducing different groups on the BODIPY core can significantly influnce the electrochemical properties.[171,172] The 2-aminoBODIPYs **3.51** and **3.58** were subject to cyclic voltammetry (CV) in order to investigate the electrochemical properties of the system (Figure 3.27). The measurements were made in acetonitrile by using a graphite (carbon) and platinum electrodes. 1.0 M Tetrabutylammonium hexafluorophosphate (TBA. PF_6) was used as the background electrolyte and ferrocene was used as an external standard. Cyclic voltammetric analysis of the BODIPY dye **3.51** showed several oxidation waves (Figure 3.27), the first is reversible ($E_{1/2}$ = 0.33 V) which is too low to be related to the oxidation of the BODIPY unit. This is most probably related to the oxidation of the amine group for the 4-methoxyaniline derivative **3.51**. Following this initial oxidation, a further two irreversible oxidations occur (E_p = 0.56 and 0.92 V) which may also be due to oxidation of the amine. A final irreversible oxidation occurs at E_p = 1.26 V and is probably due to one electron oxidation of the BODIPY.

The oxidation behaviour of the alkylamine derivative **3.58** is broadly similar (Figure 3.27) with a reversible oxidation at $E_{1/2}$ = 0.26 V, one irreversible oxidation at E_p = 0.61 V associated with the amine and an irreversible oxidation at E_p = 0.97 V.

At a negative voltage one redox peak is observed for each of the BODIPYs **3.51** and **3.58**, showing one fully reversible one electron reduction ($E_{1/2}$ = -1.48 and -1.55 V respectively). The cyclic voltammograms of **3.51** and **3.58** were recorded by Patrycja Stachelek (Prof. A Harriman's group, Newcastle University).

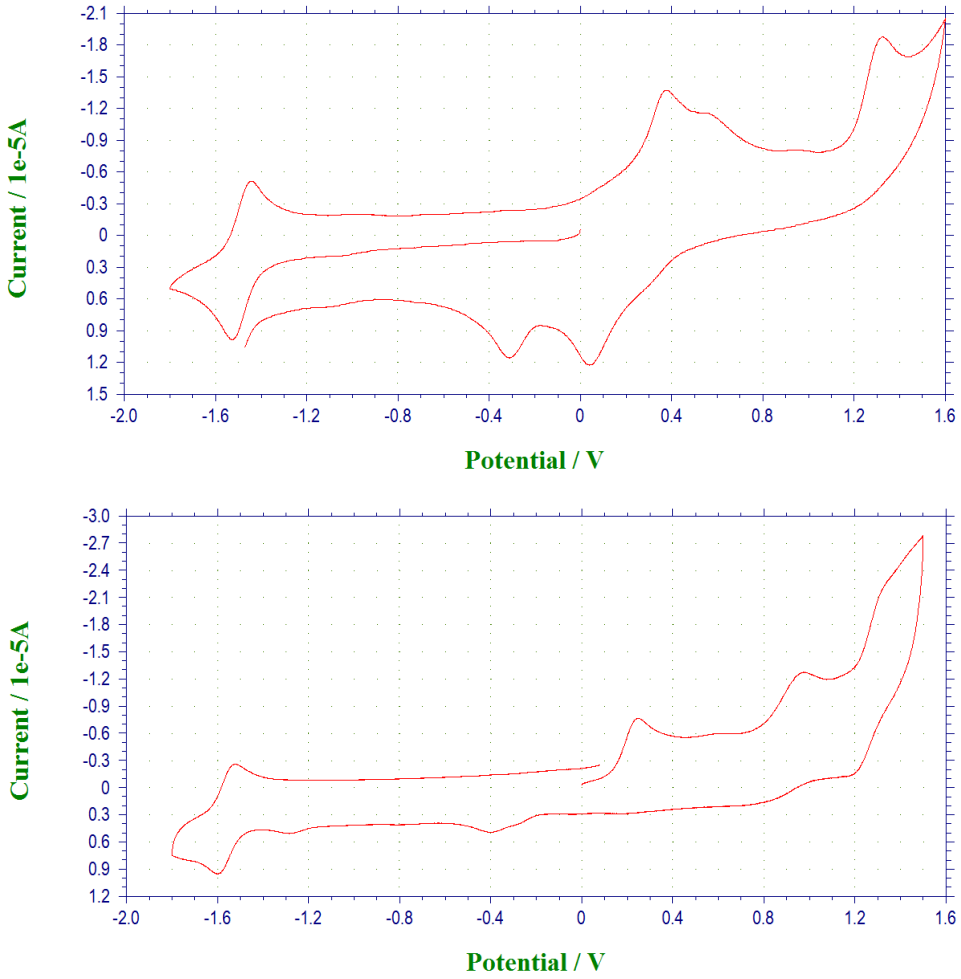

Figure 3.27: Cyclic voltammetry: oxidation waves (V>O) and reduction waves (V<O) of the 2-aminoBODIPYs **3.51** (top) and **3.58** (bottom) in acetonitrile and 1.0 M tetrabutylammonium hexafluorophosphate (TBA PF6) as electrolyte at room temperature and referenced to the potential of ferrocene/ferrocenium couple. Scan rate 0.2 vs^{-1}.

For the 4-methoxyaniline derivative **3.51**, the reversible one electron reduction of the BODIPY occurs ar -1.48 V. The fitted absorption spectrum (in MeCN) indicates an energy for the BODIPY $\pi \rightarrow \pi^*$ transition of 19,215 cm^{-1} = 2.38 eV. On this basis, the BODIPY oxidation potential would be expected to occur at approximately 2.38-1.48 = + 0.9 V. This value does correspond to the oxidation peak seen for the alkylamino-derivative **3.58** but not to the value (+1.26 V) ascribed to BODIPY oxidation in the arylamino derivative **3.51**. It may be that the multiple initial oxidation events associated with the arylamine sufficiently perturb the system such that the final oxidation cannot be regarded as a simple BODIPY oxidation.

3.13.2.4. Quantum chemical calculations of 2-aminoBODIPYs

In order to shed light on the interesting absorption features of the 2-aminoBODIPY **3.51**, we explored their structures by using density functional theory (DFT) at the B3LYP/6-31G(d) level, applying the polarizable continuum model (IEFPCM, with solvent = THF) to account for solvent effects (calculation were performed by Dr Julian Knight). Figure 3.28 shows the the HOMO and LUMO orbitals and energies for the 2-unsubstituted BODIPY **3.49** and the 2- aminoBODIPYs **3.51** and **3.61** (as a model for alkylamine substitution).

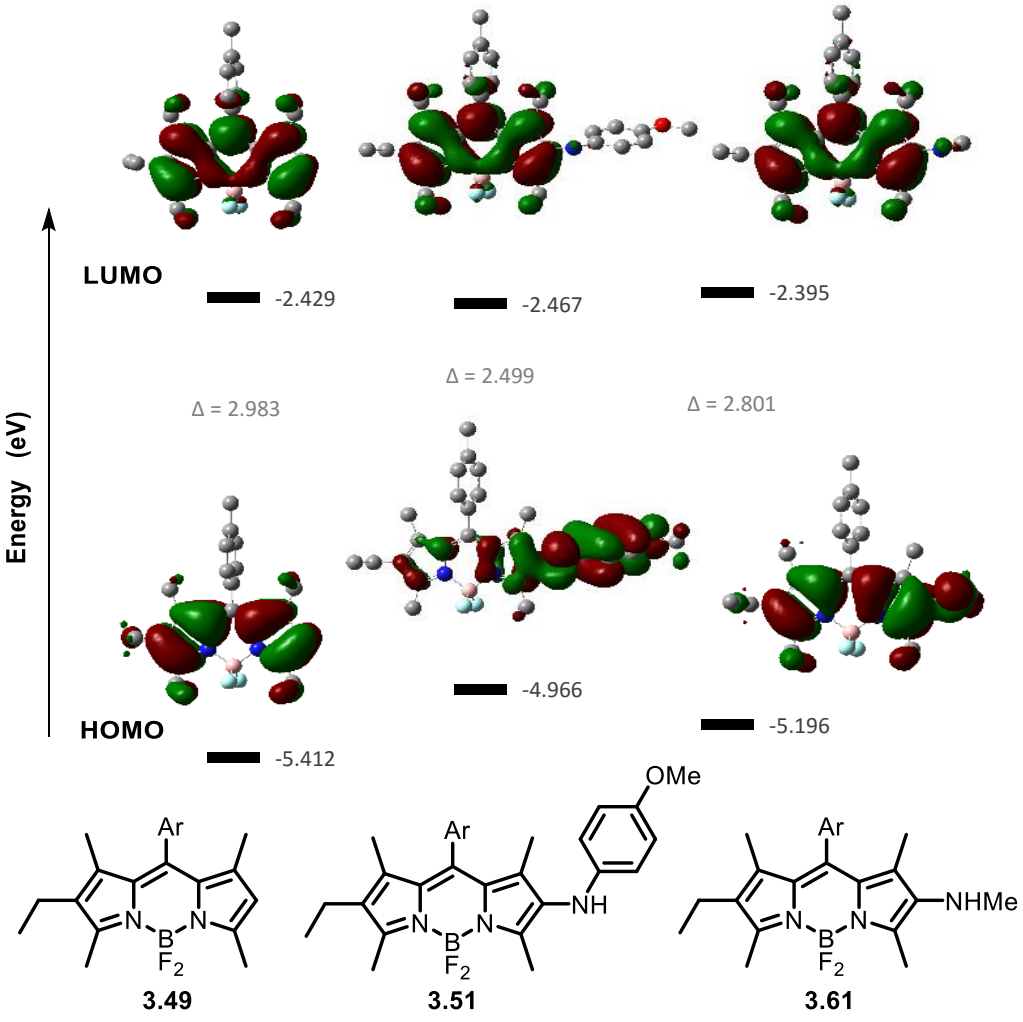

Figure 3.28: HOMO and LUMO molecular orbitals and energies (eV) for **3.49**, **3.51**, and the 2-NHMe model BODIPY **3.61**.

As expected for 1,3-dimethylated systems, the amine (NHR) and the BODIPY core are not coplanar, the calculated dihedral angle between the aryl carbon–amino nitrogen bond and the C2-C3 bond of the BODIPY pyrrole was < CNCC = 103.6° and 105.7° for compounds **3.51** (4-MeOC$_6$H$_4$NH-BODIPY) and **3.61** (MeNH-BODIPY) respectively. Such twisting reduces conjugation between the nitrogen and the BODIPY and consequently the nitrogen in the alkyl amine derivative **3.61** is significantly pyramidalized (the sum of bond angles at the nitrogen is 336.4°). Inspection of the orbitals (Figure 3.28) indicates that the 2-amino substituent has a minimal effect on the energy and topology of the LUMO whereas the HOMO is substantially delocalised onto the substituent and raised in energy. The destabilization of the HOMO relative to the LUMO is expected to result in a red-shift in the absorption spectrum, which is in qualitative agreement with the experimental observations.

Overall, the structural, spectral, electrochemical and quantum chemical behaviour of these 2-amino BODIPYs is consistent with a significant charge transfer state which completely quenches the fluorescence.

3.14. Conclusion

3-AminoBODIPYs have been synthesised successfully via a rather unusual copper catalysed vicarious nucleophilic substitution of the 2-iodoBODIPY. This approach also succeeded with less nucleophilic nitrogen nucleophiles such as anilines and an amide in many cases in high yields. Nevertheless, this approach does not produce any singly or doubly aminated product when using a 2,6-diiodoBODIPY. This observation allows straightforward separation of this by-product of the preceding iodination reaction after the amination.

In addition, 2-aminoBODIPYs derivatives have been prepared successfully via Buchwald–Hartwig amination of the 2-iodoBODIPY (fully blocked). Aniline nucleophiles were highly reactive under the Pd catalysed amination conditions, and primary amine (hexyl amine) readily participated in the Pd amination. However, secondary amines failed to substitute the 2-iodoBODIPY under the given conditions. The absorption and emission spectra for 2 and 3-aminoBODIPY were measured. The presence of the nitrogen group in both positions gives a broadened red-shifted absorption maximum and the fluorescence of the 3-aminoBODIPYs is low and sometimes quenched, while the fluorescence of the 2-aminoBODIPY is quenched.

Quenched fluorophores have often been used for sensing of a wide variety of analytes including heavy metals, oxygen and NO, and can also be used as pH sensors. In the next chapter, the use of a 2-aminoBODIPY as switch on sensor is discussed.

Chapter 4: Application of 2-aminoBODIPY derivatives

4.1. Introduction

Due to the great flexibility of BODIPY synthesis there is an extensive range of applications in biomolecular labels, drug delivery agents, cation sensors, laser dyes, electroluminescent films and fluorescent switches.[6,12,152,173–182]

In recent years, there has been an increasing interest in the development of BODIPY derivatives for the detection of heavy metal ions due to their biological importance and potential for environmental harm. Several examples of BODIPY derivatives are known in which the fluorescence is 'switched off or on' or does not change on coordination.[12] Particularly, the possibility to introduce nitrogen nuclophiles at the BODIPY core can be of interest as substitution at these positions directly influences the spectral properties of the dye. Surprisingly, there are no reports of BODIPY-based phosgene sensors, nor of the use 2-aminoBODIPYs for heavy metal ion sensing.

In previous chapters we have explored a new approach towards the synthesis of 2-aminoBODIPYs. In this chapter the synthesis of a reactive novel 2-aminoBODIPY and its applications will be reported.

4.2. Synthesis of a functionalised 2-aminoBODIPY

In designing a potential metal-ion sensor based on the 2-aminoBODIPY architecture, simple incorporation of an amino aryl substituent with additional substitution suitable for chelation to a metal was envisaged.

In the first attempt to synthesise such a functionalised 2-aminoBODIPY, 1.5 equivalents of 2-aminophenol were added to the 2-iodoBODIPY **3.50**, in the presence of SPhos **L8**, μ-OMs dimer **3.54** $(LPdOMs)_2$ (1.2 mol%) and Cs_2CO_3 in 1,4-dioxane at 95℃ for 16 h (scheme 4.1) which gave a new spot on TLC. Purification using column chromatography gave 64% of a purple product.

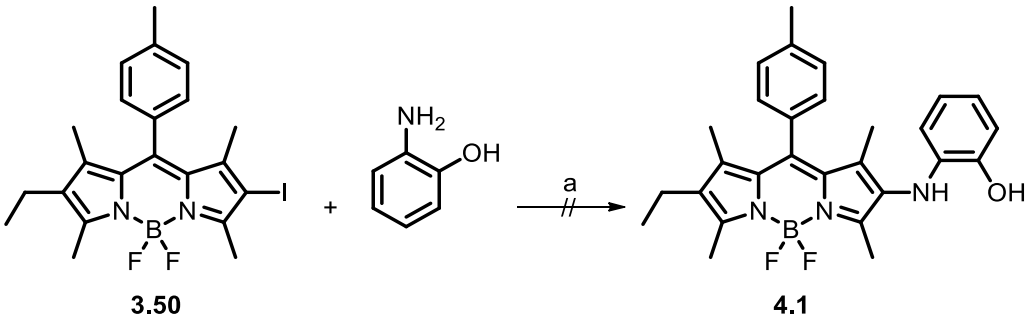

Scheme 4.1: Attempt to synthesise 2-aminoBODIPY **4.1**. Conditions and reagents: BODIPY **3.50** (0.20 mmol), amine (1.01 mmol), $(LPdOMs)_2$ **3.54** (1.2 mol%), SPhos **L8** (1.1 mol per mol Pd), Cs_2CO_3 (0.35 mmol), 1,4-dioxane (2 mL), 95 ℃, 16 h.

The ^{1}H NMR spectrum of this purple compound showed the appearance of four additional aromatic protons, however, the ^{11}B NMR spectrum had changed from a quartet as seen in all 2-aminoBODIPY derivatives to a singlet at 5.1 ppm and there were no signals in the ^{19} F NMR spectrum. This indicates that the two fluorine atoms in a BODIPY were substituted with 2-aminophenol to produce the *N*,*O*-coordinated BODIPY **4.2** (Scheme 4.2).

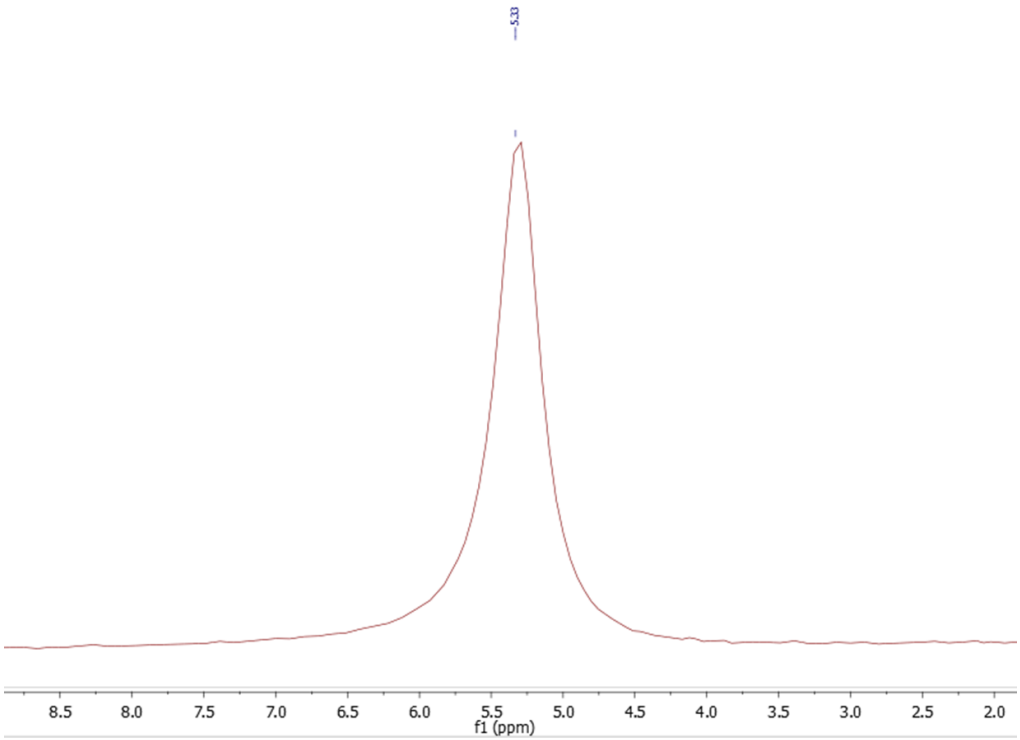

Figure 4.1: ^{11}B NMR spectrum of BODIPY **4.2**.

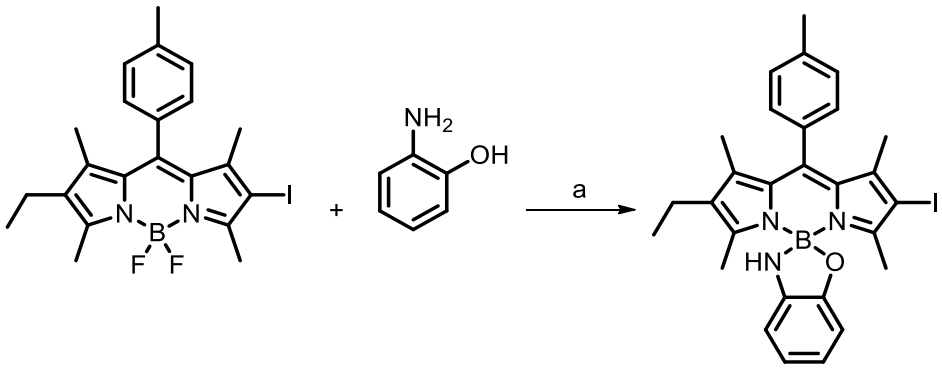

3.50 **4.2**

Scheme 4.2: Synthesis of *N*,*O*-coordinated BODIPY **4.2**. Conditions and reagents: BODIPY **3.50** (0.23 mmol), amine (1.01 mmol), $(LPdOMs)_2$ **3.54** (1.2 mol%), SPhos **L8** (1.1 mol per mol Pd), Cs_2CO_3 (0.35 mmol), 1,4-dioxane (2 mL), 95 ℃, 16 h, 64%.

The replacement of the fluorine atoms to give BODIPY **4.2** was confirmed by X-ray structure determination, after crystal growth through slow diffusion of petroleum ether into a solution of the BODIPY in DCM (Figure 4.2).

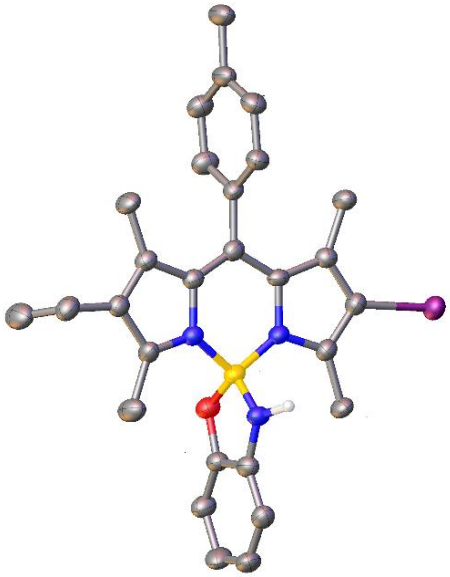

Figure 4.2: molecular structure of BODIPY **4.2**, confirming substitution of fluorine by 2-aminophenol. Hydrogen atoms have been omitted for clarity.

In reviewing the literature, there is no published data on BODIPY dyes in which the fluorine atoms have been substituted with 2-aminophenol. On the other hand, the fluorine atom in a BODIPY has been substituted with other groups including alcohols.[28,183–193] Several examples of the substitution of the fluorine atoms at the boron centre have been reported to give alkoxy or aryloxy BODIPY derivatives (*O*-BODIPY) under very harsh conditions.[28,183–193] Unsurprisingly, the boron-halogen bond strengths decrease in the order F > Cl > Br > I .[193] Thus, B-Cl bonds are much more labile than B-F. However, it was reported that the yields of formation of *O*-BODIPY compounds are often low. For instance, in 2007 Bonnet reported that refluxing BODIPY **4.3** with various alcohols in the presence of $AlCl_3$ led to a mixture of monosubstituted **4.4** and disubstituted product **4.5** (Scheme 4.3).

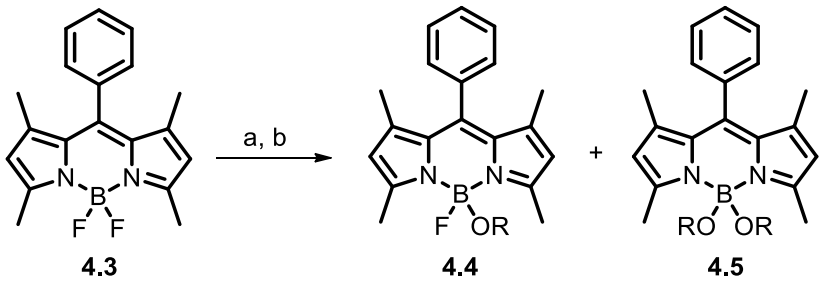

Scheme 4.3: Replacement of fluorine by oxygen nucleophiles. Conditions and reagents: a) BODIPY **4.3**, DCM, $AlCl_3$ (1.5 eq), reflux, 5 min, b) ROH, r.t.

In one recent publication the authors investigated three different methods for the synthesis of alkoxy BODIPY derivatives (*O*-BODIPY) as shown in Scheme 4.4.[187] Method A involves addition of NaOMe in refluxing MeOH, method B employs refluxing dichloromethane in presence of $AlCl_3$ followed by addition of MeOH as nucleophile, and method C uses trimethylsilyltrifluoromethanesulfonate (TMSOTf) for activation of the BODIPY in refluxing toluene followed by adding MeOH. The yields achieved depend on the structure of the BODIPYs.[187]

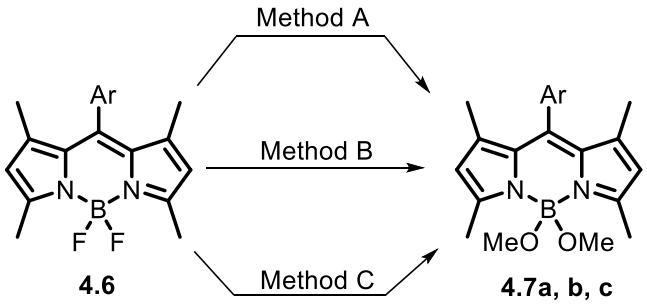

a: Ar= C_6H_5
b: Ar=3,4-$(MeO)_2$ C_6H_3
c: Ar= 4-$(MeO_2C)C_6H_4$

Scheme 4.4: Synthesis of BODIPYs **4.7**. Conditions and reagents: method A: MeONa, MeOH, reflux, 12 h. Method B: a) $AlCl_3$, DCM, reflux, 15 min. b) MeOH, reflux, 15-30 min. Method C: a) TMSOTf, toluene, reflux, 30 min. b) MeOH, DIPEA, r.t., 1 h.

The absorption spectrum of *N,O*-BODIPY **4.2** is represented in Figure 4.3. The low-energy maximum (λ_{abs}) of *N,O*-BODIPY **4.2** is 528 nm which is assigned to the S_0-S_1 (π-π^*) electronic transition associated with the BODIPY core and has a high molar absorption coefficient (ε) (34,745 $M^{-1}cm^{-1}$). *N,O*-BODIPY **4.2** is non-fluorescent which might be due to either the replacement of the two fluorine atoms with nitrogen and oxygen atoms or due to the presence of the iodine atom (heavy atom). Future work will investigate the optimised conditions for the synthesis of this type of *N,O*-BODIPY.

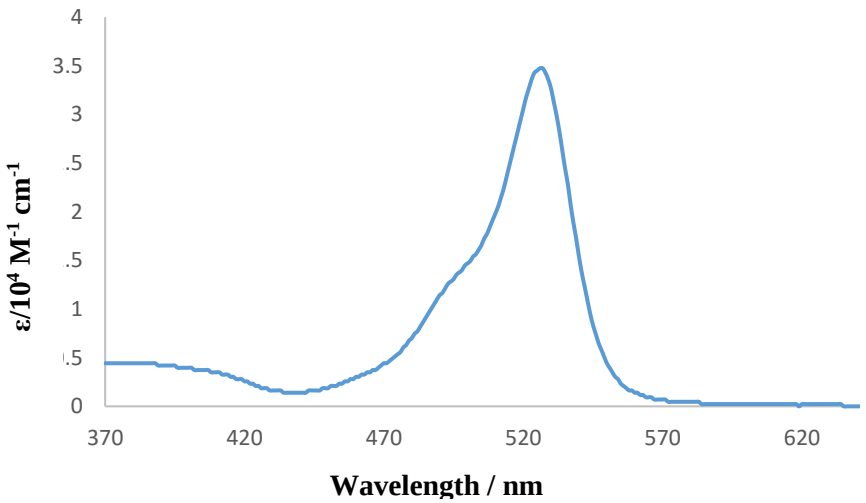

Figure 4.3: The absorption spectrum in terms of the molar absorption coefficient (ε) of the *N-O*-BODIPY **4.2**, recorded in tetrahydrofuran at room temperature.

Despite the successful incorporation of primary amines and anilines in the previous chapter, preparation 2-(*ortho*-aminophenol)BODIPY **4.1** by using *ortho*-aminophenol was shown to be unsuccessful under our conditions. We then decided to examine other anilines to synthesise a functionalized 2-aminoBODIPY. Therefore, the palladium catalysed nucleophilic amination was attempted by applying our reaction conditions, using SPhos **L8**, μ-OMs dimer $(LPdOMs)_2$ **3.54** to the reaction of the 2-iodoBODIPY **3.50** with *ortho*-nitroaniline to give the 2-((2-nitrophenyl)amino)-BODIPY **4.8** as a dark orange solid in 67% yield (Scheme 4.5).

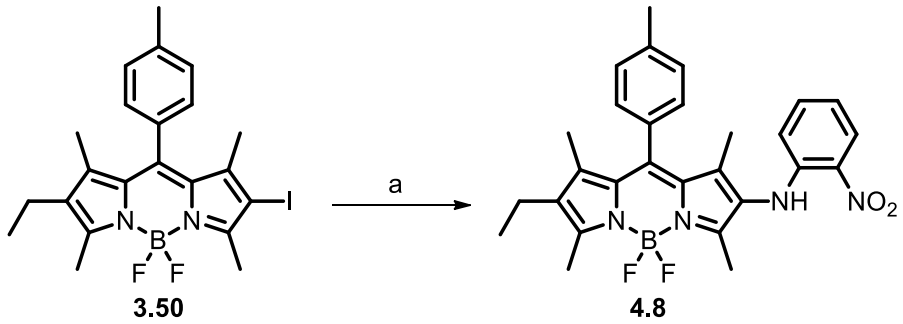

3.50 **4.8**

Scheme 4.5: Synthesis of BODIPY **4.8**. Conditions and reagents: BODIPY **3.50** (0.20 mmol), amine (1.01 mmol), $(LPdOMs)_2$ **3.54** (1.2 mol%), SPhos **L8** (1.1 mol per mol Pd), Cs_2CO_3 (0.35 mmol), 1,4-dioxane (2 mL), 95 ℃, 16 h.

Hydrogenation of 2-nitroaniline BODIPY **4.8** by using Pd/C and H_2 in DCM and MeOH for 2 h at room temperature gave the 2-aminoanilineBODIPY **4.9** as a dark purple solid in high yield (96%) (Scheme 4.6).

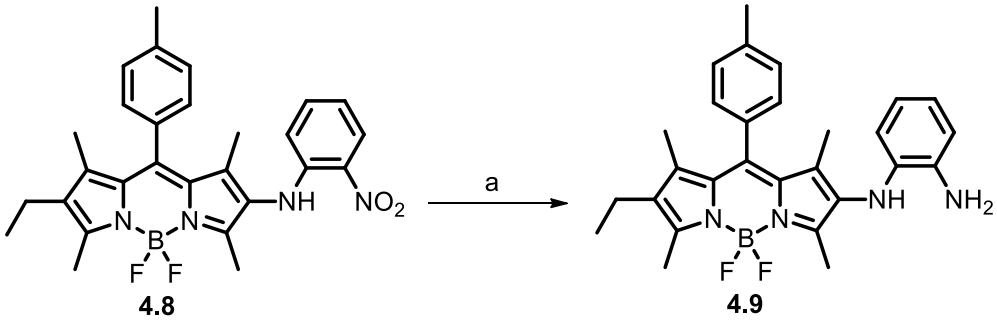

4.8 **4.9**

Scheme 4.6: Synthesis of 2-aminoBODIPY **4.9**. Conditions and reagents: a) H_2 (1 atm), 10% Pd/C, MeOH-CH_2Cl_2, r.t., 2 h (95%).

The absorption spectrum of 2-aminoBODIPY **4.9** is represented in Figure 4.4. The low-energy maximum (λ_{abs}) of 2-aminoBODIPY **4.9** is 524 nm and is assigned to the S_0-S_1 (π-π^*) electronic transition associated with the BODIPY core. The high molar absorption coefficient (ε) is 29,894 $M^{-1}cm^{-1}$.

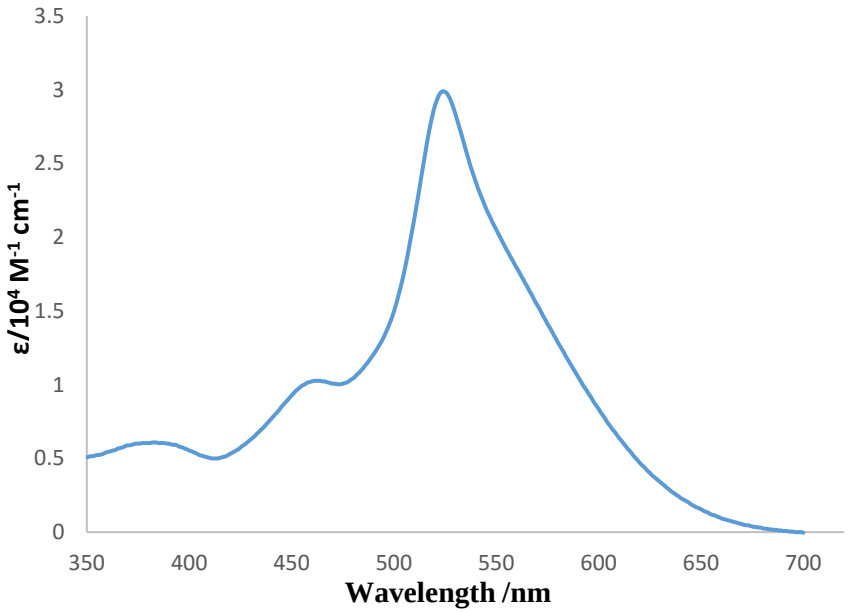

Figure 4.4: The absorption spectrum in terms of the molar absorption coefficient (ε) of the 2-aminoBODIPY **4.9**, recorded in tetrahydrofuran at room temperature.

The novel 2-aminoBODIPY **4.9**, is dark purple coloured and appears to be non fluorescent during column chromatography. We attempted to measure the fluorescence quantum yield of 2-aminoBODIPY **4.9** in tetrahydrofuran, however, the fluorescence is strongly quenched.

The key features of the novel 2-aminoBODIPY **4.9** are that it is nonfluorescent and contains two adjacent reactive functional groups, one of which is an NH group attached directly to the BODIPY core. This novel compound **4.9** might be used for many different applications such as for sensing phosgene, heavy metals and pH.

4.3. 2-AminoBODIPY 4.9 for rapid visual detection of phosgene

Phosgene ($COCl_2$) is a colourless, suffocating gas. This highly toxic[194] compound was responsible for about 85% of the 100,000 deaths caused by chemical weapons during World War I. Exposure to phosgene can cause severe damage to lungs and respiratory tract, the lethal dose for humans is 2 ppm. Phosgene is an important industrial chemical, with several million tons produced globally each year. The main commercial use of phosgene is in the synthesis of other chemicals such as pesticides, herbicides, medicines, plastics and dyes.[195] It is perhaps surprising that there are few reports of the use of fluorescence-based sensors for phosgene.

In 2007, Zhang and Rudkevich designed a new system of phosgene sensors based on fluorescent resonance energy transfer (FRET).[196] It includes a selective reaction between fluorescent donor and an acceptor fluorophore and phosgene as shown in Figure 4.5.

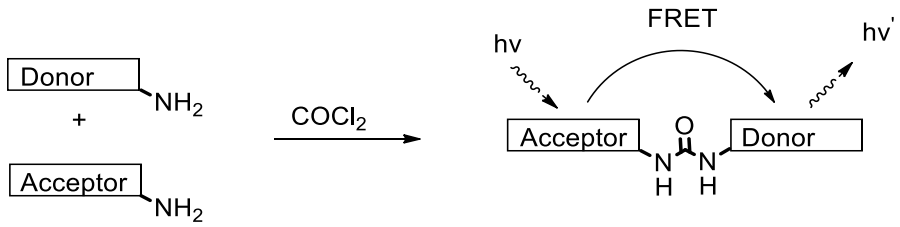

Figure 4.5: A fluorescent resonance energy transfer based approach to the detection of phosgene.[196]

For instance, coumarin **4.10** and coumarin **4.11** rapidly react with phosgene and form urea **4.12** which leads to changes in fluorescence emission spectra (limit of detection 5×10^{-5} M) (Scheme 4.7).[196]

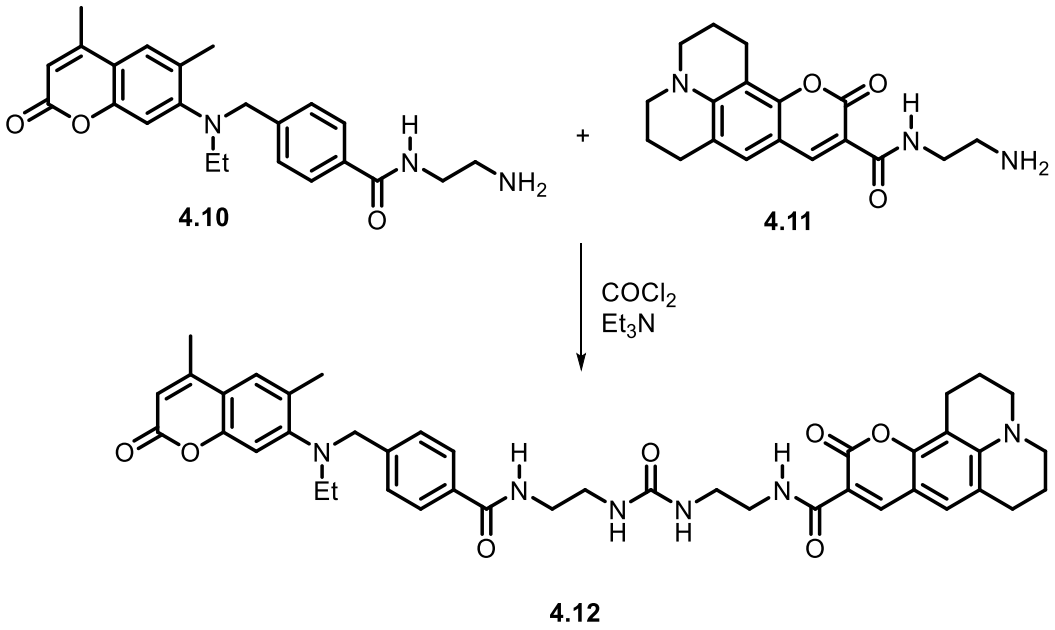

Scheme 4.7: A reaction between coumarins **4.10** and **4.11** and phosgene with the formation of urea **4.12**.[196]

In 2012, Han reported a highly sensitive chemodosimeter for rapid detection of phosgene (limit of detection 50 nM).[197] A deep-coloured and highly fluorescent species was formed by treatment of *N*-(rhodamine B)-deoxylactam-ethylenediamine **4.13** (dRB-EDA, colourless) with phosgene (Scheme 4.8)[197]

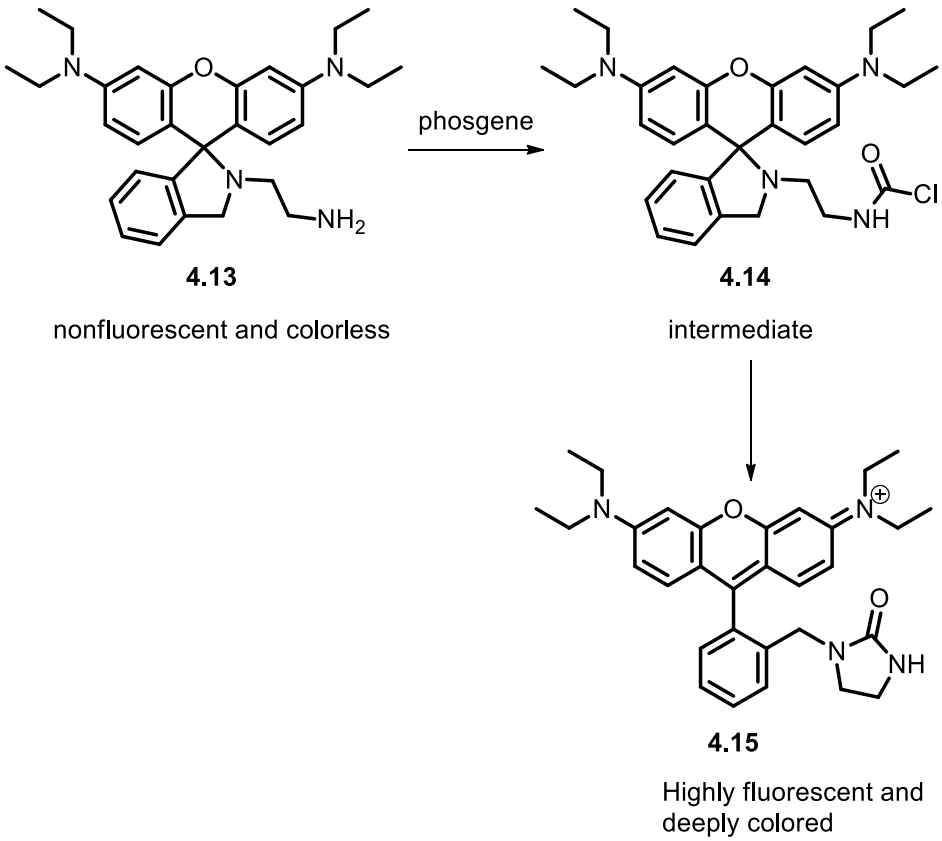

Scheme 4.8: chromo-fluorogenic detection of phosgene with dRB-EDA.[197]

In 2012, Kundu and Hwang reported rational design of unimolecular fluorescent phosgene sensors.[198] The cyclisation of an hydroxycinnamic acid (nonfluorescent) with phosgene gave a fluorescent coumarin (limit of detection 1 nM) (Scheme 4.9).[198]

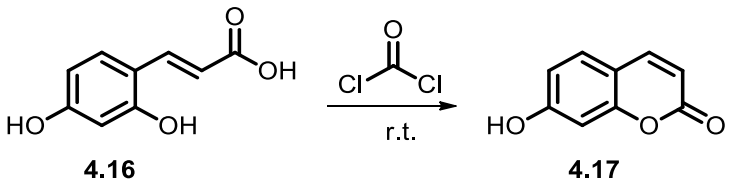

Scheme 4.9: Chemical reaction of 2,4-dihydroxy cinnamic acid **4.16** with phosgene to produce coumarin **4.17**.[198]

Interestingly, there are no reports of a BODIPY-based phosgene sensor. As we explained in the previous chapter, the presence of an amino group at the 2-position quenches the fluorescence emission of BODIPY **4.9** by resonance energy transfer, however, the nucleophilic attack of a 2-aminoBODIPY **4.9** on phosgene would decrease the electron-donor ability of the substituent and thus reduce fluorescence-quenching, potentially leading to fluorescence 'switch-on'.

In order to explore this possibility, the 2-aminoaniline-drived BODIPY **4.9** was reacted with triphosgene in the presence of triethylamine to give the corresponding benzimidazolone-substituted BODIPY **4.18** in excellent yield (98%) (Scheme 4.10).

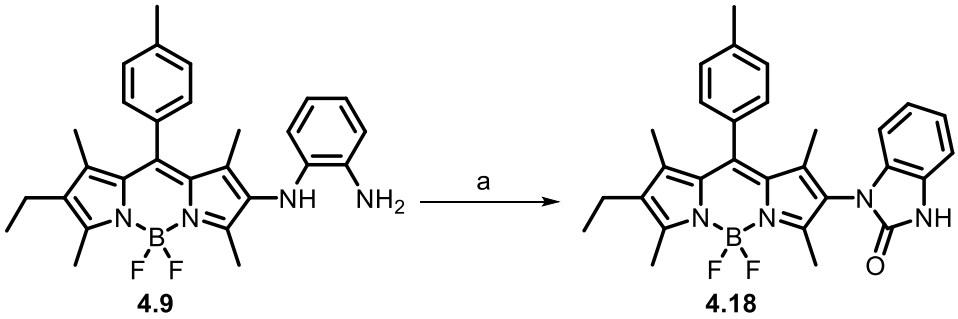

Scheme 4.10: Synthesis of the benzimidazolone BODIPY **4.18**. Conditions and reagents: a) $(Cl_3CO)_2CO$, Et_3N, CH_2Cl_2, r.t., 10 min (98%).

The ^{19}F NMR spectrum of BODIPY **4.18** consists of 16 peaks due to the two different fluorine atoms coupling to each other and also coupling to the boron atom (Figure 4.6) as explained in chapter 2. Inequivalence of the two fluorine atoms implies restricted rotation of the imidazolone substituent around the C2-N bond.

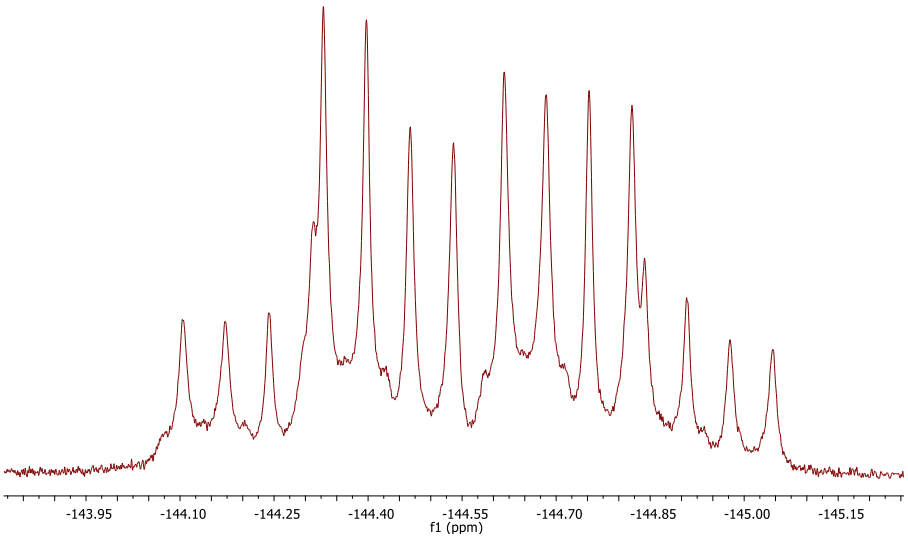

Figure 4.6: ^{19}F NMR spectrum of the benzimidazolone BODIPY **4.18**, in $CDCl_3$.

In order to measure the barrier to rotation for the benzimidazole group a variable temperature (VT) ^{19}F NMR experiment was performed using d_8-toluene from 298 to 373 K (Figure 4.7). However, no sign of coalescence or broadening of the peaks was observed which indicates that restricted rotation of the benzimidazole/BODIPY bond, even at high temperature results in the two fluorine atoms being inequivalent.

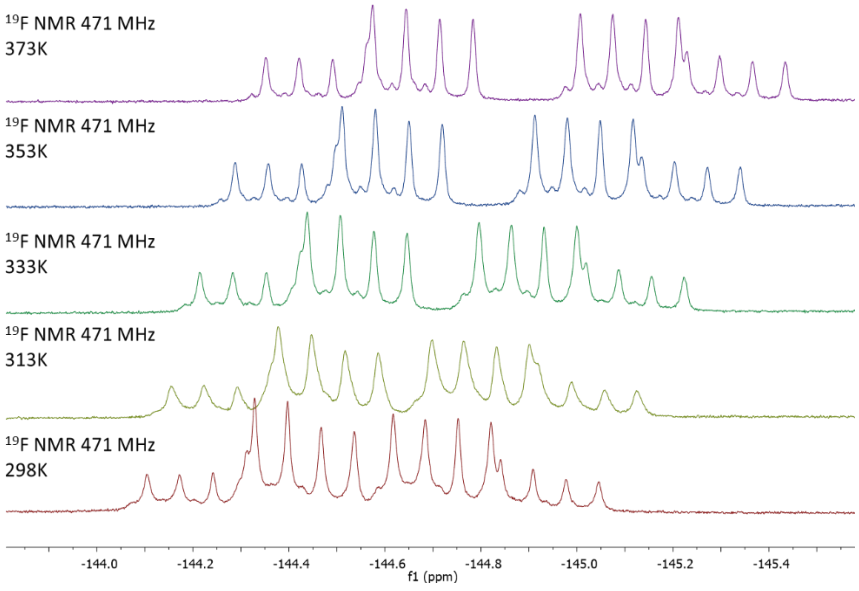

Figure 4.7: ^{19}F VT NMR spectra of the benzimidazolone BODIPY **4.18**, in d_8-toluene.

We also studied variable temperature ^{1}H NMR spectra in order to confirm the previous result. The VT study was again performed in d_8-toluene (from 298 to 373 K) (Figure 4.8). As we expected there was no coalescence or broadening of the peaks and hence rotation around the benzimidazole/BODIPY bond is restricted. This restriction is caused by the steric bulk of the benzimidazole ring in conjunction with the methyl groups at C1 and C3 of the BODIPY.

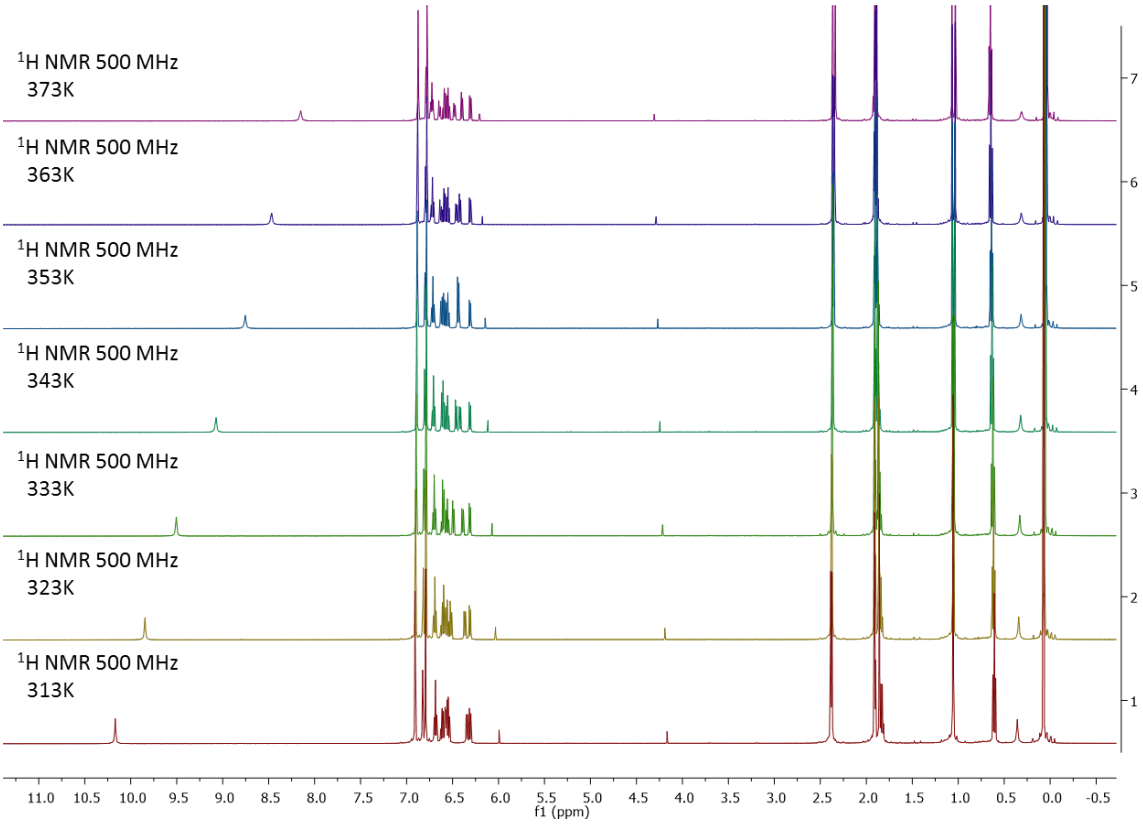

Figure 4.8: ^{1}H VT NMR spectra of the benzimidazolone BODIPY **4.18**, in d_8-toluene.

The 2-aminoaniline BODIPY **4.9** is dark purple and nonfluorescent, and instantly turned orange and strongly fluorescent in dichloromethane (DCM) upon addition of triphosgene. The low-energy maximum (λ_{abs}) of beznimidazolone **4.18** is 515 nm and is assigned to the S_0-S_1 (π-π^*) electronic transition associated with the BODIPY core. The molar absorption coefficient (ε) is 64,024 $M^{-1}cm^{-1}$. Figure 4.9 shows the normalised absorption and emission spectra of the bezimidazolone **4.18** and the parent BODIPY **3.49**.

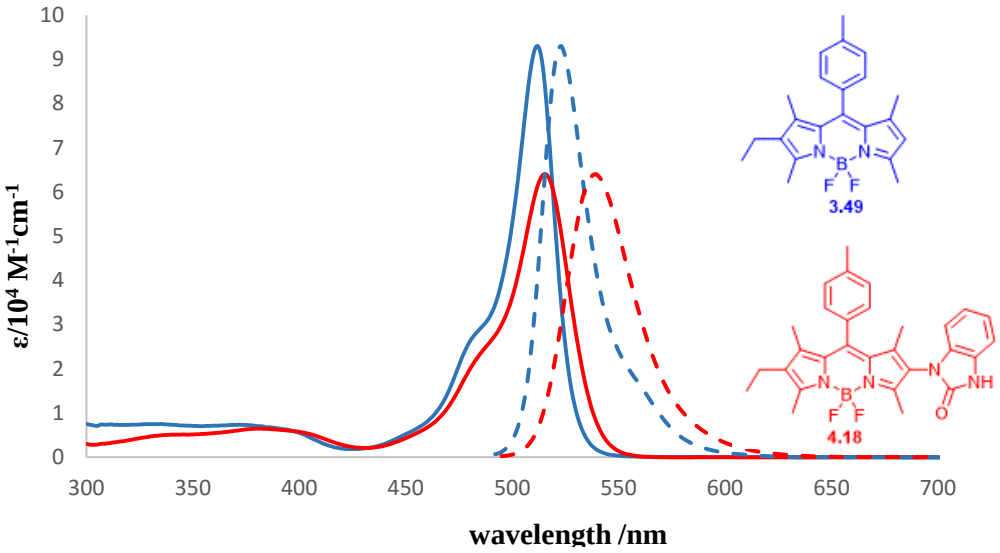

Figure 4.9: Absorption spectrum (solid lines) in terms of the molar absorption coefficient (ε) and normalised fluorescence spectrum (dashed lines) for **3.49** (—) and **4.18** (—) in THF.

As Figure 4.9 illustrates the benzimidazolone-substituted BODIPY **4.18** showed strong absorption bands. In comparison to the parent BODIPY **3.49**, the presence of benzimidazolone-substituent in the 2 position of the BODIPY core leads to a very small red-shift (3 nm, 114 cm^{-1}) of the absorption maximum and a 23 nm (585 cm^{-1}) red-shift of the emission maximum.

In addition to fluorescence spectroscopy, the response of 2-aminoaniline BODIPY **4.9** to triphosgene can be easily visualized even with the naked eye (Figure 4.10). The bright yellow fluorescence intensity was clearly observed within few seconds after the addition of triphosgene.

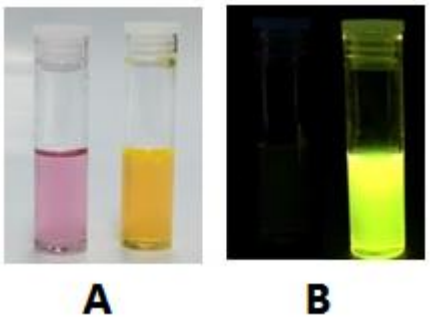

Figure 4.10: The ‘‘naked eye’’ detection of triphosgene. Optical images inset: solution of the BODIPY **4.9** (50 µM in CH_2Cl_2 containing 3% Et_3N) before (left) and after (right) addition of triphosgene (25 µM). **A** visible light illumination; **B** illumination with hand-held lamp at 365 nm.

Limit of Dectection (LoD) is the term used to describe the lowest amount or concentration of a substance that can be reliably distinguished from the absence of that substance (a blank value).[199] In order to determine the detection limit, we have recorded the fluorescence emission of 2-aminoaniline BODIPY **4.9** on treatment with varying concentrations of triphosgene in acetonitrile. Figure 4.11 displays that the fluorescence emission intensity at 534 nm increased as a function of phosgene concentration. In this case, the Limit of Dectection for phosgene was calculated according to Equation 4.1.[199]

$$3s_B/m \qquad \textbf{Equation 4.1}$$

Where s_B is the standard deviation of the blank measurement (dye solution in the absence of analyte) and m is the slope of the calibration curve.[199]

On the basis of the fluorescence titration (Figure 4.11, inset) the Limit of Detection for phosgene was found to be 160 nM.

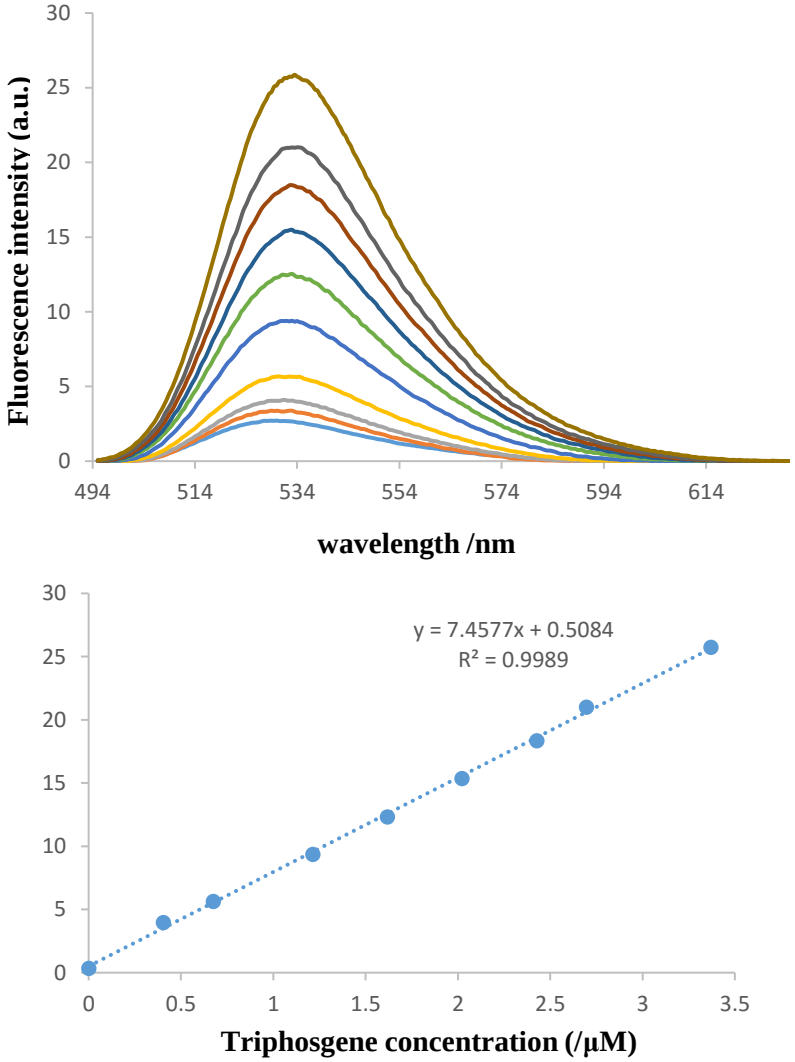

Figure 4.11: Fluorescence emission spectra of the 2-aminoaniline **4.9** (0.01 mg mL^{-1}, 21 µM) in the presence of triphosgene (3.4, 2.7, 2.4, 2.0, 1.6, 1.2, 0.7, 0.4, 0.1 µM from the top to the bottom) in MeCN containing 3% Et_3N. Graphical inset: fluorescence emission intensity at 534 nm vs triphosgene concentration (λ_{ex} = 490 nm).

4.4. Synthesis of 2-aminoBODIPYs for heavy metal sensing

Recently, researchers have shown an increased interest in the design and synthesis of BODIPY derivatives for the recognition of metal ions with high selectivity and sensitivity because these ions play essential roles in many biological system or have potential to be toxic. Figure 4.12 shows several examples of polydentate nitrogen based BODIPY derivatives,[174,200–203] these compounds act as molecular switches for a different metal cation by producing kinetically stable complexes. They work on the basis of internal charge transfer (ICT) or photoinduced electron transfer (PET) processes. In the absence of metal, both types of BODIPY derivatives show reduced fluorescence due to the efficient quenching process (ICT or PET) in the excited state. There are no published reports of applying metal coordination chemistry to a functionalized 2-aminoBODIPY. Herein we report the synthesis of suitably functionalised 2-aminoBODIPYs and also the attempts to study their complexation properties towards different metal ions.

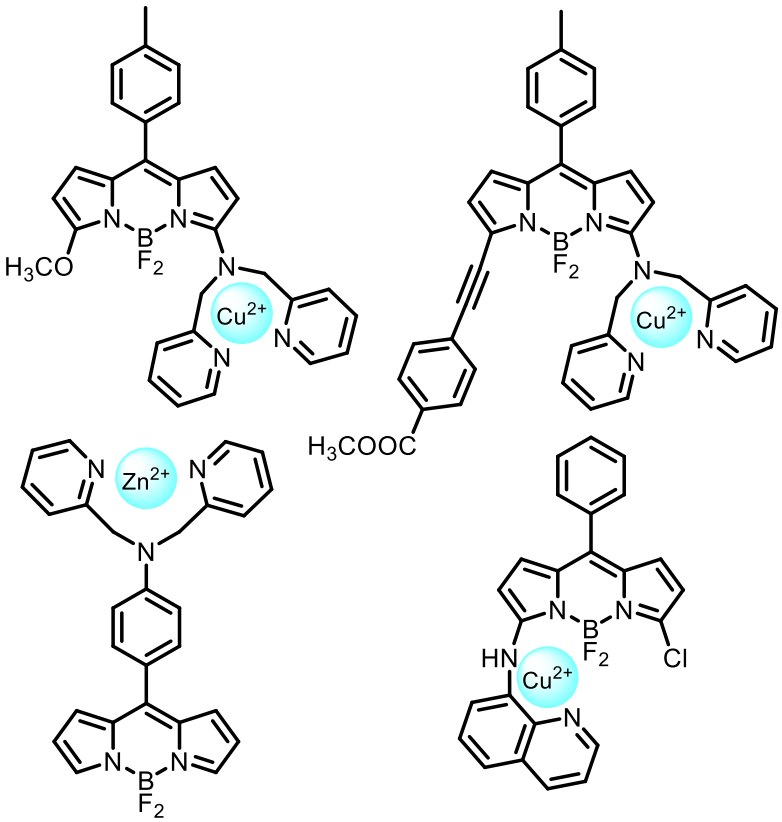

Figure 4.12: Several examples of polydentate nitrogen based BODIPY derivatives.[174,200–203]

In addition, Schiff base ligands have been reported to form complexes with several metal ions, such as Mg^{2+}, Al^{3+}, Co^{2+}, Ni^{2+}, Mn^{2+}, Fe^{2+}, Ag^{+}, Cd^{2+}, Zn^{2+}, Hg^{2+}, Pb^{2+} and Cu^{2+}. For example, Kim developed a turn on fluorescence method with high selectivity to quantify the presence of Al^{3+} by using a simple salicylimine based chemosensor (Scheme 4.11).[204]

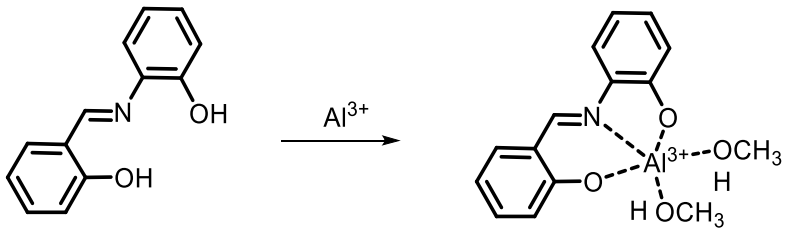

4.19 **4.20**

Scheme 4.11: Chemical structures of the receptor *o*-phenolsalicylimine and a 1:1 complex of *o*-phenolsalicylimine and Al^{3+} in CH_3OH:H_2O.[204]

Zhu reported two salen based ligands **4.21** and **4.22** which act as fluorescent sensors for rapid detection of Mg^{2+} (Figure 4.13).[205]

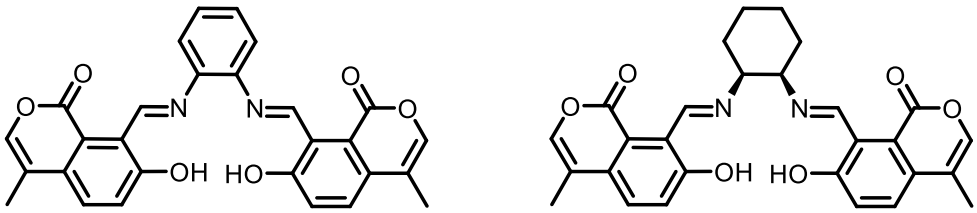

4.21 **4.22**

Figure 4.13: Chemical structure of two coumarin salen-based Mg^{2+} sensors.[205]

Schiff bases combined with a BODIPY have been published as on/off type for optical sensing of Cu^{2+} over other common cations (Scheme 4.12).[206]

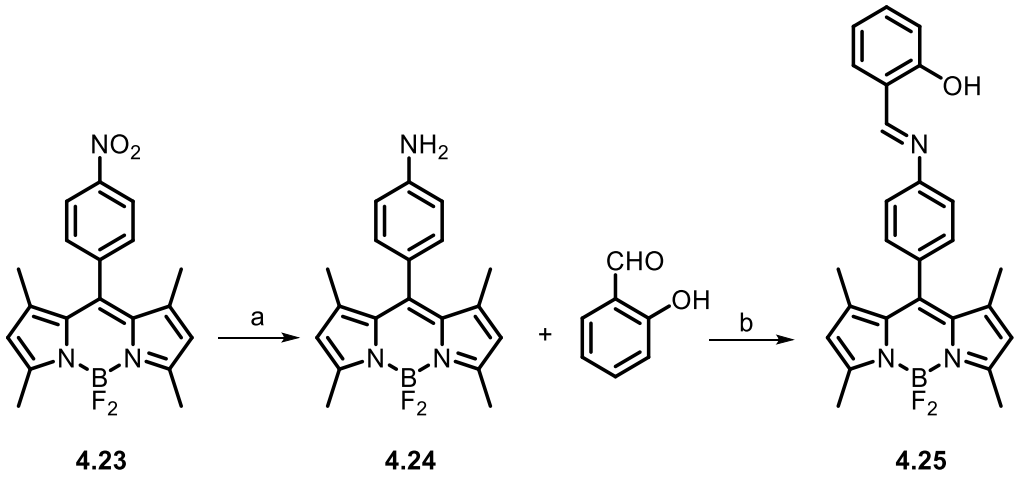

Scheme 4.12: An example of synthesis of a Schiff base combined with BODIPY **4.25**.[206] Conditions and reagents: a) $NH_2NH_2.H_2O$, 10% Pd/C. b) EtOH, 6 h, reflux.

Following this literature precedent, we chose to synthesise an ortho-hydroxy aromatic Schiff base, commonly used as a chelator.[205] Azomethine-BODIPY **4.26** was prepared successfully by the condensation of the primary amine **4.9** and salicylaldehyde (Scheme 4.13). Purification using column chromatography gave the desired azomethine-BODIPY **4.26** in high yield (73%).

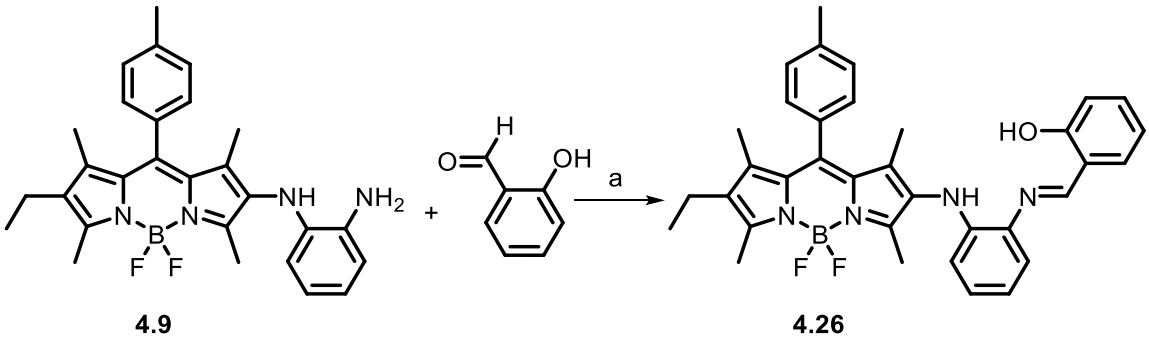

Scheme 4.13: Synthesis of the azomethine-BODIPY **4.26**. Conditions and reagents: a) salicylaldehyde (1 equivalent), AcOH, EtOH, 78℃, 20 h (73%).

The azomethine-BODIPY **4.26** was a dark red colour and nonfluorescent and the solid product was allowed to dry in air overnight. Surprisingly, an orange and fluorescent compound was formed. Figure 4.14 illustrates the ^{1}H NMR spectrum for azomethine-BODIPY **4.26** immediately after being columned and after being dried in air overnight,

which indicated disappearance of the singlet peak at 8.7 ppm corresponding to the CHN group (Figure 4.14).

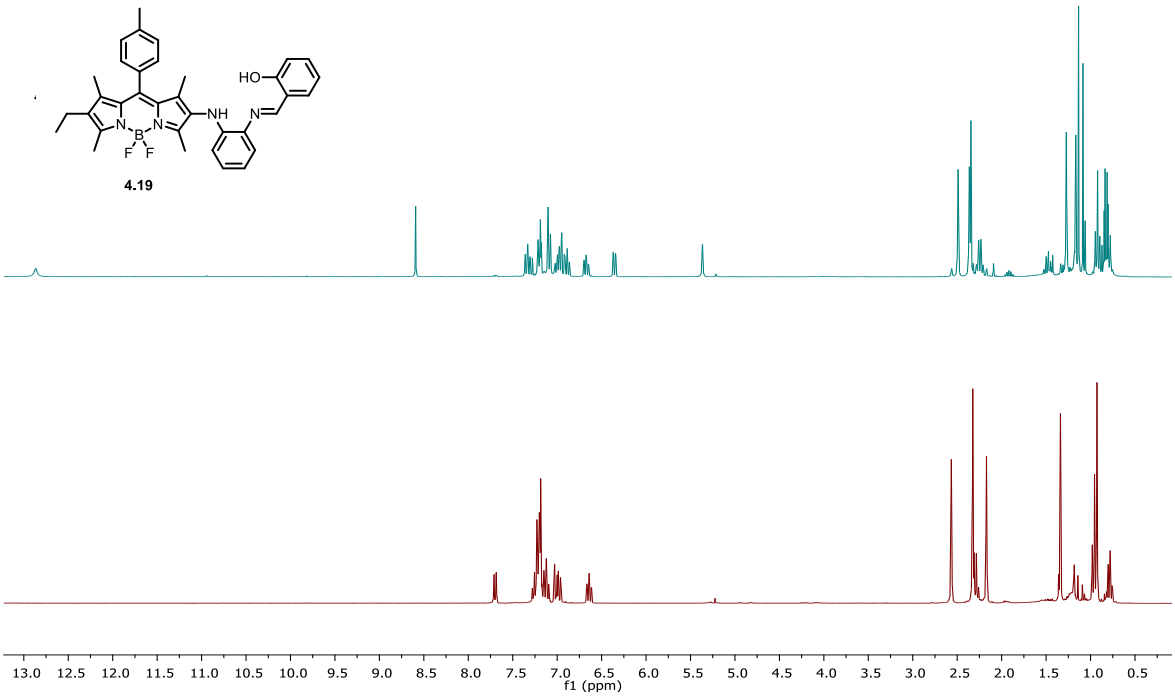

Figure 4.14: ^{1}H NMR spectra of azomethine-BODIPY **4.26** immediately after column chromatography (top) and after drying in air (bottom).

A possible explanation for this might be that nucleophilic attack by the secondary amine NH tends to cause ring closure to give a dihydrobenzimidazole **4.26b** which then undergoes oxidation by air to form a benzimidazole **4.27**.

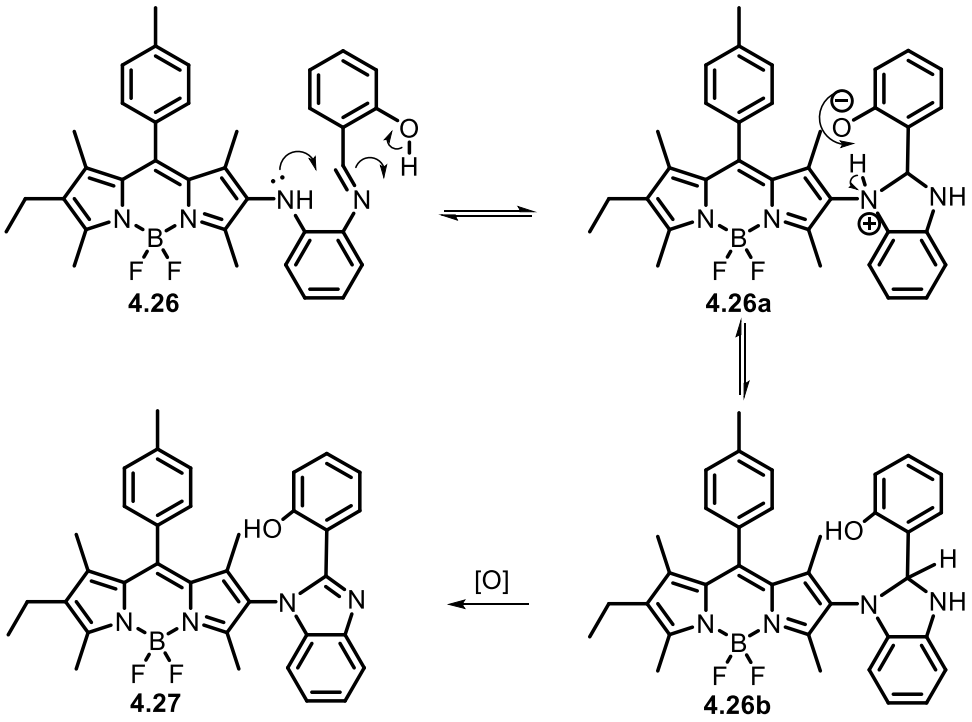

Scheme 4.14: proposed mechanism for synthesis of the BODIPY **4.27**. Conditions and reagents: air, $CHCl_3$, r.t., overnight (89%).

As shown in the above scheme, the proximal phenol may assist in the cyclisation step by protonating the imine nitrogen.

This result seem to be consistent with other research[207] which found that the preparation of the 3-benzimidazole dipyrromethane **4.29** was successfully achieved simply by treating 1,9-diformyl dipyrromethane **4.28** in methanol with *o*-phenylene diamine in the presence of a catalytic amount of TFA. The authors offered no explanation for the oxidative transformation of the formyl groups to ester and benzimidazole simply on treatment under acidic conditions. The BODIPY **4.30** was formed by subsequent oxidation with DDQ and then BF_2 chelation (Scheme 4.15). 3-Benzimidazole BODIPY **4.30** shows good selectivity toward Hg(II) in *vitro* and in *vivo*.[207]

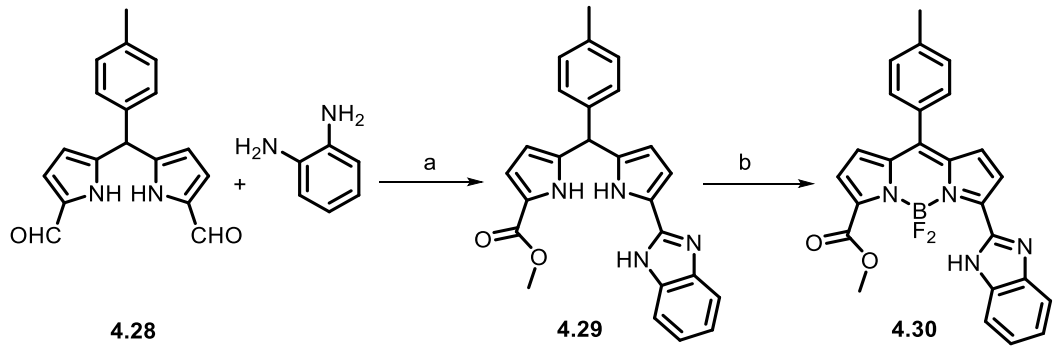

Scheme 4.15: Synthesis of the 3-benzimidazole BODIPYs **4.30**. Conditions and reagents: a) MeOH, TFA. b) DCM, DDQ, TEA and $BF_3.OEt_2$.

BODIPY **4.26** was synthesised successfully in good yield, however, it was not stable in air. Therefore, in the second attempt of synthesis of a polydentate nitrogen based BODIPY we decided to choose *bis*(pyridin-2-ylmethyl)amine, commonly known as di-(2-picolyl)amine (DPA), as a chelator.

Regioselective alkylation of BODIPY **4.9** with 3 equivalents of 2-chloromethyl pyridine hydrochloride produced the double alkylated BODIPY **4.31** together with a minor amount of the mono alkylated BODIPY **4.30** which were separable by column chromatography (Scheme 4.16). Immediately it was observed that the compounds are a dark purple colour and not fluorescent, in line with spectroscopic results for the other 2-aminoBODIPYs.

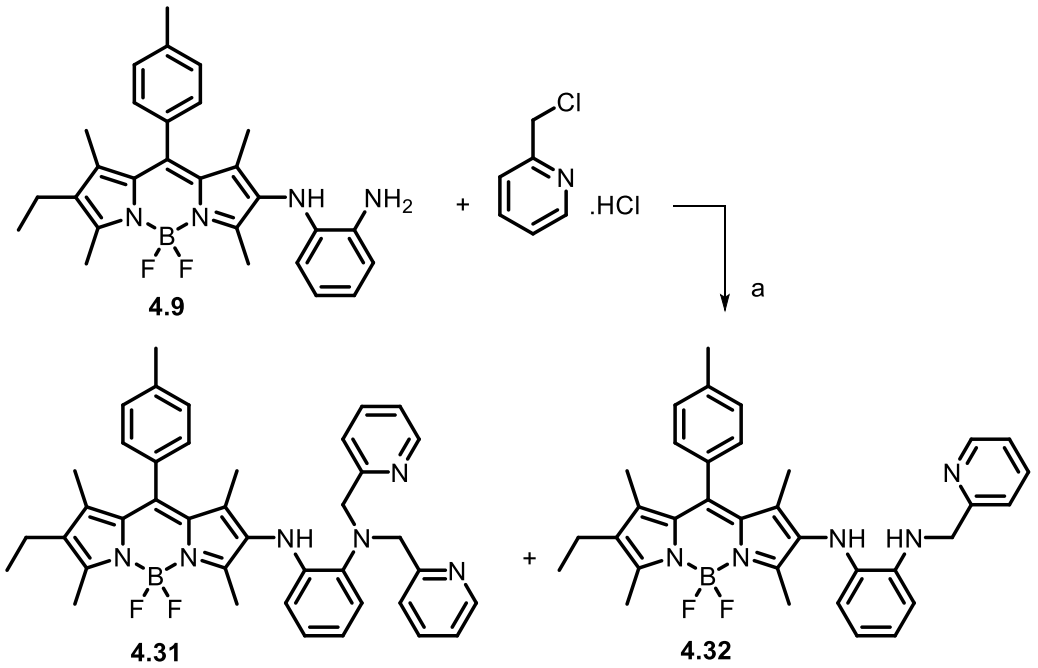

Scheme 4.16: Synthesis of the BODIPYs **4.31** and **4.32**. Conditions and reagents: a) 2-chloromethyl pyridine hydrochloride, MeCN, K_2HPO_4, reflux, overnight (**4.31** 69% and **4.32** 17%).

The absorption spectrum of dialkylated BODIPY **4.31** is represented in Figure 4.15. The low-energy maximum (λ_{abs}) occurs at 526 nm and is assigned to the S_0-S_1 (π-π^*) electronic transition associated with the BODIPY core. The molar absorption coefficient (ε) is 20,574 $M^{-1}cm^{-1}$. The BODIPY **4.31** is slightly fluorescent in THF solution with a maximum (λ_{em} = 522 nm) located at 526 nm and a low quantum yield Φ_f of 0.002.

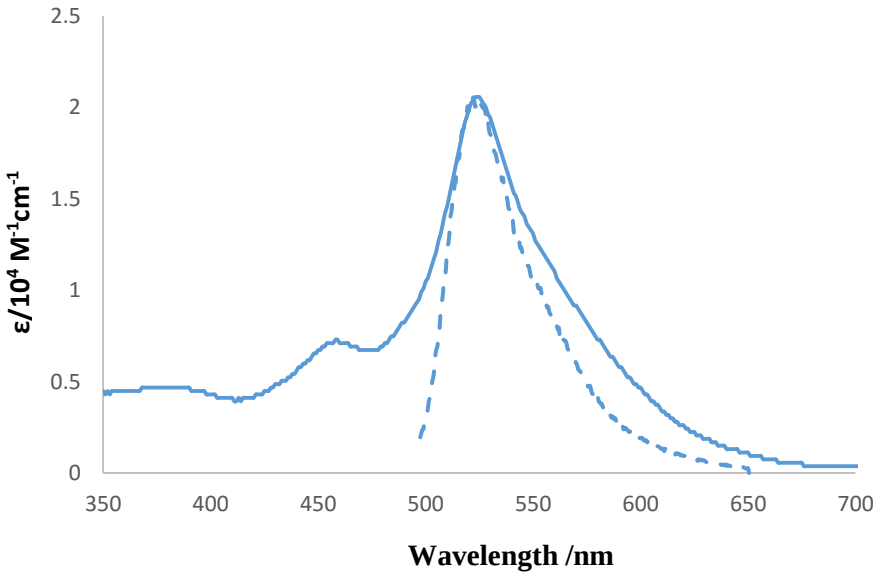

Figure 4.15: Absorption spectrum (solid lines) in terms of the molar absorption coefficient (ε) and normalised fluorescence spectrum (dashed lines) for **4.31** in THF at room temperature (λ_{ex}= 485nm).

4.5. Binding properties

Firstly, using visual examination, we checked for colour changes of BODIPY **4.31** under both naked eye and UV light, with the addition of the various metal ions (Ca^{2+}, Cu^{2+}, Fe^{2+}, Fe^{3+}, Li^{+}, Hg^{2+}, Mg^{2+}, Mn^{2+}, Ni^{2+}, Pb^{2+}, Na^{+}, Sn^{+2}, Zn^{2+}). We established that an obvious colour change (from pink to yellow or orange) of the BODIPY **4.31** solution occurs in the presence of Cu(II) and Fe(II) respectively (Figure 4.16). Nonetheless, the change of colour due to the presence of Fe(II) was not as obvious as that for Cu(II), which shows that BODIPY **4.31** might act as a sensor for copper ions.

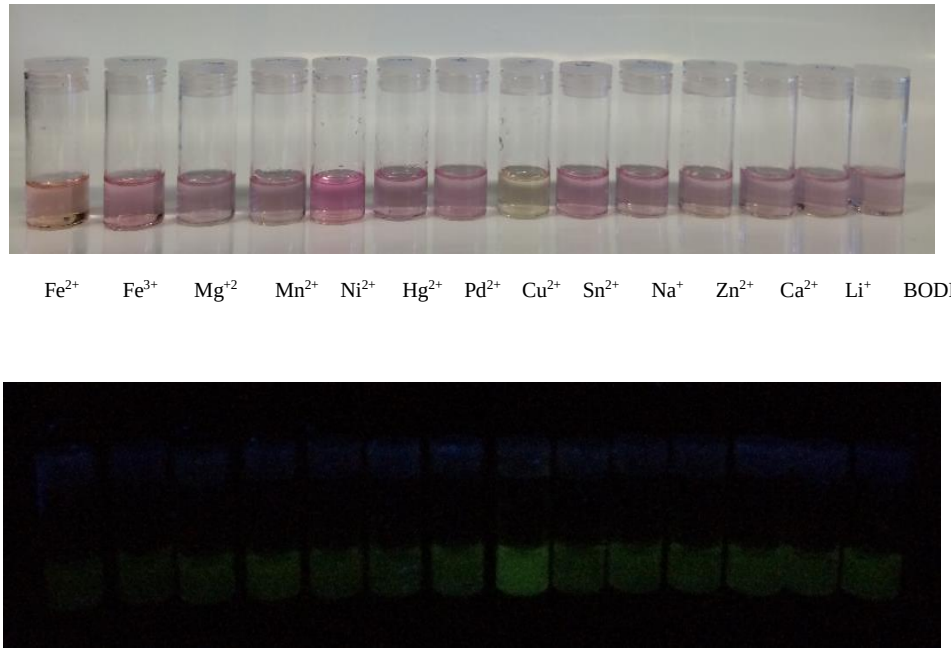

Figure 4.16: Photographs of solutions of **4.31** in HEPES-CH_3CN upon addition of various metal ions. Upper row: optical image and the lower row fluorescence observed upon excitation at 365 nm.

This result encouraged us to further investigate the selectivity of BODIPY **4.31** for Cu(II) using different spectrophotometric techniques. The emission spectra of BODIPY **4.31** in the presence of different metal ions (Ca^{2+}, Cu^{2+}, Fe^{2+}, Fe^{3+}, Li^{+}, Hg^{2+}, Mg^{2+}, Mn^{2+}, Ni^{2+}, Pb^{2+}, Na^{+}, Sn^{2+}, Zn^{2+}) were measured under simulated physiological conditions (HEPES-water/CH_3CN 9:1), (20 mM HEPES buffer pH 7.2). A stock solution of BODIPY **4.31** (1.68×10^{-4} mM) in acetonitrile was prepared and used to prepare the sample solution for the binding experiment. The fluorescence emission was recorded 120 seconds after adding each metal ion. There was a slight increase in the fluorescence emission of BODIPY **4.31** upon addition of excess of various metal ions (Ca^{2+}, Fe^{2+}, Mn^{2+}, Ni^{2+}) (Figure 4.17). However, under the same conditions, the largest increase in fluorescence intensity of BODIPY **4.31** was formed in the presence of Cu^{2+} (Figure 4.17).

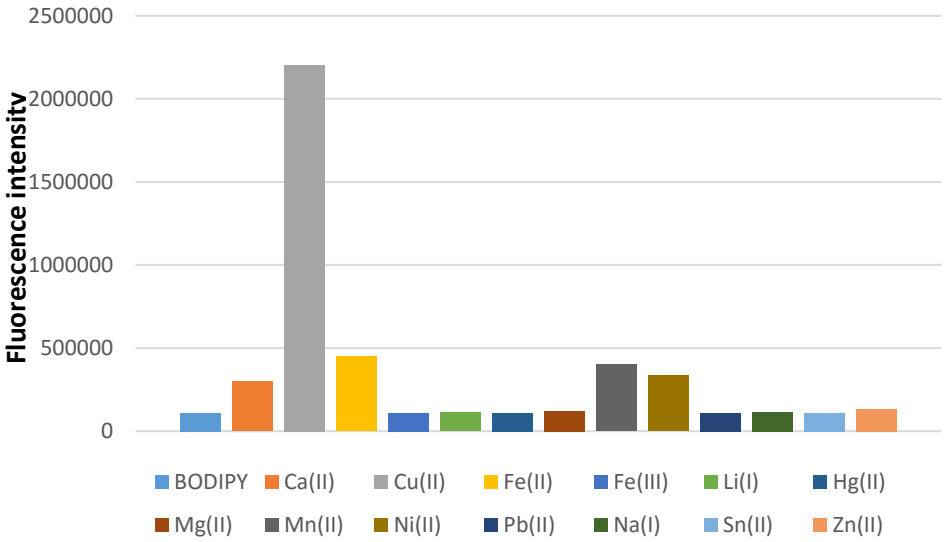

Figure 4.17: Selectivity of BODIPY **4.31** toward Cu^{2+} and other metal ions: fluorescence intensity of the BODIPY **4.31** (0.21 μM in HEPES-CH_3CN pH 7.2) after treatment with metal ions (25 eq).

Future effort will involve competitive binding experiments by addition of excess amounts of different metal ions in the presence of a small amount of Cu(II), to investigate whether the sensor can specifically detect copper ions even in the presence of excess amount of other metal ions. We will also study the binding and detection of copper ions by titration measurements of BODIPY **4.31** using spectrophotometric assays.

4.6. Conclusion

A new type of *N,O*-BODIPY **4.2** has been formed accidentally by treating 2-iodoBODIPY **3.50** with 2-aminophenol in the presence of SPhos **L8**, μ-OMs dimer $(LPdOMs)_2$ **3.54** and Cs_2CO_3. In the future, the optimised conditions for the synthesis of this type of *N,O*-BODIPY will be investigated.

The reactive novel 2-aminoBODIPY **4.9** was synthesized in good yield (95%) from the corresponding BODIPY **4.8**. Reaction of this compound with triphosgene gave the corresponding benzimidazolone-substituted BODIPY **4.18** in excellent yield (98%). The bright yellow fluorescence of the triphosgene reaction product **4.18** can be easily visualized by the naked eye. The detection limit for phosgene is 160 nM in solution at room temperature.

Moreover, the synthesis of polydentate nitrogen based BODIPY **4.31** has been achieved in excellent yields *via* the reduction of the BODIPY **4.8**, and subsequent alkylation of the diaminoBODIPY **4.9**. This route could be an excellent route to a library of new polydentate nitrogen based-BODIPY derivatives. The novel BODIPY **4.31** showed promise as a sensor for Cu^{2+} ions. Future work will test these complexes for use in diagnostic imaging and therapy.

Chapter 5: Summary

5.1 General summary

This study covers the synthesis of chiral and amino-substituted BODIPIY dyes.

The first aim of this project was to investigate synthetic approaches to chiral BODIPYs. Ultimately, these routes might be applicable to the synthesis of functionalised BODIPYs capable of interacting or coupling with non-fluorescent chiral analytes for use in enantioselective applications. Towards this end, four approaches to the synthesis of novel chiral BODIPY dyes were investigated.

The C2-symmetric axially chiral 2,6-bis(2-methoxyphenyl) BODIPY **2.6** was synthesized via Suzuki coupling of the corresponding 2,6-dibromo BODIPY with 2-methoxyphenyl boronic acid. ^{19}F NMR revealed that this compound had been produced as a 50:50 mixture of diastereoisomers (corresponding to the methoxy groups being syn and anti across the BODIPY plane). Variable temperature ^{19}F NMR indicated that these isomers did not interconvert up to 373 k, as expected due to steric hindrance to rotation around the BODIPY C2-aryl bond. Unfortunately, the stereoisomers could not be separated by chiral HPLC. The unsymmetrical axially chiral quinoline-BODIPY **2.15** was synthesized via Suzuki coupling of the corresponding 2-bromoBODIPY with phenyl boronic acid. Although some separation of the enantiomeric form of this BODIPY could be seen by chiral HPLC the resolution was not sufficient to allow isolation of pure individual enantiomers.

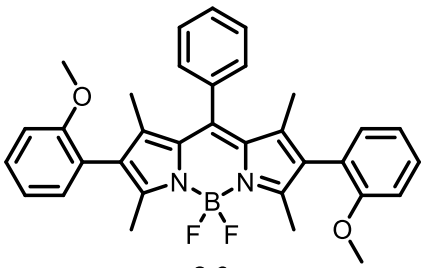

2.6

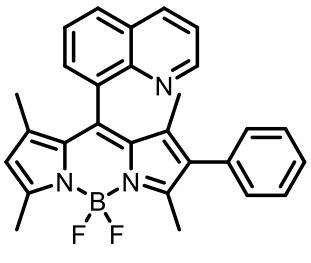

2.15

The known helically chiral aza-BODIPY compounds **2.25a, b** were synthesized successfully following the literature route. Unfortunately, all attempts to synthesise more heavily functionalized aza-BODIPY **2.26,** which carries amino groups which might interact with a chiral analyte, were unsuccessful. 2-Hydroxy-5-methyl-3-nitroacetophenone was converted to the corresponding chalcone by reaction with benzaldehyde, and then subsequently converted to the γ-nitroketone by conjugate addition of nitromethane. Further transformation to the azaBODIPY was not successful, perhaps due to interference by the second nitro group on the aromatic ring.

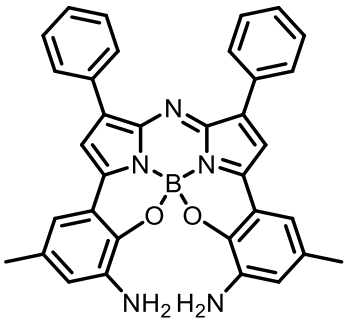

2.26

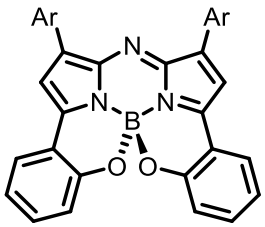

2.25a-b

a b
Ar= Ph, 4-MeOC$_6$H$_4$

A new synthetic route was developed to *N,N,O,O*-BODIPY's **2.49a-c**. Preparation of the 3,5-dibromoBODIPY's **2.56a-c** enabled late stage introduction of 2-methoxyphenyl groups by Suzuki coupling and then demethylation using BBr_3 to form the helically chiral *N,N,O,O*-BODIPYs in good yield. In comparison to the corresponding *N,N,F,F*-BODIPYs the *N,N,O,O*-systems displayed significantly red-shifted absorption and emission maxima and retained high extinction coefficients and fluorescence quantium yields. Both the p-tolyl (**2.49a**) and pyridyl-substituted systems (**2.49b**) were resolved by chiral HPLC. The enantiomeric forms of each BODIPY (**2.49a** and **b**) displayed mirror image ECD spectra and the configuration of the enantiomers was assigned on the basis of the agreement between the experimental and calculated ECD (calculations and measurement were made in the group of W. Herrebout, University of Antwerp).

The resolved enantiomers of **2.49a,b** also displayed circularly polarised luminescence (CPL) with luminescence dissymmetry factor $|g_{lum}|$ of 0.0043 (637 nm) and 0.0042 (675 nm) respectively (measured by Prof. R. D. Peacock, University of Glasgow).

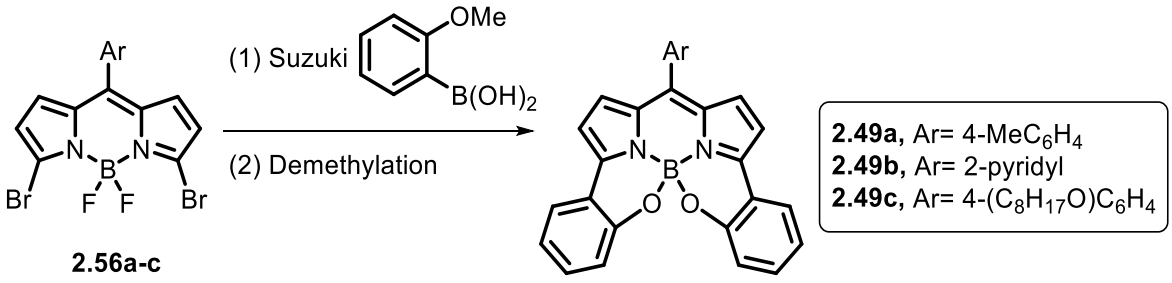

2.56a-c

Extension of our synthetic approach to *N*,*N*,*O*,*O*-BODIPYs in order to synthesise the corresponding *N*,*N*,*N*,*N*-BODIPY **2.63** was investigated. Suzuki coupling of the 3,5-dibromoBODIPY **2.56a** with 2-nitrobenzeneboronic acid followed by palladium catalysed hydrogenation gave the diamine **2.62**. Unfortunatly, due to time constraints, conversion of this compound into the *N*,*N*,*N*,*N*-BODIPY **2.63** was not accomplished.

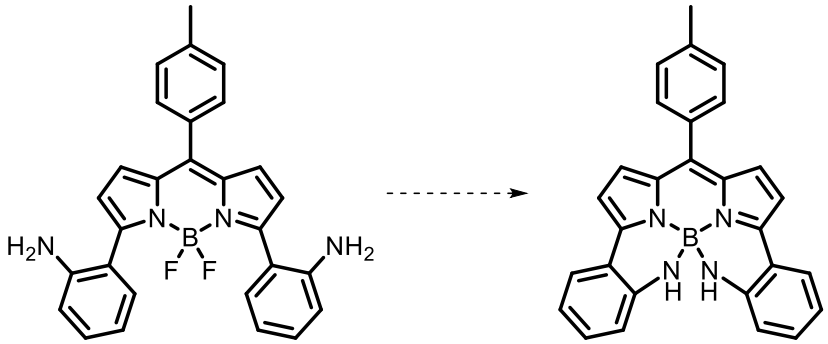

2.62 2.63

The final novel helically chiral BODIPY to be synthesised was the 'half-strapped' *N*,*N*,*O*,*F* system **2.74** which was synthesised by stepwise elaboration of the unsymmetrical BODIPY **2.69a** using a sequence of regioselective halogenation and Suzuki coupling reactions.

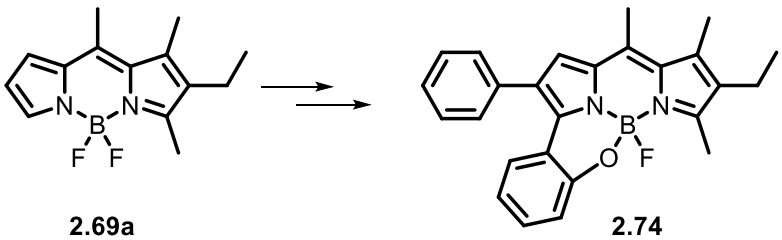

2.69a 2.74

Analytical chiral HPLC of the BODIPY **2.74** indicated that it should be possible to separate the enantiomers of this compound for further study.

The second aim of this research was to investigate the synthesis of amino-BODIPYs via metal catalysed amination reactions for use as a new strategy towards fluorescence-quenched BODIPY dyes. Attempted copper catalysed amination of the 2-iodoBODIPY **3.17** was found unexpectedly to produce the corresponding 3-aminoBODIPY **3.19** by a rather unusal vicarious nucleophilic substitution. The product distribution from reaction of a 6-deutero-2-iodoBODIPY indicated that this reaction takes place by initial nucleophilic attack at either C3 or C5, with attack at C3 predominating. Using this reaction, a range of new 3-aminoBODIPYs was synthesised and the reaction was shown to be successful with less nucleophilic nitrogen nucleophiles such as anilines and even an amide, in many cases in good yield.

In agreement with reports in the literature, the presence of the amine in the 3-position of the BODIPY leads to a broadened red-shifted absorption maximum and the fluorescence is weak and sometimes quenched.

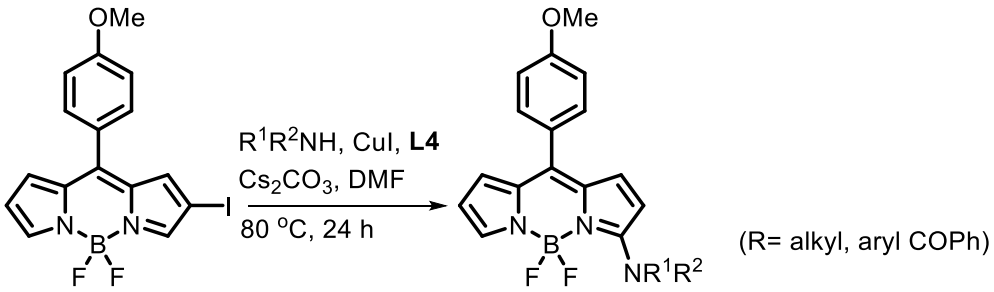

3.17 **3.19a-n**

A series of fluorescence-quenched 2-aminoBODIPY dyes was synthesised via palladium catalysed Buchwald–Hartwig amination of the corresponding 2-iodoBODIPY **3.49** (fully blocked) with anilines and a primary amine. Secondary amines were found not to react with 2-iodoBODIPY **3.50** under the given conditions.

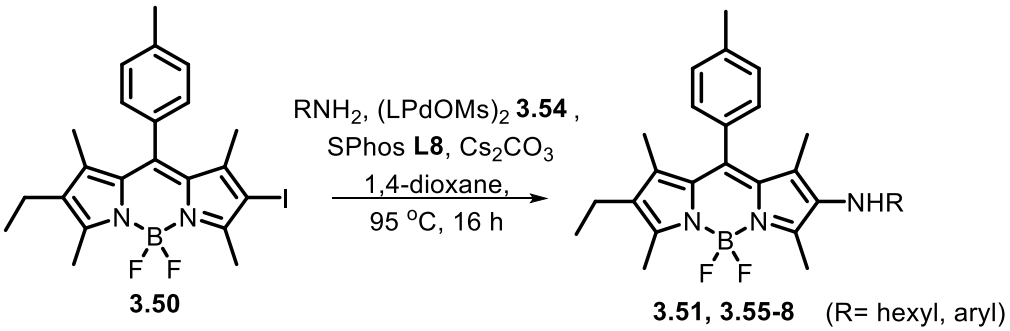

3.50 **3.51, 3.55-8** (R= hexyl, aryl)

The presence of the 2-amino group leads to broadened absorption bands and small red-shift of the absorption maximum. These compounds were found to be non-emissive which may be due to quenching via charge transfer from the electron rich amino substituent. Cyclic voltammetry indicated a very facile oxidation process, presumably associated with the amine and much lower in energy than the typical BODIPY oxidation.The modular synthesis of these quenched fluorophores allows them to be used for a wide-range of applications.

An attempt to convert the 2-iodoBODIPY **3.50** into a more highly functionalised 2-amino derivative by palladium catalysed reaction with 2-aminophenol produced instead the novel *N*,*N*,*N*,*O*-BODIPY **4.2**. It is likely that this transformation does not require palladium catalysis, and is simply base-mediated however, due to time constraints, the optimised conditions for the synthesis of this type of BODIPY have yet to be identified. The structure of this species was confirmed by x-ray crystallography and it was observed to be non-emissive.

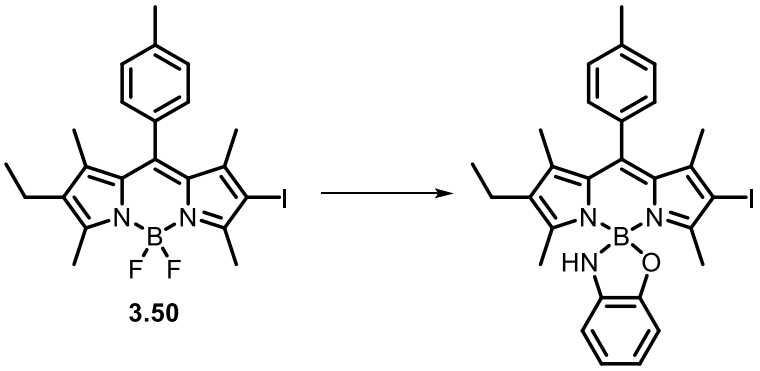

3.50 **4.2**

The 2-aminoBODIPY **4.9**, incorporating an ortho-phenylenediamine substituent, was suceessfully prepared by palladium catalysed amination of the 2-iodoBODIPY **3.50** with 2-nitroaniline followed by hydrogenation of the nitro group. Compound **4.9** was found to be non-emissive, as expected, but reacts rapidly with triphosgene to form the strongly fluorescent benzimidazolone derivative **4.18**. Fluorescence titration of the aminoBODIPY **4.9** revealed a limit of detection of 160 nM for phosgene. The bright yellow fluorescence of the triphosgene reaction product **4.18** can be easily visualized by the naked eye.

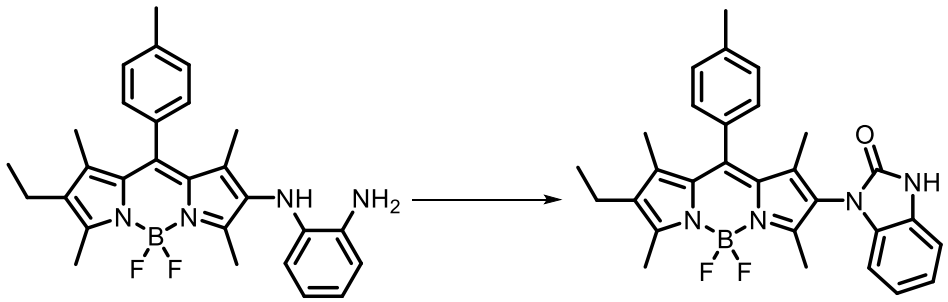

4.9 **4.18**

The regioselective alkylation of the 2-aminoBODIPY **4.9** with 2-chloromethyl pyridine hydrochloride gave doubly alkylated BODIPY **4.31** together with a minor amount of the mono alkylated BODIPY **4.32**. The novel BODIPY **4.31** showed promise as a sensor for Cu^{2+} ions. Further work needs to be done to establish whether the BODIPY **4.31** can specifically detect copper ions.

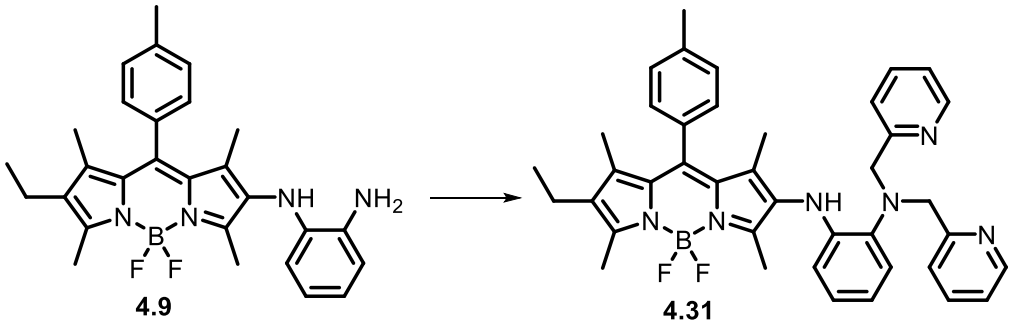

4.9 **4.31**

Chapter 6: Experimental Section

6.1. Materials and Methods

All chemicals were purchased from commercial suppliers (Sigma Aldrich, Apollo, Fluorochem and Alfa Aesar) and used without further purification except where indicated. All manipulations involving air-sensitive materials were carried out using standard Schlenk line techniques under an atmosphere of nitrogen in flame-dried glassware. Where necessary, solvents were dried prior to use.

Chloroform ($CHCl_3$), dichloromethane (CH_2Cl_2) and triethylamine (NEt_3) were distilled from calcium hydride (CaH_2); methanol (MeOH) and ethanol (EtOH) from magnesium; 1,4-dioxane, diethyl ether (Et_2O) and tetrahydrofuran (THF) from Na/benzophenone; toluene from sodium; and acetonitrile (MeCN) from K_2CO_3, under an atmosphere of nitrogen. Dimethyl formamide (DMF) was dried over activated 4 Å molecular sieves and stored under nitrogen.

IR spectra were recorded on a Varian 800 FT-IR Scimitar Series infrared spectrometer. ^{1}H, $^{13}C\{^{1}H\}$, $^{19}F\{^{1}H\}$ and $^{11}B\{^{1}H\}$NMR spectra were recorded on a JEOL ECS 400 or a Bruker Avance 300 or a Jeol Lambda 500 or a Bruker Avance 700 MHz instrument. All ^{1}H NMR were referenced relative to $CDCl_3$ ($\delta H = 7.26$, $\delta C = 77.16$). Data for ^{1}H NMR spectra are reported as follows: chemical shifts measured in ppm from internal tetramethylsilane on the δ scale, integration, multiplicity (br = broad, s = singlet, d = doublet, t = triplet, q = quartet, p = pentet and m = multiplet). ^{13}C NMR chemical shifts are reported in ppm from tetramethylsilane on the δ scale, using solvent resonance as the internal standard [deuterated chloroform ($CDCl_3$) at 77.16 ppm]. The ^{11}B NMR chemical shift is referenced to $BF_3.Et_2O$ (δ = 0ppm) and the ^{19}F NMR chemical shift is given relative to $CFCl_3$ (δ = 0 ppm).

Mass spectrometry analysis was performed using a Micromass LCT premier Mass Spectrometer in Electrospray (ES) mode. Thin layer chromatography was performed on EM reagent 0.25 mm silica gel 60F plates. Visualisation was accomplished with UV light and aqueous potassium permanganate (VII) solution. UV-vis and fluorescence spectra were recorded at 20 °C on a Shimadzu UV-1800 and Hitachi F2500 machines respectively. Relative fluorescence quantum yields (Φ_f) were determined using dilute

solutions with an absorbance below 0.1 at the excitation wavelength and using Rhodamine 6G (Φ_f = 0.95) or Rhodamine B (Φ_f = 0.65) in ethanol or MgTPP in toluene (Φ_f = 0.15) as standard. Flash column chromatography was perfomed on Fluorochem LC3025 (40-63 μm) silica gel.

4,4-Difluoro-1,3,5,7-tetramethyl-8-phenyl-4-bora-3a,4a-diaza-*s*-indacene 2.4.

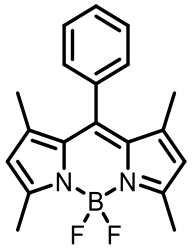

Benzoyl chloride (1.48 g, 10.5 mmol) was dissolved in dry CH_2Cl_2 (75 mL) and 2,4-dimethylpyrrole (2.00 g, 21.0 mmol) was added and the mixture was stirred at room temperature for 13 h. The mixture was then cooled to 0 ℃ and *N*,*N*-diisopropylethylamine (9.20 g, 71.4 mmol) and $BF_3.OEt_2$ (11.5 g, 80.9 mmol) were added and stirred for an additional 1 h. The reaction mixture was poured into water (100 mL). The organic layer was dried ($MgSO_4$) and the solvent was removed under reduced pressure. The product was purified using column chromatography (petroleum ether:CH_2Cl_2 1:1) to give the title compound **2.4** as a green solid (1.00 g, 30%), mp 175-176 ℃ (lit.[1] 176-177 ℃). R_f = 0.43 (petroleum ether:CH_2Cl_2 1:1). ^{1}H NMR (400 MHz, $CDCl_3$) δ 7.49 – 7.46 (m, 3H), 7.29 – 7.25 (m, 2H), 5.97 (s, 2H, pyrrole-H), 2.54 (s, 6H), 1.36 (s, 6H).^{13}C NMR (101 MHz, $CDCl_3$) δ 154.70, 142.45, 141.03, 134.27, 130.72, 128.42, 128.22, 127.21, 120.50, 13.78, 13.51.^{11}B NMR (96 MHz, $CDCl_3$) δ -0.79 (t, $J_{B\text{-}F}$ = 33.1 Hz). ^{19}F NMR (282 MHz, $CDCl_3$) δ -146.33 (q, $J_{F\text{-}B}$ = 33.1 Hz). IR (neat): υ_{max}/cm^{-1}: 2991, 1979, 1684, 1586, 1540, 1506, 1400, 1298, 1151, 969, 721. HRMS-ES Calcd for $C_{19}H_{19}N_2{}^{11}B^{19}F_2$ + H^+: 325.1688, found: 325.1685.

The spectroscopic data obtained for this compound were consistent with those reported in the literature.[55]

2,6-Dibromo-4,4-difluoro-1,3,5,7-tetramethyl-8-phenyl-4-bora-3a,4a-diaza-*s*-indacene 2.5.

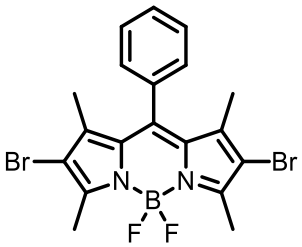

4,4-Difluoro-1,3,5,7-tetramethyl-8-phenyl-4-bora-3a,4a-diaza-*s*-indacene **2.4** (0.34 g, 1.06 mmol) was dissolved in dry CH_2Cl_2 (60 mL). Br_2 (0.67 g, 4.24 mmol) in dry CH_2Cl_2 (15 mL) was added dropwise to the mixture over 1 h. The mixture was stirred at room temperature for an additional 2 h. The mixture was washed with an aqueous solution of sodium thiosulfate (50 mL), and extracted by CH_2Cl_2 (100 mL). The organic layer was dried ($MgSO_4$), filtered and the solvent removed under reduced pressure. The product was purified using column chromatography (petroleum ether:ethyl acetate 7:1) to give the title compound **2.5** as a red solid (0.15 g, 90%), mp 230-232 ℃ (lit.[2] mp 229-231 ℃). R_f = 0.75 (petroleum ether:ethyl acetate 7:1). ^{1}H NMR (300 MHz, $CDCl_3$) δ 7.57-7.53 (m, 3H), 7.32 – 7.24 (m, 2H), 2.65 (s, 6H), 1.40 (s, 6H).^{13}C NMR (101 MHz, $CDCl_3$) δ 154.03, 142.18, 140.73, 134.45, 130.48, 129.63, 129.58, 127.83, 111.87, 13.79, 13.76. ^{11}B NMR (96 MHz, $CDCl_3$) δ 0.50 (t, $J_{B\text{-}F}$ = 32.2 Hz). ^{19}F NMR (282 MHz, $CDCl_3$) δ -146.02 (q, $J_{F\text{-}B}$ = 32.2 Hz). IR (neat): υ_{max}/cm^{-1}: 3666, 2981, 1527, 1463, 1349, 1171, 1071, 721. HRMS-ES Calcd for $C_{19}H_{17}N_2{}^{11}B^{79}Br^{81}Br^{19}F_2$ + H^+: 482.9877, found: 482.9861.

The spectroscopic data obtained for this compound were consistent with those reported in the literature.[56]

4,4-Difluoro-2,6-bis(2-methoxyphenyl)-1,3,5,7-tetramethyl-8-phenyl-4-bora-3a,4a-diaza-*s*-indacene 2.6.

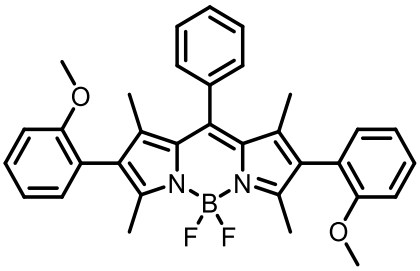

2,6-Dibromo-4,4-difluoro-1,3,5,7-tetramethyl-8-phenyl-4-bora-3a,4a-diaza-*s*-indacene **2.5** (0.10 g, 0.21 mmol) was dissolved in dry toluene (5 mL). Then 2-methoxyphenyl-boronic acid (0.10 g, 0.63 mmol), 11-dicyclohexylphosphino-12-phenyl-9,10-dihydro-9,10-ethenoanthracene (Kitphos) (0.12 g, 0.03 mmol, 12.5 mol%), $Pd(OCOCH_3)_2$ (2.00 mg, 0.01 mmol, 5 mol%), and K_3PO_4 (0.18 g, 0.83 mmol) were added. The mixture was heated under reflux for 20 h and then allowed to cool to room temperature. The solution was diluted with CH_2Cl_2 (50 mL) and washed with water (40 mL). The organic layer was dried ($MgSO_4$) and the solvent was removed under reduced pressure. The purple crude product was purified by column chromatography (petroleum ether:ethyl acetate 7:1) to give the title compound **2.6** as a pink solid (0.04 g, 36%), mp 268-272 ℃, R_f = 0.25 (petroleum ether:ethyl acetate 7:1). ^{1}H NMR (300 MHz, $CDCl_3$) δ 7.47 – 7.35 (m, 3H), 7.35 – 7.28 (m, 2H), 7.28 – 7.19 (m, 2H), 7.02 – 6.94 (m, 2H), 6.58-6.91 (m, 4H), 3.69 (s, 6H), 2.37 (s, 6H), 1.15 (s, 6H).^{13}C NMR (101 MHz, $CDCl_3$) δ 157.47, 154.99, 141.44, 135.71, 132.25, 131.30, 130.03,129.12, 129.02, 128.87, 128.40, 128.29, 122.52, 120.39, 110.91, 55.40, 13.53, 12.91.^{11}B NMR (128 MHz, $CDCl_3$) δ 0.06 (apparent t, J = 32.7 Hz).^{19}F NMR (471 MHz, $CDCl_3$) δ -145.35 (dq, $J_{F\text{-}F}$ = 109.96, $J_{F\text{-}B}$= 32.5 Hz), -145.93 (q, $J_{F\text{-}B}$ = 31.5), -146.54 (dq, $J_{F\text{-}F}$ = 109.92, $J_{F\text{-}B}$= 32.8 Hz). IR (neat): υ_{max}/cm^{-1}: 3735, 2970, 2360, 1717, 1532, 1463, 1245, 1174, 1006, 722. HRMS-ES Calcd for $C_{33}H_{31}N_2{}^{11}BO_2F_2 + H^+$: 537.2525, found: 537.2512.

Quinoline-8-carbonyl chloride hydrochloride 2.12.

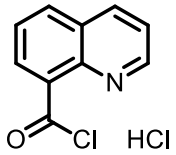

2-Quinoline carboxylic acid (0.20 g, 1.15 mmol) was dissolved in $SOCl_2$ (0.88 g, 7.39 mmol) and the mixture was stirred at room temperature under N_2 for 48 h. Hexane (5 mL) was added to the solution, a precipitate was formed and the solvent was removed using a cannula. The precipitate was dried under vacuum to give the title compound **2.12** as a tan solid (0.22 g). The product was used without further purification.

4,4-Difluoro-8-(quinolin-8-yl)-1,3,5,7-tetramethyl-4-bora-3a,4a-diaza-*s*-indacene 2.13.

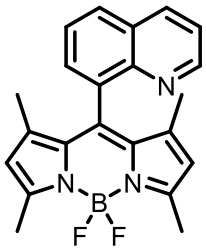

Quinoline-8-carbonyl chloride hydrochloride **2.12** (0.20 g, 0.88 mmol) was dissolved in a mixture of dry CH_2Cl_2 (75 mL) and *N*,*N*-diisopropylethylamine (0.11 g, 0.88 mmol). 2,4-Dimethylpyrrole (0.17 g, 1.75 mmol) was added and the mixture was stirred at room temperature for 24 h. The mixture was then cooled to 0 ℃ and *N*,*N*-diisopropylethylamine (0.77 g, 5.96 mmol) and $BF_3.OEt_2$ (0.96 g, 6.75 mmol) were added and stirred for an additional 2 h. The reaction mixture was poured into water (10 mL). The organic layer was dried ($MgSO_4$) and the solvent was removed under reduced pressure. The product was purified using column chromatography (CH_2Cl_2) to give the title compound **2.13** as an orange solid (1.00 g, 30%), mp 276-277 ℃. R_f = 0.32 (CH_2Cl_2). ^{1}H NMR (400 MHz, $CDCl_3$) δ 8.89 (dd, *J* = 4.2, 1.8 Hz, 1H), 8.20 (dd, *J* = 8.3, 1.8 Hz, 1H), 7.95 (dd, *J* = 6.3, 3.4 Hz, 1H), 7.70-7.60 (m, 2H), 7.43 (dd, *J* = 8.3, 4.2 Hz, 1H), 5.91 (s, 2H), 2.56 (s, 6H), 0.99 (s, 6H). ^{13}C NMR (101 MHz, $CDCl_3$) δ 155.03, 151.20, 146.74, 142.26, 140.28, 136.11, 134.69, 132.18, 129.61, 129.38, 128.38, 126.74, 121.77, 121.02, 14.66, 13.98 .^{11}B NMR (128 MHz, $CDCl_3$) δ -0.05 (t, $J_{B\text{-}F}$ = 32.2 Hz). ^{19}F NMR (282 MHz, $CDCl_3$) δ -145.26 (dq, $J_{F\text{-}F}$ = 108.9, J_{FB} = 32.2 Hz), -147.02 (dq, $J_{F\text{-}F}$ = 108.9, J_{FB} = 33.2 Hz). IR (neat): υ_{max}/cm^{-1}: 2991, 2918, 2360, 1535, 1497, 1296, 1154, 966. 745. HRMS-ES Calcd for $C_{22}H_{20}N_3{}^{11}B^{19}F_2 + Na^+$: 398.1616, found: 398.1607.

2-Bromo-4,4-difluoro-8-(quinolin-8-yl)-1,3,5,7-tetramethyl-4-bora-3a,4a-diaza-*s*-indacene 2.14.

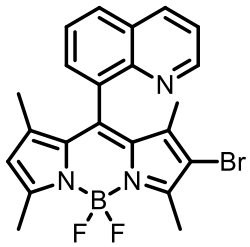

4,4-Difluoro-8-(quinolin-8-yl)-1,3,5,7-tetramethyl-4-bora-3a,4a-diaza-*s*-indacene **2.13** (0.10 g, 0.27 mmol) was dissolved in dry acetonitrile (45 mL). $CuBr_2$ (0.11 g, 0.79 mmol) and K_2CO_3 were added and the mixture was stirred at room temperature for an additional 2 h. The solvent was removed under reduced pressure. The residue was dissolved in ethyl acetate (20 mL) and washed with water (30 mL). The organic layer was dried ($MgSO_4$), filtered and the solvent removed under reduced pressure. The product was purified using column chromatography (petroleum ether:ethyl acetate 5:1) to give the title compound **2.14** as an orange solid (0.16 g, 60%), mp 248-249℃. R_f = 0.29 (petroleum ether:ethyl acetate 5:1). ^{1}H NMR (400 MHz, $CDCl_3$) δ 8.89 (dd, *J* = 4.1, 1.7 Hz, 1H), 8.22 (dd, *J* = 8.3, 1.7 Hz, 1H), 7.98 (dd, *J* = 7.9, 1.7 Hz, 1H), 7.71 – 7.58 (m, 2H), 7.45 (dd, *J* = 8.3, 4.2 Hz, 1H), 5.97 (s, 1H), 2.60 (s, 3H), 2.58 (s, 3H), 1.00 (s, 3H), 0.99 (s, 3H). ^{11}B NMR (96 MHz, $CDCl_3$) δ 0.81 (t, $J_{B\text{-}F}$ = 31.9 Hz). ^{19}F NMR (282 MHz, $CDCl_3$)) δ -145.18 (dq, $J_{F\text{-}F}$ = 108.9, $J_{F\text{-}B}$ = 31.9), -145.18 (dq, $J_{F\text{-}F}$ = 108.9, $J_{F\text{-}B}$ = 31.9 Hz). IR (neat): υ_{max}/cm^{-1}: 2970, 2922, 2360, 1733, 1538, 1461, 1302, 1161, 969, 805, 744. HRMS-ES Calcd for $C_{22}H_{19}N_3{}^{11}B^{81}Br^{19}F_2 + Na^+$: 478.0701, found: 478.0707.

4,4-Difluoro-8-(quinolin-8-yl)-2-phenyl-1,3,5,7-tetramethyl-4-bora-3a,4a-diaza-*s*-indacene 2.15.

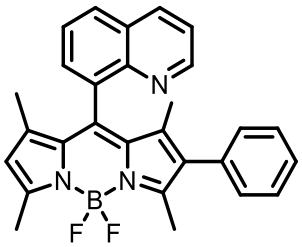

2-Bromo-4,4-difluoro-8-(quinolin-8-yl)-1,3,5,7-tetramethyl-4-bora-3a,4a-diaza-*s*-indacene **2.14** (0.10 g, 0.22 mmol) was dissolved in dry toluene (3 mL) and THF (3 mL). Then phenylboronic acid (0.09 g, 0.73 mmol), $Pd(PPh_3)_4$ (0.01 g, 0.01 mmol, 5 mol%), and aqueous Na_2CO_3 (1 M, 1.0 mL, 1.0 mmol) were added. The mixture was heated under reflux for 24 h and then allowed to cool to room temperature. The solution was diluted with CH_2Cl_2 (60 mL) and washed with brine (30 mL). The organic layer was dried ($MgSO_4$) and the solvent was removed under pressure. The orange crude product was purified by column chromatography (petroleum ether:CH_2Cl_2 1:1) to give the title compound **2.15** as an orange solid (0.06 g, 86%), mp 190-192 °C, R_f = 0.37 (petroleum ether:CH_2Cl_2, 1:1). ^{1}H NMR (300 MHz, $CDCl_3$) δ 8.85 (dd, *J* = 4.2, 1.8 Hz, 1H), 8.14 (dd, *J* = 8.3, 1.7 Hz, 1H), 7.89 (dd, *J* = 7.2, 2.5 Hz, 1H), 7.69 – 7.53 (m, 2H), 7.37 (dd, *J* = 8.3, 4.2 Hz, 1H), 7.30 – 7.13 (m, 4H), 7.07 – 6.99 (m, 1H), 5.87 (s, 1H), 2.52 (s, 3H), 2.46 (s, 3H), 0.93 (s, 3H), 0.88 (s, 3H). ^{13}C NMR (75 MHz, $CDCl_3$) δ 155.18, 153.75, 151.09, 147.14, 142.19, 140.65, 138.33, 135.78, 135.26, 134.02, 133.44, 132.56, 131.90, 130.15, 129.66, 129.08, 128.43, 128.08, 126.80, 126.56, 121.60, 121.00, 14.46, 13.74, 13.20, 11.96. ^{11}B NMR (96 MHz, $CDCl_3$) δ 0.81 (apparent t, $J_{B\text{-}F}$ = 32.5 Hz).^{19}F NMR (376 MHz, $CDCl_3$) δ -145.30 (dq, $J_{F\text{-}F}$ = 110.0, $J_{F\text{-}B}$ = 33.6 Hz), -146.91 (dq, $J_{F\text{-}F}$ = 110.0, $J_{F\text{-}B}$ = 32.2 Hz). IR (neat): υ_{max}/cm^{-1}: 2969, 2360, 1538, 1494, 1302, 1162, 980, 744. HRMS-ES Calcd for $C_{28}H_{24}N_3{}^{11}BF_2$ + Na^+: 474.1929, found: 474.1929.

1-(2-Hydroxyphenyl)-3-phenylpropenone 2.22a.

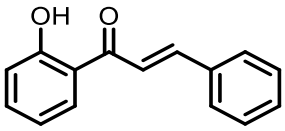

An aqueous solution of NaOH (60%, 30.0 g, 750 mmol in 50 mL of water) was added to a solution of 2'-hydroxyacetophenone (1.85 g, 13.6 mmol) in MeOH (50 mL). The resulting yellow solution was cooled to room temperature and benzaldehyde (1.75 g, 16.5 mmol) was added. The mixture was stirred at room temperature for 48 h. The solution was poured into a mixture of water (30 mL) and ice. Conc. HCl (80 mL) was added until the pH was adjusted to 2. The solution was extracted with chloroform (124 mL) and the organic extract was washed with saturated aqueous $NaHCO_3$ (2 x 80 mL). The organic extract was dried (Na_2SO_4) and the solvent was removed under reduce pressure. The crude product was recrystallized from EtOH to give the title compound **2.22a** as a yellow solid (1.60 g, 52%), mp 85-87 ^oC (lit.[3] 81-83 ^oC). ^1H NMR (400 MHz, $CDCl_3$) δ 12.83 (s, 1H), 7.92 (d, *J* = 15.4 Hz, 1H), 7.93 (dd, *J* = 8.2, 1.8 Hz, 1H), 7.66 (d, *J* = 15.5 Hz, 1H), 7.68 – 7.65 (m, 2H), 7.50 (ddd, *J* = 8.6, 7.2, 1.6 Hz, 1H), 7.46 – 7.41 (m, 3H), 7.03 (dd, *J* = 8.4, 1.0 Hz, 1H), 6.95 (ddd, *J* = 8.2, 7.3, 1.1 Hz, 1H). ^{13}C NMR (101 MHz, $CDCl_3$) δ 193.83, 163.70, 145.59, 136.54, 134.66, 131.06, 129.77, 129.15, 128.78, 120.16, 120.10, 118.98, 118.74. IR (neat): υ_{max}/cm^{-1}: 3051, 2879, 1638, 1570, 1485, 1437, 1340, 1202, 1152, 976, 729. HRMS-ES Calcd for $C_{15}H_{12}O_2 + H^+$: 225.0916, found: 225.0907.

The spectroscopic data obtained for this compound were consistent with those reported in the literature.[73]

1-(2-Hydroxyphenyl)-3-(4-methoxyphenyl)propanone 2.22b.

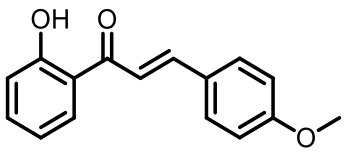

An aqueous solution of potassium hydroxide (21.0 g, 374 mmol in 30 mL of water) was added to a solution of 2'-hydroxyacetophenone (16.4 g, 120 mmol) in ethanol (300 mL). The resulting yellow solution was cooled to room temperature and 4-methoxybenzaldehyde (16.4 g, 120 mmol) was added. The mixture was stirred at room temperature for 24 h. The solution was poured into a mixture of water (1500 mL) and ice. Conc.HCl was added until the pH was adjusted to 2. The resulting orange precipitate was filtered and washed with water. The crude product was recrystallized from EtOH to give the title compound **2.22b** as a yellow solid (15.0 g, 54%), mp 93-95℃ (lit.[4] 93-94℃). ^{1}H NMR (400 MHz, $CDCl_3$) δ 12.97 (s, 1H), 7.91 (d, *J* = 15.5 Hz, 1H), 7.93 (d, *J* = 7.8 Hz, 1H), 7.66 (d, *J* = 8.4 Hz, 2H), 7.57 (d, *J* = 15.5 Hz, 1H), 7.54 – 7.48 (m, 1H), 7.04 (d, *J* = 8.2Hz, 1H), 7.01 – 6.95 (m, 3H), 3.89 (s, 3H).^{13}C NMR (75 MHz, $CDCl_3$) δ 193.64, 163.61, 162.12, 145.22, 135.94, 130.43, 129.53, 127.49, 120.26, 118.59, 117.87, 114.26, 114.00, 55.34. IR (neat): υ_{max}/cm^{-1}: 2840, 2754, 1635, 1607, 1558, 1492, 1423, 1202, 984, 757. HRMS-ES calcd for $C_{16}H_{14}O_3 + H^+$: 255.1021, found: 255.1012.

The spectroscopic data obtained for this compound were consistent with those reported in the literature.[72]

1-(2-Hydroxyphenyl)-4-nitro-3-phenylbutan-1-one 2.23a.

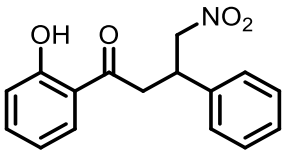

1-(2-Hydroxyphenyl)-3-phenylpropenone **2.22a** (4.00 g, 17.8 mmol) was dissolved in methanol (40 mL). Then diethylamine (1.90 g, 70.3 mmol) and nitromethane (1.07 g, 70.3 mmol) were added. The mixture was heated under reflux for 17 h and then allowed to cool to room temperature. 2M HCl was added until the pH was adjusted to 4 and CH_2Cl_2 (100 mL) was added. The organic layer was dried (Na_2SO_4) and the solvent was removed under reduced pressure. The green crude product was recrystallized from methanol to give the title compound **2.23a** as a white crystals (2.50 g, 55%), mp 78-80℃ (lit.[4] 76-77℃). ^{1}H NMR (300 MHz, $CDCl_3$) δ 11.99 (s, 1H), 7.74 (dd, *J* = 8.1, 1.6 Hz, 1H), 7.50 (ddd, *J* = 8.6, 7.2, 1.6 Hz, 1H), 7.41 – 7.28 (m, 5H), 7.00 (dd, *J* = 8.5, 1.0 Hz, 1H), 6.92 (ddd, *J* = 8.2, 7.2, 1.1 Hz, 1H), 4.84 (dd, *J* = 12.5, 6.9 Hz, 1H), 4.71 (dd, *J* = 12.5, 7.7 Hz, 1H), 4.30 – 4.18 (m, 1H), 3.64 – 3.39 (m, 2H).^{13}C NMR (75 MHz, $CDCl_3$) δ 202.72, 162.59, 138.83, 136.76, 129.57, 129.11, 127.97, 127.39, 119.08, 118.73, 79.52, 41.16, 39.26. IR (neat): υ_{max}/cm^{-1}: 3297, 3032, 2282, 1643, 1550, 1292, 1160, 702. HRMS-ES Calcd for $C_{16}H_{15}NO_4$ + Na^+: 308.0899, found: 308.0898.

The spectroscopic data obtained for this compound were consistent with those reported in the literature.[72]

1-(2-Hydroxyphenyl)-3-(4-methoxyphenyl)-4-nitrobutan-1-one 2.23b.

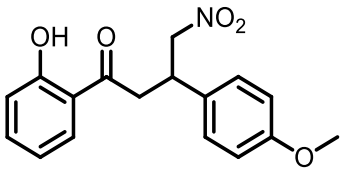

1-(2-Hydroxyphenyl)-3-(4-methoxyphenyl)propanone **2.22b** (15.0 g, 58.9 mmol) was dissolved in methanol (500 mL). Then diethylamine (20.2 g, 276 mmol) and nitromethane (16.8 g, 275 mmol) were added. The mixture was heated under reflux for 17 h. 2M HCl was added until the pH was adjusted to 4 and CH_2Cl_2 (100 mL) was added. The organic layer was dried (Na_2SO_4) and the solvent was removed under reduced pressure. The green crude product was recrystallized from methanol to give the title **2.23b** as a white crystals (15.0 g, 80%), mp 88-89℃ (lit.[4] 84-86℃). ^{1}H NMR (300 MHz, $CDCl_3$) δ 12.01 (s, 1H), 7.73 (d, *J* = 8.1 Hz, 1H), 7.50 (t, *J* = 7.2 Hz, 1H), 7.21 (d, *J* = 8.7 Hz, 2H), 6.99 (d, *J* = 8.4 Hz, 1H), 6.92 (t, *J* = 6.2 Hz, 1H), 6.88 (d, *J* = 8.6 Hz, 2H), 4.80 (dd, *J* = 12.4, 6.9 Hz, 1H), 4.66 (dd, *J* = 12.4, 7.8 Hz, 1H), 4.20 (apparent p, *J* = 7.1 Hz, 1H), 3.80 (s, 3H), 3.57 – 3.38 (m, 2H). ^{13}C NMR (101 MHz, $CDCl_3$) δ 202.81, 162.64, 162.56, 136.67, 130.56, 129.69, 128.56, 119.45, 118.81, 114.85, 79.88, 55.36, 41.30, 38.53. IR (neat): υ_{max}/cm^{-1}: 2981, 2404, 1646, 1615, 1581, 1549, 1512, 1244, 1157, 972, 723. HRMS-ES Calcd for $C_{17}H_{17}NO_5 + Na^+$: 338.1004, found: 338.1013.

The spectroscopic data obtained for this compound were consistent with those reported in the literature.[72]

[5-(2-Hydroxyphenyl)-3-phenyl-1H-pyrrol-2-yl]-[5-(2-hydroxyphenyl)-3-phenylpyrrol-2-ylidene]amine 2.24a.

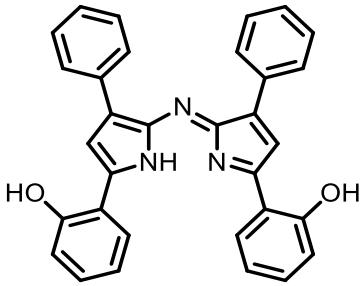

1-(2-Hydroxyphenyl)-4-nitro-3-phenylbutan-1-one **2.23a** (1.50 g, 5.90 mmol) and ammonium acetate (16.0 g, 205 mmol) were heated under reflux in cumene (3 mL) for 3 h. The resulting dark blue mixture was cooled to room temperature, diluted with CH_2Cl_2 (80 mL) and the organic solution was then washed with water (4 x 120 mL). The organic layer was dried (Na_2SO_4) and the solvent was removed under reduced pressure. The resulting solid was triturated with cold methanol (25 mL) and filtered to give the title compound as a dark blue solid **2.24a** (0.11 g, 11%), mp >260℃ (lit.[4] mp >230℃). ^{1}H NMR (400 MHz, $CHCl_3$) δ 8.02 – 7.96 (m, 4H), 7.80 – 7.75 (m, 2H), 7.43 – 7.33 (m, 6H), 7.27 – 7.21 (m, 7H), 7.01 – 6.95 (m, 4H). Due to insolubility a ^{13}C NMR spectrum was not obtained. IR (neat): υ_{max}/cm^{-1}: 3418, 3061, 1953, 1602, 1535, 1479, 1290, 1135, 909, 741. HRMS-ES Calcd for $C_{32}H_{23}N_3O_2$ + Na^+: 504.1688, found: 504.1694.

The spectroscopic data obtained for this compound were consistent with those reported in the literature.[72]

[5-(2-Hydroxyphenyl)-3-(4-methoxyphenyl)-1H-pyrrol-2-yl]-[5-(2-hydroxyphenyl)-3-(4-methoxyphenyl)-pyrrol-2-ylidene]amine 2.24b.

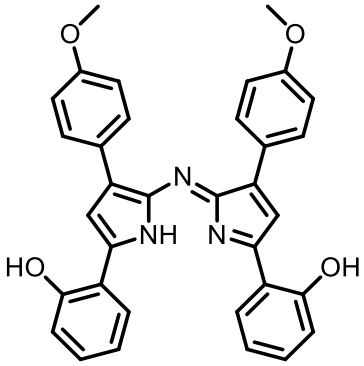

1-(2-Hydroxyphenyl)-4-nitro-3-phenylbutan-1-one **2.24b** (2.00 g, 6.34 mmol) and ammonium acetate (16.0 g, 205 mmol) were heated under reflux in cumene (3 mL) for 3 h. The resulting dark blue mixture was cooled to room temperature, diluted with CH_2Cl_2 (60 mL) and the organic solution was then washed with water (4 x 120 mL). The organic layer was dried (Na_2SO_4) and the solvent was removed under reduced pressure. The resulting solid was triturated with cold methanol (25 mL) and filtered to the title compound as a dark blue solid **2.24b** (0.7g, 20%), mp > 260℃ (lit.[4] > 240℃). ^{1}H NMR (300 MHz, $CDCl_3$, OH and NH signals not observed) δ 8.02 – 7.95 (m, 4H), 7.78 (dd, *J* = 8.3, 1.6 Hz, 2H), 7.24 (d, *J* = 7.5 Hz, 2H), 7.21 (s, 2H), 7.01 (d, *J* = 2.0 Hz, 2H), 6.99 – 6.94 (m, 7H), 3.91 (s, 6H).^{13}C NMR spectrum was not obtained for the product due to insolubility. IR (neat): υ_{max}/cm^{-1}: 3575, 3432, 2981, 2891, 1606, 1505, 1285, 965, 748. HRMS-ES Calcd for $C_{34}H_{27}N_3O_4 + H^+$: 542.2080, found: 542.2078.

The spectroscopic data obtained for this compound were consistent with those reported in the literature.[72]

Boron chelated [5-(2-hydroxyphenyl)-3-phenyl-1H-pyrrol-2-yl]-[5-(2-hydroxyphenyl)-3-phenylpyrrol-2ylidene]amine 2.25a.

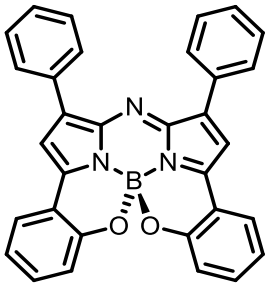

[5-(2-Hydroxyphenyl)-3-phenyl-1*H*-pyrrol-2-yl]-[5-(2-hydroxyphenyl)-3-phenylpyrrol-2-ylidene]amine **2.24a** (0.10 g, 0.20 mmol) was dissolved in toluene (20 mL). Diisopropylethylamine (0.27 g, 2.01 mmol) and $BF_3.Et_2O$ (0.41 g, 2.90 mmol) were then added. The solution was heated under reflux for 2 h. The solution was cooled to room temperature and washed with water (3 × 120 mL). The organic layer was dried (Na_2SO_4) and the solvent was removed under reduce pressure. The crude product was purified by column chromatography with (petroleum ether:ethyl acetate 2:1) to give the title compound **2.25a** as a brown solid (0.08 g, 82%), mp 261-263 ℃ (lit.[4] mp >230 ℃). R_f = 0.67 (petroleum ether:ethyl acetate 2:1). ^{1}H NMR (300 MHz, $CDCl_3$) δ 8.21 – 8.14 (m, 4H), 7.90 (dd, *J* = 7.8, 1.6 Hz, 2H), 7.55 – 7.40 (m, 8H), 7.27 (s, 2H), 7.15 (td, *J* = 7.5, 1.1 Hz, 2H), 7.05 (dd, *J* = 8.2, 1.1 Hz, 2H). ^{13}C NMR (101 MHz, $CDCl_3$) δ 156.04, 149.88, 144.93, 142.22, 133.27, 132.45, 129.20, 129.01, 128.65, 126.52, 120.84, 120.23, 118.93, 113.28. IR (neat): υ_{max}/cm^{-1}: 2961, 2927, 1728, 1607, 1487, 1427, 1136, 1099, 749. HRMS-ES Calcd for $C_{32}H_{20}BN_3O_2 + H^+$: 490.1727, found: 490.1727.

The spectroscopic data obtained for this compound were consistent with those reported in the literature.[72]

Boron chelated [5-(2-hydroxyphenyl)-3-(4-methoxyphenyl)-1H-pyrrol-2-yl]-[5-(2-hydroxyphenyl)-3-(4-methoxyphenyl)-pyrrol-2-ylidene]amine 2.25b.

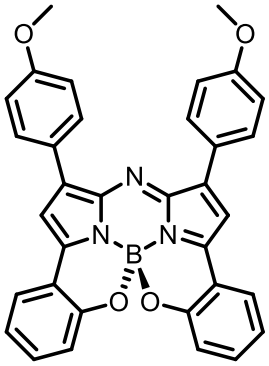

[5-(2-Hydroxyphenyl)-3-(4-methoxyphenyl)-1*H*-pyrrol-2-yl]-[5-(2-hydroxyphenyl)-3-(4-methoxyphenyl)-pyrrol-2-ylidene]amine **2.24b** (0.16g, 0.30 mmol) was dissolved in toluene (60 mL). Diisopropylethylamine (0.54g, 4.17 mmol) and $BF_3.Et_2O$ (0.42 g, 2.98 mmol) were then added. The solution was heated under reflux for 2 h. The solution was cooled to room temperature and washed with water (3 × 120 mL). The organic layer was dried (Na_2SO_4) and the solvent was removed under reduced pressure. The crude product was purified by column chromatography (petroleum ether:ethyl acetate 2:1) to give the title compound **2.25b** as a purple solid (0.12 g, 73%), mp 264-266℃ (lit.[4] mp >230℃). R_f = 0.52 (petroleum ether:ethyl acetate 2:1). ^{1}H NMR (300 MHz, $CDCl_3$) δ 8.15-8.20 (m, 4H), 7.87-7.91 (m, 2H), 7.41 (t, *J* = 7.0 Hz, 2H), 7.17 – 7.08 (m, 4H), 7.03 (m, 6H), 3.92 (s, 6H). ^{13}C NMR (101 MHz, $CDCl_3$) δ 160.81, 156.09, 149.67, 144.75, 142.03, 133.19, 130.62, 126.66, 125.40, 120.92, 120.27, 119.07, 114.36, 111.66, 55.53. IR (neat): υ_{max}/cm^{-1}: 2961, 2840, 1603, 1482, 1454, 1235, 1135, 1021, 748. HRMS-ES Calcd for $C_{34}H_{24}BN_3O_4$ + Na^+: 572.1758, found: 572.1779.

The spectroscopic data obtained for this compound were consistent with those reported in the literature.[72]

1-(2-Hydroxy-3-nitro-5-methylphenyl)-3-phenylpropenone 2.27.

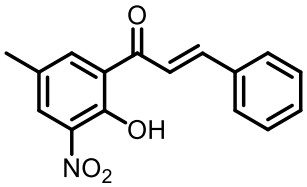

An aqueous solution of potassium hydroxide (0.89 g, 15.4 mmol in 1.3 mL of water) was added to a solution of 2-hydroxy-5-methyl-3-nitroacetophenone (1.0 g, 5.12 mmol) in ethanol (60 mL). The resulting orange solution was cooled to room temperature and benzaldehyde (0.54 g, 5.12 mmol) was added. The mixture was stirred at room temperature for 24 h. The solution was poured into a mixture of water (20 mL) and ice. Conc. HCl was added until the pH was adjusted to 2. The resulting yellow precipitate was filtered and washed with water. The crude product was recrystallized from MeOH to give the title compound **2.27** as a yellow solid (1.30 g, 89%), mp 162-165℃. ^{1}H NMR (400 MHz, $CDCl_3$) δ 13.07 (s, 1H), 8.04 (d, *J* = 2.1 Hz, 1H), 7.94 (s, 1H), 7.91 (d, *J* = 15.5 Hz, 1H), 7.68-7.66 (m, 2H), 7.57 (d, *J* = 15.5 Hz, 1H), 7.47-7.44 (m, 3H), 2.42 (s, 3H). ^{13}C NMR (101 MHz, $CDCl_3$) δ 192.31, 154.53, 146.83, 136.70, 134.32, 131.47, 131.12, 129.22, 128.99, 128.45, 124.90, 121.33, 20.47. IR (neat): υ_{max}/cm^{-1}: 3410, 3359, 2981, 2889, 2360, 1684, 1560, 1267, 1029, 716. HRMS-ES calcd for $C_{16}H_{13}NO_4$ + H^+: 284.0923, found: 284.0912.

1-(2-Hydroxy-5-methyl-3-nitrophenyl)-4-nitro-3-phenylbutan-1-one 2.28.

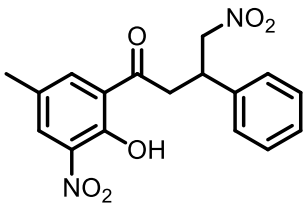

1-(2-Hydroxy-3-nitro-5-methylphenyl)-3-phenylpropenone **2.27** (0.50 g, 1.76 mmol) was dissolved in dry methanol (10 mL). Diethylamine (0.52 g, 7.06 mmol) and nitromethane (0.43 g, 7.06 mmol) were then added. The mixture was heated under reflux for 17 h and then allowed to cool to room temperature. 2M HCl was added until the pH was adjusted to 4 and CH_2Cl_2 (100 mL) were added. The organic layer was dried (Na_2SO_4) and the solvent was removed under reduced pressure. The brown crude product was purified by column chromatography (petroleum ether:CH_2Cl_2 1:4) to give the title compound **2.28** as a tan solid (0.45 g, 74%), mp 150-152℃. ^{1}H NMR (400 MHz, $CDCl_3$) δ 12.09 (s, 1H), 8.03 (s, 1H), 7.80 (s, 1H), 7.39 – 7.20 (m, 5H), 4.72 – 4.65 (m, 2H), 4.27 – 4.15 (m, 1H), 3.64 – 3.45 (m, 2H), 2.35 (s, 3H). ^{13}C NMR (101 MHz, $CDCl_3$) δ 199.26, 153.38, 138.67, 137.78, 136.06, 130.99, 129.30, 129.23, 128.14, 127.54, 125.30, 79.62, 44.67, 39.28, 20.34. IR (neat): υ_{max}/cm^{-1}: 3072, 2931, 1655, 1584, 1550, 1530, 1466, 1353, 1272, 1162, 702. HRMS-ES Calcd for $C_{17}H_{16}N_2O_6$ + Na^+: 367.0906, found: 367.0912.

3-Amino-2-hydroxy-5-methylacetophenone 2.39.

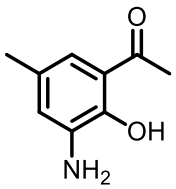

2-Hydroxy-5-methyl-3-nitroacetophenone (0.50 g, 2.56 mmol) was dissolved in dry ethanol (30 mL). Tin chloride dihydrate (2.89 g, 12.8 mmol) was added. The mixture was heated under reflux for 3 h and then allowed to cool to room temperature. 2M $NaHCO_3$ was added until the pH was adjusted to 7 and ethyl acetate (100 mL) was added. The organic layer was dried ($MgSO_4$) and the solvent was removed under reduced pressure. The brown crude product was purified by column chromatography (CH_2Cl_2) to give the title compound **2.39** as a yellow solid (0.32 g, 75%), mp 52-54 ℃ (lit.[5] mp 55-57 ℃). ^{1}H NMR (400 MHz, $CDCl_3$) δ 12.28 (s, 1H), 6.92 (s, 1H), 6.72 (s, 1H), 3.85 (s, 2H), 2.58 (s, 3H), 2.23 (s, 3H). ^{13}C NMR (101 MHz, $CDCl_3$) δ 205.13, 148.51, 136.14, 128.02, 121.38, 119.47, 118.77, 26.89, 20.93. IR (neat): υ_{max}/cm^{-1}: 3453, 3369, 2919, 1607, 1471, 1372, 1314, 1280, 1222, 1186, 1151, 1017, 781. HRMS-ES Calcd for $C_9H_{11}NO_2$ + H^+: 166.0868, found: 166.0861.

The spectroscopic data obtained for this compound were consistent with those reported in the literature.[208]

3-*N*-Boc-amino-2-hydroxy-5-methylacetophenone 2.40.

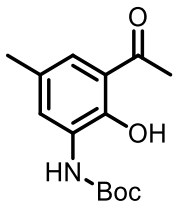

3-Amino-2-hydroxy-5-methylacetophenone **2.39** (0.20 g, 1.21 mmol) was dissolved in dry CH_2Cl_2 (8 mL). Triethylamine (0.13 g, 1.34 mmol) was added. Di-*tert*-butyl dicarbonate (0.29 g, 1.34 mmol) in CH_2Cl_2 (3 mL) was added to the mixture dropwise over 10 min and the mixture was stirred at room temperature for 48 h. The solution was poured into water (10 mL). The aqueous layer was extracted with dichloromethane (2 × 30 mL). The combined organic layers were dried ($MgSO_4$) and the solvent was removed under reduced pressure. The crude product was purified by column chromatography (petroleum ether:CH_2Cl_2 1:4) to give the title compound **2.40** as a white solid (0.096 g, 30%), mp 107-108℃. R_f = 0.52 (petroleum ether:CH_2Cl_2 1:4). ^{1}H NMR (400 MHz, $CDCl_3$) δ 7.75 (s, 1H), 7.53 (s, 1H), 2.68 (s, 3H), 2.40 (s, 3H), 1.65 (s, 9H).^{13}C NMR (101 MHz, $CDCl_3$) δ 194.29, 148.85, 147.56, 134.53, 128.39, 124.78, 120.28, 119.56, 86.80, 30.96, 28.01, 21.56. IR (neat): υ_{max}/cm^{-1}: 2978, 2935, 1750, 1686, 1472, 1368, 1275, 1146, 1116, 762. HRMS-ES Calcd for $C_{14}H_{19}NO_4$ + Na^+: 288.1212, found: 288.1216.

***N*-*tert*-Butoxycarbonyl-2-bromopyrrole 2.51 and *N*-tert-butoxycarbonyl-3-bromopyrrole 2.52.**

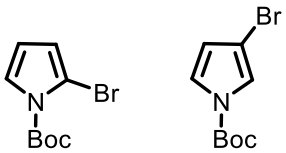

Pyrrole (45 g, 67.2 mmol) was dissolved in dry THF (180 mL) and the flask was evacuated and purged with nitrogen. Then, the mixture was cooled to -78℃ and azoisobutyronitrile (AIBN) (0.1 g, 0.001 mmol) was added and the mixture stirred for 5 min. 1,3-Dibromo-5,5-dimethylhydantoin was added over 20 min. via a solids addition funnel and the mixture was stirred for 10 min. The light green mixture was allowed to warm to room temperature and stirred for an additional 2 h. The solution was filtered by suction into a dry 250 mL three neck round bottom flask. Triethylamine (2.71 g, 26.9 mmol) and di-*tert*-butyl dicarbonate (20.4 g, 93.9 mmol) and 4-dimethylaminopyridine (0.1 g, 0.012 mmol) were added and the mixture was stirred for 8 h at room temperature. The solvent was removed under reduced pressure. The crude product was dissolved in hexane (100 mL) and washed with water (3 × 100 mL). The organic layer was dried ($NaSO_4$) and the solvent removed under reduced pressure. The crude product was purified by column chromatography (petroleum ether) to give a 70:30 mixture of the 2-bromo and 3-bromo BOC-pyrrole **2.51** and **2.52** respectively as a colorless oil (14.1 g, 85.5%, ratio determined by ^{1}H NMR). For the mixture: ^{1}H NMR (400 MHz, $CDCl_3$) δ 7.29 (dd, *J* = 3.6, 2.0 Hz, 1H, **2.51**), 7.23 – 7.20 (m, 1H, **2.52**), 6.27 (dd, *J* = 3.1, 2.3 Hz, 1H, **2.51**), 6.22 (s, 1H, **2.52**), 6.21 – 6.18 (m, 1H, **2.52**), 6.13 (t, *J* = 3.8 Hz, 1H, **2.51**), 1.63 (s, 9H, **2.52**), 1.59 (s, 9H, **2.51**). HRMS-ES Calcd for $C_9H_{12}N^{79}BrO_2 + H^+$: 246.0130, found: 246.0120.

***N*-*tert*-Butoxycarbonyl-2-(2-methoxyphenyl)pyrrole 2.45.**

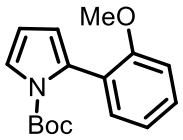

N-*tert*-Butoxycarbonyl-2-bromopyrrole **2.51** (1.50 g, 6.10 mmol) was dissolved in dry toluene (20 mL) and THF (5 mL). 2-Methoxyphenylboronic acid (1.39 g, 9.15 mmol), $Pd(PPh_3)_4$ (0.35 g, 0.31 mmol, 5 mol%), and aqueous Na_2CO_3 (2 M, 6.1 mL, 12.2 mmol) were then added. The mixture was heated under reflux for 24 h and then allowed to cool to room temperature. The solution was diluted with CH_2Cl_2 (60 mL) and washed with brine (30 mL). The organic layer was dried ($MgSO_4$) and the solvent was removed under reduced pressure. The orange crude product was purified by column chromatography (petroleum ether:ethyl acetate 9:1) to give the title compound **2.45** as a colorless oil (1.2 g, 73%), R_f = 0.45 (petroleum ether:ethyl acetate 9:1). ^{1}H NMR (400 MHz, $CDCl_3$) δ 7.46 (dd, *J* = 3.3, 1.8 Hz, 1H), 7.42 – 7.35 (m, 2H), 7.05 (td, *J* = 7.4, 1.0 Hz, 1H), 6.94 (d, *J* = 8.2 Hz, 1H), 6.33 (t, *J* = 3.3 Hz, 1H), 6.24 (dd, *J* = 3.2, 1.8 Hz, 1H), 3.81 (s, 3H), 1.42 (s, 9H).^{13}C NMR (101 MHz, $CDCl_3$) δ 157.54, 149.63, 131.39, 130.42, 129.17, 124.40, 122.00, 120.42, 114.02, 110.55, 110.09, 82.88, 55.37, 27.69. IR (neat): υ_{max}/cm^{-1}: 2978, 2937, 2838, 1734, 1599, 1464, 1313, 1241, 1146, 1114, 1024, 752. HRMS-ES Calcd for $C_{16}H_{19}NO_3 + H^+$: 274.1443, found: 274.1444.

2-(2-Methoxyphenyl)-1H-Pyrrole 2.46.

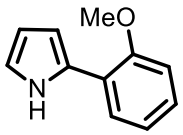

N-tert-Butoxycarbonyl-2-(2-methoxyphenyl)pyrrole **2.45** (1.24 g, 4.54 mmol) was dissolved in mixture of dry THF (15 mL) and dry methanol (4 mL). Sodium methoxide (0.73 g, 13.6 mmol) was added and the mixture stirred at room temperature for 6 h. The solvent was removed under reduced pressure and the residue dissolved in ether (30 mL) and washed with water (2 × 20 mL). The organic layer was dried ($MgSO_4$) and the solvent removed under reduced pressure. The crude product was purified by column chromatography (petroleum ether:ethyl acetate 10:1) to give the title compound **2.46** as a light green solid (0.39 g, 50%), mp 65-66 ℃ (lit.[6] mp 66-67). R_f = 0.51 (petroleum ether:ethyl acetate 10:1). ^{1}H NMR (400 MHz, $CDCl_3$) δ 9.88 (s, 1H), 7.74 (dd, *J* = 7.7, 1.7 Hz, 1H), 7.28 – 7.17 (m, 1H), 7.06 (t, *J* = 7.0 Hz, 1H), 7.02 (t, *J* = 8.7 Hz, 1H), 6.97 – 6.89 (m, 1H), 6.71 (s, 1H), 6.41 – 6.34 (m, 1H), 3.97 (s, 3H).^{13}C NMR (101 MHz, $CDCl_3$) δ 154.86, 130.00, 126.85, 126.75, 121.59, 121.25, 117.98, 111.80, 109.00, 106.29, 55.79. IR (neat): υ_{max}/cm^{-1}: 3445, 2935, 1490, 1232, 1110, 1019, 755, 722. HRMS-ES Calcd for $C_{11}H_{11}NO$ + H^+: 174.0919, found: 174.0916

The spectroscopic data obtained for this compound were consistent with those reported in the literature.[209]

1,9-Di(2-methoxyphenyl)-5-(4-methylphenyl)dipyrromethene 2.47.

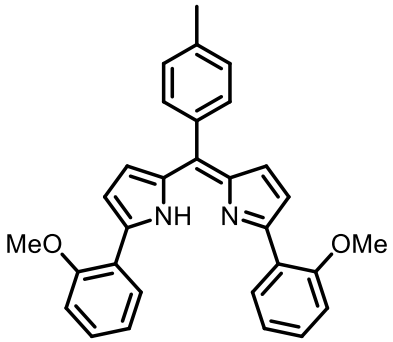

4-Methylbenzoyl chloride (0.55 g, 3.57 mmol) and 2-(2-methoxyphenyl)-1H-pyrrole **2.46** (0.31 g, 1.78 mmol) were dissolved in 1,2-dichloroethane (DCE) (6 mL). The mixture was heated under reflux for 5 h and then allowed to cool to room temperature. The solution was diluted with CH_2Cl_2 (60 mL) and washed with water (2×50 mL). The organic layer was dried ($MgSO_4$) and the solvent was removed under reduced pressure. The purple crude product was purified by column chromatography (CH_2Cl_2:ethyl acetate 9:1) to give the title compound **2.47** as a dark purple solid (0.33 g, 20%), mp 127-129 ^oC, R_f = 0.35 (CH_2Cl_2:ethyl acetate 9:1). ^1H NMR (300 MHz, $CDCl_3$) δ 13.65 (s, 1H), 7.67 (d, *J* = 7.2 Hz, 2H), 7.30 (d, *J* = 8.2 Hz, 2H), 7.25 – 7.19 (m, 4H), 6.93 (t, *J* = 7.2 Hz, 2H), 6.84 (d, *J* = 8.4 Hz, 2H), 6.74 (d, *J* = 4.5 Hz, 2H), 6.40 (d, *J* = 4.7 Hz, 2H), 3.69 (s, 6H), 2.33 (s, 3H). IR (neat): υ_{max}/cm^{-1}: 3258, 2963, 2360, 1736, 1609, 1551, 1507, 1480, 1449, 1315, 1261, 1172, 1014, 968, 734. HRMS-ES Calcd for $C_{30}H_{26}N_2O_2 + H^+$: 447.2073, found: 447.2072.

2,2'-((4-Methylphenyl)methylene)bis(1H-pyrrole) 2.54a.

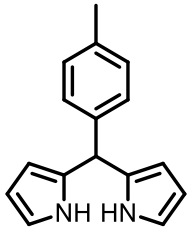

4-Methylbenzaldehyde (1.60 ml, 1.73 g, 13.6 mmol) was added to pyrrole (24.0 mL, 346 mmol) and the mixture was stirred at room temperature for 25 min. $BF_3.Et_2O$ (0.14 g, 1.40 mmol) was added to the mixture and stirred for 30 min. The solvent was removed under reduced pressure and the resulting material was partitioned between CH_2Cl_2 (50 mL) and NaOH (200 mL). The organic extract was dried ($MgSO_4$) and the solvent was removed under reduced pressure. The brown oil crude product was purified by column chromatography (petroleum ether:ethyl acetate:Et_3N 9:1:0.1) to give the title compound **2.54a** as a tan solid (2.2 g, 69%), mp 108-110℃ (lit.[7] 110-111℃). R_f = 0.23 (petroleum ether:ethyl acetate:Et_3N 9:1:0.1). ^1H NMR (300 MHz, $CDCl_3$) δ 7.94 (bs, 2H, NH), 7.17-7.11 (m, 4H), 6.67-6.74 (m, 2H), 6.18 (q, *J*=2.8 Hz, 2H), 5.92-5,97 (m, 2H), 5.47 (s, 1H), 2.35 (s, 3H, CH_3). ^{13}C NMR (101 MHz, $CDCl_3$) δ 139.15, 136.68, 132.80, 129.43, 128.37, 117.21, 108.48, 107.18, 43.66, 21.15. IR (neat): υ_{max}/cm^{-1}: 3655, 3342, 2980, 2981, 1682, 1553, 1513, 1111, 717. HRMS-ES Calcd for $C_{16}H_{16}N_2 + H^+$: 237.1392, found: 237.1397. The spectroscopic data obtained for this compound were consistent with those reported in the literature.[86]

1,9-Dibromo-5-(4-methylphenyl)dipyrrin 2.55a.

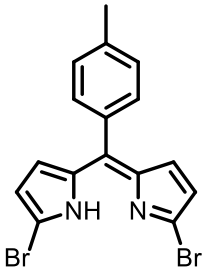

2,2'-((4-Methylphenyl)methylene)bis(1H-pyrrole) **2.54a** (1.00 g, 4.24 mmol) was dissolved in dry THF (100 mL) and cooled to -78 °C. *N*-Bromosuccinimide (1.52 g, 8.54 mmol) was added to the mixture in two portions over 1 h. DDQ (0.98 g, 4.3 mmol) in THF (10 mL) was added to the mixture dropwise over 10 min. The reaction mixture was warmed to room temperature and the solvent was removed under reduced pressure. The orange crude product was purified by column chromatography (CH_2Cl_2) to give the title compound **2.55a** as an light brown solid (1.33 g, 80%), mp 112-114℃. R_f = 0.92 (CH_2Cl_2). ^{1}H NMR (300 MHz, $CDCl_3$) δ 12.47 (s, 1H), 7.26 (d, *J* = 8.5 Hz, 2H), 7.17 (d, *J* = 8.5 Hz, 2H), 6.44 (d, *J* = 4.2 Hz, 2H), 6.26 (d, *J* = 4.2 Hz, 2H), 2.37 (s, 3H, CH_3). IR (neat): υ_{max}/cm^{-1}: 3130, 2980, 1717, 1573, 1595, 1414, 1308, 1246, 1111, 1041, 778. HRMS-ES Calcd for $C_{16}H_{12}N_2Br_2 + H^+$: 390.9445, found: 390.9454.

3,5-Dibromo-4,4-difluoro-8-(4-methylphenyl)-4-bora-3a,4a-diaza-*s*-indacene 2.56a.

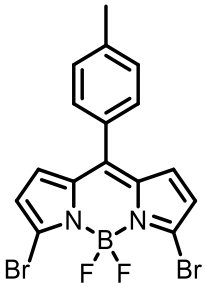

N,*N*-Diisopropylethylamine (2.14 g, 16.6 mmol) and $BF_3.Et_2O$ (3.14 g, 22.1 mmol) were added to a solution of 1,9-dibromo-5-(4-methylphenyl)dipyrrin **2.55a** (1.08 g, 2.76 mmol) in dry CH_2Cl_2 (20 mL) and the mixture was stirred at room temperature for 2 h. The mixture was then washed with 0.1 M NaOH (50 mL) and water (100 mL). The aqueous layer was extracted with dichloromethane (2 × 150 mL). The combined organic layers were dried ($MgSO_4$) and the solvent was removed under reduced pressure. The orange crude product was purified by column chromatography (CH_2Cl_2:petroleum ether 1:1) to give the title compound **2.56a** as an orange solid (1.05 g, 86%), mp 208-210℃ (lit.[8] mp 210-211℃). R_f = 0.30 (petroleum ether:CH_2Cl_2 1:1). ^{1}H NMR (300 MHz, $CDCl_3$) δ 7.37 (d, *J* = 7.9 Hz, 2 H), 7.31 (d, *J* = 7.8 Hz, 2H), 6.80 (d, *J* = 4.3 Hz, 2H), 6.52 (d, *J* = 4.3 Hz, 2H), 2.45 (s, 3H).^{13}C NMR (101 MHz, $CDCl_3$) δ 143.68, 141.67, 135.57, 132.32, 131.78, 130.57, 129.67, 129.41, 122.66, 21.59. ^{11}B NMR (128 MHz, $CDCl_3$) δ -0.36 (t, $J_{B\text{-}F}$ = 28.5 Hz). ^{19}F NMR (282 MHz, $CDCl_3$) δ -146.80 (q, $J_{F\text{-}B}$ =28.5 Hz). IR (neat): υ_{max}/cm^{-1}: 3139, 2446, 1530, 1446, 1381, 1312, 1093, 1063, 736. HRMS-ES Calcd for $C_{16}H_{11}N_2{}^{11}B^{79}Br^{81}Br^{19}F_2$ + Na^+: 462.9227, found: 462.9222.

The spectroscopic data obtained for this compound were consistent with those reported in the literature.[87]

4,4-Difluoro-3,5-di(2-methoxyphenyl)-8-(4-methylphenyl)-4-bora-3a,4a-diaza-*s*-indacene 2.48a.

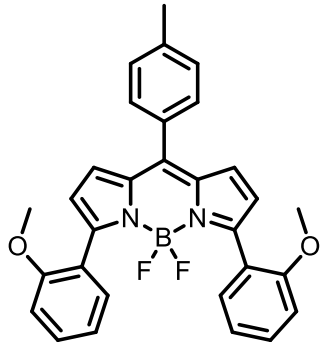

3,5-Dibromo-4,4-difluoro-8-(4-methylphenyl)-4-bora-3a,4a-diaza-*s*-indacene **2.56a** (0.10 g, 0.23 mmol) was dissolved in dry toluene (5 mL). 2-Methoxyphenylboronic acid (0.08 g, 0.54 mmol), $Pd(PPh_3)_4$ (13.0 mg, 0.01 mmol, 5 mol%), and aqueous Na_2CO_3 (1 M, 1.0 mL, 1.0 mmol) were then added. The mixture was heated under reflux for 4 h and then allowed to cool to room temperature. The solution was diluted with CH_2Cl_2 (60 mL) and washed with brine (30 mL). The organic layer was dried ($MgSO_4$) and the solvent was removed under reduced pressure. The pink crude product was purified by column chromatography (petroleum ether:ethyl acetate 4:1) to give the title compound **2.48a** as a pink solid (0.11 g, 98%), mp 190-192 ℃, R_f = 0.37 (petroleum ether:ethyl acetate 4:1). ^{1}H NMR (300 MHz, $CDCl_3$) δ 7.65 (d, *J* = 7.6 Hz, 2H), 7.44 (d, *J* = 8.4 Hz, 2H), 7.30 – 7.21 (m, 4H), 6.92 (apparent t, *J* = 7.6 Hz, 2H), 6.84 (d, *J* = 8.4 Hz, 2H), 6.80 (d, *J* = 4.8 Hz, 2H), 6.51 (d, *J* = 4.8 Hz, 2H), 3.70 (s, 6H), 2.41 (s, 3H). ^{13}C NMR (100 MHz, $CDCl_3$) δ 157.60, 155.11, 143.88, 140.32, 135.54, 132.03, 131.98,131.83, 130.70, 130.59, 129.71, 128.99, 122.18, 120.31, 111.03, 55.89, 21.56. ^{11}B NMR (128 MHz, $CDCl_3$) δ 0.14 (t, $J_{B\text{-}F}$ = 31.0 Hz). ^{19}F NMR (376 MHz, $CDCl_3$) δ -135.22 (q, $J_{F\text{-}B}$ = 31.0 Hz). IR (neat): υ_{max}/cm^{-1}: 3325, 2360, 1635, 1589, 1423, 1249, 1217. HRMS-ES Calcd for $C_{30}H_{25}BN_2O_2F_2 + H^+$: 495.2055, found: 495.2055.

***B,O*-Chelated BODIPY 2.49a.**

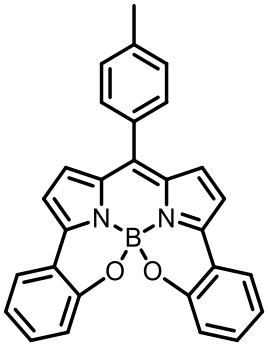

4,4-Difluoro-3,5-di(2-methoxyphenyl)-8-(4-methylphenyl)-4-bora-3a,4a-diaza-*s*-indacene **2.48a** (0.11 g, 0.22 mmol) was dissolved in dry dichloromethane (7 mL) and the solution was cooled to 0 °C. BBr_3 (0.57 g, 2.27 mmol) was added dropwise and the mixture was stirred at room temperature for 5 h. The reaction was quenched with ice (30 g) and the solution was extracted with ethyl acetate (2 x 30 mL). The combined organic extracts were washed with saturated aqueous NH_4Cl (30 mL), dried ($MgSO_4$) and the solvent was removed under reduced pressure. The crude product was purified by column chromatography (petroleum ether:ethyl acetate 4:1) to give the title compound **2.49a** as a dark red solid (0.11 g, 96% yield), mp 190-192 ℃, R_f = 0.56 (petroleum ether:ethyl acetate 4:1). ^{1}H NMR (400 MHz, $CDCl_3$) δ 7.77 (d, *J* = 7.7 Hz, 2H), 7.65 (d, *J* = 7.5 Hz, 2H), 7.28-7.36 (m, 4H), 7.09 (d, *J* = 4.0 Hz, 2H), 7.04 (t, *J* = 7.5 Hz, 2H), 6.95 (d, *J* = 8.3 Hz, 2H), 6.89 (d, *J* = 4.0 Hz, 2H), 2.48 (s, 3H). ^{13}C NMR (126 MHz, $CDCl_3$) δ 154.18, 149.67, 141.12, 139.06, 134.23, 132.09, 130.96, 130.63, 130.12, 129.49, 125.74, 120.42, 119.75, 119.72, 116.34, 21.52.^{11}B NMR (128 MHz, $CDCl_3$) δ -1.84 (s). IR (neat): υ_{max}/cm^{-1}: 3273, 2920, 2851, 1682, 1426, 1171, 1042, 762. HRMS-ES Calcd for $C_{28}H_{19}BN_2O_2$ + H^+: 427.1618, found: 427.1612.

2,2'-((2-Pyridyl)methylene)bis(1H-pyrrole) 2.54b.

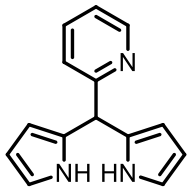

Pyridine-2-carboxaldehyde (4.28 g, 40.0 mmol) was added to pyrrole (53.6 g, 800 mmol) and the mixture was stirred at room temperature for 24 h. The excess pyrrole was removed by distillation (60 °C) to give the crude product as a crimson oil. The product was purified by column chromatography (petroleum ether:ethyl acetate 7:3) to give the title compound **2.54b** as a sand-coloured solid (5.56 g, 62%), mp 117-119 ℃ (lit.[9] 115-116 ℃). R_f = 0.55 (petroleum ether:ethyl acetate 7:3). ^{1}H NMR (300 MHz, $CDCl_3$) δ 8.87 (br.s, 2H), 8.60 (br d, *J* = 5.1 Hz, 1H), 7.69 (br t, *J* = 7.6 Hz, 1H), 7.28 (d, *J* = 7.8 Hz, 1H), 7.19-7.25 (m, 1H), 6.71-6.76 (m, 2H), 6.12–6.17 (m, 2H), 5.93-5.97 (m, 2H) 5.54 (s, 1H). ^{13}C NMR (75 MHz, $CDCl_3$) δ 161.27, 149.38, 137.19, 131.71, 123.25, 122.01, 117.50, 108.19, 106.55, 45.41. IR (neat): υ_{max}/cm^{-1}: 3432, 3103, 2984, 2861, 1593, 1437, 1262, 1029, 722. HRMS-ES Calcd for $C_{14}H_{13}N_3 + H^+$: 224.1188, found: 224.1182.

The spectroscopic data obtained for this compound were consistent with those reported in the literature.[210]

1,9-Dibromo-5-(2-pyridyl)dipyrromethane 2.55b.

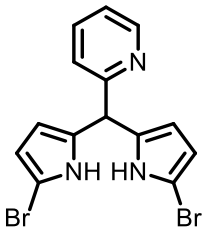

2,2'-((2-Pyridyl)methylene)bis(1H-pyrrole) **2.54b** (0.50 g, 2.20 mmol) was dissolved in dry THF (35 mL) and cooled to -78 °C. *N*-Bromosuccinimide (0.79 g, 4.50 mmol) was added to the mixture in two portions over 1 h. The reaction mixture was warmed to room temperature and the solvent was removed under reduced pressure. The brown crude product was purified by column chromatography (CH_2Cl_2) to give the title compound **2.55b** as a yellow solid (0.60 g, 76%), mp 117-120 ℃, R_f = 0.87 (CH_2Cl_2). ^{1}H NMR (300 MHz, $CDCl_3$) δ 8.90 (br. s, 2H), 8.51 (d, *J*= 4.6 H_z, 1H), 7.62 (td, *J* = 7.7, 1.8 Hz, 1H), 7.23 – 7.10 (m, 2H), 6.02-5.92 (m, 2H), 5.78 (t, *J* = 3.0 Hz, 2H), 5.30 (s, 1H). ^{13}C NMR (101 MHz, $CDCl_3$) 159.92, 149.32, 137.84, 132.46, 123.44, 122.56, 110.39, 108.67, 97.74, 45.25. IR (neat): υ_{max}/cm^{-1}: 3343, 3059, 2950, 2689, 1571, 1474, 1005, 818. HRMS-ES Calcd for $C_{14}H_{11}N_3{}^{79}Br^{81}Br + H^+$: 381.9377, found: 381.9368

3,5-Dibromo-4,4-difluoro-8-(2-pyridyl)-4-bora-3a,4a-diaza-*s*-indacene 2.56b.

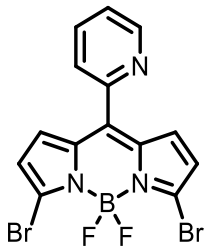

1,9-Dibromo-5-(2-pyridyl)dipyrromethane **2.55b** (1.00 g, 2.62 mmol) was dissolved in dry toluene (20 mL) followed by the addition of a solution of DDQ (0.60 g, 2.62 mmol) in dry toluene (20 mL). The mixture was stirred at room temperature for 1h. Diisopropylethylamine (2.35 g, 18.2 mmol) and $BF_3.Et_2O$ (2.35 g, 18.2 mmol) were added, and the mixture was stirred for an additional 1 h. The reaction mixture was washed with 0.1 M NaOH (2 × 100 mL) and the aqueous layer was extracted with toluene (2 × 60 mL). The combined organic extracts were dried ($MgSO_4$) and the solvent was removed under reduced pressure to give the crude product as a purple solid. The product was purified by column chromatography (petroleum ether:ethyl acetate 2:3) to give the title compound **2.56b** as a dark purple solid (0.55 g, 50%), mp 217-220 °C, R_f = 0.47 (petroleum ether:ethyl acetate 2:3). ^{1}H NMR (300 MHz, $CDCl_3$) δ 8.80 (d, *J* = 7.8 Hz, 1H), 7.90 (td, *J* = 7.7, 1.7 Hz, 1H), 7.65-7.50 (m, 2H), 6.92 (d, *J* = 4.9 Hz, 2H), 6.56 (d, *J* = 4.3 Hz, 2H). ^{13}C NMR (75 MHz, $CDCl_3$) δ 151.33, 150.36, 139.78, 136.72, 135.38, 133.49, 132.01, 126.38, 125.10, 123.14. ^{11}B NMR (128 MHz, $CDCl_3$) δ -0.35 (t, $J_{B\text{-}F}$= 27.8 Hz). ^{19}F NMR (282 MHz, $CDCl_3$) δ -146.75 (q, $J_{F\text{-}B}$= 27.8 Hz). IR (neat): υ_{max}/cm^{-1}: 3139, 2927, 1725, 1540, 1381, 1307, 1249, 1077, 713. HRMS-ES Calcd for $C_{14}H_8N_3{}^{79}Br^{81}Br^{11}BF_2 + H^+$: 427.9204, found: 427.9210.

4,4-Difluoro-3,5-bis(2-methoxyphenyl)-8-(2-pyridyl)-4-bora-3a,4a-diaza-*s*-indacene 2.48b.

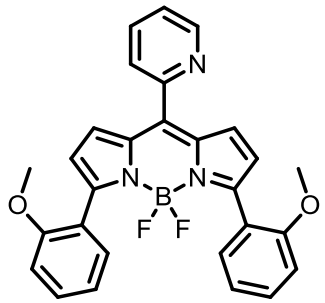

3,5-Dibromo-4,4-difluoro-8-(2-pyridyl)-4-bora-3a,4a-diaza-*s*-indacene **2.56b** (0.13 g, 0.31 mmol) was dissolved in dry toluene (5 mL). 2-Methoxyphenylboronic acid (0.11 g, 0.72 mmol), 2-dicyclohexylphosphino-2',6'-dimethoxybiphenyl (SPhos) (15.6 mg, 0.04 mmol, 12.5 mol%), $Pd(OAc)_2$ (3.40 mg, 0.02 mmol, 5 mol%), and K_3PO_4 (0.26 g, 1.29 mmol) were then added. The mixture was heated under reflux for 4 h and then allowed to cool to room temperature. The solution was diluted with CH_2Cl_2 (60 mL) and washed with brine (30 mL). The organic layer was dried ($MgSO_4$) and the solvent was removed under reduced pressure. The pink crude product was purified by column chromatography (petroleum ether:ethyl acetate 4:1) to give the title compound **2.48b** as a purple solid (0.40 g, 81 %), mp 210-212℃, R_f = 0.37 (petroleum ether:ethyl acetate 4:1). ^{1}H NMR (300 MHz, $CDCl_3$) δ 8.76 (ddd, *J* = 4.9, 1.7, 0.9 Hz, 1H), 7.81 (td, *J* = 7.7, 1.8 Hz, 1H), 7.67 (d, *J* = 7.5 Hz, 2H), 7.62 (dt, *J* = 7.8, 1.1 Hz, 1H), 7.41 (ddd, *J* = 7.6, 4.8, 1.2 Hz, 1H), 7.30-7.22 (m, 2H), 6.92 (td, *J* = 7.6, 1.0 Hz, 2H), 6.86 (s, 2H), 6.83 (d, *J* = 4.0 Hz, 2H), 6.55 (d, *J* = 4.0 Hz, 2H), 3.69 (s, 6H). ^{13}C NMR (126 MHz, $CDCl_3$) δ 157.60, 156.02, 153.46, 149.97, 136.27, 131.91, 131.46, 130.64, 129.51, 128.59, 126.22, 124.25, 122.75, 122.03, 120.26, 111.05, 55.83. ^{11}B NMR (160 MHz, $CDCl_3$) δ 1.07 (t, $J_{B\text{-}F}$ = 30.8 Hz). ^{19}F NMR (282 MHz, $CDCl_3$) δ -135.02 (q, $J_{F\text{-}B}$= 30.8 Hz). IR (neat): υ_{max}/cm^{-1}: 3625, 2839, 2364, 2338, 2163, 1988, 1553, 1469, 1248, 1137, 1072, 754. HRMS-ES Calcd for $C_{28}H_{22}{}^{11}BN_3O_2{}^{19}F_2 + H^+$: 482.1851, found: 482.1855.

***B,O*-Chelated BODIPY 2.49b.**

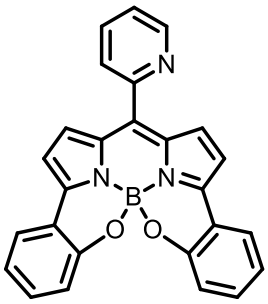

4,4-Difluoro-3,5-bis(2-methoxyphenyl)-8-(2-pyridyl)-4-bora-3a,4a-diaza-*s*-indacene **2.48b** (0.05 g, 0.11 mmol) was dissolved in dry dichloromethane (7 mL) and the solution was cooled to 0 °C. BBr_3 (0.38 g, 1.52 mmol) was added dropwise and the mixture was stirred at room temperature for 5 h. The reaction was quenched with ice (30 g) and the solution was extracted with ethyl acetate (2 x 30 mL). The combined organic extracts were washed with saturated aqueous NH_4Cl (30 mL), dried ($MgSO_4$) and the solvent was removed under reduced pressure. The crude product was purified using column chromatography (petroleum ether:ethyl acetate 2:3) to give the title compound **2.49b** as a dark red solid (0.026 mg, 60%) mp 240-241 ℃, R_f = 0.56 (petroleum ether:ethyl acetate 2:3).^{1}H NMR (500 MHz, $CDCl_3$) δ 8.89 (br d, *J* = 4.7 Hz, 1H), 7.92 (td, *J* = 7.6, 1.5 Hz, 1H), 7.86 (d, *J* = 7.8 Hz, 1H), 7.81 (dd, *J* = 7.7, 1.5 Hz, 2H), 7.53 – 7.48 (m, 1H), 7.39 – 7.34 (m, 2H), 7.27 (d, *J* = 4.4 Hz, 2H), 7.08 (t, *J* = 7.3 Hz, 2H), 6.99 (d, *J* = 8.2 Hz, 2H), 6.96 (d, *J* = 4.4 Hz, 2H). ^{13}C NMR (101 MHz, $CDCl_3$) δ 154.39, 152.91, 150.60, 150.52, 136.75, 135.35, 134.52, 132.46, 130.27, 126.45, 126.01, 124.64, 120.57, 119.86, 119.67, 116.93. ^{11}B NMR (96 MHz, $CDCl_3$) δ -0.83 (s). IR (neat): υ_{max}/cm^{-1}: 3432, 2963, 2855, 2360, 1716, 1593, 1569, 1499, 1437, 1260, 1087, 1029, 758. HRMS-ES Calcd for $C_{26}H_{16}{}^{11}BN_3O_2 + H^+$: 414.1414, found: 414.1434.

2,2'-((4-(Octyloxy)phenyl)methylene)bis(1H-pyrrole) 2.54c.

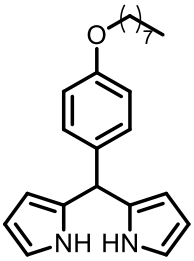

4-Octyloxybenzaldehyde (0.50 g, 2.13 mmol) was added to pyrrole (3.57 g, 53.3 mmol) and the mixture was stirred at room temperature for 25 min. $BF_3.Et_2O$ (0.03 g, 0.21 mmol) was added to the mixture and stirred for 30 min. The solvent was removed under reduced pressure and the resulting material was partitioned between CH_2Cl_2 (50 mL) and NaOH (200 mL). The organic extract was dried ($MgSO_4$) and the solvent was removed under reduced pressure. The dark green oil crude product was purified by column chromatography (petroleum ether:CH_2Cl_2 3:2) to give the title compound **2.54c** as a tan solid (0.46 g, 62%); mp 79-80 ℃ (lit.[10] mp 78-80 °C). R_f = 0.35 (petroleum ether:CH_2Cl_2 3:2). ^{1}H NMR (300 MHz, $CDCl_3$) δ 7.84 (s, 2H), 7.05 (d, *J* = 8.6 Hz, 2H), 6.77 (d, *J* = 8.6 Hz, 2H), 6.62 (dd, *J* = 4.0, 2.6 Hz, 2H), 6.08 (dd, *J* = 5.8, 2.6 Hz, 2H), 5.85 (s, 2H), 5.36 (s, 1H), 3.86 (t, *J* = 6.5 Hz, 2H), 1.77 – 1.63 (m, 2H), 1.43 – 1.14 (m, 10H), 0.81 (t, *J* = 5.7 Hz, 3H). ^{13}C NMR (75 MHz, $CDCl_3$) δ 158.14, 134.06, 133.03, 129.41, 117.19, 114.61, 108.39, 107.12, 68.13, 43.17, 31.91, 29.46, 29.34, 26.15, 22.75, 14.21. IR (neat): υ_{max}/cm^{-1}: 3339, 2923, 2854, 1608, 1553, 1509, 1249, 1023, 721. HRMS-ES Calcd for $C_{23}H_{30}N_2O$ + Na^+: 373.2256, found: 373.2249.

The spectroscopic data obtained for this compound were consistent with those reported in the literature.[211]

3,5-Dibromo-4,4-difluoro-8-(4-(octyloxy)phenyl)-4-bora-3a,4a-diaza-*s*-indacene 2.56c.

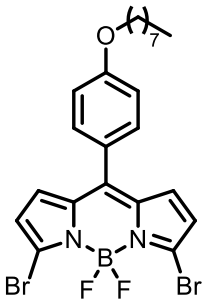

2,2'-((4-(Octyloxy)phenyl)methylene)bis(1H-pyrrole) **2.54c** (0.38 g, 1.09 mmol) was dissolved in dry THF (24 mL) and cooled to -78 °C. *N*-Bromosuccinimide (0.47 g, 2.64 mmol) was added to the mixture in two portions over 1 h. DDQ (0.27 g, 1.21 mmol) was added to the mixture and stirred for 1h. The reaction mixture was warmed to room temperature and the solvent was removed under reduced pressure. The orange crude product was dissolved in dry CH_2Cl_2 (24 mL) and neutralized with *N*,*N*-diisopropylethylamine (0.75 g, 6.59 mmol) and treated with $BF_3.Et_2O$ (1.12 g, 8.72 mmol). The mixture was stirred at room temperature for 3 h and washed with 0.1 M NaOH (50 mL) and water (100 mL). The aqueous layer was extracted with dichloromethane (2 × 150 mL). The combined organic layers were dried ($MgSO_4$) and the solvent was removed under reduced pressure. The orange crude product was purified using column chromatography (petroleum ether:ethyl acetate 10: 1) to give the title compound **2.56c** as an orange solid (0.37 g, 61%), mp 116-117℃. ^{1}H NMR (300 MHz, $CDCl_3$) δ 7.36 (d, *J* = 8.8 Hz, 2H), 6.94 (d, *J* = 8.8 Hz, 2H), 6.76 (d, *J* = 4.3 Hz, 2H), 6.46 (d, *J* = 4.3 Hz, 2H), 3.97 (t, *J* = 6.5 Hz, 2H), 1.82 – 1.70 (m, 2H), 1.45 – 1.16 (m, 10H), 0.82 (t, *J* = 6.8 Hz, 3H). ^{13}C NMR (75 MHz, $CDCl_3$) δ 161.82, 143.51, 135.44, 132.31, 131.79, 131.55, 124.59, 122.44, 114.67, 68.42, 31.82, 29.34, 29.24, 29.14, 26.04, 22.67, 14.12. ^{19}F NMR (282 MHz, $CDCl_3$) δ -146.67 (q, $J_{F\text{-}B}$ =28.4 Hz). ^{11}B NMR (96 MHz, $CDCl_3$) δ 0.60 (t, $J_{B\text{-}F}$ = 28.4 Hz). IR (neat): υ_{max}/cm^{-1}: 3048, 2924, 2854, 1602, 1571, 1538, 1505, 1380, 1251, 1176, 1096, 738. HRMS-ES Calcd for $C_{23}H_{25}{}^{11}B^{19}F_2{}^{79}Br^{81}BrN_2O + Na^+$: 577.0272, found: 577.0285.

3,5-Bis(2-methoxyphenyl)-4,4-difluoro-8-(4-(octyloxy)phenyl)-4-bora-3a,4a-diaza-*s*-indacene 2.48c.

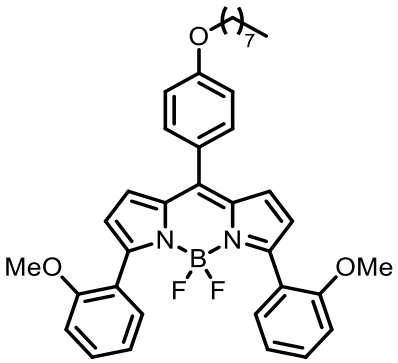

3,5-Dibromo-4,4-difluoro-8-(4-(octyloxy)phenyl)-3a,4a-diaza-*s*-indacene **2.56c** (0.20 g, 0.36 mmol), 2-methoxyphenylboronic acid (0.22 g, 1.44 mmol), K_3PO_4 (0.33 g, 1.44 mmol) and chloro(2-dicyclohexylphosphino-2',4',6'-triisopropyl-1,1'-biphenyl)[2-(2'-amino-1,1'-biphenyl)]palladium(II) (LPd(XPhos)Cl) **3.54** (0.01 g, 0.014 mmol, 5 mol%) were dissolved in THF (6 mL) and water (3 mL). The mixture was heated under reflux for 6 h and then allowed to cool to room temperature. The solution was diluted with CH_2Cl_2 (60 mL) and washed with brine (30 mL). The organic layer was dried ($MgSO_4$) and the solvent was removed under reduced pressure. The pink crude product was purified by column chromatography (petroleum ether:CH_2Cl_2 2:1) to give the title compound **2.48c** as a pink solid (0.10 g, 45%), mp 110-111 ^{o}C. ^{1}H NMR (300 MHz, $CDCl_3$) δ 7.65 (d, *J* = 8.8 Hz, 2H), 7.49 (d, *J* = 8.7 Hz, 2H), 7.30 – 7.21 (m, 2H), 6.96 (d, *J* = 8.9 Hz, 2H), 6.90 (dd, *J* = 7.5, 1.0 Hz, 2H), 6.84 (d, *J* = 7.5 Hz, 2H), 6.82 (s, 2H), 6.52 (d, *J* = 4.1 Hz, 2H), 3.99 (t, *J* = 6.5 Hz, 2H), 3.70 (s, 6H), 1.78 (p, *J* = 6.8 Hz, 2H), 1.37 – 1.18 (m, 10H), 0.86 – 0.80 (m, 3H). ^{13}C NMR (75 MHz, $CDCl_3$) δ 159.87, 156.49, 153.68, 134.41, 131.22, 130.89, 129.40, 128.53, 125.77, 122.66, 121.16, 120.90, 119.19, 113.17, 109.96, 67.24, 54.79, 30.81, 28.35, 28.22, 25.06, 21.66, 13.10. ^{11}B NMR (96 MHz, $CDCl_3$) δ 1.04 (t, $J_{B\text{-}F}$ = 31.6 Hz). ^{19}F NMR (282 MHz, $CDCl_3$) δ -135.24 (q, $J_{F\text{-}B}$ = 31.6 Hz). IR (neat): υ_{max}/cm^{-1}: 3027, 2924, 2854, 1602, 1573, 1544, 1506, 1246, 1137, 1070, 797. HRMS-ES Calcd for $C_{37}H_{39}{}^{11}B{}^{19}F_2N_2O_3 + Na^+$: 631.2919, found: 631.2897.

***B,O*-Chelated BODIPY 2.49c.**

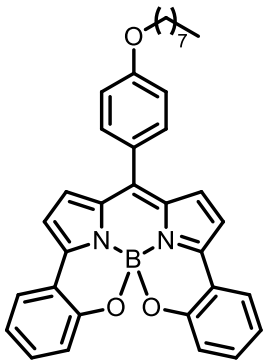

3,5-Bis(2-methoxyphenyl)-4,4-difluoro-8-(4-(octyloxy)phenyl)-4-bora-3a,4a-diaza-*s*-indacene **2.48c** (0.04 g, 0.07 mmol) was dissolved in dry dichloromethane (2 mL) and the solution was cooled to 0 °C. BBr_3 (0.85 mL, 0.85 mmol) was added dropwise and the mixture was stirred at room temperature for 5 h. The reaction was quenched with ice (30 g) and the solution was extracted with CH_2Cl_2 (2 x 30 mL). The combined organic extracts were washed with saturated aqueous NH_4Cl (30 mL), dried ($MgSO_4$) and the solvent was removed under reduced pressure. The crude product was purified using column chromatography (petroleum ether:CH_2Cl_2 2:1) to give the title compound **2.49c** as a dark green solid (0.02 g, 67% yield), mp 120-121 °C. ^{1}H NMR (300 MHz, $CDCl_3$) δ 7.70 (dd, *J* = 7.7, 1.6 Hz, 2H), 7.64 (d, *J* = 8.7 Hz, 2H), 7.29 – 7.21 (m, 2H), 7.03 (d, *J* = 4.3 Hz, 2H), 7.01 – 6.94 (m, 4H), 6.88 (dd, *J* = 8.3, 0.8 Hz, 2H), 6.83 (d, *J* = 4.3 Hz, 2H), 3.99 (t, *J* = 6.5 Hz, 2H), 1.84 – 1.71 (m, 2H), 1.30-1.17 (m, 10H), 0.83 (t, *J* = 6.8 Hz, 3H).^{11}B NMR (96 MHz, $CDCl_3$) δ -0.94 (s). IR (neat): υ_{max}/cm^{-1}: 3043, 2917, 2847, 1432, 1309, 1202, 1108, 1021, 997, 908. HRMS-ES Calcd for $C_{35}H_{33}{}^{11}BN_2O_3 + Na^+$: 563.2482, found: 563.2475.

4,4-Difluoro-8-(4-methylphenyl)-3,5-bis(2-nitrophenyl)-4-bora-3a,4a-diaza-*s*-indacene 2.61.

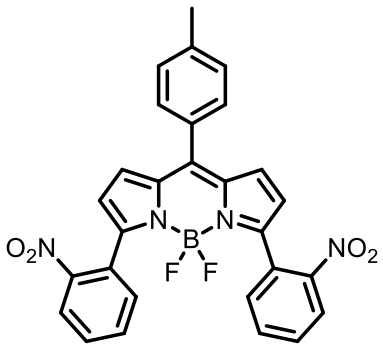

3,5-Dibromo-4,4-difluoro-8-(4-methylphenyl)-4-bora-3a,4a-diaza-*s*-indacene **2.56a** (0.20 g, 0.45 mmol), 2-nitrophenylboronic acid (0.38 g, 2.27 mmol), K_3PO_4 (0.42 g, 1.82 mmol) and chloro(2-dicyclohexylphosphino-2',4',6'-triisopropyl-1,1'-biphenyl)[2-(2'-amino-1,1'-biphenyl)]palladium(II) (LPd(XPhos)Cl) **3.54** (0.02 g, 0.03 mmol, 6 mol%) were dissolved in THF (6 mL) and water (3 mL). The mixture was heated under reflux for 24 h and then allowed to cool to room temperature. The solution was diluted with CH_2Cl_2 (60 mL) and washed with brine (30 mL). The organic layer was dried ($MgSO_4$) and the solvent was removed under reduced pressure. The orange crude product was purified by column chromatography (petroleum ether:CH_2Cl_2 1:1) to give the title compound **2.61** as an orange solid (0.18 g, 75%), mp 275-277 ^{o}C, ^{1}H NMR (300 MHz, $CDCl_3$) δ 8.00 (d, J = 7.9 Hz, 2H), 7.58 – 7.42 (m, 8H), 7.30 (d, J = 7.2 Hz, 2H), 6.92 (d, J = 3.6 Hz, 2H), 6.37 (d, J = 3.8 Hz, 2H), 2.43 (s, 3H). ^{13}C NMR (176 MHz, $CDCl_3$) δ 153.65, 148.18, 146.76, 141.18, 135.61, 132.65, 132.28, 131.18, 131.06, 130.79, 130.06, 129.17, 127.90, 124.40, 119.93, 21.51. ^{11}B NMR (96 MHz, $CDCl_3$) δ 0.49 (t, $J_{B\text{-}F}$ = 30.4 Hz). IR (neat): υ_{max}/cm^{-1}: 2981, 2927, 2360, 1528, 1502, 1452, 1250, 1136, 1101, 1035, 748. HRMS-ES Calcd for $C_{28}H_{19}{}^{11}B^{19}F_2N_4O_4 + H^+$: 525.1546, found: 525.1544.

3,5-Bis(2-aminophenyl)-4,4-difluoro-8-(4-methylphenyl)-4-bora-3a,4a-diaza-*s*-indacene 2.62.

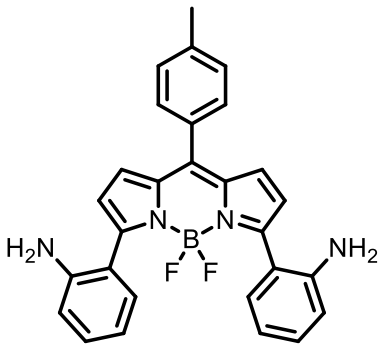

4,4-Difluoro-8-(4-methylphenyl)-3,5-bis(2-nitrophenyl)-4-bora-3a,4a-diaza-*s*-indacene **2.61** (0.10 g, 0.19 mmol) was dissolved in CH_2Cl_2 (2 mL) and MeOH (2 mL). 10% Pd/C (0.10 g) was added. The mixture was stirred under nitrogen for 15 min and the nitrogen line was replaced with a hydrogen-filled balloon. The mixture was stirred at room temperature for 1 h and then filtered through Celite, washing with CH_2Cl_2 (30 mL). The solvent was removed under reduced pressure. The crude product was purified by column chromatography (CH_2Cl_2) to give the title compound **2.62** as dark purple solid (0.07 g, 80%). R_f = 0.25 (CH_2Cl_2). ^{1}H NMR (300 MHz, $CDCl_3$) δ 7.45 (d, *J* = 8.0 Hz, 2H), 7.28-2.30 (m, 4H), 7.08 (td, *J* = 8.0, 1.5 Hz, 2H), 6.90 (d, *J* = 4.1 Hz, 2H), 6.72 (t, *J* = 7.1 Hz, 2H), 6.65 (d, *J* = 8.0 Hz, 2H), 6.51 (d, *J* = 4.1 Hz, 2H), 3.57 (s, 4H), 2.42 (s, 3H). ^{13}C NMR (75 MHz, $CDCl_3$) δ 156.08, 144.88, 144.48, 140.88, 135.85, 131.34, 131.08, 130.95, 130.70, 130.40, 129.13, 121.06, 119.19, 118.50, 116.18, 21.51.^{11}B NMR (96 MHz, $CDCl_3$) δ 0.89 (t, $J_{B\text{-}F}$ = 30.6 Hz). ^{19}F NMR (282 MHz, $CDCl_3$) δ -138.25 (q, $J_{F\text{-}B}$ = 30.6 Hz). IR (neat): υ_{max}/cm^{-1}: 3781, 3036, 2925, 2840, 2393, 2249, 1544, 1424, 1264, 1149, 1118, 992, 798. HRMS-ES Calcd for $C_{28}H_{24}$ $^{11}B^{19}F_2N_4$ + Na^+: 465.2062, found: 465.2061.

2-Acetylpyrrole 2.68a.

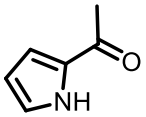

To ZnO (0.06 g, 0.5 mmol), pyrrole (1.76 g, 1.82 mmol) and acetyl chloride (1.81 g, 1.82 mmol) were added simultaneously and the mixture stirred for 5 min. The resulting material was dissolved in CH_2Cl_2 (200 mL) and washed with saturated aqueous $NaHCO_3$ (100 mL). The organic layer was dried ($MgSO_4$) and the solvent removed under reduced pressure. The crude product was purified using column chromatography (CH_2Cl_2) to give the title compound **2.68a** as a white solid (0.108 g, 55%), mp 89-92℃ (lit.[11] 91-92℃), R_f = 0.45 (CH_2Cl_2). ^{1}H NMR (300 MHz, $CDCl_3$) δ 9.34 (s, 1H), 6.96 (dt, *J* = 1.3, 2.6 Hz, 1H), 6.86-6.83 (m, 1H), 6.23-6.20 (m, 1H), 2.40 (s, 3H). ^{13}C NMR (96 MHz, $CDCl_3$) δ 188.52, 132.16, 124.73, 116.84, 110.65, 25.46. IR (neat): υ_{max}/cm^{-1}: 3264, 3116, 2976, 1634. HRMS-ES Calcd for $C_6H_7NO + H^+$: 110.0606, found: 110.0606.

The spectroscopic data obtained for this compound were consistent with those reported in the literature.[212]

2-(4-Methylbenzoyl)pyrrole 2.68b.

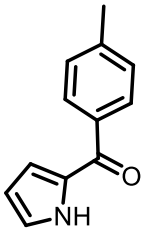

To ZnO (0.60 g, 7.45 mmol), pyrrole (2.0 g, 29.8 mmol) and 4-methylbenzoyl chloride (4.6 g, 29.8 mmol) were added simultaneously and the mixture stirred for 5 min. The resulting material was dissolved in CH_2Cl_2 (300 mL) and washed with $NaHCO_3$ (200 mL). The organic layer was dried ($MgSO_4$) and the solvent was removed under reduced pressure. The crude product was purified using column chromatography (CH_2Cl_2) to give the title compound **2.68b** as a white solid (2.94 g, 53%), mp 118-120 ℃ (lit.[12] 119-121 ℃), R_f = 0.45 (CH_2Cl_2). ^{1}H NMR (400 MHz, $CDCl_3$) δ 9.76 (s, 1H), 7.82 (d, *J* = 8.2 Hz, 2H), 7.28 (d, *J* = 8.2 Hz, 2H), 7.12 (dd, *J* = 4.0, 2.6 Hz, 1H), 6.91 – 6.86 (m, 1H), 6.35 – 6.31 (m, 1H), 2.43 (s, 3H). IR (neat): υ_{max}/cm^{-1}: 3301, 3122, 1601, 1562, 1536, 1421, 1131, 1055, 749. HRMS-ES Calcd for $C_{12}H_{11}NO + Na^+$: 208.0738, found: 208.0742.

The spectroscopic data obtained for this compound were consistent with those reported in the literature.[213]

2-Ethyl-4,4-difluoro-1,3,8-trimethyl-4-bora-3a,4a-diaza-*s*-indacene 2.69a.

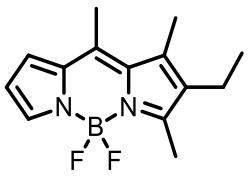

2-Acetylpyrrole **2.68a** (0.16 g, 1.42 mmol) was taken in dry CH_2Cl_2 (15 mL). 3-Ethyl-2,4-dimethyl-1H-pyrrole (0.23 g, 1.85 mmol) and $BF_3.OEt_2$ (0.02 g, 0.14 mmol) were added and the resulting solution was stirred at room temperature for 1 h. The mixture was then neutralized with *N*,*N*-diisopropylethylamine (1.10 g, 8.52 mmol) and treated with $BF_3.OEt_2$ (1.3 g, 11.36 mmol). The mixture was stirred at room temperature for 16 h and washed with water (150 mL). The aqueous layer was extracted with dichloromethane (2 × 50 mL). The combined organic layers were dried ($MgSO_4$) and the solvent was removed under reduced pressure. The orange crude product was purified by column chromatography (CH_2Cl_2:petroleum ether 1:1) to give the title compound **2.69a** as an orange solid (0.24 g, 66%), mp 153-154 °C (lit.[13] 155-156℃), R_f = 0.37 (CH_2Cl_2:petroleum ether 1:1). ^{1}H NMR (300 MHz, $CDCl_3$) δ 7.49 (s, 1H), 6.96 (d, *J* = 3.5 Hz, 1H), 6.33 (dd, *J* = 3.5, 2.1 Hz, 1H), 2.50 (s, 6H), 2.35 (q, *J* = 7.6 Hz, 2H), 2.28 (s, 3H), 0.99 (t, *J* = 7.6 Hz, 3H). ^{13}C NMR (75 MHz, $CDCl_3$) δ 160.40, 140.79, 140.38, 136.67, 135.10, 134.09, 122.70, 114.97, 17.06, 16.64, 14.58, 14.09, 13.11.^{11}B NMR (96 MHz, $CDCl_3$) δ 0.38 (t, $J_{B\text{-}F}$ = 31.2 Hz). ^{19}F NMR (282 MHz, $CDCl_3$) δ -146.33 (q, $J_{F\text{-}B}$ = 31.2 Hz). IR (neat): υ_{max}/cm^{-1}: 2974, 1566, 1454, 1393, 1291, 1209, 1174, 1102, 1059, 958, 757. HRMS-ES Calcd for $C_{14}H_{17}{}^{11}B^{19}F_2N_2O_3$ + H^+: 263.1531, found: 263.1532.
The spectroscopic data obtained for this compound were consistent with those reported in the literature.[214]

2-Ethyl-4,4-difluoro-1,3-dimethyl-8-(4-methylphenyl)-4-bora-3a,4a-diaza-*s*-indacene 2.69b.

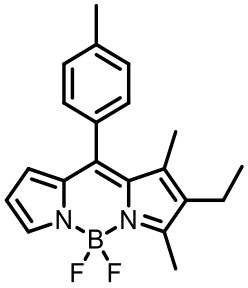

2-(4-Methylbenzoyl)pyrrole **2.68b** (0.36 g, 1.92 mmol) was taken in dry CH_2Cl_2 (50 mL). 3-Ethyl-2,4-dimethyl-1H-pyrrole (0.31 g, 2.50 mmol) and $BF_3.OEt_2$ (0.02 g, 0.19 mmol) were added and the resulting solution was stirred at room temperature for 2 h. The mixture was then neutralized with *N*,*N*-diisopropylethylamine (1.50 g, 11.6 mmol) and treated with $BF_3.OEt_2$ (1.77 g, 15.4 mmol). The mixture was stirred at room temperature for 16 h and washed with water (250 mL). The aqueous layer was extracted with dichloromethane (2 × 80 mL). The combined organic layers were dried ($MgSO_4$) and the solvent was removed under reduced pressure. The green crude product was purified by column chromatography (CH_2Cl_2:petroleum ether 1:1) to give the title compound **2.69b** as an orange solid (0.35 g, 55%), mp 146-147 °C, R_f = 0.45 (CH_2Cl_2:petroleum ether 1:1). ^{1}H NMR (300 MHz, $CDCl_3$) δ 7.54 (s, 1H), 7.22 (d, *J* = 8.3 Hz, 2H), 7.15 (d, *J* = 8.3 Hz, 2H), 6.31 – 6.22 (m, 2H), 2.54 (s, 3H), 2.38 (s, 3H), 2.28 (q, *J* = 7.6 Hz, 2H), 1.41 (s, 3H), 0.95 (t, *J* = 7.6 Hz, 3H). ^{13}C NMR (75 MHz, $CDCl_3$) δ 142.37, 142.15, 139.26, 137.14, 135.70, 134.70, 131.41, 129.04, 128.79, 128.79, 125.89, 118.05, 115.21, 21.45, 17.14, 14.29, 13.27, 12.56. ^{11}B NMR (96 MHz, $CDCl_3$) δ 0.53 (t, $J_{B\text{-}F}$ = 31.2 Hz). ^{19}F NMR (282 MHz, $CDCl_3$) δ -145.77 (q, $J_{F\text{-}B}$ = 31.2 Hz). IR (neat): υ_{max}/cm^{-1}: 3032, 2964, 2927, 2872, 1717, 1545, 1455, 1388, 1291, 1150, 1074, 980, 744.

6-Ethyl-4,4-difluoro-2-iodo-5,7,8-trimethyl-4-bora-3a,4a-diaza-*s*-indacene 2.70a.

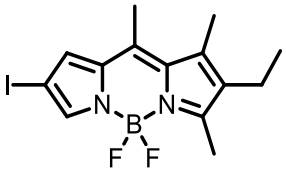

2-Ethyl-4,4-difluoro-1,3,8-trimethyl-4-bora-3a,4a-diaza-*s*-indacene **2.69a** (0.14 g, 0.52 mmol) was taken in dry CH_2Cl_2 (10 mL). *N*-Iodosuccinimide (0.15 g, 0.68 mmol) was added to the mixture and stirred for 16 h. The solvent was then removed under reduced pressure. The brown crude product was purified by column chromatography (CH_2Cl_2:petroleum ether 1:2) to give the title compound **2.70a** as an orange solid (0.12 g, 60%), mp 168-169 ℃ (lit.[14] 160.2-160.7 ℃). R_f =0.35 (CH_2Cl_2:petroleum ether 1:1). ^{1}H NMR (300 MHz, $CDCl_3$) δ 7.40 (s, 1H), 6.96 (s, 1H), 2.49 (s, 3H), 2.41 (s, 3H), 2.34 (q, *J* = 7.6 Hz, 2H), 2.25 (s, 3H), 0.98 (t, *J* = 7.6 Hz, 3H). ^{13}C NMR (75 MHz, $CDCl_3$) δ 162.74, 142.02, 139.64, 138.91, 136.27, 135.24, 134.65, 127.55, 66.63, 17.10, 16.37, 14.46, 14.20, 13.32. ^{11}B NMR (96 MHz, $CDCl_3$) δ -0.03 (t, $J_{B\text{-}F}$ = 30.7 Hz). ^{19}F NMR (282 MHz, $CDCl_3$) δ -146.07 (q, $J_{F\text{-}B}$ = 30.7 Hz). IR (neat): υ_{max}/cm^{-1}: 3115, 2962, 1867, 1557. HRMS-ES Calcd for $C_{14}H_{16}{}^{11}B^{19}F_2N_2{}^{127}I + H^+$: 389.0498, found: 389.0512.

The spectroscopic data obtained for this compound were consistent with those reported in the literature.[122]

6-Ethyl-4,4-difluoro-2-iodo-5,7-dimethyl-8-(4-methylphenyl)-4-bora-3a,4a-diaza-*s*-indacene 2.70b.

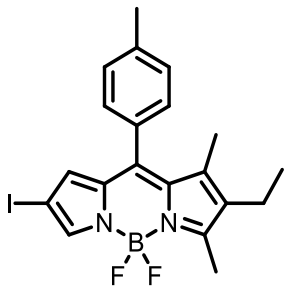

2-Ethyl-4,4-difluoro-1,3-diimethyl-8-(4-methylphenyl)-4-bora-3a,4a-diaza-*s*-indacene **2.69b** (0.32 g, 0.94 mmol) was taken in dry CH_2Cl_2 (20 mL). *N*-Iodosuccinimide (0.26 g, 0.12 mmol) was added to the mixture and stirred for 16 h. The solvent was then removed under reduced pressure. The brown crude product was purified by column chromatography (CH_2Cl_2:petroleum ether 1:1) to give the title compound **2.70b** as an orange solid (0.27 g, 85%); mp 214-215℃. R_f =0.37 (CH_2Cl_2:petroleum ether 1:1). ^{1}H NMR (300 MHz, $CDCl_3$) δ 7.47 (s, 1H), 7.22 (d, *J* = 7.9 Hz, 2H), 7.13 (d, *J* = 7.9 Hz, 2H), 6.32 (s, 1H), 2.55 (s, 3H), 2.38 (s, 3H), 2.28 (q, *J* = 7.6 Hz, 2H), 1.42 (s, 3H), 0.95 (t, *J* = 7.6 Hz, 3H). ^{13}C NMR (75 MHz, $CDCl_3$) δ 164.42, 143.23, 140.99, 140.21, 139.65, 136.65, 135.80, 133.93, 130.77, 130.49, 129.24, 128.68, 67.06, 21.46, 17.18, 14.16, 13.50, 12.69. ^{11}B NMR (96 MHz, $CDCl_3$) δ 0.19 (t, $J_{B\text{-}F}$= 30.9 Hz). ^{19}F NMR (282 MHz, $CDCl_3$) δ -145.69 (q, $J_{F\text{-}B}$ = 30.9 Hz). IR (neat): υ_{max}/cm^{-1}: 3128, 2963, 2457, 2292, 1552, 1519, 1449, 1346, 1293, 1156, 2094, 980, 749. HRMS-ES Calcd for $C_{20}H_{20}{}^{11}B^{19}F_2N_2{}^{127}I$ + H^+: 465.0811, found: 465.0818.

6-Ethyl-4,4-difluoro-5,7,8-trimethyl-2-phenyl-4-bora-3a,4a-diaza-*s*-indacene 2.71.

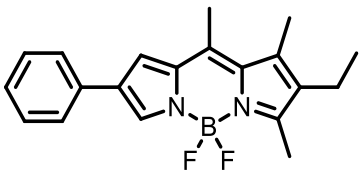

6-Ethyl-4,4-difluoro-2-iodo-5,7-dimethyl-8-(4-methylphenyl)-4-bora-3a,4a-diaza-*s*-indacene **2.70a** (0.20 g, 0.52 mmol), phenylboronic acid (94.0 mg, 0.77 mmol), K_3PO_4 (0.24 g, 1.03 mmol) and chloro(2-dicyclohexylphosphino-2',4',6'-triisopropyl-1,1'-biphenyl)[2-(2'-amino-1,1'-biphenyl)]palladium(II) (LPd(XPhos)Cl) **3.54** (7.00 mg, 0.01 mmol, 2 mol%) were dissolved in THF (6 mL) and water (3 mL). The mixture was heated under reflux for 16 h and then allowed to cool to room temperature. The solution was diluted with CH_2Cl_2 (60 mL) and washed with brine (30 mL). The organic layer was dried ($MgSO_4$) and the solvent was removed under reduced pressure. The red crude product was purified by column chromatography (CH_2Cl_2:petroleum ether 1:1) to give the title compound **2.71** as a red solid (0.159 g, 83%), mp 202-204 ^oC, R_f = 0.37 (CH_2Cl_2:petroleum ether 1:1). ^1H NMR (300 MHz, $CDCl_3$) δ 7.78 (s, 1H), 7.46 (d, *J* = 7.2 Hz, 2H), 7.28 (d, *J* = 7.2 Hz, 2H), 7.19 – 7.13 (m, 1H), 7.12 (s, 1H), 2.49 (s, 3H), 2.45 (s, 3H), 2.31 (q, *J* = 7.6 Hz, 2H), 2.21 (s, 3H), 0.97 (t, *J* = 7.6 Hz, 3H). ^{13}C NMR (75 MHz, $CDCl_3$) δ 160.71, 141.00, 140.14, 135.25, 134.77, 134.37, 133.97, 133.79, 130.66, 128.80, 126.55, 125.13, 118.26, 17.05, 16.54, 14.58, 14.07, 13.16. ^{11}B NMR (96 MHz, $CDCl_3$) δ 0.33 (t, $J_{B\text{-}F}$ = 30.9 Hz). ^{19}F NMR (282 MHz, $CDCl_3$) δ -146.32 (q, $J_{F\text{-}B}$ = 30.9 Hz). IR (neat): υ_{max}/cm^{-1}: 3038, 2968, 2933, 2871, 1572, 1450, 1422, 1364, 1305, 1169, 1059, 1004, 970, 756. HRMS-ES Calcd for $C_{20}H_{21}{}^{11}B^{19}F_2N_2{}^{23}$ + Na^+: 361.1664, found: 361.1649.

6-Ethyl-3-iodo-4,4-difluoro-5,7,8-trimethyl-2-phenyl-4-bora-3a,4a-diaza-*s*-indacene 2.72.

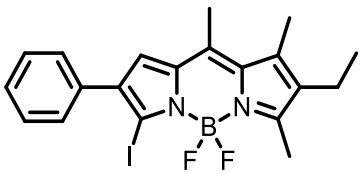

6-Ethyl-4,4-difluoro-5,7,8-trimethyl-2-phenyl-4-bora-3a,4a-diaza-*s*-indacene **2.71** (0.15 g, 0.41 mmol) was taken in dry CH_2Cl_2 (15 mL). *N*-Iodosuccinimide (0.12 g, 0.54 mmol) was added to the mixture and stirred for 16 h. The solvent was then removed under reduced pressure. The brown crude product was purified by column chromatography (CH_2Cl_2) to give the title compound **2.72** as an orange solid (0.15 g, 78%), mp 190-192 ℃. R_f = 0.45 (CH_2Cl_2). ^{1}H NMR (300 MHz, $CDCl_3$) δ 7.47-7.44 (m, 2H), 7.37-7.26 (m, 3H), 6.94 (s, 1H), 2.53 (s, 3H), 2.45 (s, 3H), 2.36 (q, J = 7.6 Hz, 2H), 2.27 (s, 3H), 1.01 (t, J = 7.6 Hz, 3H). ^{11}B NMR (96 MHz, $CDCl_3$) δ 0.30 (t, $J_{B\text{-}F}$ = 31.1 Hz). ^{19}F NMR (282 MHz, $CDCl_3$) δ -143.96 (q, $J_{F\text{-}B}$ = 31.1 Hz). IR (neat): υ_{max}/cm^{-1}: 3115, 2962, 1867, 1557. HRMS-ES Calcd for $C_{20}H_{20}{}^{11}B^{19}F_2N_2 + Na^+$: 487.0630, found: 487.0635.

6-Ethyl-4,4-difluoro-3-(2-hydroxyphenyl)-5,7,8-trimethyl-2-phenyl-4-bora-3a,4a-diaza-*s*-indacene 2.73.

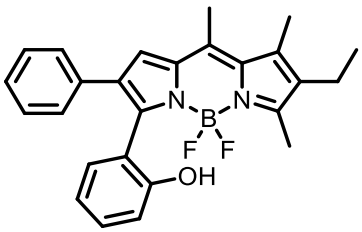

6-Ethyl-3-iodo-4,4-difluoro-5,7,8-trimethyl-2-phenyl-4-bora-3a,4a-diaza-*s*-indacene **2.72** (0.10 g, 0.21 mmol), 2-hydroxyphenylboronic acid (0.04 g, 0.32 mmol), K_3PO_4 (91.0 mg, 426 μmol) and chloro(2-dicyclohexylphosphino-2',4',6'-triisopropyl-1,1'-biphenyl)[2-(2'-amino-1,1'-biphenyl)]palladium(II) (LPd(XPhos)Cl) **3.54** (3.20 mg, 4.20 μmol) were dissolved in THF (3 mL) and water (1.5 mL). The mixture was heated under reflux for 16 h and then allowed to cool to room temperature. The solution was diluted with CH_2Cl_2 (20 mL) and washed with brine (10 mL). The organic layer was dried ($MgSO_4$) and the solvent was removed under reduced pressure. The red crude product was purified by column chromatography (CH_2Cl_2) to give the title compound **2.73** as a red solid (0.032 g, 25%), mp 203-205 ^oC, R_f = 0.35 (CH_2Cl_2). ^1H NMR (300 MHz, $CDCl_3$) δ 7.28 (d, J = 7.9 Hz, 1H), 7.23 – 7.18 (m, 2H), 7.14 – 7.04 (m, 5H), 6.96 (d, J = 8.2 Hz, 1H), 6.88 (t, *J* = 7.5Hz, 1H), 5.43 (d, *J* = 8.4 Hz, 1H), 2.57 (s, 3H), 2.40 (s, 3H), 2.34 (q, *J* = 7.6 Hz, 2H), 2.30 (s, 3H), 0.97 (t, *J* = 7.6 Hz, 3H).^{13}C NMR (176 MHz, $CDCl_3$) δ 161.53, 154.13, 142.89, 140.76, 139.28, 135.91, 134.44, 134.41, 134.05, 131.85, 131.10, 130.76, 128.33, 127.27, 126.56, 121.22, 121.02, 120.67, 116.92, 17.09, 16.41, 14.50, 14.13, 13.18. ^{11}B NMR (96 MHz, $CDCl_3$) δ 0.56 (apparent t, $J_{B\text{-}F}$ = 32.5 Hz). ^{19}F NMR (282 MHz, $CDCl_3$) δ -143.04 (dq, $J_{F\text{-}F}$ = 108.1, $J_{F\text{-}B}$ = 32.8 Hz), 143.96 (dq, $J_{F\text{-}F}$ = 108.1, $J_{F\text{-}B}$ = 32.3 Hz). IR (neat): υ_{max}/cm^{-1}: 3279, 3040, 2925, 2854, 2402, 1692, 1602, 1566, 1503, 1451, 1404, 1150, 1102, 750. HRMS-ES Calcd for $C_{26}H_{25}{}^{11}B{}^{19}F_2N_2O + Na^+$: 453.1926, found: 453.1928.

***N,N,O,F*-Chelated BODIPY 2.74.**

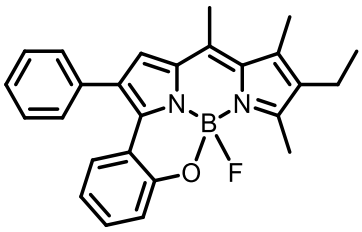

6-Ethyl-4,4-difluoro-3-(2-hydroxyphenyl)-5,7,8-trimethyl-2-phenyl-4-bora-3a,4a-diaza-*s*-indacene **2.73** (10.0 mg, 24.0 μmol) was taken in dry CH_2Cl_2 (1.5 mL). *N*,*N*-diisopropylethylamine (3.6 mg, 2.8 μmol) was added and the mixture was stirred. $BF_3.OEt_2$ (2.7 mg, 2.4 μmol) was added. The mixture was heated under reflux for 10 min and then allowed to cool to room temperature. The solution was diluted with CH_2Cl_2 (10 mL) and washed with $NaHCO_3$ (15 mL). The organic layer was dried ($MgSO_4$) and the solvent was removed under reduced pressure. The purple crude product was purified by column chromatography (ethyl acetate:petroleum ether 1:8) to give the title compound **2.74** as a purple solid (6.0 mg, 50%), R_f = 0.35 (ethyl acetate:petroleum ether 1:8). ^{1}H NMR (500 MHz, $CDCl_3$) δ 7.41-7.38 (m, 3H), 7.35 (t, *J* = 7.5 Hz, 2H), 7.32 – 7.27 (m, 1H), 7.21 (d, *J* = 8.2 Hz, 1H), 7.12 (d, *J* = 8.2 Hz, 1H), 7.00 (s, 1H), 6.67 (t, *J* = 8.1 Hz, 1H), 2.69 (s, 3H), 2.55 (s, 3H), 2.41 (q, *J* = 7.6 Hz, 2H), 2.33 (s, 3H), 1.02 (t, *J* = 7.6 Hz, 3H). ^{11}B NMR (160 MHz, $CDCl_3$) δ 0.25 (d, $J_{B\text{-}F}$ = 49.1 Hz). ^{19}F NMR (471 MHz, $CDCl_3$) δ -143.70 (q, $J_{F\text{-}B}$ = 49.1 Hz).

2,2'-((4-Methoxyphenyl)methylene)bis(1H-pyrrole) 3.15.

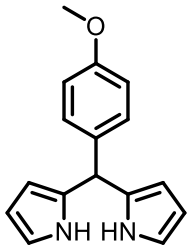

A flame dried Schlenk flask was charged with 4-methoxybenzaldehyde (2.7 mL, 22 mmol) and pyrrole (38.2 mL, 551 mmol) and the resulting solution was stirred at room temperature for 25 min. Thereafter, $BF_3.OEt_2$ (0.2 mL, 2.00 mmol) was added to the mixture and stirred for 4 h. The solvent was removed under reduced pressure and the resulting material was pratitioned between CH_2Cl_2 (100 mL) and 0.1M NaOH (300 mL). The organic extract was dried ($MgSO_4$) and the solvent was removed under reduced pressure. The resulting green oil was purified by column chromatography (CH_2Cl_2: petroleum ether 7:3) to to give the title compound **3.15** as a light grey solid (4.80 g, 87%), mp 97-98 °C (lit.[15] 98-99 °C), R_f = 0.4 (CH_2Cl_2:petroleum ether 7:3). ^{1}H NMR (300 MHz, $CDCl_3$) δ 7.85 (s, 2H), 7.06 (d, *J* = 8.7 Hz, 2H), 6.78 (d, *J* = 8.7 Hz, 2H), 6.63-6.60 (m, 2H), 6.10-6.07 (m, 2H), 5.84 (s, 2H), 5.36 (s, 1H), 3.72 (s, 3H). ^{13}C NMR (101 MHz, $CDCl_3$) δ 158.60, 134.34, 133.02, 129.51, 117.28, 114.08, 108.47, 107.19, 55.42, 43.21. IR (neat): υ_{max}/cm^{-1}: 3341, 2922, 2853, 1610, 1511, 1461, 1252, 1176, 1032, 842, 723. HRMS-ES Calcd for $C_{16}H_{16}N_2O + Na^+$: 275.1160, found: 275.1167.

The spectroscopic data obtained for this compound were consistent with those reported in the literature.[215]

4,4-Difluoro- 8-(4-methoxyphenyl)-4-bora-3a,4a-diaza-*s*-indacene 3.16.

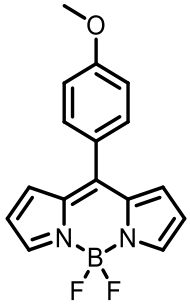

2,2'-((4-Methoxyphenyl)methylene)bis(1H-pyrrole) **3.15** (4.30 g, 17.3 mmol) was taken in dry CH_2Cl_2 (200 mL) and cooled to 0 °C. A solution of DDQ (3.92 g, 17.3 mmol) in CH_2Cl_2 (70 mL) was added to the mixture dropwise over 30 min. The mixture was then neutralized with *N*,*N*-diisopropylethylamine (25.7 g, 199 mmol) and treated with $BF_3.OEt_2$ (39.7 g, 280 mmol). The mixture was stirred at room temperature for 2 h and then washed with 0.1 M NaOH (150 mL) and water (100 mL). The aqueous layer was back extracted with CH_2Cl_2 (2 × 150 mL). The combined organic layers were dried ($MgSO_4$) and the solvent was removed under reduced pressure. The resulting orange crude product was purified by column chromatography (CH_2Cl_2:petroleum ether 4:1) to give the title compound **3.16** as an orange solid (4.00 g, 78%), mp 135-136 °C (lit.[16] mp 137-138 °C). R_f = 0.6 (CH_2Cl_2:petroleum ether 4:1).^{1}H NMR (400 MHz, $CDCl_3$) δ 7.91 (s, 2H), 7.53 (d, *J* = 8.8 Hz, 2H), 7.04 (d, *J* = 8.8 Hz, 2H), 6.96 (d, *J* = 4.2 Hz, 2H), 6.54 (d, *J* = 5.5 Hz, 2H), 3.90 (s, 3H).^{13}C NMR (101 MHz, $CDCl_3$) δ 162.17, 147.51, 143.49, 134.92, 132.52, 131.45, 126.40, 118.38, 114.15, 55.63.^{11}B NMR (128 MHz, $CDCl_3$) δ -0.67 (t, $J_{B\text{-}F}$ = 29.0 Hz).^{19}F NMR (376 MHz, $CDCl_3$) δ -145.00 (q, $J_{F\text{-}B}$ = 29.0 Hz). IR (neat): υ_{max}/cm^{-1}: 3017, 2841, 1601, 1574, 1537, 1473, 1384, 1256, 1220, 1112, 1065, 977, 844, 779. HRMS-ES Calcd for $C_{16}H_{13}BN_2OF_2$ + Na^+: 321.0987, found: 321.0975. The spectroscopic data obtained for this compound were consistent with those reported in the literature.[216]

4,4-Difluoro-2-iodo-8-(4-methoxyphenyl)-4-bora-3a,4a-diaza-*s*-indacene 3.17 and 4,4-difluoro-2,6-diiodo-8-(4-methoxyphenyl)-4-bora-3a,4a-diaza-*s*-indacene 3.18.

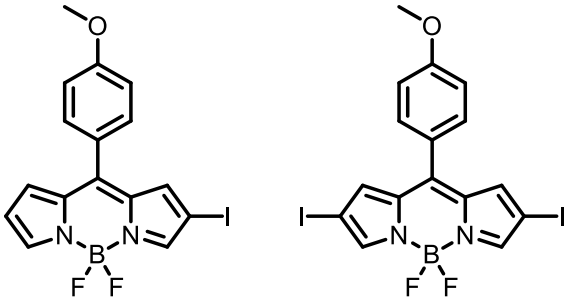

4,4-Difluoro-8-(4-methoxyphenyl)-4-bora-3a,4a-diaza-*s*-indacene **3.16** (0.20 g, 0.67 mmol) was taken in dry CH_2Cl_2-MeOH (1:1, 48 mL). A solution of ICl (0.11 g, 0.67 mmol) in MeOH (5 mL) was added to the mixture dropwise. The mixture was stirred at room temperature for 2 h. The solvent was then removed under reduced pressure and the crude product was dissolved in CH_2Cl_2 (50 mL) and washed with H_2O (2 × 100 mL). The organic layer was dried ($MgSO_4$) and the solvent was removed under reduced pressure. The resulting red crude product was purified by column chromatography (CH_2Cl_2: petroleum ether 1:1) to give: First eluted, the 2, 6-diiodide **3.18** as a pink solid (0.06 g, 15%), mp 246–248 °C. R_f = 0.4 (CH_2Cl_2:petroleum ether 1: 1). ^{1}H NMR (400 MHz, $CDCl_3$) δ 7.85 (s, 2H), 7.52 (d, *J* = 8.5 Hz, 2H), 7.13 (s, 2H), 7.06 (d, *J* = 8.5 Hz, 2H), 3.91 (s, 3H).^{13}C NMR (101 MHz, $CDCl_3$) δ 162.86, 147.74, 145.96, 137.50, 135.93, 132.64, 125.62, 114.57, 72.07, 55.75. ^{11}B NMR (128 MHz, $CDCl_3$) δ −1.27 (t, J_{B-F} = 28.0 Hz). ^{19}F NMR (376 MHz, $CDCl_3$) δ −144.63 (q, J_{F-B} = 28.0 Hz). IR (neat): υ_{max}/cm^{-1}: 3113, 2930, 1725, 1596, 1566, 1528, 1466, 1342, 1246, 1074, 984, 896, 707. HRMS-ES Calcd for $C_{16}H_{11}BN_2OF_2I_2$ + Na^+: 572.8920, found: 572.8920. Second eluted, the monoiodide **3.17** as a red solid (0.185 g, 65%), mp 206–208 °C. R*f* = 0.3 (CH_2Cl_2: petroleum ether 1: 1). ^{1}H NMR (400 MHz, $CDCl_3$) δ 7.96 (s, 1H), 7.81 (s, 1H), 7.52 (d, *J* = 8.8 Hz, 2H), 7.05 (d, *J* = 8.8 Hz, 4H), 6.59 (d, *J* = 4.3 Hz, 1H), 3.91 (s, 3H). ^{13}C NMR (101 MHz, $CDCl_3$) δ 162.51, 146.73, 146.11, 145.22, 135.99, 135.78, 135.08, 133.00, 132.57, 125.95, 119.46, 114.36, 70.73, 55.69. ^{19}F NMR (376 MHz, $CDCl_3$) δ -144.72 (q, J_{F-B} = 28.0 Hz). ^{11}B NMR (128 MHz, $CDCl_3$) δ -1.26 (t, J_{B-F} = 28.0 Hz). IR (neat): υ_{max}/cm^{-1}: 3109, 2849, 1721, 1603, 1573, 1532, 1470, 1400, 1349, 1250, 1062, 982, 706. HRMS-ES Calcd for $C_{16}H_{12}BN_2OF_2I$ + Na^+: 446.9953, found: 446.9961.

2-Bromo-4,4-difluoro-8-(4-methoxyphenyl)-4-bora-3a,4a-diaza-*s*-indacene 3.23.

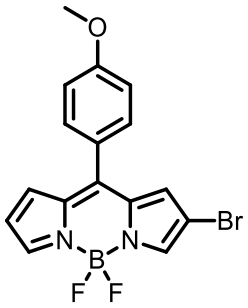

4,4-Difluoro-8-(4-methoxyphenyl)-4-bora-3a,4a-diaza-*s*-indacene **3.16** (0.30 g, 1.01 mmol) was taken in dry CH_2Cl_2/MeCN (1:1, 50 mL). A solution of NBS (0.25 g, 1.20 mmol) in CH_2Cl_2 (10 mL) was added to the mixture dropwise. The mixture was stirred at room temperature for 90 min and then the solvent was removed under reduced pressure. The crude product was dissolved in CH_2Cl_2 (60 mL) and washed with H_2O (3 x 100 mL). The organic layer was dried ($MgSO_4$) and the solvent was removed under reduced pressure. The resulting orange crude product was purified by column chromatography (CH_2Cl_2:petroleum ether 1:1) to give the title compound **3.23** as an orange solid (0.28 g, 73%), mp 246-248 °C. R_f = 0.5 (CH_2Cl_2:petroleum ether 1:1). ^{1}H NMR (400 MHz, $CDCl_3$) δ 7.96 (s, 1H), 7.75 (s, 1H), 7.51 (d, *J* = 8.5 Hz, 2H), 7.04 (d, *J* = 8.7 Hz, 3H), 6.91 (s, 1H), 6.59 (d, *J* = 4.3 Hz, 1H), 3.90 (s, 3H). ^{13}C NMR (101 MHz, $CDCl_3$) δ 162.55, 147.30, 145.45, 141.46, 135.24, 134.22, 133.05, 132.58, 130.20, 125.87, 119.41, 114.38, 105.77, 55.70. ^{11}B NMR (128 MHz, $CDCl_3$) δ -0.96 (t, J_{B-F} = 28.1 Hz). ^{19}F NMR (376 MHz, $CDCl_3$) δ -144.91 (q, J_{F-B} = 28.1 Hz). IR (neat): υ_{max}/cm^{-1}: 3227, 1603, 1573, 1536, 1474, 1400, 1356, 1246, 1060, 981. HRMS-ES Calcd for $C_{16}H_{12}BN_2OF_2Br$ + Na^+: 398.0128, found: 398.0136.

The spectroscopic data obtained for this compound were consistent with those reported in the literature.[56]

General procedure for copper catalysed amination

4,4-Difluoro-2-iodo-8-(4-methoxyphenyl)-4-bora-3a,4a-diaza-*s*-indacene **3.17** (0.10 g, 0.26 mmol), the amine (0.47 mmol), CuI (2.20 mg, 0.01 mmol, 5 mol%) Cs_2CO_3 (0.15 g, 0.47 mmol), and 1, 10-phenanthroline (8.50 mg, 0.05 mmol, 20 mol%) were taken in a flame-dried Schlenk tube and flushed with N_2 several times. Dry DMF (0.8 mL) was then added and the mixture was stirred at 80 °C for 24 h. The mixture was dissolved in ethyl acetate (30 mL) and washed with water (2 × 100 mL). The organic layer was dried ($MgSO_4$) and the solvent was removed under reduced pressure. The crude product was purified by column chromatography. In all cases the 3-amino-6-iodo by-product **3.22** eluted from the column first and the 3-amino compound **3.19** second.

4,4-Difluoro-3-(hexylamino)-8-(4-methoxyphenyl)-4-bora-3a,4a-diaza-*s*-indacene 3.19a.

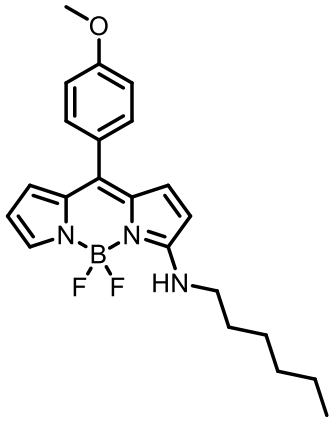

According to the general procedure for copper catalysed amination, 4,4-difluoro-2-iodo-8-(4-methoxyphenyl)-4-bora-3a,4a-diaza-*s*-indacene **3.17** (0.10 g, 0.26 mmol) was reacted with hexylamine (0.05 g, 0.47 mmol). The crude product was purified by column chromatography (CH_2Cl_2:petroleum ether 1:1) to give the title compound **3.19a** as a dark yellow solid (0.06 g, 60%), mp 202–204 °C; ^{1}H NMR (400 MHz, $CDCl_3$) δ 7.45–7.37 (m, 3H), 6.97 (dd, *J* = 6.7, 4.7 Hz, 2H), 6.94 (s, 1H), 6.44 (d, *J* = 3.5 Hz, 1H), 6.33 (dd, *J* = 3.6, 2.4 Hz, 1H), 6.23 (s, 1H), 6.16 (d, *J* = 5.0 Hz, 1H), 3.86 (s, 3H), 3.38 (dd, *J* = 13.5, 6.8 Hz, 2H), 1.75–1.62 (m, 2H), 1.45–1.35 (m, 2H), 1.34–1.25 (m, 4H), 0.89 (dd, *J* = 9.0, 4.5 Hz, 3H). ^{13}C NMR (101 MHz, $CDCl_3$) δ 161.67, 160.49, 136.12, 133.40, 132.80, 132.75, 131.75, 130.84, 127.15, 119.78, 113.74, 113.39, 110.06, 55.47, 44.82, 31.44, 30.18, 26.32, 22.59, 14.08. ^{11}B NMR (128 MHz, $CDCl_3$) δ −0.01 (t, $J_{B\text{-}F}$ = 33.5 Hz). ^{19}F NMR (376 MHz, $CDCl_3$) δ −149.24 (q, $J_{F\text{-}B}$ = 33.5 Hz). IR (neat): υ_{max}/cm^{-1}: 3413, 3127, 2923, 1606, 1524, 1471, 1397, 1372, 1243, 1178, 1021, 977, 759. HRMS-ES Calcd for $C_{22}H_{26}BN_3OF_2$ + Na^+: 419.2071, found: 419.2060.

4,4-Difluoro-3-(hexylamino)-6-iodo-8-(4-methoxyphenyl)-4-bora-3a,4a-diaza-*s*-indacene 3.22a.

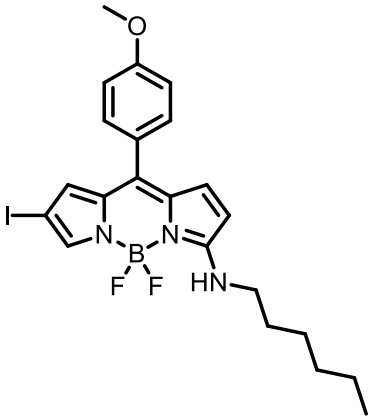

According to the general procedure for copper catalysed amination, 4,4-difluoro-2-iodo-8-(4-methoxyphenyl)-4-bora-3a,4a-diaza-*s*-indacene **3.17** (0.10 g, 0.26 mmol) was reacted with hexylamine (0.05 g, 0.47 mmol). The crude product was purified by column chromatography (CH_2Cl_2:petroleum ether 1:1) to give the title compound **3.22a** as a dark yellow solid (6.00 mg, 5%), ^{1}H NMR (400 MHz, $CDCl_3$) δ 7.42–7.34 (m, 3H), 7.01–6.93 (m, 3H), 6.47 (s, 1H), 6.31 (s, 1H), 6.23 (d, *J* = 5.0 Hz, 1H), 3.40 (q, *J* = 6.8 Hz, 2H), 1.68 (p, *J* = 7.3 Hz, 2H), 1.43–1.28 (m, 6H), 0.93–0.86 (m, 3H).^{13}C NMR (101 MHz, $CDCl_3$) δ 162.04, 160.65, 136.78, 134.61, 134.21, 133.74, 131.67, 131.05, 126.57, 124.84, 113.92, 111.30, 65.08, 55.51, 44.97, 31.41, 30.19, 26.30, 22.57, 14.07. HRMS-ES Calcd for $C_{22}H_{25}BN_3OF_2 + Na^+$: 546.1001, found: 546.1005.

4,4-Difluoro-8-(4-methoxyphenyl)-3-((4-methylphenyl)amino)-4-bora-3a,4a-diaza-*s*-indacene 3.19b.

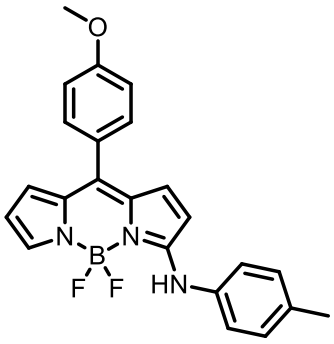

According to the general procedure for copper catalysed amination, 4,4-difluoro-2-iodo-8-(4-methoxyphenyl)-4-bora-3a,4a-diaza-*s*-indacene **3.17** (0.10 g, 0.26 mmol) was reacted with *p*-toluidine (0.05 g, 0.47 mmol). The crude product was purified by column chromatography (CH_2Cl_2:petroleum ether 1:1) to give the title compound **3.19b** as an orange solid (0.08 g, 84%), mp 186–188 °C; ^{1}H NMR (300 MHz, $CDCl_3$) δ 7.86 (s, 1H), 7.43 (s, 1H), 7.39 (d, *J* = 8.7 Hz, 2H), 7.15 (d, *J* = 8.4 Hz, 2H), 7.09 (d, *J* = 8.5 Hz, 2H), 6.92 (d, *J* = 8.8 Hz, 2H), 6.89 (s, 1H), 6.47 (d, *J* = 3.3 Hz, 1H), 6.35–6.30 (m, 1H), 6.28 (d, *J* = 4.9 Hz, 1H), 3.81 (s, 3H), 2.30 (s, 3H). ^{13}C NMR (101 MHz, $CDCl_3$) δ 160.74, 158.94, 136.20, 135.72, 135.01, 134.70, 133.13, 132.91, 132.17, 131.83, 130.38, 126.96, 122.89, 121.24, 113.97, 113.85, 111.16, 55.50, 21.08. IR (neat): υ_{max}/cm^{-1}: 3368, 2914, 2839, 1606,1580,1523,1489, 1397, 1293, 1241, 1175, 1032, 973, 787. ^{19}F NMR (376 MHz, $CDCl_3$) δ −148.37 (q, $J_{F\text{-}B}$ = 33.0 Hz). ^{11}B NMR (128 MHz, $CDCl_3$) δ 0.06 (t, $J_{B\text{-}F}$ =33.0 Hz). HRMS-ES Calcd for $C_{23}H_{20}BN_3OF_2$ + H^+: 404.1742, found: 404.1740.

4,4-Difluoro-6-iodo-8-(4-methoxyphenyl)-3-((4-methylphenyl)amino)-4-bora-3a,4a-diaza-*s*-indacene 3.22b.

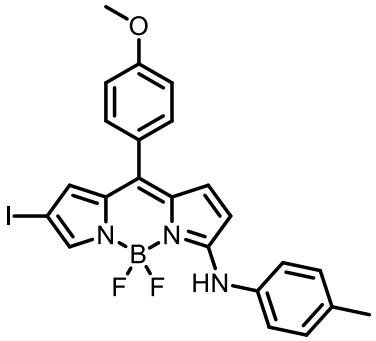

According to the general procedure for copper catalysed amination, 4,4-difluoro-2-iodo-8-(4-methoxyphenyl)-4-bora-3a,4a-diaza-*s*-indacene **3.17** (0.10 g, 0.26 mmol) was reacted with *p*-toluidine (0.05 g, 0.47 mmol). The crude product was purified by column chromatography (CH_2Cl_2:petroleum ether 1:1) to give the title compound **3.22b** as a purple solid (7.00 mg, 5%), ^{1}H NMR (400 MHz, $CDCl_3$) δ 7.99 (s, 1H), 7.42 (d, *J* = 3.8 Hz, 2H), 7.40 (s, 1H), 7.22 (d, *J* = 8.1 Hz, 2H), 7.15 (d, *J* = 8.2 Hz, 2H), 6.99 (s, 1H), 6.98 (d, *J* = 8.4 Hz, 2H), 6.56 (s, 1H), 6.37 (d, *J* = 4.9 Hz, 1H), 3.87 (s, 3H), 3.79 (s, 1H), 2.37 (s, 3H).^{13}C NMR (101 MHz, $CDCl_3$) δ 160.88, 159.64, 136.79, 136.39, 135.70, 134.56, 134.26, 133.53, 132.88, 131.73, 130.44, 126.43, 126.06, 123.28, 114.00, 112.47, 65.60, 55.52, 21.10. IR (neat): υ_{max}/cm^{-1}: 3374, 2934, 1712, 1604, 1519, 1477, 1251, 1032, 733. HRMS-ES Calcd for $C_{23}H_{19}BN_3OF_2I$ + Na^+: 551.0568, found: 551.0565.

4,4-Difluoro-8-(4-methoxyphenyl)-3-(N-benzamido)-4-bora-3a,4a-diaza-*s*-indacene 3.19c.

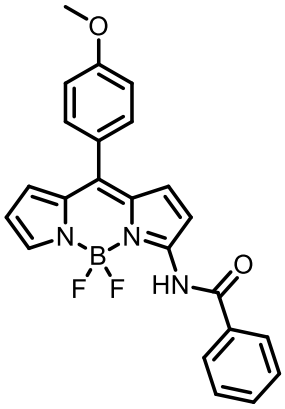

According to the general procedure for copper catalysed amination, 4,4-difluoro-2-iodo-8-(4-methoxyphenyl)-4-bora-3a,4a-diaza-*s*-indacene **3.17** (0.10 g, 0.26 mmol) was reacted with benzamide (0.06 g, 0.47 mmol). The crude product was purified by column chromatography (CH_2Cl_2:petroleum ether 1:1) to give the title compound **3.19c** as an orange solid (15.0 mg, 15%); ^{1}H NMR (400 MHz, $CDCl_3$) δ 9.61 (s, 1H), 7.97 (d, *J* = 7.8 Hz, 2H), 7.67 (s, 1H), 7.63 (d, *J* = 7.5 Hz, 1H), 7.56 (d, *J* = 7.0 Hz, 2H), 7.51 (d, *J* = 8.4 Hz, 2H), 7.39 (d, *J* = 4.7 Hz, 1H), 7.09 (d, *J* = 4.7 Hz, 1H), 7.03 (d, *J* = 8.4 Hz, 2H), 6.79 (d, *J* = 3.8 Hz, 1H), 6.53–6.40 (m, 1H), 3.90 (s, 3H). ^{13}C NMR (101 MHz, $CDCl_3$) δ 164.04, 161.68, 152.47, 142.51, 137.46, 135.05, 133.70, 133.35, 132.55, 132.22, 131.26, 129.28, 127.61, 127.01, 126.29, 116.29, 114.09, 113.34, 55.60. ^{11}B NMR (128 MHz, $CDCl_3$) δ −0.15 (t, $J_{B\text{-}F}$ = 33.1 Hz). ^{19}F NMR (376 MHz, $CDCl_3$) δ −146.81 (q, $J_{F\text{-}B}$ = 33.1 Hz). IR (neat): υ_{max}/cm^{-1}: 3402, 2919, 1692, 1588, 1503, 1444, 1348, 1287, 1250, 1176, 1057, 1033 977, 699. HRMS-ES Calcd for $C_{23}H_{18}BN_3O_2F_2$ + Na^+: 440.1358, found: 440.1360.

3-(Benzylamino)-4,4-difluoro-8-(4-methoxyphenyl)-4-bora-3a,4a-diaza-*s*-indacene 3.19d.

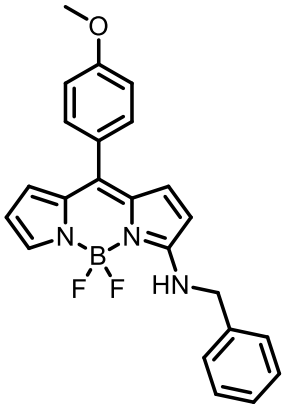

According to the general procedure for copper catalysed amination, 4,4-difluoro-2-iodo-8-(4-methoxyphenyl)-4-bora-3a,4a-diaza-*s*-indacene **3.17** (0.10 g, 0.26 mmol) was reacted with benzylamine (0.05 g, 0.47 mmol). The crude product was purified by column chromatography (CH_2Cl_2:petroleum ether 1:1) to give the title compound **3.19d** as an orange solid (61.0 mg, 61%), mp 132–134 °C; ^{1}H NMR (400 MHz, $CDCl_3$) δ 7.44 (s, 1H), 7.42 (d, *J* = 8.7 Hz, 2H), 7.40–7.36 (m, 1H), 7.34 (d, *J* = 6.6 Hz, 2H), 7.33–7.28 (m, 2H), 6.97 (d, *J* = 8.5 Hz, 2H), 6.92 (d, *J* = 4.9 Hz, 1H), 6.64 (s, 1H), 6.48 (d, *J* = 3.6 Hz, 1H), 6.34 (dd, *J* = 3.5, 2.5 Hz, 1H), 6.11 (d, *J* = 4.9 Hz, 1H), 4.60 (d, *J* = 6.3 Hz, 2H), 3.86 (s, 3H).^{13}C NMR (101 MHz, $CDCl_3$) δ 161.71, 160.60, 136.81, 136.14, 133.85, 133.28, 132.85, 131.78, 131.51, 129.15, 128.16, 127.02, 126.93, 120.55, 113.78, 113.68, 110.04, 55.48, 48.22. ^{11}B NMR (128 MHz, $CDCl_3$) δ 0.02 (t, $J_{B\text{-}F}$ = 33.5 Hz). ^{19}F NMR (376 MHz, $CDCl_3$) δ −148.95 (q, $J_{F\text{-}B}$ = 33.5 Hz). IR (neat): υ_{max}/cm^{-1}: 3360, 2970, 1705, 1619, 1466, 1379, 1160, 1128, 951, 816. HRMS-ES Calcd for $C_{23}H_{20}BN_3OF_2$ + Na^+: 426.1565, found: 426.1584.

4,4-Difluoro-8-(4-methoxyphenyl)-3-((2-(thiophen-2-yl)ethyl)amino)-4-bora- 3a,4a-diaza-*s*-indacene 3.19e.

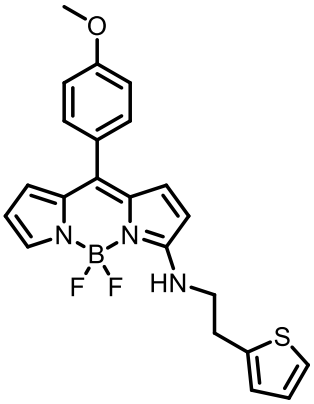

According to the general procedure for copper catalysed amination, 4,4-difluoro-2-iodo-8-(4-methoxyphenyl)-4-bora-3a,4a-diaza-*s*-indacene **3.17** (0.10 g, 0.26 mmol) was reacted with 2-thiopheneethylamine (0.06 g, 0.47 mmol). The crude product was purified by column chromatography (CH_2Cl_2:petroleum ether 1:1) to give the title compound **3.19e** as an orange solid (65.0 mg, 65%), mp 119–120 °C; ^{1}H NMR (400 MHz, $CDCl_3$) δ 7.41 (dd, *J* = 9.0, 2.4 Hz, 3H), 7.18 (dd, *J* = 5.1, 1.3 Hz, 1H), 6.96 (t, *J* = 7.1 Hz, 3H), 6.91 (dd, *J* = 2.9, 2.2 Hz, 2H), 6.46 (d, *J* = 3.5 Hz, 1H), 6.36 (s, 1H), 6.33 (dd, *J* = 3.7, 2.3 Hz, 1H), 6.06 (d, *J* = 5.0 Hz, 1H), 3.86 (s, 3H), 3.65 (q, *J* = 6.6 Hz, 2H), 3.18 (t, *J* = 6.7 Hz, 2H).^{13}C NMR (101 MHz, $CDCl_3$) δ 161.45, 160.55, 139.31, 136.06, 133.32, 132.79, 131.78, 131.21, 127.53, 127.04, 126.43, 124.69, 120.20, 113.77, 113.58, 109.73, 55.50, 46.23, 30.84. ^{11}B NMR (128 MHz, $CDCl_3$) δ −0.04 (t, $J_{B\text{-}F}$ = 33.2 Hz), ^{19}F NMR (376 MHz, $CDCl_3$) δ −148.47 (q, $J_{F\text{-}B}$ = 33.2 Hz). IR (neat): υ_{max}/cm^{-1}: 3361, 2923, 178, 1606, 1401, 1293, 1257, 1025, 792. HRMS-ES Calcd for $C_{22}H_{20}BN_3OF_2S$ + H^+: 424.1466, found: 424.1456.

3-(Cyclohexylamino)-4,4-difluoro-8-(4-methoxyphenyl)-4-bora-3a,4a-diaza-*s*-indacene 3.19f.

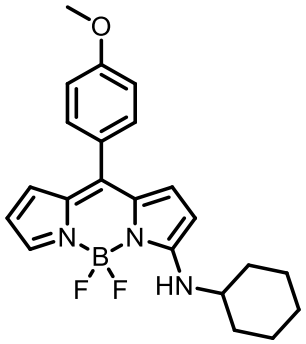

According to the general procedure for copper catalysed amination, 4,4-difluoro-2-iodo-8-(4-methoxyphenyl)-4-bora-3a,4a-diaza-*s*-indacene **3.17** (0.10 g, 0.26 mmol) was reacted with cyclohexylamine (0.05 g, 0.47 mmol). The crude product was purified by column chromatography (CH_2Cl_2:petroleum ether 1:1) to give the title compound **3.19f** as an orange solid (73.0 mg, 78%), mp 130–131 °C; ^{1}H NMR (400 MHz, $CDCl_3$) δ 7.40 (d, *J* = 8.4 Hz, 2H), 6.96 (d, *J* = 8.6 Hz, 2H), 6.93 (d, *J* = 5.0 Hz, 1H), 6.43 (d, *J* = 3.3 Hz, 1H), 6.32 (dd, *J* = 3.6, 2.4 Hz, 1H), 6.19 (s, 1H), 6.16 (d, *J* = 5.0 Hz, 1H), 3.86 (s, 2H), 3.43 (d, *J* = 8.8 Hz, 1H), 2.02 (d, *J* = 10.2 Hz, 2H), 1.81 (d, *J* = 13.3 Hz, 2H), 1.63 (d, *J* = 16.3 Hz, 1H), 1.53–1.14 (m, 4H).^{13}C NMR (101 MHz, $CDCl_3$) δ 160.76, 160.45, 136.09, 133.34, 132.78, 132.47, 131.73, 130.67, 127.19, 119.56, 113.74, 113.29, 110.49, 55.47, 53.79, 33.62, 25.21, 24.53. ^{11}B NMR (128 MHz, $CDCl_3$) δ −0.01 (t, $J_{B\text{-}F}$ = 30.0 Hz). ^{19}F NMR (376 MHz, $CDCl_3$) δ −149.24 (q, $J_{F\text{-}B}$ = 30.0 Hz). IR (neat): υ_{max}/cm^{-1}: 2931, 2858, 1718, 1604, 1511, 1293, 1253, 1175, 1062, 1027, 839, 795. HRMS-ES Calcd for $C_{22}H_{24}BN_3OF_2$ + Na^+: 418.1878, found: 418.1879.

3-(Cyclohexylamino)-4,4-difluoro-6-iodo-8-(4-methoxyphenyl)-4-bora-3a,4a-diaza-*s*-indacene 3.22f.

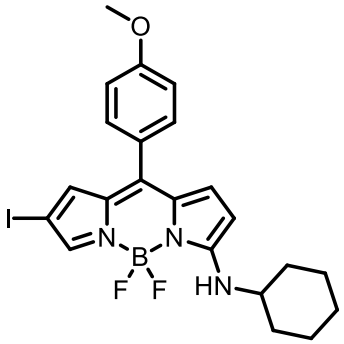

According to the general procedure for copper catalysed amination, 4,4-difluoro-2-iodo-8-(4-methoxyphenyl)-4-bora-3a,4a-diaza-*s*-indacene **3.17** (0.10 g, 0.26 mmol) was reacted with cyclohexylamine (0.05 g, 0.47 mmol). The crude product was purified by column chromatography (CH_2Cl_2:petroleum ether 1:1) to give the title compound **3.22f** as a yellow solid (5.00 mg, 4%), ^{1}H NMR (400 MHz, $CDCl_3$) δ7.35 (s, 1H), 7.37 (d, *J* = 8.8 Hz, 2H), 6.96 (d, *J* = 7.8 Hz, 2H), 6.97 (s, 1H), 6.46 (s, 1H), 6.23 (s, 2H), 3.86 (s, 3H), 3.52–3.38 (m, 1H), 2.08–1.98 (m, 2H), 1.86–1.75 (m, 2H), 1.65 (d, *J* = 12.8 Hz, 1H), 1.50–1.21 (m, 5H). ^{13}C NMR (101 MHz, $CDCl_3$) δ 161.11, 160.61, 136.72, 134.45, 134.21, 133.70, 131.66, 130.77, 126.62, 124.63, 113.91, 111.71, 65.00, 55.51, 54.04, 33.64, 25.14, 24.53. IR (neat): υ_{max}/cm^{-1}: 3373, 2916, 1608, 1574, 1519, 1480, 1392, 1252, 1101. HRMS-ES Calcd for $C_{22}H_{23}BN_3OF_2I$ + Na^+: 544.0845, found: 544.0850.

4,4-Difluoro-8-(4-methoxyphenyl)-3-(morpholino)-4-bora-3a,4a-diaza-*s*-indacene 3.19g.

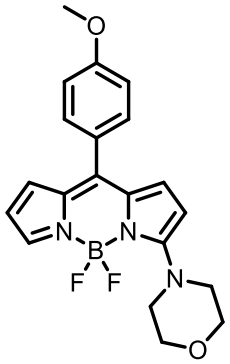

According to the general procedure for copper catalysed amination, 4,4-difluoro-2-iodo-8-(4-methoxyphenyl)-4-bora-3a,4a-diaza-*s*-indacene **3.17** (0.10 g, 0.26 mmol) was reacted with morpholine (0.04 g, 0.47 mmol). The crude product was purified by column chromatography (CH_2Cl_2:petroleum ether 1:1) to give the title compound **3.19g** as an orange solid (76.0 mg, 85%), mp 214–215 °C; ^{1}H NMR (400 MHz, $CDCl_3$) δ 7.45 (s, 1H), 7.40 (d, *J* = 8.6 Hz, 2H), 6.97 (d, *J* = 8.6 Hz, 2H), 6.92 (d, *J* = 5.1 Hz, 1H), 6.42 (d, *J* = 3.3 Hz, 1H), 6.37–6.33 (m, 1H), 6.20 (d, *J* = 5.1 Hz, 1H), 3.93 (d, *J* = 5.1 Hz, 4H), 3.88 (d, *J* = 5.1 Hz, 4H), 3.87 (s, 3H).^{13}C NMR (101 MHz, $CDCl_3$) δ 162.07, 160.50, 135.83, 135.11, 133.61, 132.07, 131.87, 131.75, 127.37, 119.51, 113.91, 113.72, 112.44, 66.87, 55.49, 50.56. ^{11}B NMR (128 MHz, $CDCl_3$) δ 0.14 (t, $J_{B\text{-}F}$ = 33.5 Hz), ^{19}F NMR (376 MHz, $CDCl_3$) δ −135.24 (q, $J_{F\text{-}B}$ = 33.5 Hz).IR (neat): υ_{max}/cm^{-1}: 3361, 2923, 2852, 2360, 1590, 1536, 1512, 1408, 1287, 1244, 1178, 1019, 902, 760. HRMS-ES Calcd for $C_{20}H_{20}BN_3O_2F_2$ + Na^+: 405.1551, found: 405.1551.

4,4-Difluoro-8-(4-methoxyphenyl)-3-(pyrrolidin-1-yl)-4-bora-3a,4a-diaza-*s*-indacene 3.19h.

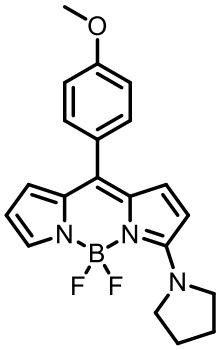

According to the general procedure for copper catalysed amination, 4,4-difluoro-2-iodo-8-(4-methoxyphenyl)-4-bora-3a,4a-diaza-*s*-indacene **3.17** (0.10 g, 0.26 mmol) was reacted with pyrrolidine (0.03 g, 0.47 mmol). The crude product was purified by column chromatography (CH_2Cl_2:petroleum ether 1:1) to give the title compound **3.19h** as a yellow solid (75.0 mg, 87%), mp 171–173 °C; ^{1}H NMR (400 MHz, $CDCl_3$) δ 7.46–7.42 (m, 1H), 7.39 (d, J = 8.7 Hz, 2H), 6.96 (d, J = 8.8 Hz, 2H), 6.90 (d, J = 5.1 Hz, 1H), 6.35 (d, J = 3.1 Hz, 1H), 6.34–6.32 (m, 1H), 6.15 (d, J = 5.1 Hz, 1H), 3.94 (br, s, 4H), 3.86 (s, 3H), 2.11–2.00 (m, 4H). ^{13}C NMR (101 MHz, $CDCl_3$) δ 160.27, 160.17, 135.53, 135.37, 132.02, 131.83, 130.89, 129.96, 127.76, 117.46, 114.35, 113.60, 113.09, 55.46, 51.35, 25.68. ^{11}B NMR (128 MHz, $CDCl_3$) δ 0.01 (t, $J_{B\text{-}F}$ = 31.0 Hz). ^{19}F NMR (376 MHz, $CDCl_3$) δ −128.23 (q, $J_{F\text{-}B}$ = 31.0 Hz). IR (neat): υ_{max}/cm^{-1}: 3360, 2923, 1577, 1510, 1395, 2350, 1251, 1094, 1028, 908, 778. HRMS-ES Calcd for $C_{20}H_{20}BN_3OF_2 + Na^+$: 490.1565, found: 490.1546.

4,4-Difluoro-3-(pyrrolidin-1-yl)-6-iodo-8-(4-methoxyphenyl)-4-bora-3a,4a-diaza-*s*-indacene 3.22h.

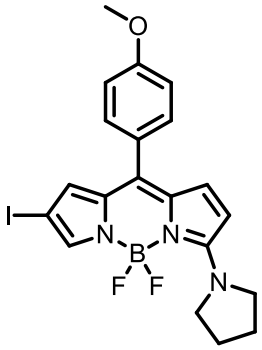

According to the general procedure for copper catalysed amination, 4,4-difluoro-2-iodo-8-(4-methoxyphenyl)-4-bora-3a,4a-diaza-*s*-indacene **3.17** (0.10 g, 0.26 mmol) was reacted with pyrrolidine (0.03 g, 0.47 mmol). The crude product was purified by column chromatography (CH_2Cl_2:petroleum ether 1:1) to give the title compound **3.22h** as a dark orange solid (5.00 mg, 4%); ^{1}H NMR (400 MHz, $CDCl_3$) δ 7.39 (s, 1H), 7.36 (d, *J* = 8.6 Hz, 2H), 6.96 (d, *J* = 8.7 Hz, 2H), 6.92 (d, *J* = 5.2 Hz, 1H), 6.39 (s, 1H), 6.21 (d, *J* = 5.1 Hz, 1H), 4.04 (s, 4H), 3.86 (s, 3H), 2.07 (t, *J* = 6.7 Hz, 4H). ^{13}C NMR (101 MHz, CDC_{l3}) δ 160.49, 160.33, 135.85, 133.82, 133.52, 132.53, 131.75, 129.11, 127.17, 122.68, 115.55, 113.77, 64.87, 55.50, 52.13, 25.75. IR (neat): υ_{max}/cm^{-1}: 2988, 2359, 1794, 1694, 1599, 1513, 1392, 1248, 1027, 779. HRMS-ES Calcd for $C_{20}H_{19}BN_3OF_2I$ + Na^+: 516.0532, found: 516.0531.

4,4-Difluoro-8-(4-methoxyphenyl)-3-((2-methylphenyl)amino)-4-bora-3a,4a-diaza-*s*-indacene 3.19i.

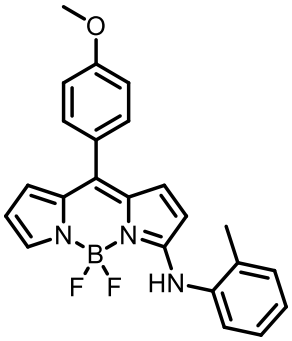

According to the general procedure for copper catalysed amination, 4,4-difluoro-2-iodo-8-(4-methoxyphenyl)-4-bora-3a,4a-diaza-*s*-indacene **3.17** (0.10 g, 0.26 mmol) was reacted with *o*-toluidine (0.05 g, 0.47 mmol). The crude product was purified by column chromatography (CH_2Cl_2:petroleum ether 1:1) to give the title compound **3.19i** as an orange solid (57.0 mg, 60%), mp 227–229 °C; ^{1}H NMR (400 MHz, $CDCl_3$) δ 7.50 (s, 1H), 7.45 (t, *J* = 7.7 Hz, 2H), 7.40 (d, *J* = 8.5 Hz, 2H), 7.35 (d, *J* = 7.7 Hz, 1H), 7.30 (d, *J* = 7.3 Hz, 2H), 6.95 (d, *J* = 8.5 Hz, 2H), 6.72 (d, *J* = 5.1 Hz, 1H), 6.41 (d, *J* = 3.4 Hz, 1H), 6.39–6.34 (m, 1H), 5.62 (d, *J* = 5.1 Hz, 1H), 3.96 (s, 2H), 3.85 (s, 2H). ^{13}C NMR (101 MHz, $CDCl_3$) δ 163.14, 160.34, 146.93, 135.59, 134.17, 132.93, 132.04, 131.82, 131.17, 130.20, 128.10, 127.57, 126.72, 118.74, 116.18, 113.65, 113.57, 55.45, 43.11. ^{11}B NMR (128 MHz, $CDCl_3$) δ 0.04 (t, $J_{B\text{-}F}$ = 33.0 Hz). ^{19}F NMR (376 MHz, $CDCl_3$) δ −148.10 (q, $J_{F\text{-}B}$ = 33.0 Hz). IR (neat): υ_{max}/cm^{-1}: 3378, 2925, 1620, 1578, 1489, 1398, 1258, 1085, 1021, 786. HRMS-ES Calcd for $C_{23}H_{20}BN_3OF_2$ + Na^+: 426.1565, found: 426.1577.

4,4-Difluoro-8-(4-methoxyphenyl)-3-((4-methoxyphenyl)amino)-4-bora-3a,4a-diaza-*s*-indacene 3.19j

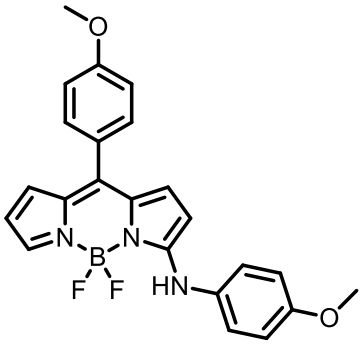

According to the general procedure for copper catalysed amination, 4,4-difluoro-2-iodo-8-(4-methoxyphenyl)-4-bora-3a,4a-diaza-*s*-indacene **3.17** (0.10 g, 0.26 mmol) was reacted with *p*-anisidine (0.06 g, 0.47 mmol). The crude product was purified by column chromatography (CH_2Cl_2:petroleum ether 9:1) to give the title compound **3.19j** as an orange solid (77.0 mg, 78%), mp 245–247 °C; ^{1}H NMR (400 MHz, $CDCl_3$) δ 7.84 (s, 1H), 7.49–7.46 (m, 1H), 7.44 (d, *J* = 8.6 Hz, 2H), 7.21 (d, *J* = 8.9 Hz, 2H), 6.98 (d, *J* = 8.7 Hz, 2H), 6.95–6.90 (m, 3H), 6.52 (d, *J* = 3.6 Hz, 1H), 6.36 (dd, *J* = 3.7, 2.3 Hz, 1H), 6.23 (d, *J* = 4.9 Hz, 1H), 3.87 (s, 3H), 3.85–3.80 (m, 3H). The compound was insufficiently soluble to determine ^{13}C NMR. ^{19}F NMR (376 MHz, $CDCl_3$) δ −148.45 (q, $J_{F\text{-}B}$ = 32.5 Hz). ^{11}B NMR (128 MHz, $CDCl_3$) δ 0.07 (t, $J_{B\text{-}F}$ = 32.5 Hz). IR (neat): υ_{max}/cm^{-1}: 3368, 2914, 1580, 1293, 1241. HRMS-ES Calcd for $C_{23}H_{20}BN_3O_2F_2$ + Na^+: 442.1514, found: 442.1499.

6-Iodo-4,4-difluoro-8-(4-methoxyphenyl)-3-((4-methoxyphenyl)amino)-4-bora-3a,4a-diaza-*s*-indacene 3.22j

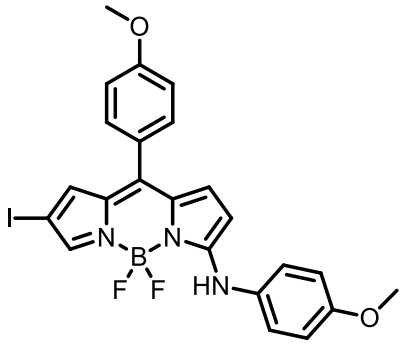

According to the general procedure for copper catalysed amination, 4,4-difluoro-2-iodo-8-(4-methoxyphenyl)-4-bora-3a,4a-diaza-*s*-indacene **3.17** (0.10 g, 0.26 mmol) was reacted with *p*-anisidine (0.06 g, 0.47 mmol). The crude product was purified by column chromatography (CH_2Cl_2:petroleum ether 9:1) to give the title compound **3.22j** as an orange solid (8.00 mg, 6%), ^{1}H NMR (400 MHz, $CDCl_3$) δ 7.91 (s, 1H), 7.42 (s, 1H), 7.41 (d, *J* = 8.9 Hz, 2H), 7.21 (d, *J* = 6.9 Hz, 2H), 6.98 (d, *J* = 6.5 Hz, 2H), 6.96 (s, 1H), 6.93 (d, *J* = 6.9 Hz, 2H), 6.55 (s, 1H), 6.27 (d, *J* = 4.9 Hz, 1H), 3.87 (s, 3H), 3.83 (s, 3H). The compound was insufficiently soluble to determine ^{13}C NMR. IR (neat): υ_{max}/cm^{-1}: 3342, 3119, 2929, 1725, 1613, 1512, 1480, 1390, 1249, 1102. HRMS-ES Calcd for $C_{23}H_{19}BN_3OF_2I + Na^+$: 568.0481, found: 568.0489.

3-((4-Chlorophenyl)amino)-4,4-difluoro-8-(4-methoxyphenyl)-4-bora-3a,4a-diaza-*s*-indacene 3.19k.

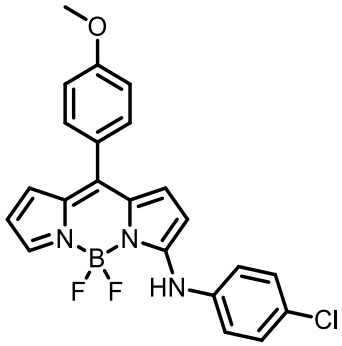

According to the general procedure for copper catalysed amination, 4,4-difluoro-2-iodo-8-(4-methoxyphenyl)-4-bora-3a,4a-diaza-*s*-indacene **3.17** (0.10 g, 0.26 mmol) was reacted with 4-chloroaniline (0.06 g, 0.47 mmol). The crude product was purified by column chromatography (CH_2Cl_2:petroleum ether 1:1) to give the title compound **3.19k** as a dark yellow solid (66.0 g, 66%), mp 178–180 °C; ^{1}H NMR (400 MHz, $CDCl_3$) δ 7.89 (s, 1H), 7.51 (s, 1H), 7.45 (d, *J* = 8.7 Hz, 2H), 7.37 (d, *J* = 8.7 Hz, 2H), 7.20 (d, *J* = 8.7 Hz, 2H), 7.02–6.96 (m, 3H), 6.58 (d, *J* = 3.7 Hz, 1H), 6.39 (dd, *J* = 3.7, 2.4 Hz, 1H), 6.34 (d, *J* = 4.9 Hz, 1H), 3.88 (s, 3H).^{13}C NMR (101 MHz, $CDCl_3$) δ 160.90, 157.99, 136.36, 136.13, 135.74, 133.16, 132.97, 132.82, 131.86, 131.34, 129.95, 126.76, 123.72, 122.37, 114.42, 113.89, 110.26, 55.52. ^{11}B NMR (128 MHz, CDCl3) δ −0.01 (t, $J_{B\text{-}F}$ = 33.0 Hz). ^{19}F NMR (376 MHz, $CDCl_3$) δ −148.10 (q, $J_{F\text{-}B}$ = 33.0 Hz). IR (neat): υ_{max}/cm^{-1}: 3348, 2926, 2860, 1726, 1578, 1519, 1476, 1385, 1292, 1251, 1180, 1096 971, 784. HRMS-ES Calcd for $C_{22}H_{17}BN_3OF_2Cl$ + Na^+: 446.1019, found: 446.1019.

3-((4-Chlorophenyl)amino)-4,4-difluoro-6-iodo-8-(4-methoxyphenyl)-4-bora-3a,4a-diaza-*s*-indacene 3.22k.

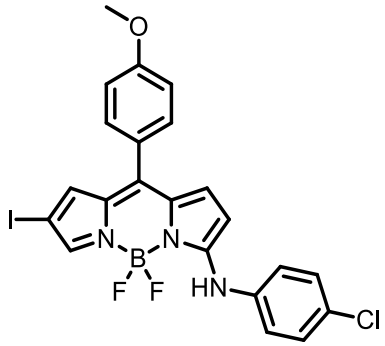

According to the general procedure for copper catalysed amination, 4,4-difluoro-2-iodo-8-(4-methoxyphenyl)-4-bora-3a,4a-diaza-*s*-indacene **3.17** (0.10 g, 0.26 mmol) was reacted with 4-chloroaniline (0.06 g, 0.47 mmol). The crude product was purified by column chromatography (CH_2Cl_2:petroleum ether 1:1) to give the title compound **3.22k** as a pink solid (13.0 mg, 13%); ^{1}H NMR (400 MHz, $CDCl_3$) δ 7.94 (s, 1H), 7.44 (d, *J* = 14.0 Hz, 2H), 7.39 (d, *J* = 9.0 Hz, 3H), 7.21 (d, *J* = 8.6 Hz, 2H), 7.01 (d, *J* = 5.2 Hz, 1H), 6.99 (d, *J* = 8.7 Hz, 2H), 6.61 (s, 1H), 6.38 (d, *J* = 5.0 Hz, 1H), 3.88 (s, 3H). ^{13}C NMR (126 MHz, $CDCl_3$) δ 161.35, 156.52, 141.60, 138.11, 136.69, 136.47, 134.33, 133.96, 132.60, 131.81, 128.85, 125.88, 121.11, 118.24, 114.10, 110.82, 108.49, 66.93, 55.51. IR (neat): υ_{max}/cm^{-1}: 3376, 2970, 1581, 1524, 1397, 1250, 1113, 1028, 785. HRMS-ES Calcd for $C_{22}H_{16}BN_3OF_2ICl + Na^+$: 571.9985, found: 571.9990.

3-((4-Cyanophenyl)amino)-4,4-difluoro-8-(4-methoxyphenyl)-4-bora-3a,4a-diaza-*s*-indacene 3.19l.

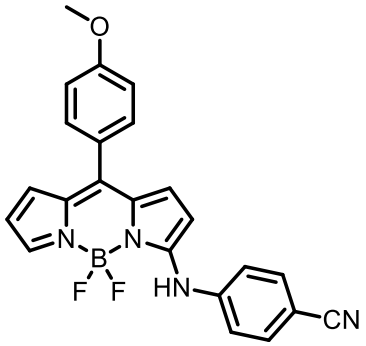

According to the general procedure for copper catalysed amination, 4,4-difluoro-2-iodo-8-(4-methoxyphenyl)-4-bora-3a,4a-diaza-*s*-indacene **3.17** (0.10 g, 0.26 mmol) was reacted with 4-cyanoaniline (0.06 g, 0.47 mmol). The crude product was purified by column chromatography (CH_2Cl_2:petroleum ether 9:1) to give the title compound **3.19l** as a pink solid (75.0 mg, 77%), mp 204–207 °C; ^{1}H NMR (400 MHz, $CDCl_3$) δ 8.06 (s, 1H), 7.68 (d, *J* = 8.8 Hz, 2H), 7.61–7.55 (m, 1H), 7.47 (d, *J* = 8.8 Hz, 2H), 7.31 (d, *J* = 8.8 Hz, 2H), 7.02 (dd, *J* = 10.7, 6.8 Hz, 3H), 6.67 (d, *J* = 4.6 Hz, 1H), 6.50 (d, *J* = 4.8 Hz, 1H), 6.43 (dd, *J* = 3.9, 2.3 Hz, 1H), 3.89 (s, 3H).^{13}C NMR (101 MHz, $CDCl_3$) δ 161.26, 155.54, 142.19, 138.61, 135.53, 135.12, 133.99, 133.21, 132.27, 131.97, 126.45,124.45, 120.55, 118.55, 115.33, 114.01, 109.54, 107.74, 55.56. ^{11}B NMR (128 MHz, $CDCl_3$) δ −0.09 (t, $J_{B\text{-}F}$ = 32.0 Hz). ^{19}F NMR (282 MHz, $CDCl_3$) δ −147.61 (q, $J_{F\text{-}B}$ = 32.0 Hz). IR (neat): υ_{max}/cm^{-1}: 3383, 3072, 2224, 1599, 1560, 1524, 1476, 1396, 1251, 1175, 1113, 1024, 936, 780. HRMS-ES Calcd for $C_{23}H_{17}BN_4OF_2$ + Na^+: 437.1361, found: 437.1367.

3-((4-Cyanophenyl)amino)-4,4-difluoro-6-iodo-8-(4-methoxyphenyl)-4-bora-3a,4a-diaza-*s*-indacene 3.22l.

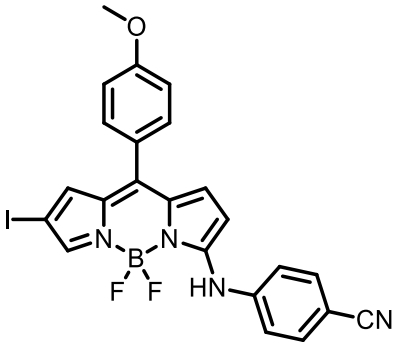

According to the general procedure for copper catalysed amination, 4,4-difluoro-2-iodo-8-(4-methoxyphenyl)-4-bora-3a,4a-diaza-*s*-indacene **3.17** (0.10 g, 0.26 mmol) was reacted with 4-cyanoaniline (0.06 g, 0.47 mmol). The crude product was purified by column chromatography (CH_2Cl_2:petroleum ether 9:1) to give the title compound **3.22l** as a pink solid (19.0 mg, 15%); ^{1}H NMR (300 MHz, $CDCl_3$) δ 8.06 (s, 1H), 7.64 (d, *J* = 8.6 Hz, 2H), 7.46 (s, 1H), 7.38 (d, *J* = 8.7 Hz, 2H), 7.27 (d, *J* = 8.7 Hz, 2H), 7.02 (d, *J* = 4.9 Hz, 1H), 6.96 (d, *J* = 8.7 Hz, 2H), 6.64 (s, 1H), 6.48 (d, *J* = 4.9 Hz, 1H), 3.83 (s, 3H). IR (neat): υ_{max}/cm^{-1}: 3366, 2995, 2227, 1597, 1566, 1474, 1394, 1253, 1101, 720. HRMS-ES Calcd for $C_{23}H_{16}BN_4OF_2I + Na^+$: 563.0328, found: 563.0323.

4,4-Difluoro-8-(4-methoxyphenyl)-3-(pyridin-2-ylamino)-4-bora-3a,4a-diaza-*s*-indacene 3.19m.

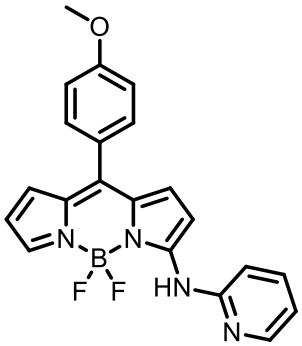

According to the general procedure for copper catalysed amination, 4,4-difluoro-2-iodo-8-(4-methoxyphenyl)-4-bora-3a,4a-diaza-*s*-indacene **3.17** (0.10 g, 0.26 mmol) was reacted with 2-aminopyridine (0.04 g, 0.47 mmol). The crude product was purified by column chromatography (CH_2Cl_2:petroleum ether 7:3) to give the title compound **3.19m** as a pink solid (55.0 mg, 60%), mp 213–215 °C; ^{1}H NMR (400 MHz, $CDCl_3$) δ 8.40–8.34 (m, 2H), 7.71–7.63 (m, 1H), 7.54 (s, 1H), 7.52 (d, J = 4.9 Hz, 1H), 7.48 (d, J = 8.4 Hz, 2H), 7.04 (d, J = 4.9 Hz, 1H), 7.02 (d, J = 3.5 Hz, 1H), 7.00 (s, 2H), 6.95 (d, J = 8.9 Hz, 1H), 6.60 (d, J = 3.6 Hz, 1H), 6.39 (dd, J = 3.5, 2.3 Hz, 1H), 3.89 (s, 3H).^{13}C NMR (101 MHz, $CDCl_3$) δ 189.77, 160.98, 155.85, 151.33, 148.49, 138.37, 137.20, 135.35, 133.61, 133.11, 132.11, 131.98, 126.85, 122.93, 118.88, 114.51, 113.89, 113.03, 55.52. ^{11}B NMR (128 MHz, $CDCl_3$) δ 0.01 (t, $J_{B\text{-}F}$ = 33.2 Hz).^{19}F NMR (376 MHz, $CDCl_3$) δ −147.12– (t, $J_{F\text{-}B}$ = 33.2 Hz). IR (neat): υ_{max}/cm^{-1}: 3385, 3029, 2356, 1629, 1603,1562, 1496, 1393, 1340, 1297, 1247, 1097, 1028, 972, 769. HRMS-ES Calcd for $C_{21}H_{17}BN_4OF_2$ + H^+: 391.1542, found: 391.1549.

4,4-Difluoro-6-iodo-8-(4-methoxyphenyl)-3-(pyridin-2-ylamino)-4-bora-3a,4a-diaza-*s*-indacene 3.22m.

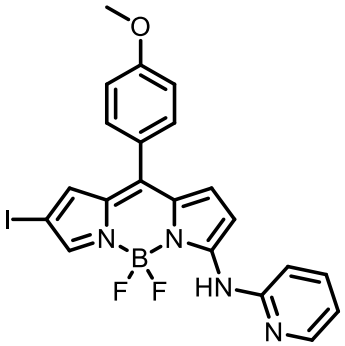

According to the general procedure for copper catalysed amination, 4,4-difluoro-2-iodo-8-(4-methoxyphenyl)-4-bora-3a,4a-diaza-*s*-indacene **3.17** (0.10 g, 0.26 mmol) was reacted with 2-aminopyridine (0.04 g, 0.47 mmol). The crude product was purified by column chromatography (CH_2Cl_2:petroleum ether 7:3) to give the title compound **3.22m** as a pink solid (17.0 mg, 14%); ^{1}H NMR (400 MHz, $CDCl_3$) δ 8.40 (s, 1H), 8.39–8.34 (m, 1H), 7.69 (td, *J* = 7.8, 1.9 Hz, 1H), 7.59 (d, *J* = 5.0 Hz, 1H), 7.47 (d, *J* = 1.1 Hz, 1H), 7.44 (d, *J* = 8.8 Hz, 2H), 7.07 (d, *J* = 5.1 Hz, 1H), 7.05–7.02 (m, 1H), 7.00 (d, *J* = 8.8 Hz, 2H), 6.96 (d, *J* = 8.2 Hz, 1H), 6.66–6.60 (m, 1H), 3.88 (s, 3H). ^{13}C NMR (101 MHz, $CDCl_3$) δ 161.14, 156.70, 150.97, 148.57, 138.51, 136.88, 136.16, 135.34, 134.38, 132.49, 131.91, 127.54, 126.31, 119.36, 115.96, 114.06, 113.29, 66.24, 55.57. IR (neat): υ_{max}/cm^{-1}: 3384, 2997, 1629, 1604, 1563, 1496, 1393, 1248, 1029, 972, 769. HRMS-ES Calcd for $C_{21}H_{16}BN_4OF_2I$ + Na^+: 539.0328, found: 539.0326.

4,4-Difluoro-8-(4-methoxyphenyl)-3-(methyl(phenyl)amino)-4-bora-3a,4a-diaza-*s*-indacene 3.19n.

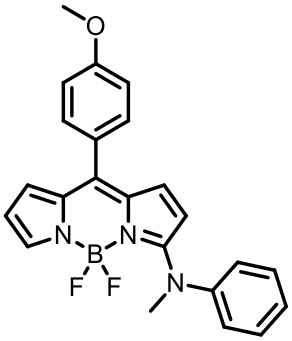

According to the general procedure for copper catalysed amination, 4,4-difluoro-2-iodo-8-(4-methoxyphenyl)-4-bora-3a,4a-diaza-*s*-indacene **3.17** (0.10 g, 0.26 mmol) was reacted with *n*-methylaniline (0.05 g, 0.47 mmol). The crude product was purified by column chromatography (CH_2Cl_2:petroleum ether 1:1) to give the title compound **3.19n** as an orange solid (38.0 mg, 40%), mp 220–221 °C; ^{1}H NMR (400 MHz, $CDCl_3$) δ 7.50 (s, 1H), 7.45 (t, *J* = 7.7 Hz, 1H), 7.40 (d, *J* = 8.5 Hz, 1H), 7.36 (t, *J* = 7.4 Hz, 1H), 7.30 (d, *J* = 7.3 Hz, 1H), 6.95 (d, *J* = 8.5 Hz, 1H), 6.72 (d, *J* = 5.1 Hz, 1H), 6.52–6.16 (m, 1H), 5.62 (d, *J* = 5.1 Hz, 1H), 3.96 (s, 1H), 3.85 (s, 1H). ^{13}C NMR (101 MHz, $CDCl_3$) δ 163.15, 160.34, 146.92, 135.59, 134.17, 132.92, 132.04, 131.82, 131.16, 130.20, 128.10, 127.56, 126.72, 118.73, 116.18, 113.65, 113.55, 55.45, 43.11. ^{11}B NMR (128 MHz, $CDCl_3$) δ 0.17 (t, $J_{B\text{-}F}$ = 32.5 Hz). ^{19}F NMR (376 MHz, $CDCl_3$) δ −129.68 (q, $J_{F\text{-}B}$ = 32.5 Hz). IR (neat): υ_{max}/cm^{-1}: 2962, 2919, 1681, 1603, 1513, 1298, 1258, 1020, 932, 794. HRMS-ES Calcd for $C_{23}H_{20}BN_3OF_2$ + Na^+: 425.1602, found: 425.1598.

6-Deuterio-4,4-difluoro-2-iodo-8-(4-methoxyphenyl)-4-bora-3a,4a-diaza-*s*-indacene 3.39 and 2,6-dideuterio-4,4-difluoro-8-(4-methoxyphenyl)-4-bora-3a,4a-diaza-*s*-indacene 3.42.

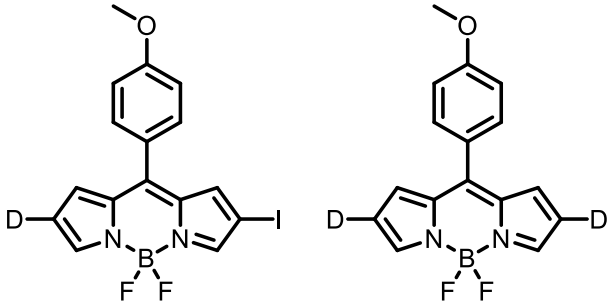

4,4-Difluoro-2,6-diiodo-8-(4-methoxyphenyl)-4-bora-3a,4a-diaza-*s*-indacene **3.18** (0.38 g, 0.69 mmol) was dissolved in CH_2Cl_2 (31 mL). Et_3N (0.09 mL, 0.69 mmol), K_2CO_3 (0.31 g, 2.25 mmol) and 10% Pd/C (0.38 g) were added. The mixture was stirred under nitrogen for 15 min and the nitrogen line was replaced with a deuterium-filled balloon. The mixture was stirred at room temperature for 4 h and then filtered through Celite, washing with CH_2Cl_2. The solvent was removed under reduced pressure and the orange crude product was purified by column chromatography eluting with CH_2Cl_2:petroleum ether (1:1) to give, first eluted: the 6-deuterio-2-iodo-BODIPY **3.39** as an orange solid (0.18 g, 60%); mp 214–215 °C; ^{1}H NMR (300 MHz, $CDCl_3$) δ 7.90 (s, 1H), 7.75 (s, 1H), 7.46 (d, J = 8.7 Hz, 2H), 7.05–6.93 (m, 4H), 3.85 (s, 3H). ^{13}C NMR (126 MHz, $CDCl_3$) δ 162.45, 146.66, 146.03, 145.07, 135.90, 135.72, 135.01, 132.81, 132.49, 125.88, 119.19, 114.29, 70.65, 55.61. ^{19}F NMR (282 MHz, $CDCl_3$) δ −144.96 (q, $J_{F\text{-}B}$ = 28.5 Hz). ^{11}B NMR (96 MHz, $CDCl_3$) δ 0.45 (t, $J_{B\text{-}F}$ = 28.5 Hz). HRMS-ES Calcd for $C_{16}H_{11}{}^2HBN_2F_2IO + Na^+$: 448.0115, found: 448.0112.

Second eluted: **2,6-dideuterio-4,4-difluoro-8-(4-methoxyphenyl)-4-bora-3a,4a-diaza-*s*-indacene 3.42.**

as an orange solid (0.04 g, 17%) mp 133–135 °C.^{1}H NMR (300 MHz, $CDCl_3$) δ 7.84 (s, 2H), 7.46 (d, J = 8.8 Hz, 2H), 6.96 (d, J = 8.8 Hz, 2H), 6.89 (s, 2H), 3.83 (s, 3H). ^{13}C NMR (75 MHz, $CDCl_3$) δ 162.11, 147.44, 143.31, 134.82, 132.44, 131.27, 126.30, 118.45, 118.12, 117.77, 114.08, 55.55. ^{11}B NMR (96 MHz, $CDCl_3$) δ 0.31 (t, $J_{B\text{-}F}$ =29.0 Hz). ^{19}F NMR (282 MHz, $CDCl_3$) δ -145.02 (q, $J_{F\text{-}B}$ = 29.0 Hz). HRMS-ES Calcd for $C_{16}H_{11}{}^2H_2BN_2F_2O + Na^+$: 323.1112, found: 323.1110.

6-Deuterio-4,4-difluoro-8-(4-methoxyphenyl)-3-(pyrrolidin-1-yl)-4-bora-3a,4a-diaza-*s*-indacene 3.43 and 2-deuterio-4,4-difluoro-8-(4-methoxyphenyl)-3-(pyrrolidin-1-yl)-4-bora-3a,4a-diaza-*s*-indacene 3.44.

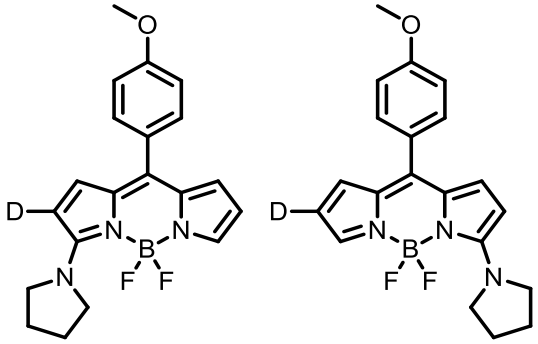

Following the General Procedure for copper catalyzed amination, 6-deuterio-4,4-difluoro-2-iodo-8-(4-methoxyphenyl)-4-bora-3a,4a-diaza-*s*-indacene **3.39** (0.11 g, 0.25 mmol) was reacted with pyrrolidine (0.04 g, 0.49 mmol). Purification by column chromatography eluting with CH_2Cl_2:petroleum ether (1:1) gave a 70: 30 mixture of the 6-deuterio and 2 deuterio-BODIPYs **3.43** and **3.44** respectively as an orange solid (0.08 g, 88%). For the mixture: ^{1}H NMR (500 MHz, $CDCl_3$) δ 7.48 (br, s, 1H), 7.41 (d, *J* = 8.7 Hz, 2H), 6.99 (d, *J* = 8.7 Hz, 2H), 6.93–6.88 (m, 1H), 6.48–6.25 (m, 1H), 6.16 (d, *J* = 5.1 Hz, 1H), 3.94 (br, s, 4H), 3.89 (s, 3H), 2.08–2.05 (m, 4H). ^{11}B NMR (96 MHz, $CDCl_3$) δ 1.00 (t, $J_{B\text{-}F}$ = 32.5 Hz). ^{19}F NMR (282 MHz, $CDCl_3$) δ -128.25 (q, $J_{F\text{-}B}$ = 32.5 Hz). HRMS-ES Calcd for $C_{20}H_{19}{}^{2}HBN_3F_2O + Na^+$: 391.1628, found: 391.1623. For the major product **3.43**: ^{13}C NMR (126 MHz, $CDCl_3$) δ 160.22 (C3), 160.13 (C4′), 135.46 (C8a), 135.24 (C1), 131.94 (C7a), 131.75 (C2′, C6′), 130.74 (C8), 129.74 (C5), 127.68 (C1′), 117.23 (C7), 114.35 (C2), 113.55 (C3′, C5′), 112.97 (C6), 55.37 (OMe), 51.26, 25.58. For the minor product **3.44**: ^{13}C NMR (126 MHz, $CDCl_3$) δ 160.17 (C3), 160.13 (C4′), 135.46 (C8a), 135.12 (C1), 131.94 (C7a), 131.75 (C2′, C6′), 130.74 (C8), 129.82 (C5), 127.68 (C1′), 117.23 (C7), 114.35 (C2), 113.55 (C3′, C5′), 112.97 (C6), 55.37(OMe), 51.26, 25.58.

4,4-Difluoro-1,3-dimethyl-8-(4-methylphenyl)-4-bora-3a,4a-diaza-*s*-indacene 3.34.

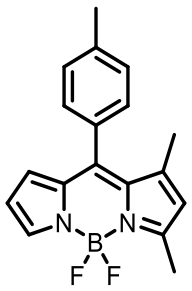

2-(4-Methylbenzoyl)pyrrole **2.64b** (0.21 g, 1.14 mmol) was taken in dry CH_2Cl_2 (50 mL). 2,4-dimethyl-1H-pyrrole (0.14 g, 1.48 mmol) and $BF_3.OEt_2$ (0.01 g, 0.11 mmol) were added and the resulting solution was stirred at room temperature for 3 h. The mixture was then neutralized with *N*,*N*-diisopropylethylamine (0.88 g, 6.86 mmol) and treated with $BF_3.OEt_2$ (1.05 g, 9.16 mmol). The mixture was stirred at room temperature for 16 h and washed with water (150 mL). The aqueous layer was extracted with dichloromethane (2 × 50 mL). The combined organic layers were dried ($MgSO_4$) and the solvent was removed under pressure. The green crude product was purified by column chromatography (CH_2Cl_2:petroleum ether 1:1) to give the title compound **3.34** as an orange solid (0.30 g, 84%), mp 146-147 °C, R_f = 0.42 (CH_2Cl_2:petroleum ether 1:1). ^{1}H NMR (300 MHz, $CDCl_3$) δ 7.59 (s, 1H), 7.21 (d, *J* = 8.1 Hz, 2H), 7.15 (d, *J* = 8.1 Hz, 2H), 6.40 – 6.25 (m, 2H), 6.05 (s, 1H), 2.54 (s, 3H), 2.37 (s, 3H), 1.49 (s, 3H).^{13}C NMR (101 MHz, $CDCl_3$) δ 161.84, 147.11, 143.87, 139.55, 138.53, 134.93, 133.67, 131.06, 129.18, 128.77, 127.12, 123.20, 116.02, 21.51, 17.14, 15.26. ^{11}B NMR (96 MHz, $CDCl_3$) δ 0.54 (t, $J_{B\text{-}F}$ = 31.1 Hz). ^{19}F NMR (282 MHz, $CDCl_3$) δ -145.95 (q, $J_{F\text{-}B}$ = 31.1 Hz). IR (neat): υ_{max}/cm^{-1}: 3116, 2963, 1544, 1455, 1390, 1141, 978, 771. HRMS-ES Calcd for $C_{18}H_{17}{}^{11}B^{19}F_2N_2$ + H^+: 311.1531, found: 311.1539.

4,4-Difluoro-2-iodo-1,3-dimethyl-8-(4-methylphenyl)-4-bora-3a,4a-diaza-*s*-indacene 3.36 and 4,4-difluoro-6-iodo-1,3-dimethyl-8-(4-methylphenyl)-4-bora-3a,4a-diaza-*s*-indacene 3.35.

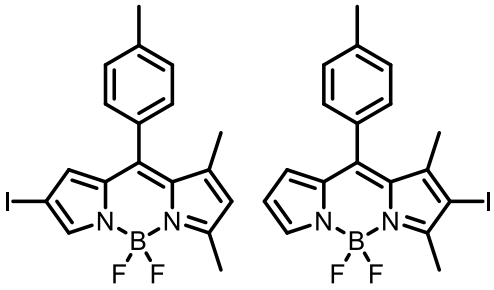

4,4-Difluoro-1,3-dimethyl-8-(4-methylphenyl)-4-bora-3a,4a-diaza-*s*-indacene **3.34** (0.17 g, 0.55 mmol) was taken in dry CH_2Cl_2 (10 mL). *N*-Iodosuccinimide (0.12 g, 0.16 mmol) was added to the mixture and stirred for 16 h. The solvent was then removed under reduced pressure. The brown crude product was purified by column chromatography (CH_2Cl_2:petroleum ether 1:1) to give, first eluted: the 4,4-difluoro-6-iodo-1,3-dimethyl-8-(4-methylphenyl)-3a,4a-diaza-*s*-indacene **3.35** as an orange solid (34.0 mg, 13%). ^{1}H NMR (400 MHz, $CDCl_3$) δ 7.58 (s, 1H), 7.25 (d, *J* = 7.8 Hz, 2H), 7.19 (d, *J* = 7.8 Hz, 2H), 6.46 (s, 1H), 6.17 (s, 1H), 2.61 (s, 3H), 2.44 (s, 3H), 1.58 (s, 3H). ^{13}C NMR (101 MHz, $CDCl_3$) δ 160.85, 148.54, 141.49, 140.33, 139.97, 135.99, 131.68, 130.46, 129.37, 129.06, 128.66, 124.18, 86.94, 21.55, 17.79, 15.39.

Second eluted: **4,4-difluoro-2-iodo-1,3-dimethyl-8-(4-methylphenyl)-4-bora-3a,4a-diaza-*s*-indacene 3.36.**

As an orange solid (0.18 g, 74%), mp 199-200 °C. ^{1}H NMR (300 MHz, $CDCl_3$) δ 7.67 (s, 1H), 7.23 (d, *J* = 7.9 Hz, 2H), 7.15 (d, *J* = 7.9 Hz, 2H), 6.45 (d, *J* = 3.8 Hz, 1H), 6.34 (dd, *J* = 4.0, 2.0 Hz, 1H), 2.63 (s, 3H), 2.39 (s, 3H), 1.50 (s, 3H). ^{13}C NMR (101 MHz, $CDCl_3$) δ 160.89, 147.84, 144.18, 140.36, 140.01, 135.01, 133.08, 131.08, 129.33, 129.08, 128.83, 117.06, 86.96, 21.59, 17.82, 16.48. ^{11}B NMR (128 MHz, $CDCl_3$) δ -0.51 (t, J_{B-F} = 30.4 Hz).^{19}F NMR (376 MHz, $CDCl_3$) δ -145.55 (q, J_{F-B} = 30.4 Hz). HRMS-ES Calcd for $C_{18}H_{15}{}^{11}BN_2{}^{19}F_2{}^{127}I + Na^+$: 584.9284, found: 584.9285.

(3,5-Dimethyl-1H-pyrrol-2-yl)(p-tolyl)methanone 3.47.

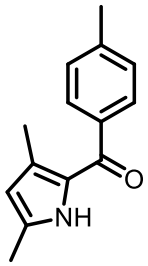

2,4-Dimethylpyrrole (0.92 g, 9.71 mmol) was dissolved in THF (20 mL). Methyl magnesium chloride solution 3.0 M in THF (3.6 mL, 10.8 mmol) was added dropwise to the reaction. The reaction mixture was then heated at reflux for 1 hour, cooled to room temperature and added via cannula to a solution of 4-methylbenzoyl chloride (1.93 g, 12.5 mmol) in THF (10 mL) and the reaction mixture was stirred at room temperature for 24 hours. The mixture was dissolved in CH_2Cl_2 (30 mL). The reaction mixture was then washed with water (2 x 60 mL) and the combined aqueous layers were back extracted with CH_2Cl_2 (60 mL). The combined organic layers were dried ($MgSO_4$) filtered and the solvent removed under reduced pressure. The resulting orange crude product was purified by column chromatography (CH_2Cl_2) to give the title compound **3.47** as a sand coloured solid (0.83 g, 40%), mp 155-157 °C (lit.[18] 158-159 ℃), R_f = 0.3 (CH_2Cl_2). ^{1}H NMR (400 MHz, $CDCl_3$) δ 9.00 (s, 1H), 7.54 (d, *J* = 7.9 Hz, 2H), 7.24 (d, *J* = 7.9 Hz, 2H), 5.85 (s, 1H), 2.41 (s, 3H), 2.28 (s, 3H), 1.96 (s, 3H).^{13}C NMR (101 MHz, $CDCl_3$) δ 185.82, 141.47, 137.30, 135.13, 130.26, 128.99, 128.51, 127.93, 112.90, 21.67, 14.14, 13.26. IR (neat): υ_{max}/cm^{-1}: 3279, 2920, 2862, 1929, 1694, 1589, 1563, 1487, 1429, 1282, 929, 762. HRMS-ES Calcd for $C_{14}H_{15}NO + H^+$: 214.1232, found: 214.1233.

The spectroscopic data obtained for this compound were consistent with those reported in the literature.[51]

(3,5-Dimethyl-1H-pyrrol-2-yl)(p-tolyl)methanone 3.47.

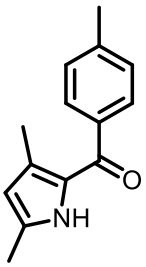

Zinc oxide (0.30 g, 3.72 mmol) was taken in a flame-dried Schlenk tube. 2,4-Dimethyl pyrrole (1.00 g, 14.9 mmol) and p-toluoyl chloride (2.30 g, 14.9 mmol) were then added and the mixture was stirred at room temperature for 5 minutes. The solid crude was dissolved in CH_2Cl_2 (60 mL) and washed with an aqueous solution of sodium bicarbonate (100 mL × 2). The aqueous layer was back extracted with CH_2Cl_2 (2 × 30 mL). The combined organic layers were dried ($MgSO_4$) and the solvent was removed under pressure. The resulting orange crude product was purified by column chromatography (CH_2Cl_2) to give the title compound **3.47** as a sand coloured solid (1.75 g, 55%).

The spectroscopic data obtained for this compound were identical with those reported above.

(4-Iodo-3,5-dimethyl-1H-pyrrol-2-yl)(p-tolyl)methanone 3.48.

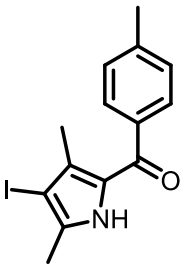

(3,5-Dimethyl-1H-pyrrol-2-yl)(p-tolyl)methanone **3.47** (0.52g, 2.45 mmol) was taken in dry CH_2Cl_2 (12 mL). *N*-Iodosuccinimide (0.55 g, 2.45 mmol) in CH_2Cl_2 (12 mL) was added over 10 minutes and the resulting solution was stirred at room temperature for 2 h. The crude product mixture was washed with water (100 mL). The aqueous layer was back extracted with CH_2Cl_2 (2 × 30 mL). The combined organic layers were dried ($MgSO_4$) and the solvent was removed under reduced pressure. The resulting brown crude product was purified by column chromatography (CH_2Cl_2) to give the title compound **3.48** as a white solid (0.81 g, 98%), mp 169-170 °C. R_f = 0.37 (CH_2Cl_2). ^{1}H NMR (400 MHz, $CDCl_3$) δ 10.07 (s, 1H), 7.55 (d, *J* = 8.0 Hz, 2H), 7.24 (d, *J* = 8.0 Hz, 2H), 2.41 (s, 3H), 2.32 (s, 3H), 1.92 (s, 3H). ^{13}C NMR (101 MHz, $CDCl_3$) δ185.73, 142.21, 137.37, 136.60, 131.77, 129.09, 128.89, 128.23, 73.97, 21.73, 16.42, 14.52. IR (neat): υ_{max}/cm^{-1}: 3240, 3035, 2945, 2918, 2853, 2567, 1592, 1549, 1511, 1588, 1421, 1382, 1284, 1049, 938, 756. HRMS-ES Calcd for $C_{14}H_{14}NO^{127}I + H^+$: 340.0198, found: 340.0259.

2-Ethyl-4,4-difluoro-1,3,5,7-tetramethyl-8-(4-methylphenyl)-4-bora-3a,4a-diaza-*s*-indacene 3.49.

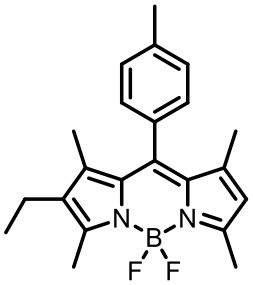

(3,5-Dimethyl-1H-pyrrol-2-yl)(p-tolyl)methanone **3.47** (2.11 g, 9.88 mmol) was taken in dry CH_2Cl_2 (60 mL). 3-Ethyl-2,4-dimethyl-1H-pyrrole (1.73 mL, 12.8 mmol) and $BF_3.OEt_2$ (1.20 mL, 12.0 mmol) were added and the resulting solution was stirred at room temperature for 2 h. The mixture was then neutralized with *N*,*N*-diisopropylethylamine (7.66 g, 59.3 mmol) and treated with $BF_3.OEt_2$ (9.10 g, 79.1 mmol) and then the mixture was stirred at room temperature for 4 h. The crude mixture was washed with water (200 mL). The aqueous layer was back extracted with CH_2Cl_2 (2 × 100 mL). The combined organic layers were dried ($MgSO_4$) and the solvent was removed under reduced pressure. The resulting orange crude product was purified by column chromatography (CH_2Cl_2:petroleum ether 1:3) to give the title compound **3.49** as an orange solid (3.13 g, 86%), mp 141-142 °C. R_f = 0.3 (CH_2Cl_2:petroleum ether 1:3). ^{1}H NMR (300 MHz, $CDCl_3$) δ 7.19 (d, *J* = 7.9 Hz, 2H), 7.05 (d, *J* = 7.9 Hz, 2H), 5.85 (s, 1H), 2.46 (s, 3H), 2.45 (s, 3H), 2.35 (s, 3H), 2.22 (q, *J* = 7.5 Hz, 2H), 1.29 (s, 3H), 1.24 (s, 3H), 0.90 (t, *J* = 7.5 Hz, 3H). ^{13}C NMR (75 MHz, $CDCl_3$) δ 155.16, 153.64, 141.98, 141.33, 139.41, 138.70, 133.34, 132.33, 131.43, 131.14, 129.75, 127.91, 120.46, 21.45, 17.09, 14.59, 14.48, 14.41, 12.62, 11.82. ^{11}B NMR (96 MHz, $CDCl_3$) δ 0.77 (t, $J_{B\text{-}F}$ = 33.1 Hz). ^{19}F NMR (282 MHz, $CDCl_3$) δ -146.02 (q, $J_{F\text{-}B}$ =33.1 Hz). IR (neat): υ_{max}/cm^{-1}: 2966, 1713, 1539, 1516, 1310, 1191, 1053, 974, 754. HRMS-ES Calcd for $C_{22}H_{25}N_2{}^{11}BF_2 + H^+$: 367.2157, found: 367.2162.

6-Ethyl-4,4-difluoro-2-iodo-1,3,5,7-tetramethyl-8-(4-methylphenyl)-4-bora-3a,4a-diaza-*s*-indacene 3.50.

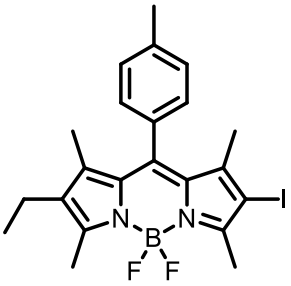

2-Ethyl-4,4-difluoro-1,3,5,7-tetramethyl-8-(4-methylphenyl)-4-bora-3a,4a-diaza-*s*-indacene **3.49** (2.16 g, 5.92 mmol) was taken in dry CH_2Cl_2 (35 mL). *N*-Iodosuccinimide (1.39 g, 5.92 mmol) in CH_2Cl_2 (40 mL) was added to the mixture dropwise. The mixture was stirred at room temperature for 4 h. The crude product mixture was washed with H_2O (3 x 100 mL). The aqueous layer was back extracted with CH_2Cl_2 (2 × 30 mL). The combined organic layers were dried ($MgSO_4$) and the solvent was removed under reduced pressure. The resulting orange crude product was purified by column chromatography (CH_2Cl_2:petroleum ether 1:1) to give the title compound **3.50** as an orange solid (2.35 g, 80%), mp 220-221 ^oC. R_f = 0.5 (CH_2Cl_2:petroleum ether 1:1). ^1H NMR (300 MHz, $CDCl_3$) δ 7.22 (d, *J* = 7.9 Hz, 2H), 7.05 (d, *J* = 7.9 Hz, 2H), 2.54 (s, 3H), 2.48 (s, 3H), 2.37 (s, 3H), 2.24 (q, *J* = 7.5 Hz, 2H), 1.30 (s, 3H), 1.25 (s, 3H), 0.92 (t, *J* = 7.5 Hz, 3H). ^{13}C NMR (75 MHz, $CDCl_3$) δ 157.80, 152.75, 141.92, 141.03, 140.98, 139.06, 134.52, 132.14, 131.92, 130.68, 129.91, 127.85, 83.38, 21.49, 17.13, 16.64, 15.69, 14.43, 12.87, 12.04. ^{11}B NMR (96 MHz, $CDCl_3$) δ 0.68 (t, $J_{B\text{-}F}$ = 32.8 Hz). ^{19}F NMR (282 MHz, $CDCl_3$) δ -145.74 (q, $J_{F\text{-}B}$ =32.8 Hz). IR (neat): υ_{max}/cm^{-1}: 2966, 2931, 1532, 1401, 1310, 1179, 1070, 976, 754. HRMS-ES Calcd for $C_{22}H_{24}N_2{}^{11}BF_2{}^{127}I + H^+$: 493.1124, found: 493.1131.

2-Ethyl-4,4-difluoro-1,3,5,7-tetramethyl-8-(4-methylphenyl)-4-bora-3a,4a-diaza-*s*-indacene 3.49 and 2-ethyl-4,4-difluoro-2-iodo-1,3,5,7-tetramethyl-8-(4-methylphenyl)-4-bora-3a,4a-diaza-*s*-indacene 3.50.

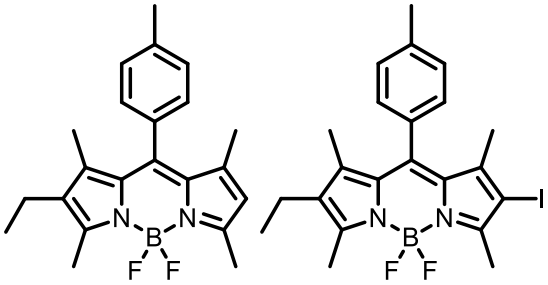

(4-Iodo-3,5-dimethyl-1H-pyrrol-2-yl)(p-tolyl)methanone **3.48** (0.06 g, 0.17 mmol) was taken in dry CH_2Cl_2 (20 mL). 3-Ethyl-2,4-dimethyl-1H-pyrrole (0.27 g, 0.22 mmol) and $BF_3.OEt_2$ (2.0 mg, 0.02 mmol) were added and the resulting solution was stirred at room temperature for 2 h. The mixture was then neutralized with *N*,*N*-diisopropylethylamine (0.12 g, 1.03 mmol) and treated with $BF_3.OEt_2$ (0.16 g, 1.37 mmol) and then the mixture was stirred at room temperature for 4 h. The crude product mixture was washed with water (100 mL). The aqueous layer was back extracted with CH_2Cl_2 (2 × 100 mL). The combined organic layers were dried ($MgSO_4$) and the solvent was removed under reduced pressure. The resulting orange crude product was purified by column chromatography (CH_2Cl_2:petroleum ether 1:3) to give: First eluted BODIPY **3.49** as an orange solid (0.02 g, 30%). Second eluted 2-iodoBODIPY **3.50** as an orange solid (0.04 g, 50%).

The spectroscopic data obtained for these compounds were identical with those reported above.

General procedure for palladium catalyzed amination

2-Ethyl-4,4-difluoro-2-iodo-1,3,5,7-tetramethyl-8-(4-methylphenyl)-4-bora-3a,4a-diaza-*s*-indacene **3.50** (0.10 g, 0.20 mmol), the amine (1.01 mmol), di((2-(2'-amino-1,1'-biphenyl))palladium(II) methanesulfonate dimer **3.54** (1.87 mg, 2.50 μmol, 1.25 mol%) Sphos (2.30 mg, 5.50 μmol, 2.75 mol %), and Cs_2CO_3 (0.11 g, 0.35 mmol) were taken in a flame-dried Schlenk tube and flushed with N_2 several times. Dry 1,4-dioxane (2 mL) was then added and the mixture was stirred at 95 °C for 16 h. The mixture was dissolved in ethyl acetate (30 mL) and washed with water (2 × 100 mL). The organic layer was dried ($MgSO_4$) and the solvent was removed under reduced pressure. The crude product was purified by column chromatography (ethyl acetate:petroleum ether 1:7).

6-Ethyl-4,4-difluoro-2-((4-methoxyphenyl)amino)-8-(4-methylphenyl)-1,3,5,7-tetramethyl-4-bora-3a,4a-diaza-*s*-indacene 3.51.

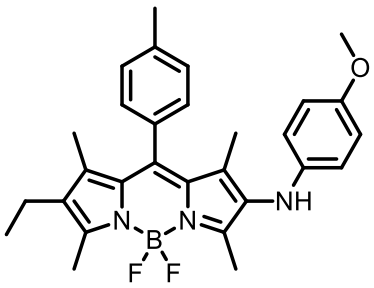

According to the general procedure for palladium catalysed amination, 2-ethyl-4,4-difluoro-2-iodo-1,3,5,7-tetramethyl-8-(4-methylphenyl)-4-bora-3a,4a-diaza-*s*-indacene **3.50** (0.10 g, 0.20 mmol) was reacted with *p*-anisidine (0.12 g, 1.01 mmol). The crude product was purified by column chromatography (ethyl acetate:petroleum ether 1:7) to give the title compound **3.51** as a dark purple solid (0.09 g, 92%), mp 240-241 ℃. R_f = 0.25 (ethyl acetate:petroleum ether 1:7). ^{1}H NMR (300 MHz, $CDCl_3$) δ 7.20 (d, *J* = 7.9 Hz, 2H), 7.08 (d, *J* = 7.9 Hz, 2H), 6.65 (d, *J* = 8.9 Hz, 2H), 6.40 (d, *J* = 8.9 Hz, 2H), 3.65 (s, 3H), 2.48 (s, 3H), 2.35 (s, 3H), 2.34 (s, 3H), 2.24 (q, *J* = 7.5 Hz, 2H), 1.26 (s, 3H), 1.15 (s, 3H), 0.92 (t, *J* = 7.5 Hz, 3H). ^{13}C NMR (101 MHz, $CDCl_3$) δ 155.50, 152.52, 151.71, 141.13, 140.86, 139.59, 138.84, 136.73, 133.31, 132.44, 131.75, 131.56, 129.84, 129.30, 128.03, 114.89, 114.31, 55.83, 21.53, 17.15, 14.67, 12.72, 11.95, 11.19. ^{11}B NMR (96 MHz, $CDCl_3$) δ 0.78 (t, $J_{B\text{-}F}$ = 32.2 Hz); ^{19}F NMR (282 MHz, $CDCl_3$) δ -145.93 (q, $J_{F\text{-}B}$ =32.2 Hz). IR (neat): υ_{max}/cm^{-1}: 3399, 2962, 2927, 2360, 1541, 1508, 1477, 1184, 1005, 798. HRMS-ES Calcd for $C_{29}H_{32}N_3{}^{11}BF_2$ O + H^+: 488.2686, found: 488.2685.

2-((4-Chlorophenyl)amino)-6-ethyl-4,4-difluoro-1,3,5,7-tetramethyl-8-(4-methylphenyl)-4-bora-3a,4a-diaza-*s*-indacene 3.55.

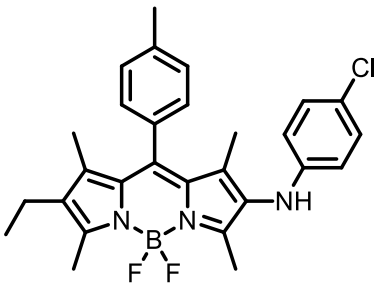

According to the general procedure for palladium catalysed amination, 2-ethyl-4,4-difluoro-2-iodo-1,3,5,7-tetramethyl-8-(4-methylphenyl)-4-bora-3a,4a-diaza-*s*-indacene **3.50** (0.10 g, 0.20 mmol) was reacted with 4-chloroaniline (0.13 g, 1.01 mmol). The crude product was purified by column chromatography (ethyl acetate:petroleum ether 1:7) to give the title compound **3.55** as a dark purple solid (0.09 g, 85%), mp 270-271℃. R_f = 0.37 (ethyl acetate:petroleum ether 1:7).^{1}H NMR (300 MHz, $CDCl_3$) δ 7.21 (d, *J* = 7.9 Hz, 2H), 7.07 (d, *J* = 7.9 Hz, 2H), 7.00 (d, *J* = 8.6 Hz, 2H), 6.37 (d, *J* = 8.6 Hz, 2H), 4.77 (s, 1H), 2.49 (s, 3H), 2.35 (s, 3H), 2.32 (s, 3H), 2.25 (q, *J* = 7.6 Hz, 2H), 1.27 (s, 3H), 1.13 (s, 3H), 0.92 (t, *J* = 7.6 Hz, 3H). ^{13}C NMR (75 MHz, $CDCl_3$) δ 156.51, 150.89, 145.55, 141.34, 140.12, 138.88, 137.01, 133.70, 132.20, 131.82, 130.03, 129.82, 129.10, 127.87, 124.83, 122.55, 114.17, 21.47, 17.08, 14.55, 12.74, 12.76, 11.94, 11.09. ^{11}B NMR (96 MHz, $CDCl_3$) δ 0.69 (t, $J_{B\text{-}F}$ = 33.0 Hz). ^{19}F NMR (282 MHz, $CDCl_3$) δ -146.05 (q, $J_{F\text{-}B}$ = 33.0 Hz). IR (neat): υ_{max}/cm^{-1}: 3357, 2962, 2923, 2360, 1661, 1597, 1539, 1490, 1259, 1074, 1009, 796. HRMS-ES Calcd for $C_{28}H_{29}N_3{}^{11}B{}^{19}F_2{}^{35}Cl + Na^+$: 514.2009, found: 514.2012.

2-((4-Cyanophenyl)amino)-6-ethyl-4,4-difluoro-1,3,5,7-tetramethyl-8-(4-methylphenyl)-4-bora-3a,4a-diaza-*s*-indacene 3.56.

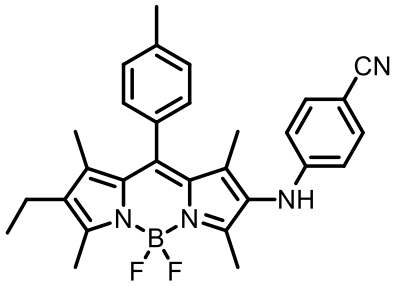

According to the general procedure for palladium catalysed amination, 2-ethyl-4,4-difluoro-2-iodo-1,3,5,7-tetramethyl-8-(4-methylphenyl)-4-bora-3a,4a-diaza-*s*-indacene **3.50** (0.10 g, 0.20 mmol) was reacted with 4-cyanoaniline (0.12 g, 1.01 mmol). The crude product was purified by column chromatography (ethyl acetate:petroleum ether 1:7) to give the title compound **3.56** as a dark red solid (0.05 g, 51%), mp 282-286℃. R_f = 0.25 (ethyl acetate:petroleum ether 1:7).^{1}H NMR (300 MHz, $CDCl_3$) δ 7.32 (d, *J* = 8.6 Hz, 2H), 7.22 (d, *J* = 7.9 Hz, 2H), 7.07 (d, *J* = 7.9 Hz, 2H), 6.45 (d, *J* = 8.6 Hz, 2H), 5.25 (s, 1H), 2.50 (s, 3H), 2.36 (s, 3H), 2.31 (s, 3H), 2.29 – 2.18 (m, 2H), 1.28 (s, 3H), 1.12 (s, 3H), 0.93 (t, *J* = 7.5 Hz, 3H). ^{13}C NMR (126 MHz, $CDCl_3$) δ 157.91, 150.61, 149.58, 141.59, 140.82, 139.05, 136.71, 134.29, 133.79, 132.25, 132.00, 129.89, 128.79, 127.94, 127.80, 120.16, 112.90, 99.97, 21.45, 17.08, 14.45, 12.84, 11.99, 11.64, 11.03. ^{11}B NMR (96 MHz, $CDCl_3$) δ 0.67 (t, $J_{B\text{-}F}$ = 32.5 Hz).^{19}F NMR (282 MHz, $CDCl_3$) δ -145.91 (q, $J_{F\text{-}B}$ = 32.5 Hz). IR (neat): υ_{max}/cm^{-1}: 3386, 2964, 2928, 2212, 1668, 1606, 1537, 1515, 1314, 1261, 1200, 1074, 1005, 800. HRMS-ES Calcd for $C_{29}H_{29}N_4{}^{11}B^{19}F_2$ + Na^+: 505.2351, found: 505.2355.

6-Ethyl-4,4-difluoro-1,3,5,7-tetramethyl-8-(4-methylphenyl)-2-((2-methylphenyl)-amino)-4-bora-3a,4a-diaza-*s*-indacene 3.57.

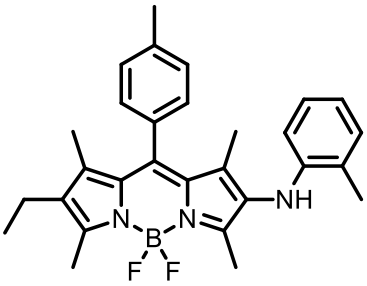

According to the general procedure for palladium catalysed amination, 2-ethyl-4,4-difluoro-2-iodo-1,3,5,7-tetramethyl-8-(4-methylphenyl)-4-bora-3a,4a-diaza-*s*-indacene **3.50** (0.10 g, 0.20 mmol) was reacted with *o*-toluidine (0.11 g, 1.01 mmol). The crude product was purified by column chromatography (ethyl acetate:petroleum ether 1:7) to give the title compound **3.57** as a dark purple solid (0.09 g, 90%), mp 201-202℃. R_f = 0.37 (ethyl acetate:petroleum ether 1:7).^{1}H NMR (300 MHz, $CDCl_3$) δ 7.20 (d, *J* = 7.9 Hz, 2H), 7.09 (d, *J* = 7.9 Hz, 2H), 6.98 (d, *J* = 7.3 Hz, 1H), 6.96 – 6.89 (m, 1H), 6.59 (td, *J* = 7.4, 1.1 Hz, 1H), 6.24 (dd, *J* = 8.0, 0.9 Hz, 1H), 4.54 (s, 1H), 2.49 (s, 3H), 2.35 (s, 3H), 2.33 (s, 3H), 2.25 (q, *J* = 7.6 Hz, 2H), 2.17 (s, 3H), 1.27 (s, 3H), 1.14 (s, 3H), 0.92 (t, *J* = 7.6 Hz, 3H). ^{13}C NMR (75 MHz, $CDCl_3$) δ 155.70, 151.54, 144.76, 141.18, 139.69, 138.79, 137.01, 133.36, 132.34, 131.56, 130.94, 130.25, 129.78, 129.23, 127.94, 127.07, 121.52, 117.85, 111.59, 21.47, 17.52, 17.09, 14.60, 12.68, 11.90, 11.82, 11.11. ^{11}B NMR (96 MHz, $CDCl_3$) δ 0.74 (t, $J_{B\text{-}F}$ = 32.5 Hz). ^{19}F NMR (282 MHz, $CDCl_3$) δ -146.13 (q, $J_{F\text{-}B}$ = 32.5 Hz). IR (neat): υ_{max}/cm^{-1}: 3410, 2962, 2972, 2868, 1535, 1475, 1323, 1303, 1179, 1054, 977, 750. HRMS-ES Calcd for $C_{29}H_{32}N_3{}^{11}B^{19}F_2 + Na^+$: 494.2555, found: 494.2561.

6-Ethyl-4,4-difluoro-2-(hexylamino)-1,3,5,7-tetramethyl-8-(4-methylphenyl)-4-bora-3a,4a-diaza-*s*-indacene 3.58.

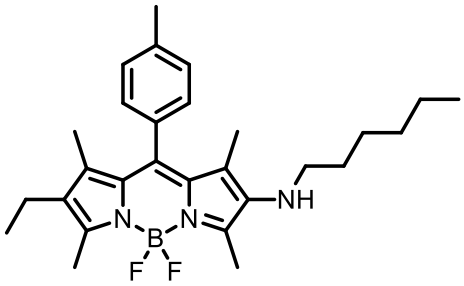

According to the general procedure for palladium catalysed amination, 2-ethyl-4,4-difluoro-2-iodo-1,3,5,7-tetramethyl-8-(4-methylphenyl)-4-bora-3a,4a-diaza-*s*-indacene **3.50** (0.10 g, 0.20 mmol) was reacted with hexylamine (0.10 g, 1.01 mmol). The crude product was purified by column chromatography (ethyl acetate:petroleum ether 1:7) to give the title compound **3.58** as a dark purple solid (0.03 g, 31%), mp 200-201℃. R_f = 0.49 (ethyl acetate:petroleum ether 1:7). ^{1}H NMR (300 MHz, $CDCl_3$) δ 7.19 (d, *J* = 8.0 Hz, 2H), 7.06 (d, *J* = 8.0 Hz, 2H), 2.81 (t, *J* = 7.4 Hz, 2H), 2.50 (s, 3H), 2.46 (s, 3H), 2.37 (s, 3H), 2.26-2.18 (m, 2H), 1.24-1.20 (m, 8H), 1.19-1.15 (m, 6H), 0.91 (t, *J* = 7.6 Hz, 3H), 0.82 – 0.76 (m, 3H). ^{13}C NMR (126 MHz, $CDCl_3$) δ 152.81, 149.75, 140.03, 139.56, 138.53, 137.95, 132.70, 132.12, 130.76, 129.78, 129.61, 128.56, 128.17, 50.02, 31.69, 30.80, 26.71, 22.62, 21.44, 17.06, 14.67, 14.04, 12.41, 12.09, 11.72, 10.85. ^{11}B NMR (96 MHz, $CDCl_3$) δ 0.70 (t, J_{B-F} = 32.5 Hz). ^{19}F NMR (282 MHz, $CDCl_3$) δ -146.13 (q, J_{F-B} = 32.5 Hz). IR (neat): υ_{max}/cm^{-1}: 3290, 2962, 2359, 1544, 1411, 1260, 1017, 797. HRMS-ES Calcd for $C_{28}H_{38}N_3{}^{11}B^{19}F_2 + H^+$: 466.3205, found: 466.3205.

6-Ethyl-4,4-difluoro-1,3,5,7-tetramethyl-8-(4-methylphenyl)-2-(2-nitrophenyl)amino)-4-bora-3a,4a-diaza-*s*-indacene 4.8.

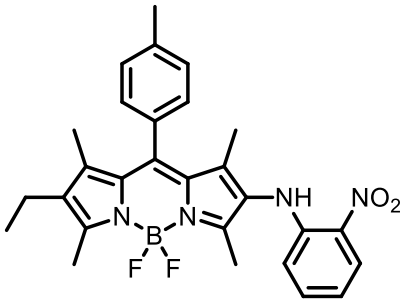

According to the general procedure for palladium catalysed amination, 2-ethyl-4,4-difluoro-2-iodo-1,3,5,7-tetramethyl-8-(4-methylphenyl)-4-bora-3a,4a-diaza-*s*-indacene **3.50** (0.10 g, 0.20 mmol) was reacted with 2-nitroaniline (0.14 g, 1.01 mmol).The crude product was purified by column chromatography (ethyl acetate:petroleum ether 1:9) to give the title compound **4.8** as a dark red solid (0.08 g, 67%), mp 220-222℃. R_f = 0.25 (ethyl acetate:petroleum ether 1:9). ^{1}H NMR (300 MHz, $CDCl_3$) δ 8.72 (s, 1H), 8.10 (dd, *J* = 8.6, 1.5 Hz, 1H), 7.31 – 7.25 (m, 1H), 7.22 (d, *J* = 8.0 Hz, 2H), 7.09 (d, *J* = 8.0 Hz, 2H), 6.63 (ddd, *J* = 8.4, 7.0, 1.2 Hz, 1H), 6.55 (dd, *J* = 8.6, 1.1 Hz, 1H), 2.51 (s, 3H), 2.36 (s, 3H), 2.34 (s, 3H), 2.26 (q, *J* = 7.6 Hz, 2H), 1.29 (s, 3H), 1.14 (s, 3H), 0.94 (t, *J* = 7.6 Hz, 3H). ^{13}C NMR (176 MHz, $CDCl_3$) δ 158.17, 149.08, 144.97, 141.65, 140.93, 139.07, 136.36, 136.10, 134.39, 132.32, 132.34, 131.97, 129.91, 128.90, 127.80, 127.13, 126.55, 116.75, 115.74, 21.46, 17.09, 14.46, 12.88, 12.02, 11.68, 11.02.^{11}B NMR (96 MHz, $CDCl_3$) δ 0.71 (t, $J_{B\text{-}F}$ = 32.6 Hz).^{19}F NMR (282 MHz, $CDCl_3$) δ -146.06 (q, $J_{F\text{-}B}$ = 32.6 Hz). IR (neat): υ_{max}/cm^{-1}: 3439, 3362, 2920, 1910, 1642, 1595, 1527, 1503, 1313, 1257, 1089, 938, 734. HRMS-ES Calcd for $C_{28}H_{29}N_4{}^{11}BF_2O_2$ + Na^+: 525.2249, found: 525.2256.

1-(1,3,2-Benzodioxaborol-2-yl)-2-[(*Z*)-(3,5-dimethyl-2*H*-pyrrol-2-ylidene)(4-iodophenyl)methyl]-3,5-dimethyl-1*H*-pyrrole 4.2.

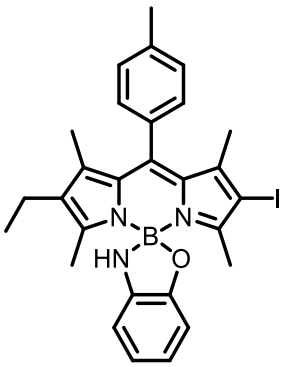

According to the general procedure for palladium catalysed amination, 2-ethyl-4,4-difluoro-2-iodo-1,3,5,7-tetramethyl-8-(4-methylphenyl)-4-bora-3a,4a-diaza-*s*-indacene **3.50** (0.10 g, 0.20 mmol) was reacted with 2-aminophenol (0.11 g, 1.01 mmol).The crude product was purified by column chromatography (CH_2Cl_2:petroleum ether 1:1) to give the title compound **4.2** as a dark purple solid (0.04 g, 64%), mp 190-191 ℃. R_f = 0.35 (CH_2Cl_2:petroleum ether 1:1). ^{1}H NMR (300 MHz, $CDCl_3$) δ 7.23 (d, *J* = 7.5 Hz, 2H), 7.09-7.03 (m, 2H), 6.64 (d, *J* = 7.5 Hz, 2H), 6.54 – 6.46 (m, 1H), 6.43 (d, *J* = 8.6 Hz, 1H), 2.38 (s, 3H), 2.18 (q, *J* = 7.5 Hz, 2H), 2.10 (s, 3H), 2.03 (s, 3H), 1.31 (s, 3H), 1.24 (s, 3H), 0.86 (t, *J* = 7.5 Hz, 3H). ^{13}C NMR (75 MHz, $CDCl_3$) δ 160.28, 154.99, 151.38, 142.16, 141.75, 140.79, 140.53, 138.94, 134.99, 132.71, 132.31, 131.22, 129.98, 129.83, 128.15, 127.81, 119.59, 115.77, 108.56, 106.15, 85.08, 21.48, 17.15, 16.99, 16.00, 14.44, 12.86, 12.16.^{11}B NMR (96 MHz, $CDCl_3$) δ 5.31 (s). IR (neat): υ_{max}/cm^{-1}: 3472, 3030, 2921, 2851, 1741, 1544, 1467, 1295, 1176, 1151, 978, 722. HRMS-ES Calcd for $C_{28}H_{29}N_3{}^{11}BO^{127}I + H^+$: 562.1527, found: 562.1532.

6-Ethyl-4,4-difluoro-1,3,5,7-tetramethyl-8-(4-methylphenyl)-2-(2-aminophenyl)-amino)-4-bora-3a,4a-diaza-*s*-indacene 4.9.

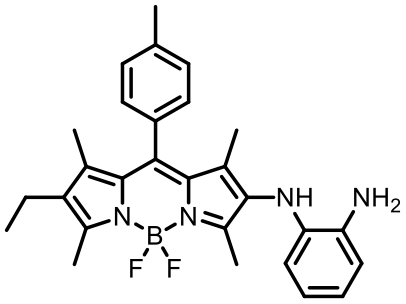

6-Ethyl-4,4-difluoro-1,3,5,7-tetramethyl-8-(4-methylphenyl)-2-((2-nitrophenyl)amino)-4-bora-3a,4a-diaza-*s*-indacene **4.8** (0.05 g, 0.10 mmol) was dissolved in CH_2Cl_2 (1 mL) and MeOH (3 mL). 10% Pd/C (0.05 g) was added. The mixture was stirred under nitrogen for 15 min and the nitrogen line was replaced with a hydrogen-filled balloon. The mixture was stirred at room temperature for 2 h and then filtered through Celite, washing with CH_2Cl_2. The solvent was removed under reduced pressure. The crude product was purified by column chromatography (CH_2Cl_2) to give the title compound **4.9** as a dark purple solid (0.05 g, 95%), mp 215-218℃. R_f = 0.25 (CH_2Cl_2). ^{1}H NMR (300 MHz, $CDCl_3$) δ 8.72 (s, 1H), 8.10 (dd, *J* = 8.6, 1.5 Hz, 1H), 7.31 – 7.25 (m, 1H), 7.22 (d, *J* = 8.0 Hz, 2H), 7.09 (d, *J* = 8.0 Hz, 2H), 6.63 (ddd, *J* = 8.4, 7.0, 1.2 Hz, 1H), 6.55 (dd, *J* = 8.6, 1.1 Hz, 1H), 2.51 (s, 3H), 2.36 (s, 3H), 2.34 (s, 3H), 2.26 (q, *J* = 7.6 Hz, 2H), 1.29 (s, 3H), 1.14 (s, 3H), 0.94 (t, *J* = 7.6 Hz, 3H). ^{13}C NMR (176 MHz, $CDCl_3$) δ 157.90, 150.61, 149.57, 141.58, 140.82, 139.05, 136.72, 134.29, 133.79, 132.24, 131.99, 129.90, 128.78, 127.92, 127.79, 120.19, 112.90, 99.92, 21.46, 17.08, 14.47, 12.85, 12.00, 11.65, 11.04. ^{11}B NMR (96 MHz, $CDCl_3$) δ 0.77 (t, $J_{B\text{-}F}$ = 32.4 Hz). ^{19}F NMR (282 MHz, $CDCl_3$) δ -146.00 (q, $J_{F\text{-}B}$ = 32.4 Hz). IR (neat): υ_{max}/cm^{-1}: 3440, 3362, 2921, 2360, 1642, 1595, 1527, 1503, 1413, 1312, 1257, 1090, 733. HRMS-ES Calcd for $C_{28}H_{31}N_4{}^{11}BF_2$ + H^+: 473.2688, found: 473.2690.

2-(2-Benzimidazolinon-l-yl)-6-ethyl-4,4-difluoro-1,3,5,7-tetramethyl-8-(4-methylphenyl)-4-bora-3a,4a-diaza-*s*-indacene 4.18.

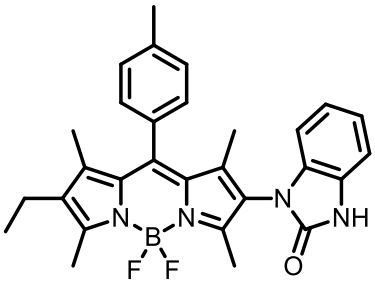

6-Ethyl-4,4-difluoro-1,3,5,7-tetramethyl-8-(4-methylphenyl)-2-((2-aminophenyl)amino)-4-bora-3a,4a-diaza-s-indacene **4.9** (0.02 g, 0.09 mmol) was dissolved in dry CH_2Cl_2 (10 mL). Triethylamine (0.09 g, 0.71 mmol) and triphosgene (8.70 mg, 0.29 mmol) in CH_2Cl_2 (1 mL) were added. The mixture was stirred at room temperature for 10 min. The solvent was removed under reduced pressure and the crude product was purified by column chromatography (CH_2Cl_2:ethyl acetate 10:1) to give the title compound **4.18** as an orange solid (0.04 g, 98%), mp 205-206℃. R_f = 0.25 (CH_2Cl_2:ethyl acetate 10:1). ^{1}H NMR (300 MHz, $CDCl_3$) δ 10.37 (s, 1H), 7.21 (d, *J* = 8.6 Hz, 2H), 7.12 (d, *J* = 8.6 Hz, 2H), 7.07 – 7.04 (m, 1H), 7.02-6.90 (m, 2H), 6.64 (d, *J* = 7.0 Hz, 1H), 2.53 (s, 3H), 2.34 (s, 6H), 2.27 (q, *J* = 7.5 Hz, 2H), 1.30 (s, 3H), 1.13 (s, 3H), 0.95 (t, *J* = 7.5 Hz, 3H). ^{13}C NMR (75 MHz, $CDCl_3$) δ 158.98, 155.23, 148.65, 142.04, 141.26, 139.05, 136.73, 134.71, 132.67, 131.89, 131.01, 129.92, 129.80, 128.90, 128.17, 128.00, 127.73, 122.69, 122.12, 121.55, 109.99, 108.91, 21.44, 17.11, 14.40, 12.97, 12.07, 11.87, 11.24. ^{11}B NMR (96 MHz, $CDCl_3$) δ 0.78 (t, $J_{B\text{-}F}$ = 32.0 Hz). ^{19}F NMR (282 MHz, $CDCl_3$) δ -145.24 (dq, $J_{F\text{-}F}$ = 107.0, $J_{F\text{-}B}$ = 32.0 Hz), -146.10 (dq, $J_{F\text{-}F}$ = 107.0, $J_{F\text{-}B}$ = 32.0 Hz). IR (neat): υ_{max}/cm^{-1}: 3440, 3362, 3233, 2917, 2274, 2119, 1707, 1641, 1594, 1569, 1531, 1503, 1387, 1257, 1089, 820, 734. HRMS-ES Calcd for $C_{29}H_{29}N_4{}^{10}B{}^{19}F_2 + Na^+$: 520.2336, found: 520.2337.

2-(2-((2-Hydroxybenzylidene)amino)phenylamino)-6-ethyl-4,4-difluoro-1,3,5,7-tetramethyl-8-(4-methylphenyl)-4-bora-3a,4a-diaza-*s*-indacene 4.26.

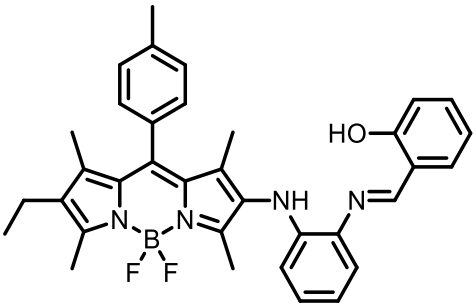

6-Ethyl-4,4-difluoro-1,3,5,7-tetramethyl-8-(4-methylphenyl)-2-((2-aminophenyl)amino)-4-bora-3a,4a-diaza-*s*-indacene **4.9** (0.03 g, 0.06 mmol) was dissolved in EtOH (2 mL). Salicylaldehyde (6.45 µL, 0.06 mmol) and a drop of AcOH were added. The mixture was stirred under reflux for 19 h. The solvent was removed under reduced pressure and the crude product was purified by column chromatography (CH_2Cl_2:petroleum ether 2:3) to give the title compound **4.26** as red solid (0.03 g, 72%). R_f = 0.25 (CH_2Cl_2:petroleum ether 2:3). ^{1}H NMR (300 MHz, $CDCl_3$) δ 12.87 (s, 1H), 8.59 (s, 1H), 7.35 (dd, *J* = 7.8, 1.8 Hz, 1H), 7.33 – 7.26 (m, 1H), 7.20 (d, *J* = 8.0 Hz, 2H), 7.09 (d, *J* = 8.0 Hz, 2H), 7.04 – 6.96 (m, 2H), 6.94 (dd, *J* = 9.0, 1.1 Hz, 1H), 6.91 – 6.85 (m, 1H), 6.67 (td, *J* = 7.6, 1.3 Hz, 1H), 6.36 (dd, *J* = 8.1, 1.1 Hz, 1H), 2.49 (s, 3H), 2.36 (s, 3H), 2.35 (s, 3H), 2.25 (q, *J* = 7.5 Hz, 2H), 1.27 (s, 3H), 1.17 (s, 3H), 0.92 (t, *J* = 7.5 Hz, 4H). ^{11}B NMR (96 MHz, $CDCl_3$) δ 0.77 (t, $J_{B\text{-}F}$ = 31.5 Hz). ^{19}F NMR (282 MHz, $CDCl_3$) δ -145.99 (q, $J_{F\text{-}B}$ = 31.5 Hz). The compound was observed to undergo slow oxidation in solution.

6-Ethyl-2-(2-(2-hydroxyphenyl)-1H-benzimidazol-l-yl)-4,4-difluoro-1,3,5,7-tetramethyl-8-(4-methylphenyl)-4-bora-3a,4a-diaza-*s*-indacene 4.27.

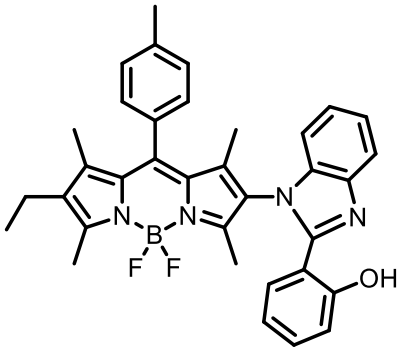

2-(2-((2-Hydroxybenzylidene)amino)phenylamino)-6-ethyl-4,4-difluoro-1,3,5,7-tetramethyl-8-(4-methylphenyl)-4-bora-3a,4a-diaza-*s*-indacene **4.26** (0.03 g, 0.05 mmol) was dissolved in $CHCl_3$ (2 mL). The mixture was left under air for 16 h. The solvent was removed under reduced pressure.The crude product was purified by column chromatography (petroleum ether:diethyl ether 4:1) to give the title compound **4.27** as a pink solid (0.02 g, 79%). R_f = 0.25 (petroleum ether:diethyl ether 4:1). ^{1}H NMR (300 MHz, $CDCl_3$) δ 13.80 (s, 1H), 7.70 (d, *J* = 7.2 Hz, 1H), 7.27 (dd, *J* = 7.3, 1.2 Hz, 1H), 7.24 – 7.16 (m, 6H), 7.16 – 7.08 (m, 2H), 7.02 (dd, *J* = 8.7, 1.2 Hz, 1H), 6.99 – 6.94 (m, 1H), 2.57 (s, 3H), 2.32 (s, 3H), 2.32 – 2.24 (m, 2H), 2.17 (s, 3H), 1.34 (s, 3H), 1.00 – 0.91 (m, 6H).^{13}C NMR (176 MHz, $CDCl_3$) δ 160.87, 159.68, 151.21, 146.53, 142.26, 139.89, 139.36, 135.80, 135.58, 134.70, 133.39, 131.63, 131.50, 129.99, 128.78, 127.70, 125.85, 125.38, 123.84, 123.46, 118.67, 118.04, 112.77, 110.42, 21.43, 17.10, 14.39, 13.13, 12.20, 11.43, 10.78.^{11}B NMR (96 MHz, $CDCl_3$) δ 0.79 (t, J_{B-F} = 32.3 Hz). ^{19}F NMR (282 MHz, $CDCl_3$) δ -145.95-145.55 (m). IR (neat): υ_{max}/cm^{-1}: 3360, 2925, 2854, 1738, 1563, 1485, 1324, 1255, 1194, 1081, 754. HRMS-ES Calcd for $C_{35}H_{33}N_4{}^{10}B{}^{19}F_2$ O + H^+: 575.2794, found: 575.2800.

6-Ethyl-4,4-difluoro-1,3,5,7-tetramethyl-8-(4-methylphenyl)-2-(2-(pyrid-2-ylmethylamino)phenylamino)-4-bora-3a,4a-diaza-*s*-indacene 4.32 and 6-ethyl-4,4-difluoro-1,3,5,7-tetramethyl-8-(4-methylphenyl)-2-((2-(di(pyrid-2-yl methyl)amino)phenylamino)-4-bora-3a,4a-diaza-*s*-indacene 4.31.

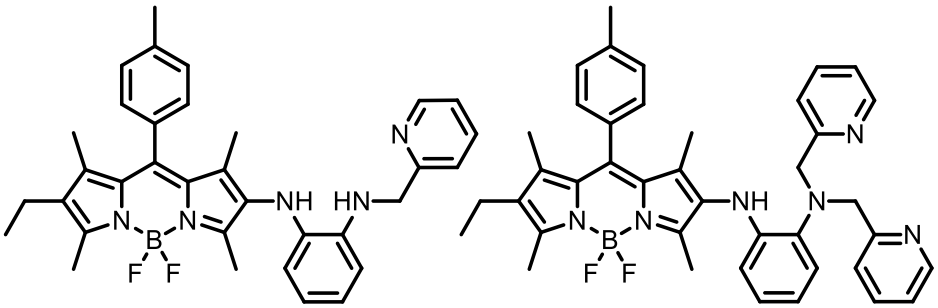

6-Ethyl-4,4-difluoro-1,3,5,7-tetramethyl-8-(4-methylphenyl)-2-((2-aminophenyl)amino)-4-bora-3a,4a-diaza-*s*-indacene **4.9** (0.02 g, 0.05 mmol) was dissolved in dry acetonitrile (5 mL). 2-Chloromethyl pyridine hydrochloride (0.02g, 0.14 mmol) and K_2HPO_4 (0.04 g, 0.23 mmol) were added. The mixture was stirred under reflux for 48 h. The solvent was removed under reduced pressure and the crude product was purified by column chromatography (CH_2Cl_2:petroleum ether 1:1) to give, first eluted: the BODIPY **4.32** as a purple solid (4.5 mg, 17%). ^{1}H NMR (300 MHz, $CDCl_3$) δ 8.55 (d, *J* = 6.8 Hz, 1H), 7.72 (td, *J* = 7.7, 1.6 Hz, 1H), 7.37 (d, *J* = 7.9 Hz, 1H), 7.25 (d, *J* = 6.9 Hz, 1H), 7.22 (d, *J* = 7.8 Hz, 2H), 7.09 (d, *J* = 7.8 Hz, 2H), 6.70 – 6.54 (m, 3H), 6.35 (d, *J* = 7.6 Hz, 1H), 5.27 (s, 1H), 5.01 (s, 1H), 4.49 (s, 2H), 2.48 (s, 3H), 2.35 (s, 3H), 2.33 (s, 3H), 2.25 (q, *J* = 7.6 Hz, 2H), 1.27 (s, 3H), 1.18 (s, 3H), 0.92 (t, *J* = 7.6 Hz, 3H). ^{11}B NMR (96 MHz, $CDCl_3$) δ 0.89 (t, $J_{B\text{-}F}$ = 30.2 Hz). ^{19}F NMR (282 MHz, $CDCl_3$) δ -145.64 (q, $J_{F\text{-}B}$ = 30.2 Hz). HRMS-ES Calcd for $C_{34}H_{36}N_5{}^{10}B^{19}F_2 + H^+$: 564.3110, found: 564.3107.

Second eluted: BODIPY **4.31** as a purple solid (0.02 g, 69%); mp >300 °C. ^{1}H NMR (700 MHz, $CDCl_3$) δ 8.39 (d, *J* = 4.2 Hz, 2H), 7.86 (s, 1H), 7.39 (t, *J* = 7.6 Hz, 2H), 7.21 (d, *J* = 7.9 Hz, 2H), 7.16 (d, *J* = 7.8 Hz, 2H), 7.12 (d, *J* = 7.9 Hz, 2H), 7.05 (d, *J* = 8.9 Hz, 1H), 7.01 – 6.96 (m, 2H), 6.78 (t, *J* = 7.7 Hz, 1H), 6.48 (t, *J* = 7.6 Hz, 1H), 6.24 (d, *J* = 9.2 Hz, 1H), 4.23 (s, 4H), 2.49 (s, 3H), 2.36 (s, 3H), 2.35 (s, 3H), 2.26 (q, *J* = 7.6 Hz, 2H), 1.27 (s, 3H), 1.17 (s, 3H), 0.93 (t, *J* = 7.6 Hz, 3H). ^{13}C NMR (176 MHz, $CDCl_3$) δ 158.82, 154.66, 152.17, 148.97, 142.27, 140.82, 139.09, 138.67, 136.57, 136.29, 135.87, 132.93, 132.54, 131.90, 131.29, 129.71, 129.61, 128.07, 124.99, 122.95, 122.09, 121.68, 116.55,

111.63, 59.39, 21.44, 17.09, 14.62, 12.60, 12.10, 11.84, 11.45. ^{11}B NMR (96 MHz, $CDCl_3$) δ 0.75 (t, $J_{B\text{-}F}$ = 32.2 Hz). ^{19}F NMR (282 MHz, $CDCl_3$) δ -146.19 (q, $J_{F\text{-}B}$ = 32.2 Hz). IR (neat): υ_{max}/cm^{-1}: 3221, 2924, 2853, 2408, 2284, 1662, 1591, 1537, 1477, 1307, 1185, 1073, 1003, 979, 753. HRMS-ES Calcd for $C_{40}H_{41}N_6{}^{10}B^{19}F_2 + H^+$: 655.3532, found: 655.3539.

7. References

1 J. R. Lakowicz, *Principles of fluorescence spectroscopy*, springer, New York, 2006.

2 B. Valeur, *Molecular Fluorescence: Principles and Applications*, Wiley-VCH, Weinheim, 2002.

3 B. Valeur and M. N. Berberan-Santos, *J. Chem. Educ.*, 2011, **88**, 731–738.

4 K. Rurack and M. Spieles, *Anal. Chem.*, 2011, **83**, 1232–1242.

5 A. T. R. Williams, S. A. Winfield and J. N. Miller, *Analyst*, 1983, **108**, 1067–1071.

6 G. Ulrich, R. Ziessel and A. Harriman, *Angew. Chem. Int. Ed.*, 2008, **47**, 1184–1201.

7 P. M. W. French and J. R. Taylor, *Opt. Commun.*, 1986, **58**, 53–55.

8 T. Ueno, Y. Urano, K. I. Setsukinai, H. Takakusa, H. Kojima, K. Kikuchi, K. Ohkubo, S. Fukuzumi and T. Nagano, *J. Am. Chem. Soc.*, 2004, **126**, 14079–14085.

9 L. Li, T. Ruzgas and A. K. Gaigalas, *Langmuir*, 1999, **15**, 6358–6363.

10 V. Bonasera, S. Alberti and A. Sacchetti, *Biotechniques*, 2007, **43**, 173–176.

11 T. Mahmood, A. Paul and S. Ladame, *J. Org. Chem.*, 2010, **75**, 204–207.

12 A. Loudet and K. Burgess, *Chem. Rev.*, 2007, **107**, 4891–4932.

13 T. E. Wood and A. Thompson, *Chem. Rev.*, 2007, **107**, 1831–1861.

14 M. Benstead, G. H. Mehl and R. W. Boyle, *Tetrahedron*, 2011, **67**, 3573–3601.

15 S. G. Awuah and Y. You, *RSC Adv.*, 2012, **2**, 11169–11183.

16 N. Boens, V. Leen and W. Dehaen, *Chem. Soc. Rev.*, 2012, **41**, 1130–1172.

17 H. Lu, J. Mack, Y. Yang and Z. Shen, *Chem. Soc. Rev.*, 2014, **43**, 4778–4823.

18 V. Lakshmi, M. Rajeswara Rao and M. Ravikanth, *Org. Biomol. Chem.*, 2015, **13**, 2501–2517.

19 V. Lakshmi and M. Ravikanth, *Chem. Phys. Lett.*, 2013, **564**, 93–97.

20 V. Lakshmi and M. Ravikanth, *J. Org. Chem.*, 2011, **76**, 8466–8471.

21 S. Y. Atsushi Wakamiya, Naoya Sugita, *Chem. Lett.*, 2008, **37**, 1094–1095.

22 Y. Gabe, T. Ueno, Y. Urano, H. Kojima and T. Nagano, *Anal. Bioanal. Chem.*, 2006, **386**, 621–626.

23 C. Tahtaoui, C. Thomas, F. Rohmer, P. Klotz, G. Duportail, Y. Mély, D. Bonnet and M. Hibert, *J. Org. Chem.*, 2007, **72**, 269–272.

24 A. Treibs and F. H. Kreuzer, *Justus Liebigs Ann. Chem.*, 1968, **718**, 208–223.

25 D. T. Gryko, D. Gryko and C.-H. Lee, *Chem. Soc. Rev.*, 2012, **41**, 3780–3789.

26 T. Uppal, N. V. S. D. K. Bhupathiraju and M. G. H. Vicente, *Tetrahedron*, 2013, **69**, 4687–4693.

27 R. Ziessel, L. Bonardi, P. Retailleau and G. Ulrich, *J. Org. Chem.*, 2006, **71**, 3093–3102.

28 C. Tahtaoui, C. Thomas, F. Rohmer, P. Klotz, G. Duportail, Y. Mely, D. Bonnet and M. Hibert, *J. Org. Chem.*, 2007, **72** , 269–272.

29 J. S. Lee, N. Y. Kang, K. K. Yun, A. Samanta, S. Feng, K. K. Hyeong, M. Vendrell, H. P. Jung and Y. T. Chang, *J. Am. Chem. Soc.*, 2009, **131**, 10077–10082.

30 R. P. Haugland, *The Handbook, A Guide to Fluorescent Probes and Labeling Technologies*, Invitrogen Corp., 2005.

31 S. Ozlem and E. U. Akkaya, *J. Am. Chem. Soc.*, 2009, **131**, 48–49.

32 G. Barin, M. D. Yilmaz and E. U. Akkaya, *Tetrahedron Lett.*, 2009, **50**, 1738–1740.

33 O. A. Bozdemir, R. Guliyev, O. Buyukcakir, S. Selcuk, S. Kolemen, G. Gulseren, T. Nalbantoglu, H. Boyaci and E. U. Akkaya, *J. Am. Chem. Soc.*, 2010, **132**, 8029–8036.

34 O. A. Bozdemir, F. Sozmen, O. Buyukcakir, R. Guliyev, Y. Cakmak and E. U. Akkaya, *Org. Lett.*, 2010, **12**, 1400–1403.

35 S. O. McDonnell, M. J. Hall, L. T. Allen, A. Byrne, W. M. Gallagher and D. F. O'Shea, *J. Am. Chem. Soc.*, 2005, **127**, 16360–16361.

36 S. P. Singh and T. Gayathri, *Eur. J. Org.Chem.*, 2014, 4689–4707.

37 Y. Kubo, D. Eguchi, A. Matsumoto, R. Nishiyabu, H. Yakushiji, K. Shigaki and M. Kaneko, *J. Mater. Chem. A*, 2014, **2**, 5204–5211.

38 J. Karolin, L. B. a Johansson, L. Strandberg and T. Ny, *J. Am. Chem. Soc.*, 1994, **116**, 7801–7806.

39 T. Ehrenschwender and H. A. Wagenknecht, *J. Org. Chem.*, 2011, **76**, 2301–2304.

40 W. Namkung, P. Padmawar, A. D. Mills and A. S. Verkman, *J. Am. Chem. Soc.*, 2008, **130**, 7794–7795.

41 L. C. D. D. L. Rezende, S. Emery and F. Emery, *Orbital Elec. J. Chem*, 2013, **5**, 62–83.

42 E. L. Eliel and S. H. Wilen, *Stereochemistry of organic compounds*, Wiley, New York, 1994.

43 J. Clayden, *Organic chemistry*, Oxford University Press, Oxford, 2001.

44 A. J. Hutt and J. Valentova, *Acta Fac. Pharm. Univ. Comen.*, 2003, **50**, 7–23.

45 D. Leung, S. O. Kang and E. V. Anslyn, *Chem. Soc. Rev.*, 2012, **41**, 448–479.

46 E. L. Izake, *J. Pharm. Sci.*, 2007, 96, 1659–1676.

47 K. Jennings and D. Diamond, *Analyst*, 2001, **126**, 1063–1067.

48 A. Accetta, R. Corradini and R. Marchelli, in *Luminescence Applied in Sensor Science*, Springer Berlin Heidelberg, 2011, vol. 300, pp. 175–216.

49 T. Bruhn, G. Pescitelli, S. Jurinovich, A. Schaumloffel, F. Witterauf, J. Ahrens, M. Broring and G. Bringmann, *Angew. Chem. Int. Ed.*, 2014, **53**, 14592–14595.

50 S. Kolemen, Y. Cakmak, Z. Kostereli and E. U. Akkaya, *Org. Lett.*, 2014, **16**, 660–663.

51 R. I. Lerrick, T. P. Winstanley, K. Haggerty, C. Wills, W. Clegg, R. W. Harrington,

P. Bultinck, W. Herrebout, A. C. Benniston and M. J. Hall, *Chem Commun.*, 2014, **50**, 4714–4716.

52 E. M. Sanchez-Carnerero, F. Moreno, B. L. Maroto, A. R. Agarrabeitia, J. Banuelos, T. Arbeloa, I. Lopez-Arbeloa, M. J. Ortiz and S. de la Moya, *Chem. Commun.*, 2013, **49**, 11641–11643.

53 A. Gossauer, F. Nydegger, T. Kiss, R. Sleziak and H. Stoeckli-Evans, *J. Am. Chem. Soc.*, 2004, **126**, 1772–1780.

54 G. Beer, J. Daub and K. Rurack, *Chem. Commun.*, 2001, 1138–1139.

55 W. Wu, H. Guo, W. Wu, S. Ji and J. Zhao, *J. Org. Chem.*, 2011, **76**, 7056–7064.

56 L. Jiao, W. Pang, J. Zhou, Y. Wei, X. Mu, G. Bai and E. Hao, *J. Org. Chem.*, 2011, **76**, 9988–9996.

57 S. Doherty, J. G. Knight, C. H. Smyth and G. A. Jorgenson, *Adv. Synth. Catal.*, 2008, **350**, 1801–1806.

58 A. C. Benniston, G. Copley, K. J. Elliott, R. W. Harrington and W. Clegg, *Eur. J. Org. Chem.*, 2008, 2705–2713.

59 A. C. Benniston, A. Harriman, V. L. Whittle and M. Zelzer, *Eur. J. Org. Chem.*, 2010, **2010**, 523–530.

60 A. Gorman, J. Killoran, C. O'Shea, T. Kenna, W. M. Gallagher and D. F. O'Shea, *J. Am. Chem. Soc.*, 2004, **126**, 10619–10631.

61 J. H. Ye, G. Wang, C. Huang, Z. Hu, W. Zhang and Y. Zhang, *Synthesis (Stuttg).*, 2012, **44**, 104–110.

62 A. Maurice and T. Rogers, *J. Chem. Soc.*, 1943, 590–596.

63 W. H. Davies and M. A. T. Rogers, *J. Chem. Soc.*, 1944, 126–131.

64 E. B. Knott, *J. Chem. Soc.*, 1947, 1196–1201.

65 T. H. Allik, R. E. Hermes, G. Sathyamoorthi and J. H. Boyer, *Proc. SPIE-Int. Soc. Opt. Eng.*, 1994, **2115**, 240–248.

66 J. Killoran, L. Allen, J. F. Gallagher, W. M. Gallagher and D. F. O′Shea, *Chem*

Commun., 2002, 1862–1863.

67 J. Killoran and D. F. O'Shea, *Chem. Commun.*, 2006, 1503–1505.

68 M. J. Hall, L. T. Allen and D. F. O'Shea, *Org. Biomol. Chem.*, 2006, **4**, 776–780.

69 J. Killoran, S. O. McDonnell, J. F. Gallagher and D. F. O'Shea, *New J. Chem.*, 2008, **32**, 483–489.

70 M. Grossi, A. Palma, S. O. McDonnell, M. J. Hall, D. K. Rai, J. Muldoon and D. F. O'shea, *J. Org. Chem.*, 2012, **77**, 9304–9312.

71 L. Gao, N. Deligonul and T. G. Gray, *Inorg. Chem.*, 2012, **51**, 7682–7688.

72 A. Loudet, R. Bandichhor, K. Burgess, A. Palma, S. O. McDonnell, M. J. Hall and D. F. O'Shea, *Org. Lett.*, 2008, **10**, 4771–4774.

73 A. I. R. N. A. Barros, A. M. S. Silva, I. Alkorta and J. Elguero, *Tetrahedron*, 2004, **60**, 6513–6521.

74 K. N. Mewett, S. P. Fernandez, A. K. Pasricha, A. Pong, S. O. Devenish, D. E. Hibbs, M. Chebib, G. A. R. Johnston and J. R. Hanrahan, *Bioorg. Med. Chem.*, 2009, **17**, 7156–7173.

75 A. R. Gholap, K. S. Toti, F. Shirazi, R. Kumari, M. K. Bhat, M. V Deshpande and K. V Srinivasan, *Bioorg. Med. Chem.*, 2007, **15**, 6705–6715.

76 H. Kim, A. Burghart, M. B. Welch, J. Reibenspies and K. Burgess, *Chem. Commun.*, 1999, 1889–1890.

77 A. K. Parhi, M. P. Kung, K. Ploessl and H. F. Kung, *Tetrahedron Lett.*, 2008, **49**, 3395–3399.

78 Y. Kubo, K. Watanabe, R. Nishiyabu, R. Hata, A. Murakami, T. Shoda and H. Ota, *Org. Lett.*, 2011, **13**, 4574–4577.

79 Y. Kubo, Y. Minowa, T. Shoda and K. Takeshita, *Tetrahedron Lett.*, 2010, **51**, 1600–1602.

80 C. Ikeda, T. Maruyama and T. Nabeshima, *Tetrahedron Lett.*, 2009, **50**, 3349–3351.

81 Y. Tomimori, T. Okujima, T. Yano, S. Mori, N. Ono, H. Yamada and H. Uno, *Tetrahedron*, 2011, **67**, 3187–3193.

82 S. Rausaria, A. Kamadulski, N. P. Rath, L. Bryant, Z. Chen, D. Salvemini and W. L. Neumann, *J. Am. Chem. Soc.*, 2011, **133**, 4200–4203.

83 C. Ikeda, S. Ueda and T. Nabeshima, *Chem. Commun.*, 2009, 2544–2546.

84 W. Chen, E. K. Stephenson, M. P. Cava and Y. A. Jackson, *Org. Synth.*, 1992, **70**, 151–154.

85 A. Burghart, H. Kim, M. B. Welch, L. H. Thoresen, J. Reibenspies, K. Burgess, F. Bergstrom and L. B. A. Johansson, *J. Org. Chem.*, 1999, **64**, 7813–7819.

86 C. H. Lee and J. S. Lindsey, *Tetrahedron*, 1994, **50**, 11427–11440.

87 M. R. Rao, S. M. Mobin and M. Ravikanth, *Tetrahedron*, 2010, **66**, 1728–1734.

88 N. C. Bruno, M. T. Tudge and S. L. Buchwald, *Chem. Sci.*, 2013, **4**, 916–920.

89 O. Ohno, Y. Kaizu and H. Kobayashi, *J. Chem. Phys.*, 1985, **82**, 1779–1787.

90 E. Bahaidarah, A. Harriman, P. Stachelek, S. Rihn, E. Heyer and R. Ziessel, *Photochem. Photobiol. Sci.*, 2014, **13**, 1397–1401.

91 B. Brizet, C. Bernhard, Y. Volkova, Y. Rousselin, P. D. Harvey, C. Goze and F. Denat, *Org. Biomol. Chem.*, 2013, **11**, 7729–7737.

92 G. P. Moss, *Pure Appl. Chem.*, 1996, **68**, 2193–2222.

93 F. S. R. James P. Riehl, *Chem. Rev.*, 1986, **86**, 1–16.

94 N. Berova, K. Nakanishi and R. W. Woody, *Circular dichroism: Principles and Applications, 2nd Edition*, Wiley-VCH, New York, 2000.

95 E. M. Sanchez-Carnerero, F. Moreno, B. L. Maroto, A. R. Agarrabeitia, M. J. Ortiz, B. G. Vo, G. Muller and S. Moya, *J. Am. Chem. Soc.*, 2014, **136**, 3346–3349.

96 F. Li, Y. Wang, Z. Wang, Y. Cheng and C. Zhu, *Polym. Chem.*, 2015, **6**, 6802–6805.

97 Y. Nagata, T. Nishikawa and M. Suginome, *Chem. Commun.*, 2014, **50**, 9951–9953.

98 S. Zhang, Y. Wang, F. Meng, C. Dai, Y. Cheng and C. Zhu, *Chem Commun*, 2015, **51**, 9014–9017.

99 Y. V. Zatsikha, V. P. Yakubovskyi, M. P. Shandura and Y. P. Kovtun, *Dye. Pigment.*, 2015, **114**, 215–221.

100 M. Shandura and V. Yakubovsky, *Org. Biomol. Chem.*, 2013, **11**, 835–841.

101 M. P. Shandura. V. P. Yakubovskyi and Y. P. Kovtun, *J. Heterocycl. Chem.*, 2009, **46**, 1386–1391.

102 S. Zhang, C. Feng, J. Cai, J. Chen, H. Hu and M. Ji, *J. Chem. Res.*, 2013, **37**, 480–482.

103 Y. Hayashi, S. Yamaguchi, W. Y. Cha, D. Kim and H. Shinokubo, *Org. Lett.*, 2011, **13**, 2992–2995.

104 T. Rohand, M. Baruah, W. Qin, N. Boens and W. Dehaen, *Chem Commun*, 2006, 266–268.

105 J. G. Knight, R. B. Alnoman and P. G. Waddell, *Org. Biomol. Chem.*, 2015, **13**, 3819–3829.

106 V. Leen, V. Z. Gonzalvo, W. M. Deborggraeve, N. Boens and W. Dehaen, *Chem. Commun.*, 2010, **46**, 4908–4910.

107 I. Esnal, J. Banuelos, I. Lopez Arbeloa, A. Costela, I. Garcia-Moreno, M. Garzon, A. R. Agarrabeitia and M. Jose Ortiz, *RSC Adv.*, 2013, **3**, 1547–1556.

108 H. Yokoi, N. Wachi, S. Hiroto and H. Shinokubo, *Chem. Commun.*, 2014, **50**, 2715–2717.

109 Y. Yu, N. Bogliotti, J. Tang and J. Xie, *Eur. J. Org. Chem.*, 2013, 7749–7760.

110 R. Gotor, P. Gavina, L. E. Ochando, K. Chulvi, A. Lorente, R. Martinez-Manez and A. M. Costero, *RSC Adv.*, 2014, **4**, 15975–15982.

111 E. Sperotto, G. P. M. Van Klink, G. Van Koten and J. G. De Vries, *Dalt. Trans.*,

2010, **39**, 10338–10351.

112 L. Kurti and B. Czako, *Strategic applications of named reactions in organic synthesis: background and detailed mechanisms*, Elsevier Academic Press, 2005.

113 D. S. Surry and S. L. Buchwald, *Chem. Sci.*, 2010, **1**, 13–31.

114 Z. Lu and R. J. Twieg, *Tetrahedron*, 2005, **61**, 903–918.

115 A. Klapars, J. C. Antilla, X. Huang, S. L. Buchwald and R. V May, *J. Am. Chem. Soc.*, 2001, 7727–7729.

116 A. Klapars, X. Huang and S. L. Buchwald, *J. Am. Chem. Soc.*, 2002, **124**, 7421–7428.

117 K. R. Crawford and A. Padwa, *Tetrahedron Lett.*, 2002, **43**, 7365–7368.

118 X. Zeng, W. Huang, Y. Qiu and S. Jiang, *Org. Biomol. Chem.*, 2011, **9**, 8224–8227.

119 M. Li, M. J. Powell, T. T. Razunguzwa and G. A. O'doherty, *J. Org. Chem.*, 2010, **75**, 6149–6153.

120 J. Kim and S. Chang, *Chem. Commun.*, 2008, 3052–3054.

121 L. Wu and K. Burgess, *Chem. Commun.*, 2008, 4933–4935.

122 M. J. Ortiz, A. R. Agarrabeitia, G. Duran-Sampedro, J. Banuelos Prieto, T. A. Lopez, W. A. Massad, H. A. Montejano, N. A. Garcia and I. Lopez Arbeloa, *Tetrahedron*, 2012, **68**, 1153–1162.

123 A. Shafir and S. L. Buchwald, *J. Am. Chem. Soc.*, 2006, **128**, 8742–8743.

124 D. Wang and K. Ding, *Chem. Commun.*, 2009, 1891–1893.

125 Y. B. Huang, C. T. Yang, J. Yi, X. J. Deng, Y. Fu and L. Liu, *J. Org. Chem.*, 2011, **76**, 800–810.

126 A. Rolfe and P. R. Hanson, *Tetrahedron Lett.*, 2009, **50**, 6935–6937.

127 J. Zhao, W. Wu, J. Sun and S. Guo, *Chem. Soc. Rev.*, 2013, **42**, 5323–5351.

128 M. Schnurch, M. Spina, A. F. Khan, M. D. Mihovilovic and P. Stanetty, *Chem.*

Soc. Rev., 2007, **36**, 1046–1057.

129 X. F. Duan and Z. B. Zhang, *Heterocycles*, 2005, **65**, 2005–2012.

130 A. John and K. M. Nicholas, *Organometallics*, 2012, **31**, 7914–7920.

131 R. Giri and J. F. Hartwig, *J. Am. Chem. Soc.*, 2010, **132**, 15860–15863.

132 T. Mutsumi, H. Iwata, K. Maruhashi, Y. Monguchi and H. Sajiki, *Tetrahedron*, 2011, **67**, 1158–1165.

133 R. Selliah, A. Dantanarayana, K. Haggard, J. Egan, E. U. Do and J. A. May, *J. Label. Compd. Radiopharm.*, 2001, **44**, 173–183.

134 M. Kosugi, M. Kameyama and T. Migita, *Chem. Lett.*, 1983, 927–928.

135 A. Guram and S. Buchwald, *J. Am. Chem. Soc.*, 1994, **116**, 7901–7902.

136 J. Louie and J. F. Hartwig, *Tetrahedron Lett.*, 1995, **36**, 3609–3612.

137 A. S. Guram, R. A. Rennels and S. L. Buchwald, *Angew. Chem. Int. Ed.*, 1995, **34**, 1348–1350.

138 Y. Sunesson, E. Lime, S. O. N. Lill, R. E. Meadows and P. O. Norrby, *J. Org. Chem.*, 2014, **79**, 11961–11969.

139 H. Shimogawa, H. Mori, A. Wakamiya and Y. Murata, *Chem. Lett.*, 2013, **42**, 986–988.

140 C. Zhang, J. Zhao, S. Wu, Z. Wang, W. Wu, J. Ma and S. Guo, *J. Am. Chem. Soc.*, 2013, **135**, 10566–10578.

141 I. P. Beletskaya and A. V. Cheprakov, *Organometallics*, 2012, **31**, 7753–7808.

142 J. P. Wolfe, S. Wagaw and S. L. Buchwald, *J. Am. Chem. Soc.*, 1996, **118**, 7215–7216.

143 D. S. Surry and S. L. Buchwald, *Angew. Chem. Int. Ed.*, 2008, **47**, 6338–6361.

144 X. Huang, K. W. Anderson, D. Zim, L. Jiang, A. Klapars and S. L. Buchwald, *J. Am. Chem. Soc.*, 2003, **125**, 6653–6655.

145 B. P. Fors and S. L. Buchwald, *J. Am. Chem. Soc.*, 2010, **132**, 15914–15917.

146 J. Louie, M. S. Driver, B. C. Hamann and J. F. Hartwig, *J. Org. Chem.*, 1997, **62**, 1268–1273.

147 P. R. Melvin, D. Balcells, N. Hazari and A. Nova, *ACS Catal.*, 2015, **5**, 5596–5606.

148 T. Kinzel, Y. Zhang and S. L. Buchwald, *J. Am. Chem. Soc.*, 2010, **132**, 14073–14075.

149 M. R. Biscoe, B. P. Fors and S. L. Buchwald, *J. Am. Chem. Soc.*, 2008, **130**, 6686–6687.

150 J. Lakowicz, *principles of fluorescence spectroscopy*, Plenum press, New York, 1983.

151 M. T. Montero, J. Hernandez and J. Estelrich, *Biochem. Educ.*, 1990, **18**, 99–101.

152 Y. Wu, X. Peng, B. Guo, J. Fan, Z. Zhang, J. Wang, A. Cui and Y. Gao, *Org. Biomol. Chem.*, 2005, **3**, 1387–1392.

153 B. Valeur, M. N. Berberan-Santos, *Molecular Fluorescence: Principles and Applications, Second Edition*, Wiley-VCH, Weinheim, 2012.

154 I. Esnal, I. Valois-Escamilla, C. F. A. Gomez-Duran, A. Urias-Benavides, M. L. Betancourt-Mendiola, I. Lopez-Arbeloa, J. Banuelos, I. Garcia-Moreno, A. Costela and E. Pena-Cabrera, *ChemPhysChem*, 2013, **14**, 4134–4142.

155 R. I. Roacho, A. Metta-Magana, M. M. Portillo, E. Pena-Cabrera and K. H. Pannell, *J. Org. Chem.*, 2013, **78**, 4245–4250.

156 I. Esnal, *J. Org. Chem.*, 2012, **77**, 5434–5438.

157 W. Qin, V. Leen, T. Rohand, W. Dehaen, P. Dedecker, M. Van Der Auweraer, K. Robeyns, L. Van Meervelt, D. Beljonne, B. Van Averbeke, J. N. Clifford, K. Driesen, K. Binnemans and N. Boens, *J. Phys. Chem. A*, 2009, **113**, 439–447.

158 X. Shao, R. Kang, Y. Zhang, Z. Huang, F. Peng, J. Zhang, Y. Wang, F. Pan, W. Zhang and W. Zhao, *Anal. Chem.*, 2015, **87**, 399–405.

159 H. Yokoi, S. Hiroto and H. Shinokubo, *Org. Lett.*, 2014, **16**, 3004–3007.

160 X. He, J. Zhang, X. Liu, L. Dong, D. Li, H. Qiu and S. Yin, *Sensors Actuators, B Chem.*, 2014, **192**, 29–35.

161 M. De Lourdes Betancourt-Mendiola, E. Pena-Cabrera, S. Gil, K. Chulvi, L. E. Ochando and A. M. Costero, *Tetrahedron*, 2014, **70**, 3735–3739.

162 Y. A. Volkova, B. Brizet, P. D. Harvey, A. D. Averin, C. Goze and F. Denat, *Eur. J. Org. Chem.*, 2013, 4270–4279.

163 L. Y. Niu, H. Li, L. Feng, Y. S. Guan, Y. Z. Chen, C. F. Duan, L. Z. Wu, Y. F. Guan, C. H. Tung and Q. Z. Yang, *Anal. Chim. Acta*, 2013, **775**, 93–99.

164 S. C. Dodani, S. C. Leary, P. A. Cobine, D. R. Winge and C. J. Chang, *J. Am. Chem. Soc.*, 2011, **133**, 8606–8616.

165 J. Banuelos, V. Martin, C. F. A. Gomez-Durán, I. J. A. Cordoba, E. Peña-Cabrera, I. Garia-Moreno, A. Costela, M. E. Perez-Ojeda, T. Arbeloa and I. L. Arbeloa, *Chemi. Eur. J.*, 2011, **17**, 7261–7270.

166 C. F. A. Gómez-Durán, I. García-Moreno, A. Costela, V. Martin, R. Sastre, J. Bañuelos, F. López Arbeloa, I. López Arbeloa and E. Peña-Cabrera, *Chem. Commun.*, 2010, **46**, 5103–5105.

167 L. Li, B. Nguyen and K. Burgess, *Bioorg. Med. Chem. Lett.*, 2008, **18**, 3112–3116.

168 D. W. Domaille, L. Zeng and C. J. Chang, *J. Am. Chem. Soc.*, 2010, **132**, 1194–1195.

169 A. M. Brouwer, *Pure Appl. Chem.*, 2011, **83**, 2213–2228.

170 X. A. Ed. J-L.Rivail, M. Ruiz-Lopez, *Quantum modeling of complex molecular systems*, springer, 2015.

171 V. Lakshmi, M. S. Shaikh and M. Ravikanth, *J. Fluoresc.*, 2013, **23**, 519–525.

172 J. Suk and A. J. Bard, *J. Solid State Electrochem.*, 2011, **15**, 2279–2291.

173 R. Ziessel, G. Ulrich and A. Harriman, *New J. Chem.*, 2007, **31**, 496–501.

174 X. Jia, X. Yu, X. Yang, J. Cui, X. Tang, W. Liu and W. Qin, *Dye. Pigment.*, 2013, **98**, 195–200.

175 J. Zhang, B. Zhao, C. Li, X. Zhu and R. Qiao, *Sensors Actuators, B Chem.*, 2014, **196**, 117–122.

176 A. S. Worthington and M. D. Burkart, *Org. Biomol. Chem.*, 2006, **4**, 44–46.

177 V. V. Martin, A. Rothe and K. R. Gee, *Bioorg. Med. Chem. Lett.*, 2005, **15**, 1851–1855.

178 N. Basarić, M. Baruah, W. Qin, B. Metten, M. Smet, W. Dehaen and N. Boens, *Org. Biomol. Chem.*, 2005, **3**, 2755–2761.

179 J. L. Bricks, A. Kovalchuk, C. Trieflinger, M. Nofz, M. Buschel, A. I. Tolmachev, J. Daub and K. Rurack, *J. Am. Chem. Soc.*, 2005, **127**, 13522–13529.

180 Y. Mei, P. A. Bentley and W. Wang, *Tetrahedron Lett.*, 2006, **47**, 2447–2449.

181 X. Qi, E. J. Jun, L. Xu, S. J. Kim, J. S. J. Hong, Y. J. Yoon and J. Yoon, *J. Org. Chem.*, 2006, **71**, 2881–2884.

182 J. Wang and X. Qian, *Org. Lett.*, 2006, **8**, 3721–3724.

183 T. W. Hudnall and F. P. Gabbai, *Chem. Commun.*, 2008, 4596–4597.

184 N. Umeda, H. Takahashi, M. Kamiya, T. Ueno, T. Komatsu, T. Terai, K. Hanaoka, T. Nagano and Y. Urano, *ACS Chem. Biol.*, 2014, **9**, 2242–2246.

185 C. A. Wijesinghe, M. E. El-Khouly, N. K. Subbaiyan, M. Supur, M. E. Zandler, K. Ohkubo, S. Fukuzumi and F. D'Souza, *Chem. Eur. J.*, 2011, **17**, 3147–3156.

186 G. Durán-Sampedro, A. R. Agarrabeitia, L. Cerdán, M. E. Pérez-Ojeda, A. Costela, I. García-Moreno, I. Esnal, J. Bañuelos, I. L. Arbeloa and M. J. Ortiz, *Adv. Funct. Mater.*, 2013, **23**, 4195–4205.

187 A. L. Nguyen, P. Bobadova-Parvanova, M. Hopfinger, F. R. Fronczek, K. M. Smith and M. G. Vicente, *Inorg. Chem.*, 2015, **54**, 3228–3236.

188 D. A. Smithen, A. E. G. Baker, M. Offman, S. M. Crawford, T. S. Cameron and A. Thompson, *J. Org. Chem.*, 2012, **77**, 3439–3453.

189 T. Lundrigan and A. Thompson, *J. Org. Chem.*, 2013, **78**, 757–761.

190 L. Yang, R. Simionescu, A. Lough and H. Yan, *Dye. Pigment.*, 2011, **91**, 264–267.

191 H. Wang, M. G. H. Vicente, F. R. Fronczek and K. M. Smith, *Chemistry*, 2014, **20**, 5064–5074.

192 C. Bonnier, W. E. Piers, M. Parvez and T. S. Sorensen, *Chem. Commun.*, 2008, 4593–4595.

193 T. Lundrigan, S. M. Crawford, T. S. Cameron and A. Thompson, *Chem. Commun.*, 2012, **48**, 1003–1005.

194 W. F. Diller, *Toxicol. Ind. Heal.*, 1985, **1**, 7–9.

195 H. Babad and A. G. Zeiler, *Chem. Rev.*, 1972, **73**, 75–91.

196 H. Zhang and D. M. Rudkevich, *Chem. Commun.*, 2007, 1238–1239.

197 X. Wu, Z. Wu, Y. Yang and S. Han, *Chem. Commun.*, 2012, **48**, 1895–1897.

198 P. Kundu and K. C. Hwang, *Anal. Chem.*, 2012, **84**, 4594–4597.

199 G. L. Long and J. D. Winefordner, *Anal. Chem.*, 1983, **55**, 712A–724A.

200 L. Zeng, E. W. Miller, A. Pralle, E. Y. Isacoff and C. J. Chang, *J. Am. Chem. Soc.*, 2006, **128**, 10–11.

201 J. Huang, B. Wang, J. Ye, B. Liu, H. Qiu and S. Yin, *Chinese J. Chem.*, 2012, **30**, 1857–1861.

202 S. Yin, W. Yuan, J. Huang, D. Xie, B. Liu, K. Jiang and H. Qiu, *Spectrochim. Acta - Part A Mol. Biomol. Spectrosc.*, 2012, **96**, 82–88.

203 R. F. Ziessel, G. Ulrich, L. Charbonniere, D. Imbert, R. Scopelliti and J. C. G. Bunzli, *Chem. Eur. J.*, 2006, **12**, 5060–5067.

204 S. Kim, J. Y. Noh, K. Y. Kim, J. H. Kim, H. K. Kang, S. W. Nam, S. H. Kim, S. Park, C. Kim and J. Kim, *Inorg. Chem.*, 2012, **51**, 3597–3602.

205 Y. Dong, J. Li, X. Jiang, F. Song, Y. Cheng and C. Zhu, *Org. Lett.*, 2011, **13**, 2252–2255.

206 Z.-H. Pan, J.-W. Zhou and G.-G. Luo, *Phys. Chem. Chem. Phys.*, 2014, **16**, 16290–16301.

207 S. Madhu, D. K. Sharma, S. K. Basu, S. Jadhav, A. Chowdhury and M. Ravikanth, *Inorg. Chem.*, 2013, **52**, 11136–11145.

208 R. E. Ford, P. Knowles, E. Lunt, S. M. Marshall, A. J. Penrose, C. A. Ramsden, A. J. H. Summers, J. L. Walker and D. E. Wright, *J. Med. Chem.*, 1986, **29**, 538–549.

209 L. Copey, L. Jean-Gérard, E. Framery, G. Pilet and B. Andrioletti, *Eur. J. Org. Chem.*, 2014, **2014**, 4759–4766.

210 D. Gryko and J. S. Lindsey, *J. Org. Chem.*, 2000, **65**, 2249–2252.

211 H. Zhao, B. Wang, J. Liao, H. Wang and G. Tan, *Tetrahedron Lett.*, 2013, **54**, 6019–6022.

212 R. G. Giles, H. Heaney and M. J. Plater, *Tetrahedron*, 2015, **71**, 7367–7385.

213 Z. Guo, X. Wei, Y. Hua, J. Chao and Di. Liu, *Tetrahedron Lett.*, 2015, **56**, 3919–3922.

214 I. Bañuelos-Prieto, A. Agarrabeitia, I. Garcia-Moreno, I. Lopez-Arbeloa, A. Costela, L. Infantes, M. Perez-Ojeda, M. Palacios-Cuesta and M. Ortiz, *Chem. Eur. J.*, 2010, **16**, 14094–14105.

215 R. Naik, P. Joshi, S. P. Kaiwar and R. K. Deshpande, *Tetrahedron*, 2003, **59**, 2207–2213.

216 E. Pena-Cabrera, A. Aguilar-Aguilar, M. Gonzalez-Dominguez, E. Lager, R. Zamudio-Vazquez, J. Godoy-Vargas and F. Villanueva-Garcia, *Org. Lett.*, 2007, **9** , 3985–3988.

8. Appendix

X-ray Crystallography Data

2,6-Dibromo-4,4-difluoro-1,3,5,7-tetramethyl-8-phenyl-4-bora-3a,4a-diaza-*s*-indacene 2.5.

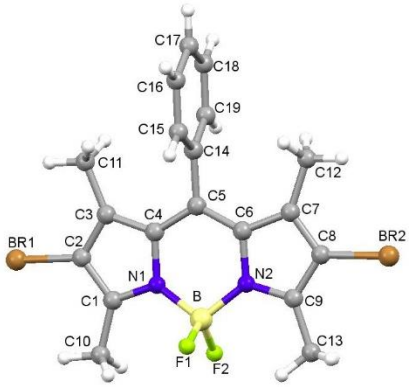

Table 1: Crystal data and structure refinement for jgk130001.

Identification code	jgk130001	
Chemical formula (moiety)	$C_{19}H_{17}BBr_2F_2N_2$	
Chemical formula (total)	$C_{19}H_{17}BBr_2F_2N_2$	
Formula weight	481.98	
Temperature	150(2) K	
Radiation, wavelength	MoKα, 0.71073 Å	
Crystal system, space group	monoclinic, $P12_1/n1$	
Unit cell parameters	a = 11.3763(5) Å	α = 90°
	b = 12.7627(6) Å	β = 93.540(4)°
	c = 12.9122(6) Å	γ = 90°
Cell volume	1871.17(15) $Å^3$	
Z	4	
Calculated density	1.711 g/cm^3	
Absorption coefficient μ	4.356 mm^{-1}	
F(000)	952	
Crystal colour and size	red, 0.32 × 0.20 × 0.20 mm^3	
Reflections for cell refinement	3775 (θ range 2.9 to 28.6°)	
Data collection method	Oxford Diffraction Gemini A Ultra	
diffractometer		
	thick-slice ω scans	
θ range for data collection	2.9 to 28.6°	
Index ranges	h –13 to 13, k –16 to 15, l –14 to 17	
Completeness to θ = 26.0°	98.3 %	
Reflections collected	10273	
Independent reflections	4000 (R_{int} = 0.0307)	
Reflections with $F^2>2\sigma$	3288	
Absorption correction	semi-empirical from equivalents	
Min. and max. transmission	0.3362 and 0.4762	
Structure solution	direct methods	

Refinement method	Full-matrix least-squares on F^2
Weighting parameters a, b	0.0287, 0.9874
Data / restraints / parameters	4000 / 0 / 235
Final R indices [$F^2>2\sigma$]	R1 = 0.0320, wR2 = 0.0658
R indices (all data)	R1 = 0.0458, wR2 = 0.0710
Goodness-of-fit on F^2	1.039
Extinction coefficient	0.0021(3)
Largest and mean shift/su	0.066 and 0.001
Largest diff. peak and hole	0.42 and –0.39 e $Å^{-3}$

3,5-Dibromo-4,4-difluoro-8-(4-methylphenyl)-4-bora-3a,4a-diaza-*s*-indacene 2.56a.

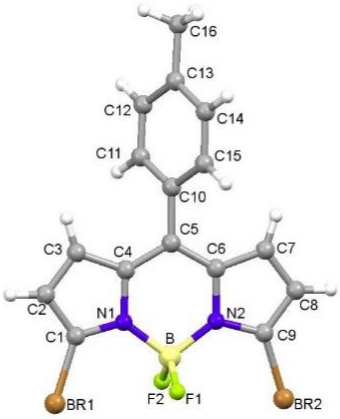

Table 2: Crystal data and structure refinement for jgk13.

Identification code	jgk130003	
Chemical formula (moiety)	$C_{32}H_{22}B_2Br_4F_4N_4$	
Chemical formula (total)	$C_{32}H_{22}B_2Br_4F_4N_4$	
Formula weight	879.80	
Temperature	150(2) K	
Radiation, wavelength	MoKα, 0.71073 Å	
Crystal system, space group	monoclinic, $P12_1/n1$	
Unit cell parameters	a = 8.5621(6) Å	α = 90°
	b = 13.1412(12) Å	β = 103.398(7)°
	c = 14.6887(9) Å	γ = 90°
Cell volume	1607.7(2) $Å^3$	
Z	2	
Calculated density	1.817 g/cm^3	
Absorption coefficient μ	5.060 mm^{-1}	
F(000)	856	
Crystal colour and size	, 0.30 × 0.30 × 0.20 mm^3	
Reflections for cell refinement	2467 (θ range 3.6 to 27.7°)	
Data collection method	Xcalibur, Atlas, Gemini ultra	
	thick-slice ω scans	
θ range for data collection	3.1 to 28.4°	
Index ranges	h –11 to 11, k –17 to 12, l –19 to 14	
Completeness to θ = 26.0°	97.6 %	
Reflections collected	8715	
Independent reflections	3387 (R_{int} = 0.0487)	
Reflections with $F^2>2\sigma$	2608	
Absorption correction	semi-empirical from equivalents	
Min. and max. transmission	0.3121 and 0.4310	
Structure solution	direct methods	
Refinement method	Full-matrix least-squares on F^2	
Weighting parameters a, b	0.0446, 3.5410	
Data / restraints / parameters	3387 / 0 / 205	
Final R indices [$F^2>2\sigma$]	R1 = 0.0471, wR2 = 0.1003	
R indices (all data)	R1 = 0.0703, wR2 = 0.1145	
Goodness-of-fit on F^2	1.042	
Extinction coefficient	0.0006(4)	

Largest and mean shift/su	0.001 and 0.000
Largest diff. peak and hole	1.00 and −1.01 e $Å^{-3}$

***B,O*-Chelated BODIPY 2.49a.**

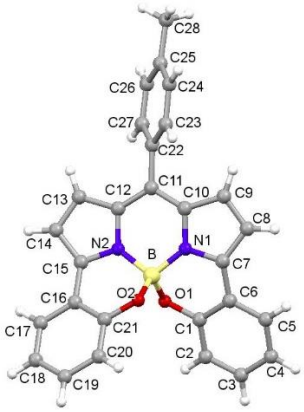

Table 3: Crystal data and structure refinement for jgk120002.

Identification code	jgk120002	
Chemical formula (moiety)	$C_{28}H_{19}BN_2O_2$	
Chemical formula (total)	$C_{28}H_{19}BN_2O_2$	
Formula weight	426.26	
Temperature	150(2) K	
Radiation, wavelength	MoKα, 0.71073 Å	
Crystal system, space group	triclinic, $P\bar{1}$	
Unit cell parameters	a = 7.9022(4) Å	α = 97.135(5)°
	b = 9.4541(6) Å	β = 98.674(5)°
	c = 14.7968(9) Å	γ = 105.621(5)°
Cell volume	1036.54(11) $Å^3$	
Z	2	
Calculated density	1.366 g/cm^3	
Absorption coefficient μ	0.086 mm^{-1}	
F(000)	444	
Crystal colour and size	red, 0.40 × 0.40 × 0.40 mm^3	
Reflections for cell refinement	3419 (θ range 3.2 to 28.6°)	
Data collection method	Xcalibur, Atlas, Gemini ultra thick-slice ω scans	
θ range for data collection	3.2 to 28.6°	
Index ranges	h −10 to 10, k −12 to 12, l −17 to 19	
Completeness to θ = 25.0°	99.7 %	
Reflections collected	9030	
Independent reflections	4338 (R_{int} = 0.0227)	
Reflections with $F^2>2\sigma$	3561	
Absorption correction	semi-empirical from equivalents	
Min. and max. transmission	0.9665 and 0.9665	
Structure solution	direct methods	
Refinement method	Full-matrix least-squares on F^2	
Weighting parameters a, b	0.0443, 0.3677	
Data / restraints / parameters	4338 / 0 / 300	
Final R indices [$F^2>2\sigma$]	R1 = 0.0415, wR2 = 0.0956	
R indices (all data)	R1 = 0.0539, wR2 = 0.1051	
Goodness-of-fit on F^2	1.024	
Extinction coefficient	0.0154(19)	

Largest and mean shift/su	0.000 and 0.000
Largest diff. peak and hole	0.30 and –0.23 e $Å^{-3}$

6-Ethyl-4,4-difluoro-5,7,8-trimethyl-2-phenyl-4-bora-3a,4a-diaza-*s*-indacene 2.70.

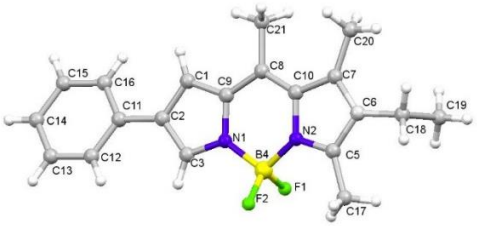

Table 4: Crystal data and structure refinement for jgk150001_fa.

Identification code	jgk150001_fa
Empirical formula	$C_{20}H_{21}BN_2F_2$
Formula weight	338.20
Temperature/K	150.0(2)
Crystal system	triclinic
Space group	P-1
a/Å	9.2603(4)
b/Å	9.7317(4)
c/Å	11.2359(4)
α/°	64.664(4)
β/°	77.921(3)
γ/°	65.199(4)
Volume/Å^3	830.23(7)
Z	2
ρ_{calc}g/cm^3	1.353
μ/mm^{-1}	0.094
F(000)	356.0
Crystal size/mm^3	0.4 × 0.18 × 0.13
Radiation	MoKα (λ = 0.71073)
2Θ range for data collection/°	6.182 to 58.602
Index ranges	-12 ≤ h ≤ 12, -12 ≤ k ≤ 13, -14 ≤ l ≤ 14
Reflections collected	26770
Independent reflections	3974 [R_{int} = 0.0389, R_{sigma} = 0.0278]
Data/restraints/parameters	3974/0/230
Goodness-of-fit on F^2	1.018
Final R indexes [I>=2σ (I)]	R_1 = 0.0439, wR_2 = 0.1003
Final R indexes [all data]	R_1 = 0.0603, wR_2 = 0.1102
Largest diff. peak/hole / e Å^{-3}	0.27/-0.22

4,4-Difluoro-2-iodo-8-(4-methoxyphenyl)-4-bora-3a,4a-diaza-*s*-indacene 3.17

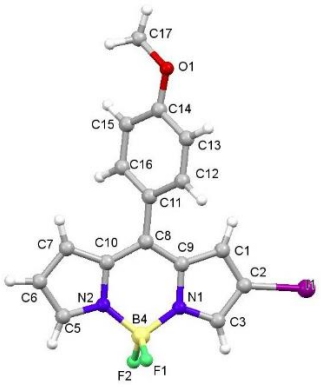

Table 5: Crystal data and structure refinement for jgk140005.

Identification code	jgk140005	
Chemical formula (moiety)	$C_{16}H_{12}BF_2IN_2O$	
Chemical formula (total)	$C_{16}H_{12}BF_2IN_2O$	
Formula weight	423.99	
Temperature	100(2) K	
Radiation, wavelength	synchrotron, 0.6889 Å	
Crystal system, space group	tetragonal, $P4_2bc$	
Unit cell parameters	a = 21.804(5) Å	α = 90°
	b = 21.804(5) Å	β = 90°
	c = 6.3692(16) Å	γ = 90°
Cell volume	3028.0(16) $Å^3$	
Z	8	
Calculated density	1.860 g/cm^3	
Absorption coefficient μ	1.912 mm^{-1}	
F(000)	1648	
Crystal colour and size	red, 0.070 × 0.010 × 0.010 mm^3	
Reflections for cell refinement	7297 (θ range 2.6 to 25.5°)	
Data collection method	Rigaku Saturn 724+ on kappa diffractometer wide-frame ω scans	
θ range for data collection	2.0 to 25.5°	
Index ranges	h –27 to 24, k –26 to 27, l –7 to 7	
Completeness to θ = 24.4°	99.1 %	
Reflections collected	25424	
Independent reflections	3065 (R_{int} = 0.0749)	
Reflections with $F^2>2\sigma$	2704	
Absorption correction	multi-scan	
Min. and max. transmission	0.883 and 0.980	
Structure solution	direct methods	
Refinement method	Full-matrix least-squares on F^2	
Weighting parameters a, b	0.0301, 2.2802	
Data / restraints / parameters	3065 / 1 / 209	
Final R indices [$F^2>2\sigma$]	R1 = 0.0303, wR2 = 0.0671	
R indices (all data)	R1 = 0.0385, wR2 = 0.0693	
Goodness-of-fit on F^2	1.042	
Absolute structure parameter	0.047(17)	
Largest and mean shift/su	0.001 and 0.000	

Largest diff. peak and hole	1.08 and −0.46 e $Å^{-3}$

4,4-difluoro-2,6-diiodo-8-(4-methoxyphenyl)-4-bora-3a,4a-diaza-*s*-indacene 3.18.

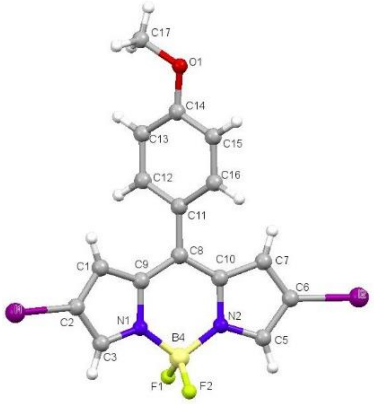

Table 6: Crystal data and structure refinement for jgk140006_4_fa.

Identification code	jgk140006_4_fa
Empirical formula	$C_{16}H_{11}BN_2OF_2I_2$
Formula weight	549.88
Temperature/K	150.01(10)
Crystal system	orthorhombic
Space group	Pnn2
a/Å	20.3020(6)
b/Å	11.2056(3)
c/Å	7.5174(4)
α/°	90
β/°	90
γ/°	90
Volume/Å^3	1710.17(11)
Z	4
ρ_{calc}mg/mm^3	2.136
m/mm^{-1}	3.703
F(000)	1032.0
Crystal size/mm^3	0.2 × 0.15 × 0.04
Radiation	MoKα (λ = 0.71073)
2Θ range for data collection	5.778 to 58.974°
Index ranges	$-27 \leq h \leq 25$, $-14 \leq k \leq 15$, $-9 \leq l \leq 10$
Reflections collected	54090
Independent reflections	4339 [R_{int} = 0.0602, R_{sigma} = 0.0316]
Data/restraints/parameters	4339/1/219
Goodness-of-fit on F^2	1.109
Final R indexes [I>=2σ (I)]	R_1 = 0.0431, wR_2 = 0.0888
Final R indexes [all data]	R_1 = 0.0560, wR_2 = 0.0941
Largest diff. peak/hole / e Å^{-3}	1.05/-1.16
Flack parameter	0.37(6)

4,4-Difluoro-3-(hexylamino)-8-(4-methoxyphenyl)-4-bora-3a,4a-diaza-*s*-indacene 3.19a.

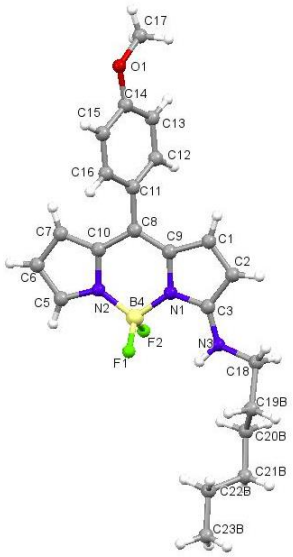

Table 7: Crystal data and structure refinement for jgk140003.

Identification code	jgk140003
Empirical formula	$C_{22}H_{26}BN_3OF_2$
Formula weight	397.27
Temperature/K	150.00(10)
Crystal system	triclinic
Space group	P-1
a/Å	9.8145(8)
b/Å	10.0842(6)
c/Å	11.3461(7)
α/°	97.195(5)
β/°	91.225(6)
γ/°	113.239(7)
Volume/Å^3	1020.62(13)
Z	2
ρ_{calc}mg/mm^3	1.293
m/mm^{-1}	0.092
F(000)	420.0
Crystal size/mm^3	0.29 × 0.21 × 0.11
Radiation	MoKα (λ = 0.71073)
2Θ range for data collection	5.932 to 57.848°
Index ranges	-12 ≤ h ≤ 12, -13 ≤ k ≤ 13, -15 ≤ l ≤ 15
Reflections collected	16496
Independent reflections	4654 [R_{int} = 0.0489, R_{sigma} = 0.0536]
Data/restraints/parameters	4654/45/284
Goodness-of-fit on F^2	1.033

Final R indexes [I>=2σ (I)]	R_1 = 0.0504, wR_2 = 0.0951
Final R indexes [all data]	R_1 = 0.0902, wR_2 = 0.1157
Largest diff. peak/hole / e $Å^{-3}$	0.22/-0.22

4,4-Difluoro-3-(hexylamino)-6-iodo-8-(4-methoxyphenyl)-4-bora-3a,4a-diaza-*s*-indacene 3.22a.

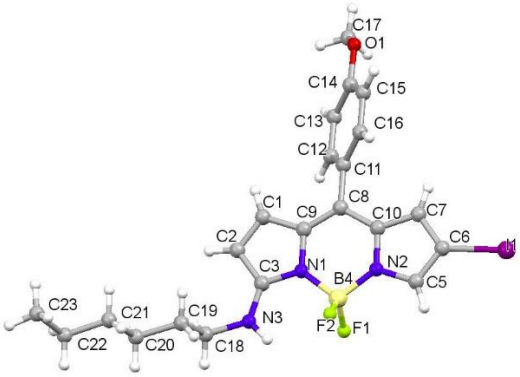

Table 8: Crystal data and structure refinement for jgk140009_fa.

Identification code	jgk140009_fa
Empirical formula	$C_{22}H_{25}BN_3OF_2I$
Formula weight	523.16
Temperature/K	150.01(10)
Crystal system	monoclinic
Space group	$P2_1$
a/Å	15.3219(4)
b/Å	17.3301(4)
c/Å	17.5462(5)
α/°	90
β/°	110.858(3)
γ/°	90
Volume/Å^3	4353.7(2)
Z	8
ρ_{calc}g/cm^3	1.596
μ/mm^{-1}	1.507
F(000)	2096.0
Crystal size/mm^3	0.31 × 0.17 × 0.13
Radiation	MoKα (λ = 0.71073)
2Θ range for data collection/°	5.598 to 59.16
Index ranges	$-20 \leq h \leq 20$, $-23 \leq k \leq 24$, $-23 \leq l \leq 24$
Reflections collected	141938
Independent reflections	21418 [R_{int} = 0.0493, R_{sigma} = 0.0376]
Data/restraints/parameters	21418/973/1090
Goodness-of-fit on F^2	1.057
Final R indexes [I>=2σ (I)]	R_1 = 0.0323, wR_2 = 0.0602
Final R indexes [all data]	R_1 = 0.0483, wR_2 = 0.0674
Largest diff. peak/hole / e Å^{-3}	0.90/-0.61
Flack parameter	0.328(11)

4,4-Difluoro-8-(4-methoxyphenyl)-3-(pyrrolidin-1-yl)-4-bora-3a,4a-diaza-*s*-indacene 3.19h.

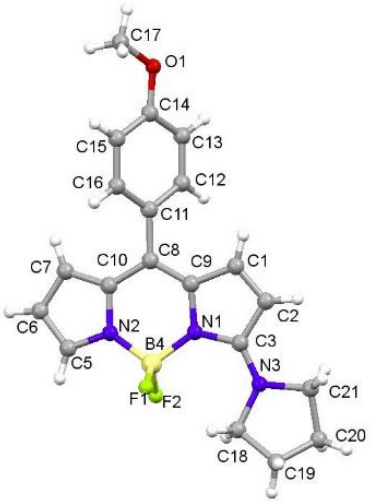

Table 9: Crystal data and structure refinement for jgk140002.

Identification code	jgk140002
Empirical formula	$C_{20}H_{20}BN_3OF_2$
Formula weight	367.20
Temperature/K	150.01(10)
Crystal system	monoclinic
Space group	$P2_1/c$
a/Å	7.8835(5)
b/Å	13.6664(9)
c/Å	15.8072(8)
α/°	90
β/°	92.063(5)
γ/°	90
Volume/Å^3	1701.96(17)
Z	4
ρ_{calc}mg/mm^3	1.433
m/mm^{-1}	0.104
F(000)	768.0
Crystal size/mm^3	0.2 × 0.18 × 0.11
Radiation	MoKα (λ = 0.71073)
2Θ range for data collection	5.958 to 57.724°
Index ranges	$-10 \leq h \leq 10$, $-17 \leq k \leq 14$, $-20 \leq l \leq 20$
Reflections collected	14534
Independent reflections	3900 [R_{int} = 0.0432, R_{sigma} = 0.0440]
Data/restraints/parameters	3900/0/245
Goodness-of-fit on F^2	1.030
Final R indexes [I>=2σ (I)]	R_1 = 0.0458, wR_2 = 0.0908

Final R indexes [all data]	R_1 = 0.0711, wR_2 = 0.1037
Largest diff. peak/hole / e Å^{-3}	0.26/-0.22

6-Ethyl-4,4-difluoro-1,3,5,7-tetramethyl-8-(4-methylphenyl)-2-((2-methylphenyl)-amino)-4-bora-3a,4a-diaza-*s*-indacene 3.57.

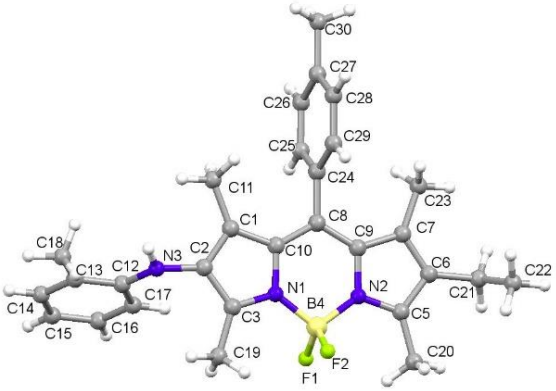

Table 10: Crystal data and structure refinement for jgk150008.

Identification code	jgk150008
Empirical formula	$C_{29}H_{32}BN_3F_2$
Formula weight	471.38
Temperature/K	150.0(2)
Crystal system	monoclinic
Space group	$P2_1/c$
a/Å	20.3605(3)
b/Å	11.6571(3)
c/Å	21.6409(8)
α/°	90
β/°	90.325(3)
γ/°	90
Volume/Å^3	5136.2(2)
Z	8
ρ_{calc}g/cm^3	1.219
μ/mm^{-1}	0.652
F(000)	2000.0
Crystal size/mm^3	0.4 × 0.19 × 0.12
Radiation	CuKα (λ = 1.54184)
2Θ range for data collection/°	8.172 to 133.924
Index ranges	$-24 \leq h \leq 17$, $-12 \leq k \leq 13$, $-25 \leq l \leq 24$
Reflections collected	37518
Independent reflections	9089 [R_{int} = 0.0362, R_{sigma} = 0.0283]
Data/restraints/parameters	9089/0/651
Goodness-of-fit on F^2	1.015
Final R indexes [I>=2σ (I)]	R_1 = 0.0384, wR_2 = 0.0947
Final R indexes [all data]	R_1 = 0.0520, wR_2 = 0.1043

Largest diff. peak/hole / e $Å^{-3}$	0.28/-0.18

1-(1,3,2-Benzodioxaborol-2-yl)-2-[(*Z*)-(3,5-dimethyl-2*H*-pyrrol-2-ylidene)(4-iodophenyl)methyl]-3,5-dimethyl-1*H*-pyrrole 4.2.

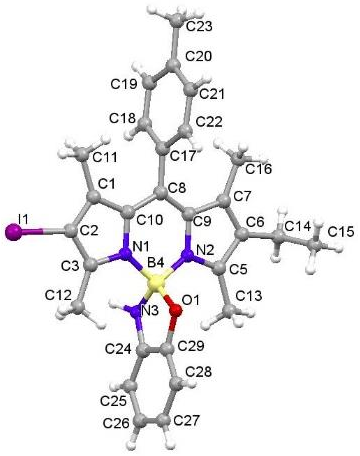

Table 11: Crystal data and structure refinement for jgk150002_fa.

Identification code	jgk150002_fa
Empirical formula	$C_{28}H_{29}BIN_3O$
Formula weight	561.25
Temperature/K	150.0(2)
Crystal system	triclinic
Space group	P-1
a/Å	8.1161(4)
b/Å	12.8348(6)
c/Å	13.4466(7)
α/°	65.729(5)
β/°	86.864(4)
γ/°	81.110(4)
Volume/Å^3	1261.50(12)
Z	2
ρ_{calc}g/cm^3	1.478
μ/mm^{-1}	10.163
F(000)	568.0
Crystal size/mm^3	0.31 × 0.11 × 0.04
Radiation	CuKα (λ = 1.54184)
2Θ range for data collection/°	7.212 to 133.87
Index ranges	-9 ≤ h ≤ 9, -15 ≤ k ≤ 14, -16 ≤ l ≤ 15
Reflections collected	17841
Independent reflections	4464 [R_{int} = 0.0529, R_{sigma} = 0.0378]
Data/restraints/parameters	4464/90/415
Goodness-of-fit on F^2	1.209
Final R indexes [I>=2σ (I)]	R_1 = 0.0492, wR_2 = 0.1154
Final R indexes [all data]	R_1 = 0.0531, wR_2 = 0.1171

Largest diff. peak/hole / e $Å^{-3}$	0.77/-0.79

UV/Vis Spectra

Compound 3.19b (THF at room temperature)

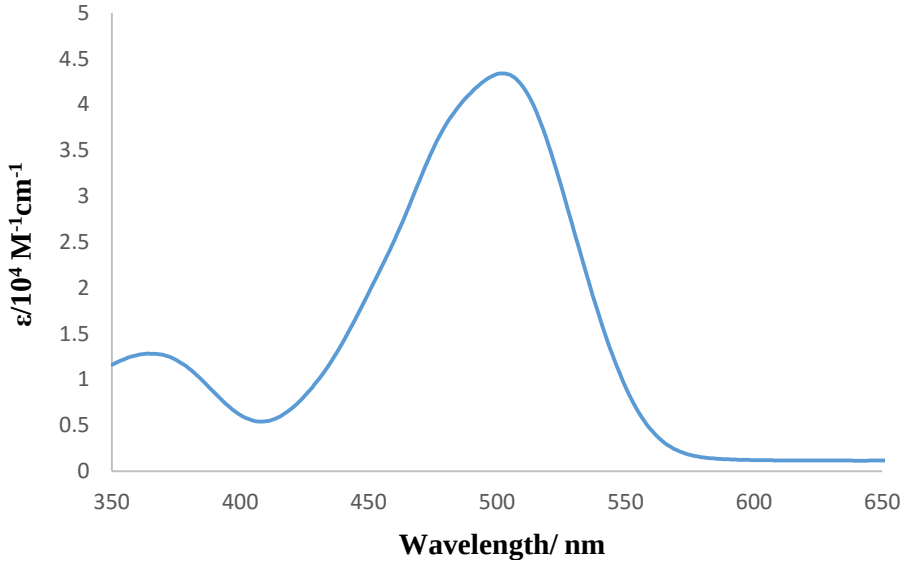

Compound 3.19c (THF at room temperature)

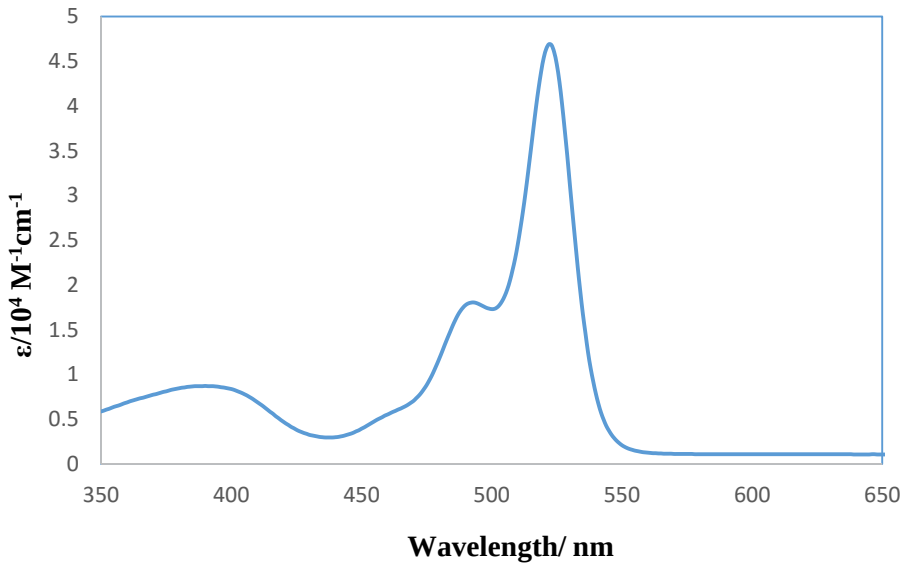

Compound3.19d (THF at room temperature)

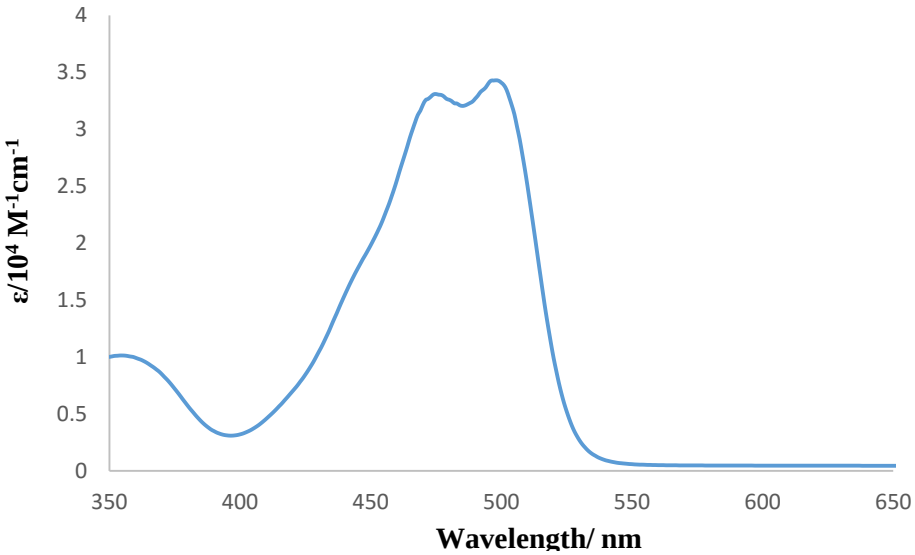

Compound 3.19e (THF at room temperature)

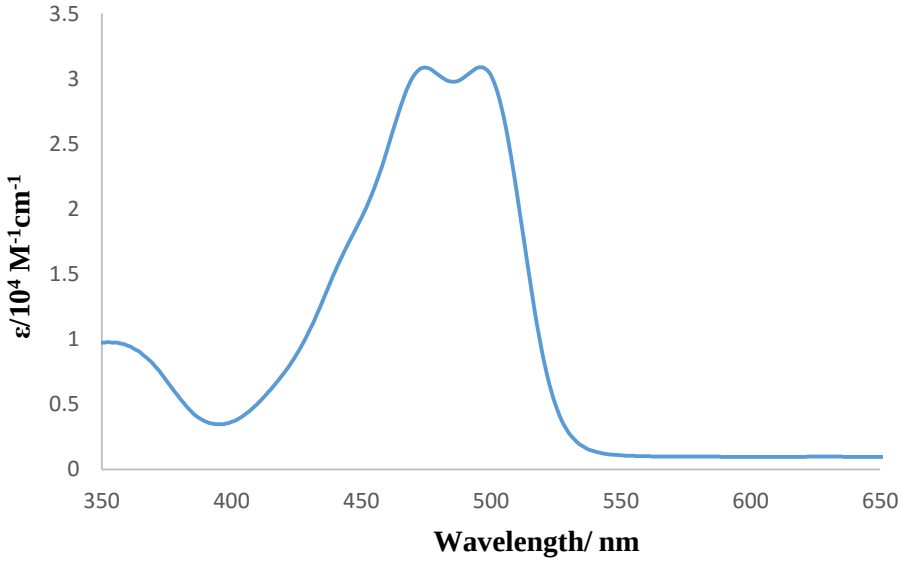

Compound 3.19f (THF at room temperature)

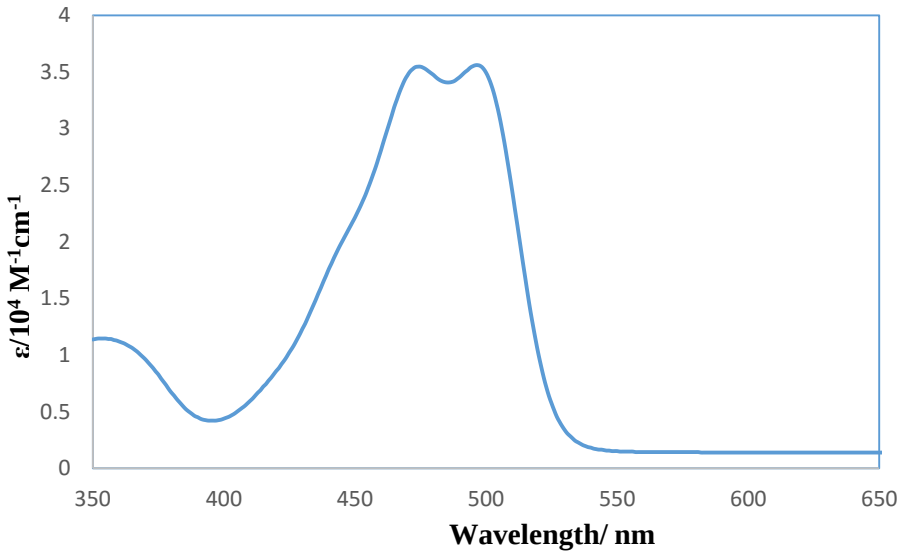

Compound 3,19g (THF at room temperature)

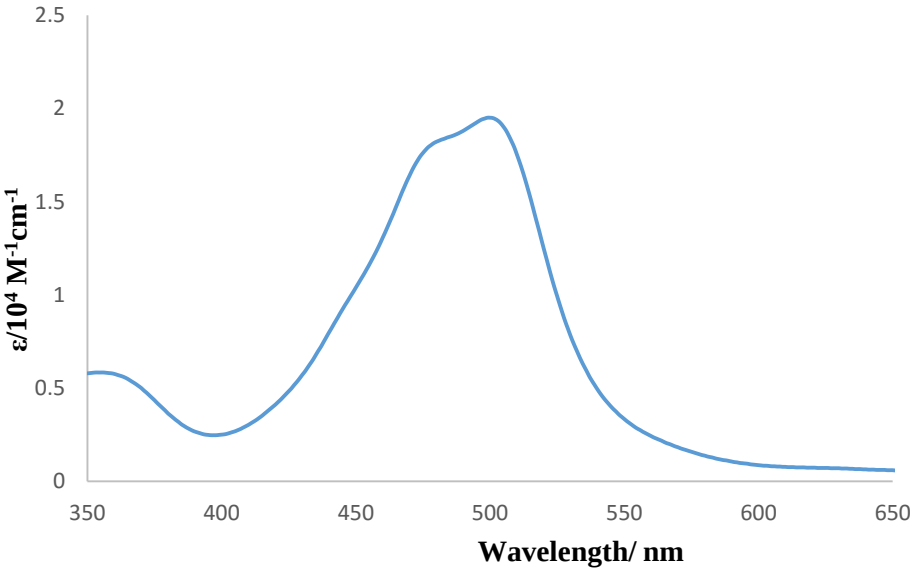

Compound 3.19h (THF at room temperature)

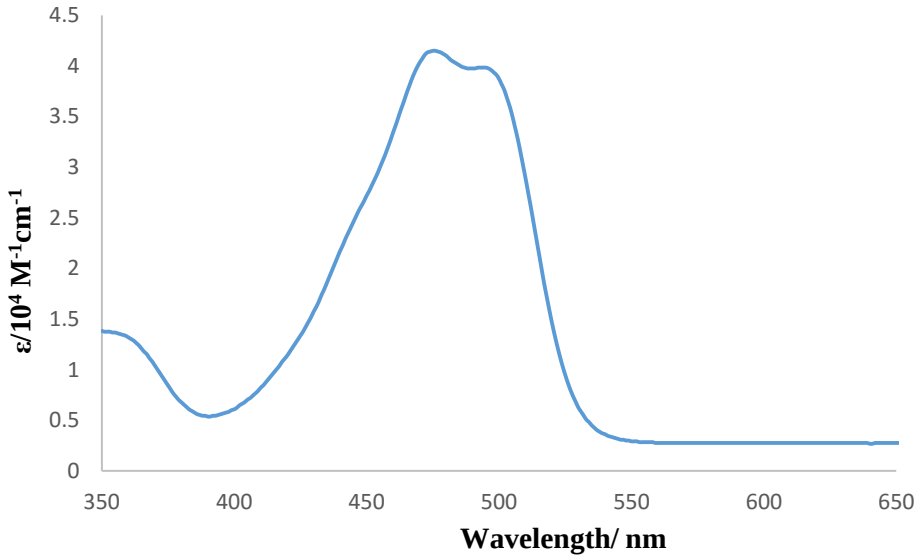

Compound 3.19j (THF at room temperature)

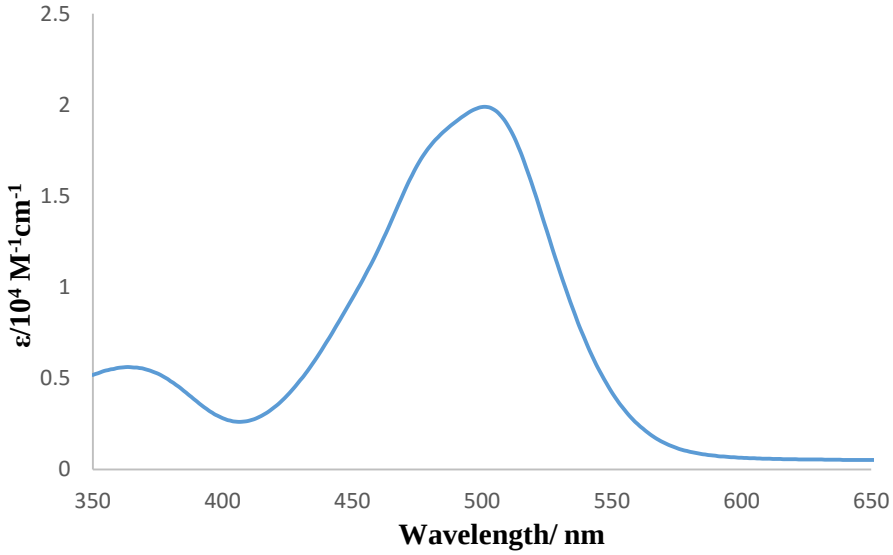

Compound 3.19m (THF at room temperature)

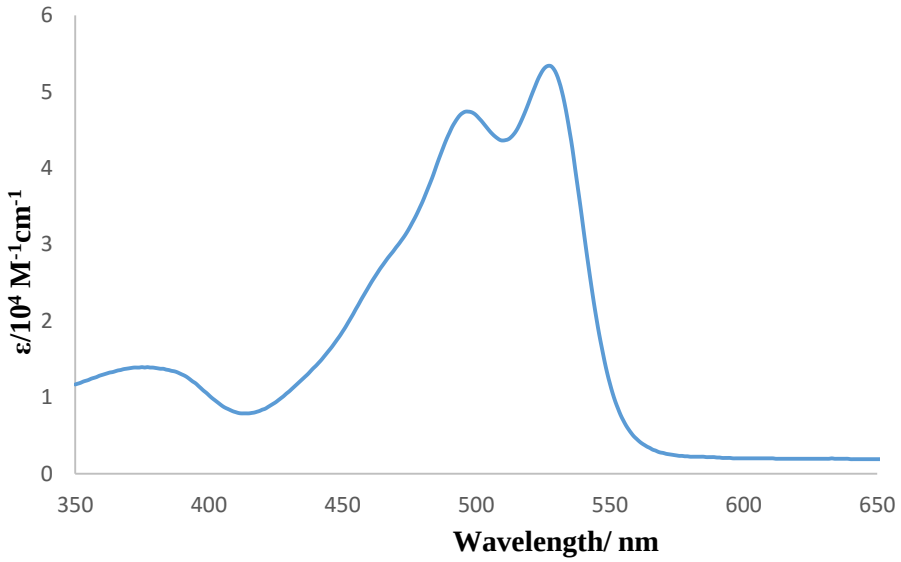

Compound 3.19n (THF at room temperature)

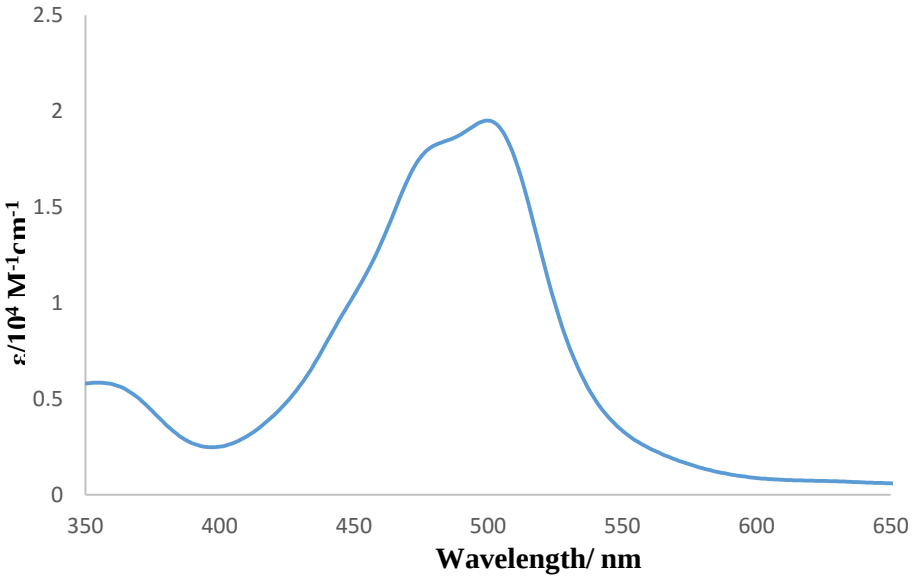

Organic & Biomolecular Chemistry

PAPER

View Article Online
View Journal | View Issue

CrossMark click for updates

Cite this: *Org. Biomol. Chem.*, 2015, **13**, 3819

Synthesis of 3-aminoBODIPY dyes *via* copper-catalyzed vicarious nucleophilic substitution of 2-halogeno derivatives†

Julian G. Knight,* Rua B. Alnoman and Paul G. Waddell

Received 18th December 2014,
Accepted 16th February 2015

DOI: 10.1039/c4ob02626h

www.rsc.org/obc

2-Halogeno BODIPYs undergo copper catalysed nucleophilic substitution with alkyl amines and anilines and an amide to give the corresponding 3-aminoBODIPY derivatives. The substrates are readily prepared by the regioselective 2-halogenation of the chemically robust, preformed BODIPYs thus providing an alternative to direct nucleophilic substitution of the corresponding 3-halogenoBODIPYs which requires regioselective 3-halogenation of the more sensitive dipyrromethane intermediate. 2-Halogenation expands the scope of vicarious substitution of BODIPYs to include weaker nitrogen nucleophiles.

Introduction

Boron dipyrromethenes (BODIPY, Fig. 1)[1] are fluorescent dyes which display high molar absorption coefficients, high fluorescence quantum yields, narrow absorption and emission bandwidths, and excitation and emission wavelengths in the visible/near infra red region.[2] The absorption and emission characteristics can be fine-tuned by modification of the substituents on the periphery of the BODIPY core. These favourable photophysical properties are complemented by chemical and photochemical robustness, including stability to air, water, and irradiation, a low tendency for self-aggregation in solution, good solubility in many organic solvents, and good synthetic accessibility. As a result, they have found extensive use as biological markers and fluorescence probes for reporting on the intracellular environment,[3] organic light emitting diodes and laser dyes,[4] and as the photosensitizer for applications in photocatalysis,[5] photodynamic therapy[6] and dye-sensitized solar cells.[7]

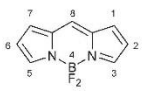

Fig. 1 Numbering scheme for 4,4-difluoro-4-bora-3a,4a-diaza-*s*-indacene (BODIPY).

BODIPYs containing a pendant amine which is able to act as an electron donor often display significant conjugative effects on the position of the absorption and emission maxima and/or fluorescence quenching due to intramolecular charge transfer. These effects can in principle be attenuated by co-ordination of the nitrogen lone pair to a Lewis or Brønsted acid, leading to restoration of the BODIPY fluorescence (switch on sensors).[8] Although the majority of the reported amine-containing BODIPYs have the nitrogen appended to a substituent, there are a number of examples in which the amine is directly substituted onto the BODIPY core and these have recently been the subject of very detailed structural and photophysical investigations motivated by the high level of current interest in elucidating the effects of the nature of the substituents on the properties of these fluorophores.[9]

The introduction of amine substituents directly linked to the BODIPY core is normally achieved by nucleophilic substitution (S_NAr) of a BODIPY carrying a suitable nucleofuge (*e.g.* halogen, methylthio, or methoxy).[9,10] In principle, because of the electronic requirements for S_NAr, aminolysis of halogenoBODIPYs is expected only to be possible in the 1,3,5,7, and 8 (meso) positions because attack at these positions allows the resulting intermediate anion to be effectively delocalised onto one of the nitrogen atoms of the BODIPY core.

An interesting alternative to S_NAr displacement of 3-halogenoBODIPYs is the vicarious oxidative nucleophilic hydrogen substitution by amines which occurs in the 3-position of unhalogenated 8-arylBODIPYs in the presence of a stoichiometric

School of Chemistry, Newcastle University, Newcastle upon Tyne, NE1 7RU, UK. E-mail: julian.knight@ncl.ac.uk

†Electronic supplementary information (ESI) available: Modified synthetic procedures for previously reported compounds **1** and **6**, X-ray crystal structure of compound **4a**, Schemes showing potential redox and base catalysed halogen dance mechanisms which were discounted by experiment, copies of NMR spectra for all compounds, and CIF files giving details of crystal data, structure solution, and refinement, atomic coordinates, bond distances, bond angles, and anisotropic displacement parameters for compounds **4a** and **5a**. CCDC 1040230–1040231. For ESI and crystallographic data in CIF or other electronic format see DOI: 10.1039/c4ob02626h

oxidant (DDQ, CAN, permanganate, or O_2). This reaction is reported to be successful for primary and secondary alkyl amines but to fail in the case of anilines.[11]

We report here a related copper catalysed amination[12] of 2-halogenoBODIPYs which allows substitution at the 3-position to take place with a wider range of amine nucleophiles than the oxidative hydrogen substitution, to include more weakly nucleophilic anilines and even an amide.

Results and discussion

Synthesis of the 2-iodoBODIPY 2

The 2-unsubstituted BODIPY **1** was prepared in good yield using a standard synthetic sequence[2b] from pyrrole and anisaldehyde *via* boron trifluoride-etherate catalysed condensation to the dipyrromethane,[13] DDQ oxidation to the corresponding dipyrromethene and reaction with boron trifluoride-etherate (Scheme 1). Regioselective iodination[10g] of **1** with ICl produced the 2-iodo-substituted BODIPY **2** together with a minor amount of the 2,6-diiodide **3** which were separable by column chromatography.

Copper catalysed amination of 2-iodoBODIPY 2

Although there are many reports of copper catalysed amination of halogenobenzene derivatives, the amination of 3-halogeno-5-membered heteroaromatic compounds is much less well studied. We first attempted to couple the iodoBODIPY **2** with hexylamine using a mixture of copper : copper(I) iodide catalyst in dimethylaminoethanol; conditions reported by Twieg for the copper catalysed amination of halothiophenes (Scheme 2).[14]

We were pleased to observe that amination had occurred, albeit in only 16% yield, but surprised to find that the product **4a** appeared to have been aminated in the 3-position. The structural assignment of **4a** was confirmed unambiguously by X-ray structure determination (Fig. S1, ESI†).

In this amination, dimethylaminoethanol acts both as a ligand for the copper and also as the solvent. In order to optimise the yield of this reaction we screened a series of bidentate ligands **L1–L4** (Fig. 2). Buchwald has reported the use of the diketone **L1** for room temperature amination of aryl halides, including 3-iodothiophene,[15] Ding has reported the use of β-ketopyridine **L2**, which is prepared in one step from tetrahydroquinoline, for amination of aryl halides,[16] and *N*,*N*′-dimethyl ethylenediamine[17] **L3** and 1,10-phenanthroline[18] **L4** are commonly used ligands for copper catalysed aminations.

Table 1 shows the results of the amination of the 2-iodoBODIPY **2** catalysed by copper(I)iodide in the presence of ligands **L1–L4**. The choice of solvent, base, catalyst and ligand

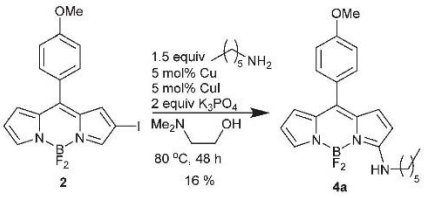

Scheme 2 Cu/CuI catalysed amination of BODIPY **2**.

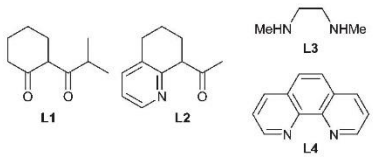

Fig. 2 Ligands screened in the amination of 2-iodoBODIPY **2**.

Table 1 Ligand variation in the amination of iodoBODIPY **2**

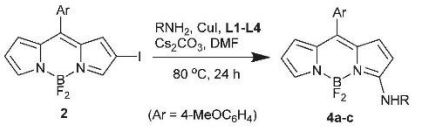

Entry[a]	R	Ligand	Product	Yield[b]
1	$CH_3(CH_2)_5$	**L1**	**4a**	30
2	$CH_3(CH_2)_5$	**L2**	**4a**	20
3	$CH_3(CH_2)_5$	**L3**	**4a**	35
4	*$CH_3(CH_2)_5$*	***L4***	***4a***	*60*
5	4-MeC_6H_4	**L1**	**4b**	6
6	4-MeC_6H_4	**L2**	**4b**	70
7	4-MeC_6H_4	**L3**	**4b**	30
8	*4-MeC_6H_4*	***L4***	***4b***	*84*
9	PhCO	**L1**	**4c**	6
10	PhCO	**L2**	**4c**	11
11	PhCO	**L3**	**4c**	10
12	*PhCO*	***L4***	***4c***	*15*

[a] Reagents and conditions: BODIPY **2** (0.235 mmol), amine/amide (0.470 mmol), CuI (5 mol%), ligand (20 mol%), Cs_2CO_3 (0.470 mmol), DMF (0.8 mL), 80 °C, 24 h. [b] Isolated yield of 3-substituted product **4**.

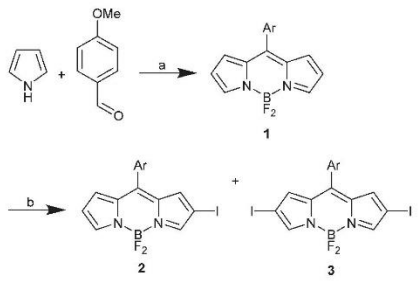

Scheme 1 Reagents: (a) $BF_3.OEt_2$, rt, 4 h (87%); DDQ, CH_2Cl_2, 0 °C, 30 min; $BF_3.OEt_2$, i-Pr_2NEt, rt, 2 h (77%); (b) ICl, CH_2Cl_2–MeOH, rt, 2 h (**2**, 65%; **3**, 15%). (Ar = 4-$MeOC_6H_4$).

loading were taken from Buchwald's report[15] using **L1**. Selection of 80 °C was based on an initial screen of reaction temperature using **L3** which indicated that no reaction with hexylamine was observed at 25 or 50 °C. It was confirmed that no reaction with hexylamine occurred at room temperature for any of these ligands.

As shown in Table 1, reaction with *n*-hexylamine, *p*-toluidine and benzamide proceeded to give the corresponding 3-substituted products **4a**, **4b**, and **4c** respectively. Ligand **L4** (1,10-phenanthroline) proved to give the highest yield regardless of the nature of the nucleophile (entries 4, 8, 12). Good yields were obtained in the case of the primary alkyl amine (entry 4) and the aniline (entry 8) and the reaction was successful even using the much more weakly nucleophilic benzamide albeit in low yield (entry 12).

The substrate scope of this reaction was investigated by applying these conditions, using phenanthroline (**L4**), to the reaction of the 2-iodoBODIPY **2** with a range of alkyl amines and anilines (Table 2).

The reaction works well with primary alkyl amines (entries 1 and 4–6) and the yields were also good with the secondary alkyl amines morpholine (entry 7) and pyrrolidine (entry 8). Yields were high for electron rich (entries 2, 10) primary anilines but were slightly lower in the cases of the less nucleophilic electron deficient anilines (entries 11, 12, 13), the more sterically hindered *ortho*-methylaniline (entry 9) and a secondary aniline (entry 14). In several cases the product **4** was accompanied by formation of a small amount of the corresponding 3-amino-6-iodoBODIPY **5** (Table 2, yields in parenthesis, Fig. 3). The structure of this by-product was confirmed unambiguously by X-ray structure determination in the case of the hexylamine derivative **5a** (Fig. 3).

Table 2 Scope of the amination of iodoBODIPY **2**

Entry[a]	R^1	R^2	Product	Yield[b]
1	$CH_3(CH_2)_5$	H	**4a**	60 (5)[c]
2	4-MeC_6H_4	H	**4b**	84 (5)[c]
3	PhCO	H	**4c**	15
4	$PhCH_2$	H	**4d**	64
5	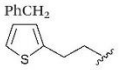	H	**4e**	65
6	Cyclohexyl	H	**4f**	78 (4)
7	$O(CH_2CH_2)_2$		**4g**	85
8	$CH_2CH_2CH_2CH_2$		**4h**	87 (4)
9	2-MeC_6H_4	H	**4i**	60
10	4-$MeOC_6H_4$	H	**4j**	78 (6)
11	4-ClC_6H_4	H	**4k**	66 (13)[c]
12	4-NCC_6H_4	H	**4l**	77 (15)[c]
13	2-Pyridyl	H	**4m**	60 (14)[c]
14	Ph	Me	**4n**	40

[a] Reagents and conditions: BODIPY **2** (0.235 mmol), amine/amide (0.470 mmol), CuI (5 mol%), phenanthroline (**L4**) (20 mol%), Cs_2CO_3 (0.470 mmol), DMF (0.8 mL), 80 °C, 24 h. [b] Isolated yield of 3-substituted product **4**. [c] Yield of 6-iodo-3-amino by-product **5** (see later).

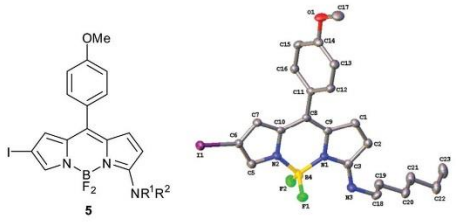

Fig. 3 Structure of 3-amino-6-iodoBODIPY by-product **5** and molecular structure of **5a**. Hydrogen atoms have been omitted for clarity. The asymmetric unit comprises four independent molecules; one is shown here as the rest are similar.

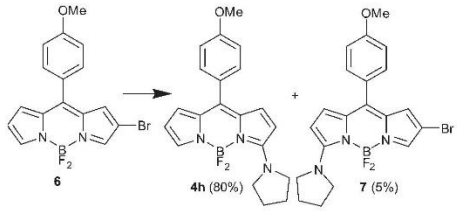

Scheme 3 Reagents and conditions: pyrrolidine (2.0 eq.), CuI (5 mol%), **L4** (20 mol%), Cs_2CO_3 (2.0 eq.), DMF, 80 °C, 24 h.

The reaction is equally successful from the 2-bromoBODIPY **6** which was prepared by treatment of the unsubstituted BODIPY **1** with NBS (73%). The 2-bromo derivative **6** reacted with pyrrolidine to give the 3-amino product **4h** in 80% yield, together with a minor amount (5%) of the corresponding 3-amino-6-bromo byproduct **7** (Scheme 3).

Surprisingly, the 2,6-diiodoBODIPY **3** is unchanged under the reaction conditions and does not produce any singly or doubly aminated products.[19]

Mechanism of reaction

No reaction occurs between the iodide **2** and pyrrolidine in the absence of copper iodide and, as Table 1 indicates, the nature of the ligand influences the amination yield. In the absence of any added ligand the amination product **4h** was formed in 50% yield (together with a trace of **5h**). If the base (Cs_2CO_3) is omitted then the product **4h** is formed in low yield (14%) together with **5h** (10%). Thus copper is obligatory for the amination to occur and the ligand and base improve the conversion.[20] Scheme 4 shows a mechanism which is similar to that proposed for the oxidative hydrogen displacement of non-halogenated BODIPYs with alkyl amines.[11] The necessity for copper catalysis suggests that the nucleophile might be an

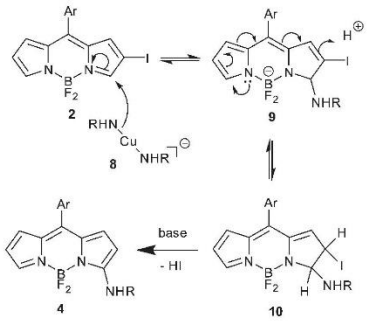

Scheme 4 Suggested mechanistic pathway initiated by nucleophilic attack.

amido copper species such as **8**.[21] Initial nucleophilic attack at C-3 leads to an anion **9** which could be copper-bound, corresponding to an amidocupration, but may be delocalised over the BODIPY π-system. In order to produce the product, iodide must be lost and this requires protonation at C-2 to give **10** followed by base-mediated elimination of HI. There are reports of the acid- or Lewis-acid-catalysed reaction of nitrogen nucleophiles with 3-haloindoles in which substitution occurs at the adjacent 2-position[22] and although these are proposed to be initiated by protonation the mechanism otherwise resembles that in Scheme 4.[23,24]

Isotopic labelling was employed to support the proposed mechanistic scheme. The 2,6-diiodoBODIPY **3** was converted to the 6-deuterio-2-iodoBODIPY **11** by palladium catalysed reduction with dideuterium (Scheme 5). A minor amount (17%) of the 2,6-dideuteriated BODIPY (2,6-$^2H_2$-**1**) was also formed but was easily separated by column chromatography. Amination of the iodide **11** with pyrrolidine produced a 70 : 30 ratio of the 3-amino-6-deuterioBODIPY **12** together with the regioisomeric 3-amino-2-deuterioBODIPY **13** (Scheme 5).

Formation of 3-amino-6-deuterioBODIPY **12** as the major product is consistent with the straightforward nucleophilic substitution mechanism (as shown in Scheme 4), but the presence of the regioisomeric 2-deuteriated product **13** indicates a minor pathway involving nucleophilic attack by the amine at C-5 in the iodoBODIPY **11** (and **2**). The unequal ratio of products **12** : **13** rules out any mechanisms involving prior dehalogenation to generate the unsubstituted BODIPY **1** *in situ*. Two other potential mechanisms, one based on a redox cycle[23] and one on a Base Catalysed Halogen Dance[24] were discounted on the basis of the results above.

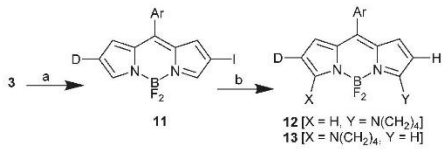

Scheme 5 Reagents: (a) D_2, Pd/C, CH_2Cl_2, rt, 5 h (60%); (b) pyrrolidine (2.0 eq.), CuI (5 mol%), **L4** (20 mol%), Cs_2CO_3 (2.0 eq.), DMF, 80 °C, 24 h (95%; **12** : **13** = 70 : 30). (Ar = 4-MeOC$_6$H$_4$).

Table 3 Absorption and fluorescence data for compounds **1**, **4a–n** in THF

BODIPY[a]	λ_{abs} (max)/ nm	$\varepsilon/10^4$ M^{-1} cm^{-1}	λ_{em} (max)/ nm	Φ_f[b] (λ_{ex})
1	494	4.59	508	0.075 (479)
4a	493	3.51	525	0.026 (484)
4a[c]	508[c]	2.09[c]	524[c]	0.058[c] (484)
4b	500	4.34	—[d]	—[d]
4c	522	4.69	534	0.050 (492)
4d	498	3.43	525	0.030 (484)
4e	496	3.09	528	0.033 (485)
4f	496	3.56	525	0.015 (484)
4g	484	3.23	—[d]	—[d]
4h	476	4.15	540	0.005 (490)
4i	500	3.07	—[d]	—[d]
4j	501	1.99	—[d]	—[d]
4k	508	4.53	565	0.007 (475)
4l	533	5.34	557	0.015 (500)
4m	527	0.97	549	0.022 (497)
4n	500	1.95	—[d]	—[d]

[a] All spectra were recorded in THF. [b] Φ_f determined *vs.* rhodamine 6G in ethanol (Φ_f = 0.95)[27] as reference. Excitation wavelength (λ_{ex}/nm) shown in brackets. [c] Value determined in cyclohexane. [d] Virtually non-fluorescent.

Photophysical properties of the 3-aminoBODIPYs 4

The absorption and fluorescence data for the 3-aminoBODIPY compounds **4a–n** and the parent unsubstituted compound **1** are summarized in Table 3.

Fig. 4 shows the absorption and fluorescence spectra for the parent 8-(4-methoxyphenyl)BODIPY **1**, and for the representative amine and aniline derivatives **4a** and **4l** respectively.

The photophysical properties of amino-substituted BODIPYs have previously been reported in detail.[9,10] As shown in Table 3, all of the compounds have low quantum yields, and some are essentially non-fluorescent which can be attributed in part to the free rotation of the aryl substituent in the

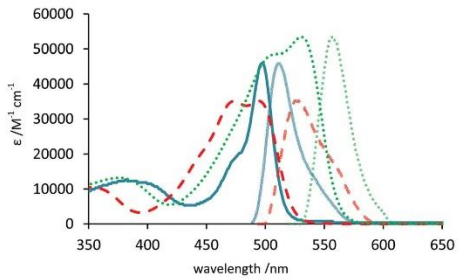

Fig. 4 Absorption spectrum (heavy lines) in terms of the molar absorption coefficient (ε) and normalised fluorescence spectrum (feint lines) for **1** (—), **4a** (----), and **4l** (·····) in THF.

8-position and partly due to the influence of the amine. Although low fluorescence of this type of BODIPY might be considered detrimental it is in fact a key feature in their use as 'switch-on' fluorescent probes and this has recently been demonstrated to good effect.[8,9g,10f,i] The red-shift in the absorption maximum, relative solvent insensitivity of the emission maximum, and slight increase in quantum yield in cyclohexane compared to the more polar THF for the hexylamine derivative **4a** (Table 3) are all in accord with reports on other 3-aminoBODIPYs.[4d,9f,10b,n,o,11]

Conclusions

2-Halogeno BODIPYs undergo copper catalysed vicarious nucleophilic substitution with alkyl amines and anilines to give the corresponding 3-aminoBODIPY derivatives. The corresponding reaction with a less nucleophilic amide also proceeded albeit in low yield. The observation that the 2,6-diiodoBODIPY does not react under these conditions allows straightforward separation of this byproduct after the amination.

There are two existing approaches to these products, but both have limitations:

(i) Direct nucleophilic substitution of the corresponding 3-halogenoBODIPYs, which requires regioselective introduction of the halogen into the 3-position which must be performed either on the somewhat sensitive dipyrromethane intermediate[28,10h] or involves lengthier synthesis of a halogenated acylpyrrole;[29]

(ii) Direct oxidative hydrogen substitution of a 3,5-unsubstituted BODIPY is known[11] but this method cannot be used with weak nitrogen nucleophiles such as anilines or amides.

Experimental

General

All manipulations involving air-sensitive materials were carried out using standard Schlenk line techniques under an atmosphere of nitrogen in flame-dried glassware. $CHCl_3$, CH_2Cl_2 and NEt_3 were distilled from CaH_2; MeOH and EtOH from magnesium; 1,4-dioxane, Et_2O and THF from Na/benzophenone; toluene from sodium; and MeCN from K_2CO_3, under an atmosphere of nitrogen. DMF was dried over activated 4 Å molecular sieves and stored under nitrogen. All other chemicals were purchased from commercial suppliers and used without further purification. ^1H and $^{13}C\{^1H\}$ NMR spectra were recorded on either a JEOL ECS 400 or a Bruker Avance 300 instrument. All NMR were referenced relative to $CDCl_3$ (δ_H = 7.26, δ_C = 77.16). IR spectra were recorded on a Varian 800 FT-IR Scimitar Series infrared spectrometer. Mass spectra were recorded on Waters ACQUITY UPLC LCT premier MS in positive ion mode. UV-vis and fluorescence spectra were recorded at 20 °C on a Shimadzu UV-1800 and Hitachi F2500 machines respectively. Relative fluorescence quantum yields (Φ_f) were determined using dilute solutions with an absorbance below 0.1 at the excitation wavelength and using Rhodamine 6G (Φ_f = 0.95)[27] in ethanol as standard. TLC was carried out on glass plates pre-coated with silica gel $60F_{254}$ and flash column chromatography was performed on Fluorochem LC3025 (40–63 μm) silica gel. Compounds **1**,[30] and **6**[10h] were prepared by modifications to the reported procedures (see ESI†).

X-ray crystal structure analysis

Single crystals were prepared by slow diffusion of hexane into a solution of the compound in chloroform. Crystal structure data was collected at 150 K on an Oxford Diffraction (Agilent Technologies) Gemini A Ultra using MoKα radiation (λ = 0.71073 Å) and equipped with an Oxford Cryosystems Cryostream open-flow N_2 cooling device. Cell refinement, data collection and data reduction were carried out using Oxford Diffraction CrysalisPro.[31] The intensities were corrected for absorption semi-empirically based on repeated, symmetry-equivalent reflections in the case of **4a** and analytically using a multi-faceted crystal model in the case of **5a**.[32]

The structures were solved *via* direct methods and refined on F^2 values for all unique data. Refinements were performed using SHELXL[33] within the Olex2 program.[34] Hydrogen atoms were positioned geometrically and defined as riding on their parent atoms.

Materials

2-Iodo-8-(4-methoxyphenyl)-4,4-difluoro-4-bora-3a,4a-diaza-*s*-indacene 2 and 2,6-diiodo-8-(4-methoxyphenyl)-4,4-difluoro-4-bora-3a,4a-diaza-*s*-indacene 3. 8-(4-Methoxyphenyl)-4,4-difluoro-4-bora-3a,4a-diaza-*s*-indacene **1** (0.200 g, 0.67 mmol) was taken in dry CH_2Cl_2–MeOH (1 : 1, 48 mL). A solution of ICl (0.11 g, 0.67 mmol) in MeOH (5 mL) was added to the mixture dropwise. The mixture was stirred at room temperature for 2 h. The solvent was then removed under reduced pressure and the crude product was dissolved in CH_2Cl_2 (50 mL) and washed with H_2O (2 × 100 mL). The organic layer was dried ($MgSO_4$) and the solvent was removed under reduced pressure. The resulting red crude product was purified by column chromatography (CH_2Cl_2–petroleum ether 1 : 1) to give:

First eluted, the 2,6-diiodide **3** as a pink solid (0.055 g, 15%), mp 246–248 °C. R_f = 0.4 (CH_2Cl_2–petrol, 1 : 1). ^1H NMR (400 MHz, $CDCl_3$) δ 7.85 (s, 2H), 7.52 (d, J = 8.5 Hz, 2H), 7.13 (s, 2H), 7.06 (d, J = 8.5 Hz, 2H), 3.91 (s, 3H).^{13}C NMR (101 MHz, $CDCl_3$) δ 162.86, 147.74, 145.96, 137.50, 135.93, 132.64, 125.62, 114.57, 72.07, 55.75. ^{11}B NMR (128 MHz, $CDCl_3$) δ −1.27 (t, J_{BF} = 28.0 Hz). ^{19}F NMR (376 MHz, $CDCl_3$) δ −144.63 (q, J_{FB} = 28.0 Hz). IR (neat): ν_{max}/cm^{-1}: 3113, 2930, 1725, 1596, 1566, 1528, 1466, 1342, 1246, 1074, 984, 896, 707. HRMS-ES Calcd for $C_{16}H_{11}BN_2OF_2I_2 + Na^+$: 572.8920. Found: 572.8920.

Second eluted, the monoiodide **2** as a red solid (0.185 g, 65%), mp 206–208 °C. R_f = 0.3 (CH_2Cl_2–petrol, 1 : 1). ^1H NMR (400 MHz, $CDCl_3$) δ 7.96 (s, 1H), 7.81 (s, 1H), 7.52 (d, J = 8.8 Hz, 2H), 7.05 (d, J = 8.8 Hz, 4H), 6.59 (d, J = 4.3 Hz, 1H), 3.91 (s, 3H). ^{13}C NMR (101 MHz, $CDCl_3$) δ 162.51, 146.73,

146.11, 145.22, 135.99, 135.78, 135.08, 133.00, 132.57, 125.95, 119.46, 114.36, 70.73, 55.69. ^{19}F NMR (376 MHz, $CDCl_3$) δ −144.72 (q, J_{FB} = 28.0 Hz). ^{11}B NMR (128 MHz, $CDCl_3$) δ −1.26 (t, J_{BF} = 28.0 Hz). IR (neat): ν_{max}/cm^{-1}: 3109, 2849, 1721, 1603, 1573, 1532, 1470, 1400, 1349, 1250, 1062, 982, 706. HRMS-ES Calcd for $C_{16}H_{12}BN_2OF_2I$ + Na^+: 446.9953. Found: 446.9961.

General procedure for copper catalysed amination

2-Iodo-8-(4-methoxyphenyl)-4,4-difluoro-4-bora-3a,4a-diaza-*s*-indacene **2** (0.100 g, 0.235 mmol), the amine (0.470 mmol), CuI (2.2 mg, 0.01 mmol, 5 mol%) Cs_2CO_3 (0.154 g, 0.470 mmol), and 1,10-phenanthroline (8.5 mg, 0.047 mmol, 20 mol%) were taken in a flame-dried Schlenk tube and flushed with N_2 several times. Dry DMF (0.8 mL) was then added and the mixture was stirred at 80 °C for 24 h. The mixture was dissolved in ethyl acetate (30 mL) and washed with water (2 × 100 mL). The organic layer was dried ($MgSO_4$) and the solvent was removed under reduced pressure. The crude product was purified by column chromatography. In all cases the 3-amino-6-iodo byproduct **5** eluted from the column first and the 3-amino compound **4** second.

3-(Hexylamino)-8-(4-methoxyphenyl)-4,4-difluoro-4-bora-3a,4a-diaza-*s*-indacene 4a. Eluted with CH_2Cl_2–petroleum ether (1 : 1). Dark yellow solid (0.056 g, 60%); mp 202–204 °C; ^{1}H NMR (400 MHz, $CDCl_3$) δ 7.45–7.37 (m, 3H), 6.97 (dd, J = 6.7, 4.7 Hz, 2H), 6.94 (s, 1H), 6.44 (d, J = 3.5 Hz, 1H), 6.33 (dd, J = 3.6, 2.4 Hz, 1H), 6.23 (s, 1H), 6.16 (d, J = 5.0 Hz, 1H), 3.86 (s, 3H), 3.38 (dd, J = 13.5, 6.8 Hz, 2H), 1.75–1.62 (m, 2H), 1.45–1.35 (m, 2H), 1.34–1.25 (m, 4H), 0.89 (dd, J = 9.0, 4.5 Hz, 3H). ^{13}C NMR (101 MHz, $CDCl_3$) δ 161.67, 160.49, 136.12, 133.40, 132.80, 132.75, 131.75, 130.84, 127.15, 119.78, 113.74, 113.39, 110.06, 55.47, 44.82, 31.44, 30.18, 26.32, 22.59, 14.08. ^{11}B NMR (128 MHz, $CDCl_3$) δ −0.01 (t, J_{BF} = 33.5 Hz). ^{19}F NMR (376 MHz, $CDCl_3$) δ −149.24 (q, J_{FB} = 33.5 Hz). IR (neat): ν_{max}/cm^{-1}: 3413, 3127, 2923, 1606, 1524, 1471, 1397, 1372, 1243, 1178, 1021, 977, 759. HRMS-ES Calcd for $C_{22}H_{26}BN_3OF_2$ + Na^+: 419.2071. Found: 419.2060.

3-(Hexylamino)-6-iodo-8-(4-methoxyphenyl)-4,4-difluoro-4-bora-3a,4a-diaza-*s*-indacene 5a. Eluted with CH_2Cl_2–petroleum ether (1 : 1). Dark yellow solid (0.006 g, 5%), ^{1}H NMR (400 MHz, $CDCl_3$) δ 7.42–7.34 (m, 3H), 7.01–6.93 (m, 3H), 6.47 (s, 1H), 6.31 (s, 1H), 6.23 (d, J = 5.0 Hz, 1H), 3.40 (q, J = 6.8 Hz, 2H), 1.68 (p, J = 7.3 Hz, 2H), 1.43–1.28 (m, 6H), 0.93–0.86 (m, 3H).^{13}C NMR (101 MHz, $CDCl_3$) δ 162.04, 160.65, 136.78, 134.61, 134.21, 133.74, 131.67, 131.05, 126.57, 124.84, 113.92, 111.30, 65.08, 55.51, 44.97, 31.41, 30.19, 26.30, 22.57, 14.07. HRMS-ES Calcd for $C_{22}H_{25}BN_3OF_2$ + Na^+: 546.1001. Found: 546.1005.

3-((4-Methylphenyl)amino)-8-(4-methoxyphenyl)-4,4-difluoro-4-bora-3a,4a-diaza-*s*-indacene 4b. Eluted with CH_2Cl_2–petroleum ether (1 : 1). Orange solid (0.080 g, 84%); mp 186–188 °C; ^{1}H NMR (300 MHz, $CDCl_3$) δ 7.86 (s, 1H), 7.43 (s, 1H), 7.39 (d, J = 8.7 Hz, 2H), 7.15 (d, J = 8.4 Hz, 2H), 7.09 (d, J = 8.5 Hz, 2H), 6.92 (d, J = 8.8 Hz, 2H), 6.89 (s, 1H), 6.47 (d, J = 3.3 Hz, 1H), 6.35–6.30 (m, 1H), 6.28 (d, J = 4.9 Hz, 1H), 3.81 (s, 3H), 2.30 (s, 3H). ^{13}C NMR (101 MHz, $CDCl_3$) δ 160.74, 158.94, 136.20, 135.72, 135.01, 134.70, 133.13, 132.91, 132.17, 131.83, 130.38, 126.96, 122.89, 121.24, 113.97, 113.85, 111.16, 55.50, 21.08. IR (neat): ν_{max}/cm^{-1}: 3368, 2914, 2839, 1606,1580,1523,1489, 1397, 1293, 1241, 1175, 1032, 973, 787. ^{19}F NMR (376 MHz, $CDCl_3$) δ −148.37 (q, J_{FB} = 33.0 Hz). ^{11}B NMR (128 MHz, $CDCl_3$) δ 0.06 (t, J_{BF} = 33.0 Hz).HRMS-ES Calcd for $C_{23}H_{20}BN_3OF_2$ + H^+: 404.1742. Found: 404.1740.

6-Iodo-3-((4-methylphenyl)amino)-8-(4-methoxyphenyl)-4,4-difluoro-4-bora-3a,4a-diaza-*s*-indacene 5b. Eluted with CH_2Cl_2–petroleum ether (1 : 1). Purple solid (0.007 g, 5%), ^{1}H NMR (400 MHz, $CDCl_3$) δ 7.99 (s, 1H), 7.42 (d, J = 3.8 Hz, 2H), 7.40 (s, 1H), 7.22 (d, J = 8.1 Hz, 2H), 7.15 (d, J = 8.2 Hz, 2H), 6.99 (s, 1H), 6.98 (d, J = 8.4 Hz, 2H), 6.56 (s, 1H), 6.37 (d, J = 4.9 Hz, 1H), 3.87 (s, 3H), 3.79 (s, 1H), 2.37 (s, 3H).^{13}C NMR (101 MHz, $CDCl_3$) δ 160.88, 159.64, 136.79, 136.39, 135.70, 134.56, 134.26, 133.53, 132.88, 131.73, 130.44, 126.43, 126.06, 123.28, 114.00, 112.47, 65.60, 55.52, 21.10. IR (neat): ν_{max}/cm^{-1}: 3374.918, 2934.681, 1712.014, 1604.078, 1519.013, 1477.763, 138.029, 1250.856, 1031.766, 733.380. HRMS-ES Calcd for $C_{23}H_{19}BN_3OF_2I$ + Na^+: 551.0568. Found: 551.0565.

3-(*N*-Benzamido)-8-(4-methoxyphenyl)-4,4-difluoro-4-bora-3a,4a-diaza-*s*-indacene 4c. Eluted with CH_2Cl_2–petroleum ether (1 : 1). Orange solid (0.015 g, 15%); ^{1}H NMR (400 MHz, $CDCl_3$) δ 9.61 (s, 1H), 7.97 (d, J = 7.8 Hz, 2H), 7.67 (s, 1H), 7.63 (d, J = 7.5 Hz, 1H), 7.56 (d, J = 7.0 Hz, 2H), 7.51 (d, J = 8.4 Hz, 2H), 7.39 (d, J = 4.7 Hz, 1H), 7.09 (d, J = 4.7 Hz, 1H), 7.03 (d, J = 8.4 Hz, 2H), 6.79 (d, J = 3.8 Hz, 1H), 6.53–6.40 (m, 1H), 3.90 (s, 3H). ^{13}C NMR (101 MHz, $CDCl_3$) δ 164.04, 161.68, 152.47, 142.51, 137.46, 135.05, 133.70, 133.35, 132.55, 132.22, 131.26, 129.28, 127.61, 127.01, 126.29, 116.29, 114.09, 113.34, 55.60. ^{11}B NMR (128 MHz, $CDCl_3$) δ −0.15 (t, J_{BF} = 33.1 Hz). ^{19}F NMR (376 MHz, $CDCl_3$) δ −146.81 (q, J_{FB} = 33.1 Hz). IR (neat): ν_{max}/cm^{-1}: 3402, 2919, 1692, 1588, 1503, 1444, 1348, 1287, 1250, 1176, 1057, 1033 977, 699. HRMS-ES Calcd for $C_{23}H_{18}BN_3O_2F_2$ + Na^+: 440.1358. Found: 440.1360.

3-(Benzylamino)-8-(4-methoxyphenyl)-4,4-difluoro-4-bora-3a,4a-diaza-*s*-indacene 4d. Eluted with CH_2Cl_2–petroleum ether (1 : 1). Dark orange solid (0.061 g, 61%); mp 132–134 °C; ^{1}H NMR (400 MHz, $CDCl_3$) δ 7.44 (s, 1H), 7.42 (d, J = 8.7 Hz, 2H), 7.40–7.36 (m, 1H), 7.34 (d, J = 6.6 Hz, 2H), 7.33–7.28 (m, 2H), 6.97 (d, J = 8.5 Hz, 2H), 6.92 (d, J = 4.9 Hz, 1H), 6.64 (s, 1H), 6.48 (d, J = 3.6 Hz, 1H), 6.34 (dd, J = 3.5, 2.5 Hz, 1H), 6.11 (d, J = 4.9 Hz, 1H), 4.60 (d, J = 6.3 Hz, 2H), 3.86 (s, 3H).^{13}C NMR (101 MHz, $CDCl_3$) δ 161.71, 160.60, 136.81, 136.14, 133.85, 133.28, 132.85, 131.78, 131.51, 129.15, 128.16, 127.02, 126.93, 120.55, 113.78, 113.68, 110.04, 55.48, 48.22. ^{11}B NMR (128 MHz, $CDCl_3$) δ 0.02 (t, J_{BF} = 33.5 Hz). ^{19}F NMR (376 MHz, $CDCl_3$) δ −148.95 (q, J_{FB} = 33.5 Hz). IR (neat): ν_{max}/cm^{-1}: 3360, 2970, 1705, 1619, 1466, 1379, 1160, 1128, 951, 816. HRMS-ES Calcd for $C_{23}H_{20}BN_3OF_2$ + Na^+: 426.1565. Found: 426.1584.

3-((2-(Thiophen-2-yl)ethyl)amino)-8-(4-methoxyphenyl)-4,4-difluoro-4-bora-3a,4a-diaza-*s*-indacene 4e. Eluted with CH_2Cl_2–petroleum ether (1 : 1). Orange solid (0.065 g, 65%); mp 119–120 °C; ^{1}H NMR (400 MHz, $CDCl_3$) δ 7.41 (dd, J = 9.0, 2.4 Hz, 3H), 7.18 (dd, J = 5.1, 1.3 Hz, 1H), 6.96 (t, J = 7.1 Hz,

3H), 6.91 (dd, J = 2.9, 2.2 Hz, 2H), 6.46 (d, J = 3.5 Hz, 1H), 6.36 (s, 1H), 6.33 (dd, J = 3.7, 2.3 Hz, 1H), 6.06 (d, J = 5.0 Hz, 1H), 3.86 (s, 3H), 3.65 (q, J = 6.6 Hz, 2H), 3.18 (t, J = 6.7 Hz, 2H).^{13}C NMR (101 MHz, $CDCl_3$) δ 161.45, 160.55, 139.31, 136.06, 133.32, 132.79, 131.78, 131.21, 127.53, 127.04, 126.43, 124.69, 120.20, 113.77, 113.58, 109.73, 55.50, 46.23, 30.84. ^{11}B NMR (128 MHz, $CDCl_3$) δ −0.04 (t, J_{BF} = 33.2 Hz), ^{19}F NMR (376 MHz, $CDCl_3$) δ −148.47–−149.21 (m). IR (neat): ν_{max}/cm^{-1}3361, 2923, 178, 1606, 1401, 1293, 1257, 1025, 792. HRMS-ES Calcd for $C_{22}H_{20}BN_3OF_2S$ + H^+: 424.1466. Found: 424.1456

3-(Cyclohexylamino)-8-(4-methoxyphenyl)-4,4-difluoro-4-bora-3a,4a-diaza-*s*-indacene 4f. Eluted with CH_2Cl_2–petroleum ether (1 : 1). Orange solid (0.073 g, 78%); mp 130–131 °C; ^{1}H NMR (400 MHz, $CDCl_3$) δ 7.40 (d, J = 8.4 Hz, 2H), 6.96 (d, J = 8.6 Hz, 2H), 6.93 (d, J = 5.0 Hz, 1H), 6.43 (d, J = 3.3 Hz, 1H), 6.32 (dd, J = 3.6, 2.4 Hz, 1H), 6.19 (s, 1H), 6.16 (d, J = 5.0 Hz, 1H), 3.86 (s, 2H), 3.43 (d, J = 8.8 Hz, 1H), 2.02 (d, J = 10.2 Hz, 2H), 1.81 (d, J = 13.3 Hz, 2H), 1.63 (d, J = 16.3 Hz, 1H), 1.53–1.14 (m, 4H).^{13}C NMR (101 MHz, $CDCl_3$) δ 160.76, 160.45, 136.09, 133.34, 132.78, 132.47, 131.73, 130.67, 127.19, 119.56, 113.74, 113.29, 110.49, 55.47, 53.79, 33.62, 25.21, 24.53. ^{11}B NMR (128 MHz, $CDCl_3$) δ −0.01 (t, J_{BF} = 30.0 Hz). ^{19}F NMR (376 MHz, $CDCl_3$) δ −149.24 (q, J_{FB} = 30.0 Hz) IR (neat): ν_{max}/cm^{-1}: 2931, 2858, 1718, 1604, 1511, 1293, 1253, 1175, 1062, 1027, 839, 795. HRMS-ES Calcd for $C_{22}H_{24}BN_3OF_2$ + Na^+: 418.1878. Found: 418.1879.

3-(Cyclohexylamino)-6-iodo-8-(4-methoxyphenyl)-4,4-difluoro-4-bora-3a,4a-diaza-*s*-indacene 5f. Eluted with CH_2Cl_2–petroleum ether (1 : 1). Dark yellow solid (0.005 g, 4%), ^{1}H NMR (400 MHz, $CDCl_3$) δ7.35 (s, 1H), 7.37 (d, J = 8.8 Hz, 2H), 6.96 (d, J = 7.8 Hz, 2H), 6.97 (s, 1H), 6.46 (s, 1H), 6.23 (s, 2H), 3.86 (s, 3H), 3.52–3.38 (m, 1H), 2.08–1.98 (m, 2H), 1.86–1.75 (m, 2H), 1.65 (d, J = 12.8 Hz, 1H), 1.50–1.21 (m, 5H). ^{13}C NMR (101 MHz, $CDCl_3$) δ 161.11, 160.61, 136.72, 134.45, 134.21, 133.70, 131.66, 130.77, 126.62, 124.63, 113.91, 111.71, 65.00, 55.51, 54.04, 33.64, 25.14, 24.53. IR (neat): ν_{max}/cm^{-1}: 3372.915, 2916.489, 1608.145, 1573.648, 1518.964, 1480.453, 1392.344, 1251.759, 1101.075. HRMS-ES Calcd for $C_{22}H_{23}BN_3OF_2I$ + Na^+: 544.0845. Found: 544.0850.

3-(Morpholino)-8-(4-methoxyphenyl)-4,4-difluoro-4-bora-3a,4a-diaza-*s*-indacene 4g. Eluted with CH_2Cl_2–petroleum ether (9 : 1). Orange solid (0.076 g, 85%); mp 214–215 °C; ^{1}H NMR (400 MHz, $CDCl_3$) δ 7.45 (s, 1H), 7.40 (d, J = 8.6 Hz, 2H), 6.97 (d, J = 8.6 Hz, 2H), 6.92 (d, J = 5.1 Hz, 1H), 6.42 (d, J = 3.3 Hz, 1H), 6.37–6.33 (m, 1H), 6.20 (d, J = 5.1 Hz, 1H), 3.93 (d, J = 5.1 Hz, 4H), 3.88 (d, J = 5.1 Hz, 4H), 3.87 (s, 3H).^{13}C NMR (101 MHz, $CDCl_3$) δ 162.07, 160.50, 135.83, 135.11, 133.61, 132.07, 131.87, 131.75, 127.37, 119.51, 113.91, 113.72, 112.44, 66.87, 55.49, 50.56. ^{11}B NMR (128 MHz, $CDCl_3$) δ 0.14 (t, J_{BF} = 33.5 Hz), ^{19}F NMR (376 MHz, $CDCl_3$) δ −135.24 (q, J_{FB} = 33.5 Hz).IR (neat): ν_{max}/cm^{-1}: 3361, 2923, 2852, 2360, 1590, 1536, 1512, 1408, 1287, 1244, 1178, 1019, 902, 760. HRMS-ES Calcd for $C_{20}H_{20}BN_3O_2F_2$ + Na^+: 405.1551. Found: 405.1551.

3-(Pyrrolidin-1-yl)-8-(4-methoxyphenyl)-4,4-difluoro-4-bora-3a,4a-diaza-*s*-indacene 4h. Eluted with CH_2Cl_2–petroleum ether (1 : 1). Dark yellow solid (0.075 g, 87%); mp 171–173 °C; ^{1}H NMR (400 MHz, $CDCl_3$) δ 7.46–7.42 (m, 1H), 7.39 (d, J = 8.7 Hz, 2H), 6.96 (d, J = 8.8 Hz, 2H), 6.90 (d, J = 5.1 Hz, 1H), 6.35 (d, J = 3.1 Hz, 1H), 6.34–6.32 (m, 1H), 6.15 (d, J = 5.1 Hz, 1H), 3.94 (br,s, 4H), 3.86 (s, 3H), 2.11–2.00 (m, 4H). ^{13}C NMR (101 MHz, $CDCl_3$) δ 160.27, 160.17, 135.53, 135.37, 132.02, 131.83, 130.89, 129.96, 127.76, 117.46, 114.35, 113.60, 113.09, 55.46, 51.35, 25.68. ^{11}B NMR (128 MHz, $CDCl_3$) δ 0.01 (t, J_{BF} = 31.0 Hz). ^{19}F NMR (376 MHz, $CDCl_3$) δ −128.23 (q, J_{FB} = 31.0 Hz).IR (neat): ν_{max}/cm^{-1}: 3360, 2923, 1577, 1510, 1395, 2350, 1251, 1094, 1028, 908, 778. HRMS-ES Calcd for $C_{20}H_{20}BN_3OF_2$ + Na^+: 490.1565. Found: 490.1546.

6-Iodo-3-(pyrrolidin-1-yl)-8-(4-methoxyphenyl)-4,4-difluoro-4-bora-3a,4a-diaza-*s*-indacene 5h. Eluted with CH_2Cl_2–petroleum ether (1 : 1). Dark orange solid (0.005 g, 4%), ^{1}H NMR (400 MHz, $CDCl_3$) δ 7.39 (s, 1H), 7.36 (d, J = 8.6 Hz, 2H), 6.96 (d, J = 8.7 Hz, 2H), 6.92 (d, J = 5.2 Hz, 1H), 6.39 (s, 1H), 6.21 (d, J = 5.1 Hz, 1H), 4.04 (s, 4H), 3.86 (s, 3H), 2.07 (t, J = 6.7 Hz, 4H). ^{13}C NMR (101 MHz, $CDCl_3$) δ 160.49, 160.33, 135.85, 133.82, 133.52, 132.53, 131.75, 129.11, 127.17, 122.68, 115.55, 113.77, 64.87, 55.50, 52.13, 25.75. IR (neat): ν_{max}/cm^{-1}: 2988.020, 2359.166, 1794.501, 1694.386, 1599.758, 1513.181, 1392.300, 1248.277, 1027.897, 779.549. HRMS-ES Calcd for $C_{20}H_{19}BN_3OF_2I$ + Na^+: 516.0532. Found: 516.0531.

3-((2-Methylphenyl)amino)-8-(4-methoxyphenyl)-4,4-difluoro-4-bora-3a,4a-diaza-*s*-indacene 4i. Eluted with CH_2Cl_2–petroleum ether (1 : 1). Orange solid (0.057, 60%); mp 227–229 °C; ^{1}H NMR (400 MHz, $CDCl_3$) δ 7.50 (s, 1H), 7.45 (t, J = 7.7 Hz, 2H), 7.40 (d, J = 8.5 Hz, 2H), 7.35 (d, J = 7.7 Hz, 1H), 7.30 (d, J = 7.3 Hz, 2H), 6.95 (d, J = 8.5 Hz, 2H), 6.72 (d, J = 5.1 Hz, 1H), 6.41 (d, J = 3.4 Hz, 1H), 6.39–6.34 (m, 1H), 5.62 (d, J = 5.1 Hz, 1H), 3.96 (s, 2H), 3.85 (s, 2H). ^{13}C NMR (101 MHz, $CDCl_3$) δ 163.14, 160.34, 146.93, 135.59, 134.17, 132.93, 132.04, 131.82, 131.17, 130.20, 128.10, 127.57, 126.72, 118.74, 116.18, 113.65, 113.57, 55.45, 43.11. ^{11}B NMR (128 MHz, $CDCl_3$) δ 0.04 (t, J_{BF} = 33.0 Hz). ^{19}F NMR (376 MHz, $CDCl_3$) δ −148.10 (q, J_{FB} = 33.0 Hz). IR (neat): ν_{max}/cm^{-1}: 3378, 2925, 1620, 1578, 1489, 1398, 1258, 1085, 1021, 786. HRMS-ES Calcd for $C_{23}H_{20}BN_3OF_2$ + Na^+: 426.1565. Found: 426.1577.

3-((4-Methoxyphenyl)amino)-8-(4-methoxyphenyl)-4,4-difluoro-4-bora-3a,4a-diaza-*s*-indacene 4j. Eluted with CH_2Cl_2–petroleum ether (9 : 1). Orange solid (0.077 g, 78%); mp 245–247 °C; ^{1}H NMR (400 MHz, $CDCl_3$) δ 7.84 (s, 1H), 7.49–7.46 (m, 1H), 7.44 (d, J = 8.6 Hz, 2H), 7.21 (d, J = 8.9 Hz, 2H), 6.98 (d, J = 8.7 Hz, 2H), 6.95–6.90 (m, 3H), 6.52 (d, J = 3.6 Hz, 1H), 6.36 (dd, J = 3.7, 2.3 Hz, 1H), 6.23 (d, J = 4.9 Hz, 1H), 3.87 (s, 3H), 3.85–3.80 (m, 3H). The compound was insufficiently soluble to determine ^{13}C NMR. ^{19}F NMR (376 MHz, $CDCl_3$) δ −148.45 (q, J_{FB} = 32.5 Hz). ^{11}B NMR (128 MHz, $CDCl_3$) δ 0.07 (t, J_{BF} = 32.5 Hz). IR (neat): ν_{max}/cm^{-1}: 3368, 2914, 1580, 1293, 1241. HRMS-ES Calcd for $C_{23}H_{20}BN_3O_2F_2$ + Na^+: 442.1514. Found: 442.1499.

6-Iodo-3-((4-methoxyphenyl)amino)-8-(4-methoxyphenyl)-4,4-difluoro-4-bora-3a,4a-diaza-*s*-indacene 5j. Eluted with CH_2Cl_2–petroleum ether (9 : 1). Orange solid (0.008 g, 6%), ^{1}H NMR (400 MHz, $CDCl_3$) δ 7.91 (s, 1H), 7.42 (s, 1H), 7.41 (d,

J = 8.9 Hz, 2H), 7.21 (d, J = 6.9 Hz, 2H), 6.98 (d, J = 6.5 Hz, 2H), 6.96 (s, 1H), 6.93 (d, J = 6.9 Hz, 2H), 6.55 (s, 1H), 6.27 (d, J = 4.9 Hz, 1H), 3.87 (s, 3H), 3.83 (s, 3H). The compound was insufficiently soluble to determine ^{13}C NMR. IR (neat): ν_{max}/cm^{-1}: 3342.169, 3119.175, 2929.044, 1725.014, 1613.144, 1511.895, 1480.277, 1390.170, 1249.831, 1101.578. HRMS-ES Calcd for $C_{23}H_{19}BN_3OF_2I + Na^+$: 568.0481. Found: 568.0489.

3-((4-Chlorophenyl)amino)-8-(4-methoxyphenyl)-4,4-difluoro-4-bora-3a,4a-diaza-*s*-indacene 4k. Eluted with CH_2Cl_2–petroleum ether (1 : 1). Dark yellow solid (0.066 g, 66%); mp 178–180 °C; ^{1}H NMR (400 MHz, $CDCl_3$) δ 7.89 (s, 1H), 7.51 (s, 1H), 7.45 (d, J = 8.7 Hz, 2H), 7.37 (d, J = 8.7 Hz, 2H), 7.20 (d, J = 8.7 Hz, 2H), 7.02–6.96 (m, 3H), 6.58 (d, J = 3.7 Hz, 1H), 6.39 (dd, J = 3.7, 2.4 Hz, 1H), 6.34 (d, J = 4.9 Hz, 1H), 3.88 (s, 3H).^{13}C NMR (101 MHz, $CDCl_3$) δ 160.90, 157.99, 136.36, 136.13, 135.74, 133.16, 132.97, 132.82, 131.86, 131.34, 129.95, 126.76, 123.72, 122.37, 114.42, 113.89, 110.26, 55.52. ^{11}B NMR (128 MHz, $CDCl_3$) δ −0.01 (t, J_{BF} = 33.0 Hz). ^{19}F NMR (376 MHz, $CDCl_3$) δ −148.10 (q, J_{FB} = 33.0 Hz).IR (neat): ν_{max}/cm^{-1}: 3348, 2926, 2860, 1726, 1578, 1519, 1476, 1385, 1292, 1251, 1180, 1096 971, 784. HRMS-ES Calcd for $C_{22}H_{17}BN_3OF_2Cl + Na^+$: 446.1019. Found: 446.1019.

6-(Iodo)-3-((4-chlorophenyl)amino)-8-(4-methoxyphenyl)-4,4-difluoro-4-bora-3a,4a-diaza-*s*-indacene 5k. Eluted with CH_2Cl_2–petroleum ether (1 : 1). Pink solid (0.013 g, 13%); ^{1}H NMR (400 MHz, $CDCl_3$) δ 7.94 (s, 1H), 7.44 (d, J = 14.0 Hz, 2H), 7.39 (d, J = 9.0 Hz, 3H), 7.21 (d, J = 8.6 Hz, 2H), 7.01 (d, J = 5.2 Hz, 1H), 6.99 (d, J = 8.7 Hz, 2H), 6.61 (s, 1H), 6.38 (d, J = 5.0 Hz, 1H), 3.88 (s, 3H). ^{13}C NMR (126 MHz, $CDCl_3$) δ 161.35, 156.52, 141.60, 138.11, 136.69, 136.47, 134.33, 133.96, 132.60, 131.81, 128.85, 125.88, 121.11, 118.24, 114.10, 110.82, 108.49, 66.93, 55.51. IR (neat): ν_{max}/cm^{-1}: 33762.294, 2970.918, 1581.968, 1524.811, 1397.159, 1250.096, 1113.533, 1028.771, 785.061. HRMS-ES Calcd for $C_{22}H_{16}BN_3OF_2ICl + Na^+$: 571.9985. Found: 571.9990.

3-((4-Cyanophenyl)amino)-8-(4-methoxyphenyl)-4,4-difluoro-4-bora-3a,4a-diaza-*s*-indacene 4l. Eluted with CH_2Cl_2–petroleum ether (9 : 1). Pink solid (0.075 g, 77%); mp 204–207 °C; ^{1}H NMR (400 MHz, $CDCl_3$) δ 8.06 (s, 1H), 7.68 (d, J = 8.8 Hz, 2H), 7.61–7.55 (m, 1H), 7.47 (d, J = 8.8 Hz, 2H), 7.31 (d, J = 8.8 Hz, 2H), 7.02 (dd, J = 10.7, 6.8 Hz, 3H), 6.67 (d, J = 4.6 Hz, 1H), 6.50 (d, J = 4.8 Hz, 1H), 6.43 (dd, J = 3.9, 2.3 Hz, 1H), 3.89 (s, 3H).^{13}C NMR (101 MHz, $CDCl_3$) δ 161.26, 155.54, 142.19, 138.61, 135.53, 135.12, 133.99, 133.21, 132.27, 131.97, 126.45, 124.45, 120.55, 118.55, 115.33, 114.01, 109.54, 107.74, 55.56. ^{11}B NMR (128 MHz, $CDCl_3$) δ −0.09 (t, J_{BF} = 32.0 Hz). ^{19}F NMR (282 MHz, $CDCl_3$) δ −147.61 (q, J_{FB} = 32.0 Hz).IR (neat): ν_{max}/cm^{-1}: 3383, 3072, 2224, 1599, 1560, 1524, 1476, 1396, 1251, 1175, 1113, 1024, 936, 780. HRMS-ES Calcd for $C_{23}H_{17}BN_4OF_2 + Na^+$: 437.1361. Found: 437.1367.

3-((4-Cyanophenyl)amino)-6-iodo-8-(4-methoxyphenyl)-4,4-difluoro-4-bora-3a,4a-diaza-*s*-indacene 5l. Eluted with CH_2Cl_2–petroleum ether (9 : 1). Pink solid (0.019 g, 15%); ^{1}H NMR (300 MHz, $CDCl_3$) δ 8.06 (s, 1H), 7.64 (d, J = 8.6 Hz, 2H), 7.46 (s, 1H), 7.38 (d, J = 8.7 Hz, 2H), 7.27 (d, J = 8.7 Hz, 2H), 7.02 (d, J = 4.9 Hz, 1H), 6.96 (d, J = 8.7 Hz, 2H), 6.64 (s, 1H), 6.48 (d, J = 4.9 Hz, 1H), 3.83 (s, 3H). IR (neat): ν_{max}/cm^{-1}: 3366.735, 2995.752, 2227.815, 1597.598, 1566.083, 1474.928, 1394.394, 1253.863, 1101.720. HRMS-ES Calcd for $C_{23}H_{16}BN_4OF_2I + Na^+$: 563.0328. Found: 563.0323.

3-(Pyridin-2-ylamino)-8-(4-methoxyphenyl)-4,4-difluoro-4-bora-3a,4a-diaza-*s*-indacene 4m. Eluted with CH_2Cl_2–petroleum ether (7 : 3). Pink solid (0.055 g, 60%); mp 213–215 °C; ^{1}H NMR (400 MHz, $CDCl_3$) δ 8.40–8.34 (m, 2H), 7.71–7.63 (m, 1H), 7.54 (s, 1H), 7.52 (d, J = 4.9 Hz, 1H), 7.48 (d, J = 8.4 Hz, 2H), 7.04 (d, J = 4.9 Hz, 1H), 7.02 (d, J = 3.5 Hz, 1H), 7.00 (s, 2H), 6.95 (d, J = 8.9 Hz, 1H), 6.60 (d, J = 3.6 Hz, 1H), 6.39 (dd, J = 3.5, 2.3 Hz, 1H), 3.89 (s, 3H).^{13}C NMR (101 MHz, $CDCl_3$) δ 189.77, 160.98, 155.85, 151.33, 148.49, 138.37, 137.20, 135.35, 133.61, 133.11, 132.11, 131.98, 126.85, 122.93, 118.88, 114.51, 113.89, 113.03, 55.52. ^{11}B NMR (128 MHz, $CDCl_3$) δ 0.01 (t, J_{BF} = 33.2 Hz).^{19}F NMR (376 MHz, $CDCl_3$) δ −147.12–−147.70 (m). IR (neat): ν_{max}/cm^{-1}: 3385, 3029, 2356, 1629, 1603,1562, 1496, 1393, 1340, 1297, 1247, 1097, 1028, 972, 769. HRMS-ES Calcd for $C_{21}H_{17}BN_4OF_2 + H^+$: 391.1542. Found: 391.1549.

6-Iodo-3-(pyridin-2-ylamino)-8-(4-methoxyphenyl)-4,4-difluoro-4-bora-3a,4a-diaza-*s*-indacene 5m. Eluted with CH_2Cl_2–petroleum ether (7 : 3). Pink solid (0.017 g, 14%); ^{1}H NMR (400 MHz, $CDCl_3$) δ 8.40 (s, 1H), 8.39–8.34 (m, 1H), 7.69 (td, J = 7.8, 1.9 Hz, 1H), 7.59 (d, J = 5.0 Hz, 1H), 7.47 (d, J = 1.1 Hz, 1H), 7.44 (d, J = 8.8 Hz, 2H), 7.07 (d, J = 5.1 Hz, 1H), 7.05–7.02 (m, 1H), 7.00 (d, J = 8.8 Hz, 2H), 6.96 (d, J = 8.2 Hz, 1H), 6.66–6.60 (m, 1H), 3.88 (s, 3H). ^{13}C NMR (101 MHz, $CDCl_3$) δ 161.14, 156.70, 150.97, 148.57, 138.51, 136.88, 136.16, 135.34, 134.38, 132.49, 131.91, 127.54, 126.31, 119.36, 115.96, 114.06, 113.29, 66.24, 55.57. IR (neat): ν_{max}/cm^{-1}: 3384.942, 2997.326, 1629.610, 1604.071, 1563.166, 1496.334, 1393.697, 1248.697, 1029.204, 972.232, 769.562. HRMS-ES Calcd for $C_{21}H_{16}BN_4OF_2I + Na^+$: 539.0328. Found: 539.0326.

3-(Methyl(phenyl)amino)-8-(4-methoxyphenyl)-4,4-difluoro-4-bora-3a,4a-diaza-*s*-indacene 4n. Eluted with CH_2Cl_2–petroleum ether (1 : 1). Orange solid (0.038, 40%); mp 220–221 °C; ^{1}H NMR (400 MHz, $CDCl_3$) δ 7.50 (s, 1H), 7.45 (t, J = 7.7 Hz, 1H), 7.40 (d, J = 8.5 Hz, 1H), 7.36 (t, J = 7.4 Hz, 1H), 7.30 (d, J = 7.3 Hz, 1H), 6.95 (d, J = 8.5 Hz, 1H), 6.72 (d, J = 5.1 Hz, 1H), 6.52–6.16 (m, 1H), 5.62 (d, J = 5.1 Hz, 1H), 3.96 (s, 1H), 3.85 (s, 1H). ^{13}C NMR (101 MHz, $CDCl_3$) δ 163.15, 160.34, 146.92, 135.59, 134.17, 132.92, 132.04, 131.82, 131.16, 130.20, 128.10, 127.56, 126.72, 118.73, 116.18, 113.65, 113.55, 55.45, 43.11. ^{11}B NMR (128 MHz, $CDCl_3$) δ 0.17 (t, J_{BF} = 32.5 Hz). ^{19}F NMR (376 MHz, $CDCl_3$) δ −129.68 (q, J_{FB} = 32.5 Hz). IR (neat): ν_{max}/cm^{-1}: 2962, 2919, 1681, 1603, 1513, 1298, 1258, 1020, 932, 794. HRMS-ES Calcd for $C_{23}H_{20}BN_3OF_2 + Na^+$: 425.1602. Found: 425.1598.

6-Deuterio-2-iodo-8-(4-methoxyphenyl)-4,4-difluoro-4-bora-3a,4a-diaza-*s*-indacene 11. 2,6-Diiodo-8-(4-methoxyphenyl)-4,4-difluoro-4-bora-3a,4a-diaza-*s*-indacene **3** (0.38 g, 0.69 mmol) was dissolved in CH_2Cl_2 (31 mL). Et_3N (0.09 mL, 0.69 mmol), K_2CO_3 (0.31 g, 2.25 mmol) and 10% Pd/C (0.38 g) were added. The mixture was stirred under nitrogen for 15 min and the nitrogen line was replaced with a deuterium-filled balloon.

The mixture was stirred at room temperature for 4 h and then filtered through Celite, washing with CH_2Cl_2. The solvent was removed under reduced pressure and the orange crude product was purified by column chromatography eluting with CH_2Cl_2–petroleum ether (1 : 1) to give, first eluted: the 6-deuterio-2-iodoBODIPY **11** as an orange solid (0.177 g, 60%) mp 214–215 °C; ^{1}H NMR (300 MHz, $CDCl_3$) δ 7.90 (s, 1H), 7.75 (s, 1H), 7.46 (d, J = 8.7 Hz, 2H), 7.05–6.93 (m, 4H), 3.85 (s, 3H). ^{13}C NMR (126 MHz, $CDCl_3$) δ 162.45, 146.66, 146.03, 145.07, 135.90, 135.72, 135.01, 132.81, 132.49, 125.88, 119.19 (t, J = 27.07 Hz), 114.29, 70.65, 55.61. ^{19}F NMR (282 MHz, $CDCl_3$) δ −144.96 (q, J_{FB} = 28.5 Hz). ^{11}B NMR (96 MHz, $CDCl_3$) δ 0.45 (t, J_{BF} = 28.5 Hz). HRMS-ES Calcd for $C_{16}H_{11}{}^2HBN_2F_2IO + Na^+$: 448.0115. Found: 448.0112.

Second eluted: **2,6-dideuterio-8-(4-methoxyphenyl)-4,4-difluoro-4-bora-3a,4a-diaza-*s*-indacene 2,6-$^2H_2$-1** as an orange solid (0.035 g, 17%) mp 133–135 °C.^{1}H NMR (300 MHz, $CDCl_3$) δ 7.84 (s, 2H), 7.46 (d, J = 8.8 Hz, 2H), 6.96 (d, J = 8.8 Hz, 2H), 6.89 (s, 2H), 3.83 (s, 3H). ^{13}C NMR (75 MHz, $CDCl_3$) δ 162.11, 147.44, 143.31, 134.82, 132.44, 131.27, 126.30, 118.45, 118.12, 117.77, 114.08, 55.55. ^{11}B NMR (96 MHz, $CDCl_3$) δ 0.31 (t, J_{BF} = 29.0 Hz). ^{19}F NMR (282 MHz, $CDCl_3$) δ −145.02 (q, J_{FB} = 29.0 Hz). HRMS-ES Calcd for $C_{16}H_{11}{}^2H_2BN_2F_2O + Na^+$: 323.1112. Found: 323.1110.

6-Deuterio-3-(pyrrolidin-1-yl)-8-(4-methoxyphenyl)-4,4-difluoro-4-bora-3a,4a-diaza-*s*-indacene 12 and 2-deuterio-3-(pyrrolidin-1-yl)-8-(4-methoxyphenyl)-4,4-difluoro-4-bora-3a,4a-diaza-*s*-indacene 13. Following the General Procedure for copper catalysed amination, 6-deuterio-2-iodo-8-(4-methoxyphenyl)-4,4-difluoro-4-bora-3a,4a-diaza-*s*-indacene **11** (0.105 g, 0.247 mmol) was reacted with pyrrolidine (0.035 g, 0.494 mmol). Purification by column chromatography eluting with CH_2Cl_2–petroleum ether (1 : 1) gave a 70 : 30 mixture of the 6-deuterio and 2-deuterio-BODIPYs **12** and **13** respectively as an orange solid (0.08 g, 88%). For the mixture: ^{1}H NMR (500 MHz, $CDCl_3$) δ 7.48 (br, s, 1H), 7.41 (d, J = 8.7 Hz, 2H), 6.99 (d, J = 8.7 Hz, 2H), 6.93–6.88 (m, 1H), 6.48–6.25 (m, 1H), 6.16 (d, J = 5.1 Hz, 1H), 3.94 (br, s, 4H), 3.89 (s, 3H), 2.08–2.05 (m, 4H). ^{11}B NMR (96 MHz, $CDCl_3$) δ 1.00 (t, J_{BF} = 32.5 Hz). ^{19}F NMR (282 MHz, $CDCl_3$) δ −128.25 (q, J_{FB} = 32.5 Hz). HRMS-ES Calcd for $C_{20}H_{19}{}^2HBN_3F_2O + Na^+$: 391.1628. Found: 391.1623. For the major product **12**: ^{13}C NMR (126 MHz, $CDCl_3$) δ 160.22 (C3), 160.13 (C4′), 135.46 (C8a), 135.24 (C1), 131.94 (C7a), 131.75 (C2′,C6′), 130.74 (C8), 129.74 (C5), 127.68 (C1′), 117.23 (C7), 114.35 (C2), 113.55 (C3′, C5′), 112.97 (C6), 55.37 (OMe), 51.26, 25.58. For the minor product **13**: ^{13}C NMR (126 MHz, $CDCl_3$) δ 160.17 (C3), 160.13 (C4′), 135.46 (C8a), 135.12 (C1), 131.94 (C7a), 131.75 (C2′,C6′), 130.74 (C8), 129.82 (C5), 127.68 (C1′), 117.23 (C7), 114.35 (C2), 113.55 (C3′,C5′), 112.97 (C6), 55.37(OMe), 51.26, 25.58.

Acknowledgements

We gratefully acknowledge the Department of Chemistry, Faculty of Science, Taibah University, Saudi Arabia for a scholarship (R.B.A.).

Notes and references

1 A. Treibs and F. H. Kreuzer, *Liebigs Ann. Chem.*, 1968, **718**, 208.
2 (*a*) G. Ulrich, R. Ziessel and A. Harriman, *Angew. Chem., Int. Ed.*, 2008, **47**, 1184; (*b*) A. Loudet and K. Burgess, *Chem. Rev.*, 2007, **107**, 4891.
3 (*a*) K. Umezawa, D. Citterio and K. Suzuki, *Anal. Sci.*, 2014, **30**, 327; (*b*) Y. Ni and J. Wu, *Org. Biomol. Chem.*, 2014, **12**, 3774; (*c*) L. D. Lavis and R. T. Raines, *ACS Chem. Biol.*, 2008, **3**, 142.
4 (*a*) I. Esnal, I. Valois-Escamilla, C. F. A. Gõmez-Durán, A. Urías-Benavides, M. L. Betancourt-Mendiola, I. Lõpez-Arbeloa, J. Bañuelos, I. García-Moreno, A. Costela and E. Peña-Cabrera, *ChemPhysChem*, 2013, **14**, 4134; (*b*) Y. Yang, L. Zhang, B. Li, L. Zhang and X. Liu, *RSC Adv.*, 2013, **3**, 14993; (*c*) G. Duran-Sampedro, A. R. Agarrabeitia, I. Garcia-Moreno, A. Costela, J. Bañuelos, T. Arbeloa, I. López Arbeloa, J. L. Chiara and M. J. Ortiz, *Eur. J. Org. Chem.*, 2012, 6335; (*d*) M. Liras, J. B. Prieto, M. Pintado-Sierra, F. L. Arbeloa, I. García-Moreno, Á. Costela, L. Infantes, R. Sastre and F. Amat-Guerri, *Org. Lett.*, 2007, **9**, 4183.
5 (*a*) J. Zhao, W. Wu, J. Sun and S. Guo, *Chem. Soc. Rev.*, 2013, **42**, 5323; (*b*) S. Guo, L. Ma, J. Zhao, B. Küçüköz, A. Karatay, M. Hayvali, H. G. Yaglioglu and A. Elmali, *Chem. Sci.*, 2014, **5**, 489.
6 (*a*) A. Kamkaew, S. H. Lim, H. B. Lee, L. V. Kiew, L. Y. Chung and K. Burgess, *Chem. Soc. Rev.*, 2013, **42**, 77; (*b*) S. G. Awuah and Y. You, *RSC Adv.*, 2012, **2**, 11169.
7 (*a*) J. F. Lefebvre, X. Z. Sun, J. A. Calladine, M. W. George and E. A. Gibson, *Chem. Commun.*, 2014, **50**, 5258; (*b*) A. M. Poe, A. M. Della Pelle, A. V. Subrahmanyam, W. White, G. Wantz and S. Thayumanavan, *Chem. Commun.*, 2014, **50**, 2913; (*c*) A. Bessette and G. S. Hanan, *Chem. Soc. Rev.*, 2014, **43**, 3342; (*d*) S. Erten-Ela, M. D. Yilmaz, B. Icli, Y. Dede, S. Icli and E. U. Akkaya, *Org. Lett.*, 2008, **10**, 3299; (*e*) S. Hattori, K. Ohkubo, Y. Urano, H. Sunahara, T. Nagano, Y. Wada, N. V. Tkachenko, H. Lemmetyinen and S. Fukuzumi, *J. Phys. Chem. B*, 2005, **109**, 15368.
8 For examples see: (*a*) R. Gotor, P. Gaviña, L. E. Ochando, K. Chulvi, A. Lorente, R. Martínez-Máñez and A. M. Costero, *RSC Adv.*, 2014, **4**, 15975; (*b*) X. Li, X. Gao, W. Shi and H. Ma, *Chem. Rev.*, 2014, **114**, 590; (*c*) H. Zhu, J. Fan, S. Zhang, J. Cao, K. Song, D. Ge, H. Dong, J. Wang and X. Peng, *Biomater. Sci.*, 2014, **2**, 89; (*d*) A. Nano, P. Retailleau, J. P. Hagon, A. Harriman and R. Ziessel, *Phys. Chem. Chem. Phys.*, 2014, **16**, 10187; (*e*) A. Barba-Bon, L. Calabuig, A. M. Costero, S. Gil, R. Martínez-Máñez and F. Sancenón, *RSC Adv.*, 2014, **4**, 8962; (*f*) W. Qin, M. Baruah, M. Van Der Auweraer, F. C. De Schryver and N. Boens, *J. Phys. Chem. A*, 2005, **109**, 7371.
9 (*a*) N. Boens, L. Wang, V. Leen, P. Yuan, B. Verbelen, W. Dehaen, M. Van Der Auweraer, W. D. De Borggraeve, L. Van Meervelt, J. Jacobs, D. Beljonne, C. Tonnelé,

R. Lazzaroni, M. J. Ruedas-Rama, A. Orte, L. Crovetto, E. M. Talavera and J. M. Alvarez-Pez, *J. Phys. Chem. A*, 2014, **118**, 1576; (*b*) I. Esnal, J. Bañuelos, I. López Arbeloa, A. Costela, I. Garcia-Moreno, M. Garzón, A. R. Agarrabeitia and M. José Ortiz, *RSC Adv.*, 2013, **3**, 1547; (*c*) I. Esnal, I. Valois-Escamilla, C. F. A. Gõmez-Durán, A. Urías-Benavides, M. L. Betancourt-Mendiola, I. Lõpez-Arbeloa, J. Bañuelos, I. García-Moreno, A. Costela and E. Peña-Cabrera, *ChemPhysChem*, 2013, **14**, 4134; (*d*) R. I. Roacho, A. Metta-Magaña, M. M. Portillo, E. Peña-Cabrera and K. H. Pannell, *J. Org. Chem.*, 2013, **78**, 4245; (*e*) C. A. Osorio-Martínez, A. Urías-Benavides, C. F. A. Gómez-Durán, J. Bañuelos, I. Esnal, I. López Arbeloa and E. Peña-Cabrera, *J. Org. Chem.*, 2012, **77**, 5434; (*f*) W. Qin, V. Leen, T. Rohand, W. Dehaen, P. Dedecker, M. Van Der Auweraer, K. Robeyns, L. Van Meervelt, D. Beljonne, B. Van Averbeke, J. N. Clifford, K. Driesen, K. Binnemans and N. Boens, *J. Phys. Chem. A*, 2009, **113**, 439; (*g*) X. Shao, R. Kang, Y. Zhang, Z. Huang, F. Peng, J. Zhang, Y. Wang, F. Pan, W. Zhang and W. Zhao, *Anal. Chem.*, 2015, **87**, 399; (*h*) M. Gupta, S. Mula, M. Tyagi, T. K. Ghanty, S. Murudkar, A. K. Ray and S. Chattopadhyay, *Chem. – Eur. J.*, 2013, **19**, 17766; (*i*) H. Yokoi, N. Wachi, S. Hiroto and H. Shinokubo, *Chem. Commun.*, 2014, **50**, 2715; (*j*) H. Yokoi, S. Hiroto and H. Shinokubo, *Org. Lett.*, 2014, **16**, 3004.

10 (*a*) X. He, J. Zhang, X. Liu, L. Dong, D. Li, H. Qiu and S. Yin, *Sens. Actuators, B*, 2014, **192**, 29; (*b*) E. Ganapathi, S. Madhu, T. Chatterjee, R. Gonnade and M. Ravikanth, *Dyes Pigm.*, 2014, **102**, 218; (*c*) M. De Lourdes Betancourt-Mendiola, E. Peña-Cabrera, S. Gil, K. Chulvi, L. E. Ochando and A. M. Costero, *Tetrahedron*, 2014, **70**, 3735; (*d*) Y. A. Volkova, B. Brizet, P. D. Harvey, A. D. Averin, C. Goze and F. Denat, *Eur. J. Org. Chem.*, 2013, 4270; (*e*) L. Y. Niu, H. Li, L. Feng, Y. S. Guan, Y. Z. Chen, C. F. Duan, L. Z. Wu, Y. F. Guan, C. H. Tung and Q. Z. Yang, *Anal. Chim. Acta*, 2013, **775**, 93; (*f*) X. Jia, X. Yu, X. Yang, J. Cui, X. Tang, W. Liu and W. Qin, *Dyes Pigm.*, 2013, **98**, 195; (*g*) M. J. Ortiz, A. R. Agarrabeitia, G. Duran-Sampedro, J. Bañuelos Prieto, T. A. Lopez, W. A. Massad, H. A. Montejano, N. A. García and I. Lopez Arbeloa, *Tetrahedron*, 2012, **68**, 1153; (*h*) L. Jiao, W. Pang, J. Zhou, Y. Wei, X. Mu, G. Bai and E. Hao, *J. Org. Chem.*, 2011, **76**, 9988; (*i*) S. C. Dodani, S. C. Leary, P. A. Cobine, D. R. Winge and C. J. Chang, *J. Am. Chem. Soc.*, 2011, **133**, 8606; (*j*) J. Bañuelos, V. Martín, C. F. A. Gómez-Durán, I. J. A. Córdoba, E. Peña-Cabrera, I. García-Moreno, A. Costela, M. E. Pérez-Ojeda, T. Arbeloa and I. L. Arbeloa, *Chem. – Eur. J.*, 2011, **17**, 7261; (*k*) C. F. A. Gómez-Durán, I. García-Moreno, A. Costela, V. Martin, R. Sastre, J. Bañuelos, F. López Arbeloa, I. López Arbeloa and E. Peña-Cabrera, *Chem. Commun.*, 2010, **46**, 5103; (*l*) D. W. Domaille, L. Zeng and C. J. Chang, *J. Am. Chem. Soc.*, 2010, **132**, 1194; (*m*) L. Li, B. Nguyen and K. Burgess, *Bioorg. Med. Chem. Lett.*, 2008, **18**, 3112; (*n*) O. Dilek and S. L. Bane, *Tetrahedron Lett.*, 2008, **49**, 1413; (*o*) T. Rohand, M. Baruah, W. Qin, N. Boens and W. Dehaen, *Chem. Commun.*, 2006, 266; (*p*) V. Goud, A. Tutar and J. F. Biellmann, *Tetrahedron*, 2006, **62**, 5084; (*q*) M. Baruah, W. Qin, R. A. L. Vallée, D. Beljonne, T. Rohand, W. Dehaen and N. Boens, *Org. Lett.*, 2005, **7**, 4377.

11 V. Leen, V. Z. Gonzalvo, W. M. Deborggraeve, N. Boens and W. Dehaen, *Chem. Commun.*, 2010, **46**, 4908.

12 For selected reviews of copper catalysed amination see: (*a*) C. Sambiagio, S. P. Marsden, A. J. Blacker and P. C. McGowan, *Chem. Soc. Rev.*, 2014, **43**, 3525; (*b*) I. P. Beletskaya and A. V. Cheprakov, *Organometallics*, 2012, **31**, 7753; (*c*) D. S. Surry and S. L. Buchwald, *Chem. Sci.*, 2010, **1**, 13; (*d*) E. Sperotto, G. P. M. Van Klink, G. Van Koten and J. G. De Vries, *Dalton Trans.*, 2010, **39**, 10338.

13 E. Kuhn, V. Bulach and M. W. Hosseini, *Chem. Commun.*, 2008, 5104.

14 Z. Lu and R. J. Twieg, *Tetrahedron*, 2005, **61**, 903.

15 A. Shafir and S. L. Buchwald, *J. Am. Chem. Soc.*, 2006, **128**, 8742.

16 D. Wang and K. Ding, *Chem. Commun.*, 2009, 1891.

17 For example, in amination of 3-bromothiophene, see: Y. B. Huang, C. T. Yang, J. Yi, X. J. Deng, Y. Fu and L. Liu, *J. Org. Chem.*, 2011, **76**, 800.

18 S. V. Ley and A. W. Thomas, *Angew. Chem., Int. Ed.*, 2003, **42**, 5400; A. Rolfe and P. R. Hanson, *Tetrahedron Lett.*, 2009, **50**, 6935.

19 A consequence of this is that amination can be performed on a mixture of the mono- and di-iodoBODIPYs **2** and **3** to give the 3-aminoBODIPY **4** and unreacted diiodide **3**, which can be easily separated by column chromatography.

20 Since iodoBODIPY compounds are known to act as initiators for photooxidation,[5] the reaction between the iodide **2** and 4-cyanoaniline was repeated with careful exclusion of light and also with a 5-cycle freeze–pump–thaw sequence to degas the solution prior to reaction. This did not significantly change the yields of the products (**4l** and **5l**) and so the reaction does not appear to be photo-initiated or require the presence of dioxygen.

21 Hartwig has suggested the intermediacy of highly reactive bisamido cuprate species in aminations catalysed by CuI/phenanthroline: R. Giri and J. F. Hartwig, *J. Am. Chem. Soc.*, 2010, **132**, 15860.

22 (*a*) V. Bocchi and G. Palla, *J. Chem. Soc., Chem. Commun.*, 1983, 1074; (*b*) M. Poirier, S. Goudreau, J. Poulin, J. Savoie and P. L. Beaulieu, *Org. Lett.*, 2010, **12**, 2334; (*c*) For a review of 'vicarious' hydrogen substitution see: M. Makosza, *Pure Appl. Chem.*, 1997, **69**, 559.

23 Reductive loss of iodine from C-2 might have been linked to oxidation of the copper(I) catalyst[25] [*e.g.* via a copper(I)/copper(III) cycle or single electron transfers involving copper(II)] (Scheme S2, ESI†). Such a mechanism would provide the oxidant required for direct nucleophilic hydrogen displacement by the amine[11] and could explain formation of the iodinated byproduct **5**. The unreactivity of the 2,6-diiodide **3**, the formation of a 1 : 1 ratio of **12** : **13** in the amination of the

deuterioBODIPY **11** (Scheme 5) and the success of the amination with aniline nucleophiles all indicate that such a mechanism does not operate.

24 A base-catalysed halogen dance[26] (BCHD) might also be envisaged involving reversible sequential deprotonations to give anionic intermediates which abstract the halogen from another molecule to set up an equilibrium of iodinated BODIPY species. The ultimate outcome of the reaction would be determined by nucleophilic interception of the 3-iodo species to give the product **4** (Scheme S3, ESI†). The insensitivity of the reaction to the nature of the halogen (Scheme 3) and the failure of an attempted copper catalysed amination of a 1 : 1 mixture of the unhalogenated BODIPY **1** and the 2,6-diiodide **3** with pyrrolidine strongly suggest that a BCHD is not involved.

25 For a related proposal see: A. John and K. M. Nicholas, *Organometallics*, 2012, **31**, 7914.

26 For a review see: M. Schnürch, M. Spina, A. F. Khan, M. D. Mihovilovic and P. Stanetty, *Chem. Soc. Rev.*, 2007, **36**, 1046.

27 M. Fischer and J. Georges, *Chem. Phys. Lett.*, 1996, **260**, 115.

28 M. Baruah, W. Qin, N. Basarić, W. M. De Borggraeve and N. Boens, *J. Org. Chem.*, 2005, **70**, 4152.

29 V. Leen, T. Leemans, N. Boens and W. Dehaen, *Eur. J. Org. Chem.*, 2011, 4386.

30 C. Yu, L. Jiao, H. Yin, J. Zhou, W. Pang, Y. Wu, Z. Wang, G. Yang and E. Hao, *Eur. J. Org. Chem.*, 2011, 5460.

31 *CrysAlisPro version 1.171.35*, Agilent Technologies, 2010.

32 R. C. Clark and J. S. Reid, *Acta Crystallogr., Sect. A: Fundam. Crystallogr.*, 1995, **51**, 887.

33 G. M. Sheldrick, *Acta Crystallogr., Sect. A: Fundam. Crystallogr.*, 2008, **64**, 112.

34 O. V. Dolomanov, L. J. Bourhis, R. J. Gildea, J. A. K. Howard and H. Puschmann, *J. Appl. Crystallogr.*, 2009, **42**, 229.

ChemPubSoc Europe

DOI: 10.1002/chem.201504484

CHEMISTRY A European Journal Communication

Chirality

Circularly Polarized Luminescence from Helically Chiral *N,N,O,O*-Boron-Chelated Dipyrromethenes

Rua B. Alnoman,[a] Sandra Rihn,[a] Daniel C. O'Connor,[a] Fiona A. Black,[a] Bernard Costello,[b] Paul G. Waddell,[a] William Clegg,[a] Robert D. Peacock,[c] Wouter Herrebout,[d] Julian G. Knight,*[a] and Michael J. Hall*[a]

Abstract: Helically chiral *N,N,O,O*-boron chelated dipyrromethenes showed solution-phase circularly polarized luminescence (CPL) in the red region of the visible spectrum (λ_{em}(max) from 621 to 663 nm). The parent dipyrromethene is desymmetrised through O chelation of boron by the 3,5-*ortho*-phenolic substituents, inducing a helical chirality in the fluorophore. The combination of high luminescence dissymmetry factors ($|g_{lum}|$ up to 4.7 $\times 10^{-3}$) and fluorescence quantum yields (Φ_F up to 0.73) gave exceptionally efficient circularly polarized red emission from these simple small organic fluorophores, enabling future application in CPL-based bioimaging.

Molecules that display circularly polarized luminescence (CPL), the spontaneous emission of right- or left-circularly polarized light, do so as a consequence of the intrinsic chirality of the excited state.[1] CPL-capable molecules and materials are of interest due to their ability to generate optical signals, which include not only wavelength and intensity but also chirality information. CPL from the condensed phase is employed in numerous applications,[2] whilst in the field of solution-phase CPL chiral lanthanide complexes[3] have proved to be popular due to their high luminescence dissymmetry factors.[4,5] However, low fluorescence quantum yields (Φ_F) and thus low CPL efficiency limits their application. Therefore, there is considerable interest in new small organic molecules, which display efficient (high $|g_{lum}|$ ($\geq 10^{-3}$) and high Φ_F) CPL (CPL-SOMs).[6] In particular, CPL-SOMs with efficient emission in the red region of the visible spectrum could be used to create new dye conjugates for CPL-based in vivo bioimaging.[7] The majority of current CPL-SOMs are based on either a BINOL or helicene scaffold. However, despite significant advances in the area,[8,9] these systems still pose significant synthetic challenges, making straightforward tuning of their photophysical or chiroptical properties difficult. Conversely, the 4,4-difluoro-4-bora-3a,4a-diaza-*s*-indacene (BODIPY) dyes are stable, tunable organic fluorophores with red to near-IR emission, high extinction coefficients and quantum yields,[10] and have been widely used in in vivo imaging,[11] photodynamic therapy,[12] analyte sensing,[13] light-harvesting arrays[14] and solar cells,[15] but have seen very limited use as chiroptical dyes. Although non-chiral BODIPYs have been co-polymerized with chiral monomers to form CPL emissive polymer materials,[16] resolved BODIPYs, which encompass an intrinsically chiral fluorophore, are rare.[17] Recently, de la Moya and co-workers reported an elegant desymmetrisation of an achiral BODIPY, by boron chelation with either (*S*)- or (*R*)-1,1′-bi-2-naphthol (BINOL).[18] The resulting long-range chiral perturbation of the fluorophore by the chelated enantiopure BINOL resulted in the first reported solution-phase CPL from the direct excitation of a BODIPY chromophore, albeit with modest efficiency ($|g_{lum}| \approx 8 \times 10^{-4}$ and $\Phi_F = 0.46$).[19]

Therefore, our aim was to develop new chiral BODIPYs capable of high-efficiency CPL (high $|g_{lum}|$ and Φ_F) in the red region of the visible spectrum (>600 nm), through the use of a direct desymmetrisation approach to induce a helical chirality in the fluorophore. Our design was inspired by the redshifted *N,N,O,O*-boron-chelated BODIPYs first reported by Burgess and co-workers,[20] involving the bonding of two 3,5-*ortho*-phenolic substituents to the central boron atom to desymmetrise our target BODIPYs **1a–d** and enforce the desired helicity. We postulated that a sterically unobtrusive, minimal substituent at the 8-position together with 1,7-di-*H*-substitution would aid in maximizing the helical pitch, increasing the $|g_{lum}|$, whilst simultaneously minimizing non-radiative decay from the S_1 excited state. Therefore, we included in our design substituents at the 8-position, which would span a range of sizes: H- (**1a**), Me- (**1b**) and two aryl groups, *p*-tolyl- (**1c**) and 2-pyridyl (**1d**; Figure 1).

[a] R. B. Alnoman, Dr. S. Rihn, D. C. O'Connor, F. A. Black, Dr. P. G. Waddell, Prof. W. Clegg, Dr. J. G. Knight, Dr. M. J. Hall
School of Chemistry, Bedson Building, Newcastle University
Newcastle upon Tyne, NE1 7RU (UK)
E-mail: julian.knight@ncl.ac.uk
m.hall@ncl.ac.uk

[b] Dr. B. Costello
Applied Photophysics Ltd., 21 Mole Business Park
Leatherhead, Surrey KT22 7BA (UK)

[c] Prof. R. D. Peacock
School of Chemistry, University of Glasgow, Joseph Black Building. University Avenue, Glasgow, G12 8QQ, Scotland (UK)

[d] Prof. W. Herrebout
Department of Chemistry, University of Antwerp, Groenenborgerlaan 171, 2020 Antwerp (Belgium)

Supporting information for this article is available on the WWW under http://dx.doi.org/10.1002/chem.201504484.

ChemPubSoc Europe

CHEMISTRY A European Journal Communication

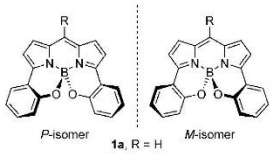

Figure 1. Target helically chiral *N,N,O,O*-boron-chelated BODIPYs **1 a–d**.

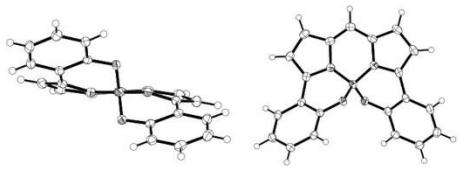

Figure 2. Two views of one molecule in the crystal structure of (*rac*)-**1 a** showing the helical chirality of the molecule (H atoms are omitted for clarity).

Our synthetic work commenced by examining routes to racemic BODIPYs **1 a–b**, which would incorporate an H or Me at the 8-position. *tert*-Butyl 2-bromo-1*H*-pyrrole-1-carboxylate (**2**) underwent Suzuki coupling with (2-hydroxyphenyl)boronic acid.[21] At high temperatures (>80 °C), only low yields of the desired Suzuki product could be obtained; however, decreasing the reaction temperature to 65 °C gave access to 5*H*-benzo[*e*]pyrrolo[1,2-*c*][1,3]oxazin-5-one (**3**), resulting from a Suzuki coupling and in situ intramolecular carbamate formation. Mild basic hydrolysis of **3** gave 2-(1*H*-pyrrol-2-yl)phenol (**4**), which was condensed with triethyl orthoformate or orthoacetate under acidic conditions and reacted with boron trifluoride to give racemic BODIPYs **1 a** and **b** (Scheme 1).

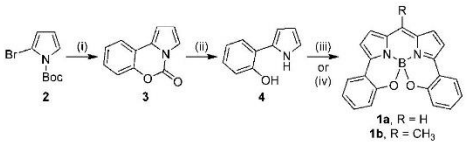

Scheme 1. Reaction conditions: i) (2-hydroxyphenyl)boronic acid, 5 mol% $[Pd(PPh_3)_4]$, K_2CO_3, toluene/EtOH/H_2O, 65 °C, 16 h, (54%); ii) NaOH, EtOH, r.t., 1 h, (72%); iii) (a) $HC(OEt)_3$, TFA, CH_2Cl_2, r.t., 45 min; (b) BF_3·OEt_2, TEA, CH_2Cl_2, r.t., 2 h, (**1 a** 18%); iv) (a) $CH_3C(OEt)_3$, TFA, CH_2Cl_2, r.t., 45 min; (b) BF_3·OEt_2, DIPEA, CH_2Cl_2, r.t., 2 h, (**1 b** 43%).

To improve overall yields and to avoid the practical difficulties associated in handling electron-rich pyrrole intermediates (such as **2**), we next examined an alternative route to the aryl-substituted BODIPYs **1 c–d**, in which the two *ortho*-phenolic groups would be introduced through a late-stage Suzuki coupling. BF_3-mediated condensation of *p*-tolualdehyde or picolinaldehyde with pyrrole gave the corresponding dipyrromethanes, which were regioselectively dibrominated at the 3,5-positions, oxidised to the dipyrromethenes with 2,3-dichloro-5,6-dicyano-1,4-benzoquinone (DDQ) and reacted with BF_3 to give dibromo-BODIPYs **5 a–b**. Suzuki coupling with 2-methoxyphenylboronic acid gave 3,5-diaryl-BODIPYs **6 a–b**, which were converted, through boron tribromide demethylation, to the racemic BODIPYs **1 c** and **d** (Scheme 2).

Crystallization experiments gave single crystals of **1 a–c** suitable for X-ray analysis (see the Supporting Information).[22] In all cases, a significant twisting of the fluorophore was observed; the twist angle between the planes defined by the two pyrrolic rings: **1 a** 11.2°, **1 b** 9.0° and **1 c** 9.8° (Figure 2).[23]

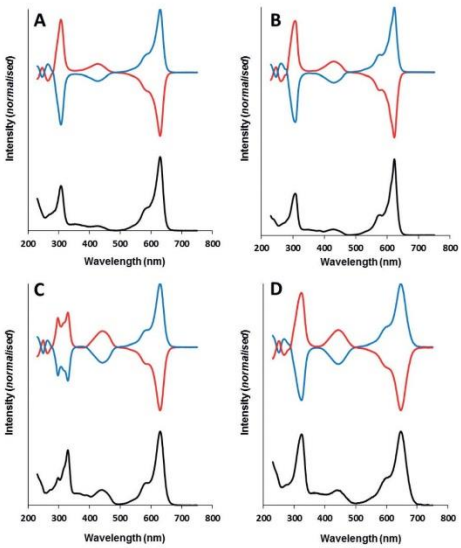

Figure 3. Normalised ECD (red and blue) and UV/Vis absorption spectra (black): a) (*M*)-**1 a** (red) and (*P*)-**1 a** (blue) [$CHCl_3$]: b) (*M*)-**1 b** (red) and (*P*)-**1 b** (blue) [hexane]: c) (*M*)-**1 c** (red) and (*P*)-**1 c** (blue) [hexane]; d) (*M*)-**1 d** (red) and (*P*)-**1 d** (blue) [$CHCl_3$].

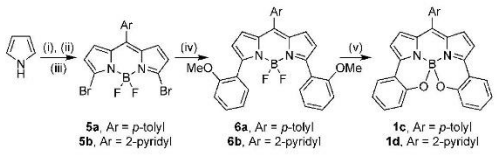

Scheme 2. Reagents: i) 4-methylbenzaldehyde or picolinaldehyde, BF_3·OEt_2, r.t., 30 min; ii) NBS, THF, −78 °C, 1 h; DDQ, THF, −78 °C to r.t.; iii) BF_3·OEt_2, DIPEA, CH_2Cl_2, r.t., 2 h, (**5 a** 47%, **5 b** 24% over three steps); iv) 2-(MeO)$C_6H_4B(OH)_2$, $[Pd(PPh_3)_4]$ (5 mol%), Na_2CO_3, toluene/H_2O, reflux, 4 h, (**6 a** 98%, **6 b** 81%); v) BBr_3, CH_2Cl_2, r.t., 5 h, (**1 c** 96%, **1 d** 60%).

ChemPubSoc Europe

CHEMISTRY A European Journal Communication

Both enantiomers of BODIPYs **1a–d** were then resolved by semi-preparative chiral HPLC to examine their chiroptical properties (see the Supporting Information). Electronic circular dichroism (ECD) spectra were measured for each of the enantiomeric samples of **1a–d**, in hexane or $CHCl_3$ as appropriate, using an Applied Photophysics Ltd. Chirascan-plus spectrometer. In each case, mirror image ECD spectra were obtained from the corresponding enantiomers, the major peaks of the ECD spectra aligning well with those of the absorption spectra (Figure 3).

Assignment of absolute configuration to the resolved enantiomers of **1a–d** was performed by a comparison of the experimental ECD with that calculated for the *P*-isomer of **1a–d**. Boltzmann-weighted ECD spectra for the *P*-isomers **1a–d** were obtained by TD-DFT calculations at the cam-B3LYP/6-311++G(3df,2pd) and M06-2X/6-311++G(3df,2pd) levels.[24] Generation of a low-energy conformation library was followed by calculation of the individual ECD spectra for each of the low-energy conformations (Figure 4). Comparison of features of the calculated ECD spectra of the *P*-isomers to the experimental spectra allowed the assignment of the absolute configuration of each of the enantiomeric samples of **1a–d**.

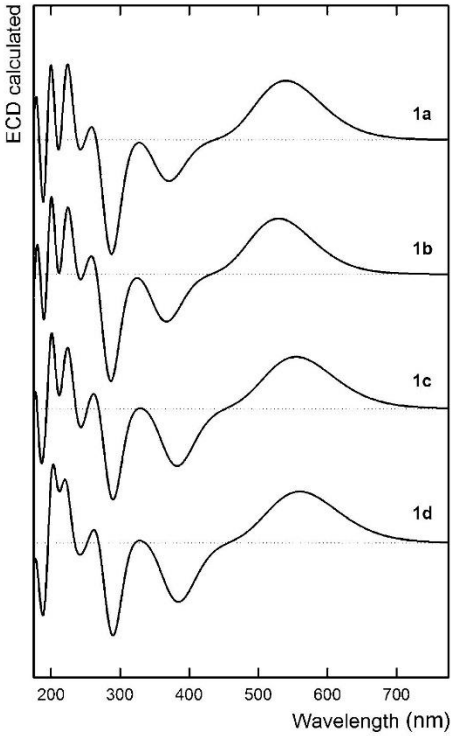

Figure 4. Boltzmann-weighted ECD spectra for the *P*-isomers **1a–d**, calculated at the cam-B3LYP/6-311++G(3df,2pd) level.

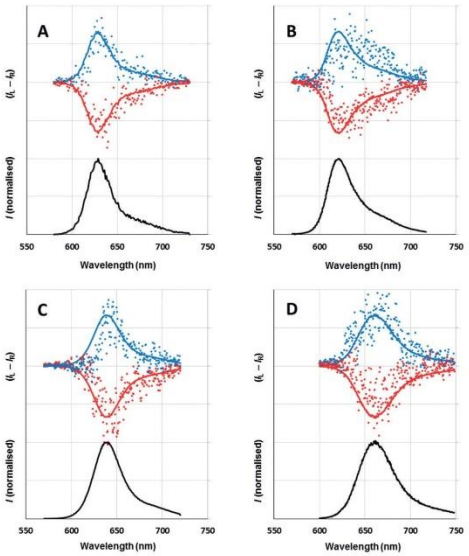

Figure 5. Normalised CPL spectra (red and blue) and normalised fluorescence spectra (black) shown (MeCN, excitation 540 nm): a) (*M*)-**1a** (red) and (*P*)-**1a** (blue); b) (*M*)-**1b** (red) and (*P*)-**1b** (blue); c) (*M*)-**1c** (red) and (*P*)-**1c** (blue); d) (*M*)-**1d** (red) and (*P*)-**1d** (blue).

CPL spectra were then measured for each pair of enantiomeric samples of **1a–d** (Figure 5). The *P*- and *M*-isomers of **1a–d** gave mirror image CPL spectra with high $|g_{lum}|$ (**1a** 0.0047 (623 nm), **1b** 0.0033 (635 nm), **1c** 0.0043 (637 nm) and **1d** 0.0042 (675 nm)). The $|g_{lum}|$ values for this series of compounds include the largest reported to date for a simple BODIPY fluorophore in solution. In the case of BODIPY **1a**, the inclusion of H- at the 8-position resulted in both a large luminescence dissymmetry factor and fluorescence quantum yield ($|g_{lum}| = 4.7 \times 10^{-3}$, $\Phi_F = 0.65$ in MeCN), making it the most efficient single-fluorophore, red-emitting CPL-SOM reported to date.[6]

In conclusion, we have shown that the helical *N,N,O,O*-boron-chelated dipyrromethenes are a privileged molecular scaffold for the creation of redshifted solution-phase CPL-SOMs and are promising motifs for future chiral fluorophore development.

Acknowledgements

The authors thank Newcastle University (NCL) and the BBSRC (BB/K013971/1) for funding, the Department of Chemistry, Faculty of Science, Taibah University, Saudi Arabia for a PhD scholarship (R.B.A.), EPSRC for X-ray crystallography facilities (EP/F03637X/1), Diamond Light Source (beamline I19), Prof. W. McFarlane and Dr. C. Wills (NCL) for NMR support, P. Stachelek

ChemPubSoc Europe

CHEMISTRY A European Journal Communication

for spectroscopy support, Prof. A. Benniston (NCL) for helpful discussions and the EPSRC UK National Mass Spectrometry Facility at Swansea University.

Keywords: absolute stereochemistry · BODIPYs · chirality · circularly polarized luminescence · luminescence

[1] a) J. P. Riehl, F. S. Richardson, *Chem. Rev.* **1986**, *86*, 1; b) H. G. Brittain, *Chirality* **1996**, *8*, 357.

[2] a) J. Liu, H. Su, L. Meng, Y. Zhao, C. Deng, J. C. Y. Ng, P. Lu, M. Faisal, J. W. Y. Lam, X. Huang, H. Wu, K. S. Wong, B. Z. Tang, *Chem. Sci.* **2012**, *3*, 2737; b) K. Okano, M. Taguchi, M. Fujiki, T. Yamashita, *Angew. Chem. Int. Ed.* **2011**, *50*, 12474; *Angew. Chem.* **2011**, *123*, 12682; c) Z. Shen, T. Wang, L. Shi, Z. Tang, M. Liu, *Chem. Sci.* **2015**, *6*, 4267.

[3] a) G. Muller, *Dalton Trans.* **2009**, 9692; b) D. Parker, R. S. Dickins, H. Puschmann, C. Crossland, J. A. K. Howard, *Chem. Rev.* **2002**, *102*, 1977; c) R. Carr, N. H. Evans, D. Parker, *Chem. Soc. Rev.* **2012**, *41*, 7673.

[4] Luminescence dissymmetry factor $g_{lum}(\lambda) = 2(I_L - I_R)/(I_L + I_R)$, in which I_L and I_R are the intensity of left and right circularly polarized emissions, respectively.

[5] a) F. Song, G. Wei, X. Jiang, F. Li, C. Zhu, Y. Cheng, *Chem. Commun.* **2013**, *49*, 5772; b) K. Okutani, K. Nozaki, M. Iwamura, *Inorg. Chem.* **2014**, *53*, 5527.

[6] a) E. M. Sánchez-Carnerero, A. R. Agarrabeitia, F. Moreno, B. L. Maroto, G. Muller, M. J. Ortiz, S. de La Moya, *Chem. Eur. J.* **2015**, *21*, 13488; b) J. Kumar, T. Nakashima, T. Kawai, *J. Phys. Chem. Lett.* **2015**, *6*, 3445.

[7] a) M. C. Heffern, L. M. Matosziuk, T. J. Meade, *Chem. Rev.* **2014**, *114*, 4496; b) M. Seitz, E. G. Moore, A. J. Ingram, G. Muller, K. N. Raymond, *J. Am. Chem. Soc.* **2007**, *129*, 15468; c) H. Tsumatori, T, Harada, J. Yuasa, Y. Hasegawa, T. Kawai, *Appl. Phys. Express* **2011**, *4*, 011601.

[8] a) H. R. Talele, S. Sahoo, A. V. Bedekar, *Org. Lett.* **2012**, *14*, 3166; b) M. S. Sundar, H. R. Talele, H. M. Mande, A. V. Bedekar, R. C. Tovar, G. Muller, *Tetrahedron Lett.* **2014**, *55*, 1760; c) Y. Kitayama, T. Amako, N. Suzuki, M. Fujiki, Y. Imai, *Org. Biomol. Chem.* **2014**, *12*, 4342.

[9] a) Y. Shen, C.-F. Chen, *Chem. Rev.* **2012**, *112*, 1463; b) N. Saleh, M. Srebro, T. Reynaldo, N. Vanthuyne, L. Toupet, V. Y. Chang, G. Muller, J. A. G. Williams, C. Roussel, J. Autschbach, J. Crassous, *Chem. Commun.* **2015**, *51*, 3754; c) N. Saleh, B. Moore, M. Srebro, N. Vanthuyne, L. Toupet, J. A. G. Williams, C. Roussel, K. K. Deol, G. Muller, J. Autschbach, J. Crassous, *Chem. Eur. J.* **2015**, *21*, 1673; d) H. Sakai, S. Shinto, J. Kumar, Y. Araki, T. Sakanoue, T. Takenobu, T. Wada, T. Kawai, T. Hasobe, *J. Phys. Chem. C* **2015**, *119*, 13937; e) T. Matsuno, Y. Koyama, S. Hiroto, J. Kumar, T. Kawai, H. Shinokubo, *Chem. Commun.* **2015**, *51*, 4607; f) K. Goto, R. Yamaguchi, S. Hiroto, H. Ueno, T. Kawai, H. Shinokubo, *Angew. Chem. Int. Ed.* **2012**, *51*, 10333; *Angew. Chem.* **2012**, *124*, 10479; g) H. Sakai, S. Shinto, Y. Araki, T. Wada, T. Sakanoue, T. Takenobu, T. Hasobe, *Chem. Eur. J.* **2014**, *20*, 10099.

[10] a) G. Ulrich, R. Ziessel, A. Harriman, *Angew. Chem. Int. Ed.* **2008**, *47*, 1184; *Angew. Chem.* **2008**, *120*, 1202; b) A. Loudet, K. Burgess, *Chem. Rev.* **2007**, *107*, 4891.

[11] a) T. Kowada, H. Maeda, K. Kikuchi, *Chem. Soc. Rev.* **2015**, *44*, 4953; b) M. Larrouy, C. Bernhard, V. Goncalves, O. Raguin, P. Provent, M. Moreau, B. Collin, A. Oudot, J. Vrigneaud, F. Brunotte, C. Goze, F. Denat, *Chem. Eur. J.* **2015**, *21*, 13091.

[12] a) A. Kamkaew, S. H. Lim, H. B. Lee, L. V. Kiew, L. Y. Chung, K. Burgess, *Chem. Soc. Rev.* **2013**, *42*, 77; b) A. Kamkaew, K. Burgess, *J. Med. Chem.* **2013**, *56*, 7608; c) S. O. McDonnell, M. J. Hall, L. T. Allen, A. Byrne, W. M. Gallagher, D. F. O'Shea, *J. Am. Chem. Soc.* **2005**, *127*, 16360.

[13] N. Boens, V. Leena, W. Dehaen, *Chem. Soc. Rev.* **2012**, *41*, 1130.

[14] a) R. Ziessel, G. Ulrich, A. Haefele, A. Harriman, *J. Am. Chem. Soc.* **2013**, *135*, 11330; b) A. Harriman, *Chem. Commun.* **2015**, *51*, 11745.

[15] a) A. Bessette, G. S. Hanan, *Chem. Soc. Rev.* **2014**, *43*, 3342; b) J.-F. Lefebvre, X.-Z. Sun, J. A. Calladine, M. W. George, E. A. Gibson, *Chem. Commun.* **2014**, *50*, 5258; c) C. J. Wood, G. H. Summers, E. A. Gibson, *Chem. Commun.* **2015**, *51*, 3915.

[16] a) A. Nagai, K. Kokado, J. Miyake, Y. Chujo, *Polym. J.* **2010**, *42*, 37; b) X. Ma, E. A. Azeem, X. Liu, Y. Cheng, C. Zhu, *J. Mater. Chem. C* **2014**, *2*, 1076.

[17] a) A. Haefele, C. Zedde, P. Retailleau, G. Ulrich, R. Ziessel, *Org. Lett.* **2010**, *12*, 1672; b) S. Kolemen, Y. Cakmak, Z. Kostereli, E. U. Akkaya, *Org. Lett.* **2014**, *16*, 660; c) R. I. Lerrick, T. P. L. Winstanley, K. Haggerty, C. Wills, W. Clegg, R. W. Harrington, P. Bultinck, W. Herrebout, A. C. Benniston, M. J. Hall, *Chem. Commun.* **2014**, *50*, 4714; d) T. Bruhn, G. Pescitelli, S. Jurinovich, A. Schaumlöffel, F. Witterauf, J. Ahrens, M. Bröring, G. Bringmann, *Angew. Chem. Int. Ed.* **2014**, *53*, 14592; *Angew. Chem.* **2014**, *126*, 14821.

[18] a) E. M. Sanchez-Carnerero, F. Moreno, B. L. Maroto, A. R. Agarrabeitia, M. J. Ortiz, B. G. Vo, G. Muller, S. de La Moya, *J. Am. Chem. Soc.* **2014**, *136*, 3346; b) E. M. Sánchez-Carnerero, L. Gartzia-Rivero, F. Moreno, B. L. Maroto, A. R. Agarrabeitia, M. J. Ortiz, J. Bañuelos, Í. López-Arbeloa, S. de La Moya, *Chem. Commun.* **2014**, *50*, 12765; c) S. Zhang, Y. Wang, F. Meng, C. Dai, Y. Cheng, C. Zhu, *Chem. Commun.* **2015**, *51*, 9014.

[19] An example of CPL from a BODIPY by indirect excitation has also been reported, the BODIPY chromophore acting as the acceptor in an electronic energy-transfer cassette based on an urobilin scaffold: A. Gossauer, F. Fehr, F. Nydegger, H. Stöckli-Evans, *J. Am. Chem. Soc.* **1997**, *119*, 1599.

[20] a) H. Kim, A. Burghart, M. B. Welch, J. Reibenspies, K. Burgess, *Chem. Commun.* **1999**, 1889; b) A. Loudet, R. Bandichhor, K. Burgess, A. Palma, S. O. McDonnell, M. J. Hall, D. F. O'Shea, *Org Lett.* **2008**, *10*, 4771.

[21] W. Chen, E. K. Stephenson, M. P. Cava, Y. A. Jackson, *Org. Synth.* **1992**, *70*, 151.

[22] CCDC 1413058, 1413059, 1413060, 1413061, 1413062 contain the supplementary crystallographic data for this paper. These data can be obtained free of charge from The Cambridge Crystallographic Data Centre via www.ccdc.cam.ac.uk/data request/cif.

[23] A survey of 60 typical BODIPY crystal structures (CCDC) showed plane/plane twist angles of one to two degrees (plane/plane twist angle is the angle between the plane normals projected onto the plane perpendicular to the vector joining the plane centroids).

[24] Gaussian 09, Revision D.01, M. J. Frisch, G. W. Trucks, H. B. Schlegel, G. E. Scuseria, M. A. Robb, J. R. Cheeseman, G. Scalmani, V. Barone, B. Mennucci, G. A. Petersson, H. Nakatsuji, M. Caricato, X. Li, H. P. Hratchian, A. F. Izmaylov, J. Bloino, G. Zheng, J. L. Sonnenberg, M. Hada, M. Ehara, K. Toyota, R. Fukuda, J. Hasegawa, M. Ishida, T. Nakajima, Y. Honda, O. Kitao, H. Nakai, T. Vreven, J. A. Montgomery, Jr., J. E. Peralta, F. Ogliaro, M. Bearpark, J. J. Heyd, E. Brothers, K. N. Kudin, V. N. Staroverov, R. Kobayashi, J. Normand, K. Raghavachari, A. Rendell, J. C. Burant, S. S. Iyengar, J. Tomasi, M. Cossi, N. Rega, M. J. Millam, M. Klene, J. E. Knox, J. B. Cross, V. Bakken, C. Adamo, J. Jaramillo, R. Gomperts, R. E. Stratmann, O. Yazyev, A. J. Austin, R. Cammi, C. Pomelli, J. W. Ochterski, R. L. Martin, K. Morokuma, V. G. Zakrzewski, G. A. Voth, P. Salvador, J. J. Dannenberg, S. Dapprich, A. D. Daniels, Ö. Farkas, J. B. Foresman, J. V. Ortiz, J. Cioslowski, D. J. Fox, Gaussian, Inc., Wallingford CT, **2009**.

Received: November 9, 2015
Published online on November 30, 2015

4